ENVIRONMENTAL GEOCHEMISTRY OF MINESITE DRAINAGE: PRACTICAL THEORY AND CASE STUDIES, *DIGITAL EDITION*

by:

Kevin A. Morin
and
Nora M. Hutt

Minesite Drainage Assessment Group/
Grupo Estudio del Drenaje de Minas

Canadian Cataloguing in Publication Data

Morin, Kevin A. (Kevin Andrew), 1955-
Environmental geochemistry of minesite drainage [computer file]

ISBN 0-9682039-1-4

1. Mine drainage -- Environmental aspects. 2. Environmental geochemistry. I. Hutt, Nora M. II. Title.
TD195.M48M67 2001 622'.5 C2001-910196-1

(ISBN for Paper Edition: 0-9682039-0-6)

Published by:
MDAG Publishing
Vancouver, British Columbia, Canada

Cover Photo Credit: BHP Minerals Canada Ltd., Island Copper Mine
(photograph by Ian Audley Horne)

Dedicated to:

1) environmentally thoughtful mining in the 21st century

2) *aloha ‘aina*
domoni ni vanua
(love of the environment)

3) future generations,
to show that we managed as best we could
the environmental legacy of our minesites
and of those bequeathed to us

TABLE OF CONTENTS

LIST OF TABLES

LIST OF FIGURES

PREFACE AND ACKNOWLEDGEMENTS

This book has three purposes. First, it is a *guidebook* for the assessment, prediction, and control of minesite-drainage chemistry. The chapters on these tasks emphasize practical, rather than theoretical, concepts. As demonstrated here, the abundant conflicting theories on drainage chemistry are, for the most part, unimportant to the practical requirements of many minesites.

Second, this is a *reference book* containing numerous case studies on various aspects of drainage chemistry. These illustrate the many different views of drainage-chemistry work around the world and are valuable in extrapolating conclusions to other minesites. Case studies are used heavily in this book to illustrate common themes and to highlight atypical findings.

Third, this is a *textbook* to present the state-of-the-art in minesite drainage to fellow students on the topic. The questions at the end of each chapter provoke additional thought and insight into important issues. No matter what level of experience and age, there is something new and informative in this book for every reader.

Based on our work with more than 130 proposed and existing minesites, and on reviews of hundreds of papers and reports by many others, these three ambitious purposes have been attained here in a reasonably compact book. We welcome copies of other papers and reports that readers consider important and valuable to future compilations.

We have noticed there is confusion sometimes between minesite-drainage chemistry and water-quality impacts. The emphasis in this book is on the chemistry of waters draining from various minesite components. In the jargon of hydrologic studies, the focus is on “headwater” chemical effects in and around a minesite. There is little emphasis on “downstream” chemistry in distant rivers and lakes, where regional water-quality and biological impacts are defined by applicable legislation and social expectations. Consistent with this view, “water quality”, which implies comparison to some standard, is rarely used here.

A book like this on theory and case studies cannot be created in isolation from other people — no one person could carry out all these studies and interpretations. Therefore, there are many people and publications that we have depended on, and learned from. Obviously, the efforts of all authors listed in the References are important and gratefully recognized. We are especially grateful to the people who provided technical and editorial comments on various chapters of this book:

Les MacPhie, Geocon/SNC—Lavalin Environment [Chapters 1 to 6]
Peri Mehling, Mehling Environmental Management [Chapters 1 and 2]
Gavin Murray, Placer Pacific Limited [Chapters 1 to 6]
Jim Robertson, Placer Dome Inc. [Chapters 3 to 6]

We also acknowledge the time and efforts of those that we have worked with professionally and personally, who are employed by mining companies, regulatory agencies, universities, consulting firms, and laboratories. With mining companies, we offer particular thanks to Jim Robertson (Placer Dome Inc.), Keith Ferguson (Placer Dome Canada), Gavin Murray (Placer Pacific Limited), Vern Coffin (Noranda Mining and Exploration), Ross Gallinger (Rio Algom Limited), Ian Horne (formerly with BHP Minerals Canada), Derek Riehm (Teck Corporation), Luc St-Arnaud (Noranda Technology Centre), and Kelvin Dushnisky (Redfern Resources Ltd.)

To those with regulatory agencies, we have particularly benefited from discussions with Bill Price (British Columbia Ministry of Employment and Investment, Energy and Minerals Division), Grant Feasby, Gilles Tremblay, and Carl Weatherell (MEND/Natural Resources Canada), and Kim Lapakko (Minnesota Department of Natural Resources).

The university professors we wish especially to thank are John Cherry and David Blowes (University of Waterloo) and Ernest Yanful (University of Western Ontario).

We have benefited greatly from discussions with fellow consultants, particularly Les MacPhie and Maciej Szymanski (Geocon/SNC-Lavalin Environment), Clem Pelletier (Rescan Environmental Services), Ron Nicholson (Beak Consultants), and Shirley Hutt (Ocean Bound Enterprises).

On a personal level, Kevin thanks Catherine, Karla, Kathy, Larry, Karen, Joe, Keith, Robin, Kirk, David, Jennifer, Christina, Laura, Kyle, Drew, Amanda, and the rest of the gang. Nora thanks Shirley, George, and Noreen.

Kevin Morin
Nora Hutt
Vancouver, British Columbia, Canada
March, 1997

CHAPTER 1
INTRODUCTION

1.1 Overview and Objectives

Mining and milling (concentrating) of ore has always been a fundamental activity of the human race, supplying the metals, nonmetals, and minerals needed to maintain and advance our standard of living. Therefore, it is no coincidence that mining activity has grown in intensity and complexity as human civilization has grown and expanded. A simple testimony to this symbiotic relationship is human epochs like the Iron and Bronze Ages. Other testimony comes from historical reports of mining.

Documented mining for raw materials reaches back to the Stone Age, with a 20,000-year-old underground flint mine reported in a limestone cave in Australia (James and Thorpe, 1994). Due to the demand for flint axes, several flint mines were operating in Western Europe by 4000 B.C., with hundreds of shafts dug to depths of 9-12 m.

Copper mining was underway at Rudna Glava, Serbia, by 4500 B.C. to depths of 60 feet (James and Thorpe, 1994). By 2600 B.C., Egyptians were mining turquoise and copper in the Negev of northern Sinai with 6-meter-diameter shafts accompanied by a system of underground workings. About the same time, rock with silver and lead was being mined near Athens using underground workings driven up to 330 feet laterally into hillsides. Cisterns for water supply and ore washing (milling) were excavated nearby into rock and lined with cement.

Underground coal mines in China are reported as early as 200 BC while Roman coal mines in Britain are reported around 100 A.D. (James and Thorpe, 1994). Ancient Romans also operated mines for iron, gold, silver, tin, copper, and lead (Thornton, 1996). These included a copper mine at Córdoba, Spain, with a 688-foot-deep shaft and a lead-silver mine at El Centenillo with workings 3500 feet long and 650 feet deep (James and Thorpe, 1994). The Romans apparently developed relatively advanced techniques for excavating, lighting, ventilating, and draining mines, such as a vertically staged series of 15-foot-diameter water wheels.

Due to our relatively short lifespan, it can be easy for people to overlook past lessons and advances. Today, many think of past mining and milling activities, even a hundred years ago, as primitive. However, by the time Agricola (1556) wrote his text on mining and milling centuries ago, these activities were already refined sciences and arts. The refinements continue today and will no doubt continue into the future.

One rapidly growing refinement is the incorporation of environmental maintenance into the economics and engineering of mining. This is a reasonable consequence of increasing environmental awareness and the increasing intensity and cumulative extent of mining. Some statistics illustrate this best. By the Year 2000, Merrington and Alloway (1994) expect that approximately 240,000 km^2 of the earth's surface will have been disturbed by mining activity. In the Canadian Province of Ontario, there are more than 6000 abandoned minesites with varying degrees of environmental, safety, and health concerns (Mitchell and Mackasey, 1995). In the USA, 17,000 abandoned mines are documented in the State of Utah alone (Vance et al., 1995). Also in the USA, aquatic life has been decimated in 4100 km of 88,000 km of streams within the Commonwealth of Pennsylvania by acidic mine drainage (Scheetz et al., 1995). The Chinese mining industry generates an estimated 2.5×10^9 m^3/yr of polluted water (Chen and Huang, 1995) and Chinese coal mining alone generates 150×10^6 t of waste a year (Hu, 1995). This intense industrial activity around the world must be accompanied by environmental protection or restoration.

In the past, mining and milling were sometimes considered sufficiently important to dismiss legally corporate responsibility for adverse effects on the local environment and health (Vranesh, 1979). It is interesting to read Weingart (1982), an ex-hardline miner, publicly confessing his “sins” and accepting environmental responsibility. There is no longer any doubt that many mining companies place major emphasis on environmental protection. For example, Robertson (1994a) reports that his company will not mine sulfide-bearing ore if the subsequent acid generation cannot be properly prevented or controlled.

Blight (1979) summarized the mining-environment issue well:

> "It is well to concede at this point that any mining or industrial activity will inevitably cause some environmental damage. The overall benefit to the country must be offset against this damage. It must also be recognized that whatever control measures are instituted, due regard must be paid to local conditions and current circumstances. The costs of the waste disposal operation in relation to the revenue-producing operation that must pay for it, the practicability of the environmental protection measures proposed, and the short and long-term consequences of these measures, both for the safety of the public and for their quality of life, must all receive careful and due consideration."

This is reflected in the current international movement for sustainable development.

There are some who oppose efforts to return the environment at old minesites as close as possible to pre-mining conditions. For example, an international organization suggests that millions of bats have been lost by closing and sealing underground mines (Taylor, 1995). Also, Banks et al. (1996) argue that minesite drainages with elevated concentrations of some metals and lower concentrations of others have historically played a beneficial roles. They have provided or augmented surface-water base flows, drinking-water supplies, water treatment, spa waters, and secondary minerals for paints and industrial processes. Nevertheless, this opposition to restoration represents a minority today.

Mining operations can have physical, chemical, and biological effects on the local environment, which consists of soil and rock (solid phase), groundwater and surface waters (liquid phase), and air and pore gases (gaseous phase). Any detailed discussion of one effect or one phase alone can fill, and has filled, several proceedings and books. In this book, the focus is primarily on the chemistry of surface and ground waters draining from minesite components.

In the fields of environmental geochemistry and environmental hydrogeology, sufficient literature on many types of mining now exists to allow a compilation of data to identify similarities and highlight site-specific differences. This, in turn, provides an opportunity to understand mining and milling operations on a large scale in order to (1) remediate closed minesites, (2) guide environmental studies at existing operations, and (3) design improved minesites for the future. The compilation of data and the conceptual chemical models of mining are the primary objectives of this book.

1.2 Organization of This Book

The next chapter, Chapter 2, describes the various minesite components whose physical and chemical characteristics affect the chemistry of their drainages. Chapter 2 also introduces the terminology used in this book. While most technical words are used consistently around the world, other terms vary widely in their meaning and usage. Therefore, clearer communication requires well-defined terminology. For example, the word *mine* is used here as a specific component (open pit or underground working), whereas *minesite* refers here to a set of components. A Glossary is provided in Appendix A to standardize technical meanings in this book.

Chapter 3 provides a brief explanation of how water drains through and from minesite components. This drainage occurs as surface and ground waters. Consequently, Chapter 3 provides the physical framework of water movement, onto which chemistry is superimposed.

The remaining chapters are dedicated to the chemistry of drainage waters. Chapter 4 describes drainage chemistry through in-field case studies of various minesite components. Chapter 5 then explains and illustrates methods for predicting drainage chemistry, and thus provides important theoretical background of a practical nature.

Chapter 6 discusses the geochemical aspects of various methods for controlling the chemistry of drainage waters. The appendices provide supporting information for these chapters.

1.3 Questions

1-1. Many metals and minerals are obtained by mining. How many objects have you encountered in your life that were not derived from, or affected by, mining? (Keep in mind that even a smooth piece of wood may have been cut or trimmed by a metallic instrument fashioned from mined metal.) Over the next 24 hours, note how few non-mining-related objects you encounter.

1-2. What would be the effect on our standard of living if various types of mining, like gold, copper, and potash mining, were halted?

1-3. What percentage of your country's economic production is derived from mining or mineral processing?

1-4. In your community and country, do most people recognize the contribution that mining makes to the economy and their standard of living?

1-5. How much would you limit mining to protect the environment near your home?

CHAPTER 2
LAYOUT OF MINESITES AND THEIR COMPONENTS

2.1 Overview and Terminology

Because mining is a worldwide industry, some terminology has evolved differently in various countries. This can lead to confusion when discussing technical issues on an international level. To minimize confusion in this book, important and relevant terms have been defined in the Glossary (Appendix A), although some simplification has been necessary. For example, this book uses the term, "ore", in a general sense so that many different types of mining operations can be conceptualized and explained in a consistent manner. In literal terms, however, coal is not often referred to as ore, and rock mined around a coal seam is often called "spoils" rather than waste rock. Nevertheless, as long as the general concepts are understood here, the selected terminology should be clear.

A *mine* is often thought of both as an area in which rock is excavated, like an open pit, and as a larger, general location where rock is excavated, ore milled, and waste material disposed. To eliminate this ambiguity, *minesite* as used in this book refers to a collection of one or more components and the *mine* itself remains limited to the area where ore is excavated.

A visit to a minesite can sometimes be confusing, because of the movement of people, equipment, rock, and/or water in many directions. The first step in lessening this confusion is the delineation of all significant components at the minesite.

The components that can form a minesite are numerous (Table 2.1-1), but not all are necessarily found at all minesites. In addition to the mine component itself, there are various sizes of mined-rock piles, ranging from lower-volume fills for roads and building foundations to larger-volume waste-rock dumps, low-grade and ore stockpiles, and dams. Tailings impoundments, when present, typically cover the largest land area at many minesites. To assess, predict, or control drainage chemistry in and around a minesite, inventories and descriptions of all components are important starting points.

The next step in the assessment or prediction of drainage chemistry is the recognition that all components are part of one industrial operation and thus interact with each other by design or coincidence. From an environmental perspective, rock, soil, and water can be transported from one component to another and then to another. Because of unique site-specific features of each minesite, all possible exchanges of liquid and solids among components cannot be defined in a general way. However, a schematic diagram of several possible exchange pathways hints at the complexity of some minesites (Figure 2.1-1). The careful delineation of these exchange pathways is a basic requirement for drainage-chemistry studies at a particular minesite.

The solid and water phases within a component of a mining operation are derived from three basic sources: the component itself, other components, and an external source given the general name of "climate" (Figure 2.1-1). Climate primarily represents precipitation, evaporation and transpiration of water, incoming runoff, and groundwater inflow. Short discussions by component will illustrate some of these sources and balances for the solid and water phases.

For the mine component, all the ore and waste rock are generated within the component and are then passed on to other components. This exposes rock walls that can affect inflowing water derived from climate, which may then be sent to a mill or a treatment plant.

The solids balance for an ore stockpile (Section 2.3) is relatively simple. Ore from the mine is delivered to the stockpile and is then fed into the mill as required. The main input of water is typically from climate, and the main outflow of water is typically groundwater drainage and/or surface water appearing near the base of the pile at springs.

TABLE 2.1-1
Examples of Minesite Components Potentially Affecting Drainage Chemistry

Types of Mines		
Open Pits	Underground Workings	Placer Mines
Solution Mines	Quarries	
Types of Mined-Rock Piles		
Ore Stockpiles	Low-Grade Ore Stockpiles	Waste-Rock Dumps
Heap-Leach Piles	Dams	Disturbed-Rock Foundations for Buildings
Airstrips	Roads and Ramps	Dikes
Mill and Mill-Waste Disposal Areas		
Mill/Processing Plant	Tailings Impoundments	Spills of Tailings and Reagents
Other Components		
Water-Treatment Plants	Sewage Systems	Industrial-waste/garbage disposal areas
Fuel storage areas	Stormwater and Seepage Ponds	Ditches surrounding or extending between other components
Laboratories	Explosives storage areas	Water-Supply Facilities

For waste-rock dumps, the solids balance can be more complex. For example, some waste rock may be taken from a dump and used for construction materials in such components as roads and dams. Additionally, there is also an option for returning some waste rock to the mine during or after mining activity.

The solids balance of a tailings impoundment primarily consists of the input of spent, processed ore, although garbage, sewage, waste fuel, process chemicals, and waste rock may also be disposed of within an impoundment. The water balance can consist of input from the mill as tailings liquid, climate, and perhaps water from other components. Water may leave an impoundment through groundwater flow systems, through surface watercourses, by climate (evaporation), and, if recirculation is employed, to the mill component.

Based on the preceding basic descriptions of major minesite components, detailed discussions can now be given. Each of the following five subsections focusses on a single component.

2.2 The Mine Component

The mine component is the fundamental portion of a minesite because virtually all ore and waste rock originate there. Without it there is no mining operation. From an environmental perspective, there are four basic types of mines: open pit, underground, placer, and solution. The first two are the most common.

Open-pit mining is used when the quantity of waste rock lying over an ore zone is relatively small and the ore zone is shallow in depth. Open-pit mining involves the vertical and/or lateral removal of layers of overburden and waste rock above an ore zone, resulting in a pit open to precipitation (Pit

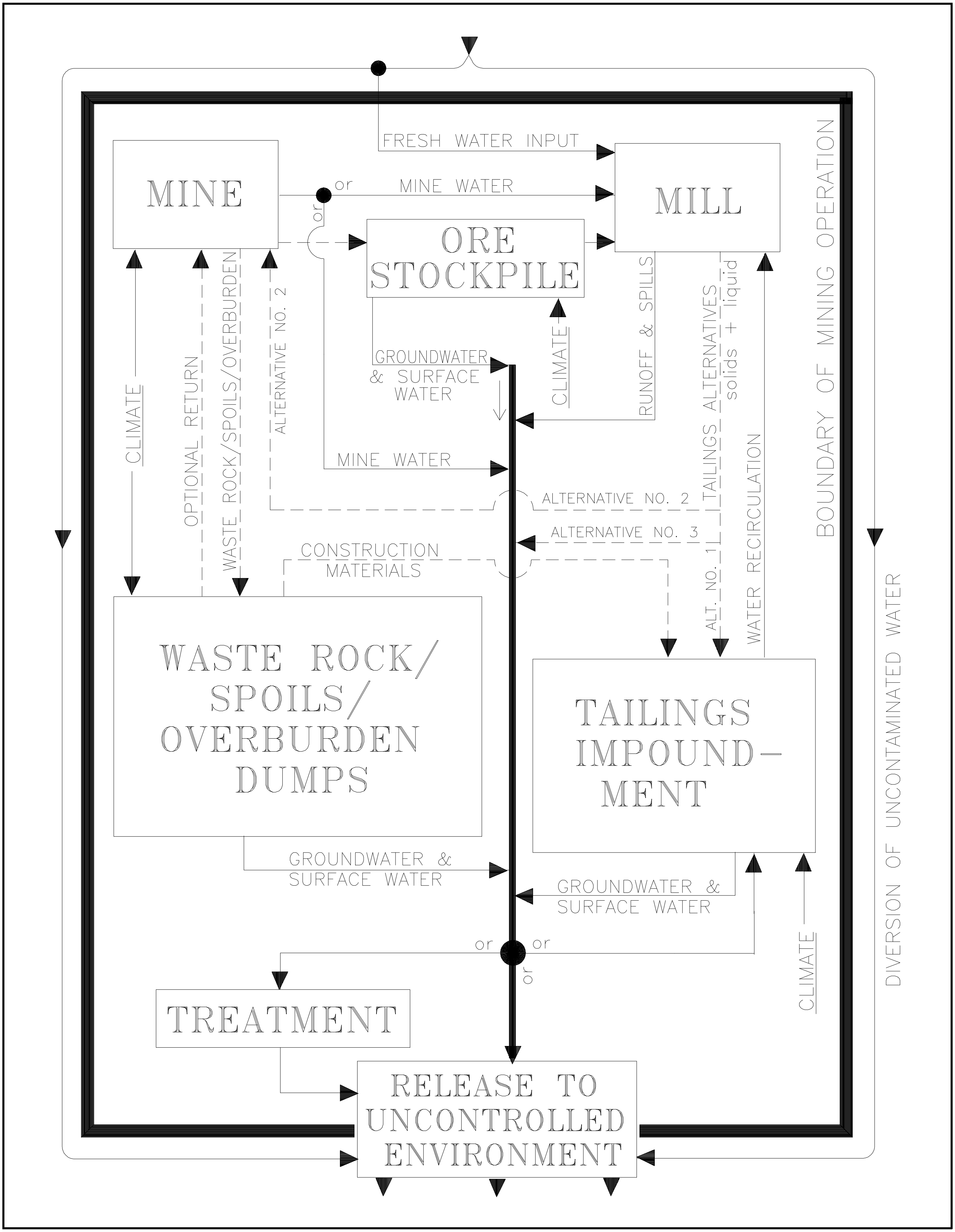

FIGURE 2.1-1. Schematic Diagram of a Minesite (after Morin, 1988a); interactions among components depicted by arrows (solid = liquid exchange; dashed = solid exchange).

Types 1 through 3, Figures 2.2-1 to 2.2-4).

The waste rock from an open pit is sent to waste-rock dumps (Section 2.3), whereas the ore, once reached, is sent directly to the mill or to ore stockpiles which provide feed to the mill (Section 2.3). Pits are expanded either laterally for long, tabular ore zones like coal seams or vertically in steps or "benches" for more localized ore zones like many base-metal deposits. Both waste and ore rock are typically mined with explosives, shovels, and trucks. From this general perspective, quarries can be considered open pits (Allen, 1983).

Where the ore is relatively deep or under a significant amount of waste rock, underground workings are created by selective blasting and excavation of rock in a three-dimensional pattern (Types 1 and 2, Figures 2.2-5 to 2.2-7). The choice between underground and open-pit mining can also be the result of other factors such as the size of the ore zone and the geotechnical stability of overburden and waste rock.

The third type, placer mining, is often limited to the shallow excavation of unconsolidated sediment for the removal of metals and minerals that have accumulated through erosional processes. The unconsolidated nature of the ore normally precludes underground and open-pit mining due to the lack of geotechnical stability. Consequently, methods like jetting or "monitoring" with high-pressure water and dredging can be used to recover the ore (Figure 2.2-8). Stream, lake, and ocean beds are frequent targets for this type of mining (Cruickshank, 1965; McFarland, 1965; Pakianathan and Simpson, 1965). Case Study 4.3-14 is one example. Because of similarities, placer mining conceptually includes sand and gravel operations (Frost, 1983).

There are five categories of placer deposits. A *remnant placer* is an ore zone reworked by weathering without significant transport from the site of formation. Such deposits may arise when elevated rock formations are weathered in place by water and/or wind. An *eluvial placer* forms directly downhill of an ore zone where mass transport processes such as creep and landslides have carried the ore away from the site of formation. An *alluvial placer* results from erosion and transport in streams and rivers, and the placer may be located in river beds, bars, floodplains, and elevated terraces (ancient floodplains). *Glacial placers* are ore zones formed by erosion and transport by glacier-related mechanisms and are often located in till, morainal deposits, and outwash. *Submerged placers* are located beneath deep fresh or sea water. They may originate as any of the above types of placers that have been submerged or through reworking of an ore zone by deep-water processes such as currents and turbidity flows. Some examples of submerged placers include gold-bearing beach sediment near Nome, Alaska (USA), tin-bearing river alluvium in Thailand, and diamond-bearing alluvium off South Africa (Cruickshank, 1965).

The mining of a placer can be an integrated operation through which a floating dredge excavates the ore of a submerged placer, mills the ore on board the dredge, and dumps the tailings off the back end. Alternatively, like open pits, the mining of an alluvial placer may proceed in a phased approach. The ore is first excavated by a shovel or dozer, transported to sluice boxes or other processing equipment, and the tailings are then disposed of elsewhere or in old excavations.

The fourth type of mine, labelled "solution mining", involves the dissolution of ore by injected process water and pumping recovered process water to a mill (Figure 2.2-8). The process water can, for example, be water for dissolving salt, or acidic or alkaline solutions for dissolving metals (Larson, 1980).

In reality, two or more of the preceding four types of mining can operate simultaneously, like the dissolution of ore in an existing underground mine (e.g., Millenacker, 1992; Boreck et al., 1990; Boreck and Goris, 1992). In all these cases, the manner in which water is used in the mining process can affect its chemistry as the water drains through or from the mine. As a result, the pathways of water drainage through a mine should be documented.

An important observation to repeat about all mines is that the ore and waste rock are disturbed in some way from their original in situ conditions and are transported to other components. Within these

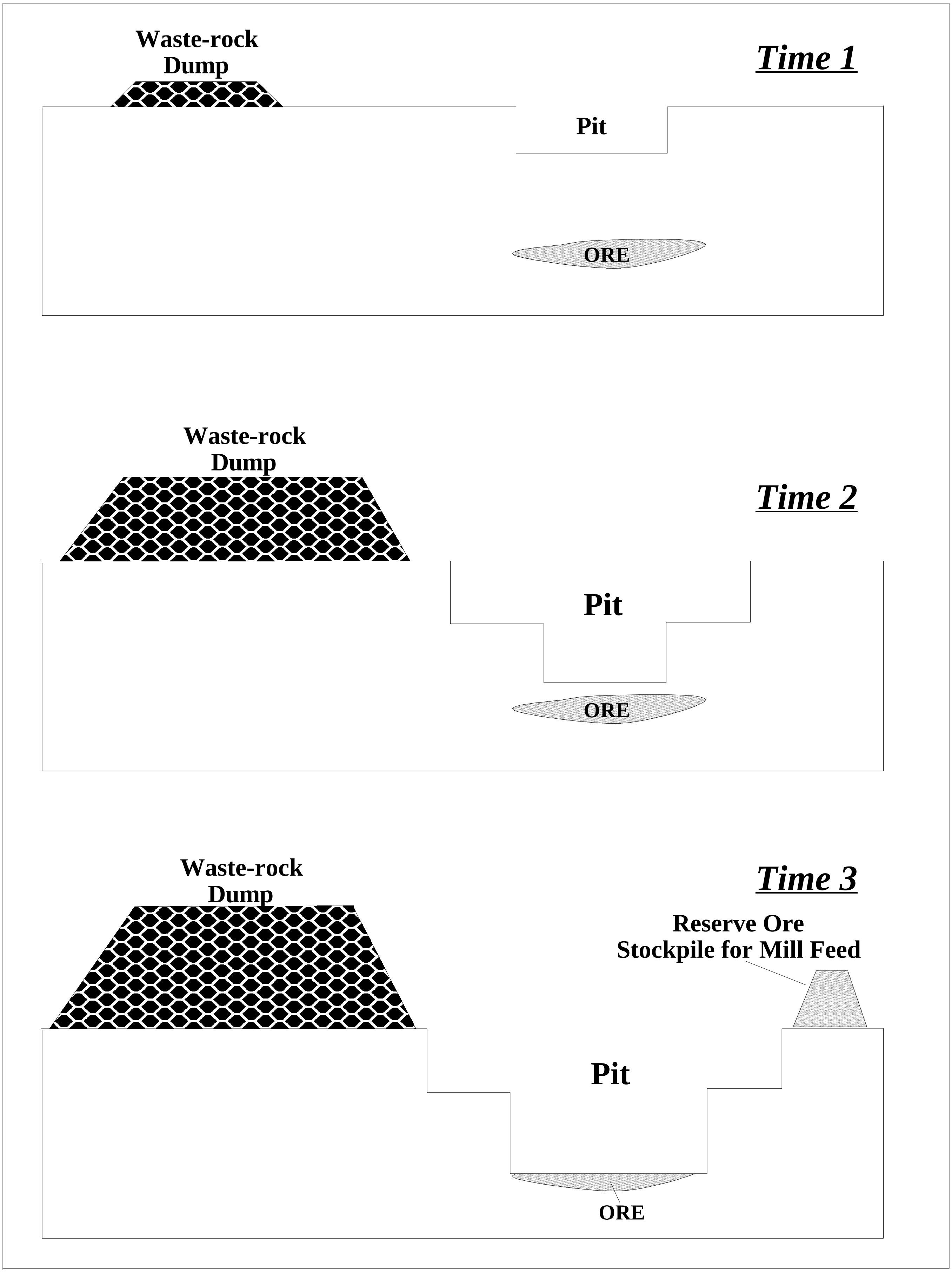

FIGURE 2.2-1. Schematic Open-Pit Mining - Type 1.

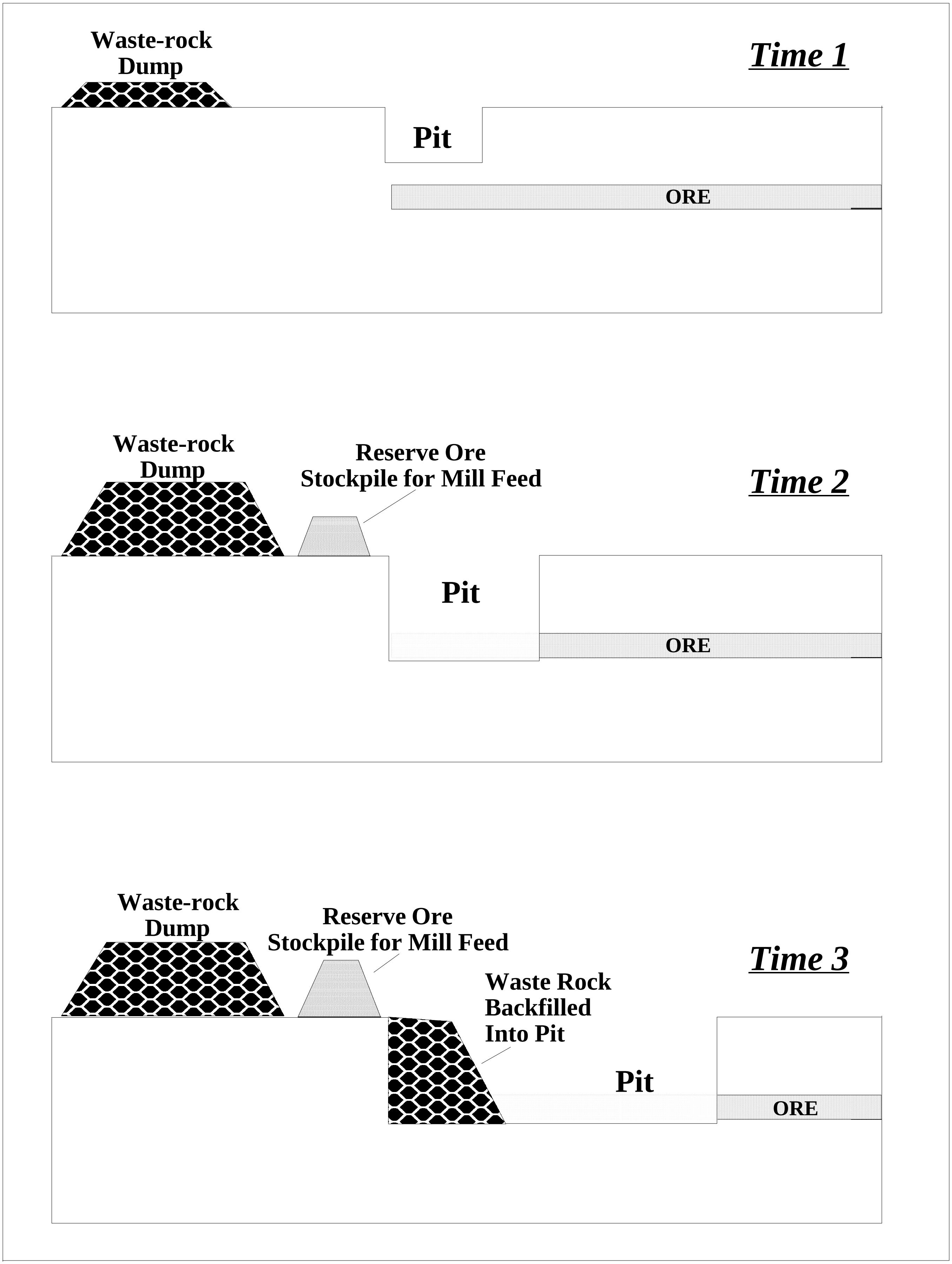

FIGURE 2.2-2. Schematic Open-Pit Mining - Type 2.

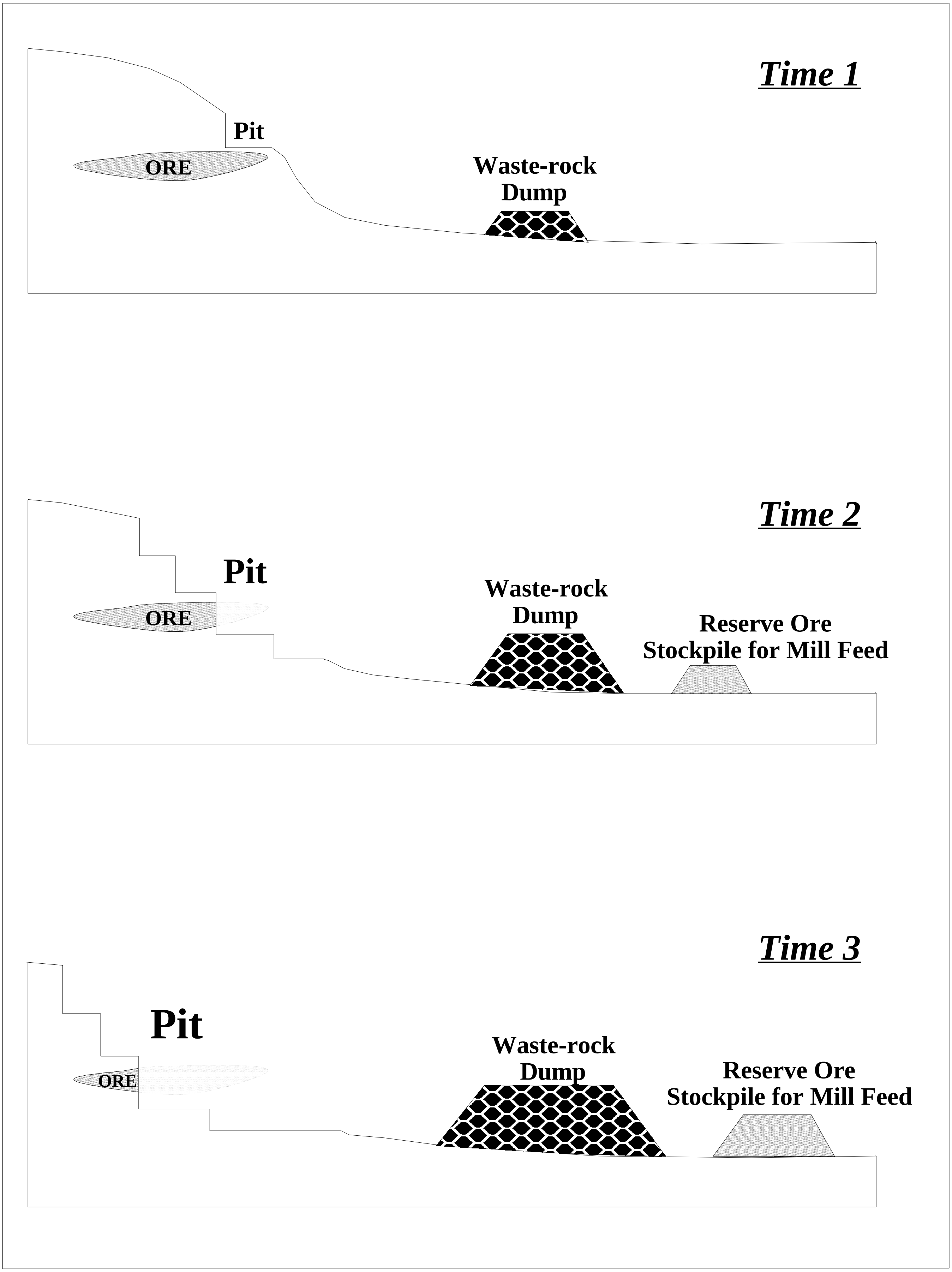

FIGURE 2.2-3. Schematic Open-Pit Mining - Type 3.

Looking Down into a Type 1 Open Pit

Looking Down and Parallel to a Type 2 Open Pit

Looking Down into a Type 3 Open Pit

FIGURE 2.2-4. Photographs of Various Types of Pits (photos by K.A. Morin).

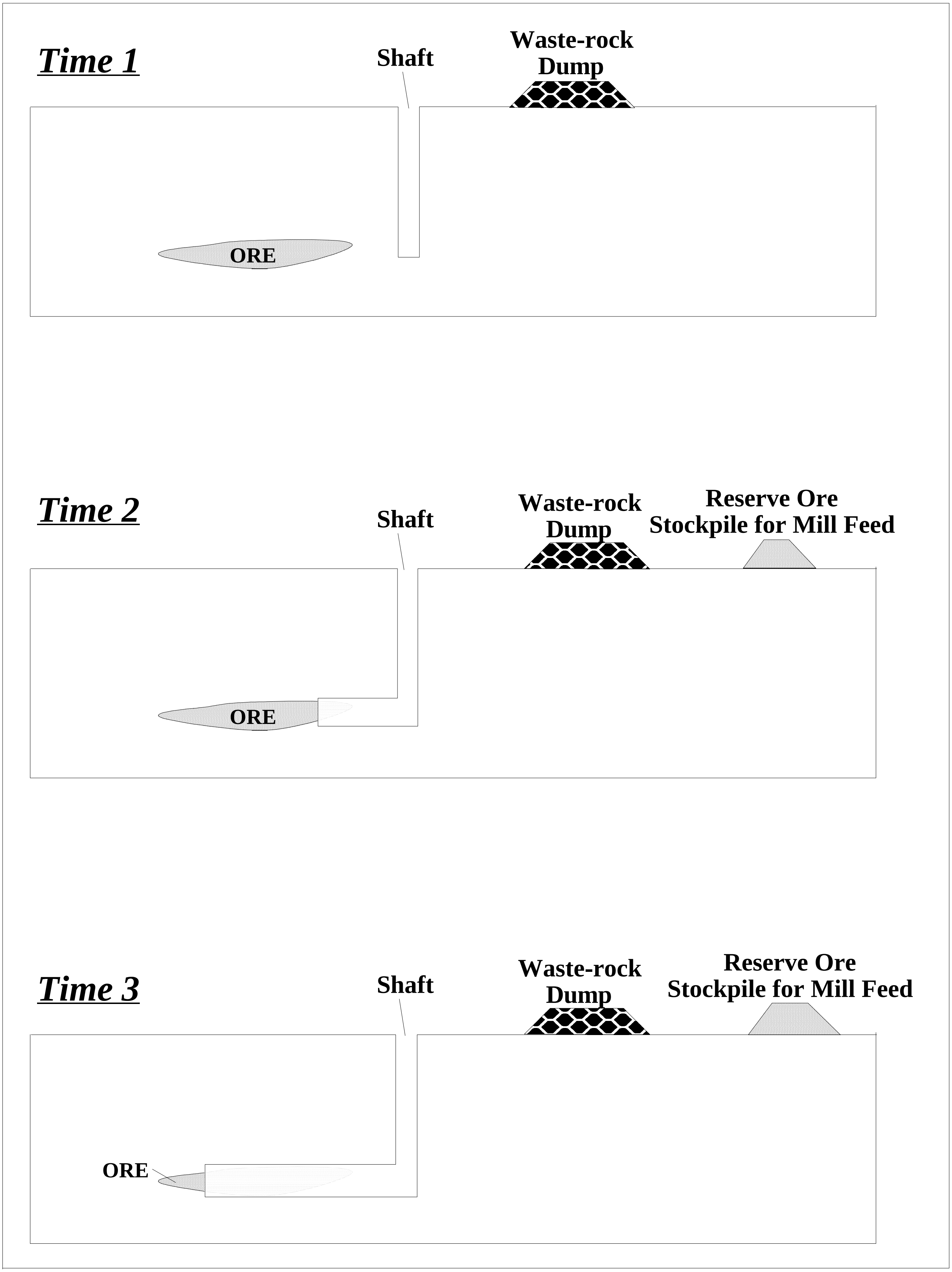

FIGURE 2.2-5. Schematic Underground Mining - Type 1.

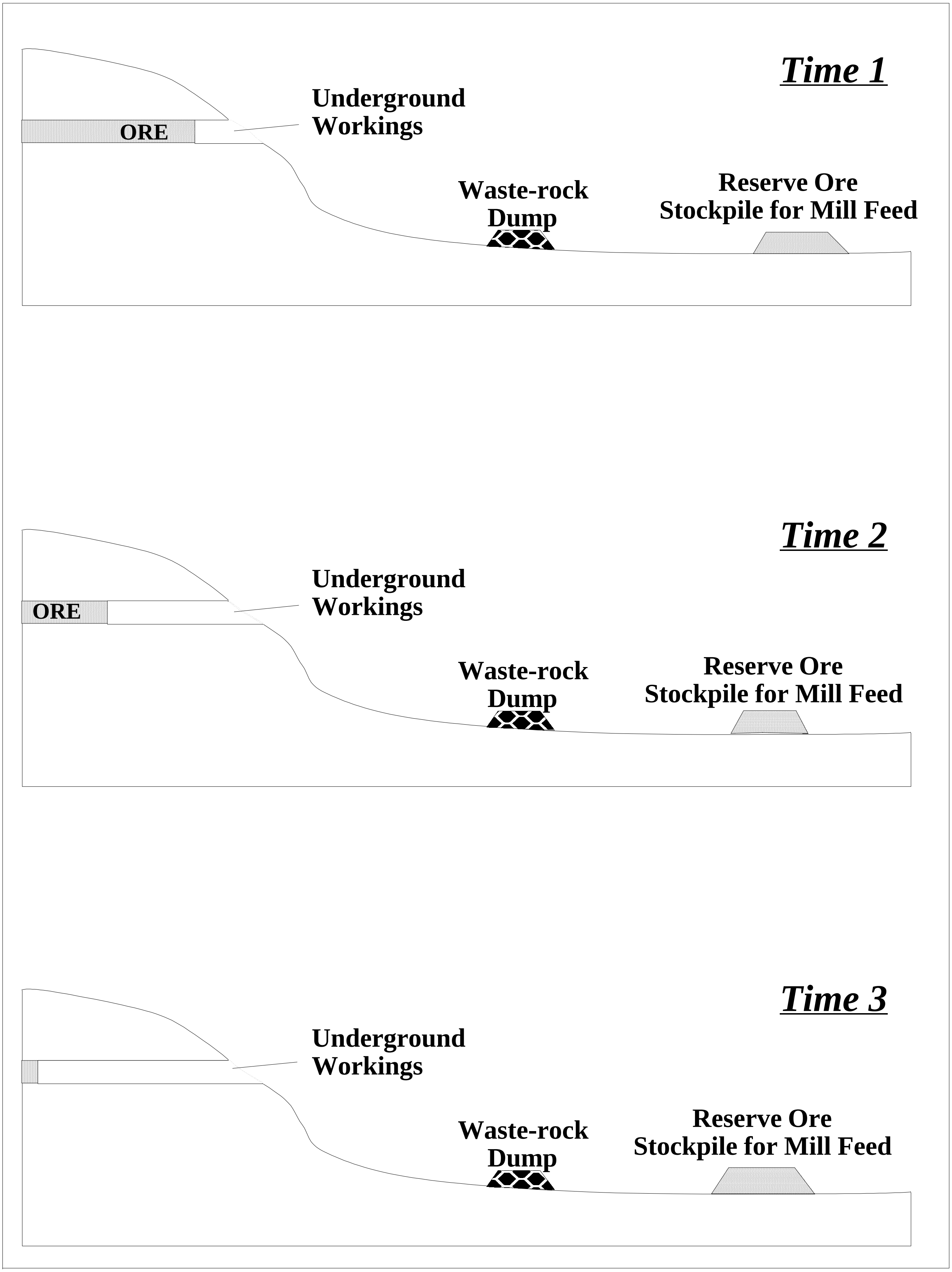

FIGURE 2.2-6. Schematic Underground Mining - Type 2.

Looking at Support Facilities above a Type 1 Underground Mine.

Looking at the Portal to a Type 2 Underground Mine;
note gravity drainage.

FIGURE 2.2-7. Photographs of Various Types of Underground Mines (photos by K.A. Morin).

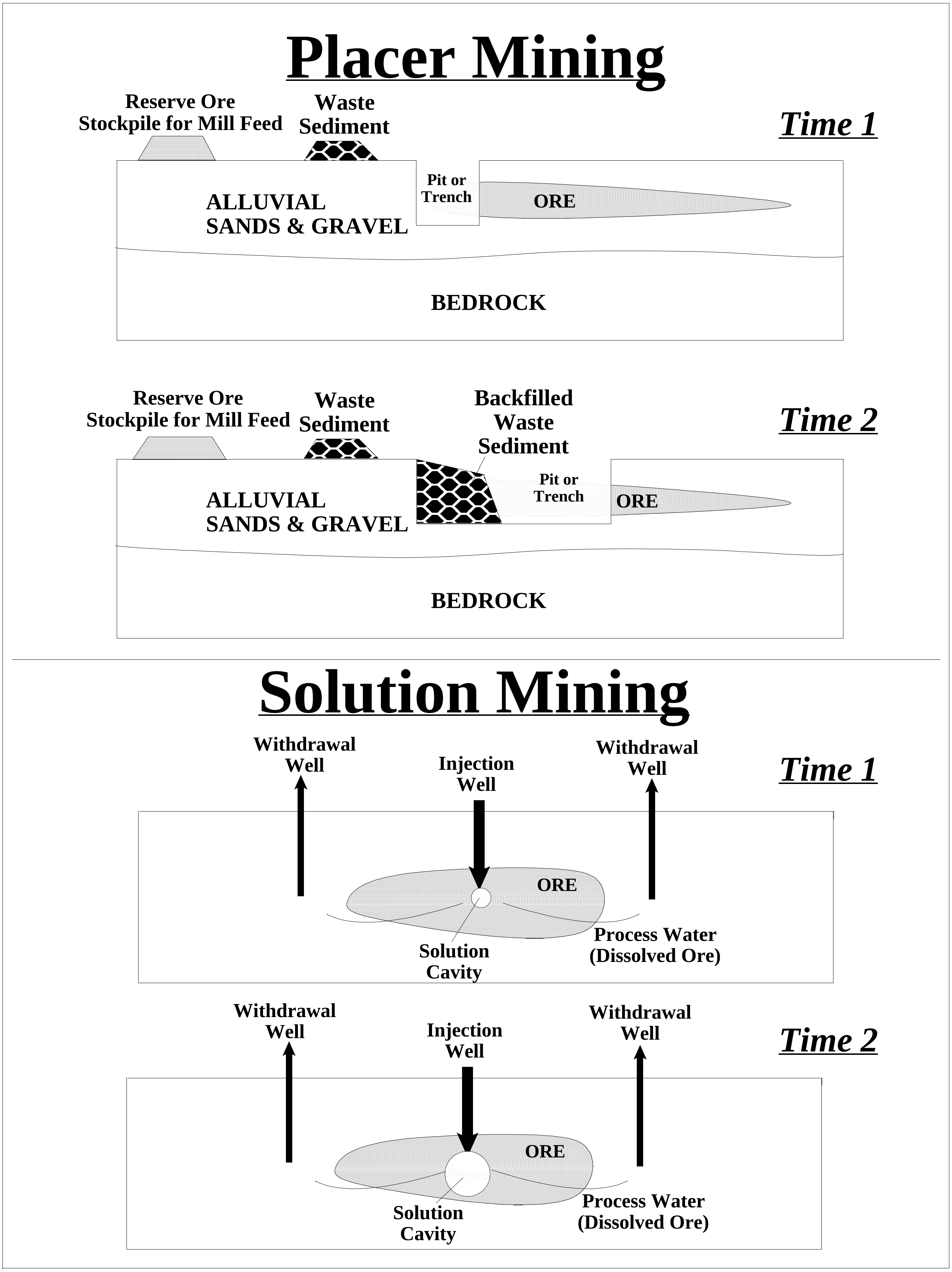

FIGURE 2.2-8. Schematic Placer and Solution Mining.

other components, the rock is exposed to new, geochemically different conditions that lead to new reactions such as accelerated physical and chemical weathering. In turn, this can have major effects on drainage chemistry from these components. This is discussed further in Sections 2.3 and 2.4.

Another important observation to repeat is that the mine component is not geochemically inert after ore and waste rock have been removed. The walls of the mine exposed to air and water can be as reactive as the adjacent rock removed during mining. As a result, mine walls can have a significant effect on the chemistry of water draining through or from a mine. The reactive surfaces in fractures behind the walls can greatly heighten this effect (Section 5.4.2). Water movement through the various types of mines (Figures 2.2-1 to 2.2-8) is discussed further in Section 3.2.

2.3 Ore Stockpiles, Low-Grade-Ore Stockpiles, and Waste-Rock Dumps

When rock or sediment is removed from the mine component (Section 2.2), it is typically separated into ore and waste. The criterion for separation, sometimes called the “cutoff grade”, is based on (1) the amount of an economical target mineral(s) or metal(s) in each unit of mined rock and (2) on the cost of mining and milling that unit. For example, rock containing 1.0 g of gold a tonne would be considered ore at one gold mine and waste at another. Consequently, every mine will have a different criterion for separating ore from waste. Additionally, ore is sometimes divided into full-grade and low-grade levels, with the latter reflecting levels of minerals or elements that may someday be economical to mill.

Full-grade ore is sent directly to the mill or is placed into stockpiles. The stockpiles act as a reserve ore supply to ensure continuous feed to the mill. Therefore, such ore stockpiles are active and usually milled quickly. As a result, ore is often exposed only for short periods during which effects on drainage chemistry may be small unless geochemical reactivity is high. Also, to improve recovery, these stockpiles are sometimes protected from precipitation so that no water enters and drains from them.

On the other hand, low-grade ore is placed in stockpiles for possible later milling. They are rarely protected from precipitation, and are sometimes never milled because mining operations cease before processing the low-grade ore. Consequently, low-grade-ore stockpiles are often long-term components that can affect the chemistry of their drainages, like waste-rock dumps.

Waste rock contains reactive minerals, but the valuable minerals are at relatively low levels. This rock is sent to disposal areas, or dumps (Figures 3.3-1 to 3.3-3), typically with the intent of no further handling. The resulting chemical effects on drainage waters may persist for as long as the dumps exist.

A variation on stockpiles and waste-rock dumps is a heap-leach stockpile. This component is composed of ore subjected to chemical leaching to remove the target elements. When recovery of the elements decreases to a certain level, leaching is halted and the spent pile virtually becomes a waste-rock dump with residual leaching chemicals.

These stockpiles and dumps can collectively be referred to as mined-rock piles. Three types of mined-rock piles based on water movement are discussed in Section 3.3.

2.4 Dams, Roads, and Building Foundations

Prior to and during operation of a minesite, certain components must be constructed to facilitate site construction and operation. These components include dams that contain water or tailings (Section 2.5), roads for access to all components, and building pads and foundations. These components may be made of waste rock from the mine component (Sections 2.2 and 2.3). As a result, they can be conceptualized as mined-rock piles. Although typically smaller than dams and dumps, roads and foundations can have significant effects on the chemistry of their drainages.

Dams sometimes present an intriguing problem from the perspective of drainage chemistry and long-term environmental protection. Whereas components such as stockpiles, dumps, and roads can often be moved or processed, dams are often created to contain water or waste materials for indefinite periods of time and are thus engineered for long-term stability. Consequently, if a dam contains unacceptably reactive rock, it will indefinitely affect the chemistry of water draining through it, with little chance of removing the rock or manipulating the dam's profile or internal water table. For this reason, the rock used in dams should be checked particularly carefully to determine its long-term effect on drainage chemistry.

The geotechnical stability of dams against physical and chemical processes is environmentally critical due to the consequences of failure. An example of a tailings-dam breach occurred on July 16, 1979 at the United Nuclear Corporation's Church Rock site in New Mexico, USA. The resulting spill contained approximately 360,000 m^3 of tailings liquid and 1,000 t of tailings solids. Tailings spilled into an adjacent arroyo, travelled down a so-called "pipeline arroyo", into the north branch of the Rio Puerco arroyo, past the convergence of the north and south Rio Puerco, travelled through the rest of New Mexico, and then approximately 35 km into the adjacent state of Arizona (Weimer et al., 1981). The initial site investigation and subsequent cleanup were based on chemical analysis of approximately 2,400 samples, primarily to monitor radionuclide levels in the contaminated materials during cleanup.

Other examples of tailings impoundment failures include:

Ø in March of 1965, ten of fourteen tailings dams in the El Cobre district of Chile failed and more than 250 people were killed as tailings flowed down an adjacent valley, caused by the failure of dam walls and the liquefaction of tailings during an earthquake (Down and Stocks, 1976);

Ù in September of 1970, 89 miners died at Mufulira, Zambia, when tailings placed over the underground workings liquefied (Down and Stocks, 1976) and moved downward as a mudrush through a "sinkhole" (Neller et al., 1973);

Ú in November of 1974, 15 people died at Impala Platinum Mine in the Transvaal by a mud slide of tailings, apparently caused by a breach in a tailings-dam retaining wall following a period of heavy rainfall (Down and Stocks, 1976);

Û in 1972, a coal-refuse dam failure at Buffalo Creek, West Virginia, USA, resulted in a release of water and coal-waste sludge that flooded and demolished 1,500 homes and killed 150 people (Popovich and Adam, 1985; Wood, 1983).

2.5 Tailings Impoundments and Mills

The ore discussed in Sections 2.1 and 2.2 is often subjected to some type of concentrating, cleaning, processing, milling, and/or smelting, simply called "milling" in this book for brevity. This milling results in some type of waste materials, often called "tailings", which are sent to surface impoundments, generally as an aqueous slurry, for indefinite disposal. Depending on the nature of a milling process, the slurry can be composed of (1) ore solids which are sometimes ground to a fine grain size and processed with added chemicals, (2) solid chemical precipitants and excess solid chemicals from the mill process, and (3) water with dissolved solids derived from the ore rock and the process chemicals. Many tailings look and feel like silt or clay.

A conceptual variation on aqueous tailings is smelter slag (e.g., Maki and Taylor, 1987) which is placed into impoundments in a molten or recently quenched form. However, the primary environmental effect of smelters is reportedly airborne particles rather than drainage from smelter slag (Fuge et al., 1996), and thus smelter drainage is not discussed in this book. Nevertheless, slag likely has some chemical effects on drainage waters.

The grinding of ore creates relatively high particle-surface areas in a unit volume compared to waste rock and mine walls, enhances climatic exposure of most minerals in the ore, and can accelerate reaction rates. Additionally, tailings impoundments are often the largest and most obvious minesite component in terms of lateral area, and thus often have the largest amount of drainage (Figure 2.5-1). As a result, tailings impoundments often generate the largest concern and environmental costs at a minesite when drainage chemistry requires active management and control (Chapter 6).

Tailings Impoundment; note active discharge pipe on right.

Oblique Air Photograph of a Tailings Impoundment.

FIGURE 2.5-1. Photographs of Tailings Impoundments.

Coal milling typically includes the physical separation of non-coal material and then washing of the coal product (Figure 2.5-2). In general, coal mining generates proportionally less waste rock and tailings than metal mining (Bell et al., 1992), because the target material is visually obvious and often occurs as discrete, easily mined strata. On the other hand, because annual tonnages in coal mining are typically much greater than metal mining, equivalent tonnages of wastes are produced. Also, as shown in Section 5, the ability of coal wastes to affect drainage chemistry is similar to that of metal-mine wastes. Therefore, the generalized concepts in this book apply well to coal mining.

To highlight the complexity in defining minesite components, older tailings, created in the past using less efficient milling, are sometimes seen as ore bodies worthy of placer mining and milling (e.g., Bean, 1972; Hutt and Morin, 1994). Such reprocessing of tailings is further discussed in Section 6.4.

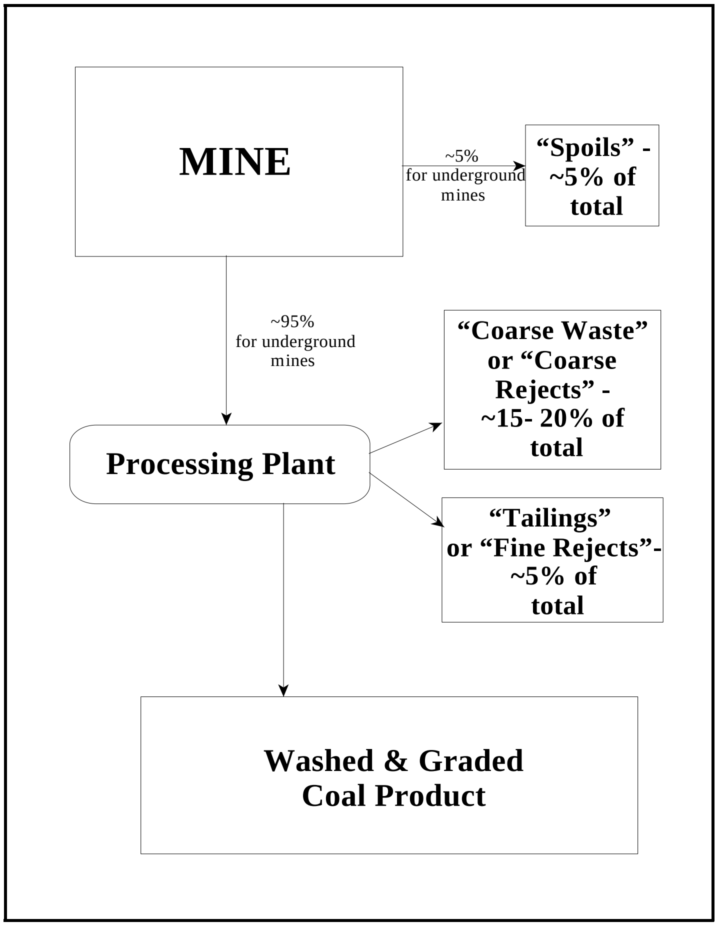

FIGURE 2.5-2. Typical Process and Terminology for Coal Milling (adapted from Bell et al., 1992).

2.6 Other Components

Other minesite components can include any excavations, quarries, and ditches, as well as any size of piled rock. In effect, any other component can be assessed as a variation on one of the three major types of components: mines, mined-rock piles, and tailings impoundments. For example, any open excavation can be conceptualized and assessed as a mine component (Section 2.2). Any rock pile can be thought of and assessed as a variation on stockpiles and dumps (Section 2.3), as can dams and roads (Section 2.4). Waste disposal areas can be conceptualized as tailings impoundments (Section 2.5). As a result, the remainder of this book will focus on these three primary types of components.

2.7 Questions

Hypothetical "Mine A": This Type 2 Underground Mine in a wet tropical climate is mined at a rate of 1000 t/day, with 90 weight-percent (wt-%) of the rock being ore grade, 5 wt-% of low-grade status, and 5 wt-% as waste rock. All rock is delivered to stockpiles and a dump. The ore is milled after an average stockpile time of 30 days, 10 wt-% of the ore is recovered as economic metal, and the remainder is sent to a tailings impoundment as a slurry with 40 wt-% water. This water for milling is obtained from the tailings impoundment (450 m^3/day) and from the underground workings (50 m^3/day), but drainages from the stockpiles and dump are discharged to the environment. Average annual rainfall is 2 m/yr.

2-1. Create a schematic diagram like Figure 2.1-1 showing rock and water balances for Mine A.

2-2. Mine A disposes of its waste rock in a dump 5 m high. After five years of mining, what will be the lateral area of the dump if disturbed bulk density is 1.7 t/m^3? Assuming no evapotranspiration and no runoff of rainfall, what will be the average annual drainage through the dump at Year 5?

2-3. Mine A mills ore, with 10 wt-% recovered as economic metal. How many tonnes a day of tailings, and cubic meters a day based on a dry bulk density of 1.3 t/m^3, are sent to the impoundment? If the tailings have a specific gravity of 2.8 and remain fully saturated after deposition, how much water in cubic meters a day is "locked" within the tailings mass and not recoverable?

2-4. When Mine A was being designed, the tailings impoundment was sized so that its lateral catchment area would be sufficient to provide 150 m^3/day to the mill from the impoundment assuming 50% evapotranspiration of annual precipitation in the impoundment and 20% of slurry water retained within the impoundment. What is the minimum area of the impoundment needed to provide the mill's requirement? Based on this minimum area and a dam height of 11 m including 1 m of freeboard that cannot be used, how many years are required to fill the impoundment to the top of the dam with tailings and water?

2-5. Further to Question 2-4, how many years are required to fill the impoundment to the top of the dam if water from the dump was diverted from the beginning of mining into the impoundment because it was unacceptable for discharge?

2-6. In light of Question 2-5, the treatment and release of unneeded water to the environment provide more storage volume for tailings solids. What is the maximum amount of water that can be treated and released to the environment each year? What is the maximum weight of tailings solids that can be placed in the impoundment?

2-7. If Mine A were a Type 1 Underground Mine, rather than a free-draining Type 2, would active pumping of water from the workings to the mill increase costs of the mining operation? Under what conditions would expansion of the tailings impoundment be justified to provide all the mill's water?

CHAPTER 3
FLOW OF MINESITE DRAINAGE

3.1 Overview

According to the classic concept of environmental water balance, precipitation falling onto a minesite component will experience three fates. First, a portion will evaporate or be transpired by vegetation, and thus will return to the atmosphere ("evapotranspiration"). A second portion will run over the surface of the component (overland "runoff"). The third portion will infiltrate into, and eventually flow from, the component ("infiltration" or "subsurface flow"). In classical hydrology, the second and third portions are collectively called "runoff", but this grouping is not appropriate at minesites as explained below. Therefore, this book distinguishes between runoff and subsurface flow, and *drainage* is the collective term for both.

Compared with runoff, subsurface flow often leads to greater contact and more chemical interaction between water and mined materials. Additionally, runoff over minesite components with rough or broken surfaces is often negligible. For these reasons, greater emphasis is placed in this chapter on subsurface flow.

Hydrogeology is the science of subsurface flow and chemistry, which defines two basic types of flow. The first is relatively smooth, laminar, Darcian flow through a porous medium of relatively fine particles or fractures. The two most important factors in Darcian flow are hydraulic gradient and hydraulic conductivity (Freeze and Cherry, 1979).

Hydraulic gradient is the change in hydraulic head between two points in a groundwater system divided by the distance between the points, which characterizes the "driving force" behind the groundwater. Values of gradients typically range over roughly four orders of magnitude (0.0001 to 1.0) and reflect site-specific conditions including recharge and discharge areas and variations in hydraulic conductivity.

Hydraulic conductivity (K) reflects the water-carrying capacity of a unit cross-sectional area of rock (1 m^2) under a hydraulic gradient of 1.0. Conductivity typically ranges over 10 orders of magnitude (roughly 10^{-12} to 10^{-2} m/s) and thus can proportionally play a greater role in regulating groundwater flow than hydraulic gradient.

The second basic type of subsurface flow is turbulent, non-Darcian flow through relatively large particles or fractures. Research in this area has attempted, with limited success, to relate turbulent flow to Darcian-type analysis, to define flow through empirical parameters, or to describe flow using novel concepts like fractal characteristics of the flow system. Turbulent flow will be defined in greater detail in the following two subsections.

Subsurface flow through each minesite component will occur entirely as one type, or as both types in various zones. Nevertheless, in a general sense, mines and coarse-grained rock piles are typically associated with turbulent flow, whereas fine-grained rock piles and tailings are associated with Darcian flow. The following subsections will illustrate these traits as well as exceptions.

3.2 Drainage Flow through and from Mines

The mine component is the center of an ongoing struggle of humans and machinery with nature. Through time and without human intervention, many mines will fill with water through groundwater seepage and precipitation and with rock and sediment through erosional and rock-failure processes. This section presents only an overview of the physical effects of mining on drainage flow, because the amount of flow is not usually critical in determining drainage chemistry (Chapter 4). On the other hand, the sizes of treatment systems to handle drainage that is unacceptable for discharge are dependent in part on the amount of flow (Chapter 6), so this issue cannot be ignored entirely. The many books and proceedings on mining engineering and hydrology can be consulted for additional details on water movement (e.g., Williams et al., 1986).

Many underground and open-pit mines are excavated into relatively impermeable rock with fractures, or relatively permeable rock with fractures. In both cases, fractures play a role in controlling the rate and direction of water flow into, through, and from a mine. For this reason, this subsection focusses on fractures rather than the traditional porous-medium concept (Section 3.1). The word, fracture, is used here is a general sense and includes narrow "cracks" to large-scale open or sealed faults.

Blasting, ore removal, and stress redistribution can cause fracturing throughout the rock mass surrounding a mine, in addition to that originally present before mining (e.g., Roberts, 1981). Also, any collapse or subsidence of rock after mining can also open new fractures. As a result, a pre-mining assessment of fractures is not a reliable indicator of future fracture and water movement. In fact, in contrast to the normal expectation, Wei and Hudson (1990) noted that in some cases deep excavation in good quality rock can cause reduced permeability, especially if the rock exhibits elastic or plastic characteristics.

Although Darcian and porous-medium concepts do not apply to fractured rock, the basic concept of hydraulic conductivity can be adapted in a general way. Bulk hydraulic conductivity of a fractured rock mass is a composite of the intrinsic conductivity of the rock, which is typically low, and the fracture conductivity, which is typically higher. As a result, bulk conductivity and its control over groundwater flow are often determined by fracture conductivity, although many examples of fractures hindering water movement are also known. In any case, fracture conductivity is determined by several factors such as fracture aperture, smoothness, and interconnectivity of one fracture to another.

Two examples of non-mining-related studies illustrate well the complexities and details of water movement through fractured rock. In a computer-based study of fractured rock, Jardine et al. (1996) presented an example showing the fracture pattern in a rock mass (Figure 3.2-1a) and the resulting volumetric flow through the mass (Figure 3.2-1b).

A detailed in-field hydrogeologic study of shallow fractured gneiss (200 x 150 x 50 m deep) included visual borehole logging of fractures and pump tests (Raven, 1986). Bulk hydraulic conductivity and calculated effective aperture were found to be lognormally distributed with geometric means of $2x10^{-9}$ m/s and 11.8 : m, respectively. The scale below which the rock resembled a relatively simple, homogeneous, and isotropic porous medium was roughly 10 m. Anisotropy ratios of conductivity were typically between 1 and 10.

Fractures exposed in mine walls can be grouped according to two endpoints in a spectrum: long, continuous, pre-existing fractures and short, mining-induced fractures. The first type of "large-scale fractures" is the result of long-term geological processes, whereas the second endpoint is caused by mining activity. The latter type is sometimes labelled "excavation response", "excavation damage zone", or salt halo in nuclear-waste-repository studies (e.g., Everitt et al., 1989; Gascoyne et al., 1995). A salt halo reflects the evaporation of water in fractures adjacent to mine walls and the accumulation of secondary minerals, which is a key aspect in predicting minesite-drainage chemistry (Chapters 4 and 5). Recent, mining-induced fractures can sometimes be distinguished by their lack of mineral infilling or alteration and by their symmetry to blast or room geometry.

The detailed delineation of all fracture characteristics for all relevant fractures surrounding a mine is beyond current technology and economics, as shown by expensive international studies for high-level radioactive waste repositories (see Case Studies 3.2.2-1 and 3.2.2-2). For example, predicted changes in hydraulic conductivity during mining at the Canadian Underground Research Laboratory (URL) based on computer modelling were opposite to observed trends. As a result, the researchers concluded that " . . . the models and/or the codes used do not correctly simulate the physical processes that occur in a fracture subjected to excavation-induced [mining] displacements" (Lang, 1989).

The assessment or prediction of water flowing into a mine can be reduced through empirical methods which do not attempt to simulate every fracture or every block of rock. For example, in an underground mine, the monitoring of flow at various

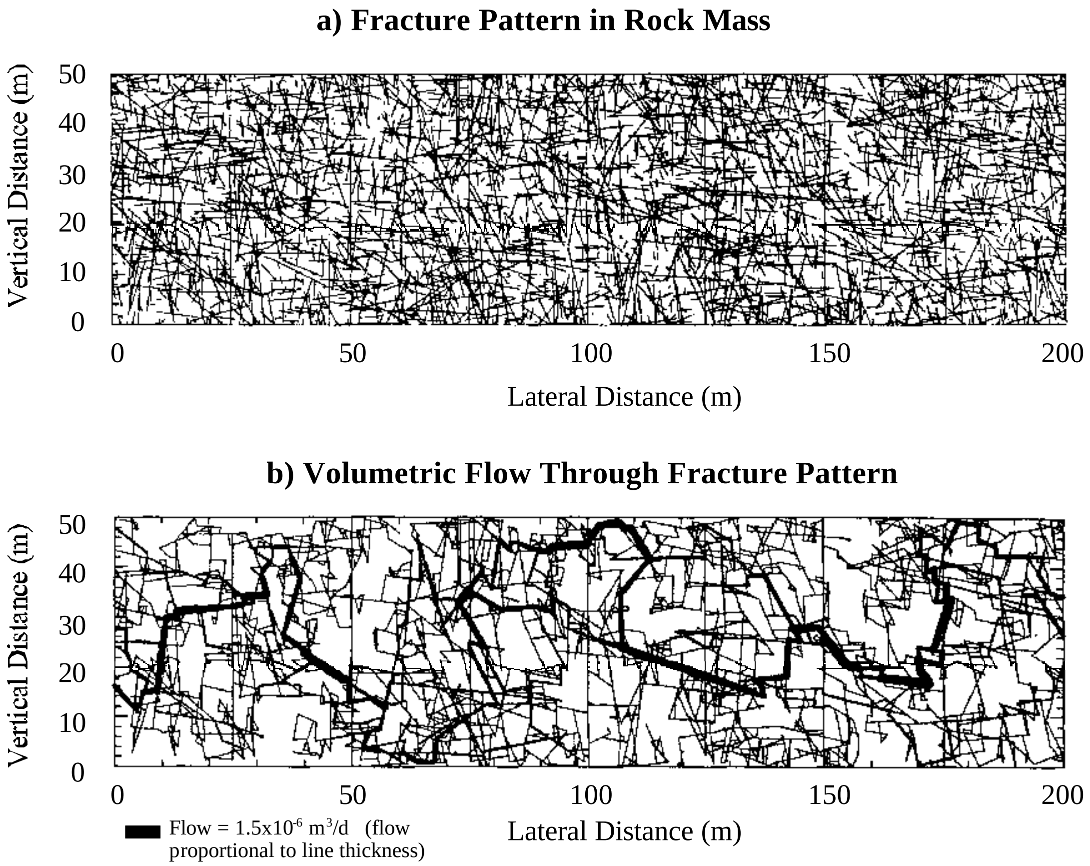

FIGURE 3.2-1. Computer-Based Example of Fractured Rock and Groundwater Flow (adapted from Jardine et al., 1996).

locations in an underground mine showed that flow increased by around a factor of 10 within 50-100 m of the portals (Northwest Geochem, 1992). As a result, the bulk conductivity of the outer 50-100 meters of each level was apparently a factor of 10 higher, presumably due to blasting and stress release. These findings affected closure planning for the site that previously included portal sealing and extensive flooding which were then dismissed. This type of empirical approach is used to describe water movement through open pits and underground workings in the following subsections.

An important reminder at this point is that, as a mine floods, changes of hydraulic pressures and gradients within the mine and the surrounding groundwater system may cause a change in fracture size and number, as well as a change of groundwater flow through the mine. Consequently, an assessment of pre-mining or mining flows will not necessarily reflect post-mining flow.

3.2.1 Drainage Flow in Open-Pit Mines

The flow of water into, through, and from an open-pit mine (Figures 2.2-1 to 2.2-4) is dependent on the rate and direction of flow from specific sources and sinks. The following paragraphs present a simple scenario for the sources and sinks, but exceptions reflecting site-specific complexities are known and are included here.

During the Operational Phase (Figure 3.2.1-1), *precipitation* is a key source of drainage into open pits. Also, any surface flow over the sloping walls

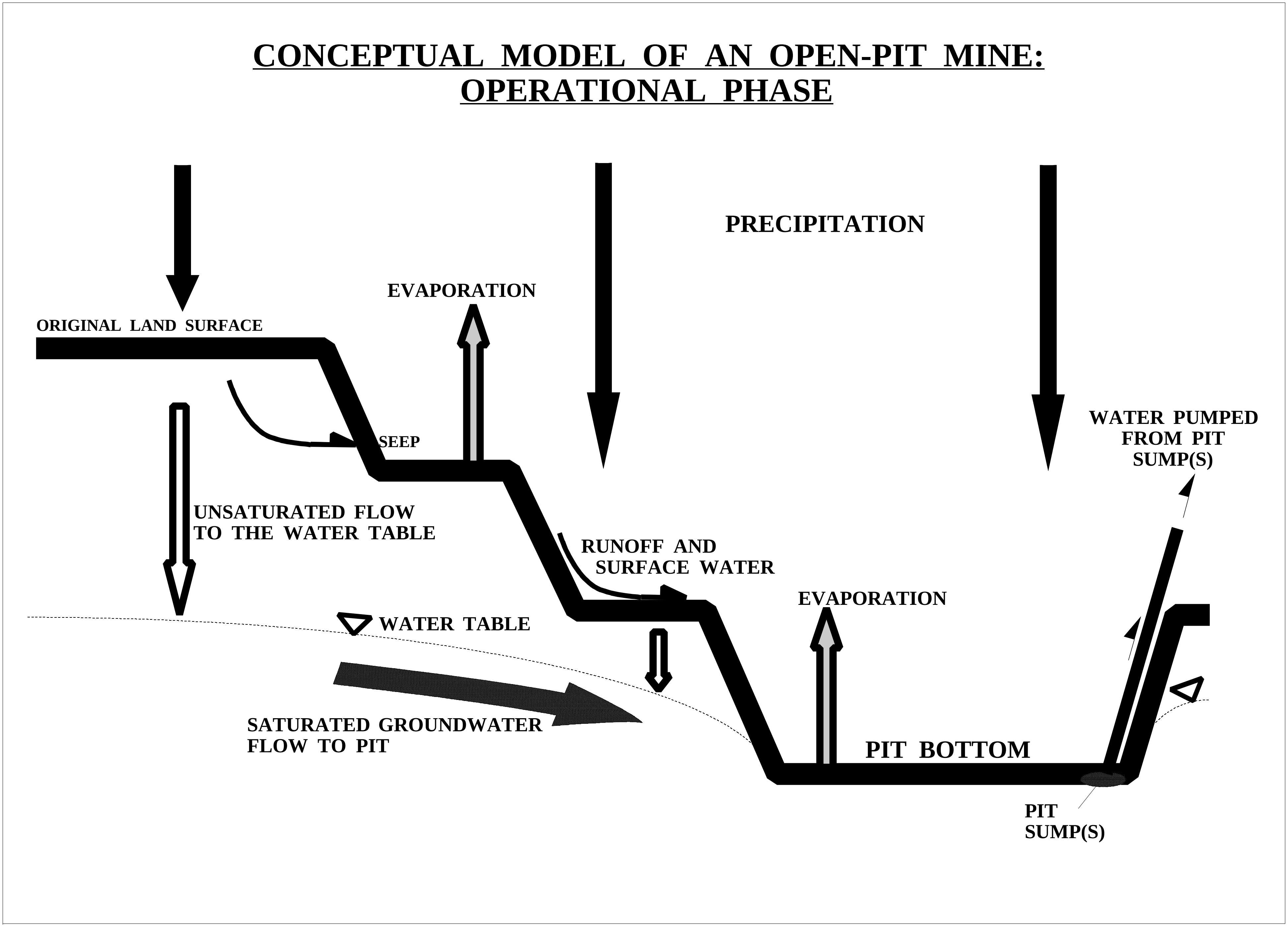

FIGURE 3.2.1-1. Schematic Water Movement In and Near Open-Pit Mines During Operation (adapted from Morin and Hutt, 1995a).

and flat benches of open pits is *runoff*, and may be augmented by seeps discharging from the pit walls. The seeps, in fact, represent an interaction of groundwater (discussed below) and *runoff*, and can be indicative of geochemical processes operating behind the walls (Section 4.2).

Runoff from surface catchment beyond a pit rim is typically diverted around the pit for safety and stability reasons and for reducing expense of pumping from the pit. Consequently, there is often little runoff to the base of the pit from an area much larger than the pit itself.

Any *precipitation* infiltrating into the ground becomes *unsaturated groundwater flow*. Some percentage of this unsaturated flow will eventually discharge from pit walls as seeps and thus be accounted for as *runoff*. The remainder can be expected eventually to reach the water table and join the regional saturated flow system which extends to the pit.

Saturated and unsaturated groundwater can play a critical role in the stability of pit walls. This is the result of (1) reduction of shear strength in rock and overburden, (2) large lateral forces exerted on rock-block surfaces by a column of water within a fracture or fault, (3) reduction of friction force in a fracture plane by the pressure exerted by a water column, and (4) transmission of hydrodynamic shock by water in fractures upon blasting (Cavers, 1987). The decreased stability caused by the presence of groundwater requires flatter pit-wall slopes, increasing the volume of waste rock removed from the pit area, which in turn increases the extent of environmental disturbance and the costs for blasting and handling. Furthermore, the movement of groundwater in the pit area can be responsible for (1) the heaving of the pit floor during excavation, (2) the erosion of walls and, during sub-zero temperatures, icing of the groundwater discharges through the pit walls, and (3) increased blasting costs because of the need for higher grade explosives in water-saturated areas (Brawner, 1979). For all of these reasons, control of groundwater movement and water-table elevation are critical topics in mine engineering.

There are three basic techniques for control of hydraulic head and groundwater movement near an open pit: (1) toe drains at the base of pit walls, (2) underground galleries within the pit walls, and (3) perimeter and in-pit pumping wells (Pentz, 1979). Although the first two techniques are usually considered gravity-driven and passive, all three techniques eventually require active pumping to lift the water to the surrounding land surface at most sites. Perimeter wells are considered practical only where hydraulic conductivities are high and hydrogeologic barriers such as clay-filled fault zones are widely separated (tens of meters or more).

In addition to the aforementioned sources of water, the important sinks during Operation are usually (1) *pumping* of water (or gravity drainage for pits in sloping terrain that are not completely surrounded by walls) and (2) *evaporation*. Without these factors, a pit would begin to fill with water. Some reports of water-table drawdowns have shown that effects can extend for more than a hundred meters vertically and dozens of kilometers laterally (Table 3.2.1-1).

As with any conceptual model like Figure 3.2.1-1, there are myriad variations. For example, Kipp et al. (1983) described pits located above the local water table. As a result, no groundwater from the saturated zone reported to them, but instead pit water was lost to the underlying unsaturated zone. Additionally, Figure 3.2.1-1 shows the water table joining the pit near its base whereas Lopaschuk (1979) reported a drawdown of only 10 meters in a 90-150 meter deep pit.

When a pit is closed upon cessation of mining and initiation of decommissioning, pit pumps may be turned off or gravity drainage may be halted. This causes the water level in the pit to rise out of the sump(s), cover the pit bottom, and progressively submerge portions of the pit wall. Filling of a pit can be accomplished through natural processes (Figure 3.2.1-2) or assisted by pumping of water into the pit (Figure 3.2.1-3). A notable example of a naturally filling pit is the Berkeley Pit in Montana, USA. Davis and Ashenberg (1989) reported that the pit's water level was rising 22 meters a year and that total water storage was expected to reach 5×10^8 m^3 of acidic water. Eventual overflow of the acidic water into the uppermost aquifer was a primary concern.

TABLE 3.2.1-1
Case Studies of Groundwater Flow to Pits
(from MEND, 1995)

Location & Type of Mining	Approximate Pit Dimensions		Maximum Drawdown (m)	Lateral Extent of Drawdown (m)	Elap-sed Time	Pump Rate (m^3/d)	Reference & Miscellaneous
	Area (m^2)	Depth (m)					
Faro Mine, Yukon - base metal & Ag	840,000	90 - 150	10	-	1-2 wks	2180	Lopaschuk,1979; 380 m^3/d from lateral drains, 1800 as inflow to pit
Whitewood, Alberta - coal	110,000	20 - 40	20	1200	> 6 yrs	410 to 685	Sumer et al., 1987; recharge = 5% of 50 cm/yr; dewater wells; model K = 10^{-6} - $5*10^{-4}$ m/s, Sy = 0.05, S = 0.001
Twin Buttes, Arizona - base metal(?)	1,170,000	230	90	300	1.3 yrs	generally < 5	Pentz, 1979; underground galleries with lateral drill holes for dewatering; K = 10^{-8}
Shirley Basin, Wyoming - uranium	150,000	90	21	> 300	1 yr	> 1440	Straskraba & Kissinger, 1982; dewater wells/lateral drains; K = $2*10^{-5}$ m/s, S = 0.00054
Southern Illinois - coal	-	-	> 24	> 300	-	-	Oertel & Hood, 1983; K < 10^{-7} m/s
Kentucky - coal	-	-	10 & rise of 1.5	-	< 1 month	-	Kipp et al., 1983; pits in unsaturated zones above wells with positive and negative effects on recharge
Haywood Pit, Scotland - coal	225,000	71	45	-	-	26,000	Norton, 1982; dewater wells
Blindwells Pit, Scotland - coal	1,200,000	60	30	< 1,000	2 yrs	35,000 to 69,000	Norton, 1982; area contains abandoned, flooded underground mines; water table stable prior to pit mining; dewatering wells
Piaski, Poland - coal	-	124	> 100	8,000	-	560,000	Seweryn, 1982; dewater wells
Nyirad, Hungary - bauxite	2 pits: 5,000,000 2,500,000	> 100 > 100	100	45,000	21 yrs	430,000	Bocker and Vizy, 1982; Paris, Karst limestone; K = 10^{-5} - 10^{-4} m/s, porosity = 2 - 4%; S = 0.00002; dewatering wells; recharge = 25% of 63 cm/yr
Queensland, Australia - limestone	10,000	27	25	> 2,000	7 yrs	1,400	Dudgeon, 1987
Victoria, Australia - coal	3,000,000	-	130	50,000	22 yrs	68,000	Evans, 1987; aquifer K = $6*10^{-6}$ - $2*10^{-4}$ m/s, S = 0.00002 - 0.0003; K of aquitard = 10^{-11} m/s
South Australia - coal, trial pit	200,000	60	40	-	1 yr	17,300	Armstrong, 1982; aquifer K = 6 - $9*10^{-5}$ m/s; aquitard K = 10^{-8}; series of emergency wells for water control
Neyveli, India - coal	7,770,000	70	49	11,000	18 yrs	160,000 to 320,000	Hofedank, 1979; Brealey, 1965; transmissivity = 0.01 m^2/s; dewatering wells

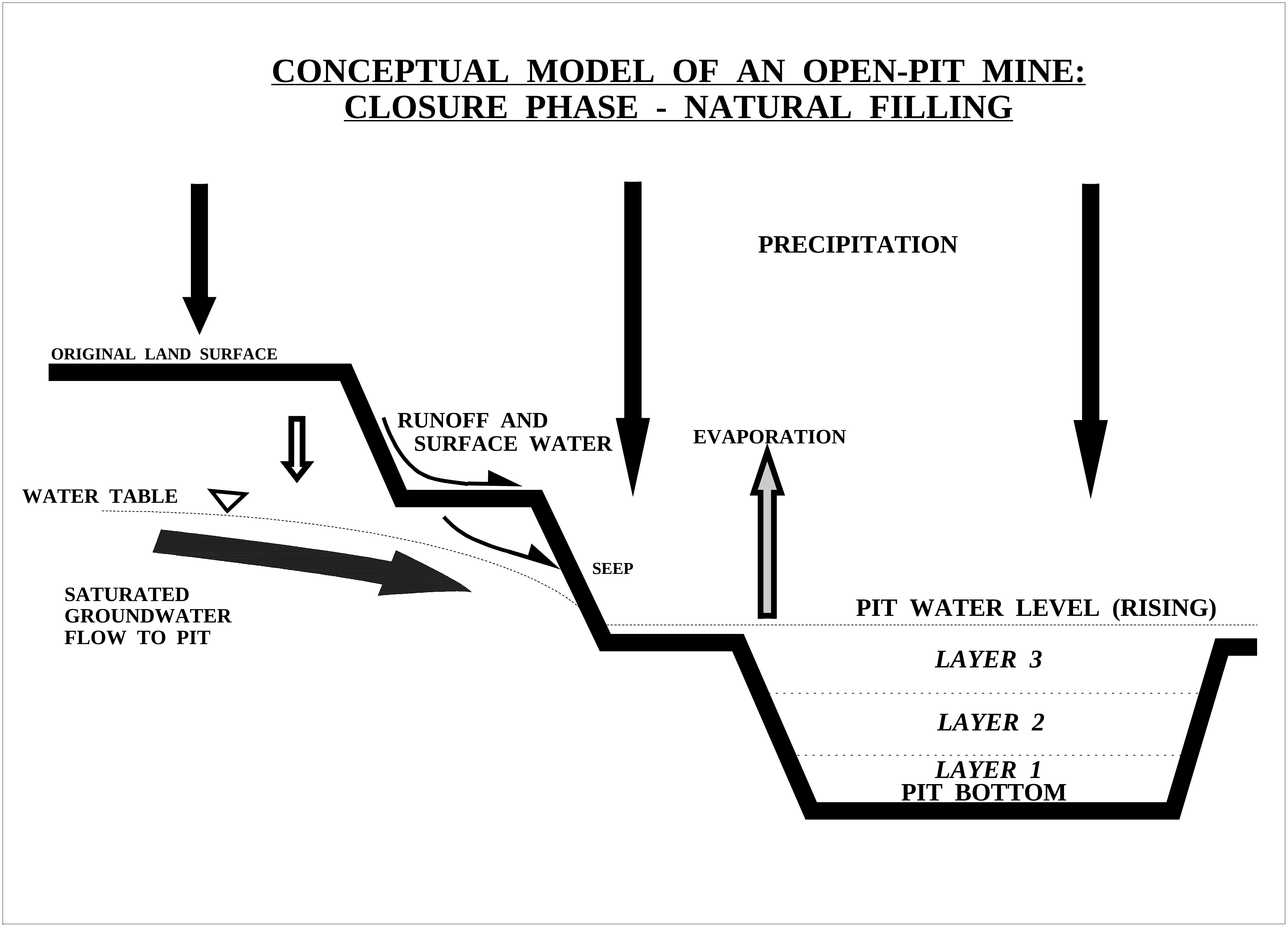

FIGURE 3.2.1-2. Schematic Pit Filling by Natural Processes During Closure (adapted from Morin and Hutt, 1995a).

CONCEPTUAL MODEL OF AN OPEN-PIT MINE: CLOSURE PHASE - ASSISTED FILLING

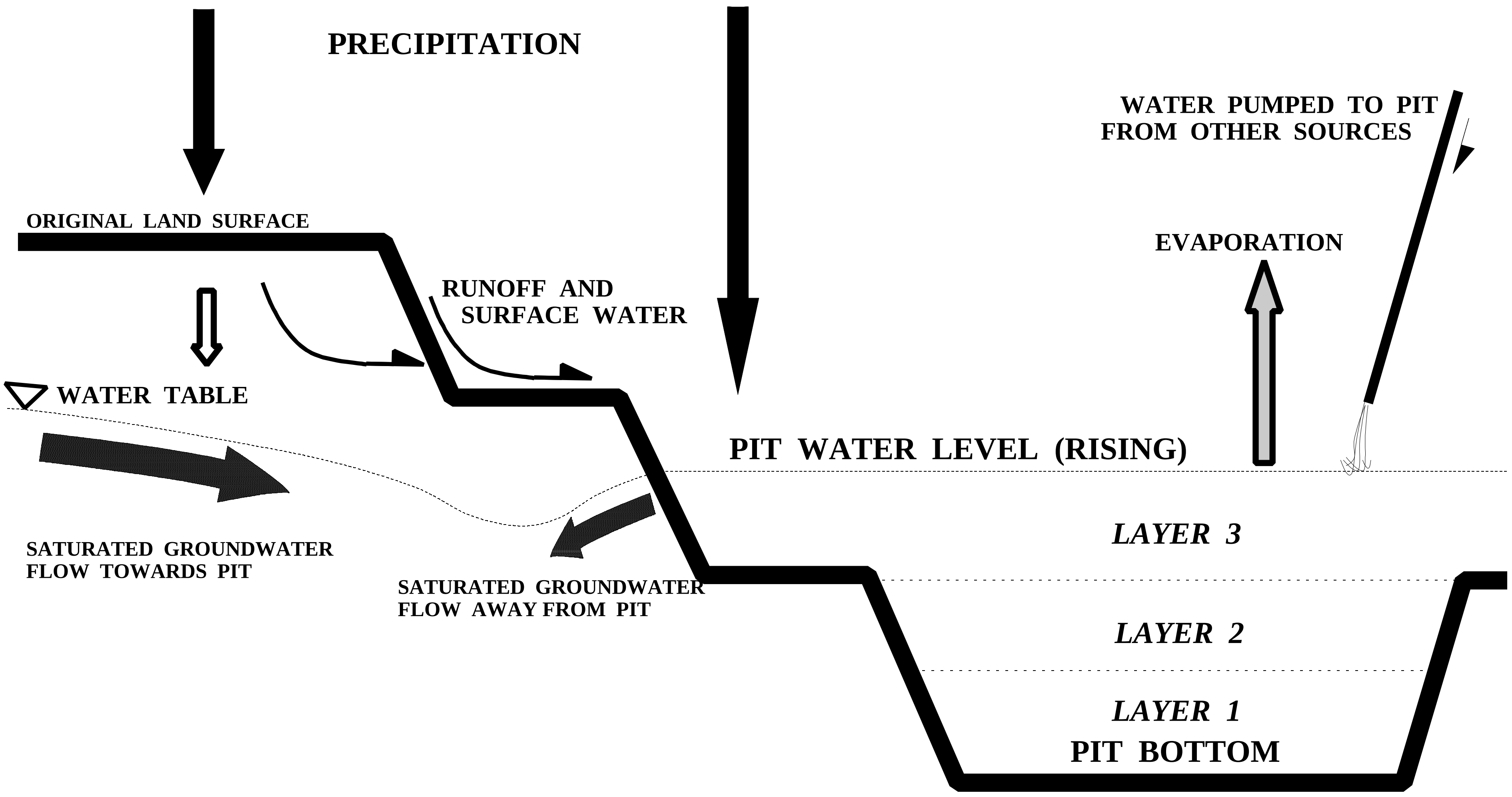

FIGURE 3.2.1-3. Schematic Pit Filling by Assisted Methods During Closure (adapted from Morin and Hutt, 1995a).

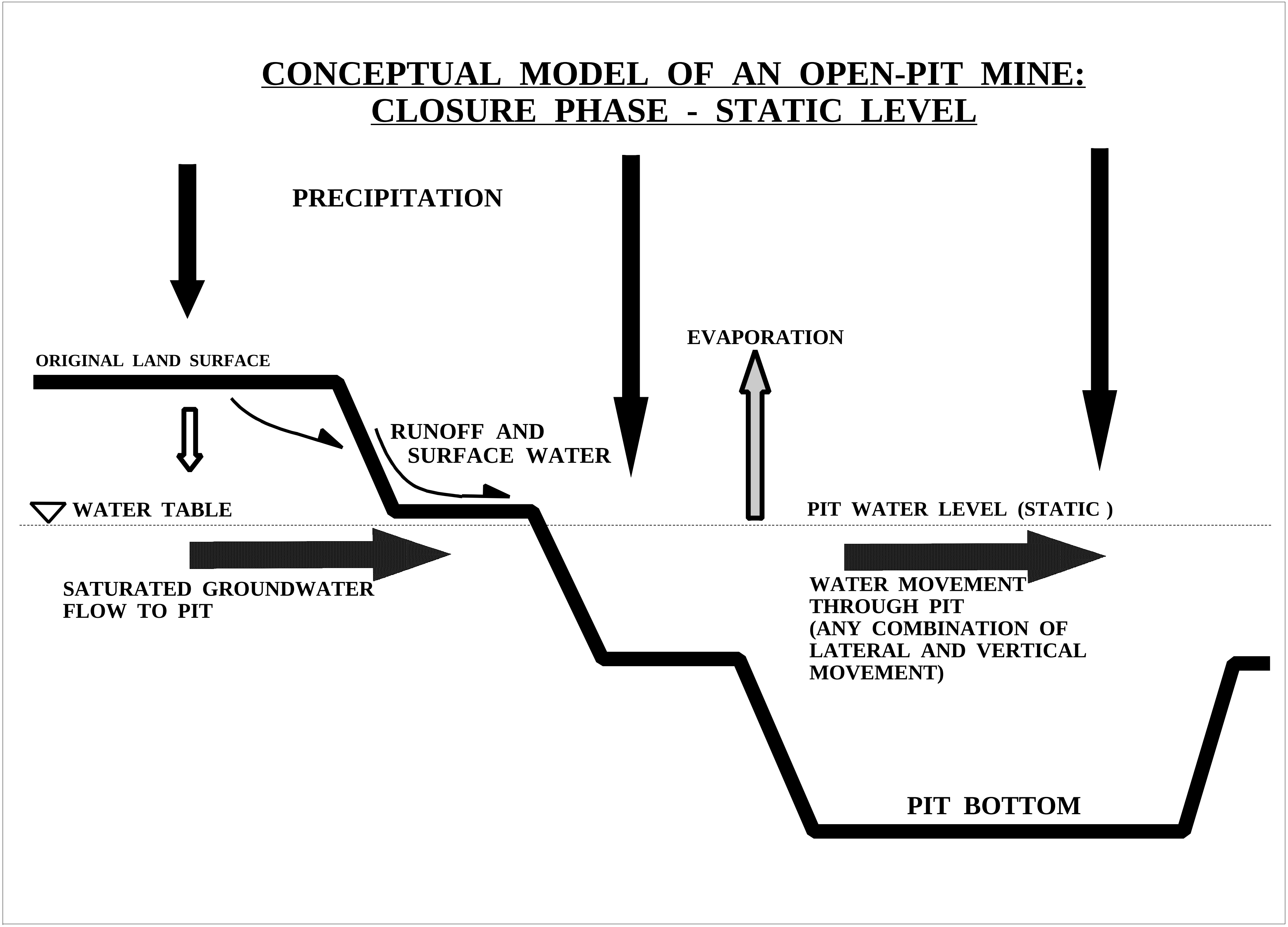

FIGURE 3.2.1-4. Schematic Pit Filled to Its Static Level (adapted from Morin and Hutt, 1995a).

The primary difference between natural and assisted filling during the Closure Phase of a pit lies in the local direction of groundwater movement close to the mine walls. During assisted filling, a temporary stagnant zone may form in the groundwater system.

As the input of water continues, the water level rises until a “static” or equilibrium level is attained (Figure 3.2.1-4). At that point, the rate of water entering the pit is generally balanced against water leaving the pit, and the water level remains relatively steady from year to year. However, “static” level is only meant in a general sense and some season-to-season and year-to-year variations can be expected. As with the Operational phase, there are myriad variations. For example, to ensure no pit water is lost to the surrounding groundwater system, ongoing pumping may be required to create an artificial static water level below the natural static level.

Water within a flooding pit can be thought of as one physical mass, but it may actually consist of several layers divided on the basis of chemical or thermal characteristics. The circulation of water is sometimes limited to within each layer or water may circulate freely among several layers. Also, if the pit water experiences physical seasonal “turnover” due to thermal instability, some or all layers may occasionally mix and thus be temporarily indistinguishable.

Case Study 3.2.1-1: Groundwater Depressurization in Pit Walls

highlights: pre-mining manipulation of groundwater flow using drillholes; control of groundwater inflow to an open pit using underground workings; effect of groundwater control on pit size, volume of waste rock, and exposed rock-surface area

The East Pit of the Twin Buttes Minesite in Arizona, USA, was designed to intercept ore in a Paleozoic sedimentary sequence, predominately composed of limestone and siltstone (Pentz, 1979). The ore rock was laterally adjacent to waste rock to the east consisting of Mesozoic arkosic and porphyritic strata, separated by a 60-meter-wide fault zone containing semi-vertical clay-filled structures.

Based on geotechnical and mining considerations, a decision was made to optimize (steepen) pit slopes in the Mesozoic rock by lowering hydraulic head in the surrounding rock. After toe drains at the base of the walls proved unsuccessful, approximately 1000 meters of underground workings were excavated for dewatering purposes and almost 8000 meters of lateral holes were drilled and screened with slotted PVC pipe to enhance drainage. In order to monitor changes in hydraulic head, 72 pneumatic piezometers were placed in multilevel installations.

Underground flow was monitored in the crosscut and drainage holes. Flow from the 21-02 crosscut had an average of 2.3 m^3/day from each meter of crosscut. Flow from drainage holes reached as high as 130 m^3/day, but decreased to less than 1 m^3/day in most holes after two months.

Observed declines in hydraulic head in the piezometers ranged from 11% to 100% with an average of 67% relative to the elevation of the underground workings. The adit discharge and hydraulic heads were modelled to obtain a bulk hydraulic conductivity of 10^{-8} m/s.

Despite the decline in hydraulic head along the east wall, the water table remained near the land surface, because the rate of infiltration was close to the rate of drainage. Nevertheless, a risk/uncertainty analysis showed that the depressurized groundwater system allowed a steeper slope in the pit, resulting in less waste rock. Additionally, the steeper slope provided less surface area for contact with rainfall, which has implications for in-pit water quality (Chapter 4).

Case Study 3.2.1-2: Pre-mining Rock Dewatering

highlights: control of groundwater movement as necessity for mining; large pumping volumes offset by markets for the water

Prior to mining at the Neyveli lignite (low-grade coal) mine in India, groundwater and geotechnical studies indicated that upward pressure on the Type 2 pit floor (Figure 2.2-2) would be approximately 50 t/m^2 (Brealey, 1965). This was expected to result in heaving and piping (wash-out) of unconsolidated material in the floor and through unsealed boreholes. Old, unsealed boreholes were considered a problem because they connected aquifers, pierced aquitards, and provided easy connections of surface-water to groundwater systems. Brealey noted that the project involved "one of the most difficult groundwater situations ever encountered in [open-pit] mining" and recommended a phased approach to groundwater evaluations involving (1) exploratory drilling, (2) formation sampling, and then (3) pump tests from installed wells.

Under the lignite at a depth of 53 m below the water table, a high-pressure (confined) aquifer was found with a transmissivity of approximately 0.026 m^2/s, based on a several-week-long pump test at approximately 1.1 m^3/s with a maximum drawdown of 49 m. During mining, electrical generators were kept on-site in case of a main power failure which would have allowed a rapid head recovery of up to 30 m in the first hour. In turn, this recovery would have created the potential for catastrophic heaving and flooding in the mine. Additionally, pontoon-mounted pumps with a total capacity of 0.6 m^3/s were kept in the pit for monsoon rains and as a contingency option in case of groundwater flooding.

To maintain low groundwater heads as the pit advanced at a rate of about 3 m/week, approximately one new well was drilled weekly and old wells were sealed when expendable. Additional wells were maintained in case water levels had to be lowered rapidly to prevent groundwater flooding through old boreholes during pit excavation.

On average, 19-32 tonnes of water were pumped for each tonne of lignite. This water was distributed to processing plants, the local township, and irrigation, which helped to offset costs.

3.2.2 Underground Mines

The physical conceptual models of water movement through underground mines resemble those for open-pit mines (Section 3.2.1), but there are important distinctions. Water movement into underground mines is not always subjected to highly variable input of water, such as caused by precipitation and snowmelt. However, mines with vertical openings to the surface or in shallow, highly fractured rock can have significant seasonal variations of inflow.

Unlike open-pit mines, underground mines have workings like *levels*, *adits*, *shafts*, *crosscuts*, *declines*, *raises*, and *portals* (see the glossary in Appendix A) oriented in three dimensions. Each level can be an independent hydraulic system or can be hydraulically connected with one or more other levels.

The two endpoints of underground mines from the perspective of water movement and drainage are (1) those that have portals through which minewater can drain by gravity ("gravity-drained mines") and (2) those containing one or more vertical shafts to which lateral levels are connected and to which water drains for pumping to the surface ("pumped mines"). These endpoints also reflect the two types of underground mining (Figures 2.2-5 to 2.2-7). As with many physical and chemical factors, there are myriad variations between these endpoints.

During the Operational Phase of an underground mine, the source of water entering gravity-drained and pumped mines is primarily through surrounding groundwater system (Figure 3.2.2-1). In some cases, the local water table or piezometric surface may remain high and thus saturated groundwater flow is the primary contributor. In other cases, the water table or piezometric surface may lie below, or eventually fall below, the mine and thus unsaturated flow will provide most of the inflow. Other potential sources of water include (1) surface water from access/ventilation/glory holes excavated near or to the land surface, (2) drillholes extending to either the surface, the saturated groundwater zone, or isolated and pressurized fault/fracture systems, and (3) drainage from any backfilled material (Brealey, 1965; Emrich and Merritt, 1969; Williams et al., 1979; Trexler, 1979).

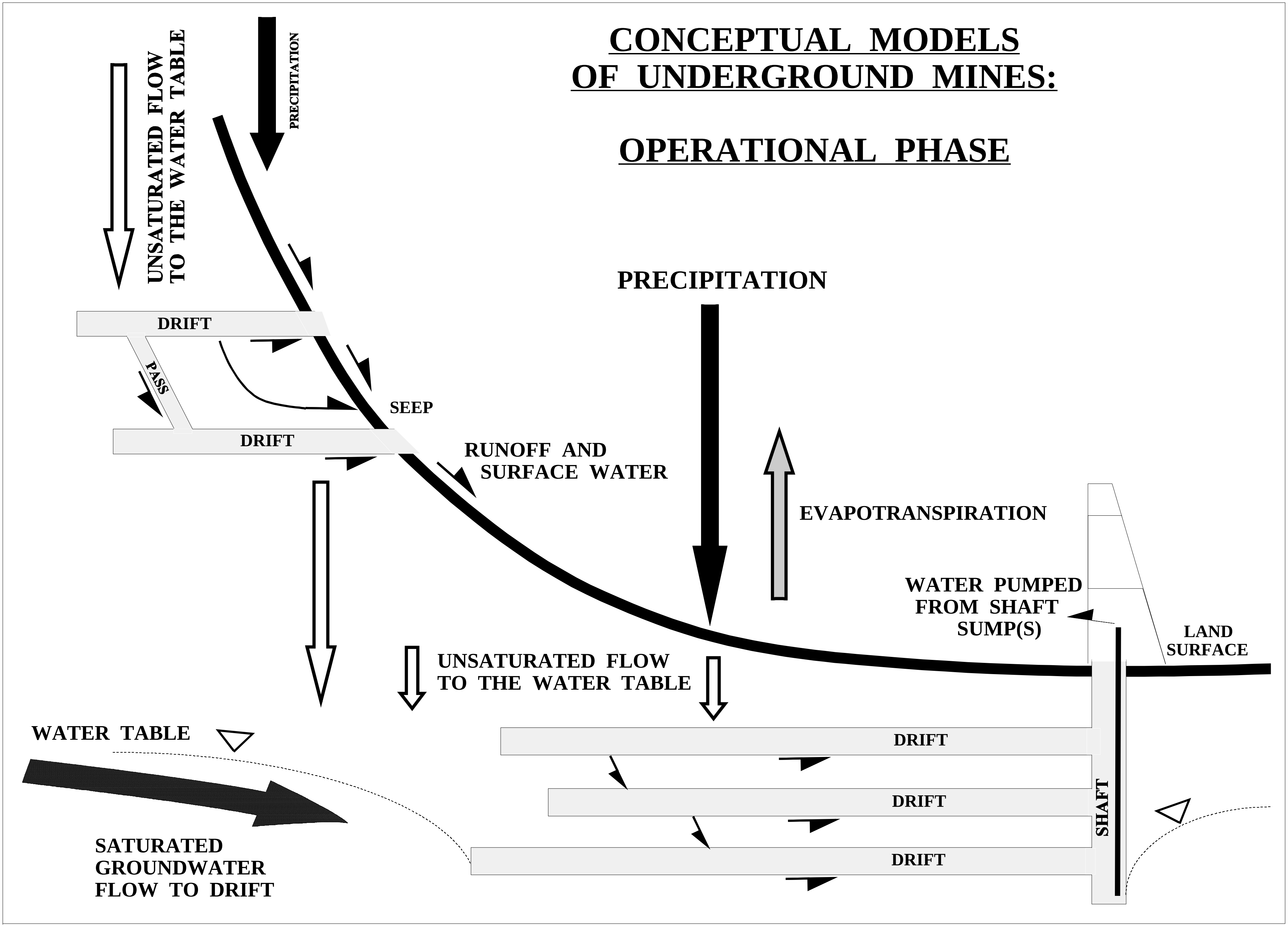

FIGURE 3.2.2-1. Schematic Underground Mines Free Draining to Surface or Shaft.

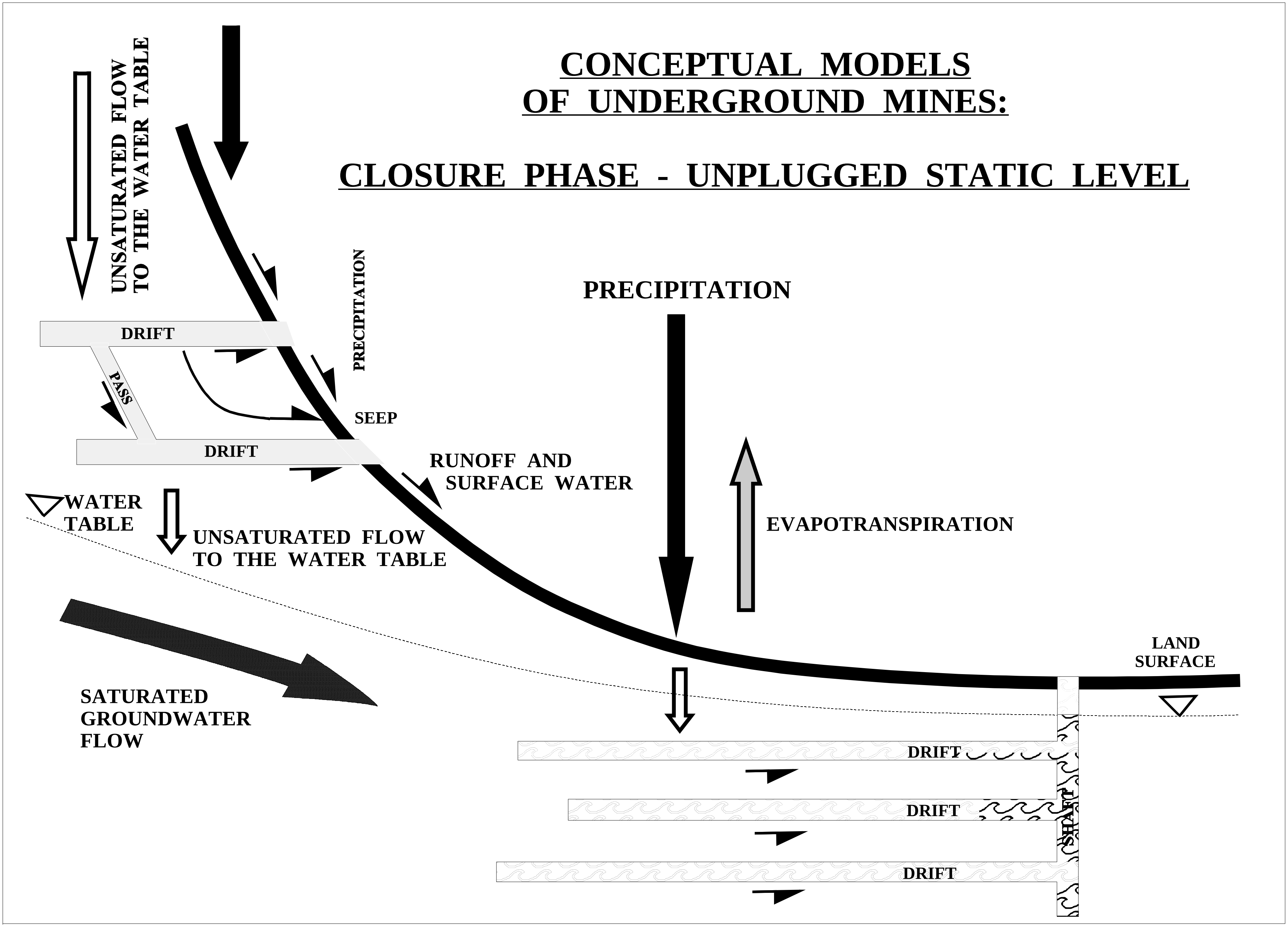

FIGURE 3.2.2-2. Schematic Underground Mines during Closure with No Portal Plugging.

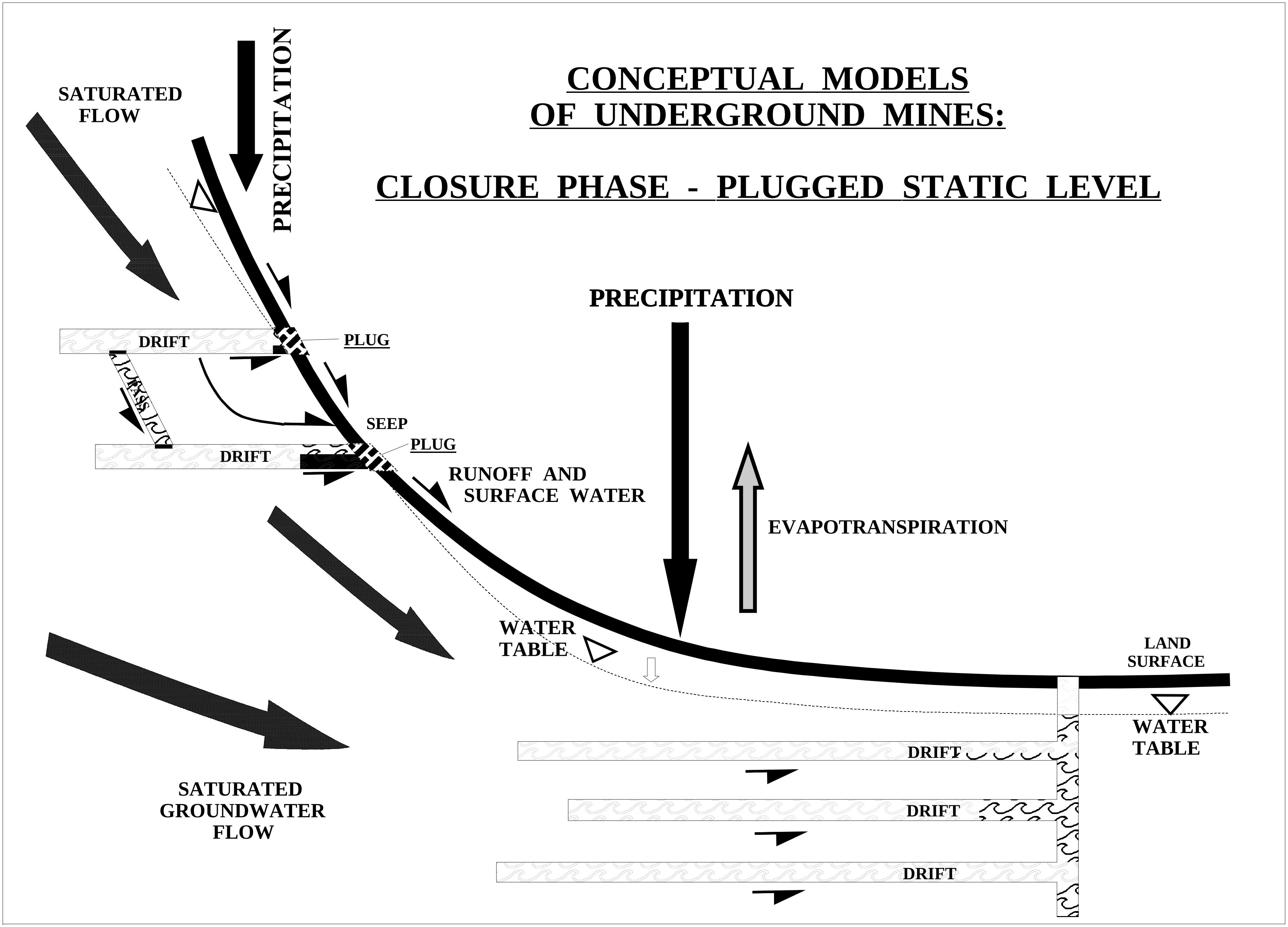

FIGURE 3.2.2-3. Schematic Underground Mines during Closure with Fully Plugged Portals .

The aforementioned classic concept of distinct and vertically stratified, unsaturated and saturated groundwater zones may not apply to underground mines, especially in rock masses where groundwater primarily flows through fractures. In such cases, fractures not connected, or poorly connected, to the main fracture system (e.g., Figure 3.2.2-6) may remain saturated or pressurized even after the local water table has fallen due to mining. If mining activity eventually intercepts such a fracture, the groundwater will quickly drain, appearing as saturated flow, and little if any water will follow as "unsaturated" flow.

During the Closure phase of underground mines, mines pumped during operation will partially or fully fill with water through time (Figures 3.2.2-2 and 3.2.2-3). The static level will generally reflect the pre-mining groundwater level modified by any surficial changes in infiltration and runoff. On the other hand, gravity-drained mines will not fill unless naturally or artificially plugged, and may only form perched water tables rather than raising the regional water table as depicted in Figure 3.2.2-2.

One process that can greatly affect water movement in and around underground mines is subsidence and accompanying fracturing due to the redistribution of stress within the remaining rock. In small, relatively stable workings, stress is oriented toward the excavation from the roof, floor, and walls, causing locally increased hydraulic conductivity. Additionally, a "pressure arch" forms above the roof (Figure 3.2.2-4) as support of overlying rock is transferred to walls or pillars (Booth, 1986). The sagging roof rock results in increased hydraulic conductivity within this pressure arch. From a porous-media perspective, this will allow more rapid draining of saturated porespaces in the pressure arch. However, long-term effects may be minimal in some cases due to the long-term dependence of groundwater inflow on regional conductivity outside the arch. On the other hand, from a fractured-media perspective, the pressure arch may connect several independent fracture networks, potentially leading to higher groundwater flows over relatively long periods of time.

When the width of an underground excavation exceeds the stable width of the pressure arch, as is done intentionally for longwall coal mining, there is a major collapse of roof rock (Figure 3.2.2-5). The critical width of the excavation is variable and is dependent on such factors as physical properties and thickness of rock, size and distribution of pillars, degree of fracturing, and groundwater conditions in and around the workings. Roof collapse consists of irregular breaking of overlying strata for tens to hundreds of meters above the ore zone. If the irregularly broken rock (sometimes called "gob" in coal mining) does not extend to the land surface, the higher strata will deform in a more regular manner.

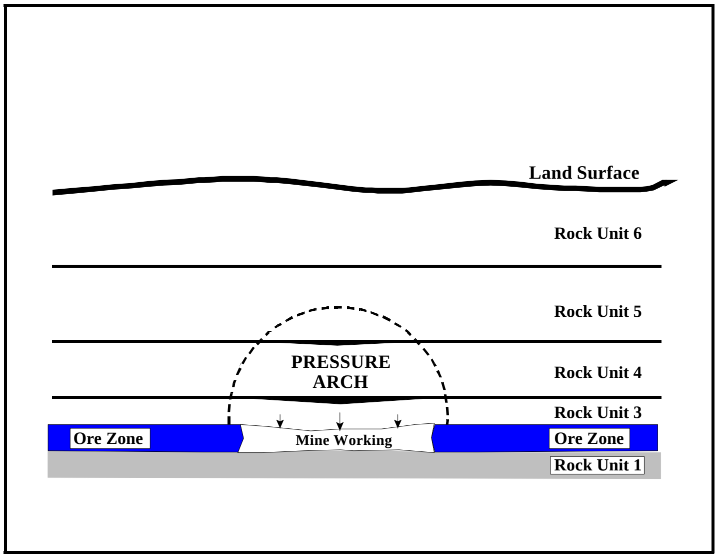

FIGURE 3.2.2-4. Formation of a Pressure Arch during Underground Mining (adapted from Booth, 1986).

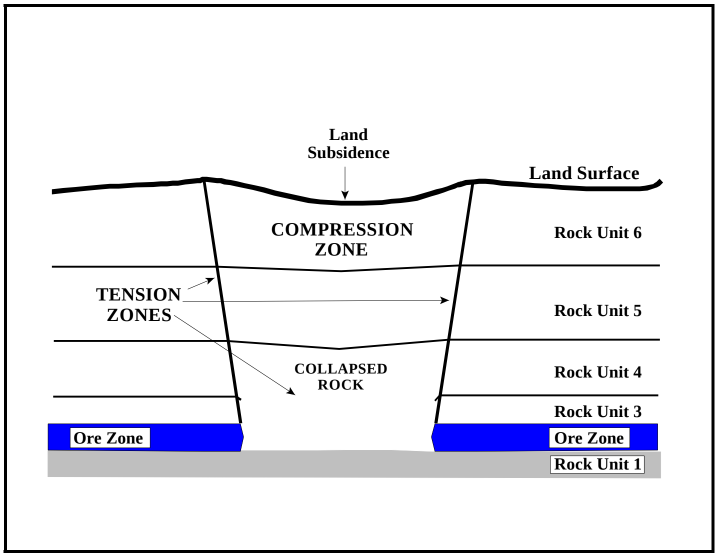

FIGURE 3.2.2-5. Rock Collapse and Tension Zones during Subsidence (adapted from Booth, 1986).

The movement will be directed downward and laterally toward the centerline of the excavation, resulting in a tension zone at the outer edges of the subsiding zone and a compression zone around the centerline. Within the broken rock, hydraulic conductivity and porosity are enhanced. Within the tension zones that extend to the surface, hydraulic conductivity is also enhanced, leading to water-table drawdown and potentially enhanced infiltration from the land surface. The width of the subsidence zone, which depends on the depth of the mine and rock characteristics, is reportedly approximately one-half of the mine depth in British coal mines (Whittaker and Reddish, 1984) and is at an angle of 25-50^o from vertical in Appalachian (USA) coal fields (Peng and Geng, 1984). The prediction of subsidence can be based on empirical data to sophisticated computer programs (e.g., Kiusalaas and Albert, 1984).

Case Study 3.2.2-1: Fracture Studies at an Underground Mine

highlights: complexity and variability of fractures in rock; irregularity of groundwater movement through fractures; technique for measuring low flows into underground workings

The Stripa Mine in central Sweden has been used as an international research facility for assessing and predicting the responses of a granitic rock mass to excavation operations (Carlsson, 1981). Research into geochemical, hydrogeologic, and geomechanic responses, as well as the development of monitoring and testing equipment, were all objectives of the project.

Nordstrom et al. (1989) described the hydrogeology of the Stripa Mine in Sweden and indicated that the total porosity of fractured rock (Figure 3.2.2-6) can be calculated from:

$$2_T = 2_K + 2_D + 2_R \qquad (3.2.2\text{-}1)$$

where 2_T = the total porosity in a fractured medium;

2_K = the effective flow porosity or kinematic porosity which represents dominant fluid flow through the fractures;

2_D = the diffusion porosity which represents limited flow through the fractures; and,

2_R = the residual porosity which also represents negligible fluid flow through the fractures.

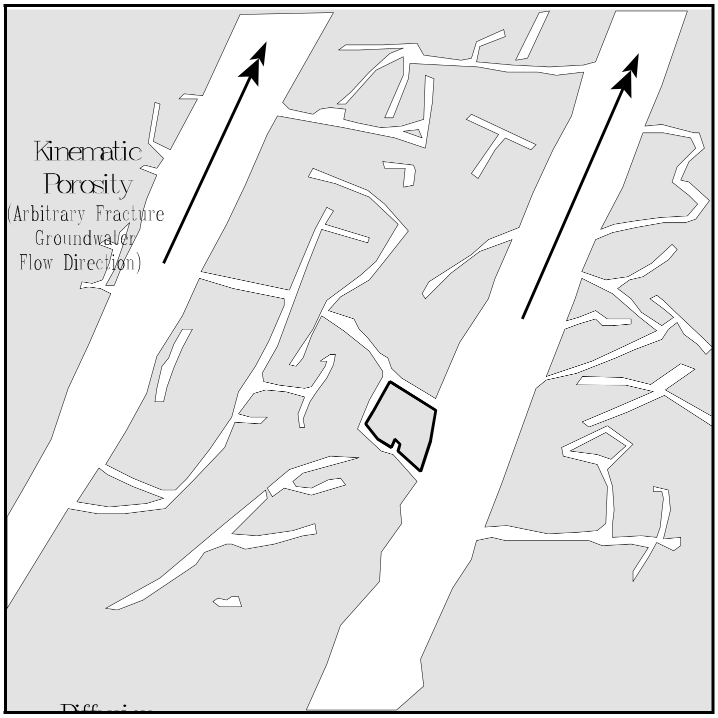

FIGURE 3.2.2-6. Example of Kinematic, Diffusion, and Residual Porosities (adapted from Nordstrom et al., 1989).

Mapping of fractures and porosity on a small scale was found to be complex (Figure 3.2.2-7). The conclusion reached was “[a]t present, it is impractical to model such ubiquitous joints as they actually exist . . . ” (Witherspoon et al., 1981).

To examine larger-scale hydrogeology of the rock at Stripa, 30-meter-long boreholes into one tunnel were sealed with multiple packers and the resulting increase in piezometric pressure in the holes were monitored over discrete intervals (Figure 3.2.2-8). The relatively low pressure increases were attributed to years of loss of pressure and water to adjacent free-draining workings. When Borehole R01 with the dominant flow was sealed later, additional increases in pressure after eight days were noted in some intervals along all boreholes around the tunnel (Figure 3.2.2-8). The additional increases apparently reflected the degree of interconnectedness of fracture zones surrounding the tunnel.

During this test at Stripa, air circulation was

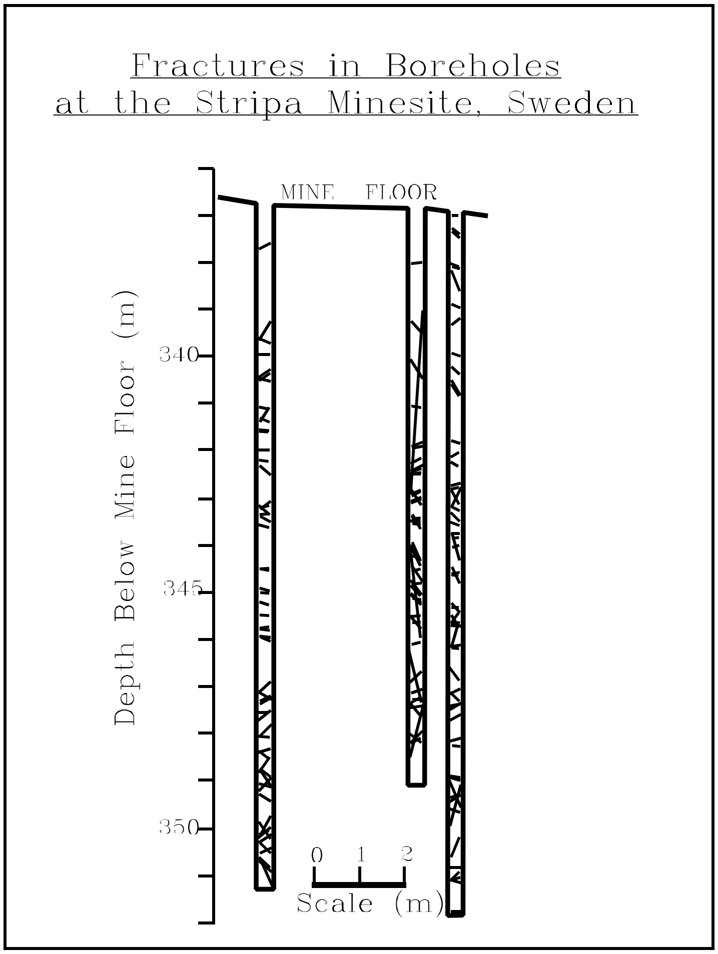

FIGURE 3.2.2-7. Fracture Patterns in Closely Spaced Boreholes at the Stripa Project (adapted from Witherspoon et al., 1981).

adjusted to evaporate all inflowing groundwater from boreholes. Based on air flow and temperature, total inflow was 50 mL a minute and, based on measured hydraulic gradients, average hydraulic conductivity of the rock was calculated to be 10^{-11} m/s (Witherspoon et al., 1981).

Case Study 3.2.2-2: Detailed Fracture Studies at Underground Research Sites

highlights: detailed characterization of fractures; transient effect of mining on fracture properties and groundwater levels

Canada has focussed on crystalline or "hard" rock for nuclear-waste repositories, and the findings can be adapted to many hard-rock mines. The regulatory and safety concerns in the repositories can be seen in the extensive physical, chemical, thermal, and mechanical studies carried out in granite at the Canada Underground Research Laboratory (URL) at Pinawa, Manitoba.

Researchers conducted a carefully planned, executed, and monitored study involving mining through a distinct fracture zone in the URL at a depth of 237 meters in granite (Lang, 1989). By prior drilling, the "Room 209 Fracture Zone" was known to have a maximum thickness of 0.4 meters, consisting of one to six en echelon fractures. The zone intersected the proposed tunnel nearly vertically, perpendicular to the length of the tunnel, and included a low-permeability "band" representing about one-half of the zone to be excavated. The zone extended at least 30 meters laterally beyond the sides of the intended tunnel, only a few meters below the floor, and roughly 30 meters above the floor where it was hydraulically connected to a shear zone.

The remainder of the rock to be exposed was reportedly virtually unfractured, with an unconfined compressive strength of 182 ± 10 (standard deviation) MPa, a tensile strength (Brazilian) of 9.1 ± 0.4 MPa, Young's modulus of 69.1 ± 1.7 GPa, a Poisson's ratio of 0.24 ± 0.02, and a coefficient of linear thermal expansion at 25°C of $(2.5 \pm 0.7) \times 10^{-6}$ $(^{\circ}C)^{-1}$. Normal stiffness of the zone was measured at 500 MPa/mm.

Excavation toward the fracture zone began from a distance of approximately 12 meters. At a distance of 4 meters (not yet reaching the zone), the fracture zone experienced a decrease in equivalent single-fracture aperture from about 59 to 53 µm within a few days. Subsequent mining through the fracture zone occurred as a "pilot tunnel" of 2.5 meters width, followed about three weeks later by "slashing" which widened the tunnel to 3.85 meters.

Modelling showed that stress changes and displacements in intact rock could be reasonably predicted, but the hydrogeologic response of the fracture zone could not. When the pilot tunnel passed from 2.5 m behind the zone to 2.5 m past the zone in one day, measured inflow increased from 0 to 300 mL/min in comparison to the predicted inflow of 2077 mL/min.

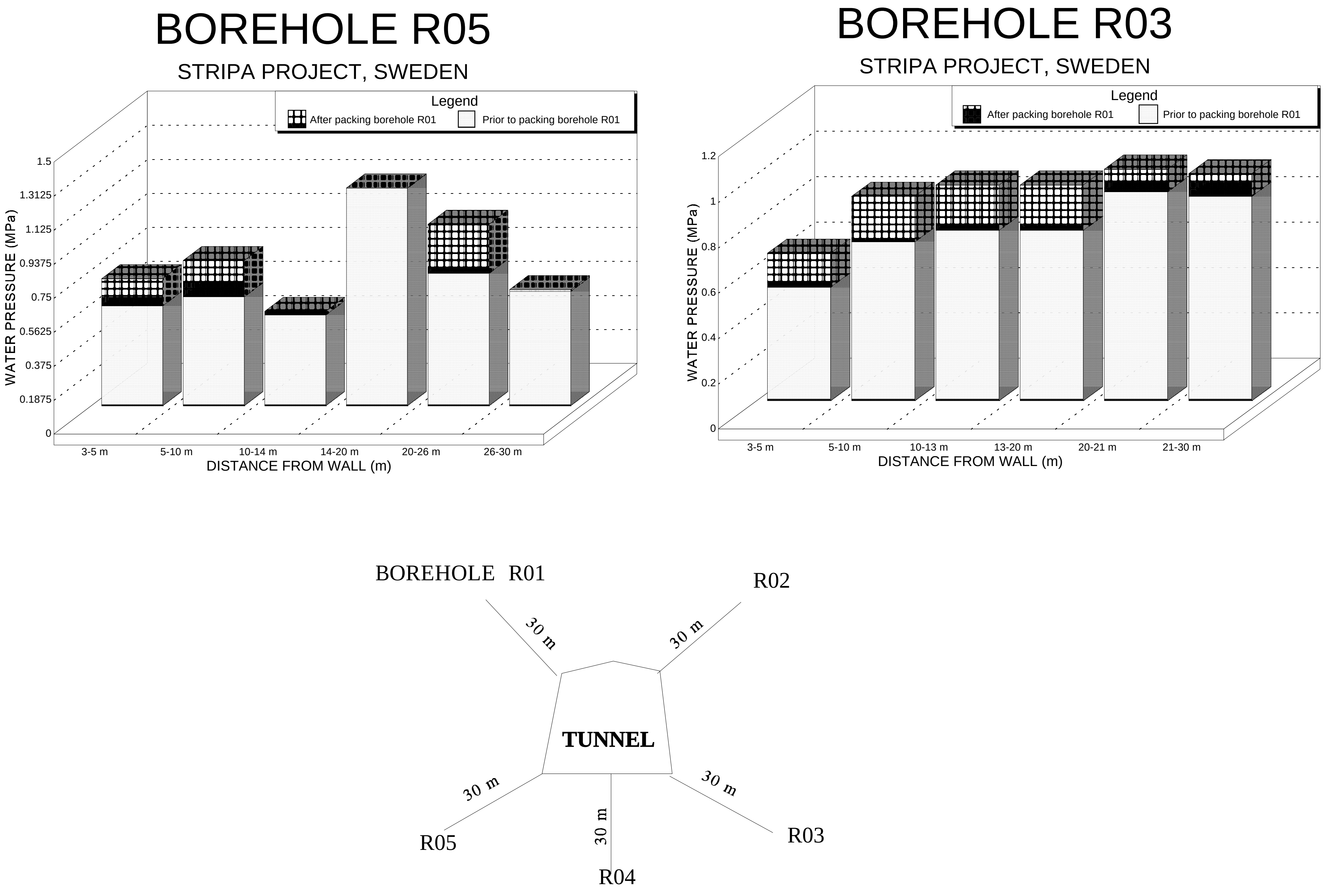

FIGURE 3.2.2-8. Changes in Water Pressure within Selected Fractures at the Stripa Project (adapted from Witherspoon et al., 1981).

Simultaneously, equivalent single-fracture apertures within 2 meters of the walls lost about 10 µm of aperture where total aperture was 60 to 100 µm, and lost about 5 µm from the portion with a total aperture of 20 µm. Because hydraulic conductivity is typically considered a function of the third power of aperture, this loss represented a significant change in conductivity. However, most of the lost aperture was recovered within a few days. Additionally, a monitoring point at 12.8 meters inside the wall showed no loss of aperture. Head losses no greater than 5 m were measured (Figure 3.2.2-9), although piezometric heads were predicted to decrease 20-50 meters during pilot excavation

The later slashing (widening) of the tunnel caused inflow to increase to 450 mL/min compared with a predicted inflow of 3565 mL/min. Like the pilot tunnel, the portion of the zone with 20 µm aperture lost roughly 5 µm, but aperture recovered within a few days. However, the 60 and 100 µm portions lost 20-30 µm and did not recover. Although measured head losses were about one-third of the predicted 7-30 m (Figure 3.2.2-9), except at two stations, the absolute values of head loss were greater than those of the pilot excavation.

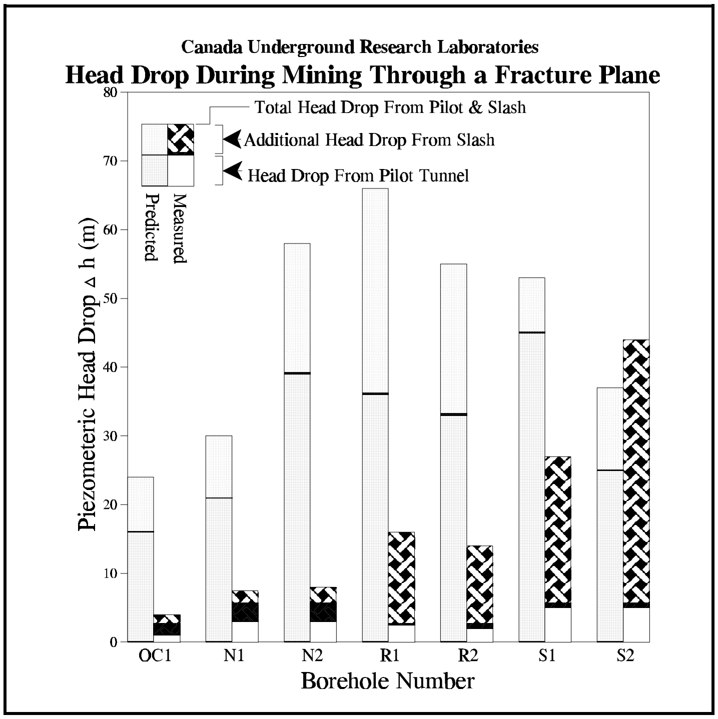

FIGURE 3.2.2-9. Predicted and Measured Head Losses during Mining through a Fracture Plane at URL (adapted from Everritt et al., 1989).

Visual inspection and monitoring after excavation indicated the walls and roof showed no visible fracturing beyond 0.2 meters. However, blasting of the floor involved less controlled methods and thus blasting-induced fracturing extended at least to one meter below the floor with the shallowest 0.3 meters having a high conductivity. Overall, Lang (1989) concluded that "the models used for predicting the hydrogeologic response did poorly" and improvements were underway.

The depth of excavation-response fracturing around a carefully blasted, circular shaft extension at URL was limited to approximately 0.3 meters (Everritt et al., 1989). This fracture depth was less than the measured 1.5 meters in the rectangular access shaft and an average of 0.5 meters (maximum of 10 meters) in access tunnels, indicating careful blasting minimizes fracturing. In addition to the average depth of fracturing, Jakubick et al. (1989) showed that the maximum depth of mining-induced fracturing was 10 meters, but such fracturing was not apparent at shallow depths (15 meters) where lithostatic pressure was minimal.

For the excavation-response fractures in the circular shaft at URL, Everritt et al. (1989) described two categories. "Microfractures" had exposed trace lengths on the wall of less than 0.05 meters, were parallel to the maximum principal compressive strength in a horizontal plane, and were believed to be extensional in origin. "Mesoscopic" fractures had exposed trace lengths of 0.29-1.5 meters, were perpendicular to the microfractures, and were of uncertain origin. The mesoscopic fractures consistently had apertures less than 0.5 mm, were described as "undulating and rough", and had roughness ratings of 4 to 5.

Jakubick et al. (1989) reported that the permeability of a discrete fracture can sometimes be determined with a vacuum-based technique. Because the technique affects a fracture plane up to a distance of a few meters, the full bulk conductivity of most excavation-response fractures can be determined. Application of the technique at the first of three sites examined excavation-response fracturing in a 60-meter-deep tunnel in horizontally bedded limestones with shaly interbeds was 0.9 m in the sidewall and 0.4 m in the roof. At the second site (URL access shaft), no excavation-response fracturing was found at a depth of only 15 meters, apparently due to the relative lack of lithostatic stress at this shallow depth. However, pre-existing discrete fractures were identified and tested (Figure 3.2.2-10). At a depth of 100 meters at the third site, a tunnel in Precambrian medium-to-coarse-grained granitic gneiss revealed lenses of pegmatite, biotite schist, and quartz. Excavation-response fracturing extended to depths of 0.5 to 1.15 meters, with other permeable zones farther behind the walls (Figure 3.2.2-11). Based on this work, Jakubick et al. concluded that the excavation-response zones should not be thought of as homogeneous anisotropic porous media displaying monotonically decreasing permeability with increasing distance from the wall.

Case Study 3.2.2-3: Types of Land-Surface Subsidence above Underground Mines

highlights: types of subsidence into underground mines; effects of mine layout on subsidence

Based on 848 case studies in the USA, Craft and Crandell (1988) described three basic types of land-surface subsidence. The first type, “pit subsidence”, closely reflects the size of the underground excavation and is reported at shallow mines. For room-and-pillar mines, surface subsidence will appear as rows of depressions above the rooms. This behavior is probably related to the intersection of the land surface with the pressure arch so that sagging within the pressure arch is expressed at the land surface.

“Sag subsidence” is usually tens to hundreds of meters in diameter and is associated with the crushing of underground pillars, which accounts for the large sphere of influence. This type of subsidence is apparently the classical longwall-type of subsidence.

“Cantilever beam subsidence” usually occurs above relatively deep mines with a well indurated (brittle) rock strata. In this situation, the crushing of certain pillars causes the indurated stratum to separate at the pivot points above stable walls and pillars as the rock collapses as a rigid beam into the open areas of the mine. This causes linear ridges of sharp subsidence above the pivot points.

For the reliable explanation and control of subsidence events, Craft and Crandall (1988) emphasized the importance of access to the mine plan which defines the locations of walls, pillars, and rooms. From an economic viewpoint, they found that access to a mine plan in one case probably saved at least US$43,000 by eliminating wasted drilling into pillars rather than rooms for grouting of the mine. They also presented several case studies showing the relationship of subsidence to the mine plan.

Case Study 3.2.2-4: Small-scale Flow on Fracture Planes

highlights: discrepancy between observed and effective apertures of fractures; lack of matrix diffusion in small-scale experiments

A block of slate measuring 1.25 x 1.05 x 0.45 m was obtained from a quarry in Cornwall, U.K. (Cliffe et al., 1993). The block contained two principal fractures which were locally iron stained, but not cemented. Before testing, the block was restressed to simulate a 10-m burial depth.

Hydraulic apertures were determined at seven locations through radial flow from small “boreholes”. At two locations, no flow occurred. At the remaining five locations, apertures of 5 to 50 :m were calculated with a mean of 24 :m. Larger-scale “effective” apertures, which were determined by bulk flow through portions of the fracture measuring 1.05 x 0.2 m, ranged from 8 to 65 :m with an average of 45 :m. The larger values of effective aperture suggested that the locally measured hydraulic apertures did not intercept the higher-aperture channels that regulate bulk water flow.

Water with tritium was used as a conservative tracer of chemical transport through the fracture system. Two flow rates, differing by a factor of 1.7, produced identical breakthrough curves at the end of the fracture with step-function changes in tritium.

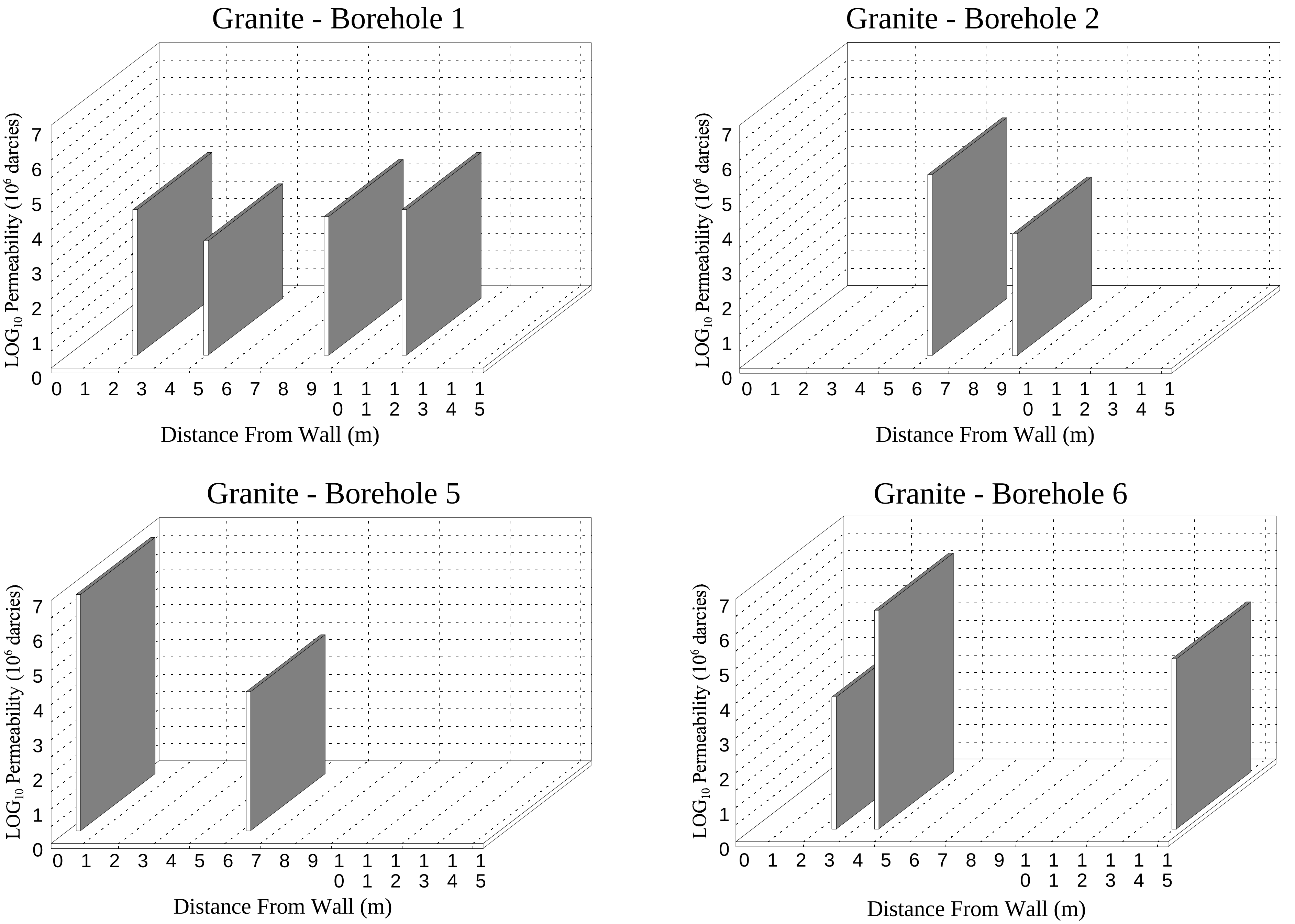

FIGURE 3.2.2-10. Discrete Fracture Permeabilities at URL; 15 m depth at shaft collar (adapted from Jakubick et al., 1989.)

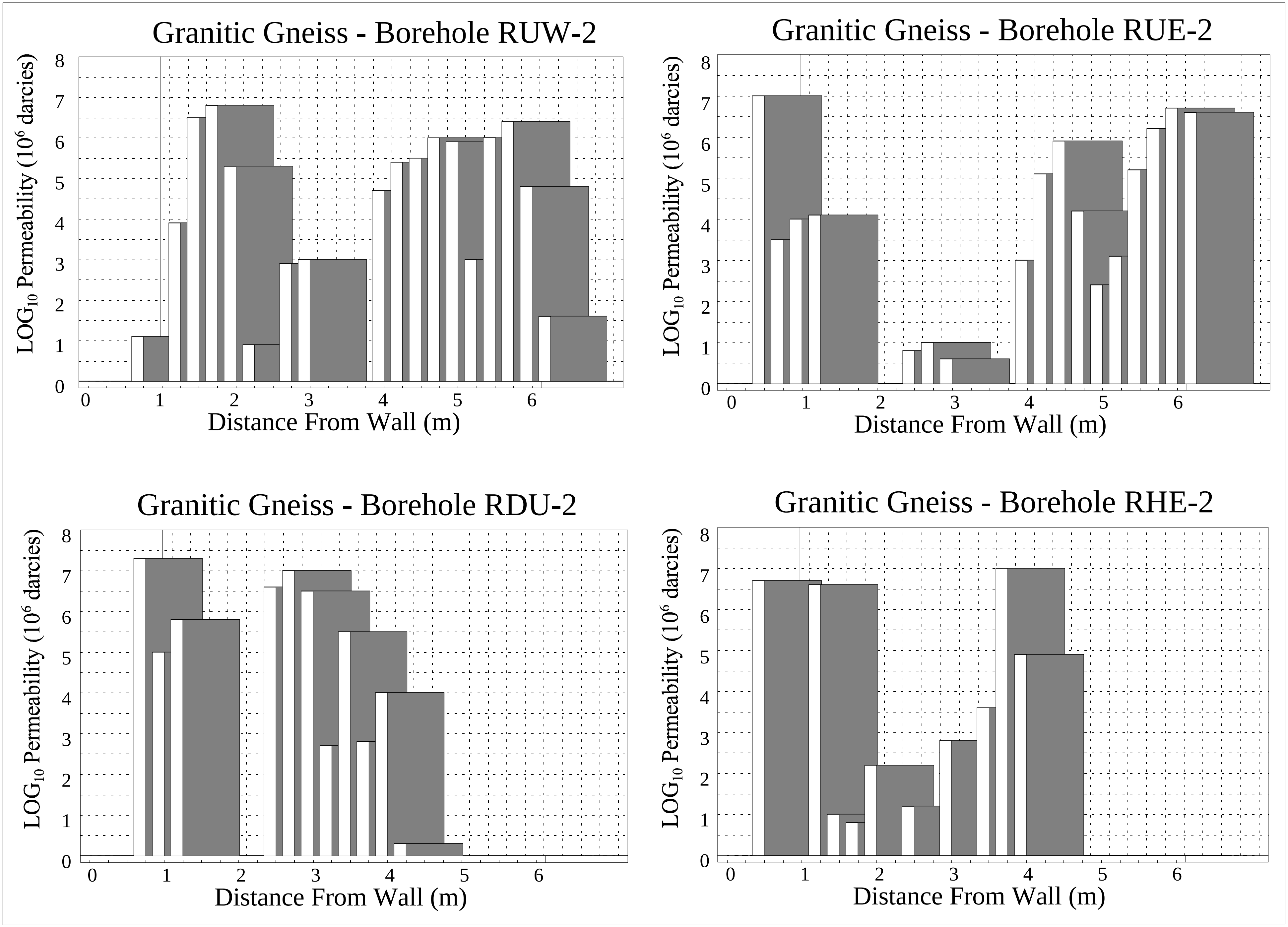

FIGURE 3.2.2-11. Fracture Permeabilities at Colorado School of Mines' Experimental Mine (adapted from Jakubick et al., 1989).

This suggested that diffusion into the rock matrix, which is often thought to be an important retardation mechanism, was not relevant in these small-scale experiments. Pulsed inputs of tritium led to similar conclusions.

Because of spatial variability in aperture as well as temporal variation implied by non-reproducible results, the flow of water through a fracture was difficult to model, but a two-channel representation of the system provided reasonable simulations (Cliffe et al., 1993). In any case, the movement of water in the fracture was complex, which is often overlooked in some models of fracture transport and rock-matrix diffusion.

Case Study 3.2.2-5: Groundwater Depressurization in an Underground Mine Through Faults

highlights: assessment of pre-mining, and prediction of intra-mining, groundwater behavior; characterization of fracture patterns; effect of underground mining on groundwater levels

During a feasibility study for an investment/mining decision of the Bouganville Copper Deposit in Papua New Guinea, a drilling program was carried out to define the geotechnical characteristics of the rock, such as acceptable pit-slope angles, and the rates of groundwater inflow from the rock to the drillholes (Pentz, 1979). Despite the usefulness of the drillholes, most of the valuable hydrogeologic data was obtained from two underground ore-sampling adits. The baseline water levels in the area before adit excavation were defined by the open drillholes and piezometers installed along and on either side of the proposed adit centerlines. During adit excavation, the change in water levels in drillholes and piezometers were monitored and the groundwater discharges from the portals and at various locations within the adits were periodically measured.

The dominant rock types in the deposit are igneous intrusives (diorite and granodiorite) and extrusive rock (andesite). These rock types are significantly fractured with 10-70 fractures in a meter-long interval. The intrusive rock generally has been less fractured, but the fractures apparently have larger apertures, resulting in equivalent porosities for all of the rock types. The bulk hydraulic conductivities of the rock range from 10^{-4} to 10^{-7} m/s, primarily attributed to the fracturing. There was no dominant orientation to the fracture planes, although many had near-vertical dip angles. The fractures were observed to be mostly open and fresh. A number of steeply dipping fault zones filled with clay act as hydrogeologic barriers at the site.

The Pan Adit was excavated near the center of the deposit. Pentz (1979) differentiates (1) the release of groundwater from storage with the associated decrease of hydraulic heads during initial drainage into the adit ("depressurization") from (2) the subsequent dewatering of pores and fractures with the associated decrease in water-table elevation ("drainage"). A depressurization phase was not seen during the excavation of the Pan Adit. Steady-state conditions at a location were attained 2-3 weeks after excavation in the area and, after excavation was completed, water levels had decreased in a concentric pattern around the underground workings (Figure 3.2.2-12).

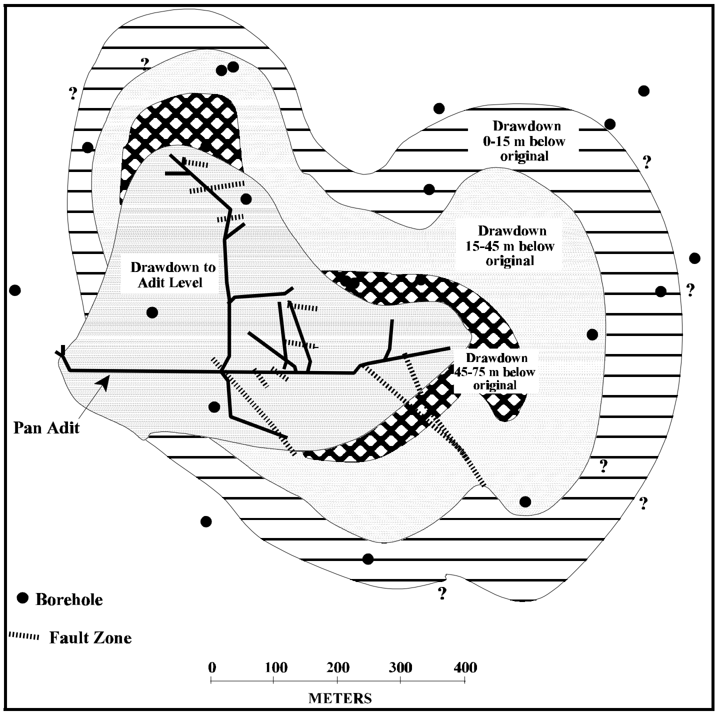

FIGURE 3.2.2-12. Piezometric Drawdowns after Excavation of the Pan Adit (adapted from Pentz, 1979).

The relatively impermeable fault zones had detectible effects on the rate of head change. A piezometer located about 140 meters from the adit portal, along the adit centerline, showed a steady decline in the local hydraulic head as the adit was advanced. When a fault zone about 45 meters from the piezometer was penetrated on Day 60 (Figure 3.2.2-13), the head decreased at a faster rate despite a slower rate of pit advance, confirming the relatively impermeable nature of the fault clay. A second fault located about 15 meters from the piezometer was penetrated on Day 100, but this had little effect on the head levels apparently because the piezometer was nearly dry and hydraulic gradients were relatively small. The maximum groundwater flow measured at the adit portal was 100 L/s, or 0.08 L/s from each meter of adit.

During excavation of the Western Adit on the west side of the ore deposit, hydraulic head decreased in a similar manner as in the Pan Adit. Upon cutting of a relatively impermeable fault zone, groundwater inflow at the head of the adit reached 50 L/s, causing discharge at the adit outflow to rise from 4 to 55 L/s. A piezometer installed near the fault zone showed declines in local hydraulic head after fault penetration (Figure 3.2.2-14).

Case Study 3.2.2-6: Techniques to Manage Flow of Groundwater in Underground Workings

highlights: tabulated methods and examples for controlling water flow into and through underground workings

Loofbourow (1979) suggested various standard and innovative controls for water in underground mines (Table 3.2.2-1). For example, underground mining beginning at the deepest level and progressing upwards takes advantage of generally less fractured, less permeable rock at depth. This provides several environmental and economic advantages such as (1) significant lowering of the shallow water table would only occur in the later stages of mining so that impacts on baseline hydrogeology are reduced, (2) as the upper levels are reached and inflow reaches its maximum rate, the exhausted lower levels can act as settling basins to clarify and, if necessary, chemically treat the water,

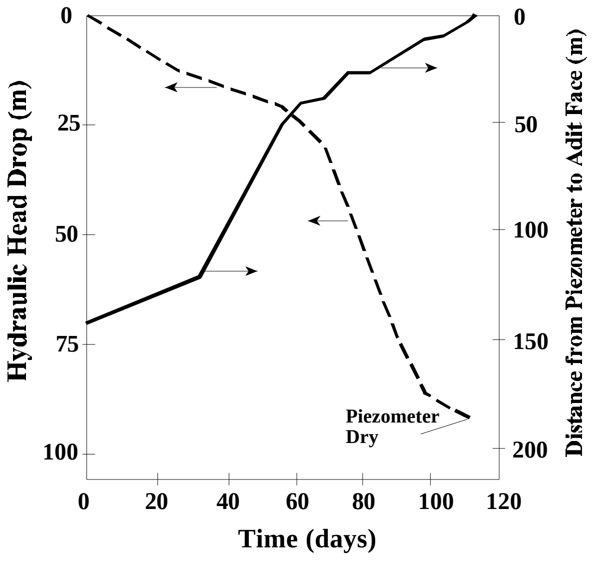

FIGURE 3.2.2-13. Drawdown As Adit Excavation Approaches Piezometer (adapted from Pentz, 1979).

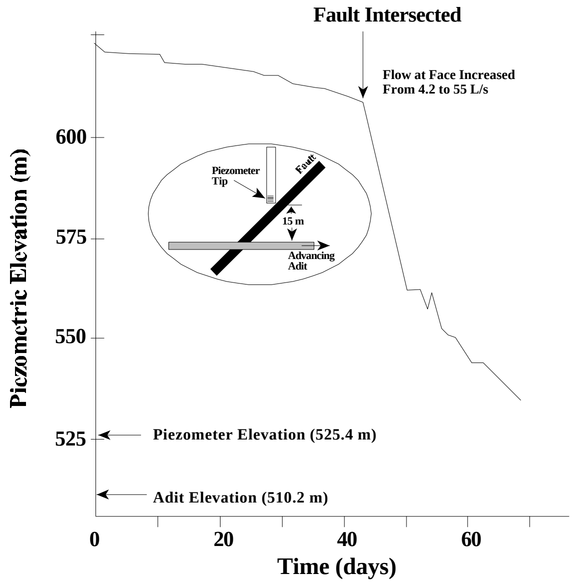

FIGURE 3.2.2-14. Piezometric Drawdowns after Excavation of the Western Adit (adapted from Pentz, 1979).

TABLE 3.2.2-1
Methods for Underground Water Control
(from Loofbourow, 1979)

Methods	Example
1. Reduce, postpone, or avoid inflow	
1a) Locate shafts or workings in impermeable rock	Naica; Kimballton; San Antonio
1b) Mine from bottom up	West Driefontein
1c) Work underwater by dredging, mining with draglines, leaching in place, slurry trenches	Alluvial gold; tin; sand; gravel; phosphate; Shirley Basin uranium; foundations in ground difficult to dewater and to support
2. Protect workings from inflow	
2a) Leave sufficient solid ground or rock between the workings and water	Wabana, Newfoundland; submarine coal in Durham, England, and Nova Scotia; metal mines in Ontario and Quebec
2b) Leave pillars on fissures to prevent or minimize water movement	South Africa gold mines
2c) Plug or case drill holes, or survey and do not mine near them	Plugging is required in many localities; most salt mines are especially careful
3. Divert, drain, or intercept water near surface	
3a) Divert rivers, drain lakes	Griffiths; Black Lake; Caland; Bancroft; Steep Rock Lake; Biwabik
3b) Cover intakes with concrete or ponded slime, with great care	Leadwood; Bancroft
3c) Clear slopes, build drains, plant trees in low, flat areas to increase evapotranspiration	Bancroft
3d) Catch water in shafts or on an upper level to prevent it moving deeper	Most wet shafts; Champion Mine, Michigan
3e) Intercept water in shallow wells	Homer Wauseca
4. Keep water from shafts with impervious linings	
4a) Pre-grout from the surface, then test and grout from the shaft bottom	Many recent South African shafts, e.g., Kinross
4b) Sink with grouting from the shaft bottom only	Venterspost; Friedensville; Deep Ruth, Meremec
4c) Freeze, sink, and set lining	European coal mines; Saskatchewan potash; some Carlsbad potash shafts
4d) Bore, usually with mud, and place casing	Beatrix Shafts, the Netherlands; Grants; Carlsbad
4e) Drop shafts, stationary slip forming	Chicago Metropolitan Sanitary Commission
5. Reduce permeability of the rock mass	
5a) Grout with cement slurry	Port Radium; Deep Creek
5b) Plug solution channels with de-sanded tailings and grouting	Leadwood
5c) Plug pores or fractures with clay	Aswan Dam and others, especially in Europe

Methods	Example
5d) Plug with chemical or bacteriological precipitate	No trial known in mining
6. Drain water through an adit (e.g., wet mines in hilly terrain)	
7. Use special practices to aid control, to reduce or prepare for surprises	
7a) Compartmentalize the mine to confine inrushes and minimize damage	Leadwood; Nova Scotia coal mines
7b) Mine from bottom up to provide space for water and time to build protection	West Driefontein
7c) Regularly get informed by outside opinion	-
7d) Regularly drill test holes in advance of work	-
7e) Regularly plot, record pertinent data on water occurrence and protection, plan and test procedures	-
7f) Maintain material, tools, and trained crew, ready to carry out protective procedures	-
8. Procedures which have been used in emergencies	
8a) Working from the surface, plug a large conduit of water	Levant, Cornwall; Moodie, Kentucky
8b) Working from the surface through pipe or drill holes, plug a large conduit in the mine	Belgian Congo; Friedensville; Indiana gypsum mine
9. Dispose of water more conveniently as by dropping it into a conduit, dropping or pumping it into an aquifer against lower pressure	

and (3) total pumpage costs are reduced because high pumping rates would be required only during the late stages of mining rather than throughout the mine life. The implementation of such innovative controls depends on the best combination of economic factors for each individual mine that minimize the overall cost of mining and environmental maintenance while maximizing profit and environmental protection. To highlight the potential financial benefit of inflow control, Loofbourow mentions an example of two mines near Grants, New Mexico, with differing degrees of groundwater inflow. Each tonne of ore removed from the wetter mine costs twice as much because of less efficient methods, more expensive equipment costs, and a greater volume of water to be raised to the surface.

Case Study 3.2.2-7: Finite-Element Modelling of Groundwater Flow

highlights: simulation of groundwater around an underground mine using porous-media concepts; enhanced fracturing and hydraulic conductivity close to the mine; simulated recovery of groundwater levels after mining

Toran and Bradbury (1988) simulated regional hydrogeologic impacts of an underground lead-zinc mine in Wisconsin, USA. A block-centered finite-difference grid in a horizontal plane was created using 957 nodes covering an area of about 25 x 10 km. The model was calibrated to the site by generally matching the pre-mining water-table elevations inferred from topography, the intra-mining elevations based on historical data, and post-mining elevations collected three years after mine closure. Within 100-200 m of the underground workings, the rock was assigned a hydraulic conductivity of about 1.5 x 10^{-3} m/s, which is a factor of 200 greater than the regional bulk conductivity, based on hydrogeologic testwork. This more conductive "skin" is the result of stress and subsidence around the underground workings. Although groundwater flow at the site is fracture-dominated, the simulation as a porous medium was justified on the basis that each finite-difference cell contained thousands of fractures, thereby approaching a consistent porous medium.

Vertical gradients were known to exist near the mine, but cannot be simulated by the horizontal grid. However, a quasi-three-dimensional model indicated the local vertical flow had negligible effect on the regional two-dimensional simulations.

The comparison of pre-mining and intra-mining scenarios showed the mine created a water-table depression of up to 60 m with a lateral extent of about 3 km. The average predicted rate of groundwater inflow to the mine during mining was 1.2 m^3/s compared with measured inflow of up to 4.3 m^3/s, which is an acceptable error considering the regional nature of the modelling. Within three years after mine closure, the simulated water table had recovered by more than 50%. The best-fit storage coefficient, which is critical for simulating water-table recovery, was found to be 0.02 during three years of recovery, typical of an unconfined system. Recovery was predicted to be essentially complete ten years after closure and the mine and its high-conductivity skin are not predicted to affect long-term regional flows.

Case Study 3.2.2-8: Hydraulic Connections Between Land Surface and an Underground Mine

highlights: enhanced flow from underground workings due to hydraulic connections with the land surface; contributions of various surface sources to flow at portal

Williams et al. (1979) examined the inactive Blackbird Mine in Idaho, mined primarily for copper and cobalt. The rock at the minesite is Precambrian metamorphic rock, predominately quartzite, with groundwater flow primarily controlled by fractures. At the minesite, there were a mill, several waste-rock piles, a tailings pile, an open pit, and several portals into the underground workings. The use of underground mining minimized the volume of waste rock by allowing the excavation of drifts to remove the lenticular and tabular ore bodies. The coarse fraction of the tailings from the mill processing was returned to the mine as backfill for structural support.

The underground workings consist of 12 levels with eight portals. The main level is at 6850' elevation and 2,200,000 tons of ore have been mined at and above this level.

The relatively high discharge of contaminated water from the mine led to a study of recharge patterns. Williams et al. (1979) found four leaky raises that connected the 6850' level to the surface and carried surface runoff and precipitation into the mine.

A second source of mine recharge was found to be surficial test pits and trenches excavated during exploration and geologic mapping to define surface trends in the ore zones and faults. Infiltration from approximately 60 test pits and trenches was estimated at 10% of mine discharge from the 6850' portal.

Another source of mine recharge was identified as enhanced surficial fracturing caused by stress and subsidence above the underground workings. This recharge was also estimated at 10% of the 6850' discharge. The loss of water from Meadow Creek into the mine accounted for 5% of discharge from the 6850' portal.

The estimated total of 23,000 m of diamond-drill holes originating at the surface was assumed to enhance mine recharge, but no estimate of the recharge was reported. Also, the open pit provided direct recharge into the 7400' and 7265' levels.

Water reaching the 7200' level normally exited the mine at the 7200' portal, but a small wall collapse blocked the outflow for several years. Instead, the water backed up and flowed down the 572R raise to the 7100' level. This flow reached a peak of approximately 1 L/s.

3.2.3 Drainage Flow in Placer and Solution Mines

For submerged placers, the effect of mining on water flow includes the disturbance and mixing of subsurface sediment and porewater with surface water. For non-submerged placers, excavations extending below the local water table can produce groundwater drawdowns and inflows, similar to open pits (Section 3.2.1). Additionally, local surface watercourses may be affected and diverted. From a chemical perspective, aqueous concentrations can be affected (Case Study 4.3-14).

3.3 Drainage Flow from Stockpiles, Dumps, and Mined-Rock Piles

To assess or predict drainage chemistry from mined-rock piles, a basic understanding is needed of (1) the manner in which water moves through the rock and (2) the interactions between this moving water and the reactive minerals. This section focusses on water movement, whereas the chemical aspects are discussed in Chapter 4.

Morin et al. (1991) defined three types of mined-rock piles based on general patterns of water movement. Type 1 piles, built on relatively flat ground, receive water only through precipitation onto the top and sides of the pile (Figure 3.3-1). This water then percolates and drains downward by gravity to the base of the rock where it leaves as groundwater flow and/or seepage into surface "toe" ditches around the base of the rock (collectively referred to as *drainage* here). Type 2 piles are located at the bottom of valleys. In these locations, groundwater can move upward into the rock and mix with downward percolating infiltration, then leave as seepage parallel to the valley axis (Figure 3.3-2). Type 3 piles are located on sloping land where downward percolating water mixes with surface and ground waters flowing down the slope and into/beneath the pile (Figure 3.3-3). This mixed water then leaves as groundwater seepage and/or surface drainage.

In a general sense, the water-balance equation for all three types of piles is:

$$D = P - R - E - dS \qquad (3.3\text{-}1)$$

where D = discharge of seepage (m^3/s)
P = precipitation onto the pile (m^3/s)
R = runoff over the surface of the pile (m^3/s)
E = evapotranspiration from the pile (m^3/s)
dS = change in the amount of water stored within the pile (m^3/s)

However, the movement of water through a pile is more complex than suggested by Equation 3.3-1.

The size of rock within mined-rock piles can be classified according to two endpoints. Some piles consist of fine-grained rock of silt and sand size, caused by crushing or natural weathering of the material. Drainage through them is relatively slow and regular, and a water table may be located within the rock. In this case, drainage flow can be predicted or assessed through standard porous-media (Darcian) approaches as used for tailings (Section 3.4).

On the other hand, some dumps consist of coarse-grained rock. Drainage passes through these piles in a more irregular, unpredictable, and turbulent pattern, pouring downwards and laterally from rock to rock. These piles rarely have elevated water tables within them. Also, the runoff (R) in Equation 3.3-1 is often negligible due to the coarseness of the rock.

The presence of turbulent flow can be assessed by the dimensionless Reynold's Number (Freeze and Cherry, 1979). For a coarse mined-rock pile with a hydraulic conductivity of 10^{-3} m/s and a gradient of 1.0, grain diameters greater than 1-15 cm (gravel) will generate turbulent flow (Morin et al., 1991).

In reality, many mined-rock piles probably have aspects of both two endpoints depending on method of dumping and height of pile (e.g., Nichols, 1986). In relatively coarse piles typical of hard-rock mining in metamorphic and igneous terrains, drainage is apparently directed into a few preferred, vertical to nearly horizontal, channels within a few meters below the top of the pile (ElBoushi, 1975; Morin and Hutt, 1994a; Smith et al., 1995).

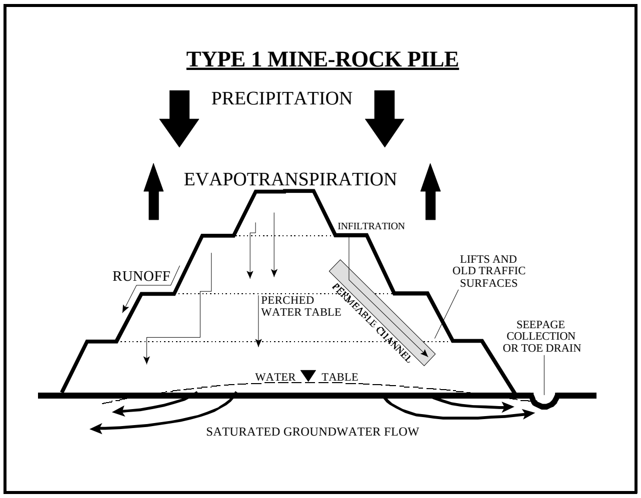

FIGURE 3.3-1a. Schematic Mined-Rock Pile - Type 1.

FIGURE 3.3-1b. Photograph of a Type 1 Mined-Rock Pile (by K.A. Morin).

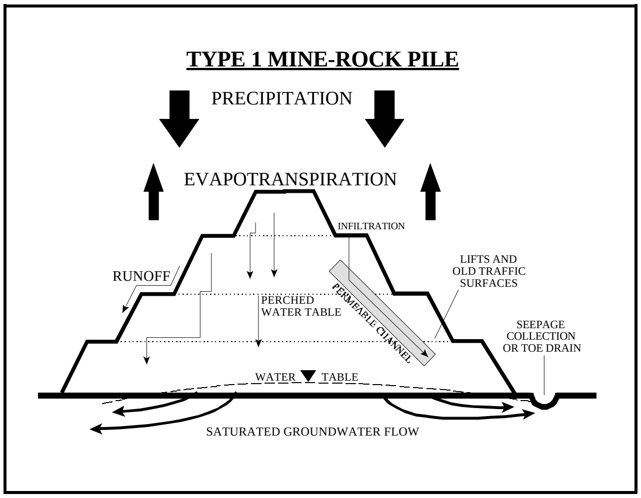

FIGURE 3.3.-2a. Schematic Mined-Rock Pile - Type 2.

FIGURE 3.3-2b. Photograph of a Type 2 Mined-Rock Pile (by K.A. Morin).

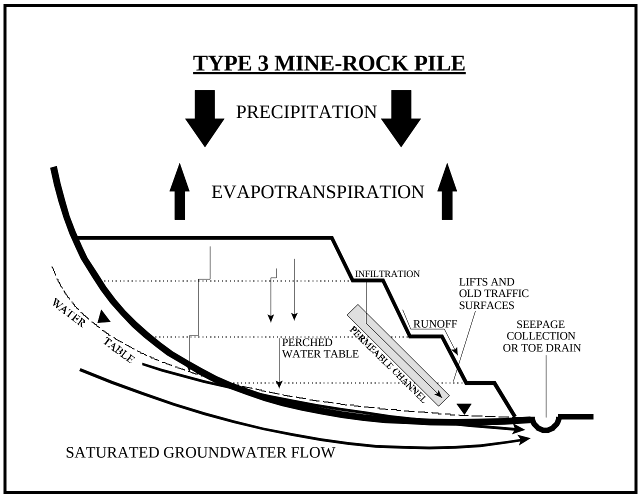

FIGURE 3.3-3a. Schematic Mined-Rock Pile - Type 3.

FIGURE 3.3-3b. Photograph of a Type 3 Mined-Rock Pile (by K.A. Morin).

These channels can then direct water to the base of the pile within several hours (Morin et al., 1994c). However, because piles are often built in layers, or "lifts", the top of a lift can contain finer rock due to vehicle traffic and enhanced weathering. These finer layers can truncate channels, create perched water tables, and slow the drainage. From this irregular heterogeneous arrangement, a simplified routing model can be formulated (Figure 3.3-4), in which the various channels or "branches" of drainage can combine, separate, and mix.

Most reported studies of mined-rock piles have taken place at Levels C, D, and E (Figure 3-4). Studies inside piles in Levels A and B are rarer, more difficult, and more expensive (Schafer et al., 1994; Morin et al., 1994c). Interestingly, such detailed studies may have to consider migration of water in the vapor phase if coarse rock and thermal gradients lead to significant internal evaporation or condensation.

Case Study 3.3-1: Small-Scale Study of Drainage Movement Through Mined-Rock Piles

highlights: amount of infiltration to initiate basal flow from a mined-rock pile; use of diluted paint to delineate channelling

ElBoushi (1975) used small rock piles and rock-filled columns to examine small-scale movement of water. Water was sprayed onto dry basaltic rock until flow was obtained from the base. For grain sizes of 3-10 mm, the spraying of water equivalent to 2-3% of the pile volume initiated flow, whereas grain sizes greater than 10 mm only required 1%-by-volume addition to create flow. On the other hand, ElBoushi noted that specific retention of the rock, that is, the amount of water retained by the rock after draining, was generally two to three times greater. As a result, not all of the rock was apparently moistened before basal flow appeared, suggesting channelling of the water.

To examine channelling further, diluted white paint was sprayed onto piles after bottom flow was observed. Disassembly of the piles and visual examinations of rock surfaces revealed that less than 20% of surfaces were coated with paint below depths of 1 m (Figure 3.3-5). This suggests that less than 20% of rock surfaces in a large pile will be contacted by infiltrating water, in general agreement with reported retention factors of chemical loads (Sections 4.2 and 5.2.4).

Case Study 3.3-2: Tracking Drainage Movement through a Mined-Rock Pile with Thermistors and Basal Monitoring Wells

highlights: detailed investigation of temperature and water levels within a Type 3 waste-rock dump; tracking internal water movement using temperature

Westmin Resources' Myra Falls Operations (base- and precious-metal mine, Figure 3.3-6) is located on Vancouver Island off the west coast of Canada. In this coastal climate, the warm, relatively dry summers are followed by cool, wet winters. Precipitation is predominantly rain, approximately 1.5-2.0 m annually, with minor snow accumulation during winter. This mine has been operating for more than 25 years.

Dump #1 (a Type 3 dump, Figure 3.3-3) contains approximately 10^7 metric tonnes of pyritic waste rock (Morin et al, 1994c). This dump was built against a valley wall, and is approximately 800 m in length parallel to the wall, approximately 300 m wide at the base, and reaches a maximum measured height of 42 m. Thermistor strings were installed in four boreholes in this dump for a total of 20 thermistors, and temperatures were transmitted to dataloggers every 12 hours. The temperature data at Thermistor T4 produced a maximum value of 51.6°C at an intermediate depth of 10 meters. This is consistent with an acidic zone identified in this area by acid-base accounting (Section 5.2.1-5) to a depth of 26 m. During infiltration events, the upper and intermediate temperatures were cooled by the infiltration, but the deeper temperatures were raised by the infiltration as it passed through the upper, warmer levels.

Four two-inch-diameter wells contained pressure transducers that transmitted basal groundwater levels to dataloggers every 12 hours. Fluctuations

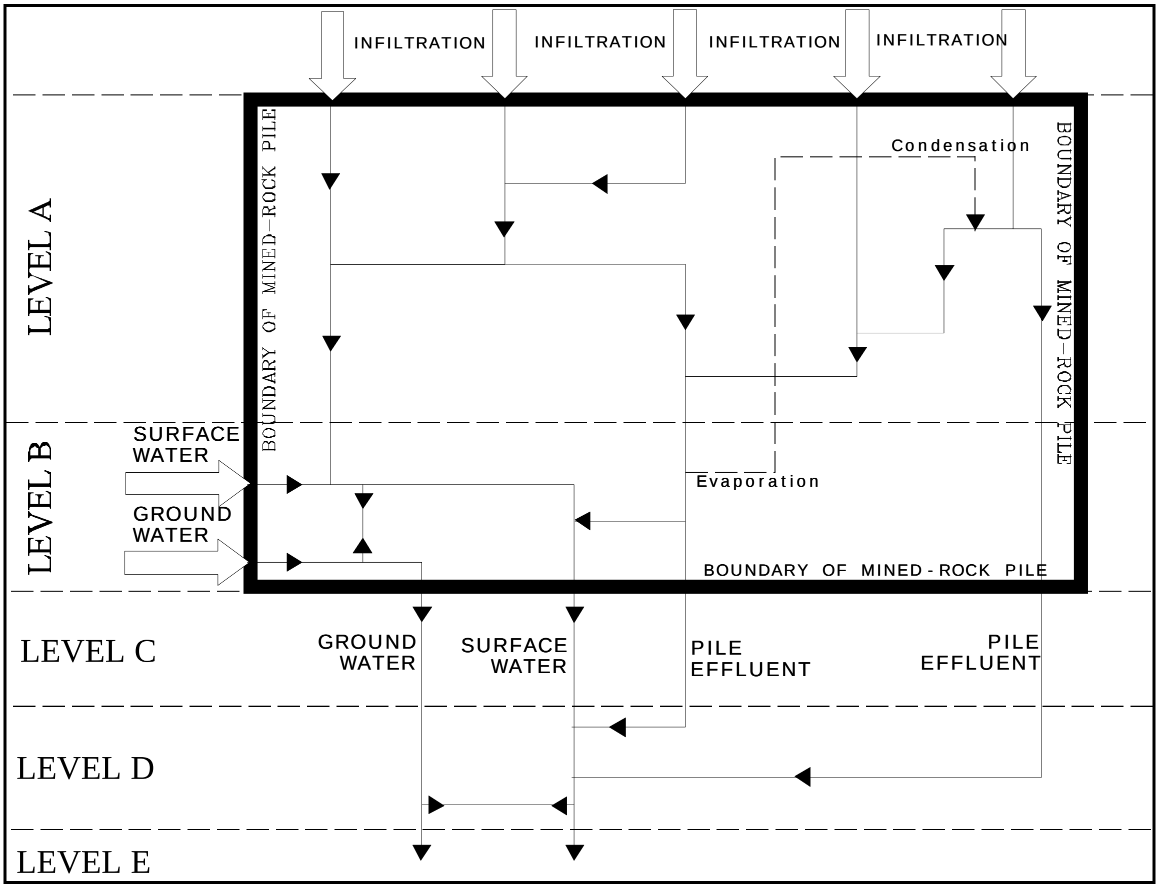

FIGURE 3.3-4. Conceptual Model of Channelized Drainage Flow through a Mined-Rock Pile

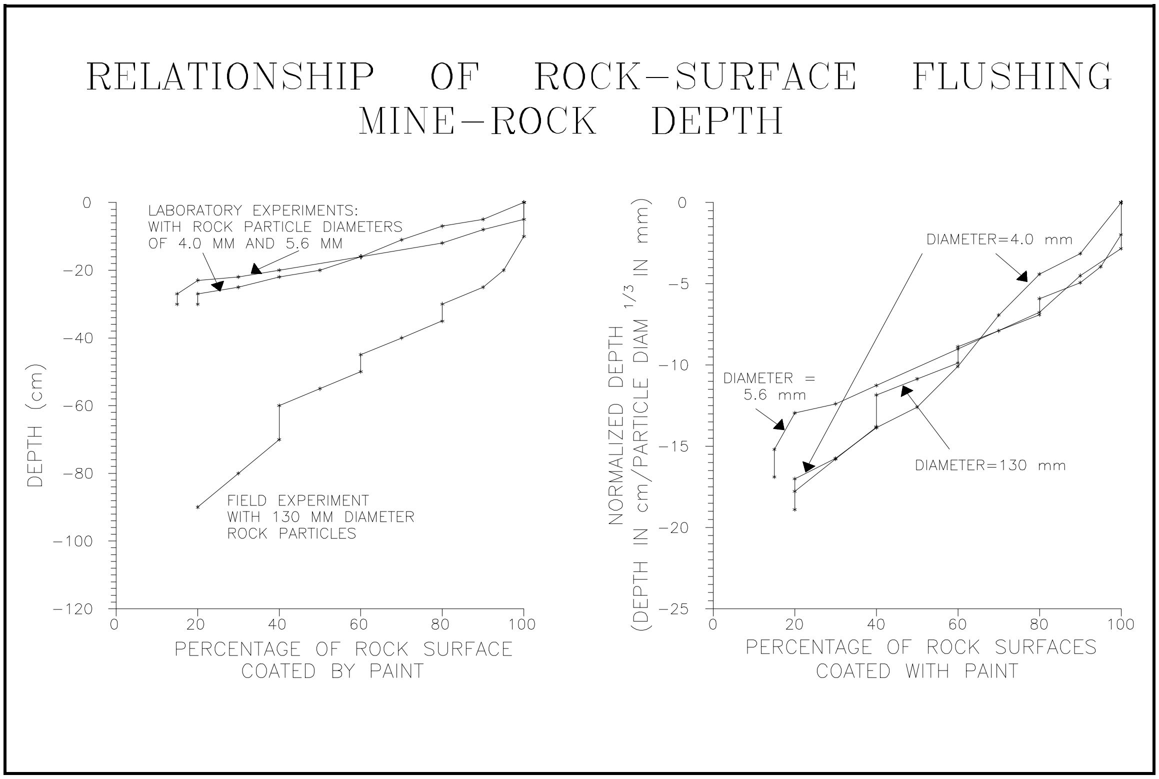

FIGURE 3.3-5. Channelling in Small-Scale Rock Piles (adapted from ElBoushi, 1975, and Morin et al., 1991).

up to 4 m were recorded during intense storm events consisting of roughly 10 cm of rain in 12 hours.

Infiltration events from major storms in 1991 were tracked downward through the dump through their effects on internal temperature (Figure 3.3-7). Since precipitation was relatively cool, the chilling effect of an infiltration event could be seen to depths of 10 m. After passing through this hottest zone, an infiltration event then produced a heating effect at greater depths.

This behavior can be seen more clearly by focussing on one storm event. During the 12-hour period centered around 00:00 on 31 January 1991, precipitation began falling and increased to approximately 7 cm over 12 hr by 00:00 on 1 February 1991 (Figure 3.3-8). Within 12 hours, this storm event caused rapid changes in temperature at T4, with temperature to depths of 10 m decreasing and temperature below 10 m increasing. There was no temperature response at 30 m depth.

Although temperatures responded within 12 hours, the water table, at a depth of approximately 45 m, did not begin responding until 24 hours later. The midpoint of the water-table response occurred at 36 hours (shaded area in Figure 3.3-8), representing a rise of approximately 0.5 m. The difference between this hydrogeologic response of 36 hours and temperature response in less than 12 hours to depths of 20 m indicated either (1) there is a perched zone between 20 and 45 m which slowed infiltration or (2) the temperature responded to an initial, minimal amount of initial infiltration whereas the water table reflected the response to volume.

Case Study 3.3-3: Tracking Water Movement Below a Type 3 Dump

highlights: example of subsurface water movement below and through a Type 3 waste-rock dump; use of bacteriophage to trace water movement

This coal waste-rock dump ("spoils pile") is a Type 3 pile (Figure 3.3-3) and forms a conical shape due to geotechnical failures lowering the angle of its slopes (Figure 3.3-9). Martin and Thomas (1974) found that groundwater movement is downgradient in natural strata, upwards into the base of the dump, then parallel to the spoils-strata contact. This groundwater then discharges as springs at the lower toe or continues through the subsurface past a boggy area.

To trace this groundwater movement, Martin and Thomas injected bacteriophage (parasites of bacteria) as a conservative tracer in upgradient Well CD16. Average linear groundwater velocities were calculated in the range of 36 to 180 m/day, generally typical of sand to gravel. Lateral spreading of the groundwater was more than 100 m over a travel distance of 680 m.

Case Study 3.3-4: A Type 2 Pile in a Dry Climate

highlights: complex movement of groundwater through coal spoils; interaction of surface and ground waters

The Diplomat coal mine is located approximately 200 km southeast of Edmonton, Canada (Trudell and Moran, 1982). After pit mining of the coal, spoil (waste rock) was returned to the pit, creating a Type 2 Pile (Figure 3.3-2). In 10 nests, a total of 33 piezometers was installed in the spoils and intact pit walls to delineate groundwater flow (Figure 3.3-10). This showed that ponds in surface depressions on the reclaimed spoils, as well as groundwater discharge from the pit walls, exerted major influences on groundwater flow directions. Toward the center of the spoils, groundwater flowed perpendicular to the plane of Figure 3.3-10. Much of the groundwater reportedly moved through the base of the spoils where rubble zones and intact, fractured coal provided conductive channels (see also Case Study 3.3-6).

Case Study 3.3-5: Importance of Delineating Subsurface Flowpaths Beneath Mined-Rock Piles

highlights: subsurface flow from one minesite component to another

The Mt. Washington Minesite on Vancouver

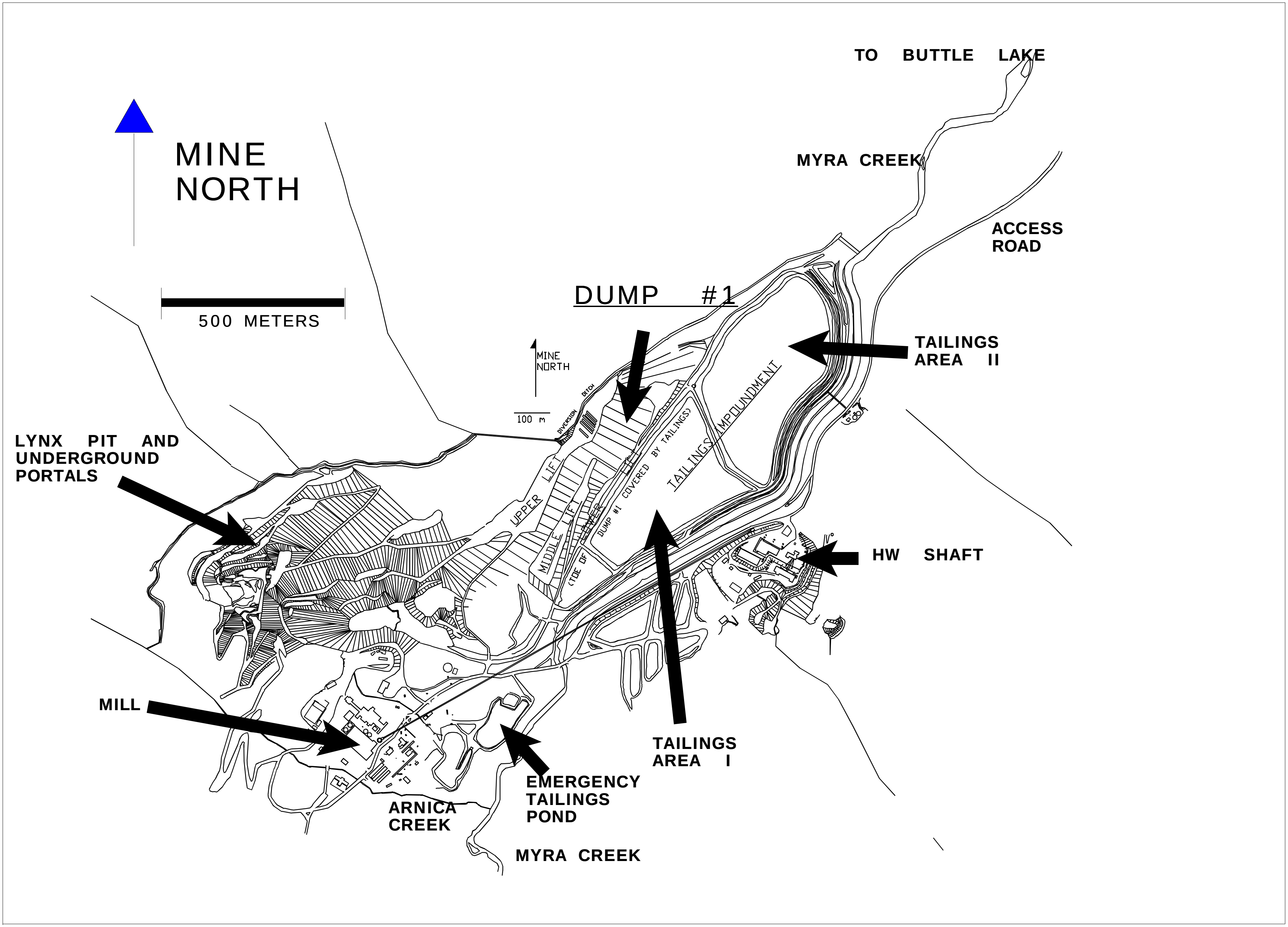

FIGURE 3.3-6. Layout of Myra Falls Operations and Dump #1 (adapted from Morin et al., 1994c).

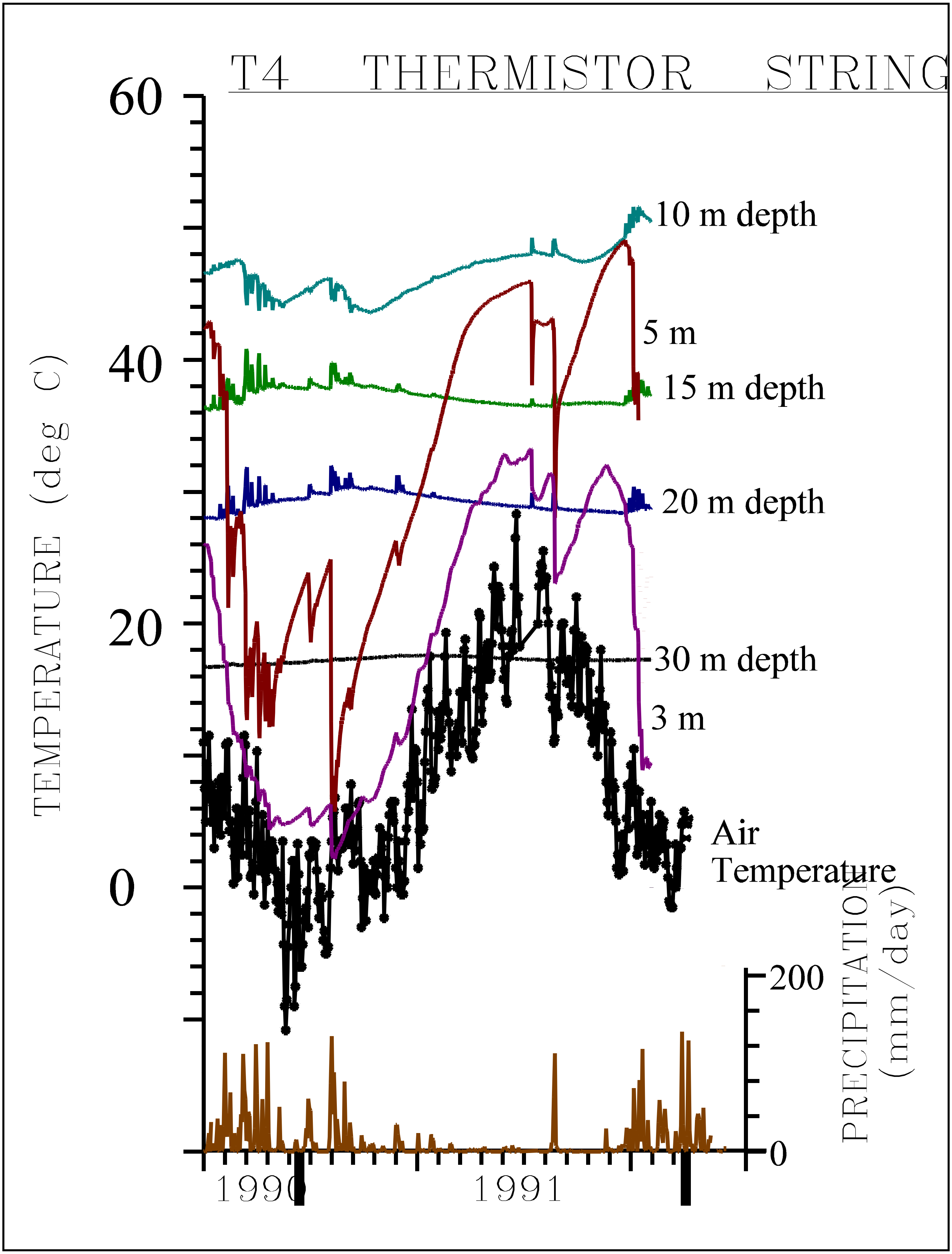

FIGURE 3.3-7. Internal Temperatures in Dump #1 Through 1991 (adapted from Morin et al., 1994c).

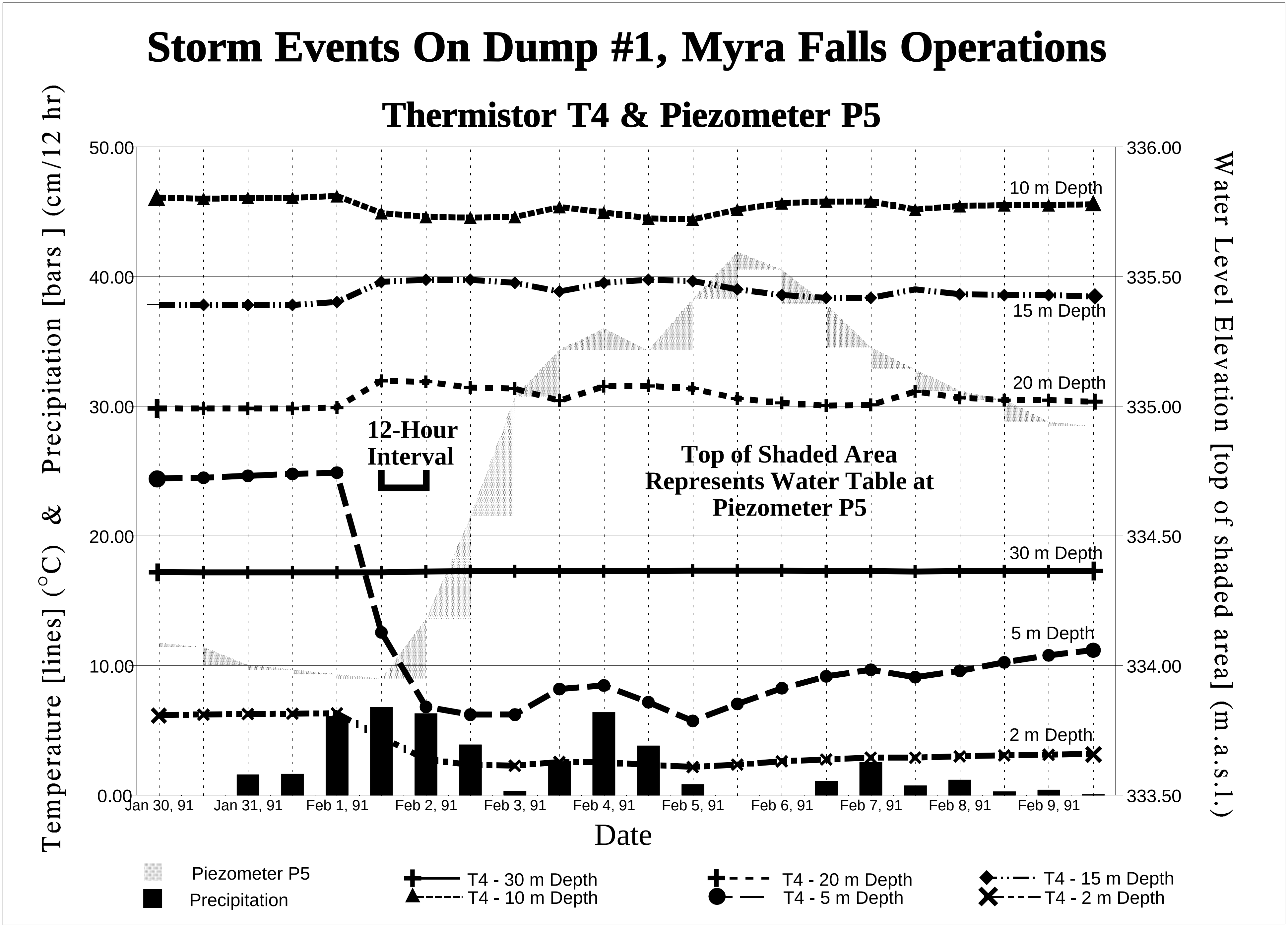

FIGURE 3.3-8. Response of Internal Temperatures and Basal Water Table in Dump 1 (adapted from Morin et al., 1994c).

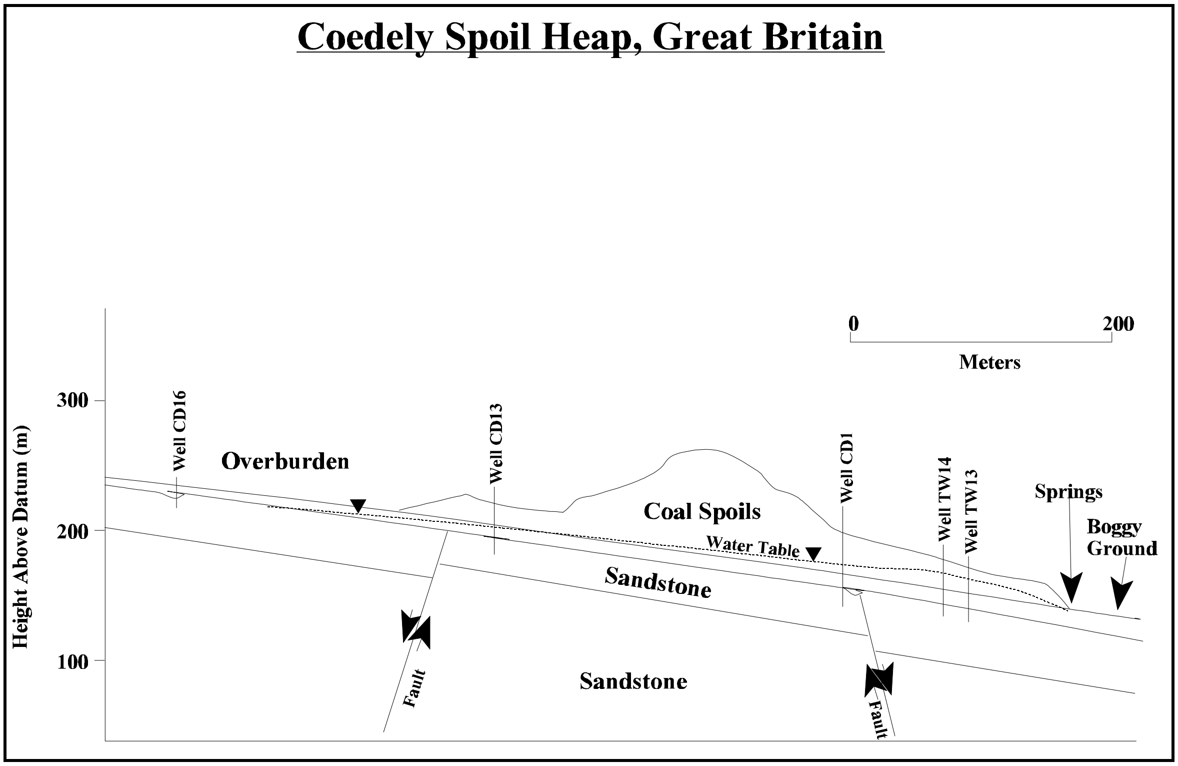

FIGURE 3.3-9. Cross-section through the Coedely Spoil Pile, Great Britain (adapted from Martin and Thomas, 1974).

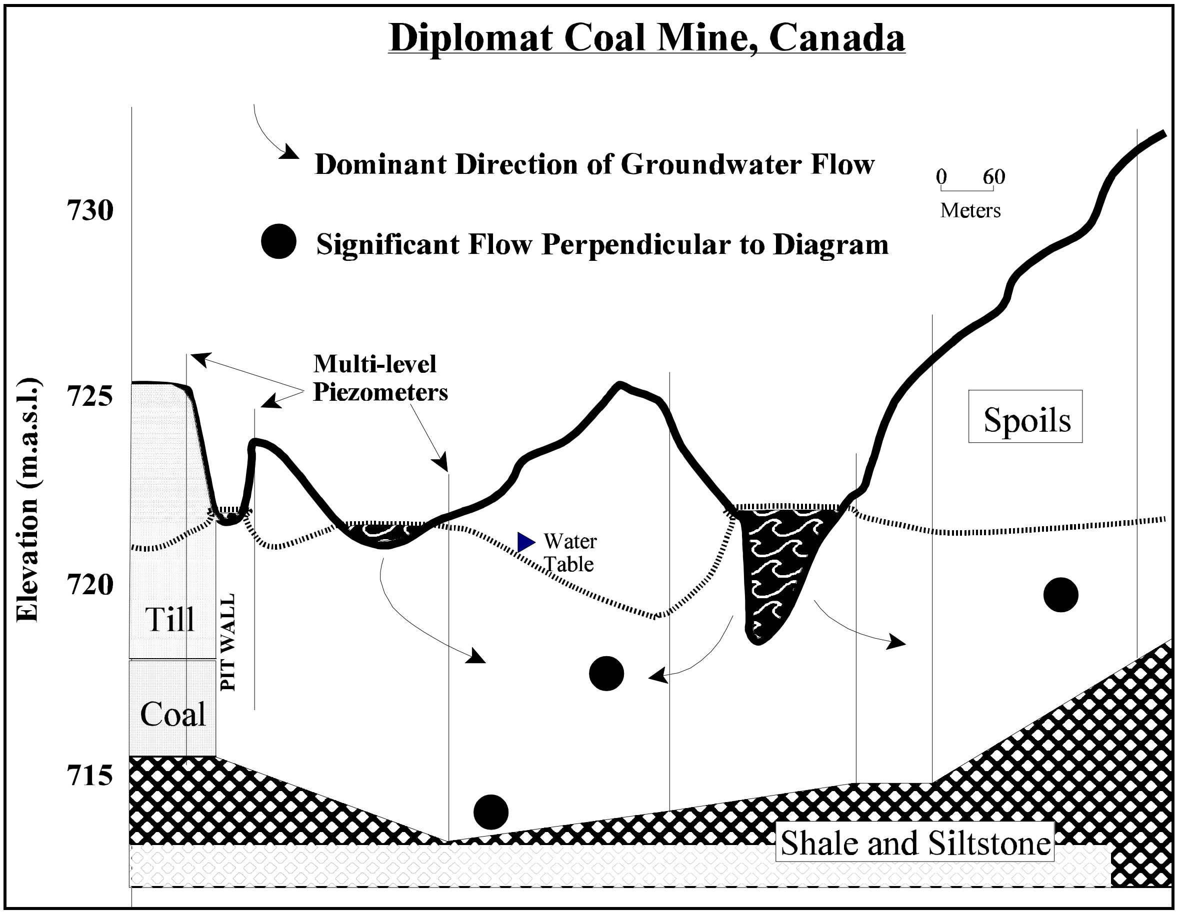

FIGURE 3.3-10. Cross-section through the Diplomat Mine Coal Spoils Pile in a Backfilled Pit (adapted from Trudell and Moran, 1982).

Island, Canada, has been inactive for a few decades and contains three Type 3 waste-rock piles: East, West, and South Dumps (Golder Associates Ltd., 1989; Galbraith, 1990). Due to the acidic drainage and dissolved copper concentrations draining from the toe of the East Dump (Figure 3.3-11), downstream fisheries had apparently declined, and remediation focussed on sealing the dumps.

Approximately 1 m of till was placed on the East Dump as a seal. Monitoring of internal temperature and poregas concentrations of oxygen and carbon dioxide over six months revealed little change from the pre-cover conditions of elevated oxygen levels. More important, the severity of the drainage did not change.

Further hydrogeologic investigations (Figure 3.3-11) showed that the major source of acidic drainage was a veneer of rock left on the upgradient Type 3 pit floor. This drainage then flowed al ong the base of this Type 3 pile and exited at its toe. Remedial activities then focussed on the pit floor.

Case Study 3.3-6: Physical Hydrogeology of Coal Spoils (Waste Rock)

> *highlights: complex flow of water through coal spoils; combination of Darcian and non-Darcian conditions within one component; interaction of surface and ground waters*

Hawkins and Aljoe (1990 and 1991) delineated the physical hydrogeology of a 3.2 ha coal waste-rock (spoils) dump in West Virginia, USA (Figure 3.3-12 and similar to Figure 2.2-2). They found that groundwater movement through the dump followed Darcian principles (Section 3.1) in some areas and turbulent, non-Darcian behavior in others. The high-conductivity, turbulent conduits were apparently not continuous and not interconnected, and were described as "pseudokarst" conditions due to similarities to carbonate-rock karst zones. Because the conduits were separated by finer-grained porous media, there was contrasting behavior at various times of the year. The conduits dominated groundwater flow patterns during high-

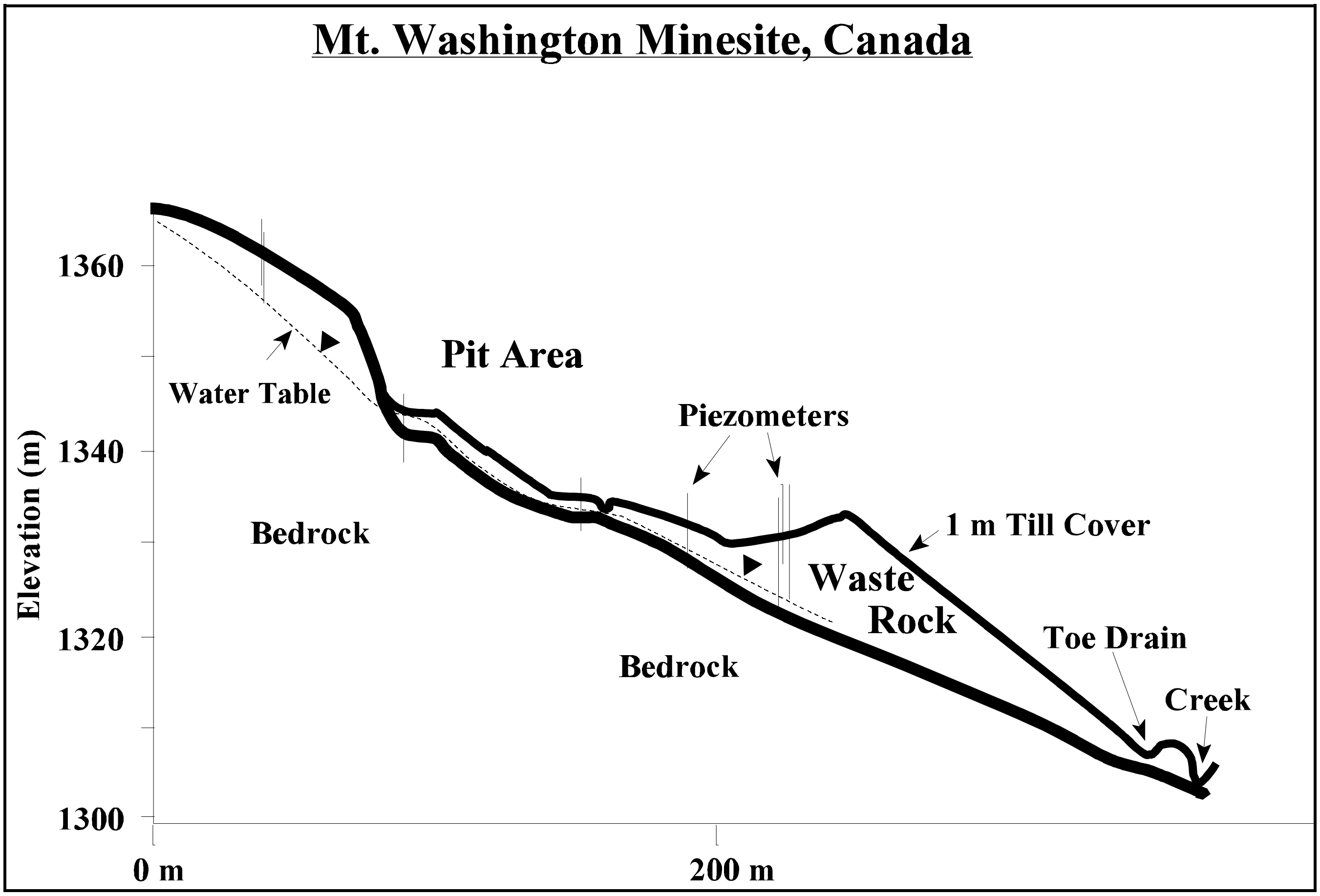

FIGURE 3.3-11. Cross-section through the Mt. Washington Minesite (adapted from Galbraith, 1990).

flow periods, whereas the intervening porous sediments dominated flow patterns during steady-state conditions. The following paragraphs illustrate the nature and extent of pseudokarst conditions in this waste-rock dump.

Drilling of boreholes by Hawkins and Aljoe (1990 and 1991) occasionally intercepted open conduits and voids, providing the first indication of the pseudokarst conditions. Later, the elevation of the water table, measured in piezometers installed in the boreholes, showed the preferential drainage effect that conduits provided by orienting water-table contours subparallel to them. These preferential drainage patterns lessened during steady-state flow.

Single-well (slug) tests in the piezometers also revealed the hydraulic effect of localized conduits by providing either normal, smooth semi-log recoveries or a very rapid response followed by a slow completion of recovery. The latter response was an indication that the localized conduits could quickly provide some water, but were then slowly refilled from the surrounding sediments. Porous-media hydraulic conductivities from the slug tests ranged from $5.7x10^{-5}$ to $2.1\ x10^{-7}$ m/s for water withdrawal and $1.3x10^{-4}$ to $3.3x10^{-7}$ m/s for injection. Pump tests of 1-2 hours duration in wells displaying pseudokarst behavior yielded conductivities of $2.8x10^{-2}$ to $5.1x10^{-3}$ m/s, except for one low value of $6.0x10^{-5}$ m/s.

One conduit extending from near the waste-rock surface to the toe of the rock was identified based on hydraulic responses. When runoff over the waste rock in surficial drainage ditches was high, the drainage in one channel infiltrated completely over a distance of 3-5 m. This water then exited at a spring 0.3 m in diameter and 1 m deep, approximately 60 m away laterally. However, when ditch flow was less than 0.2-0.3 L/s, the spring had standing water, but no overflow. When the ditch was dry, the spring was dry. Similar water chemistries in the ditch and spring also confirmed the hydraulic connection.

Injection of 73 kg of NaCl into a fracture on the pit wall (Figure 3.3-12) was used to define overall groundwater velocity through the waste rock over lateral distances of 60-100 m. The peak arrival times of the NaCl in various wells yielded average linear velocities of $1.2x10^{-5}$ to $4.9x10^{-5}$ m/s. This relatively slow velocity over the large distances indicated conduits were not interconnected. Nevertheless, two-dimensional analytical simulations of groundwater movement showed that dump-wide conductivities had to be increased by a factor of ten over the porous-medium values.

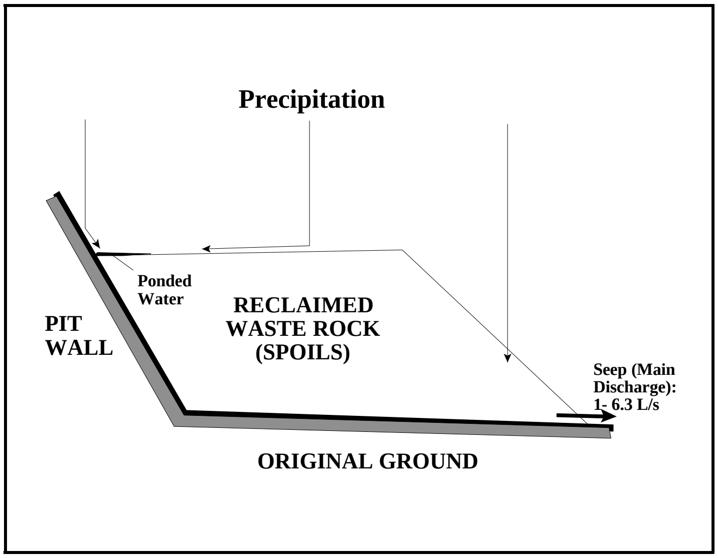

FIGURE 3.3-12. Schematic Cross-section of a Coal Waste-Rock Dump (adapted from Hawkins and Aljoe, 1990).

3.4 Drainage Flow from Tailings Impoundments

In many types of mining, the ore must be crushed, ground, or segregated to sand or silt size to maximize recovery of the economic minerals or elements (e.g., Figure 3.4-1). In placer mining, the ore is often already sand size or smaller. Therefore, in nearly all cases, these solid-waste materials from milling, often labelled “tailings”, accumulate and must therefore be disposed and managed. The volume of tailings at a minesite can be high, up to $1x10^9$ t or more at the largest mines. This is because economic metals like copper and gold often comprise a relatively small proportion of the ore, so the volume of tailings is equivalent to the amount of ore mined. For other types of mining like coal, the amount of tailings, resulting from some grinding and washing to remove impurities, is dependent on the amount of impurities.

The flow of water over and through tailings impoundments is markedly different from flows in most mines (Section 3.2) and mined-rock piles (Section 3.3). Instead of fractured rock with planar pathways or coarse-grained rock, tailings typically consist of relatively small grains with porespaces, or a “porous medium”. As a result, standard non-turbulent, or Darcian-style, analyses of groundwater flow can be applied (Section 3.1). Also, because of the low hydraulic conductivity of tailings, there is typically less infiltration, and more runoff and ponding, than for other minesite components.

In many ways, tailings behave like soils and thus well established sciences like hydrology, hydrogeology, and soil science exist for the examination and characterization of water movement. Consequently, this movement over and through tailings is not typically assessed or predicted in the empirical manner of the other components. While this technically advanced approach may seem to lend greater credibility to tailings studies, there are complexities that reduce that credibility.

Tailings are typically discharged along the perimeter of an impoundment, through one or more pipes from a mill. The pipes may occasionally be moved so that tailings are more evenly distributed. However, the effects of specific gravity and inertia lead to heterogeneities along discharge pathways, which later have significant effects on the movement and chemistry of drainage waters. In effect, larger particles and heavier minerals settle out quickly near the discharge point, whereas smaller particles and lighter minerals are carried farther (Figure 3.4-2). This leads to a rim of coarse-grained, better-draining materials, partially to fully encircling an impoundment, causing the internal water table to be lower near the perimeter. This effect was well known by the early 1970's (Ralston and Morilla, 1974). Also, because heavy-metal and sulfide minerals have high specific gravities, the rim may contain preferential levels of acid-generating minerals exposed to relatively rapid water flushing and air entry. This enhances the potential for metal-laden or acidic drainage from the impoundment (Chapter 4).

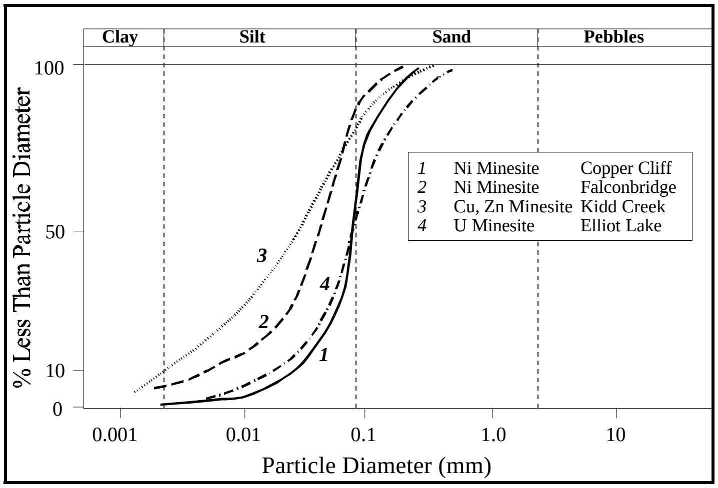

FIGURE 3.4-1. Examples of Tailings Grain Sizes from Metal Mines (adapted from Robertson, 1994b).

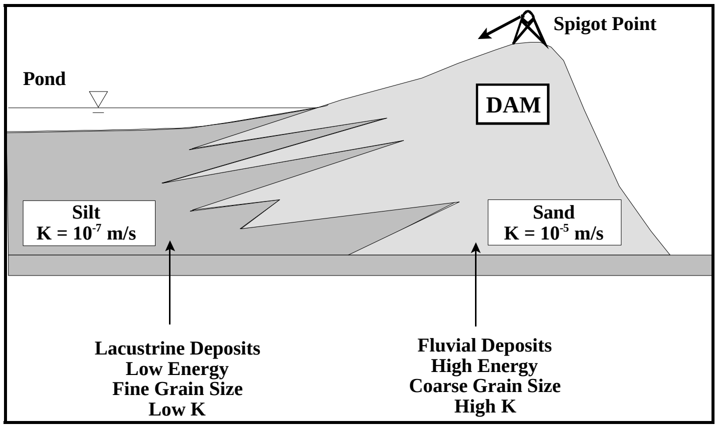

FIGURE 3.4-2. Particle-Size Segregation in a Tailings Impoundment (adapted from Robertson, 1994b).

To reduce segregation by inertia and specific gravity, dewatered “thickened” tailings with reduced moisture content can be deposited in a cone shape from a central point (Case Study 3.4-1). At the Kidd Creek Mine in Ontario, Canada, Al et al. (1994) reported on stratification of hydraulic conductivity in thickened tailings (Figure 3.4-3). One limb of the cone maintained a conductivity between 10^{-8} and 10^{-7} m/s from the discharge point almost to the retaining dam.

To maximize storage volumes relative to dam construction, engineered tailings impoundments are often located in topographic depressions like valleys. As a result, surrounding runoff is often toward the impoundment from higher areas unless interception ditches carry it elsewhere. Through time and mine life, however, the elevation of the tailings surface may increase until the impoundment becomes topographically high. In this way, drainage through surface and groundwater pathways migrates outward from the impoundment (Figures 3.4-4 and 3.4-5). In many cases, surface drainage is captured in an internal pond and recirculated to the mill in order to reduce the water requirements of milling and the discharge of minewater to the surrounding environment (Figure 2.1-1).

Case Study 3.4-1: Runoff from Thickened Tailings

> *highlights: hydrogeologic properties of thickened tailings; interactions of surface and ground waters; transient contributions of porewaters to runoff*

Woyshner and St-Arnaud (1994) and Al and Blowes (1995) reported on studies of groundwater and runoff over a thickened-tailings impoundment (see preceding discussion of thickened tailings). This impoundment contains $100x10^6$ t of sulfide-rich tailings over a 1200 ha area, deposited in a conical shape as thickened tailings at the Kidd Creek Mine, Ontario, Canada. Because of the thickening, obtained through dewatering before discharge, these tailings have a more uniform grain-size distribution (clay to fine sand, Figure 3.4-3) and hydraulic conductivity ($5x10^{-9}$ to $5x10^{-7}$ m/s), a thick capillary fringe (water-tension zone) above the water table, and a cone-shaped surface. Runoff thus occurs in a radial distribution around the cone in small ephemeral channels. Woyshner and St-Arnaud (1994) indicated that normally 42% of precipitation was lost as runoff, 51% evaporated, and 7% infiltrated into the tailings.

To determine the proportion of tailings porewater in the runoff due to a rapid rise of the water table, a chemical mass-balance technique was used on the hydrograph of three storm events at the lower end of a channel. The selected channel was 3500 m long, 0.5-0.75 m deep, and predominantly dendritic with intermittent braiding. No vegetation was present.

The percentage of porewater in the runoff ranged from virtually zero for short-term intense rainfall to 25% for less intense rainfall (Al and Blowes, 1995). This was in contrast to the 50-75% in runoff on conventional, unthickened tailings. The rapid delivery of porewater to the surface at Kidd Creek, despite downward hydraulic gradients in the

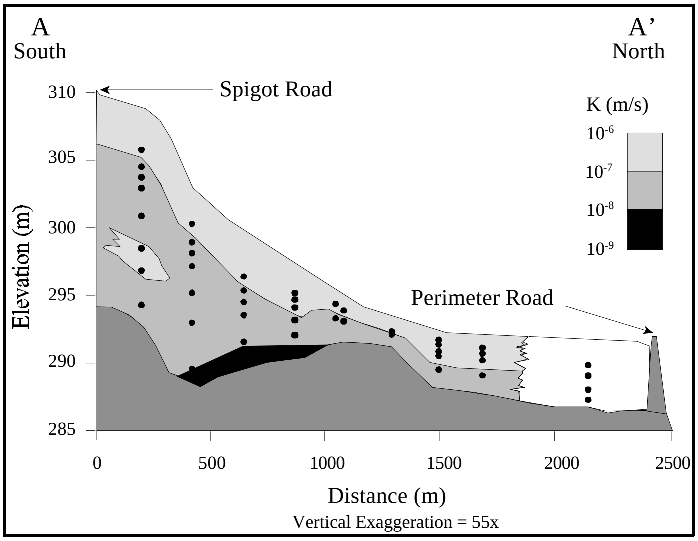

FIGURE 3.4-3. Hydraulic-Conductivity Pattern in Thickened Tailings (adapted from Al et al., 1994).

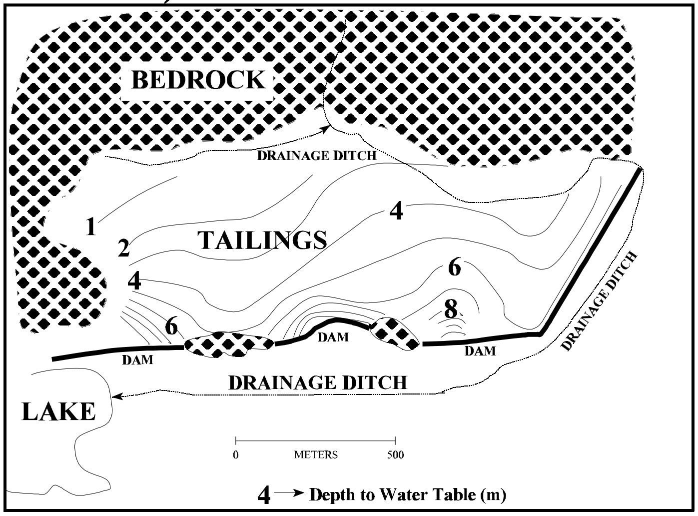

FIGURE 3.4-4. Depth to Water Table in a Tailings Impoundment (adapted from Cherry et al., 1980).

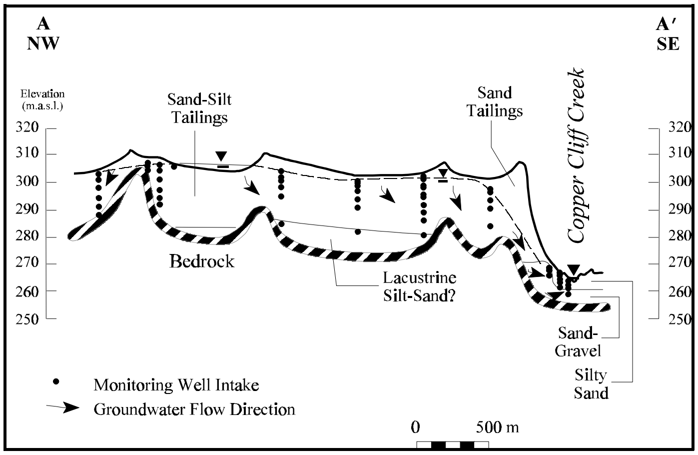

FIGURE 3.4-5. Vertical Cross-section Showing Groundwater Movement through a Tailings Impoundment (adapted from Robertson, 1994b).

porewater, was attributed to desiccation fractures to depths of 1-2 m filled with coarser tailings particles. The loadings of ferrous iron from porewater during the three events ranged from 23 to 2800 mg/s.

Average linear groundwater velocities were calculated around 12 cm/yr. The water table was typically a few meters below the tailings surface, but fluctuated with time and infiltration. Because of the consistent fine-grained composition, the capillary fringe often extended to within a meter, even near the peak of the central cone, which accounted for the rapid rise of the water table during a relatively small addition of infiltration. This also means that the thickness of tailings available for oxygen entry and oxidation was generally limited and was expected to remain so after closure of the impoundment. Nevertheless, Williams (1996) points out that this thickness of oxidation was still sufficient to generate acidity and thus affect drainage chemistry (Case Study 6.2-8).

3.5 Questions

Hypothetical Type 1 Pit "A": This perfectly circular open-pit mine has ten benches (or "steps", see Figure 3.2.1-1). Each bench consists of a ten-meter-high vertical wall and a ten-meter-wide horizontal terrace. At Pit Bottom, the elevation is 0 m above sea level and the diameter of the pit at this elevation is 100 m. The Total Pit Limit is defined by the uppermost, or 10th, bench at +100 m elevation. Hydraulic Inputs (+) and Outputs (-) are: Precipitation = +1.0 m/yr, Saturated Groundwater Flow = +700 m^3/day (always constant), and Evaporation = -0.5 m/yr.

3-1. Draw a vertical profile for Pit "A" and calculate the cumulative volume at the top of each bench. What is the total volume of the pit?

3-2. Based on the flow data for Pit "A", how many years are required to fill the pit to elevation a) +20 m, b) +60 m, and c) +100 m?

3-3. Assuming the pit must be filled within three years to improve water chemistry, what average additional flow is needed from other sources (e.g., Figure 3.2.1-3)?

3-4. At an equilibrium, or "static", elevation (Figure 3.2.1-4) of +85 m, the pit water will begin flowing into the surrounding shallow groundwater system. If the chemistry of the pit water is unacceptable for release to the environment, the pit-water level must be maintained at +75 m. Based on no flow from additional sources (i.e., ignoring Question 3-3), at what year will +75 m be reached? What pumping rate from the pit to a water-treatment plant would be required to maintain the level at +75 m?

Hypothetical Type 2 Underground Mine "B": This mine consists of one adit with a length of 300 m and a rectangular vertical cross-section of 3 m by 4 m. The rock surrounding this mine has an average fractured hydraulic conductivity of 10^{-6} m/s.

3-5. What is the volume and wall surface area of Mine "B"?

3-6. If groundwater moves into Mine "B" under a hydraulic gradient of 1.0, how many years are needed to flood this mine after the portal is sealed?

Hypothetical Type 1 Mined-Rock Pile "C": This waste-rock dump is 10 m high with a lateral area of 100 m by 100 m, and contains 170,000 t of rock. Occasional rainfall events are 0.1 m/d and occur continuously and evenly over 24 hours. Evapotranspiration consumes 25% of this precipitation, another 25% becomes runoff, and 50% infiltrates into the dump. Runoff begins immediately as the rain begins and ends six hours after the rain ends. Infiltration reaches and begins flowing from the base of the dump 24 hours after precipitation begins and continues at a constant rate for 48 hours.

3-7. Draw a graph depicting drainage flow (runoff plus subsurface seepage) exiting the edge of Pile "C" through time during and after one rainfall event.

3-8. Draw a similar graph for three consecutive rainfall events.

Hypothetical Tailings Impoundment "D" (e.g., Figure 3.4-2): The lateral area of this impoundment is 500 m by 500 m, with 5% of the area consisting of vertically continuous sandy tailings and the remainder consisting of vertically continuous silty tailings. The hydraulic conductivity of the sandy tailings is 10^{-5} m/s, but is 10^{-7} m/s for the silty tailings. Groundwater moves vertically downward throughout the entire impoundment under a hydraulic gradient of 0.1.

3-9. Over a 24-hour period, what is the volume of vertical groundwater drainage from a) the silty tailings and b) the sandy tailings within Impoundment "D"?

3-10. If rainfall over this 24-hour period was 0.01 m, what is the volume of precipitation left ponded above, or running of, the top of the tailings in Impoundment "D"?

CHAPTER 4
DESCRIPTION AND ASSESSMENT OF DRAINAGE CHEMISTRY

4.1 Overview

Minesite-drainage chemistry is remarkable from a geochemical perspective, because it spans such large ranges of conditions. Reports of drainage chemistry show that pH can extend from -3 (negative three) to 12, with aqueous concentrations of cations and anions from less than one microgram a liter (µg/L) to more than 100,000 milligrams a liter (mg/L). This is a range of more than eight orders of magnitude. In the Colorado Mineral Belt (USA) alone, pH varies from 1.7 to 7.8 and copper and zinc range from <1 to 700,000 µg/L (Ficklin et al., 1994). Consequently, there is no attempt at listing "typical" concentrations in this book, even for specific mining areas.

The large observed range in chemistry is due to the combination of (1) human activity, (2) exposure of fresh minerals, and (3) climatic conditions. Minerals form in a vast array of environments, from volcanic cores to deep oceans, from deserts to arctic permafrost. They form in "equilibrium" with the geologic or climatic conditions that created them. Upon mining, often long after their formation, these "primary" minerals are exposed to different conditions than those under which they formed, and thus are no longer in equilibrium. They begin to dissolve or alter to other, "secondary" minerals at various rates. These basic processes of primary-mineral dissolution and secondary-mineral formation are inevitable after mining and lead to measurable chemical concentrations in drainage waters. Therefore, these processes are the key to assessing, predicting, and controlling drainage chemistry.

4.2 General Description

With such large ranges of concentrations, the assessment, prediction, and control of minesite-drainage chemistry may seem daunting. However, there are basic principles that simplify the tasks, focussing specifically on (1) primary mineral dissolution and (2) formation of secondary minerals. With a general understanding of these principles, drainage chemistry is not so bewildering.

4.2.1 Kinetic and Equilibrium Reactions

Minerals can dissolve into, and can precipitate from, water under two basic conditions: kinetic or equilibrium (Table 4.2.1-1). The critical features of equilibrium conditions are that aqueous concentrations are constant through time and not dependent on the relative and absolute amounts of water and minerals. This subject to the obvious condition that sufficient minerals must be present to allow dissolution to equilibrium. Also, through time, kinetic reactions approach equilibrium conditions (Figure 4.2.1-1). Dissolution of many primary minerals at minesites like sulfides (Table 4.2.1-2) and aluminosilicates is a kinetic process. Other primary minerals like oxides may follow either kinetic or equilibrium dissolution.

Probably the greatest complexity in this scenario for minesite drainage is that drainage often moves and comes in contact with various minerals along flowpaths. As a result, a rapidly evolving series of equilibrium conditions on a small scale can appear incorrectly as a kinetic condition on a larger scale.

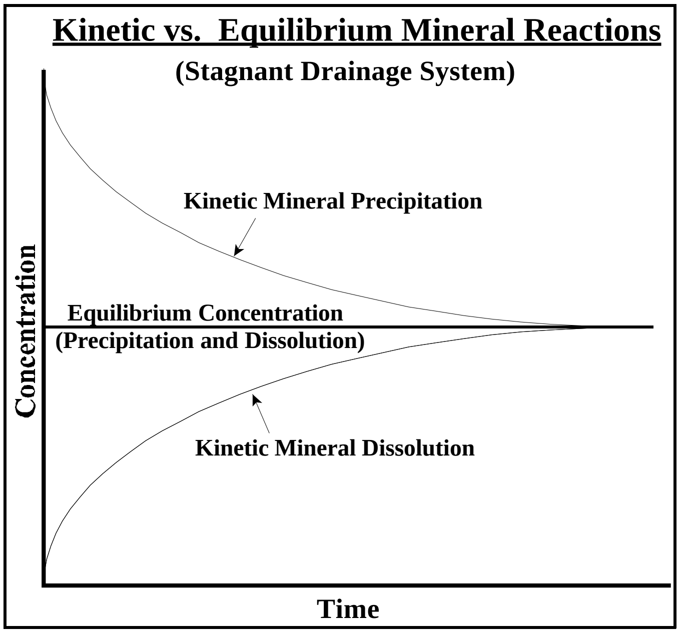

FIGURE 4.2.1-1. Evolution of Kinetic to Equilibrium Conditions.

TABLE 4.2.1-1
Kinetic vs. Equilibrium Mineral Reactions

Kinetic	Equilibrium
aqueous concentrations (as mg/L) change with time	aqueous concentrations (as mg/L) do not change with time
aqueous concentrations (as mg/L) can depend on the ratio of water to mineral	aqueous concentrations (as mg/L) are independent of the amount of water and mineral
if water remains in contact with minerals long enough (stagnant drainage), equilibrium will eventually be reached (Figure 4.2.1-1)	if drainage moves into contact with other minerals, equilibrium will change, resulting in either new equilibrium or kinetic conditions

TABLE 4.2.1-2
Examples of Sulfide Minerals
(from Lowson, 1982)

Name	Composition	Name	Composition
Realgar	AsS	Pyrrhotite	$Fe_{(0.8-1.0)}S$
Orpiment	As_2S_3	Troilite	FeS
Greenockite	CdS	Greigite	Fe_3S_4
Cobaltite	CoAsS	Arsenopyrite	FeAsS
Linnaeite	Co_3S_4	Violarite	$FeNi_2S_4$
Covellite	CuS	Cinnabar	HgS
Chalcocite	Cu_2S	Alabandite	MnS
Chalcopyrite	$CuFeS_2$	Hauerite	MnS_2
Cubanite	$CuFe_2S_3$	Molybdenite	MoS_2
Bornite	Cu_3FeS_4	Millerite	NiS
Enargite	Cu_3AsS_4	Galena	PbS
Tennantite	$Cu_2As_2S_{13}$	Stibnite	Sb_2S_3
Pyrite	FeS_2	Sphalerite	ZnS
Marcasite	FeS_2	Wurtzite	ZnS

Also because of drainage movement, concentrations quickly can deceptively appear as equilibrium, and this condition is often called “pseudoequilibrium”. These complexities are discussed later.

4.2.2 Three Stages of Drainage Chemistry

The second important principle in minesite drainage is the formation of secondary minerals. Primary minerals can be far from equilibrium upon mining and subsequent exposure to air, precipitation, and temperature fluctuations. As a result, their kinetic reaction rates are initially high and then become relatively stable for an extended period of time (Rate1, First Stage, Figure 4.2.2-1). Over this period, the rates typically exceed the solubility of various secondary minerals (“supersaturation”) like sulfates, carbonates, hydroxides (Table 4.2.2-1), causing them to precipitate within the minesite component. The remaining amounts of elements in the drainage then create the observed drainage chemistry exiting the component (Rate2, Figure 4.2.2-1). This is the First Stage of drainage chemistry, which apparently can last for years to millennia. The difference between Rate1 and Rate2, multiplied by the number of years for the First Stage, reflects the mass of accumulated minerals.

The Second Stage begins after most of the reactive primary minerals have either dissolved or dissolve at negligible rates (Figure 4.2.2-1). At this point, the accumulated secondary minerals begin dissolving. Because the precipitation and dissolution of many secondary minerals are equilibrium processes, Rate2 can remain relatively constant and predictable through the First and Second Stages of drainage chemistry, which apparently can last for decades to millennia.

The Third Stage of drainage chemistry begins when only low-reactivity primary and secondary minerals like quartz remain. As a result, drainage concentrations are relatively low. This stage is seen frequently with natural rock outcrops exposed and weathered for extended periods.

In some cases, Rate1 may not be sufficiently high to exceed secondary-mineral solubility, or secondary solubility is very high as with potash and salt minesites (e.g., Case Study 4.2-3). As a result, Rate2 is equal to, and limited by, Rate1. In this situation, no Second Stage develops since there is no secondary accumulation. This is not expected at many minesites because frequent and thorough rinsing of all reactive surfaces within a component is unlikely by natural infiltration. Well-rinsed heap-leach piles may be an exception (see Case Study 4.4-6).

4.2.3 Four Classes of Drainage Chemistry

There are four classes of drainage chemistry, classified by the effect that primary minerals have on pH (Table 4.2.3-1). Non-neutral-pH drainages (acidic and alkaline) are often greater concerns for minesites and regulatory agencies, perhaps due to the obvious violation of water-quality requirements based on a simple, fast measurement of pH.

The class that raises the greatest concern in the mining industry is acidic drainage, which seems unwarranted because drainage chemistry of the other classes can sometimes be more severe and toxic. For example, drainage from potash tailings can carry hundreds of thousands of mg/L of sodium and chloride, which is toxic to most life, renders surface and ground waters undrinkable, and corrodes stainless steel within a few months. Also, pH-neutral drainage can carry tens of mg/L of toxic heavy metals. In any case, acidic drainage is the focus of most research and monitoring of drainage chemistry, as demonstrated by many of the case studies in this book.

Acidic drainage at minesites is also known as acid mine drainage (AMD), or acid rock drainage (ARD) where its connection with natural acidic drainage is emphasized. AMD is a natural consequence of the oxidation of some sulfide minerals (particularly pyrite, pyrrhotite, and marcasite: Table 4.2.1-2) in the presence of air (oxygen) and water:

$$\text{sulfide mineral + oxygen + water} = \text{sulfate + acidity + metals} \qquad (4.2.3\text{-}1)$$

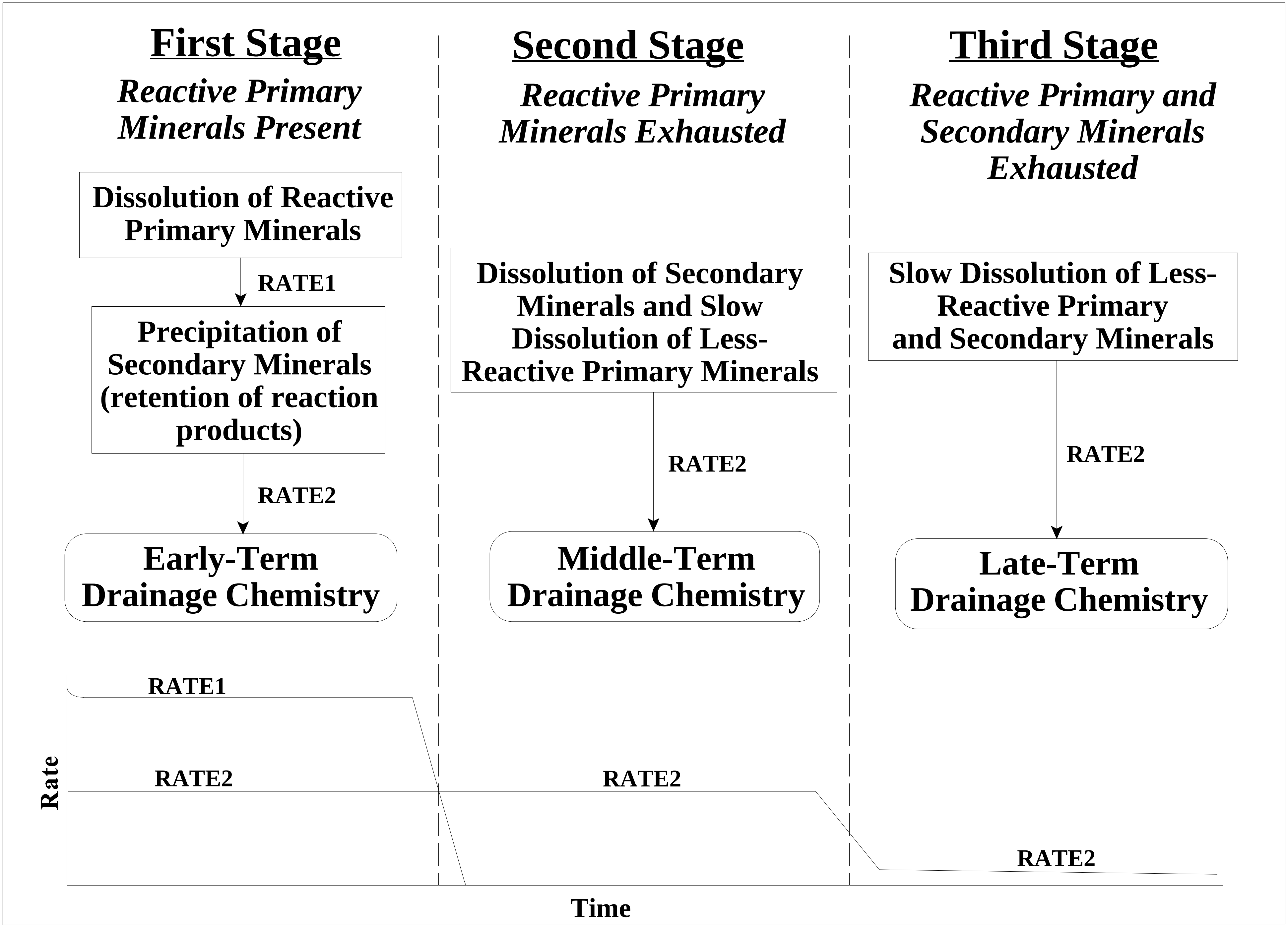

FIGURE 4.2.2-1. Three Stages in Minesite-Drainage Chemistry.

TABLE 4.2.2-1
Examples of Secondary Minerals[1]
(compiled from Jambor and Blowes, 1994)

Carbonates		
Calcite [$CaCO_3$]	Aragonite [$CaCO_3$]	Magnesite [$MgCO_3$]
Rhodocrosite [$MnCO_3$]	Siderite [$FeCO_3$]	Otavite [$CdCO_3$]
Gaspeite [$NiCO_3$]	Smithsonite [$ZnCO_3$]	Strontianite [$SrCO_3$]
Witherite [$BaCO_3$]	Cerrusite [$PbCO_3$]	Sphaerocobaltite [$CoCO_3$]
Dolomite [$CaMg(CO_3)_2$]	Kutnohorite [$CaMn(CO_3)_2$]	Ankerite [$Ca(Fe,Mg)(CO_3)_2$]
Minrecordite [$CaZn(CO_3)_2$]	Malachite [$Cu_2(OH)_2CO_3$]	Azurite [$Cu_3(OH)_2(CO_3)_2$]
Hydrozincite [$Zn_5(OH)_6(CO_3)_2$]	Aurichalcite [$(Zn,Cu)(OH)_6(CO_3)_2$]	Hydrocerrusite [$Pb_3(OH)_2(CO_3)_2$]
Sulfur-Bearing		
Gypsum [$CaSO_4 \cdot 2H_2O$]	Bassanite [$2CaSO_4 \cdot H_2O$]	Anhydrite [$CaSO_4$]
Melanterite [$FeSO_4 \cdot 7H_2O$]	Siderotil [$FeSO_4 \cdot 5H_2O$]	Ferrohexahydrite [$FeSO_4 \cdot 6H_2O$]
Rozenite [$FeSO_4 \cdot 4H_2O$]	Szomolnokite [$FeSO_4 \cdot H_2O$]	Römerite [$Fe^{2+}Fe_2^{3+}(SO_4)_4 \cdot 14H_2O$]
Bilinite [$Fe^{2+}Fe_2^{3+}(SO_4)_4 \cdot 22H_2O$]	Copiapite [$Fe^{2+}Fe_4^{3+}(SO_4)_6(OH)_2 \cdot 20H_2O$]	Voltaite [$K_2Fe_5^{2+}Fe_4^{3+}(SO_4)_{12} \cdot 18H_2O$]
Coquimbite [$Fe_2(SO_4)_3 \cdot 9H_2O$]	Kornelite [$Fe_2(SO_4)_3 \cdot 7H_2O$]	Rhomboclase [$HFe(SO_4)_2 \cdot 4H_2O$]
Fibroferrite [$FeOHSO_4 \cdot 5H_2O$]	Amarantite [$FeOHSO_4 \cdot 3H_2O$]	Schwertmannite [$Fe_8O_8(OH)_6SO_4$]
Jarosite [$KFe_3(SO_4)_2(OH)_6$][2]	Ferricopiapite [$Fe_5O(OH)(SO_4)_6 \cdot 20H_2O$]	Unknown[$(Cu,Fe)(SO_4,AsO_4,PO_4)$]
Alunite [$KAl_3(SO_4)_2(OH)_6$][2]	Halotrichite [$FeAl_2(SO_4)_4 \cdot 22H_2O$]	Alunogen [$Al_2(SO_4)_3 \cdot 18H_2O$]
Jurbanite [$AlOHSO_4 \cdot 5H_2O$]	Basaluminite [$Al_4(OH)_{10}SO_4 \cdot H_2O$]	Hydrobasaluminite [$Al_4(OH)_{10}SO_4 \cdot 12\text{-}36H_2O$]
Elemental sulfur [S]	Anglesite [$PbSO_4$]	Barite [$BaSO_4$]
Celestite [$SrSO_4$]	Osarizawaite [$PbCuAl_2(SO_4)_2(OH)_6$]	Beaverite [$PbCuFe_2(SO_4)_2(OH)_6$]
Goslarite [$ZnSO_4 \cdot 7H_2O$]	Bianchite [$ZnSO_4 \cdot 6H_2O$]	Gunningite [$ZnSO_4 \cdot H_2O$]
Epsomite [$MgSO_4 \cdot 7H_2O$]	Hexahydrite [$MgSO_4 \cdot 6H_2O$]	Chalcanthite [$CuSO_4 \cdot 5H_2O$]
Antlerite [$Cu_3(OH)_4SO_4$]	Brochantite [$Cu_4(OH)_6SO_4$]	Langite [$Cu_4(OH)_6SO_4 \cdot 2H_2O$]
Posnjakite [$Cu_4(OH)_6SO_4 \cdot H_2O$]	Morenosite [$NiSO_4 \cdot 7H_2O$]	Retgersite [$NiSO_4 \cdot 6H_2O$]
Thenardite [Na_2SO_4]	Mirabilite [$Na_2SO_4 \cdot 10H_2O$]	Amorphous [FeS]
Mackinawite [$(Fe,Ni)_9S_8$]	Smythite [$(Fe,Ni)_9S_{11}$]	Greigite [$Fe^{2+}Fe_3^{3+}S_4$]
Pyrite [FeS_2]	Marcasite [FeS_2]	Violarite [Ni_2FeS_4]
Millerite [NiS]	Chalcocite [Cu_2S]	Djurleite [$Cu_{31}S_{16}$]

Sulfur-Bearing (continued)		
Digenite [$(Cu,Fe)_{1.8}S$]	Anilite [$Cu_{1.75}S$]	Geerite [$Cu_{1.60}S$]
Spionkopite [$Cu_{1.39}S$]	Yarrowite [$Cu_{1.12}S$]	Covellite [CuS]
Oxides/Hydroxides		
Amorphous [$Fe(OH)_3$]	Goethite ["-FeO(OH)]	Lepidocrosite [(-FeO(OH)]
Feroxyhyte [*-FeO(OH)]	Ferrihydrite [$5Fe_2O_3 \cdot 9H_2O$]	Akaganéite [$-FeO(OH,Cl)]
Hematite ["-Fe_2O_3]	Maghemite [(-Fe_2O_3]	Magnetite [$FeO \cdot Fe_2O_3$]
Amorphous [$Al(OH)_3$]	Nordstrandite [$Al(OH)_3$]	Doyleite [$Al(OH)_3$]
Bayerite [$Al(OH)_3$]	Gibbsite [$Al(OH)_3$]	Boehmite [$AlO(OH)$]
Diaspore [$AlO(OH)$]	Corundum [Al_2O_3]	Cristobalite/quartz [SiO_2]
Pyrolusite [MnO_2]	Hausmannite [Mn_3O_4]	Manganite [(-MnO(OH)]
Pyrochroite [$Mn(OH)_2$]	Todorokite [$(Mn^{2+},Ca,Mg)Mn_3^{4+}O_7 \cdot H_2O$]	Rancieite [$(Ca,Mn^{2+})Mn_4^{4+}O_9 \cdot 3H_2O$]
Tenorite [CuO]	Cuprite [Cu_2O]	Delafossite [$CuFeO_2$]
Bunsenite [NiO]	Theophrastite [$Ni(OH)_2$]	Jamborite [$(Ni^{2+},Ni^{3+},Fe)(OH)_2(OH,S,H_2O)$]
Aluminosilicates		
Mica-Clay minerals	Kaolinite [$Al_2Si_2O_5(OH)_4$]	
Phosphates, Arsenates, and Halides		
Vivianite [$Fe_3(PO_4)_2 \cdot 8H_2O$]	Strengite [$FePO_4 \cdot 2H_2O$]	Variscite [$AlPO_4 \cdot 2H_2O$]
Berlinite [$AlPO_4$]	Crandallite [$CaAl_3(PO_4)_2(OH)_5 \cdot H_2O$]	Svanbergite [$SrAl_3PO_4(OH)_6SO_4$]
Corkite [$PbFe_3PO_4(OH)_6SO_4$]	Pseudomalachite [$Cu_5(PO_4)_2(OH)_4 \cdot H_2O$]	Woodhouseite [$CaAl_3PO_4(OH)_6SO_4$]
Pyromorphite [$Pb_5(PO_4)_3Cl$]	Scorodite [$FeAsO_4 \cdot 2H_2O$]	Mansfieldite [$AlAsO_4 \cdot 2H_2O$]
Pharmacosiderite [$KFe_4(AsO_4)_3(OH)_4 \cdot 6\text{-}7H_2O$]	Beudantite [$PbFe_3AsO_4SO_4(OH)_6$]	Atacamite [$Cu_4Cl_2(OH)_6$]
Chlorargyrite [$Ag(Cl,Br,I)$]	Bromargyrite [$AgBr$]	Boleite [$Pb_{26}Ag_9Cu_{24}Cl_{62}(OH)_{48}$]
Other		
Native copper [Cu]	Native silver [Ag]	

[1] Some minerals represent end members of solid-solution series or cation substitutions. Therefore, many other secondary minerals exist, some of which have not yet been identified. Also, many of these minerals can occur as primary minerals.

[2] In jarosite and alunite, K can be replaced by Na, H, Ag, NH_4, $Pb_{0.5}$ and other metals.

TABLE 4.2.3-1
Four Classes of Minesite Drainage Based on pH Effects of Primary Minerals

Class	Details/Examples
Acidic	drainage pH < 6.0 with acidity generated through mineral oxidation, particularly oxidation of sulfides (Table 4.2.1-2); aqueous metal levels often but not always higher than in near-neutral drainage; greatest international attention of all classes; associated with many metal mines and pyrite mines
Alkaline	drainage pH > 9.0-10.0 with high levels of alkalinity generated through mineral dissolution, particularly oxides, hydroxides, and some silicates; sometimes associated with diamond (kimberlite) mining, fly ash from coal combustion, bauxite milling (“red mud”), and smelter slag within a minesite component; levels of some metals like aluminum may be higher than in near-neutral drainage
Near-Neutral	6.0 < drainage pH < 9.0-10.0; drainage where acid-generating minerals cannot overcome acid-neutralizing minerals or where base-generating minerals cannot overcome base-neutralizing minerals; can become acidic or alkaline with time depending on mineral abundances and reaction rates; aqueous metal concentrations can sometimes exceed toxic levels
Other	pH generally irrelevant, but may affect aqueous concentrations; non-metal mining like potash, halite, borate, other evaporites, bentonite, kaolinite, sand/gravel, and clays.

Also, other oxidants like aqueous ferric iron may substitute for air in the reaction:

sulfide mineral + ferric iron + water =
sulfate + acidity + metals (4.2.3-2)

Apparently, these reactions can operate even with minimal levels of oxygen or water (e.g., Leatherwood and Kunzler, 1989).

The oxidation of sulfide minerals and the accompanying acid generation are often viewed as environmental concerns. However, to illustrate an opposing viewpoint, Castelo Branco et al. (1996) reported that these processes can yield nutrients in degraded soils.

In contrast to AMD, alkaline mine drainage (LMD) is the result of the dissolution of oxide, hydroxide, or silicate minerals like magnesium-rich olivine and brucite:

oxide/hydroxide mineral + water =
alkalinity + metals (4.2.3-3)

silicate mineral + water =
alkalinity + metals + aqueous silica (4.2.3-4)

However, if neutralizing minerals are present in the system, some acidity from Equations 4.2.3-1 or 4.2.3-2 or some alkalinity from Equations 4.2.3-3 or 4.2.3-4 will be consumed and some metals may be precipitated as secondary minerals. In the presence of excess amounts of neutralizing minerals, AMD and LMD will not appear even if kinetic rates are high. This is discussed further in Sections 4.5 and 5.2.

4.2.4 Bacterial Contributions to Drainage Chemistry

One problem in studies of minesite drainage relates to the effects of bacteria. *Thiobacillus* *ferrooxidans* which can accelerate the oxidation of sulfide and ferrous iron to create acidic drainage (Equations 4.2.3-1 and 4.2.3-2) can be used to illustrate and resolve the contributions.

A study still referenced frequently today, Singer and Stumm (1970), suggested that *T. ferrooxidans* greatly accelerated sulfide oxidation by orders of magnitude at acidic pH. However, aspects of that study were discredited long ago (Morth et al., 1972). Also, recent studies under laboratory and field conditions with sterile and non-sterile samples show similar oxidation rates over a large range of pH from 1 to 8 (Nicholson, 1994; Van Stempvoort and Krouse, 1994; Kwong et al., 1995), which contradict the widely believed effect of *T. ferrooxidans* at acidic pH.

This is not surprising, because the basic principles of bacterial populations are ignored in many geochemical studies. For example, bacteria do not react simply to an energy source like sulfide minerals, but adjust their activity based on population size, removal of waste products from their environment, and other factors. Therefore, the free-for-all bacterial activity depicted in some acidic-drainage literature is not realistic.

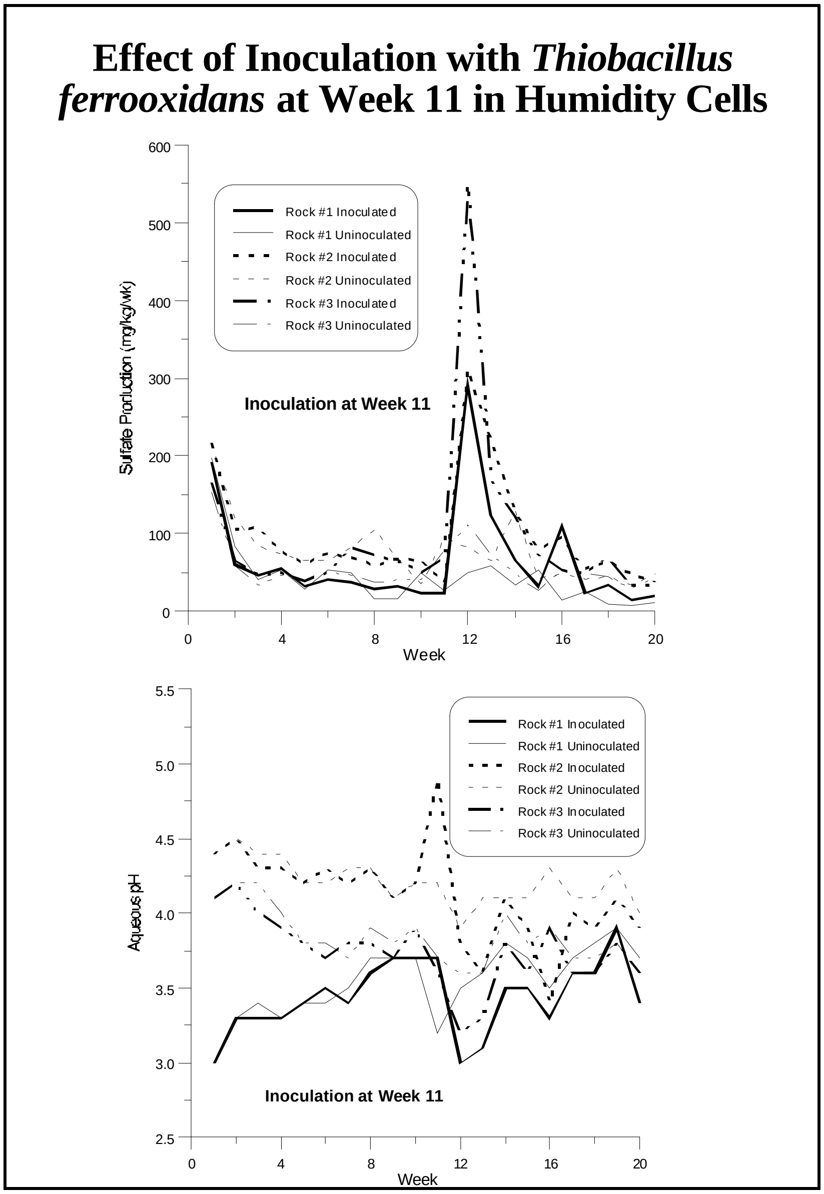

FIGURE 4.2.4-1. Example of Short-Term Effects from Inoculating Humidity Cells with *Thiobacillus ferrooxidans*.

Furthermore, debates such as whether laboratory tests (e.g., Section 5.3.1) should be inoculated and whether full-scale components can be rendered sterile are unimportant, because bacteria are ubiquitous and will often flourish in spite of attempts to stop them. For example, three sets of duplicate laboratory humidity cells were operated with one cell of each set inoculated with *Thiobacillus ferrooxidans* at Week 11 (Figure 4.2.4-1). This work showed that the inoculated cells experienced a rapid acceleration in sulfide oxidation with some decrease in pH, but the bacterial population apparently readjusted to that of the uninoculated cells within a few weeks. As another complication, the bacteria were probably present and active in all cells from early weeks, but could not be detected due to the high detection limits common to bacterial enumeration.

Furthermore, dozens of species of bacteria at any pH, like *T. ferrooxidans*, are probably involved in mineral-water reactions, and some have not yet been studied in any detail. In fact, roughly 95% of bacteria associated with acidic drainage are reportedly not *T. ferrooxidans* and their contributions to drainage chemistry remain unknown.

For all these reasons, detailed study of bacterial populations in assessments and predictions of drainage chemistry is in its infancy and is of little practical value and consequence. This is not because bacterial contributions are necessarily unimportant, but because (1) bacteria are always present in our environment, (2) bacterial effects on aqueous chemistry cannot be reliably detected and quantified at this time, and (3) bacteria cannot be eliminated from minesite components. In other words, bacterial activity can be considered another factor in the generation of minesite-drainage chemistry, but whose overall contribution is apparently constant under natural environmental conditions according to recent studies.

4.2.5 General Trends in Minesite-Drainage Chemistry

Complications involving a series of secondary-mineral equilibrium reactions along flowpaths were mentioned in Section 4.2.1 and are examined in greater detail in Section 4.5 as the sub-region concept of neutralization. However, for this section, a more simple, empirical approach to describing and assessing drainage chemistry at a minesite is discussed here.

As explained above and depicted in Figure 4.2.2-1, the precipitation and dissolution of secondary minerals, often as an equilibrium process, causes a relatively constant range of concentrations to appear year after year at minesites. This range, depicted simply as Rate2 in Figure 4.2.2-1, is easily defined even if the identities of the secondary minerals are not known.

For example, Morin et al. (1994a, 1994b, 1995a, 1995b) found that annual means and standard deviations of drainage chemistry at monitoring sites within two minesites were relatively constant as long as pH remained generally steady. This recurrence of the annual statistical values was observed at monitoring stations adjacent to a single component, as well as at a station receiving mixed drainage from several waste-rock dumps and an open pit (Table 4.2.5-1).

If pH changed through time at a monitoring station, however, the annual mean value changed also. This simply reflects the significant effect that pH has on some metal concentrations. As a result, scatterplots of many aqueous parameters against pH often show some correlation. This correlation can be impressive when up to 25 years of drainage chemistry at all monitoring locations (all minesite components) are compiled (Figure 4.2.5-1). Although correlations with pH are seen, these correlations for a particular metal are not the same among minesites (Figure 4.2.5-2), indicating site-specific differences in secondary minerals.

The site-specific differences do not necessarily indicate that different secondary minerals are precipitating or dissolving. Identical minerals can generate different pH levels and metal concentrations depending on many factors. For example, some waste-rock dumps can reach 60°C internally (Case Study 4.4-7) and such temperature variations affect solubilities. Also, small amounts of impurities like zinc and sulfate coprecipitated within ferric hydroxide affect the solubility of the secondary iron minerals. Morin and Cherry (1986) reported that a small amount of ferrous iron within calcite can lower its solubility by one order of magnitude.

Figures 4.2.5-1 and 4.2.5-2 reveal much more about drainage chemistry, and Rate2 in Figure 4.2.2-1, than just correlations. As indicated previously, annual mean concentrations and standard deviations have been observed to remain generally steady from year to year when pH fluctuates little. In Figures 4.2.5-1 and 4.2.5-2, the mean annual concentrations at each pH are reflected in the “best-fit line” (left-side diagrams), and the distribution of datapoints around the best-fit line is depicted as the “variability” (right-side diagrams). Interestingly, best-fit diagrams often show clustering of datapoints around a near-neutral and an acidic pH for each minesite (pH 7.5 and 4.0 in Figure 4.2.5-2a and pH 7.0 and 3.0 in Figure 4.2.5-2b). This clustering is also seen in parameters like acidity (e.g., Figure 4.4-5). The transient datapoints between the clusters reflect a progressive onset of acidification with partial neutralization, explained as the sub-region concept in Section 4.5.

TABLE 4.2.5-1
Annual Statistics for Drainage Chemistry at a Monitoring Station Receiving Drainages from Several Waste-Rock Dumps and an Open Pit
(adapted data from Morin et al., 1994a and 1995a)

	Log_{10} Mean[1]				Log_{10} Standard Deviation[1]			
	90-91	91-92	92-93	93-94	90-91	91-92	92-93	93-94
pH	6.27	6.93	7.08	6.86	0.71	0.85	0.67	0.69
Conductivity	3.06	3.09	3.1	3.16	0.12	0.09	0.11	0.06
Alkal. (mg/L)	1.74	1.71	1.7	1.62	0.07	0.45	0.36	0.35
Acidity (mg/L)	1.32	1.33	1.51	1.6	0	0.33	0.24	0.05
Cu (mg/L)	-0.94	-1.23	-1.49	-1.43	0.41	0.46	0.42	0.46
Zn (mg/L)	0.41	0.22	0.25	0.41	0.38	0.44	0.4	0.34
Cd (mg/L)	-1.74	-1.82	-1.79	-1.72	0.17	0.22	0.23	0.21
Sulfate (mg/L)	2.89	2.9	2.91	2.93	0.06	0.09	0.08	0.08
Ca (mg/L)	2.37	2.39	2.43	2.44	0.04	0.09	0.06	0.07
Mg (mg/L)	1.46	1.51	1.59	1.6	0.04	0.16	0.07	0.07
Al (mg/L)	-0.78	-0.71	-0.56	-0.57	0.68	0.33	0.35	0.37

[1] All values are logarithms except pH

Many variability diagrams (right-side diagrams of Figures 4.2.5-1 and 4.2.5-2) resemble normal distributions using logarithms, or "lognormal distributions". This allows the calculation of standard deviations and the use of standard probability tables, with adjustments for logarithmic values that can be complex (Aitchison and Brown, 1976; Morin et al., 1994b and 1995b). As explained below, this standard deviation for a best-fit line, which reflects seasonal variations in concentration, is important in the assessment and description of annual drainage chemistry.

The annual standard deviation is generally independent of pH (e.g., Figure 4.2.5-2b), although the average annual concentration is not. This is not necessarily obvious from scatterplots that have more datapoints within one pH range than within another. According to probabilities of normal distributions, the greater the number of datapoints within a pH range, the greater the range in measured concentrations in that range. This is apparent in the left-side diagrams of Figures 4.2.5-1 and 4.2.5-2.

The annual fluctuations defined by the logarithmic standard deviations are caused by natural processes, like temperature variations, and artificial factors like analytical error (Morin et al., 1995b) or filtration effects (Hall et al., 1996). Each of these factors contributes to the standard deviation based on their weighting factors (e.g., Morgan and Henrion, 1990):

$$(\text{log standard deviation})^2 = \text{weight}_{\text{factor1}} * \text{variation}_{\text{factor1}} + \text{weight}_{\text{factor2}} * \text{variation}_{\text{factor2}} + \ldots \qquad (4.2.5\text{-}1)$$

While it would be scientifically satisfying to determine the contribution of each natural and artificial factor to the standard deviation, this is not a practical possibility. In an open-environment systems like a minesite components, the variations and weighting factors of all relevant factors cannot

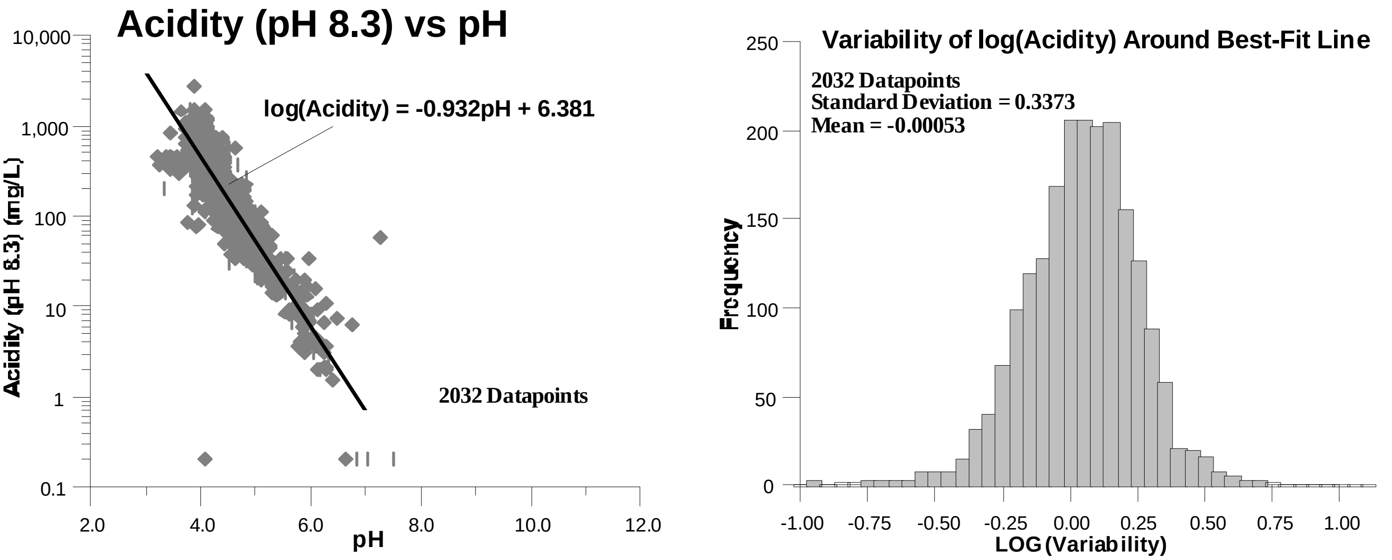

a) an empirical relationship of acidity to pH (adapted from Morin et al., 1995a)

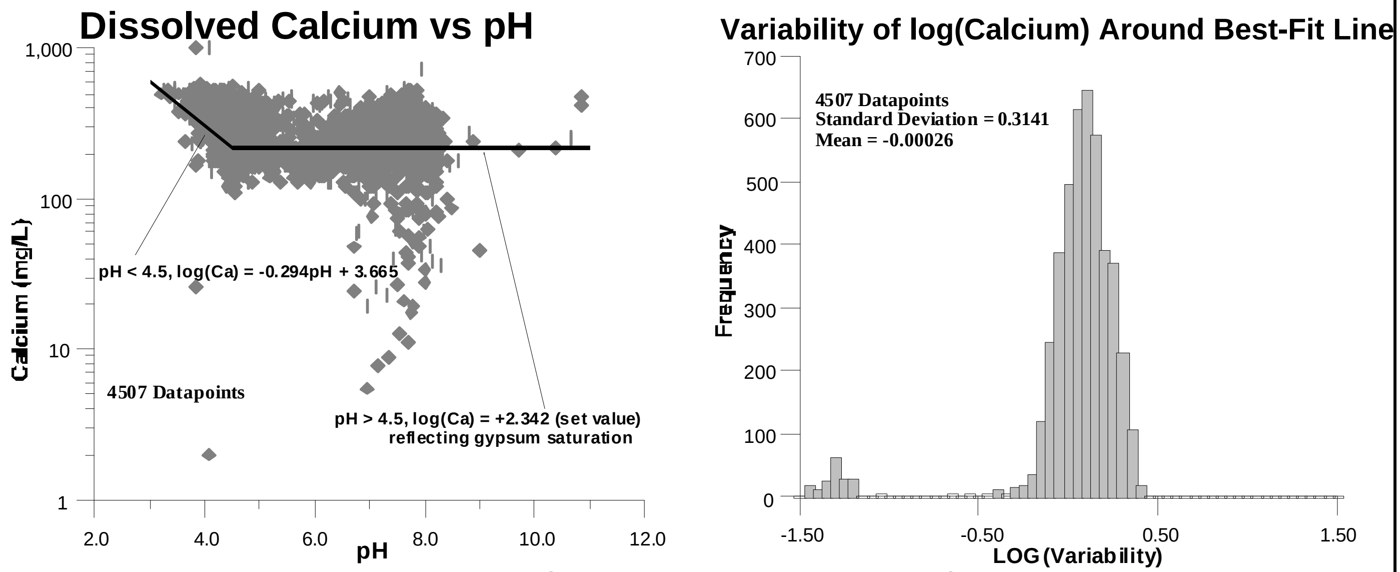

b) an empirical relationship of calcium to pH (adapted from Morin et al., 1995a)

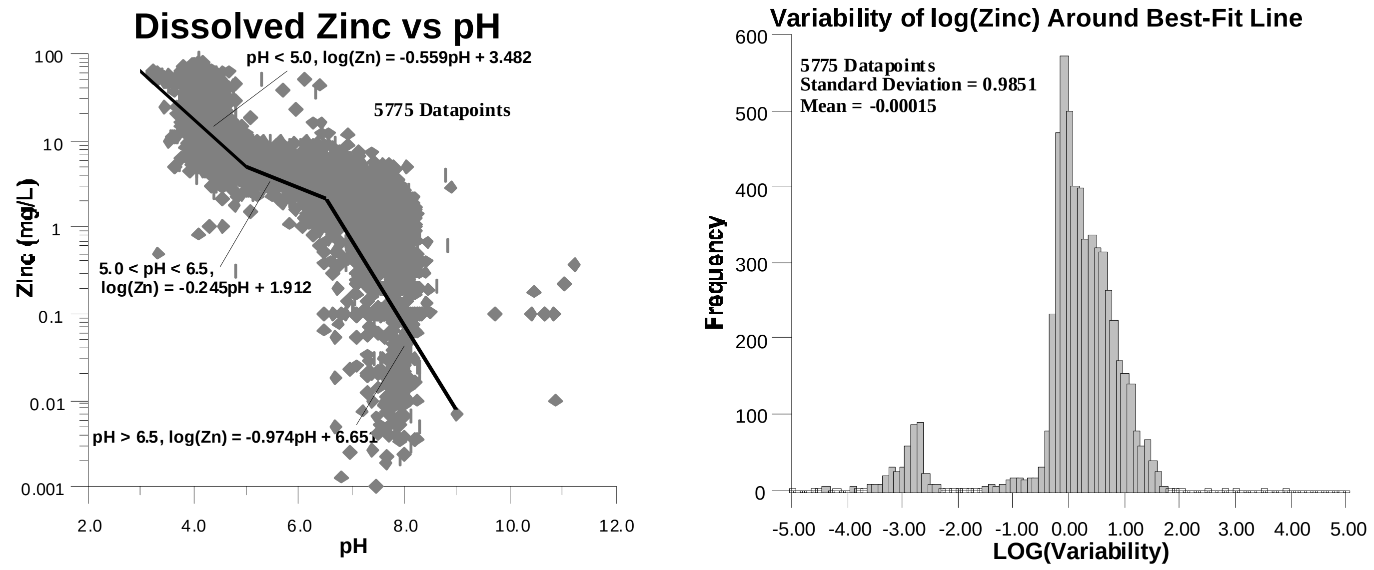

c) an empirical relationship of zinc to pH (adapted from Morin et al., 1995a)

FIGURE 4.2.5-1. Examples of Empirical Drainage-Chemistry Correlations with pH.

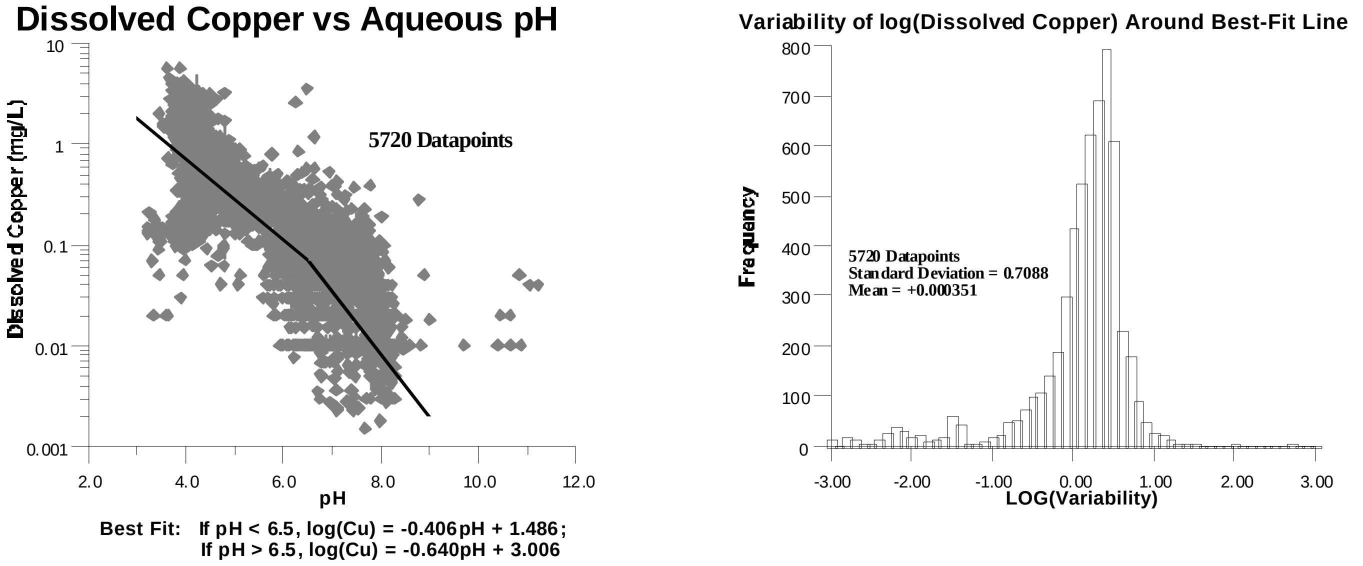

a) empirical relationship of copper and pH at Island Copper Mine (adapted from Morin et al., 1995a)

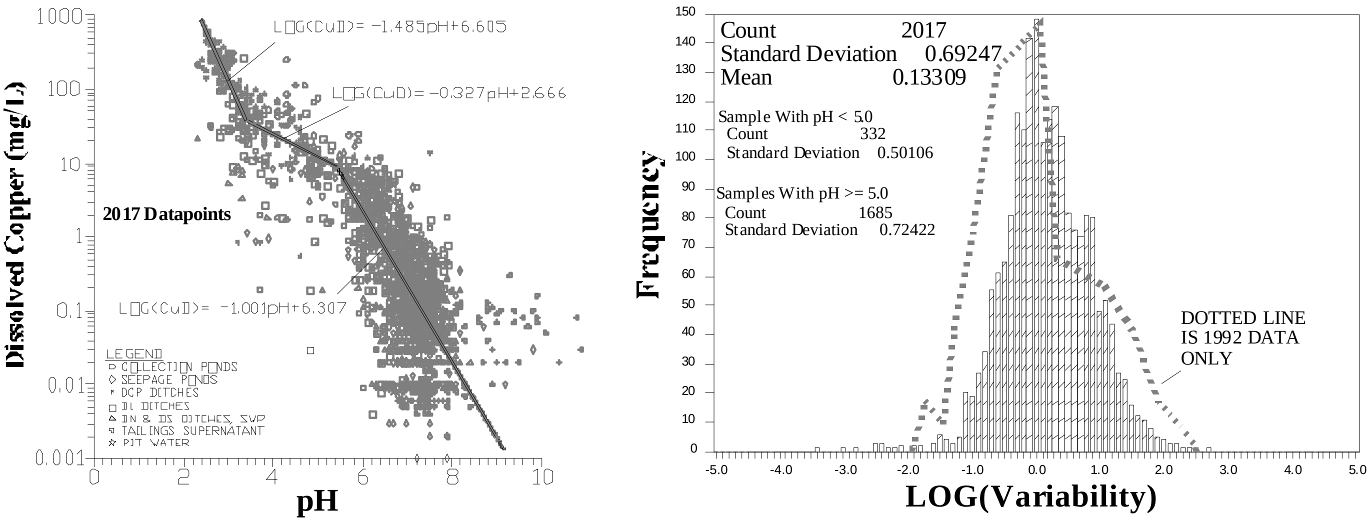

b) empirical relationship of copper and pH at Bell Mine (adapted from Morin et al., 1995b)

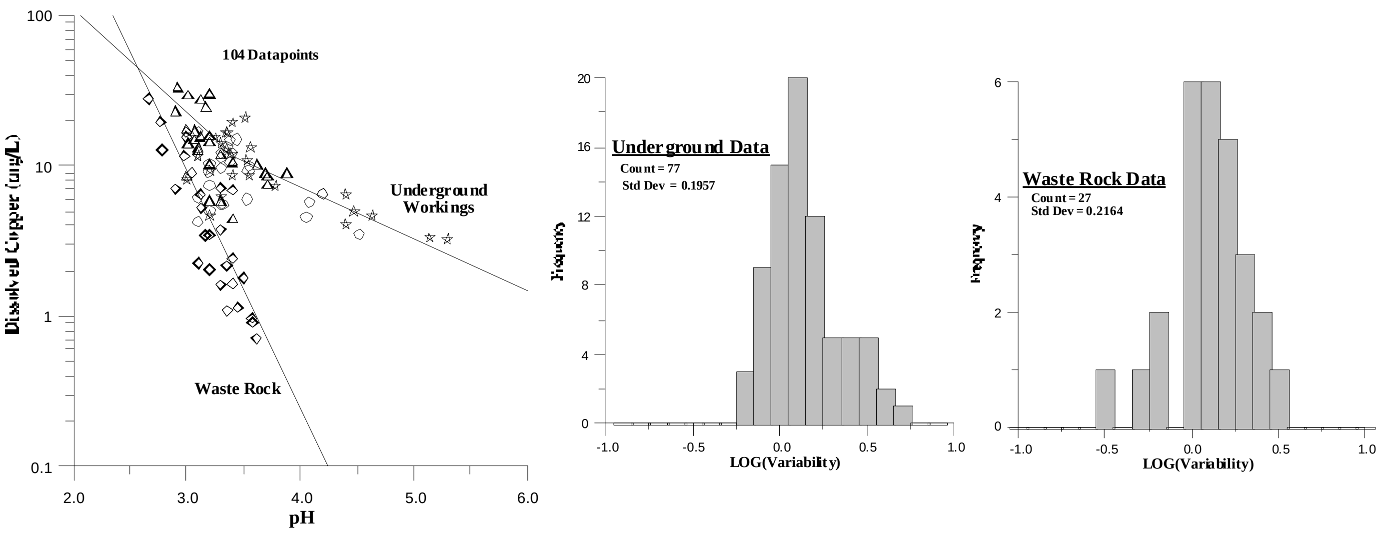

c) empirical relationship of copper and pH at Mine C

FIGURE 4.2.5-2. Examples of Copper vs. pH Correlations at Three Minesites.

be delineated to the level needed for Equation 4.2.5-1. Even if, for example, the standard deviation correlates well with the variation in temperature and thus temperature is given a large weighting factor, this does not rule out the existence of a major factor that mimics the variation of temperature and should thus be given a high weighting. As a result, unless all relevant factors are monitored in detail, any detailed explanation for a standard deviation remains suspect.

Because there are likely several dozen potentially relevant factors affecting drainage chemistry, and because some factors have probably not yet been identified or examined in any detail, there are no detailed examples or case studies on the application of Equation 4.2.5-1. In contrast to this argument, others have stated that all important factors have already been identified and quantified (D.K. Nordstrom, personal communication, 1995).

Despite the foregoing pessimistic view of explaining variations in drainage chemistry, important conclusions can be drawn and emphasized about the annual log standard deviation. No matter what factors contribute to it, the standard deviation has been observed to remain generally constant from year to year at some minesites, even during changes in pH. Therefore, the standard deviation defines, in an empirical manner, the combined seasonal effect of all natural and artificial factors operating at a particular minesite. Independent evaluations of factors like temperature and data quality are therefore not necessary for empirically describing and assessing drainage chemistry.

A compilation of best-fit lines and corresponding standard deviations (e.g., Table 4.2.5-2) is labelled an “empirical drainage-chemistry model” which summarizes the past and current chemistry and is important for future predictions (Chapter 5). It is important to note that Table 4.2.5-2 shows that some parameters do not correlate well with pH. Instead they are relatively constant across the observed range of pH, or correlate better with another parameter like sulfate.

Norecol, Dames, and Moore (1996) examined empirical drainage-chemistry models from a more academic perspective, and suggested statistical refinements that are interesting but cannot be justified at this time. This work also showed that the derivation and use of empirical drainage-chemistry models may not be physically meaningful or statistically valid at minesites with less than a few hundred datapoints. However, Norecol, Dames, and Moore evaluated three datasets with less than 70 metal analyses, one set with 228 analyses, and one dataset with more than 1000 calculated concentrations. As a result, many conclusions and recommendations are questionable. Additionally, there were a few misconceptions in the study on (1) dismissal of values below detection and (2) the use of standard deviation and standard error at a particular pH.

Two related issues arise at this point about the log standard deviation: its physical relevance and the frequency of monitoring needed to obtain it. The physical relevance lies in probability tables for estimating maximum or minimum concentrations over one day or one week. The relevance also includes the probability that a particular concentration will be encountered through a year. Standard probability tables applied to one year (Table 4.2.5-3) indicate that the maximum concentration of one-week duration will be 2.34 log standard deviations above the best-fit line. For example, with dissolved copper at pH 5.0 in Table 4.2.5-2, the average annual concentration is:

$$\begin{aligned}\log(\text{avg. annual copper, mg/L}) &= \\ &= -0.327\text{pH} + 2.666 \qquad (4.2.5\text{-}2)\\ &= -0.327*5.0 + 2.666\\ &= +1.03\end{aligned}$$

Avg. annual copper = 10.7 mg/L

The corresponding maximum one-week-duration concentration of dissolved copper at pH 5.0 is:

$$\begin{aligned}\log(\text{max. one-week-duration copper}) &= \\ &= -0.327\text{pH} + 2.666 + (2.34*0.692) \qquad (4.2.5\text{-}3)\\ &= -0.327*5.0 +2.666 + (2.34*0.692)\\ &= +2.65\end{aligned}$$

Max. one-week-duration copper = 447 mg/L

This approach was confirmed when drainage chemistry was analyzed every four hours, at several sites of waste-rock drainage, for three years (Morin et al., 1993; Morin et al., 1994a; Morin et al., 1995a).

TABLE 4.2.5-2
Example of an Empirical Drainage-Chemistry Model
Including an Open Pit, Several Waste-Rock Dumps, and a Tailings Impoundment
(adapted from Morin et al., 1995b)

Parameter	pH Range	Best-Fit Equation	Log(Std Dev)
Acidity	pH < 3.5	log(Acid) = -0.932pH +5.864	0.345
	pH > 3.5	log(Acid) = -0.360pH + 3.862	
Alkalinity	pH > 4.5	log(Alk) = +0.698pH - 3.141	0.654
Dissolved Aluminum	pH < 6.0	log(Al) = -0.925pH + 4.851	0.429
	pH > 6.0	Al = 0.2 mg/L	
Dissolved Arsenic		< 0.2 mg/L	0
Dissolved Cadmium	pH < 3.0	Cd = 0.07 mg/L	0
	pH > 3.0	Cd = 0.015 mg/L	
Dissolved Calcium		log(Ca) = +0.619log(SO_4) + 0.524	0.375
Dissolved Copper	pH < 3.4	log(Cu) = -1.485pH + 6.605	0.692
	3.4<pH<5.4	log(Cu) = -0.327pH + 2.666	
	pH > 5.4	log(Cu) = -1.001pH + 6.307	
Total Copper		log(CuT) = +0.962log(CuD) + 0.180	0.23
Dissolved Iron	pH < 4.4	log(Fe) = -1.429pH + 6.286	0.807
	pH > 4.4	log(Fe) = -0.455pH +2.000	
Total Iron		If diss Fe>1.0, total Fe=diss Fe	0
Dissolved Lead		Pb = 0.05 mg/L	0
Dissolved Nickel		log(Ni) = -0.317pH + 0.853	0.607
Total Nickel		total Ni = diss Ni	0.613
Dissolved Selenium		Se = 0.2 mg/L	
Dissolved Silver		Ag = 0.015 mg/L	
Dissolved Zinc		log(Zn) = -0.441pH + 1.838	0.667
Total Zinc		total Zn = diss Zn	0.144

TABLE 4.2.5-3
Probability Levels and Corresponding Time Intervals within a Year

Time interval	1 Year	1 Month	1 Week	1 Day	1 Hour
Probability	100%	8.3%	1.9%	0.27%	0.011%
No. Of std. deviations above/below mean[1]	0.00	1.73	2.34	3.00	3.85

[1] From normal-distribution tables (e.g., Pollard, 1977) after dividing probability by 2

Although normal and lognormal distributions theoretically continue to positive and negative infinity, distributions of aqueous concentrations cannot. At lower values, the distribution is truncated by analytical detection limits. At higher values, the distribution is truncated by the maximum solubilities of secondary minerals, and thus the actual concentrations for durations of one second, one minute, and one hour may be the same despite the differing statistical estimates.

The second issue on the standard deviation is the frequency of sampling required to obtain it. Obviously, two samples a year would be sufficient to calculate a standard deviation, but this value may be found inaccurate if more frequent sampling were conducted. Therefore, high-frequency sampling and analysis are theoretically required, which is not always practical and affordable. This leads to a practical alternative that requires only weekly or monthly sampling.

The annual standard deviation calculated from four samples collected in each quarter (each three-month period) should be within a certain "error bar" of the annual deviation calculated from 12 samples collected each month and within another error bar of the deviation calculated from 52 samples collected each week. This approach was used by Morin et al. (1993) and Morin et al. (1994a), who compared all these standard deviations to the "real" deviation obtained from sampling every four hours. For each time interval (quarter, month, week, and day), they calculated 25 values of the deviation: one using the midpoint samples of the intervals and 24 using a random-number generator for sample selection (Figure 4.2.5-3, left side). This showed that the error, or range, in the calculated deviation decreased with increasing frequency, and the range converged on a central value. This trend was also noted for the calculation of the annual average concentration (Figure 4.2.5-3, right side).

Anomalies were noted at this monitoring station, however, because lime was occasionally added upstream of the station and caused pH to rise from approximately 6 to above 10. The selection of an alkaline sample can be seen in the occasionally high datapoint for standard deviations.

This analysis showed that, for an acceptable level of error equivalent to typical analytical error, weekly to monthly analyses would be sufficient to obtain reasonably accurate standard deviations and means. No special timing of the sampling was needed.

4.2.6 Relationship of Drainage Chemistry to Flow and Loading

One factor that can affect drainage chemistry is the flowrate of drainage through and from a minesite component. In a fundamental sense, there is no drainage chemistry if there is no drainage. However, available studies have shown that there is little correlation between flow and concentration (e.g., Figure 4.2.6-1), probably reflecting the stronger effects of other factors like equilibrium reactions. This general independence, or minimal dependence, of concentrations to flow has not been widely tested for, so it is not known whether it is common. Nevertheless, where a correlation exists, the effect of flow is automatically included as part of the annual standard deviation using the approach of Section 4.2.5.

One parameter, dependent on both flow and concentration, is "loading" (concentration multiplied

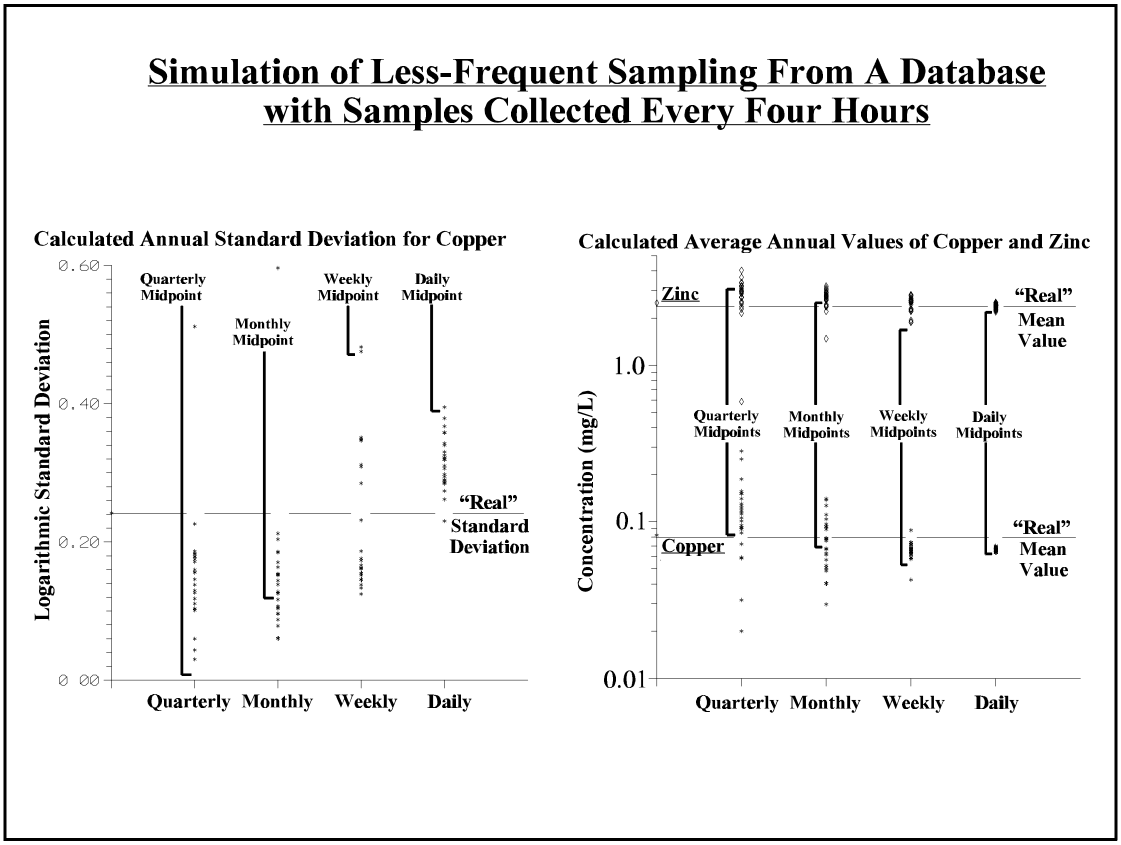

FIGURE 4.2.5-3. Simulations of Less-Frequent Sampling with a Database of Samples Collected Every Four Hours (adapted from Morin et al., 1993).

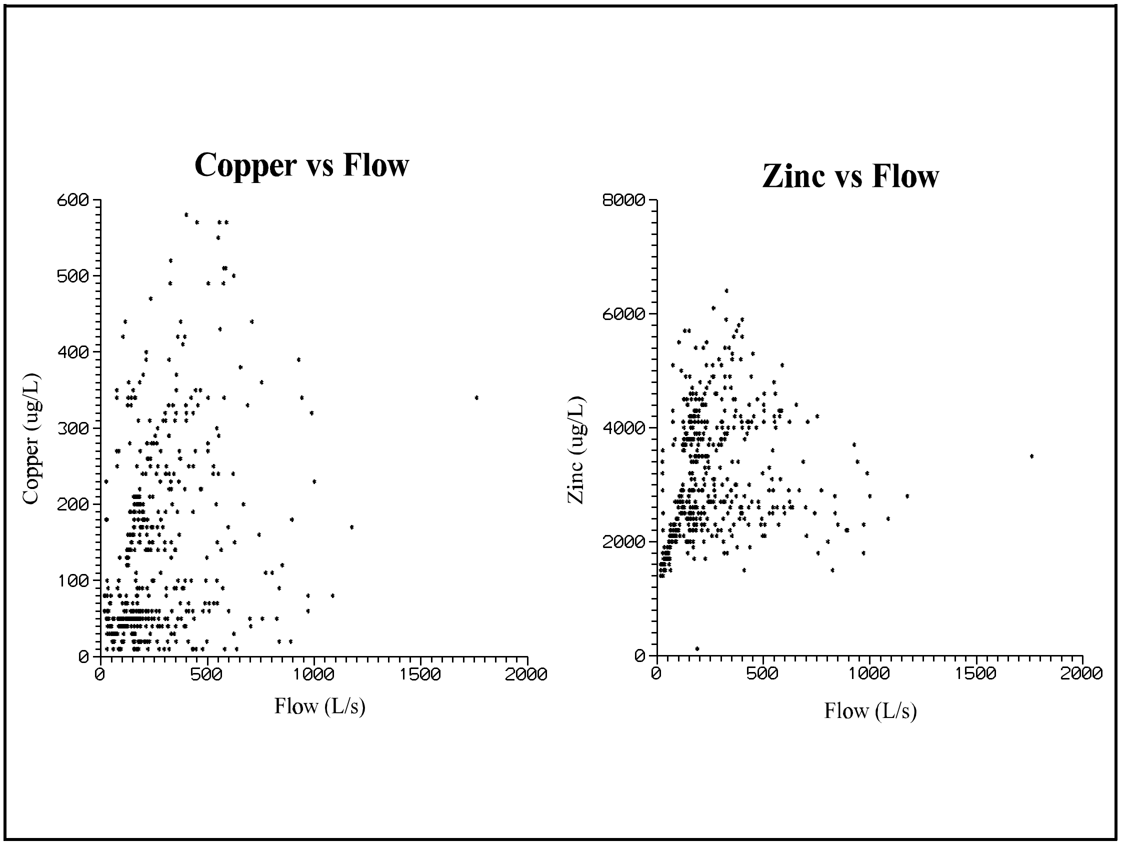

FIGURE 4.2.6-1. Scatterplots of Flow against Copper and Zinc (adapted from Morin et al., 1994a).

by flow), which can be important in aspects of minesite-drainage chemistry, like the costs for some reactive controls on drainage chemistry (Chapter 6). The calculation or prediction of loading requires assessments or predictions of both flow (Chapter 3) and concentrations (Chapters 4 and 5).

Case Study 4.2-1: Chemical Effect of Secondary Minerals at a Reclaimed Coal Minesite

highlights: attempted control of acid generation and sulfide oxidation using sewage sludge; effect of secondary minerals on drainage chemistry

Cravotta (1994) reported a groundwater study at a reclaimed surface coal mine in northwestern Pennsylvania, USA. Sewage sludge had been applied to the overlying topsoil to reduce oxygen flux to the pyrite through organic consumption of oxygen. Despite dissolved oxygen concentrations of less than 1 mg O_2/L, aqueous concentrations of sulfate and acidity increased with depth below the local water table. This was attributed to the dissolution of secondary minerals, the oxidation of deeper pyrite by Fe^{3+}, and the hydrolysis of Fe^{3+}. Mineral-saturation indices from groundwaters in a multilevel well suggested that the sub-region concept of neutralization (defined in Section 4.5) applied in this groundwater system.

Case Study 4.2-2: Behavior of Cyanide in Minesite Drainage

highlights: use of cyanide in milling; mobilization of metals as cyanide complexes; mechanisms to reduce toxicity of cyanide

Cyanide (CN) has received particular attention in minesite-drainage studies of tailings impoundments and heap leaching due to its toxicity (e.g., Case Study 4.4-4). Its complex chemical behavior also provides a challenge in assessing and predicting concentrations.

Cyanide is typically used in milling of precious-metal ores, often added as NaCN to the mill process or to heap-leach solutions in order to complex and carry solid-phase gold into solution. However, due to its complexing ability, cyanide also mobilizes other metals like iron, cadmium, copper, and zinc. There are apparently dozens of metal complexes (Smith, 1994). Cyanide also forms cyanate (CNO^-) when oxidized and thiocyanate (SCN^-) when in contact with sulfide and other reduced-sulfur species. In its free form, cyanide occurs predominantly as HCN^0 below pH 9.3 and as CN^- at higher pH. A hybrid form, known as Weak Acid Dissociable (WAD) cyanide, includes free and weakly complexed forms, and is sometimes used in water-quality criteria because it generally reflects overall toxicity.

Published literature discusses various mechanisms capable of “degrading” cyanide in minesite drainages, although some of the mechanisms like precipitation and complexation do not lead to true destruction. A more appropriate term would be “toxicity-reduction mechanisms”, which are: (1) volatilization of HCN into the atmosphere, (2) strong aqueous complexes with metals, (3) precipitation of relatively insoluble metal-cyanide compounds, (4) biodegradation, (5) adsorption to mineral and soil surfaces, (6) hydrolysis at low pH to formate compounds, and (7) formation of cyanate and thiocyanate (Smith, 1994). The latter mechanism can operate in reverse and, especially at high concentrations, toxic levels of free cyanide can then be re-created. Some proposed water-quality criteria include cyanate and thiocyanate.

Under field conditions in warmer tropical climates, volatilization and biodegradation of free cyanide can be dramatic in their ability to reduce aqueous concentrations (Case Study 6.2-1). In other cases where complexes represent a large proportion of total cyanide (Table 4.2.5-4), the loss of free or WAD cyanide lessens toxicity but does not significantly affect total cyanide.

Case Study 4.2-3: Drainage Chemistry at Potash Mines

highlights: mining of highly soluble chloride minerals; high concentrations in drainage chemistry; migration of potash-tailings drainage as a density plume

TABLE 4.2.5-4
Example of Cyanide Degradation in Tailings Drainage,
Golden Cross Project, New Zealand
(from Smith, 1994)

Days of Exposure	pH[1]	Total CN (mg/L)	WAD CN (mg/L)
0	10.2	29.4	6.8
1	8	29.4	-
3	8.2	30	-
7	8.2	30	-
14	8	31.9	-
28	7.3	32	0.33

[1] Volatilization of free cyanide is enhanced below pH 9.

Potash (KCl) mining involves the removal of salt beds and subsequent milling to separate the economic KCl from the major, uneconomic NaCl, minor K-bearing impurities, and minor "slimes" (sulfate, carbonate, silica, and/or clay minerals). Either underground or solution mining (Section 2.2) is typically used to remove the salt beds. Tallin et al. (1990) reported that potash mining in the Canadian Province of Saskatchewan annually generated $28x10^6$ t of tailings and $11x10^6$ m^3 of concentrated drainage.

Unlike most types of tailings, potash tailings are highly soluble because they often consist of more than 90% NaCl with other minor chloride minerals and clayey "slimes" (Johnson, 1984). Thus they can generate drainages with up to hundreds of thousands of mg/L of sodium, potassium, and chloride (Vonhof, 1983; Pufahl and Johnson, 1987; Morin, 1988a; Case Study 6.1.1-3).

The tailings are often fractured due to drying and shrinkage. Rainfall may be directed into vertical fractures, where it dissolves and widens them. This probably accounts for reports of "caverns" within potash tailings piles. However, within relatively unfractured tailings, groundwater displays Darcian behavior (Section 3.1) with hydraulic conductivities (for brine) around 10^{-4} m/s (Wong and Barbour, 1987). Because the formation of secondary minerals is apparently not significant, there will often be no significant Second Stage (Figure 4.2.2-1) for potash-tailings drainage.

The concentrated drainage derived from infiltration of precipitation and mill discharge behaves differently in the environment than most types of minesite drainage. Due to the high concentrations, the drainage can migrate as a distinct, dense mass, similar to dense non-aqueous-phase liquids (DNAPLs). Consequently, the drainage may "sink" through shallow aquifers or migrate along the bottom of surface watercourses beneath dilute water. Eventually, mixing and dilution with background water will eliminate the distinct mass, but significant distances and time can be required due to the several orders-of-magnitude contrast in total dissolved solids.

For reactive control of potash-tailings drainage, the drainage can be intercepted by standard techniques like seepage-collection ditches and pump wells (Tallin et al, 1990; Case Study 6.1.1-3). Also, to minimize environmental effects, emphasis has been placed on backfilling underground workings with tailings and injecting drainage and dissolved tailings into deep geologic formations (Prugger, 1992).

Case Study 4.2-4: Effect of Freezing and Permafrost on Drainage Chemistry

highlights: lack of control on drainage chemistry by frozen conditions; acidic drainage noted at minesites and mining projects in permafrost areas; deep oxidation of natural sulfide deposits in frozen ground

Because drainage chemistry is determined by reactions of primary and secondary minerals, any process that slows these reactions could affect concentrations. Cold climates, particularly permafrost regions, have been long thought to be effective controls on drainage chemistry. However, a recent review of studies at minesites and mining projects in permafrost, and of general studies of geochemistry in cold climates, revealed that freezing conditions do not necessarily limit mineral reactions and aqueous concentrations (Dawson and Morin, 1996).

Based on literature, Dawson and Morin (1996) could attribute significant reaction rates and elevated drainage concentrations to combinations of (1) expulsion of porewater during freezing, (2) unfrozen water contents even at temperatures below -10°C that could result in effective hydraulic conductivities of nearly 10^{-7} m/s, (3) effective ionic diffusion coefficients of $2\text{x}10^{-11}$ m^2/s at -15°C which can be enhanced by thermal gradients, (4) the increasing aqueous solubility of dissolved oxygen with decreasing temperature, (5) increased reactive surfaces due to frost shattering, and (6) acclimation of bacteria to cold temperatures such as *Thiobacillus ferrooxidans* (Section 4.2.4) to temperatures below +12°C.

A survey of 15 minesites in northern Canada with the potential to generate net acidity revealed that seven had acidic drainage. Additionally, for tailings and waste rock in permafrost climates, detailed field and laboratory studies at several minesites and mining projects showed that metal leaching and/or acid generation were viable environmental concerns. Occasionally, the laboratory testwork predicted no degradation of drainage chemistry, whereas field data confirmed the degradation.

Furthermore, naturally occurring massive sulfide deposits in permafrost climates, exposed at the surface for thousands of years, were still releasing acidic drainage with elevated metal concentrations. Cameron (1977 and 1979) reported that pH in surrounding surface waters and soils were as low as 2.4 and speculated that oxidation and acid generation were occurring at depths of up to tens of meters. Shastkewich (1966) reported that sulfide oxidation was occurring in Russian deposits to depths of 70 m. This is discussed further in Case Study 4.5-5. Nevertheless, on the effect of permafrost, Cameron (1977) concluded,

> "Permafrost is no deterrent to active oxidation of sulphide bodies. In fact O_2 is more soluble in cold water and the exothermic nature of many oxidation processes provides a continuing energy source. In frozen ground, thin, intergranular water films allow chemical processes to be active, even in winter. . . . The presence of springs and sink holes in the vicinity of the mineralization show that taliks (thawed channels) exist in the permafrost."

4.3 Drainage Chemistry from Mines

The patterns of drainage into, through, and from mines were described in Section 3.2. Although these patterns can be site-specific and complex, Section 4.2.6 explained that the chemistry of the drainage is not often strongly dependent on its flow. Therefore, a great deal of theory pertaining solely to the mine component is not needed. Instead, this section focusses on case studies. Additional, related information can be found in Section 5.4.2.

Case Study 4.3-1: Chemical Effect of Groundwater Drawdown Around Mine Components

highlights: effect of groundwater drawdown on groundwater chemistry near mines; anomalous upgradient effects on water chemistry near open pits

McCurry and Rauch (1986) and O'Steen and Rauch (1983) evaluated more than 100 groundwater samples from wells near open-pit and underground mines in West Virginia, USA. Although groundwater drawdown (Sections 3.2.1) conceptually prevents the migration of any contaminated water from a mine, these researchers identified chemical effects outside pits up to 460 m laterally and 30 m vertically based on sulfate concentrations. The concentrations decreased exponentially with distance from the pits. However, because even upgradient wells showed effects, the cause of increasing sulfate may not be migration from pits, but the exposure of fresh rock to air in the drawdown cone (e.g., Figure 3.2.1-1). Water-chemistry effects of underground mines were less than those from the open pits.

Case Study 4.3-2: Pit Backfilled with Waste Rock

> *highlights: placement of acid-generating waste rock into a mined-out open pit, followed by flooding; delineation of groundwater movement around and through the pit; subsequent groundwater contamination downgradient of the pit*

The closed base-metal Solbec Mine in Quebec, Canada, and was operated from 1962 to 1970. A total of 1.5×10^6 metric tonnes of rock was extracted through underground cut-and-fill (Type 1, Figure 2.2-5). An additional 4.0×10^5 t was removed from a Type 1 pit (Figure 2.2-1) in 1964 and 1965 (Figure 4.3-1). The Solbec mill continued operating by processing ore from three nearby mines until 1977, processing a total of 4.9×10^6 t of ore. In 1988, 276,000 m^3 of waste rock and mine wastes, mostly of sand to cobble size with sulfide minerals, was placed into the dewatered open pit at the site, in effect creating a Type 2 dump (Figure 3.3-2). A till dyke installed around the pit perimeter allowed the pit-water level to be raised to 1.5 m above the backfilled rock after a 5-cm layer of non-dolomitic limestone was placed as a cap.

Ross et al. (1994) described a study of the physical and chemical hydrogeology of this backfilled pit (Figure 4.3-1). The pit walls and floor were fractured chloritic schist and sericite. Drillholes into the backfill revealed that up to 6 m of fine material had accumulated in the pit prior to backfilling. A small proportion of this material was attributed to deposition of 1×10^4 m^3 of mine wastes during the last stages of mining and milling.

The underground workings were at least 10 m below the pit floor. However, some shafts extended from the pit floor into the workings providing hydraulic connections, although these shafts may have been filled and covered with till before the placement of waste rock. Other shafts extended from ground surface around the pit to the workings.

Ross et al. (1994) drilled five boreholes: two inside the pit and three around the pit perimeter (Figure 4.3-1). Multilevel piezometers were placed in four of the five holes. Based on piezometers, groundwater flow was generally lateral from north to south through the backfilled rock, with some variable vertical gradients along the flowpaths. Based on hydraulic conductivities of 1×10^{-6} to 1×10^{-7} m/s in the surrounding fractured bedrock which limited flow, a maximum porosity of 0.01, and a hydraulic gradient of 0.03, the average linear groundwater velocity was estimated at 10-95 m/yr. Total volume of groundwater flow was estimated at 1.2×10^4 m^3/yr. Perturbations of groundwater movement caused by the underground workings could not be determined with the available piezometer network.

An electromagnetic survey revealed that groundwater contamination extended 120-160 m south from the pit perimeter, which was consistent with contaminated piezometer samples to the southeast of the pit. Porewater in the submerged waste rock contained more than 1 mg/L dissolved oxygen and thus ongoing oxidation of sulfide minerals was considered a possible source of the groundwater contamination. Also, since the waste rock was a past source of acidic drainage and leached metals before placement in the pit, the simple flushing of accumulated reaction products could account for the downgradient contamination. Further monitoring was recommended to distinguish between the two causes.

Ross et al. (1994) provided little water-chemistry data. However, bar charts presented for a few parameters suggest the concentrations are regulated by chemical equilibrium.

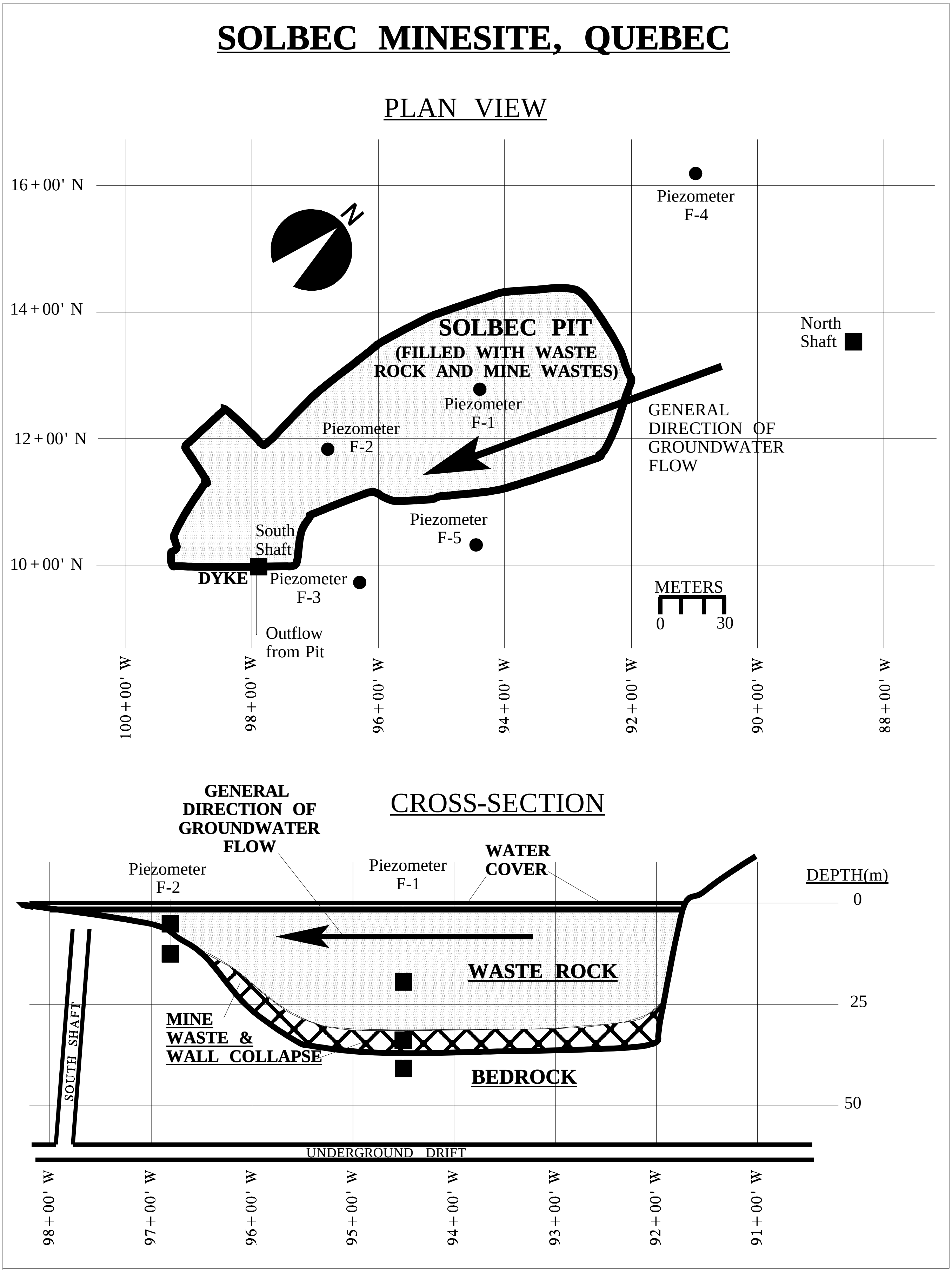

FIGURE 4.3-1. Plan and Cross-Section of the Solbec Pit (adapted from Ross et al., 1994).

Case Study 4.3-3: General Assessment of an Open Pit and Surrounding Minesite Components

highlights: integrated hydrogeologic study of an open pit and surrounding minesite components; prediction of water levels in a flooding pit; delineation of subsurface drainage with more than 100 mg Zn/L

The No. 6 Minesite (Figure 4.3-2) in New Brunswick, Canada, began operating in 1966 and closed in November 1983 (St-Arnaud and Aiken, 1991). The geology of the minesite is dominated by coarse-grained, quartz-rich meta-gabbro of Ordovician age. The orebody contained massive interlayered sulfide beds consisting mostly of pyrite, pyrrhotite, chalcopyrite, galena, and sphalerite. Local faulting was identified with up to 30 m of displacement that also brecciated the nearby sulfide beds up to a width of 1 m. Overburden covering the rock is predominantly compact sandy silty basal till.

Ore containing economic levels of zinc, lead, copper, and silver was mined from a Type 1 pit (Figure 2.2-1) with limited underground workings, for a total of 1.21×10^7 tonnes. At the same time, approximately 3.0×10^6 m^3 of waste rock and waste sulfides from the operation were placed in the North, East, and Pyrite Waste Dumps (Types 1 and 3, Figures 3.3-1 and 3.3-3). An additional 2.1×10^5 m^3 was used for roads and foundations and lesser amounts were placed in the South waste pad. Approximately 8×10^4 m^3 of tailings from a pilot-scale milling operation was also placed on the site.

Maximum depth of the No. 6 Pit was 185.4 m and lateral surface area at the overflow elevation of 2581.7 m was estimated at 11.1 ha. The underground workings joined the south side of the pit near the base. Total volume of the pit excluding the workings was 8.5×10^6 m^3. The water level in the pit was approximately 50 m below its overflow elevation, but was expected to reach it by the Year 2000.

Identified or suspected sources of acidic drainage at the site were: mine walls, the waste-rock dumps and pads, the pyrite dump, the tailings pond, acid-water holding and settling ponds, a natural on-site pond, roads, and building foundations (Figure 4.3-2). Acidic drainage from the site was treated seasonally with lime and an average of 3.7×10^5 m^3 of treated water was annually discharged into the pit for settling of precipitants (secondary minerals). Additionally, high-pyrite acidic waste rock was dumped into the southeast corner of the flooded pit.

St-Arnaud and Aiken (1991) conducted a hydrogeologic study of the minesite with 36 monitor wells and a few samples of pit water. Most groundwater was expected to flow through the fractured, shallow bedrock, with hydraulic conductivities between 10^{-4} and 10^{-7} m/s and a mean (apparently geometric average) of 1.27×10^{-5} m/s. Because vertical hydraulic gradients were negligible, groundwater flow was expected to be predominantly lateral at calculated average velocities of 100-1000 m/yr.

Groundwater levels in the wells indicated drawdown caused groundwater only within roughly 100-200 m of the pit to move into it (e.g., Figure 3.2.1-2). The shape of the drawdown cone around the pit showed marked anisotropy with relatively steep hydraulic gradients to the north and west of the pit. When the pit fills to its equilibrium level, groundwater is predicted to migrate southward through the pit area toward a brook more than 500 m away.

The rate of groundwater flow into the pit was calculated through the "equivalent well approach" attributed to Singh and Reed (1988) and modified from the Dupuit Equation for lateral flow in an unconfined aquifer:

$$Q(t) = BK\,(H^2 - h^2(t))\,\ln(R(t)/r) \qquad (4.3\text{-}1)$$

$$r = (2/B)\,(Y * W)^{0.5} \qquad (4.3\text{-}2)$$

where Q(t) = flow ("t" accompanying a variable indicates its value changes through time)
K = bulk hydraulic conductivity
H = regional elevation of water table
h(t) = pit-water level at a specific time
R(t) = radius of groundwater drawdown caused by the pit
r = "equivalent-well radius" of the pit
Y = length of the pit
W = width of the pit

Based on flows from this model plus precipitation, treatment discharge, and the addition of waste rock, and subtracting evaporation, the June 1990 water-level elevation was accurately predicted by St-Arnaud and Aiken (1991). This meant that an average volume of 470,000 m^3 was accumulating in the pit each year. As a result, the pit-water level was expected to rise to the regional water-table level in 1995 and continue rising until the pit overflows in 1999. Flow from the pit would then follow both subsurface and surface pathways. Before that time, control measures will likely be implemented, involving collection of contaminated water within the pit with seasonal pumping to a treatment plant.

Pit-water analyses showed zinc exceeding 59 mg/L and pH less than 4. All physical and chemical parameters were relatively constant in each lateral plane, but pH and total iron were consistently lower at depths less than 4.3 m. This difference at shallow depths was attributed to iron oxidation and acidic rain.

Around most of the minesite, aqueous sulfate concentrations in groundwater exceeded 2000 mg/L, showing that the effect of sulfide oxidation was pervasive. However, groundwater with pH less than 5.0 and zinc greater than 100 mg/L was limited to the north and east of the pit (Figure 4.3-2), apparently reflecting subsurface acidic drainage from the North, East, and Pyrite Waste Dumps and the tailings area. Maximum reported zinc concentration in groundwater was 3240 mg/L beneath the North Waste Dump.

Case Study 4.3-4: Series of Type 1 Pits and Other Downgradient Components at One Minesite

highlights: drainage movement from pit to pit at a uranium minesite; trends in water-column chemistry within flooded pits

The inactive Midnite Minesite is located on the Spokane Indian Reservation, approximately 40 miles northwest of Spokane, Washington (Sumioka, 1991). The minesite has approximately 130 ha of disturbed land and lies at an altitude of approximately 850 m. The site has warm, dry summers and clear, cold winters with snow. Average precipitation at a nearby town was 49 cm/yr over a 29-year period. The mine is mostly limited to one topographic basin which is drained by three small streams that converge (Figure 4.3-3).

Ore-grade uranium was discovered in 1954 at geologic contacts between Precambrian metasedimentary rock and intruded quartz monzonite. Near the surface, uranium occurs as autunite and meta-autunite, whereas at greater depth it occurs as uraninite and coffinite and is associated with pyrite and marcasite. Quaternary alluvium covers the rock in places.

Mining for uranium was conducted between 1956 and 1982 except during a shutdown period from 1962 to 1969. The site contains two pits (Pit 4 and the larger Pit 3), one ore stockpile, and two waste-rock dumps (Figure 4.3-3).

In 1978, a yellow-white precipitant was noted in a creek bed draining the site, extending several hundred meters below the mine boundary. This precipitant was found to contain aluminum-bearing minerals, gypsum, and 3-6% uranium oxide, which was taken as evidence of significant metal leaching. As a result, a retention pond and dam were constructed and water from this pond and Pit 4 was occasionally pumped to Pit 3. Nevertheless, a small flow of surface water with total dissolved solids of approximately 6,000 mg/L still bypassed the dam.

Pit 3 is located near the center of the minesite. It has a maximum depth of approximately 170 m, a lateral area of 3.6 ha at full water level, and an estimated volume of 4.4×10^5 m^3. Pit 4 at the north end of the site has a maximum depth of roughly 140 m, a lateral area of 2.4 ha at full water level, and an estimated volume of 1.8×10^5 m^3. The southern rim of Pit 4 was raised 12-15 m with fill in 1982 to prevent surface overflow. The retention pond below these pits has a maximum depth of 9 m, a surface area of 0.4 ha, and a volume of 1.8×10^4 m^3.

Sumioka (1991) reported on a detailed physical and chemical study of the hydrogeology and hydrology of the minesite. Most of the study focussed on site-wide water balance and downstream water chemistry. However, there were chemical analyses of the water columns in Pits 3 and

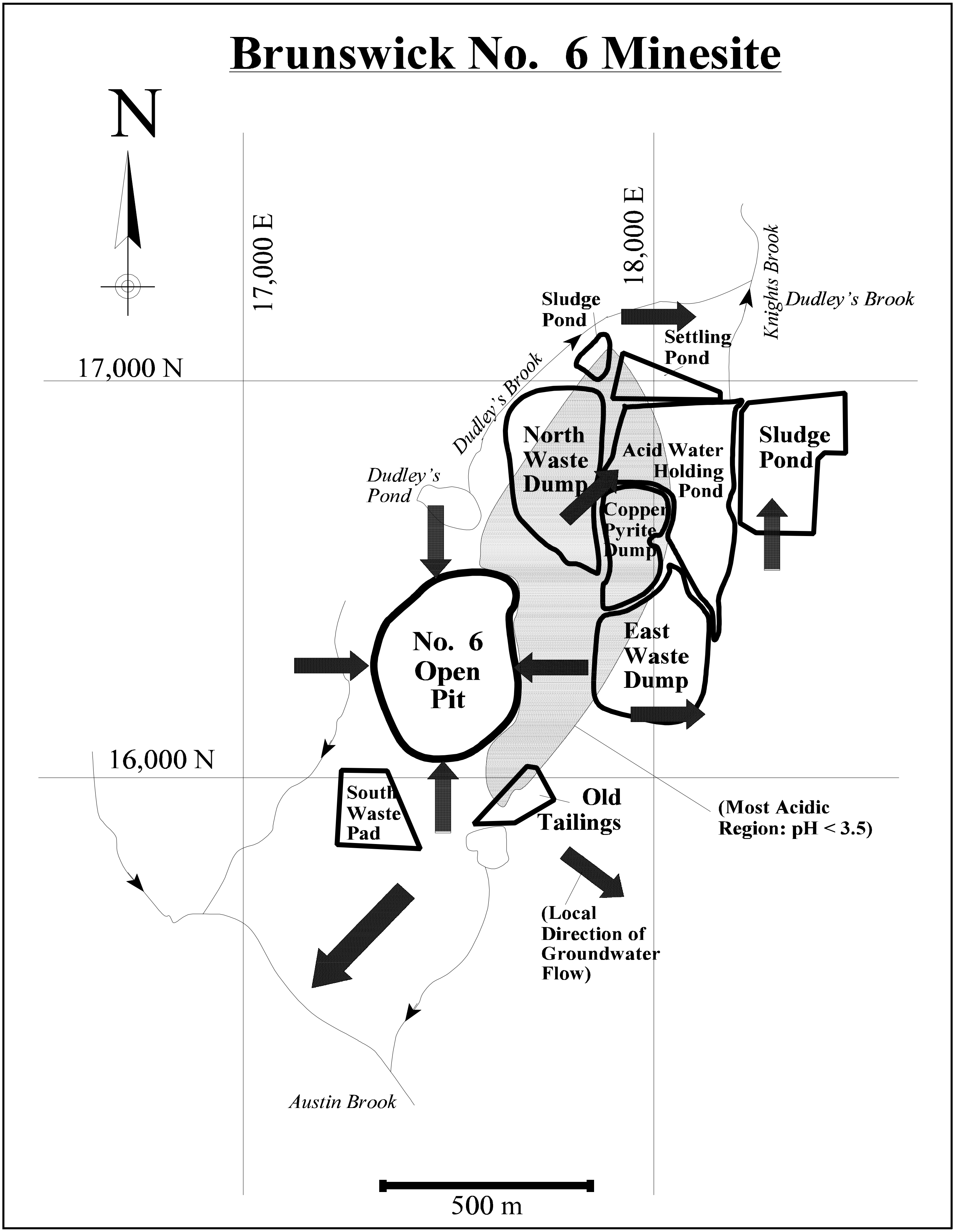

FIGURE 4.3-2. Map, Groundwater Flow, and Acidic Zone at Brunswick No. 6 Minesite; shaded zone indicates the most acidic region (adapted from St-Arnaud and Aiken, 1991).

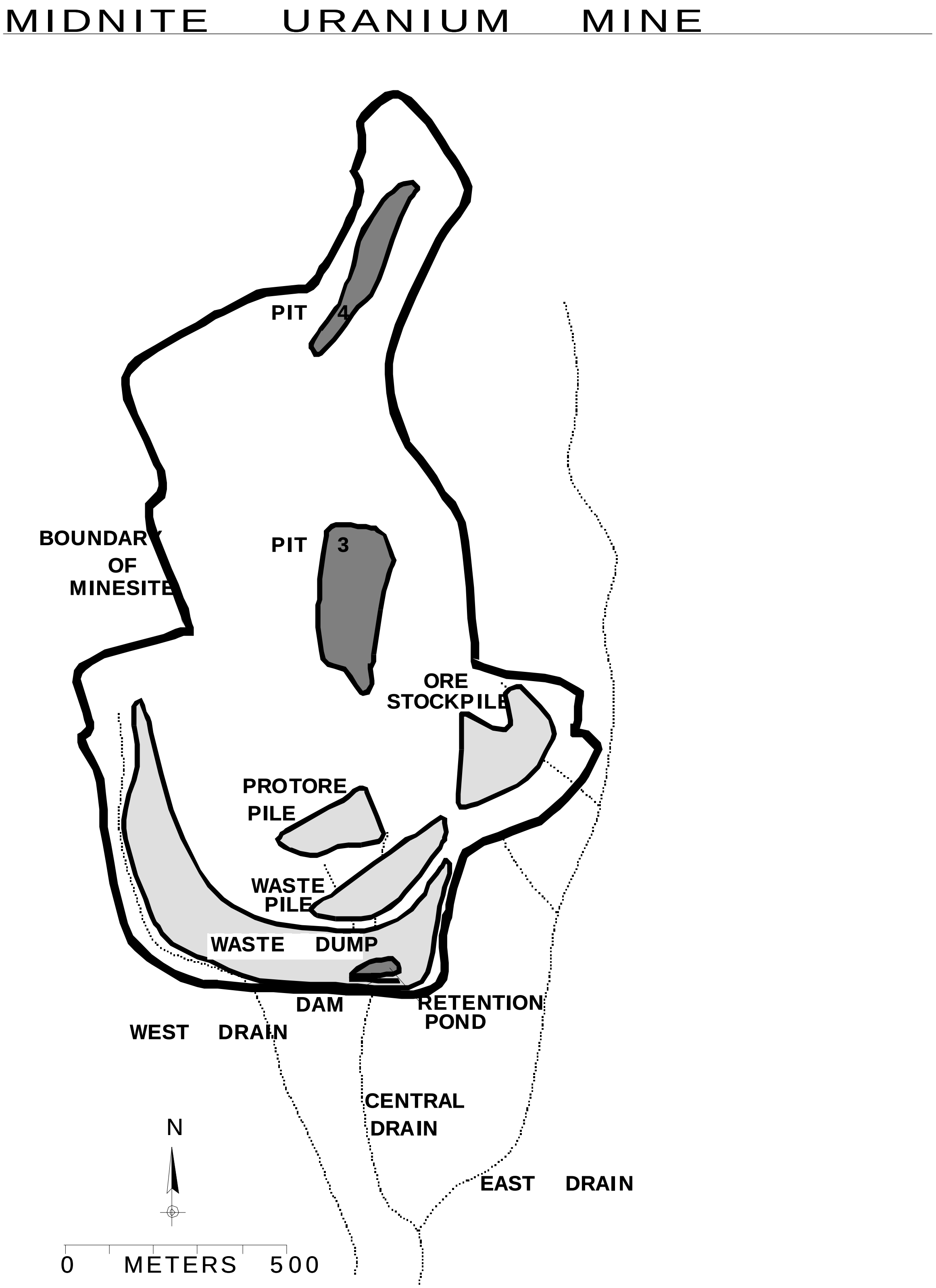

FIGURE 4.3-3. Map of the Midnite Minesite (adapted from Sumioka, 1991).

4, and in the retention pond.

In Pit 4, conductance and pH (~7) were generally steady through time and depth. However, with increasing depth, temperature and dissolved oxygen decreased, while total dissolved solids, ^{226}Ra, and U increased. These trends suggested a relatively stable water column with chemoclines (changes in chemistry, Section 5.4.2) and thermoclines (changes in temperature), and more reducing conditions mobilizing uranium with depth.

In contrast to Pit 4, Pit 3 showed relatively few or minor trends of any parameters through time and depth. The measured pH remained around 4.5. As a result, Pit 3 appeared to remain well mixed with little stratification.

The retention pond showed some decrease of dissolved oxygen and increase of suspended solids with depth. However, like Pit 3, most parameters remain generally steady with pH around 3.6.

Case Study 4.3-5: Trends of Mine-Floor pH in an Underground Mine

highlights: an old base-metal underground mine with more than 240 km of workings; local pH of water on mine floors; water balance for the workings; dye tracer tests to identify water sources

The underground Bunker Hill Mine in northern Idaho, USA, was mined for lead and zinc beginning in 1885. The rock is highly faulted and fractured metamorphic quartzites with interbedded argillites. Annual precipitation in the area is approximately 0.76 m, mostly as snow.

By 1979, the mine had more than 240 km of workings to depths of approximately 1.6 km, representing roughly 180 km^3 of rock. The yearly rate of new drifting and drilling were roughly 6 km and 18 km, respectively. Portions of the underground workings have been backfilled with sand since 1961 and with mined rock before 1961. Some of the mined rock contained elevated levels of lead, zinc, and pyrite, which contributed to acidic drainage and metal leaching from the upper levels.

Trexler et al. (1974) reported more than 400 pH measurements on a simplified two-dimensional vertical profile of the mine (Figure 4.3-4). Acidic pH was encountered most often in the upper levels and near the No. 2 Shaft, but at least one acidic pH was found on most levels.

The availability of water to flush reaction products of acid generation and metal leaching was identified as the major control on water chemistry. On the other hand, Williams (1979) pointed out that the three-dimensional distributions of two orebodies within the mine determines where acidic pH is detected, which has also been noticed at other underground mines (Case Study 4.3-8). Nevertheless, reclamation activities focussed on identification and elimination of surface-water access to the workings.

Drainage from the mine according to two studies was 0.17 m^3/s at an average pH of 3.3 (Trexler et al., 1974), and 0.13-0.16 m^3/s at pH 4.0-4.7 with minimum of 3.3 (Trexler, 1979). The sources of this flow were: surface-water inflow through fractures and faults (69.1%), groundwater inflow (19.0%), and drainage of sand backfill (11.9%).

The main drainage pathways for the mine are the Cherry Ditch, which drains the upper levels, and the Kellogg Tunnel. Hydrographs for the Ditch and Tunnel, and for Milo Creek which drains part of the land surface above the mine, showed a close correlation with more pronounced variations in Milo Creek. General, but more subdued, correlations were noted for deeper levels. This indicated underground flow was hydraulically connected to surface water with the connection decreasing with depth. Potential connections were then identified: (1) fractures between the surface and the upper workings due to surface subsidence, (2) faults between the surface and the upper workings, and (3) a drift and stope on 4 level extending close to surface.

The subsided "Caving Area", measuring 60 m in diameter and 12 m deep, apparently received water from tributaries of Milo Creek. During winter months, a "vapor cloud" of mine air could be seen issuing from this area.

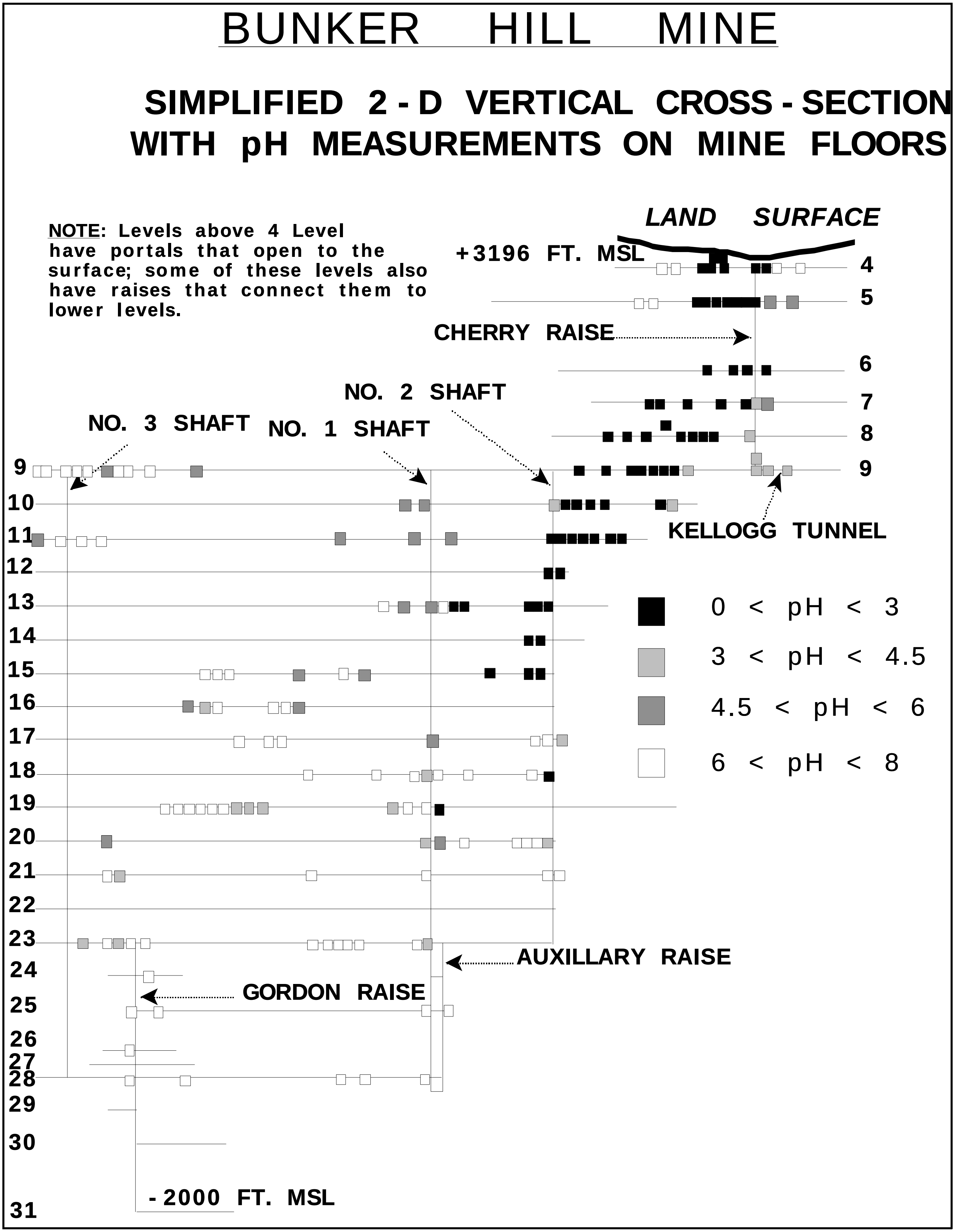

FIGURE 4.3-4. Simplified Vertical Cross-section through Part of the Bunker Hill Mine with Mine-Floo Measurements (adapted from Trexler et al., 1974).

A dye tracer test in the tributaries through the Caving Area then showed that creek water reached 4 level within 15 minutes and 5 level in 30 minutes. In January of 1973, continuous flow monitoring revealed that at least 99% of surface drainage water was caught by the depression and surrounding fractures.

In another portion of Milo Creek, constant dye-release tests in May and July 1973 confirmed that creek water was lost into fractures and a fault zone. Losses ranged from 29-76% of streamflow (0.028-0.093 m^3/s). In adjacent Deadwood Creek, dye tracer tests showed that creek water required 12-36 hours to reach 9 level, located 370 m below and 610 m laterally away from the creek.

Case Study 4.3-6: Natural Flooding of a Large Open Pit

highlights: unwanted natural flooding of a large open pit; water-column chemistry in the pit, including chemoclines and thermoclines; seasonal variation in shallow pit water

The Berkeley Pit in southwestern Montana is reportedly the second largest pit in the USA (Davis and Ashenberg, 1989). Maximum depth is 542 m and lateral dimensions are 1.8 km by 1.4 km. The lower 38 m of the pit had been filled due to collapse of wall material. Underground workings are connected to the pit.

In 1987, the lower 340 m of the pit had been flooded and the water level was rising 22 m/yr due to inflow of groundwater and surface waters (David and Ashenberg, 1989). Total inflow was estimated at 28,700 m^3/day including an estimated loss to evaporation of 300 m^3/day.

Depth-specific samples indicated many parameters generally increased with depth including pH (~3), suspended solids, conductance, aluminum, calcium, total and ferrous iron, and sulfate (e.g., Table 4.3-1). On the other hand, dissolved oxygen and Eh decreased with depth. This demonstrated the presence of chemoclines and a thermocline (Section 5.4.2), and the development of reducing conditions.

Due to metal leaching, concentrations of cadmium, copper, and zinc reached concentrations of 1.9, 214, and 500 mg/L, respectively. Concentrations of iron, calcium, aluminum, potassium, and sulfate were apparently regulated by mineral solubility of ferric hydroxide, gypsum, jurbanite, and jarosite. The presence of reduced sulfur (sulfide), which may lower metal concentrations through precipitation of relatively insoluble sulfide minerals, was not mentioned and thus the pit may not be meromictic or sufficiently reducing.

Changes in appearance and chemistry of the shallowest pit water were noted seasonally. For example, formation of ice cover resulted in the reduction of ferric iron to ferrous iron, with the reverse reaction occurring during summer months. Below a depth of 30 m, water chemistry was relatively steady.

Case Study 4.3-7: Assisted Flooding of a Small Open Pit

highlights: flooding of a pit by storm runoff; groundwater movement in and around the pit; chemistry of pit-water column and bottom sediments; sulfate concentrations in groundwater during and after mining

The Cluff Lake uranium minesite is located in northwestern Saskatchewan, Canada. Mining of one relatively small, shallow orebody at Cluff Lake, named "D", began in April of 1980 (Saskatchewan Environment, 1990 and 1993). D Pit lies in a faulted metamorphic zone that reportedly contains uraninite, selenides, gold, tellurides, nickel-sulfur arsenides, jordisite, minor pyrite, and chalcopyrite.

The cold, boreal climate at Cluff Lake produces cool, short summers and long, cold winters with relatively dry subhumid moisture. Mean monthly temperatures are usually below zero from November to April. Total annual precipitation is approximately 400 mm and evaporation, which is limited to May through September, consistently exceeds total precipitation based on evaporation-pan data. The average annual precipitation and evaporation represent roughly 3.8% and 6.5% of the pit volume,

TABLE 4.3-1
Water Chemistry in the Flooding Berkeley Pit
(from Davis and Ashenberg, 1989)

Depth (m)	pH	Eh (V)	Fe^{2+} (mg/L)	Fe^{3+} (mg/L)	Total Fe (mg/L)
0	2.76	0.82	0.25	196	196
1	2.72	0.72	60	142	202
3	2.84	0.64	262	14	276
15	2.95	0.57	622	28	650
31	3.08	0.50	900	10	910
66	3.15	0.46	938	-	854
100	3.15	0.47	944	14	958
130	3.14	0.46	962	24	986

respectively.

Excavation of D Pit was temporarily halted in October of 1980, but began again in May of 1981. By September 1981, mining was completed after removal of approximately 107,800 tonnes of ore grading roughly 7% U_3O_8. The final pit had a lateral extent of 200 meters by 90 meters with a maximum depth of 23 meters. At the overflow elevation of 332.5 m, the volume was roughly 177,400 m^3.

Active dewatering of D Pit continued until November 1982, then the pit began filling. During spring of 1983, a nearby creek overflowed and filled the pit in 24 hours. A berm was later built to prevent creek water from entering the pit again.

Ice cover usually appears around October 20-30 and open water usually appears around April 17 to May 9. During spring months, snowmelt from the surrounding watershed generated a volume of water exceeding 1000 m^3 causing the pit to overflow. All surface water and groundwater around D Pit move generally westward toward Cluff Lake. Most of the groundwater is believed to move through the shallow overburden due to its elevated hydraulic conductivity (1 to 5 x 10^{-4} m/s) over the fractured bedrock (2 x 10^{-7} to less than 2 x 10^{-9} m/s). The relationship between groundwater and pit water is discussed in more detail later in this case study.

The north wall of D Pit above its flooded, equilibrium water level exposes 10 meters of rock composed of garnet-rich aluminous gneiss with seven fault zones. The dominant fault zone is F-1, containing a one-meter thickness of clays, slightly mineralized breccias, and gersdorffite. F-1 has been identified as a source of metals for pit water, and is assumed to extend to the base of the pit. Part of the east side of the pit is covered with dumped waste rock, which like F-1 has been identified as a source of metals to pit water. On the south and west sides, no rock is exposed above the water level. Iron precipitant on the overburden in the southeast wall indicates groundwater is entering the pit there and apparently exiting through the southwestern wall of overburden.

Monitoring of the flooded pit began in 1983. Results through 1988 are reported by Saskatchewan Environment (1990) and partial results through 1992 are reported by Saskatchewan Environment (1993).

Based on the pit-water chemistry, several conclusions were reached. First, a thermocline forms in D Pit during early spring and summer. As winter approaches, an ice cover forms and the thermal gradient approaches equilibrium across the water column. Second, major ions, metals, and radionuclides occur in higher concentration at depth after spring runoff and rainstorm events. Third, the likely sources of the contaminants are (1) seepage from the nearby waste rock dump and (2) dissolution of materials in the faults and wall rock along the north side of the pit. Another potential source, that required further study, is the possible resuspension of bottom sediments into the water column due to spring and fall turnover.

A sample of bottom sediments obtained with an Eckman dredge showed that the sediment was predominately composed of silicon, aluminum, and iron (Table 4.3-2). The relatively high moisture content and loss on ignition suggested the mineral phases were amorphous or associated with water. Under the assumptions that silicon occurs as silicon dioxide (quartz or an amorphous phase), and that aluminum and iron occur as hydroxides ($Al(OH)_3$ and $Fe(OH)_3$), these three mineral phases would comprise 95% of the bottom sediment and would indicate the presence of significant secondary-mineral precipitants.

The presence of mineral precipitants was further supported by an analysis of suspended sediment (Table 4.3-2), which showed enrichment of arsenic and uranium over the underlying sediments. Because these two elements are more often regulated by solubility and redox conditions than radium, their higher levels suggested they may be precipitating in, and settling from, the water column. In agreement, water-column analyses also revealed a redox “front” at a depth of 19 m in the pit.

Piezometers installed near the edge of D Pit during operation showed effects such as elevated sulfate concentrations. This apparently can be attributed to water-table drawdown around the pit and the resulting entry of oxygen into the walls. After pit flooding, piezometers approximately 400 m downgradient showed a peak about 3 years after the pit-edge piezometers, then decreased in sulfate concentrations. This was consistent with hydraulic conductivities and gradients in the shallow overburden.

Case Study 4.3-8: Complex Seasonal Changes of Drainage through an Underground Mine

highlights: flow and chemistry of water on underground mine floors; bulk hydraulic conductivities based on changes in flow; potential misinterpretations based solely on portal monitoring

Northwest Geochem (1992) conducted a detailed hydrogeologic assessment of the upper levels of the Lynx Underground at the Myra Falls Operations, British Columbia, Canada. Eight upper levels (Type 2, Figure 2.2-6), with portals opening onto the walls of a Type 3 pit (Figure 2.2-3), were examined to measure pH and flow from stopes, drillholes, fractures, and along the mine floor (e.g., Figure 4.3-5).

On a few levels, weirs were installed on the mine floor and periodically monitored for flow and water chemistry. These allowed mass-balance calculations along the length of the mine floor to identify specific areas of diffuse (non-point-source) gain and loss of water (Section 5.4.2).

Based on the diffuse gains of water on several levels, a bulk hydraulic conductivity of $1x10^{-6}$ m/s was calculated for the rock under an assumed hydraulic gradient of 1.0. Within 100 m of the portals, within the perimeter of a Type 3 pit (Figure 2.2-3) that lies above the workings, diffuse gains suggested that hydraulic conductivity increased by one order of magnitude, presumably reflecting additional fracturing from mining.

Interestingly, this study highlighted the potential for incorrect interpretations based solely on flow and chemistry at a portal (Figure 4.3-6). The Level 8 Portal suggested that, as flow increased during early winter months, there was a flushing of accumulated acidity from the level and pH then recovered before flow peaked in December.

In reality, the flow originating on Level 8 in September was pH-neutral, and flow was negligible from two acidic stopes (Stopes X and Y, pH 2.33) bottoming on Level 8 and connected to the surface. As heavy rains began in October, flow rose quickly from Stopes X and Y, causing increased flow at the portal (Figure 4.3-7).

TABLE 4.3-2
Chemical Analyses of Bottom and Suspended Sediment in D Pit
(from Saskatchewan Environment, 1993)

Parameter	Concentration	Parameter	Concentration
Bottom Sediment			
Al (%)	4.6	Si (%)	35.2
As (µg/g)	192	Zn (µg/g)	60
Carbon, inorganic (%)	0.009	Pb 210 (total, Bq/g)	4.0
Carbon, organic (%)	0.80	Ra 226 (total, Bq/g)	4.5
Cu (µg/g)	30	Th (µg/g)	30
Fe (%)	3.1	U (total, µg/g)	279
Mn (µg/g)	300	Moisture (%)	47.8
Mo (µg/g)	14	Loss on Ignition (LOI, %, @ 550°C)	4
Ni (µg/g)	170		
Suspended Sediment (just above pit bottom)			
As (µg/g)	1090	U (total, µg/g)	922
Ra 226 (total, Bq/g)	7.0		

However, the portal flow did not reflect the actual flow through Level 8, because a significant amount was now spilling down a raise just inside the portal to Level 9. As flow from the stopes and other sources increased into December, most of the flow from the stopes reversed on Level 8 and poured down another raise to Level 9. Consequently, less acidic water was reaching the portal and its pH increased.

Northwest Geochem (1992) concluded that there were two primary causes of acidic drainage from the workings. First, stagnation of water on levels allowed it to accumulate acidity and eventually become acidic. The most acidic pH was measured on an abandoned level with no visible flow. Second, a zone of rock with a lateral extent of roughly 10,000 m^2 was often associated with depressed pH, even in moving water. This zone extended diagonally downwards from one level to the next. Acidic Stope Y discussed above was located in this zone. Such a zone also exists at the Bunker Hill Mine (Case Study 4.3-5).

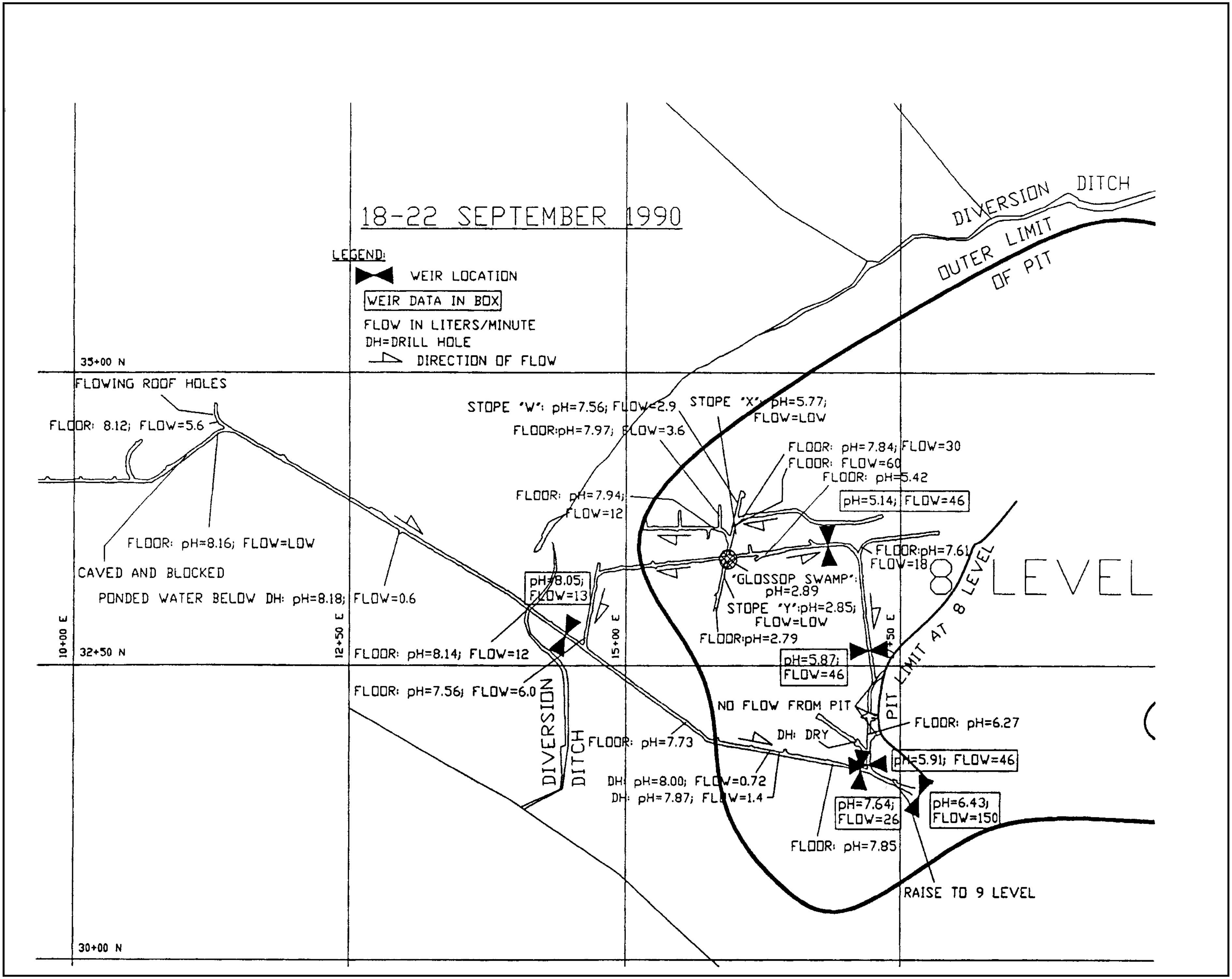

FIGURE 4.3-5. Monitoring of Flow and Chemistry on Level 8, Myra Falls Operations (adapted from Northwest Geochem, 1992).

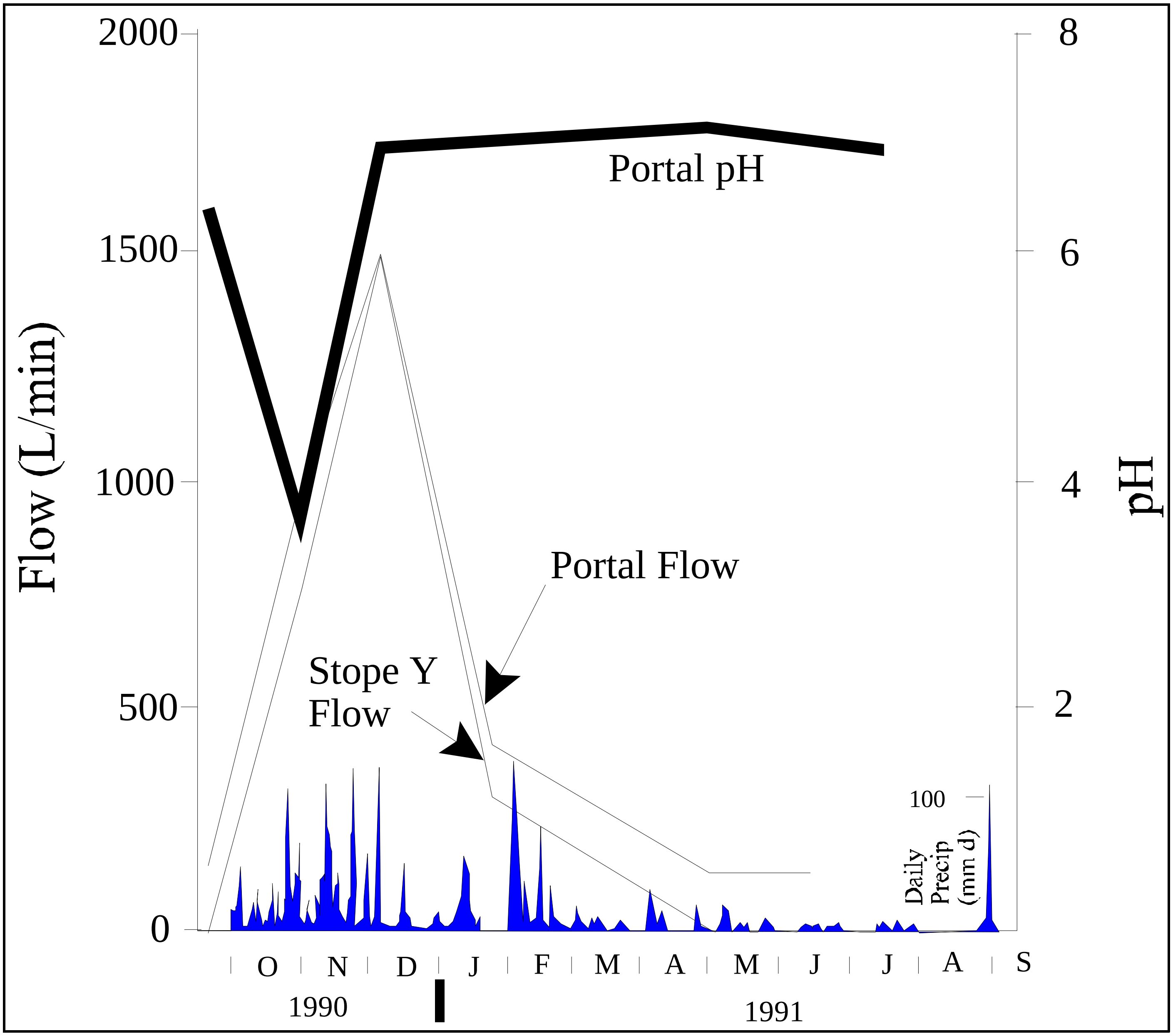

FIGURE 4.3-6. Flow and pH at Portal, Flow at Stope Y, and Daily Precipitation, Myra Falls Operation (adapted from Northwest Geochem, 1992).

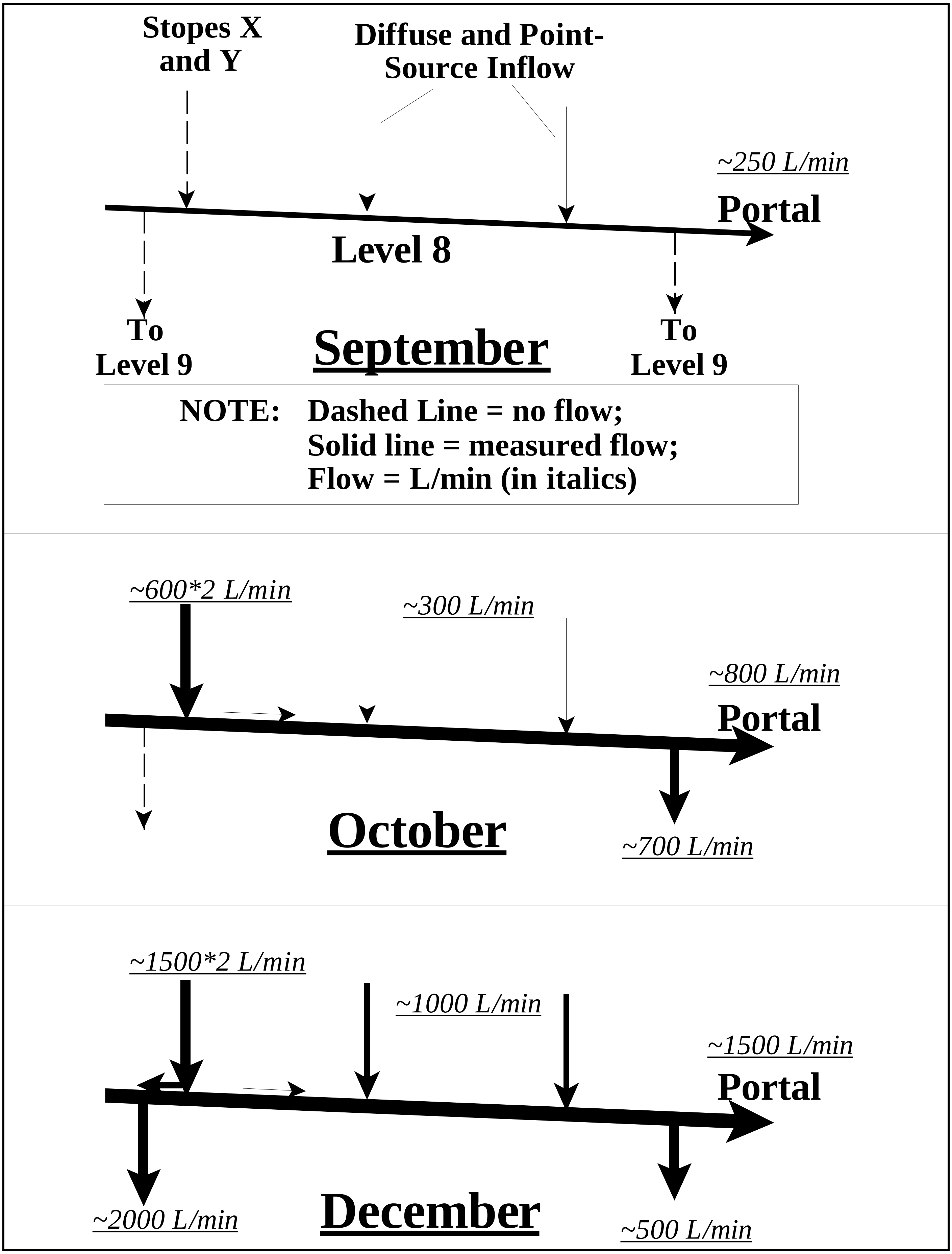

FIGURE 4.3-7. Schematic Flow through Time on Level 8, Myra Falls Operations.

Case Study 4.3-9: Nitrogen in Drainage from Explosives

highlights: sources of nitrogen in drainage from mines; average loss of nitrogen from explosives to drainage

Forsyth et al. (1995) pointed out that much of the nitrate found at minesites is derived from explosives. The explosives typically fall into three categories: (1) highly soluble ANFO (ammonium nitrate - fuel oil) with 33 wt-% nitrogen, (2) watergels/slurries with 20-30 wt-% nitrogen, and (3) emulsions with 20-30 wt-% nitrogen.

The pattern of explosives usage varies between underground and open-pit mines. Underground mining often requires small quantities of explosives at high frequencies, whereas pit mining requires large quantities at low frequency. The amount of explosive lost to drainage waters is dependent on the pattern of usage, drainage flow, handling, and blasting efficiency. Field studies have shown that roughly 5% of total nitrogen in explosives is often lost to drainage, with high losses reaching 15%.

Case Study 4.3-10: An Extremely Acidic Underground Mine

highlights: lowest published pH for minesite drainage; estimated bulk rates for oxidation and heat generation; high costs for control of drainage chemistry

Probably the preeminent case of acidic drainage from underground workings in the USA is Iron Mountain (Alpers et al., 1994; Nordstrom and Alpers, 1995). This drainage is reportedly the most acidic and metal-laden anywhere in the world. The climate includes hot, dry summers and cool, rainy winters with occasional snow. Average annual precipitation is 1.52 m, with a range of 0.71 to 3.30m from 1944-1990.

Host rock at Iron Mountain is hydrothermally altered volcanic rock of the Kuroko type (marine formation of metal-sulfide rock). The dominant mineralogy is albite, sericite, quartz, kaolinite, epidote, chlorite, and minor calcite (Nordstrom and Alpers, 1995). Two sulfide-rich areas (90-99% by volume of sulfide minerals) are the Richmond and Hornet deposits (Figure 4.3-8), with the Brick Flat deposit nearby. The metal-enriched gossan at the top of Iron Mountain was mined for silver in the 1880's. This was followed by underground mining of the Hornet area for copper from 1907 to 1926. In the 1940's, the Richmond deposit was mined for copper and zinc. Finally, the Brick Flat deposit was open-pit mined for pyrite from 1950 to 1962. Totals of approximately 5.2x10^6 t of sulfide ore, 2.6x10^6 t of gossan, and 9.5x10^6 t of waste rock were mined at Iron Mountain.

Underground mining involved a series of adits into the ore zones through the Richmond and

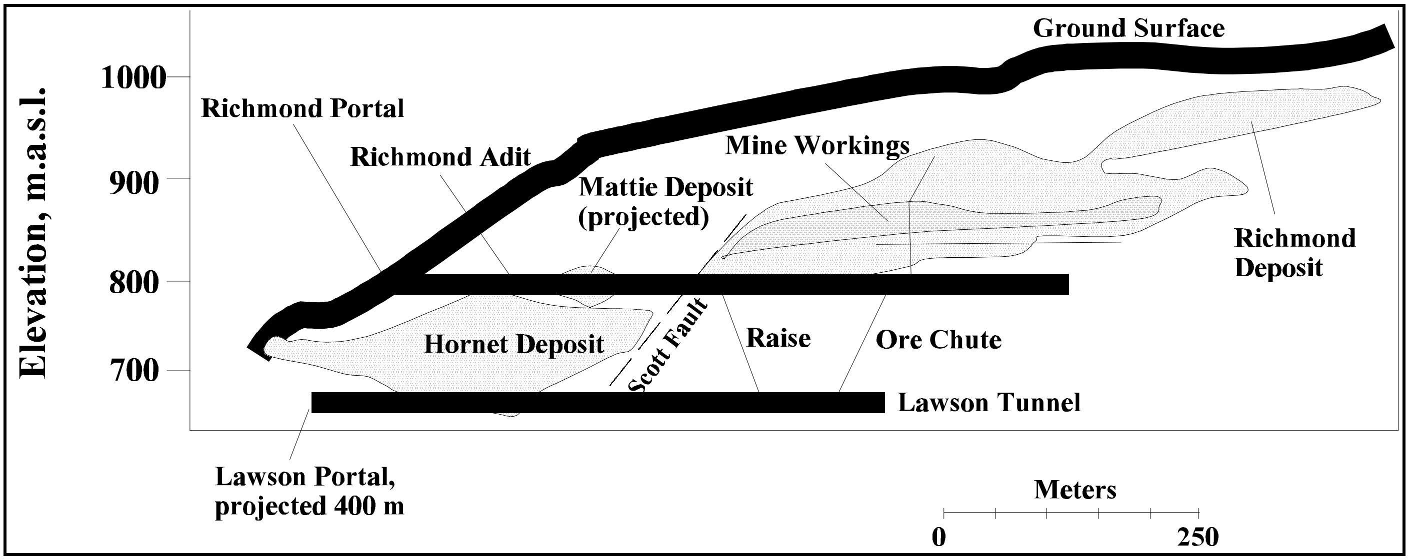

FIGURE 4.3-8. Cross-section through Iron Mountain (adapted from Alpers et al., 1994).

Lawson Portals. The Type 2 workings (Figure 2.2-6) are shown in cross-section in Figure 4.3-8. During the dry season, flows from the Lawson Portal are about twice those from the Richmond Portal, showing that the lower Lawson intercepts more background groundwater flow. During the wet season from October to April, flow increases from both portals, but the more variable flow from the Richmond Portal indicates a closer connection with surface waters.

Roughly 300 t/yr of dissolved cadmium, copper, and zinc drained from the workings. Consequently, in September of 1983, the Iron Mountain area was placed on the U.S. EPA National Priority List for remediation. Efforts began by renovating the workings, providing access for inspection and monitoring. This monitoring of dripping water within the workings yielded aqueous pH with negative values, between -0.45 to -3.4 (Table 4.3-3). Flow from the Richmond Portal has pH 0.02 to 1.5 with more than 100,000 mg/L of total dissolved solids. Based on ranges of concentrations from 1983 to 1991 (Table 4.3-4), drainage chemistry has remained relatively constant, which is consistent with expectations in Section 4.2.5.

The total oxidation rate of pyrite at Iron Mountain is estimated at nearly 300 kg/hr (2400 mol/hr). Based on a factor of 1500 kJ/mol pyrite, this is equivalent to 1 kW/hr (Nordstrom and Alpers, 1995). This heat energy accounts for drainage temperatures up to 47°C and past fires with temperatures of 221°C measured at the ore surface.

Various options have been considered for rehabilitating the workings, including placement of lime underground, plugging portals, and air-sealing the workings (Nordstrom and Alpers, 1995). These have been rejected due to risks (e.g., a large mine pool of roughly 600,000 m^3 of highly acidic water placing pressure on plugs and forcing drainage through rock fractures) and technical issues (e.g., accumulation and pressurization of carbon dioxide during neutralization). At this time, the preferred rehabilitation includes the diversion of surface water around the area, lime treatment, and eventual surface capping of the site, with costs estimated at US$150,000,000. Periods of heavy rain still stress the current treatment system.

Case Study 4.3-11: Natural Acidic Drainage

highlights: non-mining-induced acidic drainage; examples of concentrations in natural acidic drainage

In 1991-1992, Koyanagi and Panteleyev (1992) collected and analyzed 77 water samples of natural drainage in an area of altered and mineralized rock in the Mount McIntosh/Pemberton Hills region of northern Vancouver Island, British Columbia, Canada. This area is roughly 20 km west of Island Copper Mine (Morin et al., 1995a; Case Study 4.4-9). The rock types identified in the area included porphyry copper/gold, base-metal skarns, and advanced argillic acid-sulfate epithermal mineralization. Minerals noted in the latter type included alunite, jarosite, gypsum, anhydrite, barite, and melanterite, suggestive of strong acid generation. Pyrite and marcasite were the primary iron-sulfide minerals.

Aqueous pH ranged from 2.0 to 6.5. The lowest pH of 2.0 was measured in a stagnant ditch and was associated with the highest measured temperature of 28.9°C, 1300 mg SO_4/L, 165 mg Ca/L, 88.8 mg Fe/L, 45.7 mg Al/L, 36.6 mg Si/L, 0.15 mg Cu/L, and 0.65 mg Zn/L. Most concentrations in the remaining 76 samples were at least an order of magnitude less than these values. A creek draining a significant area (no size or flow given) had pH values as low as 3.1.

Case Study 4.3-12: Flooded Underground Mines (Mine Pools)

highlights: spatial and temporal trends in drainage chemistry in flooded underground mines; slow to no improvement of water chemistry after flooding; difficulty in studying underground mines after flooding; tracer tests through flooded mines; difficulties in sealing mines

Type 1 underground mines (Figure 2.2-5) will naturally flood after mining ceases if groundwater and/or surface water flow into them (Figures 3.2.2-1 to 3.2.2-3). On the other hand, Type 2 underground mines (e.g., Figure 2.2-6) will flood only if the rate

TABLE 4.3-3
Examples of Drainage Chemistry from Underground Workings at Iron Mountain (from Alpers et al., 1994 and Nordstrom and Alpers, 1995)

Parameter (mg/L)	Richmond Portal	Drip Water	Drip Water	Drip Water	Drip Water
Temp (°C)	34.8	41.8	32.2	28	-
pH (pH units, field)	0.48	-0.35	-0.7	-	-2.6
Al	2210	4710	6680	6470	-
Sb	4	11	16	15	-
As (III)	8.14	27.2	38	74	-
As (total)	56.4	169	154	850	340
Ba	0.068	0.25	0.1	<0.10	-
Be	0.026	0.1	0.1	<0.1	-
B	1.5	2.5	2.5	-	-
Cd	15.9	43	48.3	370	210
Ca	183	424	330	443	-
Cr	0.12	4.5	0.75	2.6	-
Co	1.3	2.2	15.5	3.6	-
Cu	290	578	2340	9800	4800
Fe (II)	18100	50800	79700	-	34500
Fe (total)	20300	55600	86200	68100	124000
Pb	3.6	4.3	3.8	8.3	12
Mg	821	1380	1450	2560	-
Mn	17.1	41.8	42.1	119	-
Mo	0.59	1	3.7	2.3	-
Ni	0.66	2.8	2.9	6.3	-
K	261	704	1170	11.1	-
Se	0.42	2.1	2.1	<2.8	-
SiO_2	170	69	34	-	-
Ag	0.16	0.49	0.65	0.7	-
Na	251	355	939	44	-

Parameter (mg/L)	Richmond Portal	Drip Water	Drip Water	Drip Water	Drip Water
Sr	0.25	0.3	0.49	-	-
SO_4	118000	420000	360000	-	760000
Tl	0.44	0.15	0.15	1.6	-
Sn	1.6	6.5	15	-	-
Ti	5.9	8.6	125	-	-
V	2.9	17	11	28	-
Zn	2010	6150	7650	49300	23500

TABLE 4.3-4
Range of Drainage Chemistry from Portals at Iron Mountain

	Flow (L/s)	pH	Zn (mg/L)	Cu (mg/L)
Richmond Portal				
Mean	4.4	0.8	1600	250
Range	0.5-50	0.02-1.5	700-2600	120-650
Lawson Portal				
Mean	2.5	1.6	540	90
Range	0.8-15	0.6-2.8	280-840	50-150

of inflow exceeds the rate of drainage. A common method to lessen the rate of drainage is “portal plugs” or “mine seals” (Section 6.4 and Case Study 3.2.2-6). However, from the perspective of drainage chemistry, mine seals do not have major effects for at least several decades after installation for several reasons. First, seals at portals are incapable of preventing oxygen entry because of natural and mining-induced fractures in the wall rock (Case Studies 3.2.2-1, 3.2.2-2, 3.2.2-8, and 4.3-8). Where unsaturated, these fractures allow “pumping” of air into sulfide-bearing mines during seasonal fluctuations in water levels. Second, flooding of mines leads to the rinsing (1) of previously dewatered fractures that may have accumulated significant reaction products (Section 5.4.2) and (2) of reactive minerals exposed on mine walls. This can generate high concentrations of metals and nonmetals in the mine water. Third, plugs that fully impound water experience high pressures as ponded water levels increase, leading to (1) elevated seepage rates through fractures and (2) higher risk of catastrophic failure of the plug or surrounding rock. Attempts to seal fractures around portals have made little difference in drainage rates and oxygen entry, because other, permeable fractures farther from the portal became conduits.

Stuart and Simpson (1961) noted that flooded Type 1 anthracite coal mines in Pennsylvania, USA, exhibited variations in pH with depth in the mine. Depth-specific samples from eleven shafts, flooded for 1 to 20 years, showed various trends in pH (Table 4.3-5), including constant, homogeneous pH. Relatively homogeneous conditions were the result of vertical mixing due to occasional pumping from

TABLE 4.3-5
Vertical pH Profiles in Flooded Underground Shafts (from Stuart and Simpson, 1961)

Mine	Shaft	Elevation of shaft collar[1]	Elevation of mine-pool surface[1]	Date of sampling	Elevation of sampling point[1]	pH	Comment[2]
Exeter	Red Ash	177.8	147.8	Jan. 9, 1961	140.2	6.8	"Pool formed after 1949 and was pumped to prevent overflow until about 7/59. "
					100.6	6.9	
					61	6.9	
					18.3	6.7	
Clear-Spring	Clear-Spring	176.2	160.9	Jan. 4, 1961	153.3	6.9	"When mine was in operation, the pH of pumped discharge was 6.5, on May 27, 1941. Pool formed before 1944; not pumped since."
					144.2	6.8	
Schooley	No. 1	170.1	128.9	Jan. 9, 1961	121.3	6.4	"When mine was in operation, the pH of pumped discharge was 6.7 on May 23, 1941. Pool formed after Jan. 1951. Pumping ceased July 1959."
					84.7	6.2	
					48.2	6.4	
					10.1	6.8	
South Wilkes-Barre	No. 5	179.5	27.1	Jan. 9, 1961	19.5	7.1	"When mine was in operation, the pH of pumped discharge was 5.1 on May 19, 1941. Pool formed after June 1958."
					-18.6	3.7	
					-71.9	4	
					-125.3	4.1	
No. 7	No. 2	166.1	154.8	Jan. 10, 1961	144.2	6.9	"When mine was in operation, the pH of pumped discharge was 3.2 on June 10, 1941. Pool formed after May 1954."
					102.1	6.3	
					56.4	6.5	
					21.9	6.4	
Henry	Red Ash	171	136.6	Apr. 19, 1960	133.5	7.4	"When mine was in operation, the pH of pumped discharge was 3.9 on May 15, 1958. Pool formed after Jan. 1959. Shaft destroyed June 1960."
					106.1	6	
					45.1	5.1	
					-49.4	5.3	
Hazelton	Hazelton	481.6	332.5	Nov. 13, 1957	326.1	3.2	"Water rises in shaft and overflows through drainage tunnel at altitude [332.5 m]."
					274.3	3.4	
					228.6	3.2	
				Jan. 10, 1961	324.9	3.6	
					291.1	3.8	
					258.5	3.6	

Mine	Shaft	Elevation of shaft collar[1]	Elevation of mine-pool surface[1]	Date of sampling	Elevation of sampling point[1]	pH	Comment[2]
Locust Gap	Locust Gap	391.4	242.9	Jan. 11, 1961	235.3	4.6	“Mine-water pool overflows through drainage tunnel at altitude [242.9 m].”
					197.2	4.5	
					159.1	5.9	
					86.6	5.5	
Reliance	Reliance	322.5	298.4	Jan. 12, 1961	290.8	6.1	“When mine was in operation, pH of pumped discharge was 2.7 on Sept. 18, 1941, and 4.0 on Sept. 23, 1946. Water pumped sporadically from shaft.”
					230.4	5.9	
					169.5	5.7	
					108.5	6	
Packer No. 5	No. 5	337.7	293.5	Jan. 13, 1961	285.9	6.7	“When mine was in operation, pH of pumped discharge was 4.9 on Sept. 16, 1941. Pool formed after Sept. 1957.”
					206.7	6.6	
					96.9	6.7	
					17.7	6.6	
Greenwood	No. 10	305.4	137.8	Jan. 12, 1961	130.1	4.2	“When mine was in operation, pH of pumped discharge was 3.6 on July 2, 1941, and 3.1 on Oct. 15, 1946. Pool formed after May 1960. Pumping at shaft ceased Nov. 1960.”
					113.4	4	
					52.4	3.8	
					12.8	2.80	

[1] Elevations are in meters above sea level

[2] Quotations taken from Stuart and Simpson (1961) with elevations converted from feet to meters.

the shafts or multiple entry points (underground levels) of water into the shaft. Interestingly, other researchers noted that multiple entry points created heterogeneous chemistry (described below).

Erickson et al. (1982) reiterated that flooding of mines was expected to lower aqueous concentrations significantly, particularly in acid-generating mines, but this had not generally happened over the span of a few decades. Returning to one region (100 km by a maximum of 8 km) examined by Stuart and Simpson (1961) above, they noted that 50×10^6 m^3 of mine pools had developed there by 1948. In some locations, this caused flooding of homes, accelerated surface subsidence, and caused overflow of acidic drainage into nearby surface watercourses. A detailed hydrogeochemical study of nine shafts in the region was undertaken in mid 1981 and compared with past analyses.

Sixty-three depth-specific water samples were collected up to depths of 170 m in the nine shafts. Vertical profiles revealed some variations in specific conductance (Figure 4.3-9) corresponded to variations in iron and sulfate (Figure 4.3-10), but pH reportedly changed little within a shaft. Sharp changes in conductance were often associated with mined-out coal seams (workings) where they joined the shaft. For redox conditions, Eh profiles frequently showed no change, or more reducing conditions with depth, although opposite trends and significant changes over 3 m depth adjacent to a working were also noted. Significant populations of fecal coliform in four shafts indicated the presence of sewage.

Comparisons of water chemistry in 1981 to 1973 data showed that the most acidic water has generally disappeared (Table 4.3-6). This required several decades to happen, and might depend on the rate of water flowing through the mine. In any case, Erickson et al. (1982) could not identify the mechanism for acidity attenuation. However, they noted that sulfate in overflow from one shaft (Askam Outfall) was constant over an order-of-magnitude change in flow, which is consistent with secondary-mineral equilibrium (Section 4.2).

Johnson and Cregger (1986) reported that more than 55 pyritic, acid-generating iron mines operated in one area of Michigan, USA, from 1882 to 1978. These mines expected that acidic drainage would be attenuated upon flooding. This did not happen.

In particular, the Dober Mine Complex consists of three interconnected mines (Figure 4.3-11): Dober (pits, shafts, adits), Isabella (pit, shaft, adit), and Hiawatha (shaft and adit), operated from 1966 to 1972 (Johnson and Cregger, 1986). The rising water levels caused the Dober Pit and surrounding sediments to fill with acidic drainage in 1972. Concurrently, water levels in the two Hiawatha shafts were 2 m higher, suggesting the acidic water was moving from deep on the 10th level of Hiawatha, upwards into the Dober Pit.

While the overall pattern of movement was correct, the actual differences in water levels could be attributed to density differences between near-neutral and acidic water in the mine. As a result, the remaining differences in corrected water head indicated the presence of strong, open hydraulic connections through the mine. As confirmation, a pumping test at 120 L/s for 13 hours caused only one-meter water-level declines throughout the mine complex as well as the cessation of overflow from the Dober Pit. The water level in the complex recovered over 4.5 days.

Depth-specific analyses in the Hiawatha No. 2 Shaft (Table 4.3-7) revealed a relatively sharp contact between near-neutral water and deeper acidic water. This confirmed that acidic water was present on the 10th level in Hiawatha.

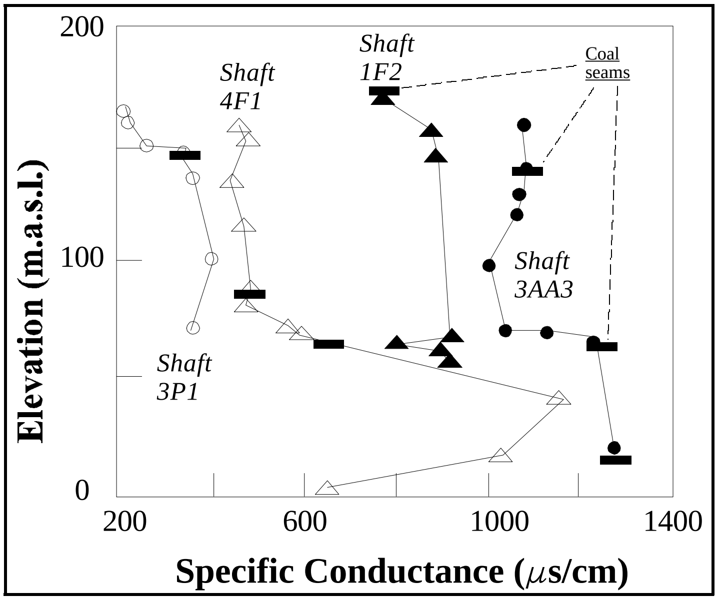

FIGURE 4.3-9. Vertical Profiles of Specific Conductance in Flooded Mine Shafts (adapted from Erickson et al., 1982).

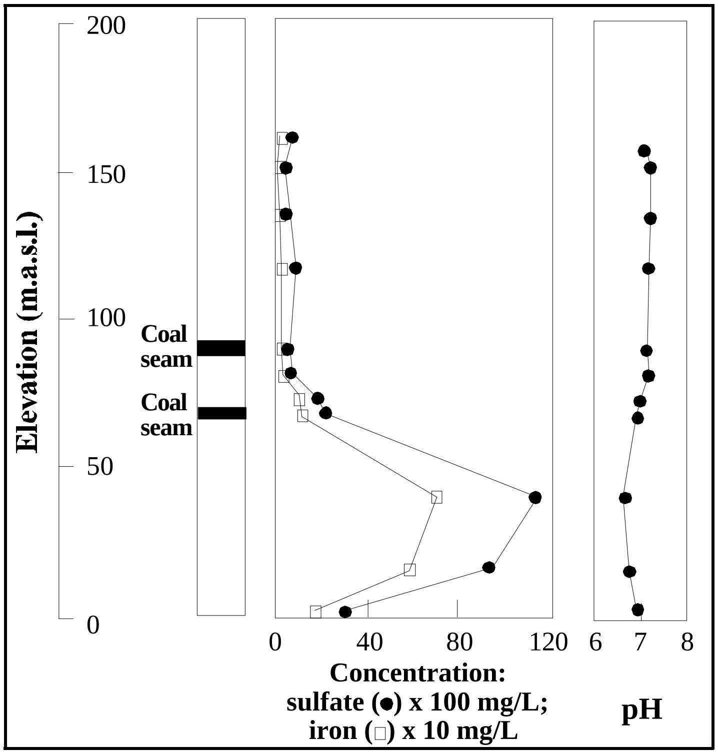

FIGURE 4.3-10. Vertical Profiles of Water Chemistry in a Flooded Shaft (adapted from Erickson et al., 1982).

TABLE 4.3-6
Temporal Trends in Mine-Pool Chemistry at Three Sites
(from Erickson et al., 1982)

Year	pH	SO_4 (mg/L)	Fe (mg/L)	Conductivity (µS/cm)
South Wilkes-Barre Boreholes				
1973	3.0-5.9	1300-3500	150-500	2400-3000
1981	5.7-5.8	1350-1460	131-143	1140-1260
Askam Outfall				
1973	3.1-5.6	1850-2950	120-420	NA
1981	5.8-6.1	1150-1540	89-119	750-1160
Buttonwood Tunnel				
1973	3.1-6.2	1000-2750	120-462	2100-2500
1981	5.7-5.9	1050-1150	73-88	940-990

The volume of workings above 10th Level, including workings backfilled with sand, was estimated around 6.3×10^5 m^3 (Johnson and Cregger, 1986). At a mine-discharge rate of 4.1 L/s and with no mixing, one mine volume would be replaced after 4.8 years. This was reportedly consistent with 50% dilution of aqueous iron (1000 mg/L in 1978 to 500 mg/L in 1983). On the other hand, this is not consistent with iron concentrations in Table 4.3-7 and ignores controls on aqueous iron by pH and secondary-mineral solubility. In any case, with the replacement time of 4.8 years, upper levels of the mine were predicted to be diluted three more times by the Year 2000, producing a 90% decrease in iron. Thus, the delay in reducing aqueous concentrations in this study was attributed to slow mixing and dilution, as a consequence of slow flow rates, compared with the large volume of mine water.

Aljoe and Hawkins (1991a and b; 1993) and Aljoe (1994) examined flooded underground mines containing acidic water, with the ultimate objective of injecting alkaline compounds into the mines. This injection would neutralize the acidity and allow the precipitated metal-bearing sludge to accumulate without requiring any handling and disposal. Previous attempts at alkaline injection into mines (and waste rock) were generally unsuccessful and were not economic relative to standard collection and treatment (Section 6.1). One potentially successful mine had such a slow flow rate that the effects of any injection on drainage may

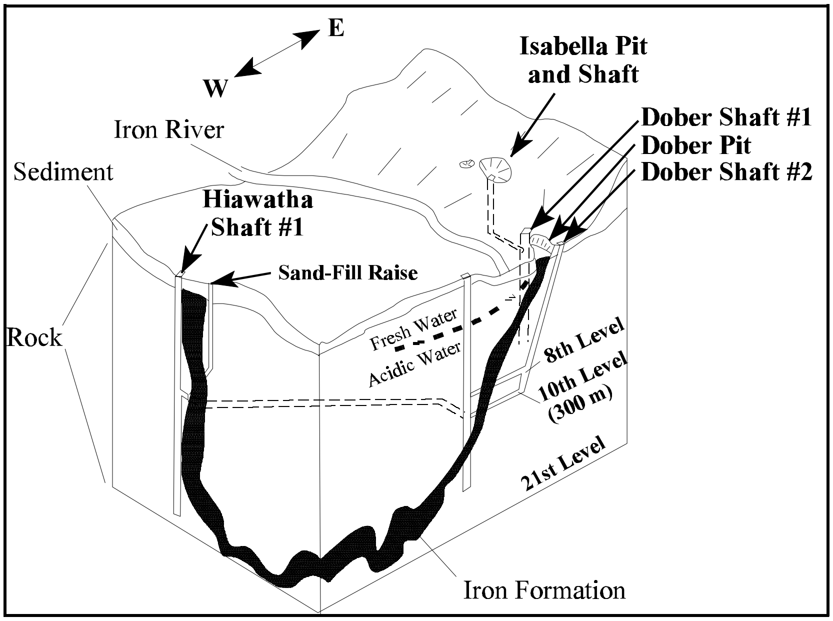

FIGURE 4.3-11. Layout of the Dober Mine Complex (adapted from Johnson and Cregger, 1986).

TABLE 4.3-7
Vertical Trends in Water Chemistry in the Dober Mine Complex
(From Johnson and Cregger, 1986)

Depth (m)	Field pH	Sp. Conduct. (µS/cm)	Acidity (mg $CaCO_3$/L)	Fe (mg/L)	Mn (mg/L)	Al (mg/L)	SO_4 (mg/L)
30	7.2	580	100	-	-	-	-
61	7.1	490	40	-	-	-	-
91	6.6	2000	200	-	-	-	-
107	6.6	2000	220	-	-	-	-
152	6.6	2020	240	-	-	-	-
160	6.7	1600	-	38	43	trace	1130
168	3.8	5900	-	1670	94	296	7290
183	3.7	5900	7200	1680	91	307	7430
213	3.7	5900	-	1670	95	299	7030
244	3.7	5900	-	1680	96	299	7500
274	3.8	5900	-	1680	86	291	7410
305	3.7	6200	-	1870	102	304	8190
335	4	6800	-	1970	99	250	8450
366	4	6800	-	2080	103	280	8670

not have be seen for 10-20 years, and thus the project was halted. Two, more accommodating mines were located in southwestern Pennsylvania, USA, and are discussed below.

The first site of Aljoe and Hawkins (1991a and b; 1993) was located in Keystone State Park. Portal seals were installed in the mid 1970's to flood this Type 2 coal mine (Figure 2.2-6) that operated from 1938 to the mid 1950's. At the same time, a grout “curtain” was injected into all fractures adjacent to the portals. In the late 1970's, water pressure behind the seals caused a major “blowout” of mine water through rock about 50 m behind the seals. A borehole was then installed at the blowout to collect the overflow and direct it into a series of pipes. These pipes eventually clogged with secondary-mineral precipitants and were replaced in 1989 (Figures 4.3-12 and 4.3-13). The new pipes included french drains to collect diffuse subsurface drainage bypassing the grout curtain and flowing

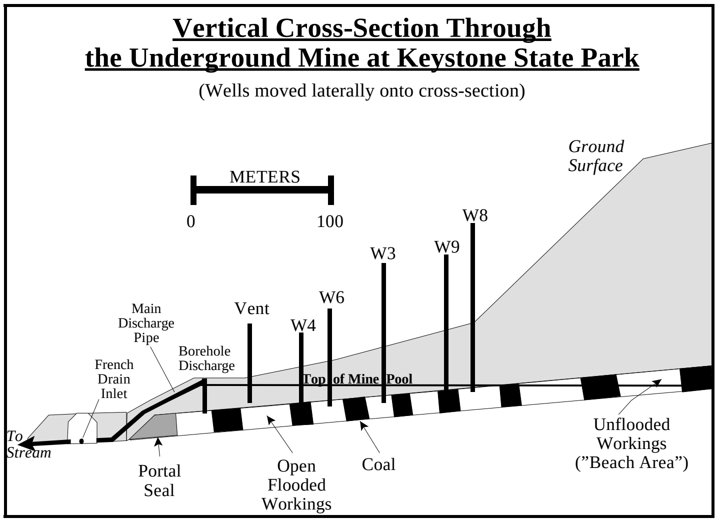

FIGURE 4.3-12. Vertical Cross-section through the Keystone Park Underground Coal Mine (adapted from Aljoe, 1994).

downgradient of the seals. The pipes empty into a nearby stream.

The mine pool at the Keystone site did not completely flood all workings because they were mined upwards at a slight angle (Figure 4.3-12). From the portal plugs to the estimated updip edge of the pool (Figure 4.3-13), the volume of mine water was calculated at 87,000-98,000 m^3. Of nine monitor wells installed into the eastern portion of the workings from the surface (Figure 4.3-13), three intercepted the main adit (W1, W2, and W6), one intercepted a submain adit (W3), and one intercepted a mined-out room (W8). These wells were constructed of pipe open at the bottom into the workings. The remaining four wells intercepted solid coal, and were constructed with standard screens and sand packs.

Water levels in all these wells, except two wells completed in coal, were virtually the same, indicating (1) no significant hydraulic gradient with this portion of the mine, (2) open hydraulic connections among the workings, and (3) hydrogeologically confined (pressurized) conditions. Wells into the workings recharged instantaneously upon water removal, confirming proper installation.

From October 1967 to August 1969 at the Keystone site, prior to portal sealing, drainage flows from the portals were typically 0.88-6.9 L/s with a median of 2.6 L/s. The lowest flows were in late summer and the highest flows took place over the first three months of the year. Flows from October 1989 to December 1990 from the drains, long after sealing, were 0.44-9.8 L/s with a median of 2.3 L/s. Thus, the seals provided little long-term reduction in flow. Mine-pool level varied by only 0.5 m from 1988 to 1990, but this minor change correlated well with drainage rates and precipitation records. Based on mass balance calculations, 7% of precipitation reached the mine pool from spring through fall, increasing to 17% during winter.

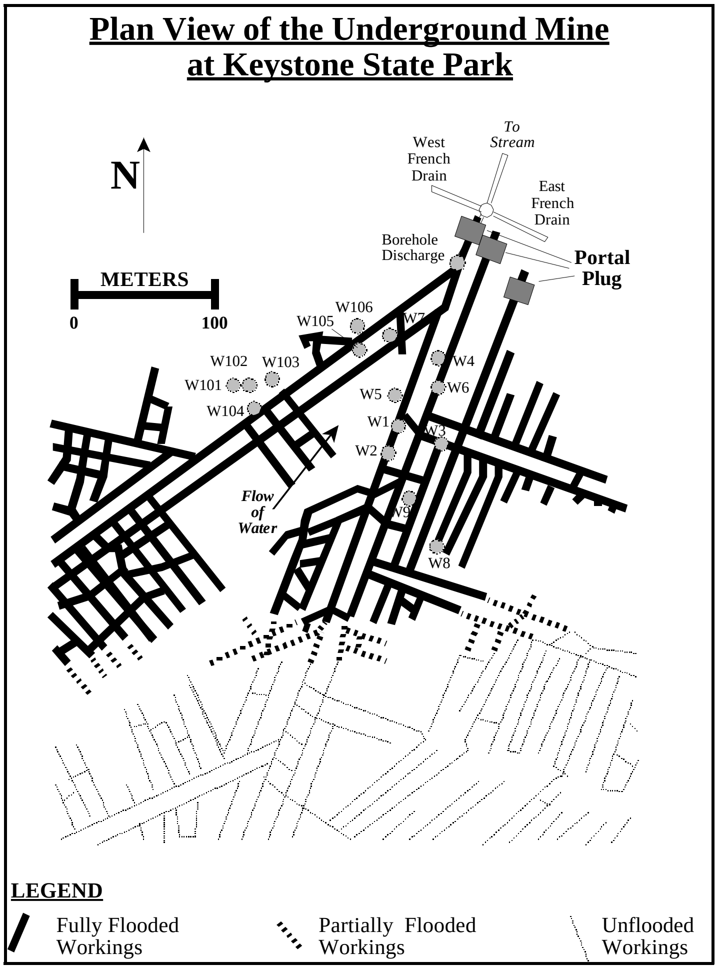

FIGURE 4.3-13. Plan View of the Keystone Park Underground Coal Mine (adapted from Aljoe, 1994).

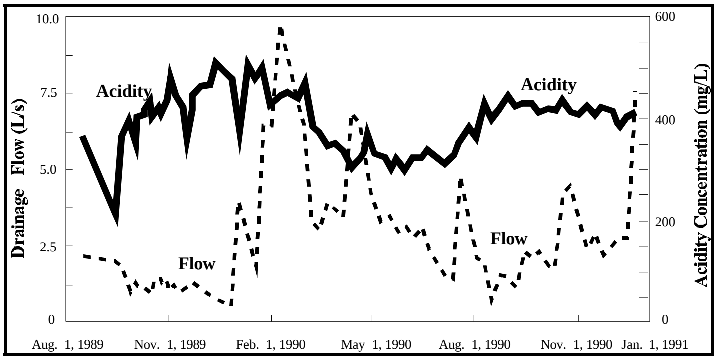

FIGURE 4.3-14. Temporal Trends of Acidity and Flow in Drainage from the Keystone Park Underground Coal Mine (adapted from Aljoe and Hawkins, 1993).

Also prior to portal sealing, from October 1967 to August 1969, drainage chemistry was generally constant. Common ranges of concentrations were 60-140 mg/L for total iron, 350-600 mg/L for acidity, 1000-1800 mg/L for sulfate. Two decades later, average drainage concentrations were 100 mg/L for total iron, 400 mg/L for acidity (with pH 3), and 1200 mg/L for sulfate. All parameters reportedly showed little variation through time, and temporal trends of parameters "were almost identical" to acidity (Figure 4.3-14). Consequently, drainage concentrations have been generally steady for decades, before and after portal sealing, in agreement with the expectations of Section 4.2. Seasonal variations yield the annual standard deviation discussed in Section 4.2.

Although drainage chemistry has been relatively constant, water chemistry varied significantly by location within the mine (Table 4.3-8). Wells W5, W7, and W9, installed in coal, had near-neutral pH with lower metal levels. These wells also had water levels up to 0.2 m higher than the mine pool. Aljoe and Hawkins (1993) concluded that the narrow unmined coal blocks were recharged from above with fresh infiltration and that the acidic pool water did not pass through them. Because this ongoing near-neutral infiltration has not diluted mine-pool chemistry, there is still a strong active control on drainage chemistry. The near-neutral drainage chemistry from the east french drain may reflect remnants of limestone and cement grout placed during portal sealing, although these materials were apparently consumed above the west french drain. The remnant limestone also accounted for higher calcium concentrations in the drains. Other differences between the two drains are discussed below.

Compared with drainage chemistry around the portals, mine-pool chemistry as sampled from the eastern wells was less acidic (up to 0.5 pH units higher and less than 50% of the acidity) with lower metal concentrations (Aljoe and Hawkins, 1991a and b; 1993). This suggested a more acidic, more dominant source of acidic water for the portal area, namely the western portions of the workings (Figure 4.3-13). This was confirmed later by additional wells (Aljoe, 1994).

The relatively stagnant conditions in the eastern portion were based on two observations. First, vertical profiles of aqueous concentrations in the eastern workings increased roughly by a factor of two from mine roof to mine floor (~2 m), indicating stratification and little vertical mixing. Second, the injection of 6 kg of sodium bromide into W3 was expected to cause peak bromide concentrations at W1, W6, and the portal drainage within several days. Instead, even after 92 days, no detectable traces of bromide were found. Interpretation of the bromide-decay curve at W3 provided a mean velocity of 0.60 m/d. According to mass balance, these workings would account for only 1.4% of average drainage.

Aljoe (1994) reported on another bromide-trace test, at Well W6, which resulted in a peak of 6.8 mg/L appearing in the west french drain after three days. In the east french drain, bromide levels rose steadily over the first 17 days, and remained relatively steady around 1.0 mg/L until Day 54. This shows that W6 has a better hydraulic connection with the portals than W3 and that chemical conditions can evolve more rapidly around the western portal area. Tracer migration away from W6 was three times faster near the mine floor than near the mine roof. Bromide occurred only near detection from the discharge borehole, indicating only a minor connection with W6. This is a good example of how water movement can be complex, but drainage chemistry remains relatively constant.

A total of 1890 kg of NaOH was injected into Wells W3 and W6 as part of alkaline-injection testwork (Aljoe and Hawkins, 1991a and b; 1993). Within six weeks, water chemistry at these wells returned to previous acidic conditions. The only change noted in portal-area drainage was two peaks in sodium concentrations, seven and 49 days after injection (Figure 4.3-15). Thus, all neutralizing capacity had been consumed within the mine.

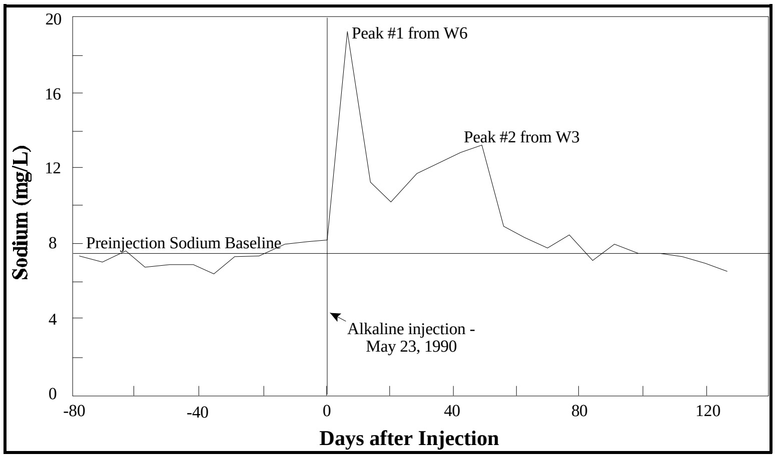

FIGURE 4.3-15. Temporal Trend of Sodium in Drainage from the Keystone Park Underground Coal Mine Following Alkaline Injection at Two Wells (adapted from Aljoe and Hawkins, 1993).

TABLE 4.3-8
Median Water Chemistry in Drainage and Monitor Wells in a Partially Flooded Underground Coal Mine
(from Aljoe, 1994)

Parameter[1]	Borehole Discharge	East French Drain	West French Drain	Wells 104 & 106[2]	Near Floor of Workings
No. of samples	141	56	57	20	84
pH	3.11	6.37	3.99	3.03	3.31
Net acidity	365	-45.5	208	303	187
Total Fe	93.8	28.9	69.4	104.5	60.3
Ferrous Fe	67.8	28.6	69.4	102.3	58.6
SO_4	1125	868	1074	1025	840
Ca	185	248	224	184	162
Mg	74.4	56.6	69.5	70.4	53.8
Na	7.5	13.5	8.2	6.6	13.1
Al	18.9	3.7	12.6	15.9	9.6
Mn	13.6	12.7	12.8	13.4	5.9

[1] Concentrations in mg/L.

[2] Wells 104 and 106 are closest to the walls of the workings.

The sodium peaks provided average water velocities of 14 m/d from W6 to the portals and 3.4 m/d from W3. Sodium mass balance indicated that approximately 1.3% of drainage flow was derived from these eastern workings, in agreement with 1.4% from the first bromide-tracer test. It also indicated that only 5.4% of injected sodium had flowed from the mine.

The second coal mine examined by Aljoe and Hawkins (1991a and b; 1993) was Friendship Hill, operated in the 1920's. Mine maps were less detailed and reliable than for the Keystone site. Nevertheless, nine of the ten monitor wells intercepted caved zones or mine workings. Extensive caving and surface subsidence apparently minimized open conduits in the workings and partially replaced them with porous media, accounting for a measurable hydraulic gradient and sloping water table through the mine.

Drainage flow from the main portal correlated well with precipitation events, but water levels in the wells showed little change. This was attributed to the large size of the mine pool that would require massive changes in water storage before levels would be significantly affected.

As at the Keystone site, drainage chemistry from the main portal was relatively constant with pH (Figure 4.3-16) remaining between 2.5 and 3.0, with little dependence on flow rate. Seasonal variations can be quantified by the standard deviation discussed in Section 4.2. Water chemistry varied from well to well and from portal to portal, although the authors did not provide pH data to determine if pH fluctuation was the primary cause of the differences. Ongoing acid generation was suspected at this site due to the extensive fracturing, caving, and subsidence which would enhance oxygen entry.

A bromide tracer test yielded a water velocity of 4.3 m/d over 30 m between two wells. However, since a single-well slug test at one well yielded a hydraulic conductivity of 1.2×10^{-4} m/s, the tracer velocity suggested the presence of an open conduit near and between the wells.

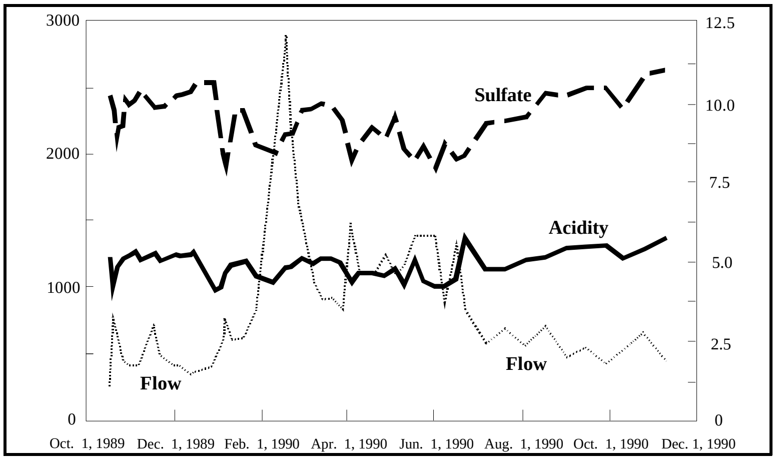

FIGURE 4.3-16. Temporal Trends of Acidity, Sulfate, and Flow in Drainage from the Friendship Hill Underground Coal Mine (adapted from Aljoe and Hawkins, 1993).

Case Study 4.3-13: Flooded Open Pit in a Wet-Dry Tropical Climate

highlights: effects of an alternating wet-dry tropical climate on pit-water chemistry; trends and exceptions

The northern portion of the Northern Territory of Australia experiences an alternating wet-dry climate with 90% of annual rainfall occurring between November and April (Parker et al., 1996). Annual high temperatures are 29-34°C and relative humidity is typically above 70% throughout the year.

Aqueous concentrations and pH were compared for several pits with sulfide-bearing walls and their surrounding groundwaters (Table 4.3-9). In general, the pit waters were found to be acidic with higher concentrations than the groundwaters. This suggested there was no net loss of pit waters into the surrounding groundwater systems, presumably due to the net inflow to the pits from high evaporation (e.g., Figure 3.2.1-2 vs. 3.2.1-4). By way of explanation for the two exceptions to acidic pits, Pine Creek was artificially flooded by diverting pH-neutral water from a nearby creek and Rum Jungle South has little capacity to generate net acidity (see also end of Case Study 6.2-2).

Case Study 4.3-14: Placer Mining of an Aquifer Used for Water Supply

highlights: effects of placer mining on groundwater chemistry; difficulty in defining background concentrations; nearby water-supply wellfield; iron as primary element of concern

The Viney Creek Mine (Fredrickson, 1996), approximately 250 km north of Sydney, Australia, is beside a national park and a wellfield supplying water to nearby areas (Figure 4.3-17). The mine consists of heavy-mineral-rich sand beds to a depth of 6 m over a 30 km^2 area. The terrain is relatively flat and the water table is typically 0.5-1.5 m below surface, rising to form ponds during the wet season.

The sands are mined in 200-meter-wide paths by removing trees and stockpiling soil to the side of the path. A dredge, floating on the water table it exposes, separates the heavy minerals physically (no chemicals) and discharges the tailings from the back to fill the path (e.g., Figure 2.2-8). The tailings are

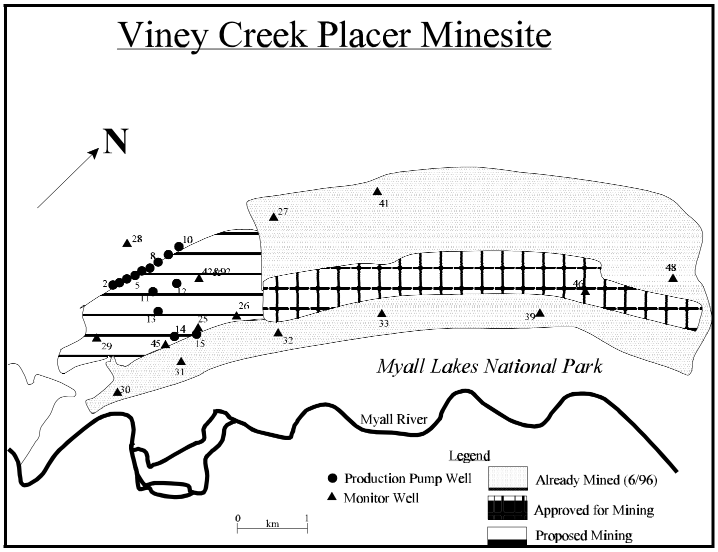

FIGURE 4.3-17. Viney Creek Placer Minesite and Nearby Water-Supply Wellfield and National Park (adapted from Fredrickson, 1996).

TABLE 4.3-9
Water Chemistry in Flooded Pits and Surrounding Groundwater Systems, Northern Territory, Australia
(from Parker et al., 1996)

Location	Conductivity (µS/cm)	pH	HCO_3^- (ppm)	SO_4^{2-} (ppm)	Total Diss. Solids (ppm)	Al (ppm)	Fe (ppm)
Goodall Gold Mine							
Pit	1800 ± 110 (21)	3.16 ± 0.06 (21)	<0.1	1170 ± 79 (15)	950 ± 140 (6)	56.1 ± 15.2 (10)	18.7 ± 3.9 (12)
Pit Dewatering Bores	270 ± 20 (12)	6.69 ± 0.12 (16)	146.6 ± 1 (11)	5.0 ± 1 (11)	173 ± 14 (15)	0.0102 ± 0.0039 (2)	0.012 ± 0 (2)
Tom’s Gully Gold Mine							
Pit	2150 ± 100 (24)	2.87 ± 0.06 (19)	<0.1	1780 ± 140 (12)	1940 ± 502 (3)	65.3 ± 15.6 (6)	27.2 ± 6.3 (5)
Pit Dewatering Bores	250 ± 10 (47)	6.86 ± 0.08 (47)	134.8 ± 6.1 (46)	4.3 ± 0.2 (39)	136 ± 6 (44)	< 0.050 (40)	< 0.050 (34)
Mount Todd Gold Mine							
Batman Pit	2850 ± 130 (7)	2.91 ± 0.03 (7)	<0.1	2400 (1)	1860 (calculated)	35.0 (1)	45.2 (1)
Production Bores	250 ± 40 (9)	6.80 ± 0.1 (9)	181.3 ± 34.9 (8)	8.8 ± 2.5 (8)	162 (calculated)	-	0.40 (1)
Cosmo Howley Gold Mine							
Chinese Pit 2	750 ± 140 (6)	3.74 ± 0.09 (6)	<0.1	180 (1)	450 (calculated)	1.60* (1)	0.260* (1)
Pit Dewatering Bore	450 ± 50 (5)	6.36 ± 0.05 (5)	145 ± 6.5 (4)	119 ± 29 (5)	270 (calculated)	<0.010 (1)	0.035 ± 0.0262 (2)
Pine Creek Gold Mine							
Pit	970 ± 250 (11)	5.56 ± 0.31 (11)	<0.1	539 ± 162 (11)	517 ± 203 (3)	0.193 ± 0.073 (6)	0.037 ± 0.016 (7)
Potable Water Bores	450 ± 10 (78)	7.34 ± 0.05 (78)	287.5 ± 3.4 (78)	4.1 ± 1 (69)	296 ± 9 (78)	< 0.050 (45)	< 0.050 (46)
Rum Jungle South							
Pit	260 ± 10 (23)	7.88 ± 0.14 (28)	109.1 ± 7.3 (24)	28.6 ± 5.2 (17)	164 (calculated)	0.066 ± 0.024 (8)	0.024 ± 0.024 (14)
Bore rn22085	490 (1)	7.30 (1)	328 (1)	8.0 (1)	270 (1)	-	-

[1] Values are written as: mean ± standard error (number of samples); all concentrations represent dissolved levels, except those marked with *.

contoured, topsoil is replaced, and natural revegetation is supplemented. By 1996, 950 ha of the area had been mined.

Because a field of 14 wells to depths of 17-20 m is nearby (Figure 4.3-17), there is ongoing monitoring of these pump wells and monitor wells to determine the effect of mining (Fredrickson, 1996). In similar situations, the main concern was increased iron concentrations. In fact, pre-mining iron concentrations of 2-5 mg/L in one study increased to 10-20 mg/L after shallow mining and to 100-200 mg/L after deep mining. These increases were attributed to oxidation of iron-sulfide minerals, which reached 1% at depth, and were redistributed throughout the tailings profile by the dredge. For Viney Creek, legal agreements are in place so that new wells and an iron-treatment system will be installed should iron levels increase significantly.

Based on reported analytical procedures by Fredrickson (1996), groundwater samples are apparently unfiltered and thus reflect total rather than dissolved concentrations. Determination of background iron concentrations of approximately 0.5 mg/L from the wells was difficult, due to the natural temporal variations and artificial effects of pumping rates and timing. Also, installation of pump and monitor wells typically created short-term peaks in iron concentrations, followed by a general trend of decreasing concentrations. Duplicate wells showed that variations of 0.2 mg/L were not

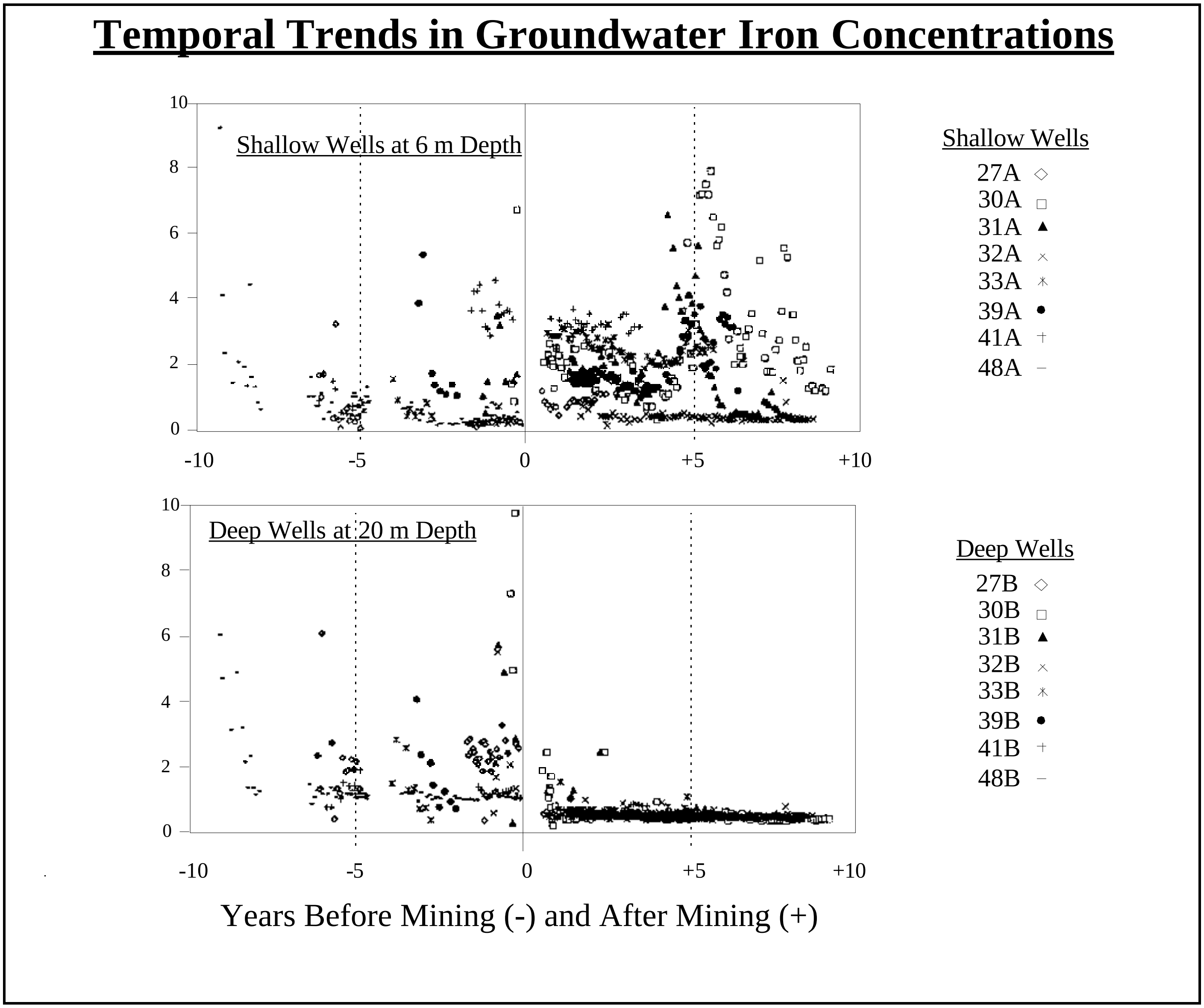

FIGURE 4.3-18. Temporal Trends in Groundwater Iron Concentrations Before and After Placer Mining at Viney Creek Minesite (adapted from Fredrickson, 1996).

significant.

The local effects of mining were determined through monitoring of shallow wells at the depth of mining (6 m), before mining and within tailings after mining. Deeper wells (20 m) monitored the effect of mining before mining and beneath the tailings after mining. In general, the shallow wells showed increased concentrations after mining (Figure 4.3-18), whereas deeper wells showed lower concentrations toward background. This behavior in the deep wells, especially when the dredge path passed within 50-150 m of two production wells, indicated mining did not affect iron concentrations in the deeper water supply. Monitoring is continuing.

4.4 Drainage Chemistry from Stockpiles, Dumps, and Mine-Rock Piles

In the conceptual routing model of Figure 3.3-4, the drainage chemistry at any one point in mined-rock piles is dependent on the conditions in all upstream branches. For acidic drainage, the chemical acidity is commonly higher than alkalinity levels in pH-neutral water, and thus an entire downstream branch can become acidic even if only one of many upstream branches become acidic. For example, one monitoring point in Level C (Figure 3.3-4) just outside the pile may remain pH-neutral whereas an adjacent point may become acidic due to one channel in Level A becoming acidic. As a result, the delineation of acidic or other types of drainage becomes highly location-specific. The following case studies illustrate this. For the same reasons, the prediction and control of drainage chemistry (Chapters 5 and 6) are difficult.

Case Study 4.4-1: Acidic Groundwater Drainage from an Acid-Generating Waste-Rock Dump

highlights: acidic groundwater drainage from a uranium waste-rock dump; sequential neutralization along flowpaths

Veska (1983) reported on an acidic waste-rock dump at a uranium mine near Bancroft, Ontario, Canada. This dump is located near a bedrock outcrop and rests on a sand aquifer (Figure 4.4-1). Groundwater flow is predominantly through the sand aquifer.

Acidic water beneath the waste rock (Table 4.4-1) is at pH 3.4, but a sulfate concentration of 627 mg/L represents relatively low strength drainage that is not in equilibrium with gypsum. Nevertheless, iron, silica, and thorium are in apparent equilibrium with amorphous $Fe(OH)_3$, amorphous SiO_2, and $Th(SO_4)_2/Th(OH)_4$, respectively (Morin, 1983). Concentrations of other minerals are presumably regulated by sorption.

The application of the sub-region concept (Section 4.5) to the migration of the acidic drainage indicated the presence of three neutralizing zones. First, precipitation/dissolution of $Fe(OH)_3$ created a

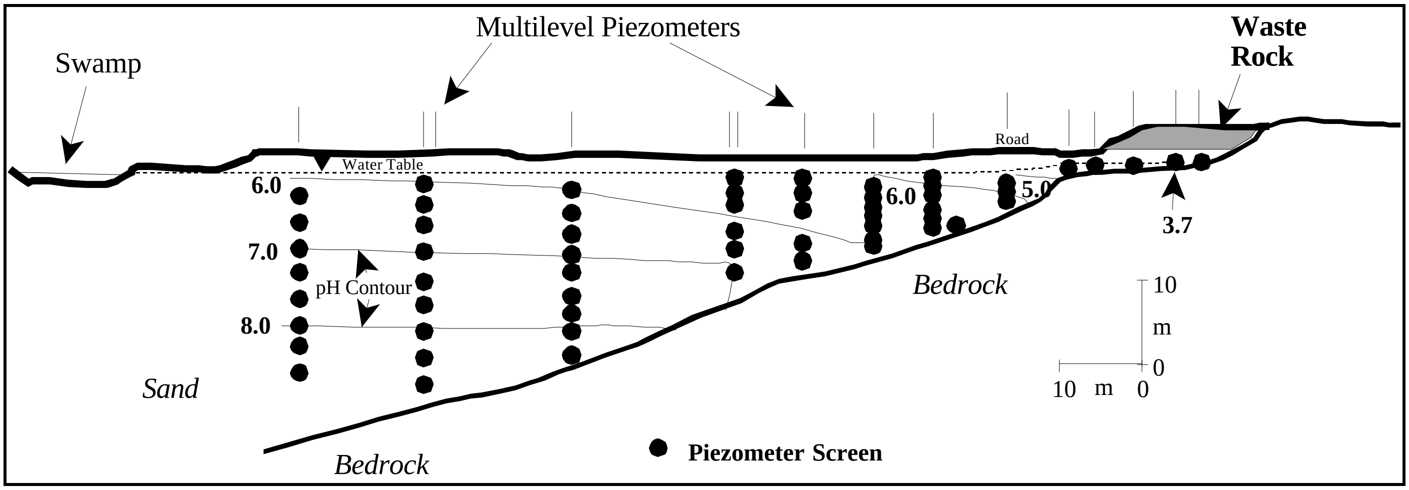

FIGURE 4.4-1. Vertical Cross-section through Acidic Groundwater Drainage from a Uranium-Mine Waste-Rock Dump (adapted from Veska, 1983).

TABLE 4.4-1
Dissolved Concentrations in Groundwater Beneath Acid-Generating Waste Rock at a Uranium Minesite
(all concentrations as mg/L unless noted; from Veska, 1983)

Parameter	Value	Parameter	Value
pH (pH units)	3.4	SO_4	627
Temp (^oC)	10	PO_4	0.002
pe (pe units)	10	Cl	1.2
SiO_2	53	F	0.2
Fe	67	Diss. Inorg. Carbon (as C)	17
Ca	112	Total Ra (molal)	$7.04\text{x}10^{-14}$
Mg	59	^{226}Ra (pCi/L)	15
K	8	Total Th (molal)	$7.60\text{x}10^{-8}$
Na	6	^{232}Th (pCi/L)	2
Mn	3	Total U (molal)	$1.25\text{x}10^{-6}$
Al	5	^{238}U (pCi/L)	100

$Fe(OH)_3$ sub-region with pH around 3.7. A downgradient siderite ($FeCO_3$) sub-region raised pH to approximately 6.1. The most-distant, calcite sub-region raised pH above 7.3.

Case Study 4.4-2: Detailed Field Studies of Acid-Generating Waste-Rock Dumps Including Oxygen Levels and Temperature

highlights: oxygen and temperature profiles in acid-generating waste-rock dumps; calculation of sulfide-oxidation rates; lack of connection of drainage chemistry to temperature and oxygen levels

Oxygen profiles in oxygen-consuming waste-rock dumps (Equation 4.2.3-1) can display various trends with depth (Ritchie, 1994a and b). A steady decrease in concentration with depth suggests diffusion-controlled oxygen transport and steady-state consumption. Also, constant atmospheric levels with depth indicate oxygen transport and supply exceed the rate of consumption, probably due to air convection. In contrast, constant oxygen with depth except for a zone of depleted oxygen points to either a high-consumption zone or a finer-grained, diffusion-controlled zone. Other irregular trends and ambiguous temporal variations have also been observed in other studies, but are often ignored because they are not explained well with current theory.

Ritchie (1994b) provided profiles for waste-rock dumps at Rum Jungle in Australia and at the Aitik Mine in Sweden (Figures 4.4-2 and 4.4-3; see also Case Study 6.2-2). At Aitik, seasonal temperature profiles to 8 m depth at one monitoring site show fluctuations of more than 2°C.

Modelling of oxygen transport and of heat, simplistically controlled only by pyrite oxidation, was conducted on four waste-rock dumps and a large column test using notably consistent input data (e.g., Table 4.4-2). The resulting large-scale oxidation rates spanned approximately one order of

TABLE 4.4-2
Measurements of Thermal Conductivity, Air Permeability, and Oxygen Diffusion Coefficients in Waste-Rock Dumps (from Ritchie, 1994a and Harries and Ritchie, 1987).

Minesite	Number of Measurements	Range
In Situ Thermal Conductivity ($W\ m^{-1}\ K^{-1}$)		
Aitik Mine, Sweden	8	0.71-1.63
Heath Steele, Canada	3	1.04-1.22
Kelian, Indonesia	7	1.57-3.31
Rum Jungle, Australia	6	1.77-3.12
Various soils in literature (0.02-0.20 wt-% moisture content)		0.2 TO 1.7
In Situ Air Permeability (m^2)		
Aitik Mine, Sweden	27	2.6×10^{-11} - 1.4×10^{-9}
Heath Steele, Canada	24	1.6×10^{-10} - 4.7×10^{-9}
Kelian, Indonesia	18	3.9×10^{-13} - 9.3×10^{-10}
Rum Jungle, Australia	144	8.89×10^{-13} - 1.49×10^{-9}
In Situ Oxygen Diffusion Coefficient ($m^2\ s^{-1}$)		
Aitik Mine, Sweden	2	$2.25\text{-}6.85 \times 10^{-6}$
Heath Steele, Canada	3	$2.65\text{-}3.35 \times 10^{-6}$
Woodlawn, Australia	2	$3.49\text{-}5.07 \times 10^{-6}$

TABLE 4.4-3
Calculated Large-scale Oxidation Rates in Waste-Rock Dumps (from Ritchie, 1994b, and Johnson et al., 1996)

Minesite	Range kg $O_2\ m^{-3}\ s^{-1}$
Aitik Mine, Sweden	$0.3\text{-}4.3 \times 10^{-8}$
Aitik Mine (large columns)	1.4×10^{-8}
Rum Jungle, Australia	$0.3\text{-}8.8 \times 10^{-8}$
Norwich Park, Australia	$0.3\text{-}2.2 \times 10^{-8}$
Woodlawn, Australia	$0.2\text{-}2.7 \times 10^{-8}$
Mount Lyell, Australia	4×10^{-9}

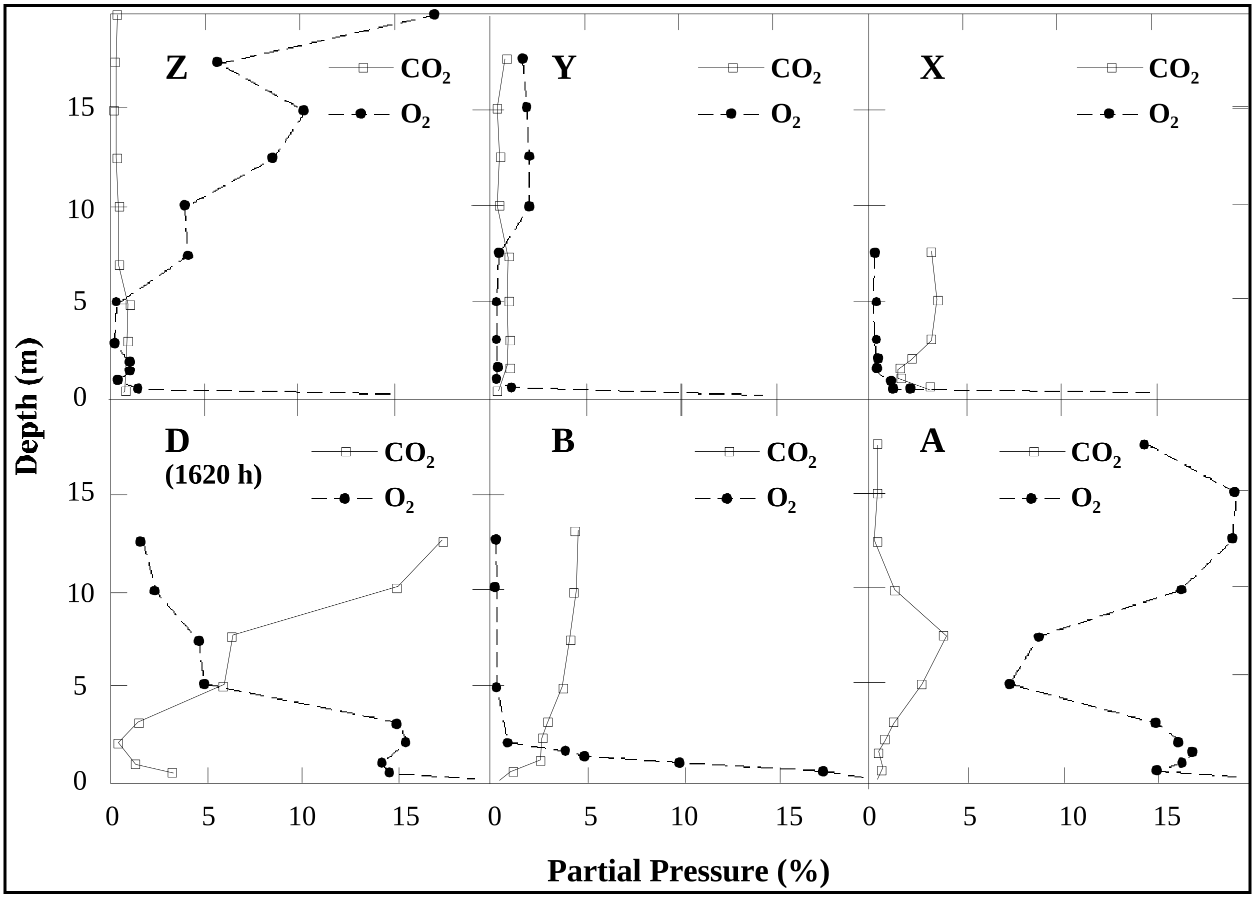

FIGURE 4.4-2. Depth Profiles of Poregas in White's (A, B, D) and Intermediate (X, Y, Z) Dumps at the Rum Jungle Minesite (adapted from Ritchie, 1994b).

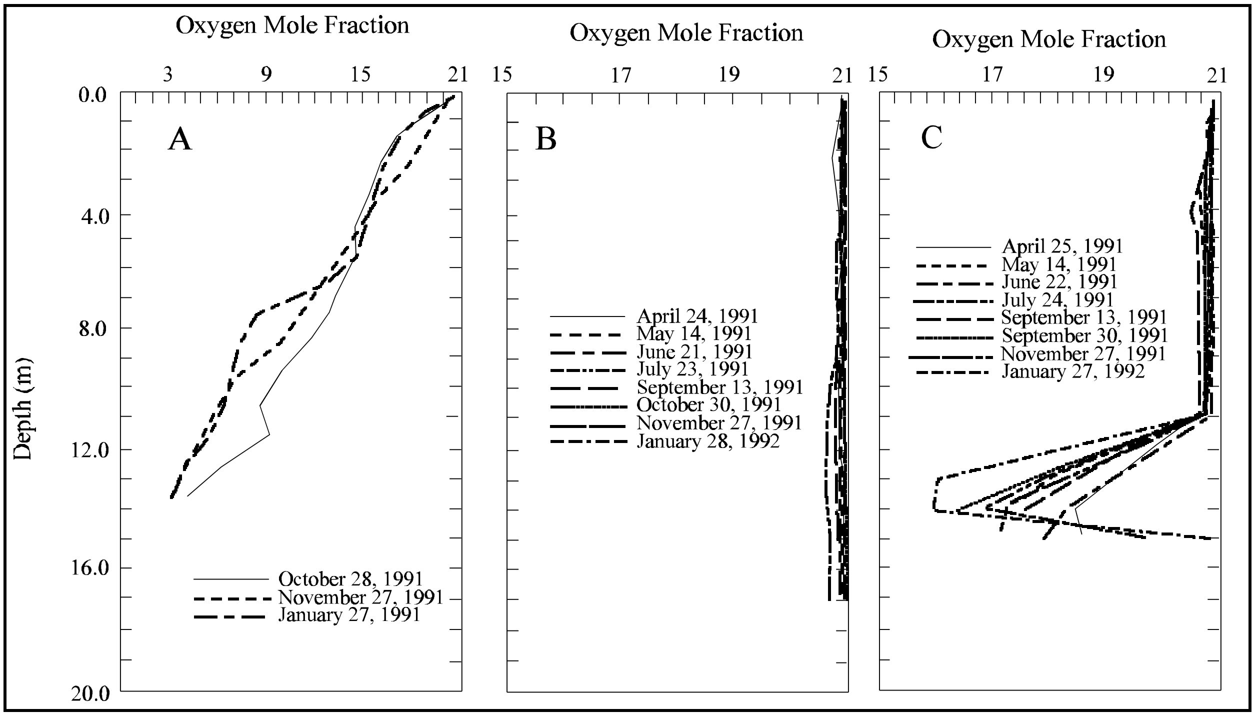

FIGURE 4.4-3. Profiles of Oxygen Levels in the Aitik Dump Through Time (adapted from Ritchie, 1994b).

magnitude (Figure 4.4-3). The agreement in values and ranges appear to be more than coincidental. As a result, either waste-rock dumps around the world have similar large-scale rates (in contrast to the International Kinetic Database, Section 5.3.3) or the technique is not detecting rates properly.

Case Study 4.4-3: Heap Leaching of Existing Mined-Rock Piles

highlights: commercial leaching of waste-rock dumps; methods for recovering leached copper; lack of acidic-water containment due to subsurface losses

Dump leaching is distinguished from heap leaching through the placement of ore directly on native soil or rock rather than on a specially installed basal liner for heap leaching (Hearn and Hoye, 1988). In 1988, there were 18 commercially active copper leaching operations in the USA, with 14 of the sites in the state of Arizona. Total production was placed at 280,000 metric tonnes a year. Approximately 23 inactive and abandoned leaching sites were also identified.

Leach dumps were typically found to cover hundreds of hectares, attain heights of more than 100 m, and contain millions of metric tonnes of ore. Hearn and Hoye (1988) visually observed leach dumps ranging in area from 8 ha at Cyprus Johnson to 850 ha at Bingham Canyon. More than 5.5 billion metric tonnes of ore were in place in leach dumps in 1988 and an estimated 40 million metric tonnes of new ore was added to the dumps annually.

Frequently only water had to be added to most dumps because internal acid generation through sulfide oxidation produced sufficient acidity for the leaching process. Copper was typically recovered by one of two processes. One process (“cementation”) used scrap iron which removed copper from solution and replaced it with iron. When recirculated to the dump, the iron typically precipitated on the surface of the dump and restricted infiltration. The second method (“solvent extraction”) used chemical complexation and chelation, usually with kerosene as a carrier, to strip the copper from the acidic water.

The loss of acidic leach water into underlying soil and rock, due to the lack of a basal liner, has been documented. Groundwater is the primary recipient of this lost water. Management of the contamination was found to be difficult and costly due to the areal extent of most dumps.

Case Study 4.4-4: Retention of Cyanide After Alkaline Heap Leaching

highlights: commercial leaching of precious metals from ore stockpiles using cyanide; retention of cyanide within stockpiles after leaching

Alkaline heap leaching with cyanide is one method for recovering gold or silver from ore piles, especially low-grade ore that is too expensive for milling. After concentrations of precious metals in the process water fall below a non-economic level, leaching is halted. However, not all cyanide is immediately removed from the heap due to internal retention by various physical and chemical processes. Slow release of retained cyanide can affect drainage chemistry from the spent heap for years. In some cases, the spent heaps are rinsed with water to remove retained cyanide. In other cases, the retained cyanide is allowed to decline gradually through processes like volatilization and degradation (Section 4.2-2).

A spent heap pile at the Trinity Silver Mine in Nevada, USA, was a focus of a detailed drilling and analytical study to determine the retention and gradual loss of cyanide (Comba et al., 1992). From September of 1987 to October of 1988, ore with a cutoff grade of 1.3 ounces of cyanide-extractable silver was crushed to less than 1.9 cm in size, agglomerated with 4.3 kg of cement per tonne, and stacked onto a lined leach pad at a rate of 2,700 t/day. The pad was 7.1 ha in area and the rock reached a maximum height of 12 m.

Leaching consisted of a 60-day primary leach at 0.003-0.005 L/s/m^2 of pile surface, a rest period of 60 days, and a secondary 60-day leach at the same flow rate. The process water (0.12% NaCN) was applied frequently through dripping and occasionally with sprinklers. Leaching was completed in early

1990.

Drilling and analysis of drill cuttings began in February 1991 (Comba et al., 1992), six months after the last application of process water. Additional drilling and analysis were conducted quarterly within specified cells of the heap until December 1991. Emphasis was placed on careful and high quality collection, storage, and analysis of drill cuttings. During this time, water was still draining from the heap, from 0.7 L/s in October 1990 to 0.3 L/s in February 1991 to 0.1 L/s in August 1991. The chemistry of this drainage was relatively constant.

Levels of weak-acid-dissociable (WAD) cyanide in the drill cuttings were similar to total cyanide, although laboratory rinsing tests indicated some of the total cyanide existed as insoluble cyanide compounds. Levels of WAD cyanide in the drill holes ranged from a minimum of 34.3 to a maximum of 115.5 mg WAD CN/kg ore, with an average of 74.2. In a few holes, cyanide was lower at shallow depth, presumably due to volatilization or degradation. However, no clear pattern of cyanide loss from the rock over the year was observed within analytical inaccuracy of approximately 10%, in agreement with the constant drainage chemistry.

Case Study 4.4-5: Alkaline Drainage from Cement

highlights: temporary neutralization of alkaline drainage passing through sandstone; identification of secondary minerals created during neutralization

Porewater from cement (pH 12 to 13) was passed through a sample of Clashach sandstone to determine the effects on the primary mineralogy, the formation of secondary minerals, and the transport of water-borne contaminants (Braney et al., 1993). The sandstone consisted predominantly of quartz with minor, highly weathered potassium feldspar, illitic clay, and iron oxide, with a mean grain diameter of 200 µm and a geometric grain-surface area of 8 m^2 kg^{-1}. Apparently, a BET or similar measurement was also made of grain-surface area, yielding 780 m^2 kg^{-1}, or a factor of 90 greater than the geometric area.

Approximately 4 L of $Ca(OH)_2$ saturated solution was passed through a rock sample of 0.1 m length and 0.076 m diameter over 280 days. The solution and rock were isolated from air to minimize ingassing of CO_2 and subsequent carbonation reactions.

The first 500 mL passed through the rock was successfully neutralized to pH 6, but then pH rose sharply to an unattenuated value of 12.0-12.5. The initial neutralization of pH was attributed to ion exchange onto phyllosilicate minerals and adsorption onto iron oxide, although modelling showed these and related processes could not account for most of the neutralization. Concentrations of calcium, silica, and potassium also followed this trend. Aluminum concentrations peaked around 22 mg/L as pH rose to 12, but quickly dropped to low levels below 1 mg/L.

Observations through scanning-electron microprobes and an energy-dispersive x-ray microanalyzer of the post-test rock revealed “extensive precipitation” of secondary minerals on the quartz and feldspar surfaces. On the other hand, the quantity of the secondary minerals was also described as “very small” with little effect on bulk porosity. In any case, the secondary minerals were identified as hydrated calcium-silicate phases, possibly containing aluminum and potassium. The exact mineralogy of these phases was not identified, but thought to be chain-structured minerals like tobermorite ($Ca_5Si_6O_{17}\cdot 10.5H_2O$) and foshagite ($Ca_4Si_3O_{10}\cdot 1.5H_2O$). The original quartz content showed only minor evidence of dissolution.

Case Study 4.4-6: A 20-Year Perspective on Heap Leaching

highlights: laboratory and field studies of acidic metal leaching over 20 years; observations on the importance of oxygen, the retention of secondary minerals, and the rinsing of particle surfaces

Cathles began modelling sulfide oxidation in heap-leach piles over 20 years ago (Cathles, 1994). His insights after two decades provide valuable lessons for understanding field-scale behavior of mined-rock piles. However, it is important to remember that heap-leach piles are subjected to high flow rates, providing greater and more extensive rinsing of particle surfaces than typically occurs in waste-rock dumps.

By the 1970's, Cathles (1994) reported that some of Kennecott Copper Corporation's heaps had been leached for over 30 years and showed a decreasing trend of copper release and recovery proportional to the square root of time. Cathles (1994) then focussed on the 12-m-high Midas Test Dump at Kennecott Copper's Bingham Canyon Mine, USA, using recycled acidic water. The success of the leaching was strongly dependent on the convective flow through the dump, with 20-40 times more air than water needed to optimize oxidation and leaching.

Poregas sampling pipes and downhole thermocouples were installed in the test heap. Within six months, internal temperatures reached 55°C, attesting to the success of oxygen and water supply. Oxygen profiles showed full-atmospheric levels (21% O_2) at the base and 50-100% depletion at the top, indicating that air was convecting laterally through the base and upwards in the center. While this behavior is not unusual, other studies have documented decreasing oxygen with increasing depth, reflecting diffusive entry from the top, irregular patterns in time and location, and atmospheric oxygen throughout (e.g., Ritchie, 1994b; Morin et al., 1994; Gélinas et al., 1994; Case Study 4.4-2). Cathles alluded to larger dumps having numerous "coherent" convection patterns with both inflow and outflow occurring across the top of the pile, similar to the observations of Case Study 4.4-7.

Second in importance after air convection was the development of "leached rims" on grain surfaces, leading to a shrinking core of unreacted material. Leached copper was found to diffuse into the unreacted portion as well as outwards, leading to the internal formation of secondary minerals like covellite and chalcocite (Table 4.2.2-1). The rate of leaching was controlled by diffusion of the oxidant, Fe^{3+}, when air convection was not limited. Modelling of the processes led to good agreement between predicted and observed depletion of copper, showing a significant decrease in copper recovery to below 0.4%/month after a year of leaching (Figure 4.4-4). The agreement improved for larger piles when the temperature limitation of *Thiobacillus ferrooxidans* around 65°C was added. Efforts to promote bacterial growth were not considered worthwhile since growth was already self-supporting.

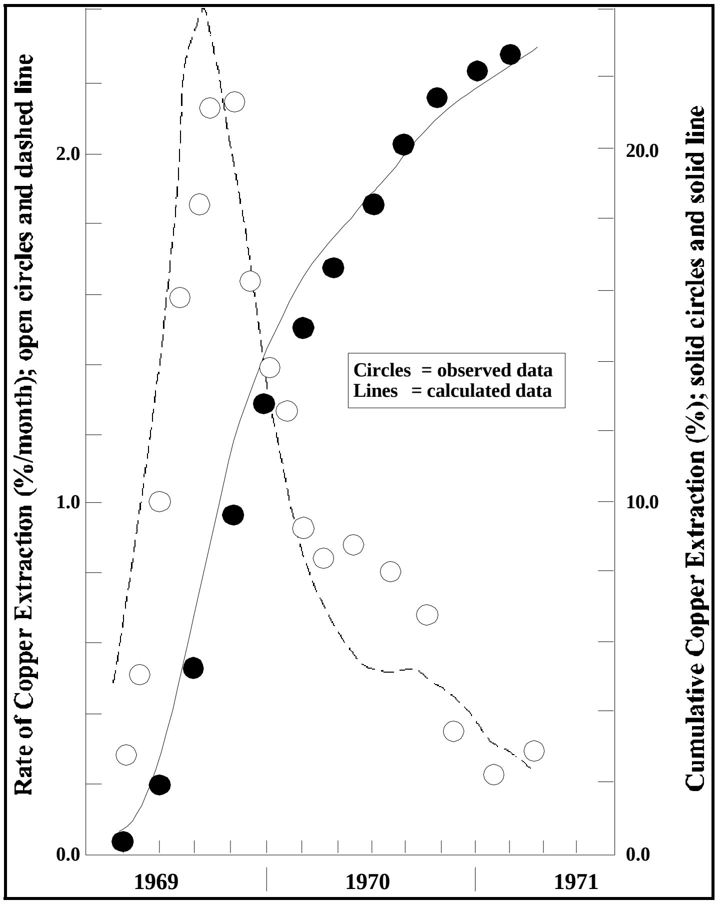

FIGURE 4.4-4. Observed and Calculated Copper Leaching from the 12-m high Midas Test Dump (adapted from Cathles, 1994).

To examine and model the leaching process further, a column experiment was designed in a well-insulated 12-m-high, 3-m-diameter stainless steel tank, holding 160 t of rock from Kennecott's Chino Mines Division in New Mexico, USA. Temperatures in the column reached 55-65°C within six months, as expected. Confusingly, a comparison of model results to two years of column operation showed that "all aspects of the leaching [were predicted] very well", although the model failed to estimate accurately the amounts and rates of copper leaching.

In any case, red dye (rhodamine-B) was added at the end of the test, and the column was carefully disassembled and inspected. Around 50% of particle surfaces were found stained with the dye compared with 57% of total copper in the column being leached. Presumably because of the shrinking-core concept, the discrepancy in percentages was evidence that flowpaths within the column shifted through time to provide more uniform rinsing of the surfaces.

Cathles (1994) provided a numerical example of secondary-mineral retention within waste-rock dumps. Based on expected oxidation rates within a coal-waste pile, pyrite was expected to oxidize fully within ten years. However, at a rainfall rate of 51 cm/yr, much of the reaction products would be precipitated as secondary minerals and then slowly released at pH 2 over 108 years. Cathles considered this behavior of waste-rock dumps as "an unconventional view of the origin of acid mine drainage [that] suggests remedial procedures very different from those in current use". To the contrary, Chapters 4 through 6 in this book show that secondary-mineral retention has been well documented for many years.

Case Study 4.4-7: Physical and Chemical Characterization of an Acid-Generating Waste-Rock Dump

highlights: strong acidic drainage from a waste-rock dump; studies of air, temperature, water, and minerals in a dump; lack of connection of drainage chemistry to oxygen and temperature

Gélinas et al. (1994) summarized various physical, mineralogical, and biological studies of the acid-generating South Waste-Rock Dump at La Mine Doyon in Quebec, Canada, to model and predict drainage chemistry. Only several dozen analyses of the actual drainage in perimeter ditches were conducted over several years of the studies, whereas over a thousand concentrations were calculated from water-chemistry relationships. This was found by Norecol, Dames, and Moore (1996) to be insufficient for detailed interpretation and modelling. Consequently, the main value of this study is in the various investigations conducted to characterize various non-drainage aspects of the dump.

Annual precipitation in 1991 for La Mine Doyon was 832 mm with monthly values ranging from 22 mm in February to 110 mm in September. Winter precipitation occurs as snow, representing 25-30% of total precipitation, and snowmelt accounts for most of the drainage through the dump.

The South Dump was constructed from 1983 to 1988, covers a lateral area of approximately 900 by 600 m with an average thickness of 30 m, and is composed of $21x10^6$ t of various volcanic rocks with roughly 5% pyrite. Approximately 35% of the dump is composed of rock with an SNPR (based on sulfide and CaNP; see also Section 5.2.1) around 2 (presumably net acid neutralizing) and the remainder with an SNPR of approximately 0.1 (net acid generating). Apparently, low-grade ore was also placed in the dump. The first evidence of acidic drainage was obtained in 1985, with acidity > 10,000 mg/L detected in 1988 (Figure 4.4-5). In 1991, drainage pH at weirs was around 2.1 and generally accompanied by 60,000 mg/L of acidity, 4,000 mg Al/L, 600 mg Ca/L, 16,000 mg Fe/L, 3,700 mg Mg/L, and 62,000 mg SO_4/L. This drainage is collected and treated with lime (Section 6.1).

Seven trenches excavated into the dump showed that the first meter of rock had a near-neutral pH, with apparent oxidation found below 3 m. Four grain-size distributions suggested most particles were between 1 and 100 mm, with d_{50} around 15-100 mm and 10% less than 1 mm. Average water content was 3.8%, except in a reactive zone with sericite schist at 7.5%, and dry bulk density was calculated at 1840 kg/m^3. Dump-wide porosity was estimated at 0.33 and, with the water content, the degree of saturation was calculated at 0.21 near the surface to 0.42 in the finer-grained reactive area at depth.

Six multilevel gas ports revealed that oxygen profiles were generally constant in time, but varied spatially. The profiles showed either increasing oxygen with depth, decreasing oxygen with depth, and depleted levels at intermediate depths of 10-20 m. Few measurements were below 2% O_2.

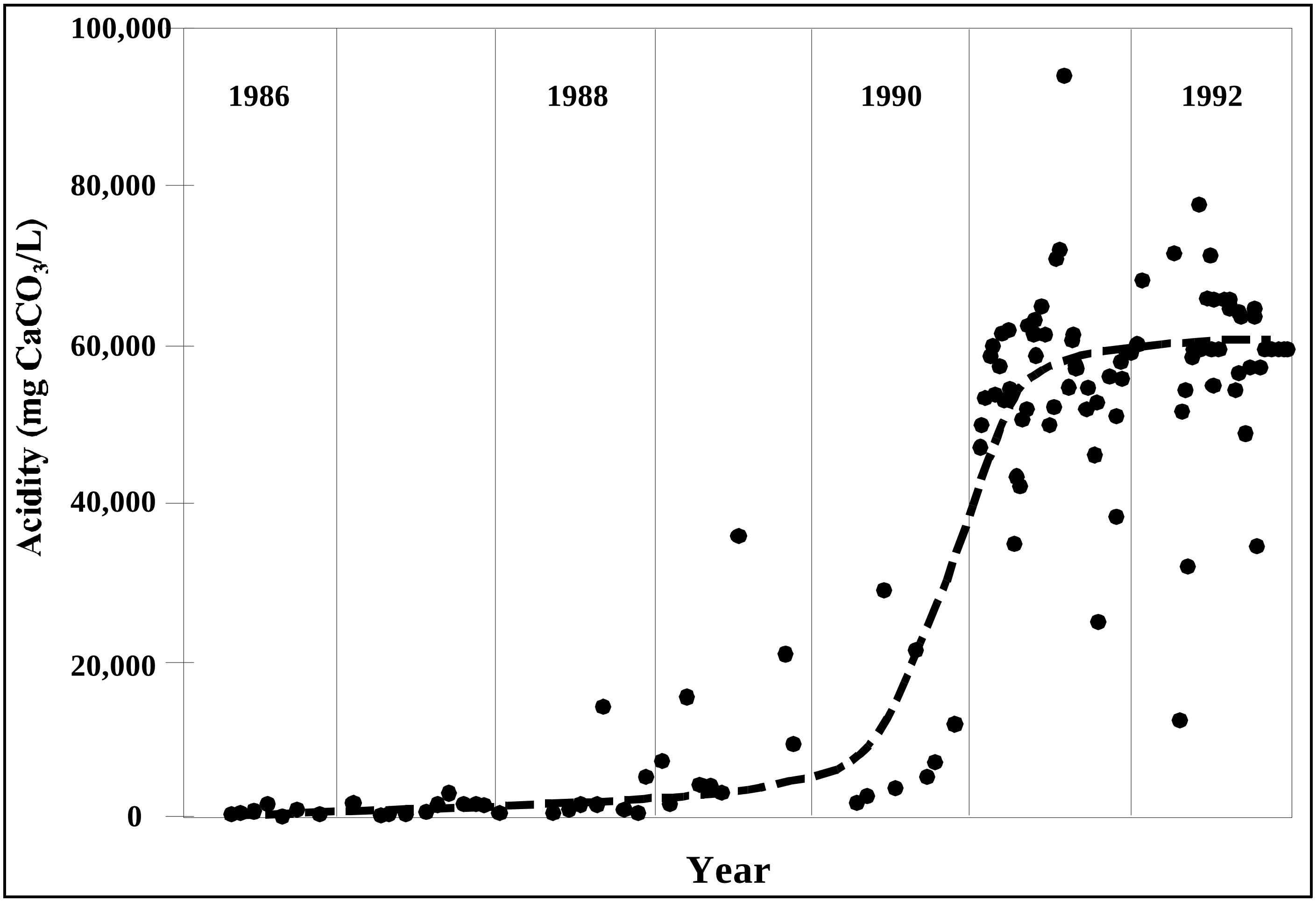

FIGURE 4.4-5. Acidity Concentrations in Dump Drainage at Mine Doyon (adapted from Gélinas et al., 1994).

Gas-pressure equipment with a precision of 2.5 Pa (later reported as 10 Pa or 10^{-4} atmospheres) only detected minor gradients between the dump surface and various depths. Consequently, permeability to air was considered high, and set in the model at 1.0×10^{-9} m^2 vertically and 2.5×10^{-9} m^2 horizontally.

The gas-pressure gradients in three boreholes indicated upward movement of air, whereas three other holes indicated downward movement (apparently a vector of lateral movement was not considered). Infrared thermography revealed "hot spots" of elevated temperatures, suggesting air entered the base of the dump at the slopes and rose upward. Further inside the dump, irregular convection cells with diameters around 10-15 m were noted. The resulting conceptual model indicated little oxygen reached below the convection-cell depth of 15 m and thus these depths were depleted of oxygen, although actual oxygen measurements in four of six boreholes contradicted this. Measurements in boreholes showed that temperatures above 40°C were typical below a depth of 5-10 m, with a maximum near 65°C. Thermal conductivities of the waste rock were typically around 2.5 W/(m°C), with extremes of 0.97 to 10.67 W/(m°C).

Unit-hydrograph analyses for rainfall-runoff events over one to five days yielded runoff coefficients for the dump around 0.05, although a maximum value of 0.62 was reported. However, this runoff was attributed to the surrounding watershed rather than the porous dump itself.

Water movement through the dump and underlying rock was modelled using a pseudo-three-dimensional Darcian flow model, which is incorrect for this coarse dump (Section 3.3). A hydraulic conductivity of 10^{-3} m/s was assigned to the waste rock, but not justified. This modelling indicated that drainage into the perimeter ditches corresponded to

199 mm of equivalent rainfall, compared to 213 mm based on hydrograph analysis, and drainage into the underlying rock was 70 mm of rainfall equivalent. Annual uptake, or "storage", of infiltration within the dump was estimated at 40-50 mm rainfall equivalent.

Acidity loadings indicated the dump released almost 10,000 t of acidity annually. Mineralogical studies found that most of the carbonate minerals were depleted and that the minor neutralization was from aluminosilicate minerals which also accounted for significant magnesium and aluminum in the drainage. Biological studies documented the presence of many acidic-based and neutral-based bacteria.

Case Study 4.4-8: Modelling of Mineral Reactions within a Waste-Rock Dump

highlights: relatively constant drainage chemistry from a waste-rock dump; geochemical modelling of mineral reaction rates and depletion times over centuries to millennia

The Aitik minesite in northern Sweden is reportedly Europe's largest copper mine. The waste-rock dump currently covers 400 ha with a 15 m height, and $14x10^6$ t is added annually (Strömberg and Banwart, 1994). This waste rock is relatively coarse, well aerated (10-20%O_2), and 0.50 m/yr to 0.68 m/yr precipitation infiltrates into and through the dump. Average summer and winter temperatures are +15°C and -15°C, with an annual average of 0°C. Temperatures in shallow waste rock are -5 to +12°C, while the base of the dump is relatively constant around 0-3°C. Warmer drainage waters indicate the presence of even hotter areas within the dump. Drainage chemistry and flowrates for the two main drainage ditches around the dump are characteristic of mild to moderate acidic drainage, and are relatively constant through time (Table 4.4-4).

The mineralogy of fresh waste rock (Table 4.4-5) is dominated by quartz, potassium feldspar, and plagioclase (70% sodium, 30% calcium). The primary acid-generating mineral is pyrite and, due to the general lack of carbonate minerals, much of the NP is provided by biotite and plagioclase.

The average particle surface area of the waste rock, based on BET measurements (Section 5.2.5), was 1 m^2/g. Based on an estimated density of 2800 kg/m^3 and porosity of 35%, this surface area is equivalent to $2x10^6$ m^2/m^3.

Geochemical modelling of the waste-rock dump involved both kinetic and equilibrium reactions. This modelling showed that the primary acid-generating reactions were ferrous-iron oxidation followed by pyrite oxidation by oxygen. The primary acid-neutralizing reactions in decreasing order of significance were biotite dissolution, outflow, plagioclase dissolution, and pyrite oxidation by ferric iron.

The reactive surface area obtained by modelling was $1.1x10^4$ m^2/m^3, or 0.6% of the BET surface area. As a result, 99.4% of particle surface areas were not reacting. Alternatively, this may represent retained reaction products (Section 4.2.2).

Overall, the time for complete dissolution based on modelling ranged from 700 years for pyrite, to 5000 years for biotite, to $3x10^6$ years for muscovite. As a result, acidic drainage may persist for several centuries.

Case Study 4.4-9: Onset of Net Acidity from a Waste-Rock Dump

highlights: temporal patterns in pH and sulfate as acidic conditions develop; early-warning observations signalling impending acidification of drainage

Monitoring of drainage chemistry at Island Copper Mine (cover photograph) on the west coast of Canada began in 1971 as the mine began operating. The monitoring network was expanded through time, particularly after the appearance of acidic drainage in 1985, and is continuing since the mine closed in 1995. Two stations, NDD and EDD, around the mine's North Dump monitored the period when some nearby rock began generating net acidity. According to the conceptual model of Figure 3.3-4, Station NDD is located on Level C, at the base of

TABLE 4.4-4
Waste-Rock Drainage Chemistry in Ditches, Aitik Minesite
(from Strömberg and Banwart, 1994)

Parameter (mg/L except pH and flow)[1]	Ditch D1 (Mean ± 1 Std Dev)	Ditch D2 (Mean ± 1 Std Dev)	Parameter (mg/L except pH and flow)[1]	Ditch D1 (Mean ± 1 Std Dev)	Ditch D2 (Mean ± 1 Std Dev)
pH	3.8±0.1	4.2±0.4	SO_4	1310±250	220±97
Ca	185±46	47±24	Mg	57±13	11±5.7
Al	75±24	6.5±4.4	Cu	19±5.0	1.2±0.8
Fe	2.0±1.0	2.8±1.9	Zn	5.8±1.6	0.40±0.3
Na	46±9.0	14±7.4	K	17±4.5	4.2±2.0
Si	19.1±7.1	16.4±8.6	Cl	27±8	5.5±3.5
Mn	12.1±3.9	2.2±1.6	Ni	1.3±0.7	0.17±0.20
Co	1.1±0.2	0.16±0.15	NO_3-N	8.2±3.1	0.49±0.26
HCO_3	<0.05	<0.05			
			(m^3/min)	Mean (hi-lo)	Mean (hi-lo)
			Flow	10 (2-50)	2 (0.5-10)

[1] Based on data collected between May 1991 and October 1993; chemistry based on 33 samples from D1 and 30 samples from D2 for SO_4, Ca, Mg, Cu, Zn, Al, Fe, and pH (other parameters based on 5 to 8 samples); flow based on 42 measurements.

TABLE 4.4-5
Mineralogy of Fresh Waste Rock at the Aitik Minesite
(from Strömberg and Banwart, 1994)

Mineral	Volume Percent (mean ± 1 Std Dev)	Mineral	Volume Percent (mean ± 1 Std Dev)
Quartz	24±14	K Feldspar	24±19
Plagioclase	19	Muscovite	10±16
Biotite	8±7	Amphibole, epidote, etc.	6±18
Chlorite, apatite, etc.	5±7	Calcite	0.1±0.5
Pyrite	0.57	Chalcopyrite	0.09

the pile (Morin et al., 1995a). Station EDD is located on Level E after flows from two distinct ditches mix.

Monitoring Station NDD is found near a discrete discharge point of subsurface water, which is in part fed by a creek that flows into the dump elsewhere. The pH values at this station apparently showed a slow drift toward lower values through the early 1980's (Figure 4.4-6). On the other hand, significantly increasing sulfate was a more reliable indicator of the impending onset of net acidity.

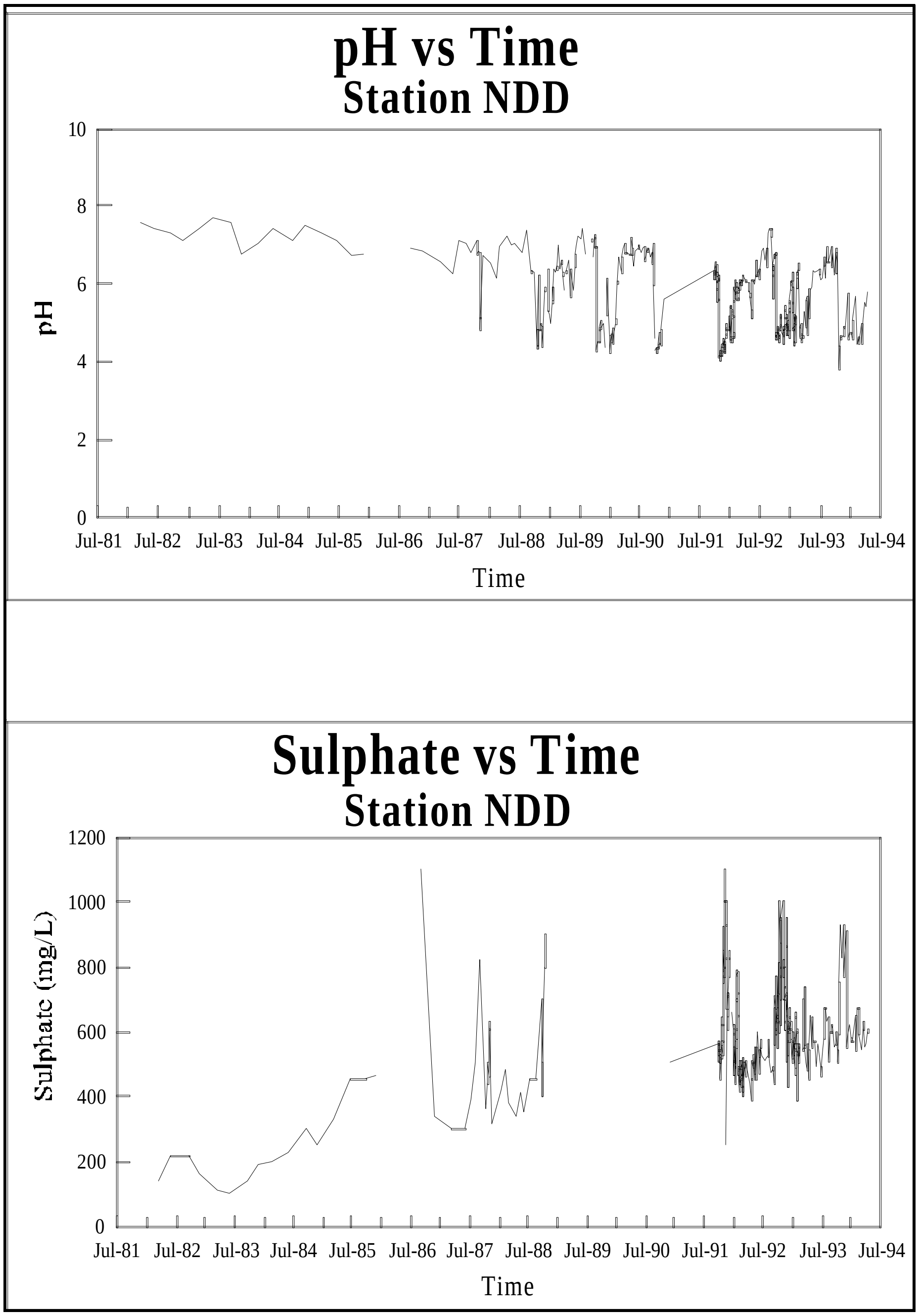

FIGURE 4.4-6. Temporal Trends of pH and Sulfate at Station NDD (adapted from Morin et al., 1995a).

Through 1994 at NDD, the annual duration of acidic pH (less than 6.0) had increased and sulfate concentrations showed a generally increasing trend. These effects can be explained by upstream branches and levels from Figure 3.3-4 that include (1) near-pH-neutral stream water flowing into the dump on Level B, (2) infiltrating water passing through carbonate-bearing till placed in this part of the North Dump on Level A, and (3) infiltrating water passing through acidic rock on Level A. Acidic conditions have persisted mostly during winter months when precipitation, infiltration, and flushing of accumulated acidity in Level A channels are highest. Therefore, the onset of acidic drainage at NDD was attributed to only a few upstream branches in Level A becoming acidic and being periodically flushed by infiltration. However, the prognosis for Station NDD is that additional branches will become acidic, resulting in more persistent acidic drainage passing through this monitoring point.

Station EDD monitors flow primarily from two upstream ditches and local catchments (Morin et al., 1995a). The trend of pH through time shows a sharp decrease in late 1987, from around 8 to almost 6 (Figure 4.4-7). In early 1988, the first acidic pH (less than 6.0) was detected. By mid 1988, pH recovered, but began a trend of fluctuation until stabilizing near pH 4.0 in late 1990. One ditch began turning acidic in late 1987. Therefore, the pH fluctuations in the late 1980's at EDD are attributable to the other ditch, which only became steadily acidic in 1990.

Although pH first showed an acidic value in late 1988, sulfate concentrations produced a sharp increase in mid 1986 by a factor of two and again in mid 1987 by another factor of two (Figure 4.4-7). As a result, sulfate provided a warning period of about two years before acidic pH was first measured. This observation is consistent with the observations at Station NDD (see also Case Study 5.3.1-1 and 5.3.1-3).

4.5 Drainage Chemistry from Tailings Impoundments

Tailings are often comprised of fine-grained particles, with elevated reactive grain-surface areas compared to an equal volume of mined rock. As a result, aqueous concentrations in tailings drainage can quickly increase to the equilibrium levels discussed in Section 4.2. Additionally, because of the relatively large lateral size and catchment area of tailings impoundments (Section 3.4), large volumes of tailings drainage with elevated concentrations can represent the greatest environmental concern at a minesite.

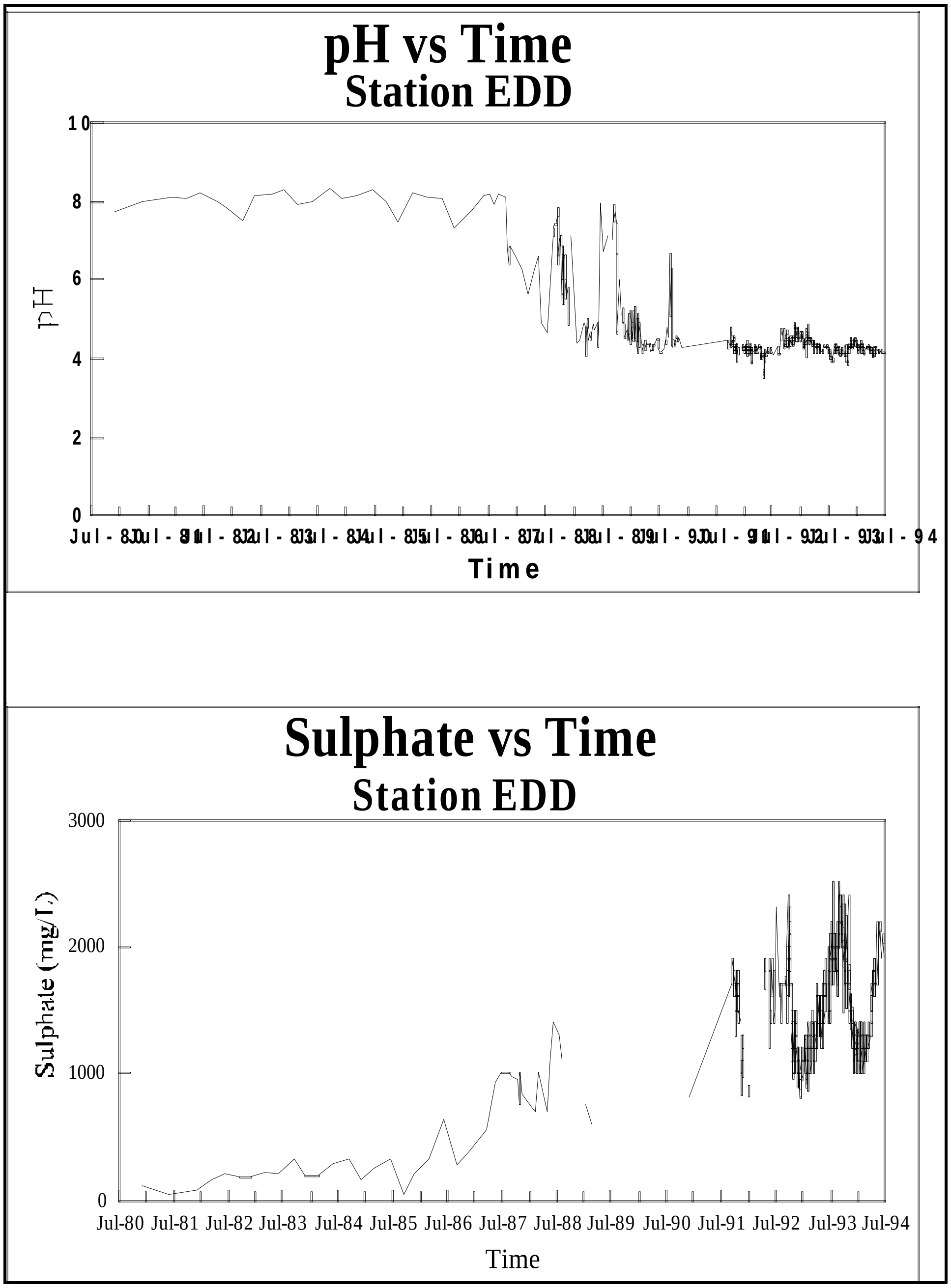

FIGURE 4.4-7. Temporal Trends of pH and Sulfate at Station EDD (adapted from Morin et al., 1995a).

In some cases in the past, tailings were discharged into open stream or river valleys. This was apparently done with the intent that surface waters would carry the tailings downstream away from the minesite, allowing more tailings to be discharged. Where the tailings were reactive, accumulation of the tailings along kilometers of floodplain resulted in widespread degradation of water and environmental quality. In the USA, Nimick and Moore (1994) discussed the effects of discharging 704,000 m^3 of metal-rich, sulfide-bearing tailings over 274 ha of floodplain along a 10 km reach of a river in Montana. This discharge occurred between 1864 and 1915 and, about a century later, represents a major source of contamination in the area.

The dissolved form of metals often represents the greatest chemical release from a tailings impoundment. For example, at two lead-zinc mines in the United Kingdom, maximum metal transport from the perimeter of unvegetated tailings (Merrington and Alloway, 1994) showed that dissolved metals dominated the water-phase transport, although aerial transport rivalled it (Table 4.5-1). In fact, the wind-blown transport of tailings

TABLE 4.5-1
Sources and Rates of Metal Release from a Tailings Impoundment (from Merrington and Alloway, 1994)

	Dissolved Metal (kg/yr)	Suspended Metal[1] (kg/yr)	Bed Load[1] (kg/yr)	Wind Blown (kg/yr)
Cadmium	4.2	0.7	0.0003	3.3
Copper	9.4	38	0.025	71
Lead	43	74	0.26	373
Zinc	1387	546	0.13	1041

[1] Suspended metals are classified as 0.45 to 62.5 µm (clay and silt), and bed load is greater than 62.5 µm

has also been a major concern for many decades, and installation of a soil or clay cover (Section 6.2) for this reason alone is often justified. For other minesite components, which typically contain coarser particles, aerial transport is a lesser concern.

Where this metal-bearing drainage is acidic, neutralizing minerals in the vicinity or along the flowpath dissolve to attenuate the acidity and precipitate metals as secondary minerals. Due to the relatively slow flowrates and Darcian behavior of groundwater flow through tailings, the neutralization reactions have been studied in greater detail than in other minesite components. The greater detail shows that neutralization of acidic drainage along flowpaths or through time often occurs as a series of equilibrium “sub-regions” (Morin et al., 1982).

After acidic drainage is generated and begins flowing through groundwater systems and surface-water channels, the local environment attenuates the acidity through time and distance (Figure 4.5-1). Elevated aqueous concentrations are attenuated by various processes like secondary-mineral precipitation, coprecipitation, adsorption to precipitated mineral surfaces, and physical dilution with background waters.

A series of equilibrium mineral reactions has been defined along flowpaths where acidic drainage encounters acid-neutralizing minerals. Each reaction zone defines its own “sub-region” of neutralization in which a relatively constant pH is created (Morin et al., 1982; Morin et al., 1988a; Morin and Cherry, 1988). Sub-region systems can develop (1) within a minesite component, (2) in a groundwater system beneath it, and (3) in surface waters beyond it. They arise in cases of acidic drainage, alkaline drainage, and even near-neutral drainage with minor pH fluctuations. However, sub-regions are not readily identifiable in minesite components where flowpaths are irregular, transient, or mixed. Consequently, they have been studied in greatest detail within and downgradient of tailings impoundments where Darcian conditions prevail.

Sub-regions for acidic drainage are best defined and are used here to illustrate the concepts, with alkaline drainage discussed afterwards. The sub-region neutralization of pH has been observed in, below, and beyond many acid-generating tailings impoundments (Morin et al., 1982; Morin, 1983; Dubrovsky, 1986; Morin et al., 1988a; Morin and Cherry, 1988; Morin, 1988b; Blowes, 1990; Blowes and Ptacek, 1994; Germain et al., 1994; Blowes et al., 1994; Jurjovec et al., 1995; De Vos et al., 1995; Bain et al., 1995; Lin and Qvarfort, 1996), fine-grained coal-waste piles (Cravotta, 1994), and streams.

In a typical situation, acidic drainage begins entering a flow system, encountering a primary carbonate mineral like calcite. As calcite dissolves, it neutralizes pH to an “equilibrium pH” reflecting the site-specific mineralogy, solubility, reaction rate, aqueous concentrations, and climate factors. As a

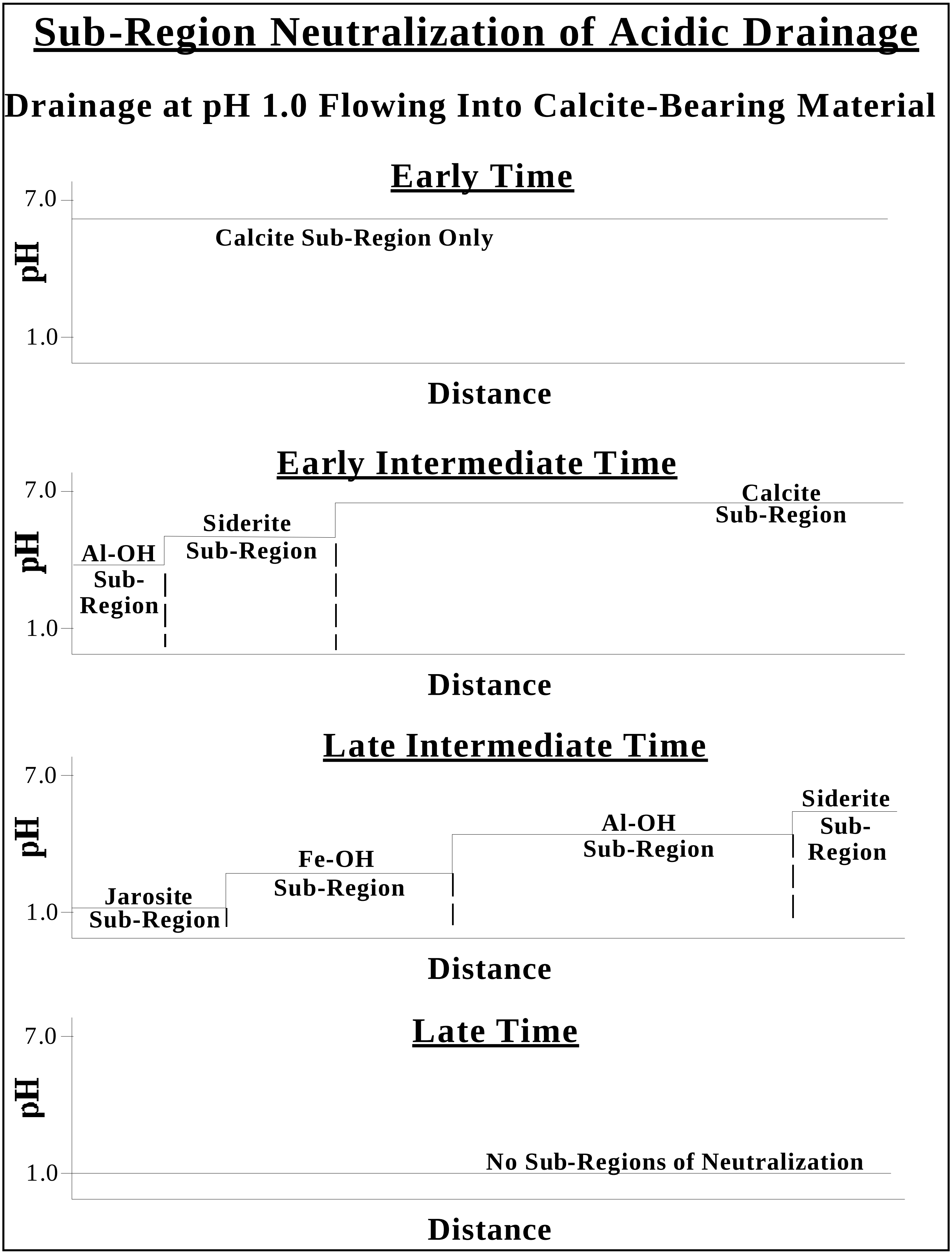

FIGURE 4.5-1. Sub-Region Neutralization of Acidic Drainage Along Flowpaths.

result, the equilibrium pH of a particular sub-region varies among minesites and the reported range for calcite sub-regions is 5.5 to 8.5 (e.g, Morin, 1983; Morin, 1988b; Jurjovec et al., 1995). As equilibrium pH is attained, the solubility of other minerals like siderite, Al-OH, and Fe-OH minerals are exceeded and they precipitate. The precipitation of OH-bearing minerals and the formation of siderite removes neutralization capacity from the water, and thus more calcite must dissolve to maintain its equilibrium pH.

After all calcite is exhausted at the head of a flow system, the next most soluble mineral begins dissolving to form another sub-region of neutralization. In anoxic groundwater systems at minesites, siderite often forms this next sub-region, and its equilibrium pH is reported in the range of 5.1 to 6.0 (e.g., Morin, 1983; Morin 1988b; Jurjovec et al., 1995). This pH is sufficient to continue the precipitation of Al-OH and Fe-OH minerals. Meanwhile, this partially neutralized water moves further along the flowpath, eventually encounters undissolved calcite, and becomes fully neutralized while dissolving a relatively small amount of calcite. This begins the creation of a step-wise neutralization of pH, from the source of the acidic drainage to the calcite sub-region (Figure 4.5-1). This has also been described mathematically as precipitation-dissolution waves (Dria et al., 1987).

In turn, when siderite is exhausted, Al-OH minerals dissolve in the pH range of 4.3 to 5.0. Of course, this occurs only if the pH of the inflowing acidic drainage is less than this. Again, when the Al-OH minerals are exhausted, Fe-OH minerals begin dissolving, creating an equilibrium pH around 3.0 to 3.7. If the inflowing acidic drainage has a pH less than 1.8, then jarosite minerals may have precipitated in the previous sub-regions (e.g., Norton et al., 1991) and would then begin dissolving with an equilibrium pH around 1.8 after the Fe-OH minerals are exhausted. Jurjovec et al. (1995) reported another, aluminosilicate sub-region around pH 1.3 in strongly acidic systems.

The formation, migration, and mass balance of each sub-region is different, with the downgradient sub-regions (calcite) moving faster than upgradient ones. As a result, a slight depression of pH is seen much sooner at longer distances along a flowpath than a marked decrease in pH. This slight depression in pH is a warning of approaching acidic drainage in the system.

As with acidic drainage, alkaline drainage also creates chromatographic profiles in pH and concentrations through time and distance (Braney et al., 1993; Bunge and Radke, 1982), although the number and types of sub-regions under alkaline conditions are not as well defined. Alkaline drainage is typically the result of the dissolution of natural or artificial oxide/hydroxide and silicate compounds with high solubility. For example, lime (CaO) can generate drainage pH values above 12, as readily illustrated by the pH of cement mixtures (Case Study 4.4-5). These highly soluble compounds are sometimes found in waste products like fly ash, smelter slag, and water-treatment sludge placed in a component. Highly alkaline minerals are also sometimes found within kimberlite, which is the typical host rock for diamonds.

Exposure to carbon dioxide in air appears to be a major source of neutralization for alkaline drainage. This is the result of ingassing of CO_2, the formation of base-neutralizing carbonic acid (H_2CO_3), and the precipitation of carbonate minerals. Also, because input concentrations are generally lower in alkaline drainage than in acidic drainage, factors other than mineral precipitation, like ion exchange, can play a major role in neutralization. In contrast, the more intense precipitation of minerals can quickly fill or cover ion exchange sites in acidic drainage.

In detailed laboratory and modelling studies of clay-bearing and nearly pure silica sands with minor iron hydroxides, ion exchange and dissolution of quartz and/or clays, rather than calcite precipitation, were found to form a neutralized sub-region. The pH reported for this ion-exchange sub-region was 6-8 compared with an input pH of 12-13 (Braney et al., 1993; Bunge and Radke, 1982). This was accompanied by the precipitation of zeolite, hydrated calcium-silica, and/or hydrated calcium-silica-aluminum minerals. Modelling and assessment did not continue beyond this two sub-region stage.

In some kimberlite and ultramafic rock, highly reactive magnesium-rich olivine (Mg_2SiO_4) and associated minerals can generate aqueous pH values up to 12 (Howe, 1997). As this alkaline drainage migrates, calcium and magnesium carbonates precipitate to form a sub-region, lowering the pH to approximately 8-9, if ingassing of CO_2 is sufficient. Otherwise, precipitation of hydroxide and silicate minerals like brucite ($Mg(OH)_2$) lowers the pH only to roughly 10-11. Upon exhaustion of the most alkaline minerals, the precipitated minerals like brucite or magnesium carbonate may begin dissolving, maintaining an elevated but less alkaline pH.

Case Study 4.5-1: Groundwater Drainage from an Acid-Generating Uranium Tailings Impoundment

highlights: long delay in release of acidic drainage from an acidic tailings impoundment; identification of primary pathways of subsurface drainage using sulfate

Cherry et al. (1982) summarized a hydrogeologic study of tailings drainage from a uranium tailings impoundment in the Shirley Basin Uranium District of Wyoming, USA (Figure 4.5-2). This impoundment lies on an alluvial sand aquifer with average groundwater velocities of 50-200 m/yr. The sand is underlain by relatively impermeable, sloping clay and thus most of the groundwater travels through the sand directly above the clay.

The tailings pond water was acidic with pH 1.8 and sulfate at 9200 mg/L (Table 4.5-2), and in equilibrium with gypsum and Al-OH-SO_4 minerals. This tailings water was draining from the impoundment through the sand, and sulfate concentrations in the resulting plume moving toward the creek confirmed this. However, all pH values in monitor wells were above 6.0 and many were greater than 7.0. As a result, the sand obviously contained sufficient neutralizing minerals at the time to neutralize the acidic drainage. Nevertheless, predictions indicated the groundwater would become acidic after a few decades if drainage from the impoundment continued.

Case Study 4.5-2: Oxygen Entry into Sulfide-Bearing Tailings

highlights: relative sulfide-oxidation rate in tailings under various exposure conditions; calculation of oxygen-diffusion rates into tailings

David and Nicholson (1995) determined in-field rates of sulfide oxidation in tailings based on porewater chemistry and poregas oxygen profiles with depth. The calculated rates for a tailings site at the East Mine in Ontario, Canada, indicated that, relative to the exposed control site, slime-covered (very fine-grained) tailings oxidized 100 times slower and submerged tailings oxidized 100-1000 times slower. Based on work by various researchers, David and Nicholson present an equation for estimating the effective diffusion coefficient for oxygen into tailings, partly dependent on the degree of saturation (see also Table 5.5.1-2 and Case Study 6.2-7):

$$D_{eff} = JD_a^o(1-S)^{"} + JD_w^o/H \qquad (4.5\text{-}1)$$

where D_{eff} = effective diffusion coefficient (m^2/s)
J and " = fitting parameters from laboratory column data of tailings from an Ontario mine (J = 0.27 and " = 3.27)
D_a^o = coefficient for free diffusion of oxygen in air ($1.78x10^{-5}$ m^2/s)
D_w^o = coefficient for diffusion of oxygen in water ($2.1x10^{-9}$ m^2/s)
S = dimensionless degree of water saturation (dry = 0.0 to saturated = 1.0)
H = modified dimensionless Henry's constant (26.32 at 10°C)

Stuparyk et al. (1995) reported a different equation, based on the work of Reardon and Moddle (1985):

$$D_{eff} = 3.98x10^{-7}[(G-0.05)/0.95]^{1.7}T^{1.5} \qquad (4.5\text{-}2)$$

where D_{eff} = effective diffusion coefficient (m^2/s)
G = gas-filled pore space
T = temperature (K)

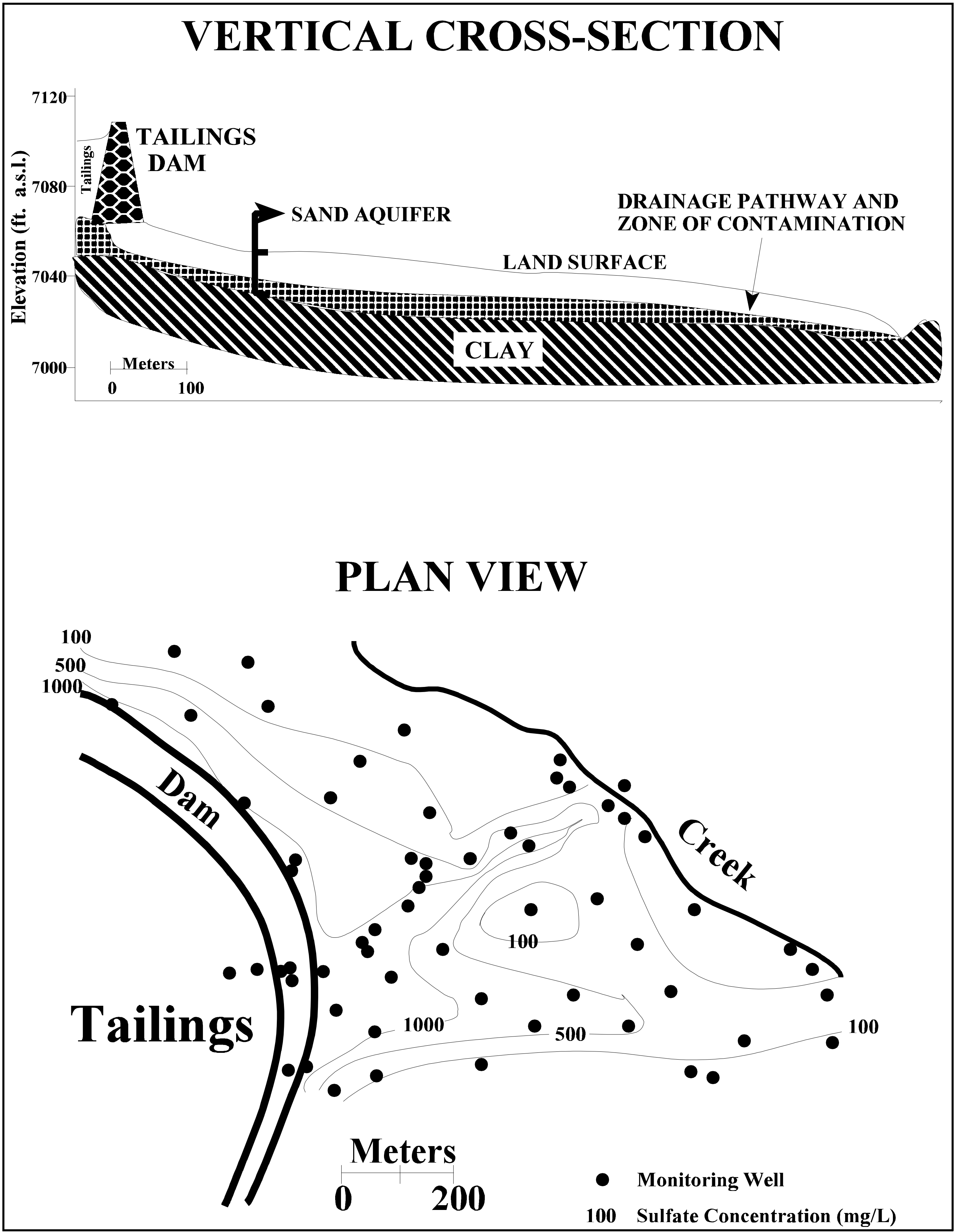

VERTICAL CROSS-SECTION

PLAN VIEW

FIGURE 4.5-2. Groundwater Seepage from a Uranium Tailings Impoundment, Wyoming, USA (adapted from Cherry et al., 1982).

TABLE 4.5-2
Concentrations in an Acidic Tailings Pond at a Uranium Mine
(all concentrations as mg/L unless noted; from Cherry et al., 1982)

Parameter	Value	Parameter	Value
pH (pH units)	1.8	Ba	0.08
SO_4	9200	Cd	0.13
Cl	1700	Cr	0.81
Fe	500	Cu	0.8
Mn	170	F	21
Al	205	Hg	0.03
K	90	Mo	0.14
Na	1400	Ni	1.6
Ca	500	Se	95
Mg	370	Zn	1.6
NH_4	0.5	U	38.2
NO_3 (as N)	2.9	^{226}Ra (pCi/L)	350
As	53	^{210}Pb (pCi/L)	200
B	0.2		

Case Study 4.5-3: Migration and Neutralization of Acidic Groundwater Drainage from an Acidic Tailings Impoundment

highlights: neutralization of acidic groundwater along flowpaths; prediction of increasing acidity with time

In 1958, a uranium-tailings impoundment began operating in a bifurcating granite-bedrock valley (Figure 4.5-3) in Wyoming, USA (Taylor and Antommaria, 1978; Taylor, 1980; and Haji-Djafari et al., 1979). The valley is filled with a complex sequence of sands and sandstones with a hydraulic conductivity around 10^{-4} m/s, in contrast to the surrounding/underlying granite with 10^{-7} m/s. Groundwater in the sand aquifer moves at approximately 180-360 m/yr and the sand contains an average of 1.6 wt-% calcite.

The tailings water is acidic with pH 1.95 and sulfate at 6000 mg/L (Table 4.5-3). Monitor wells at distances of 0 (Well WN-6S), 400 (WN-14H), and 1000 m (WN-1HDA) from the impoundment, along drainage flowpaths, showed progressive neutralization of acidity. This was consistent with the sub-region concept of neutralization (Section 4.5), with a siderite sub-region around pH 5.3 and a calcite sub-region around 6.4. As the acidic drainage continues to enter the sand, the sub-regions will migrate downgradient and a larger portion of the aquifer will become acidic (Morin, 1983).

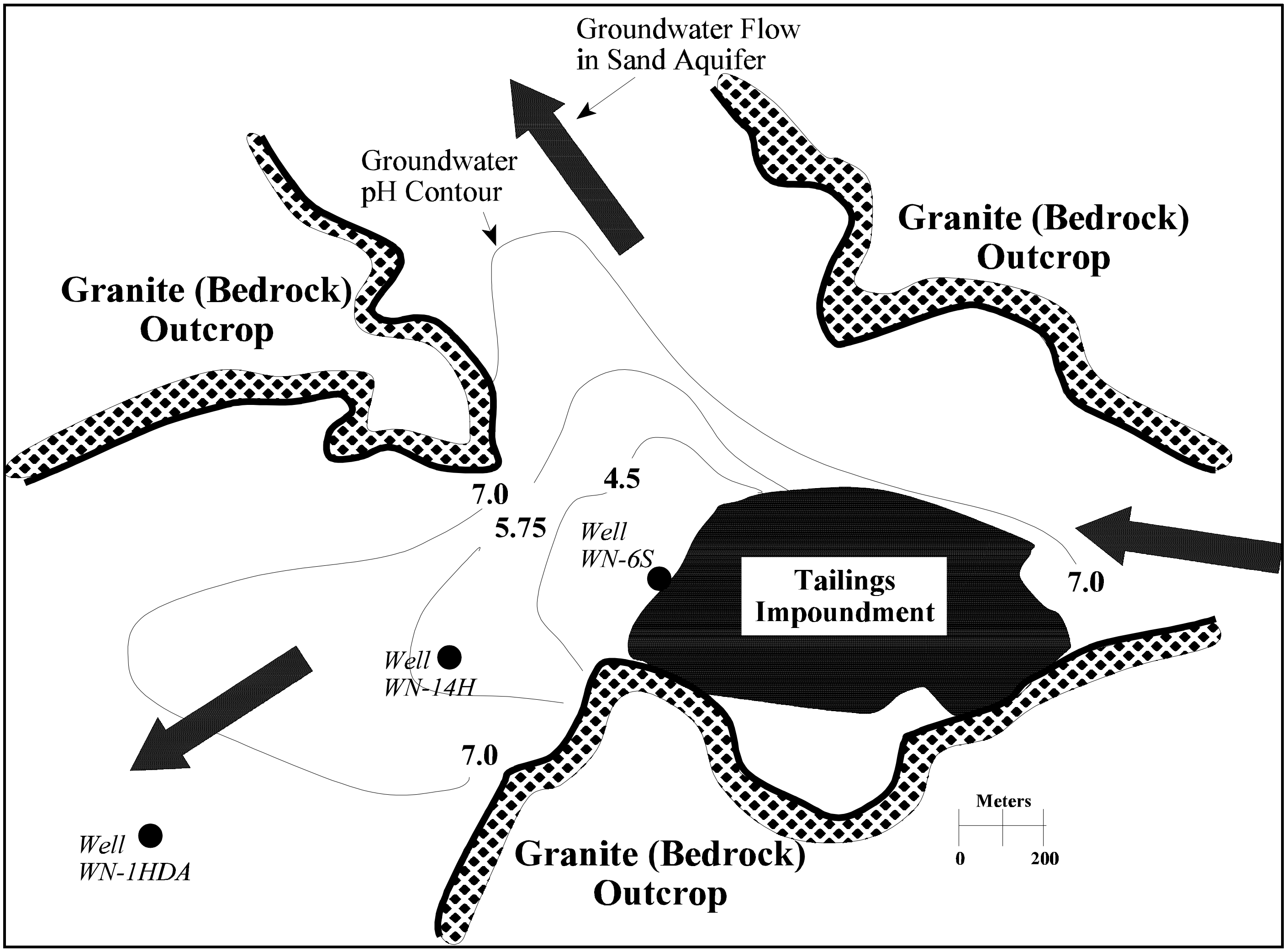

FIGURE 4.5-3. Migration and Progressive Neutralization of Acidic Groundwater Drainage from an Acidic Tailings Impoundment (adapted from Taylor, 1980).

Case Study 4.5-4: Detailed Hydrogeologic and Porewater Studies at a High-Sulfide Tailings Impoundment

highlights: trends in oxygen and porewater chemistry with depth in high-sulfide tailings; limitations of oxygen entry using woodwaste and sewage sludge

The East Sullivan tailings impoundment near Val-d'Or, Quebec, Canada, contains 15x10^6 t of tailings deposited from 1949 to 1966 (Germain et al., 1994). The impoundment covers 136 ha with tailings thicknesses ranging from 2.1 to 13.5 m (average of 7.3 m). Relatively impermeable clay and bedrock underlie the area. As a result, the water table is elevated within the impoundment, often at depth of a few meters, and groundwater drains down and toward the perimeter (Figure 4.5-4).

Around the impoundment, the grain size of tailings was relatively constant. Fine to very fine silt (median diameter of 3.5-17 µm) in layers of 1-15 cm thickness was interbedded with very fine sand to coarse silt (median diameter of 11-153 µm) in layers of 1-17 cm thickness. In contrast to the consistent grain size, the ratio of total thickness of coarse tailings to that of fine tailings varied from 0.3 near the basin center to 3.1 at the impoundment perimeter, based on cores. This coarsening toward the perimeter is consistent with specific-gravity and inertia effects from perimeter discharge of tailings. Falling-head hydraulic conductivities ranged from 1.2x10^{-6} to 9.1x10^{-6} m/s.

TABLE 4.5-3
Attenuation of Acidic Drainage from a Tailings Impoundment along a Groundwater Flowpath (all concentrations as mg/L unless noted; from Taylor, 1980)

Parameter	Tailings Pond	Wells		
		WN-6S	WN-14H	WN-1HDA
Lateral Distance from Tailings (m)	0	0	400	1000
Temperature (ºC)	22	13	13	13
pH (pH units)	1.95	3	5.5	7.2
Conductivity (µmhos/cm)	20200	4690	4600	2380
Dissolved Oxygen	6.1	-	-	-
HCO3	0	0	81	407
B	0.3	0.29	0.52	0.13
Cl	64.8	97.8	48.7	<0.5
CN	<0.005	<0.005	<0.005	<0.005
F	0.1	0.4	2.4	0.2
NH_3 (as N)	374	18.7	289	8.5
NO_3 (as N)	43.5	3	2.2	1.1
SO_4	6000	3100	3100	620
As	1.44	0.94	0.02	0.007
Cd	0.02	<0.01	0.02	<0.01
Ca	560	420	540	310
Fe	280	358	128	0.04
Pb	1.07	0.15	<0.05	<0.05
Mg	120	150	120	55
Mn	15.5	12.9	86	1.58
Mo	1	0.4	0.1	<0.1
Se	0.178	0.125	0.003	<0.002
V	0.5	0.2	<0.1	<0.1
U	10.4	8.5	2.8	0.27
^{226}Ra (pCi/L)	4800	1240	0.1	0.8
^{230}Th (pCi/L)	44100	10700	32	6.4

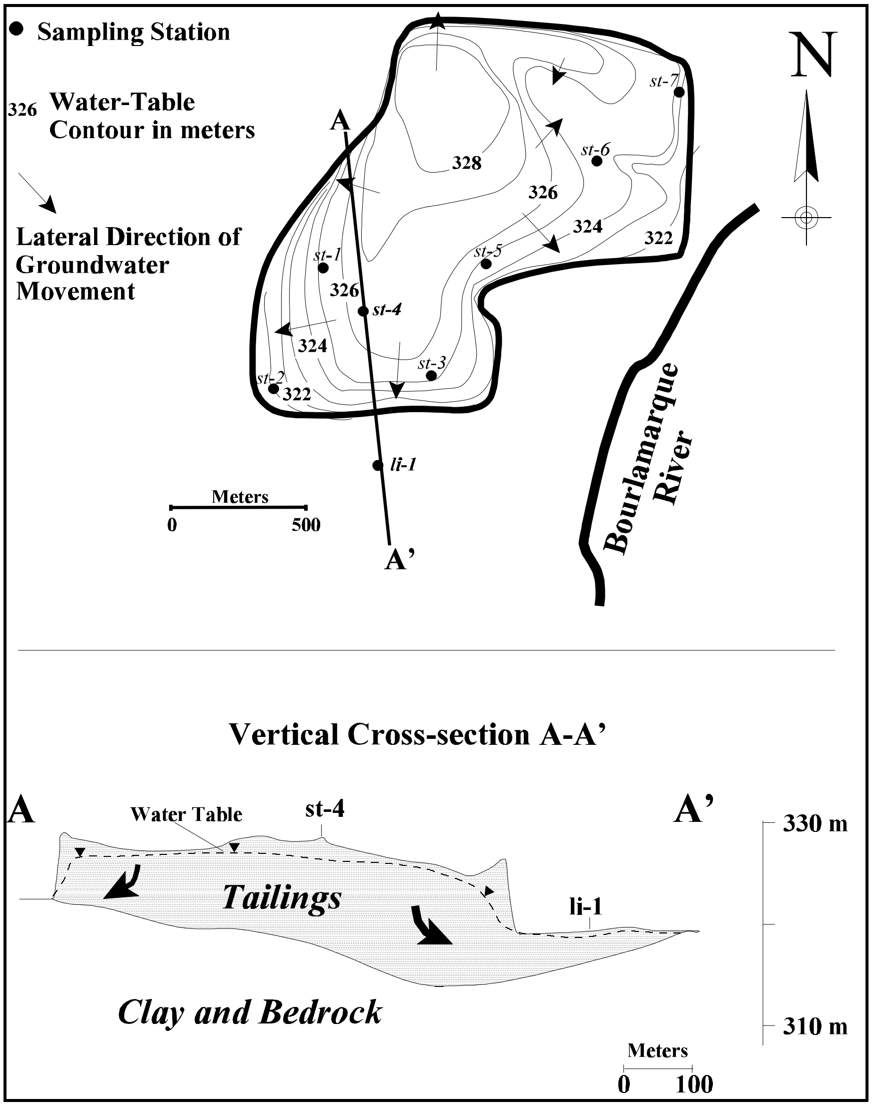

FIGURE 4.5-4. Plan Map and Vertical Cross-section through the East Sullivan Tailings Impoundment (adapted from Germain et al., 1994).

Ore at the minesite contained approximately 50% pyrite and pyrrhotite. As a result, the tailings contain sulfide minerals capable of net acid generation. Other primary minerals found in the tailings included quartz, chlorite, micas, and feldspars, with occasional trace amounts of calcite, dolomite, and amphibole. The carbonate minerals were detected only near the bottom of cores, reflecting the shallow generation of acidity. Secondary minerals were primarily jarosite and gypsum, suggesting a highly acidic environment, and were detectible only in the near-surface tailings. Goethite and hematite were detected in only one sample (although goethite was later reported as a major secondary mineral).

Oxygen levels in pore gases declined sharply with depth, to <5 volume-% at depths of 40-60 cm. Conversely, carbon dioxide increases from 0.15 % to a maximum of 24% at 2 m depth.

Porewater chemistry (Figure 4.5-5) showed that pH rose from 2 in the shallow, unsaturated zone to 5-7 at depth below the water table. Aqueous sulfate and iron generally showed trends of increasing, then decreasing, concentrations with depth. Mineralogical data and saturation indices of minerals indicated carbonate minerals were dissolving as acidic porewaters moved downwards. The neutralization with depth is consistent with the sub-region concept of neutralization along flowpaths. As the deeper carbonate and NP are consumed, the extent of net acidity and acidic drainage is expected to increase. Additionally, acidic drainage due simply to the precipitation of aqueous iron from neutral drainage was noted in some locations.

Recent remediation of this site involved widespread covers composed of wood waste and sewage sludge (Tremblay, 1994; see also Case Study 6.2-5). Although this reportedly eliminated oxygen entry and the acidic-drainage problem, near-neutral drainage with phenol and organic acids, as well as aesthetics, are apparently new concerns.

Case Study 4.5-5: Natural Massive-Sulfide Deposits and Gossans as Natural Analogs for the Distant Future of Minesite Components

highlights: acid generation for thousands of years; gossans as long-term natural analogs for minesite components

Studies of natural massive-sulfide deposits and gossans can provide important analogs for future geochemical conditions in and around high-sulfide minesite components (Cameron, 1977, 1979; Boyle,

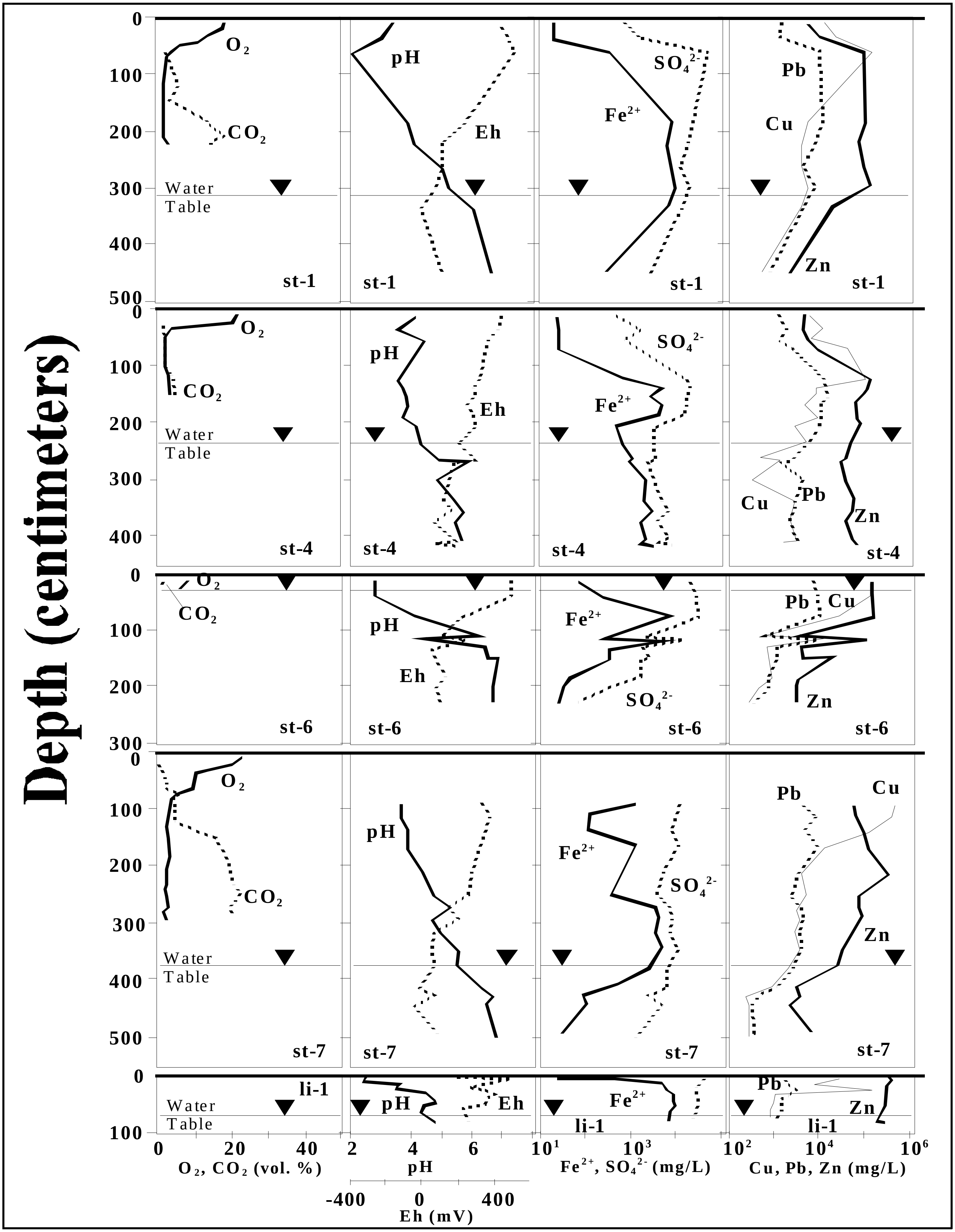

FIGURE 4.5-5. Vertical Profiles of Pore Gases and Porewater Concentrations in the East Sullivan Tailings (adapted from Germain et al., 1994).

1994; Dumaresq and Michel, 1994). The basic concept is that these old, deeply weathered deposits contained mineralogy similar to some components, particularly sulfide-rich tailings, so the geochemical evolution of the components should lead to similar ends. This is a particularly valuable undertaking, because most predictive testwork (Chapter 5) often spans only a few years at most, and rarely a decade.

Cameron (1977) reported a study of a massive sulphide body, named the Agricola Lake prospect, approximately 480 km northeast of Yellowknife, Northwest Territories, Canada. This deposit is found in continuous permafrost, but, in spite of this, “intensive” sulphide oxidation was occurring near the surface and at depth. Due to this oxidation and the lack of carbonate minerals in the area, there was natural acidic drainage and metal leaching around the deposit. Presumably, this oxidation had been occurring since glacial retreat several thousands of years ago and was actively continuing.

Measurements of moist-soil pH revealed a minimum pH of 2.4 with values commonly between 3 and 4. More important, the presence of jarosite minerals indicated that pH, at least on a local scale, may be less than 2.0. A groundwater spring near the deposit had a pH of 3.4. At greater distances from the deposit, soil pH typically increased to 5-6.

Cameron (1977) attributed the increased thickness of the thawed permafrost “active layer” over the body to heat generation through sulphide oxidation. Cameron thus concluded that freezing conditions and permafrost was not a solution to acidic drainage, because heat generation and even thin water films around grains were sufficient to maintain chemical weathering and oxidation. Additionally, patterned ground at Agricola Lake like mudboils suggested that vertical convection of massive-sulphide material may replenish the surface exposure of sulphide minerals. The boils were largest directly over the massive sulphide body, presumably indicating the greatest rate of convection.

In a similar study, Cameron (1979) examined massive sulphide deposits on Melville Peninsula, Northwest Territories, Canada. These deposits were in continuous permafrost like Agricola Lake. Around an outcrop of metasedimentary rock containing one massive-sulphide deposit, surface waters had a pH as low as 3.1. However, calcareous outcrops and till successfully neutralized the acidity by the time it reached nearby lakes. Although the active layer in the area was roughly 1 m thick, Cameron hypothesized that oxidation was occurring at depths of meters to tens of meters. This was attributed to abundant graphite and/or various sulphide minerals that acted as inert conductors of electrons, which passed from the deep sulphide minerals to atmospheric oxygen. Such electrochemical potentials have been invoked elsewhere, as mentioned below. Like Cameron's 1977 work at Agricola Lake, this study indicated that freezing conditions and permafrost were not deterrents to sulfide oxidation.

Boyle (1994) discussed natural oxidation of massive-sulfide deposits to depths of 25 m in the Bathurst mining area, New Brunswick, Canada, as well as up to 400-500 m deep in other areas. The oxidation occurred beneath water tables and in the absence of atmospheric and dissolved oxygen. Like Cameron (1977 and 1979), the evidence again pointed to oxygen-free electrochemical oxidation, leading to deep acidic drainage that can persist for millennia.

Boyle (1994) also addressed weathering of in-situ massive-sulfide deposits over tens of thousands to millions of years, much longer times than Cameron. This approach, discussed below, may reflect the general geochemistry of high-sulfide minesite components in the very distant future.

The Bathurst mining area of New Brunswick, Canada, contains 37 massive-sulfide deposits containing zinc, lead, copper, and silver (Boyle, 1994). Ten of these deposits have been mined (Case Study 4.3-3), with Brunswick Mining and Smelting No. 12 being the largest at $161x10^6$ t. Several of these deposits are capped by weathered gossan and supergene-sulfide zones (Table 4.5-4).

The gossan zones of the Bathurst area have lost 50-60% of their mass due to oxidation and weathering over 40,000 years, based on comparisons of specific gravity and conservative (non-leached) elements in the gossans and underlying unweathered

TABLE 4.5-4
Zones and Mineralogy of Gossan and Supergene Zones of Massive-Sulfide Deposits of the Bathurst Area, New Brunswick, Canada (adapted from Boyle, 1994)

Zone (maximum thickness in m)	Typical Mineralogy
[TOP] Ferruginized Wallrock (20)	Quartz sericite/chlorite schist
Gossan (15)	Primarily oxides and sulfates: goethite, primary quartz, secondary silica, K-Fe-Pb-Sb-As-(Hg) hydroxy-sulfates, K-Ag jarosites, scorodite, woodhouseite, native Au-Ag-Bi, cassiterite [SnO_2], cinnabar, barite
Massive-Sulfide Gossan (45)	Primarily sulfides and sulfates: covellite, chalcocite, digenite, enargite, luzonite, beaverite, meta-aluminite, acanthite, anglesite, scorodite, goethite, litharge [PbO], hinsdalite, brochantite
Sulfide-Quartz Sand (4)	(not described)
Altered Massive Sulfide (20)	(not described)
Fresh Massive Sulfide (120)	Primarily sulfides and carbonates: pyrite, marcasite, arsenopyrite, sphalerite, chalcopyrite, galena, tetrahedrite group, pyrrhotite, cassiterite, stannite, Pb-Sb-As-Ag sulfosalts, quartz, ankerite, siderite, calcite, magnetite, chlorite, sericite
[BOTTOM] Footwall	Quartz chlorite schist

zones. After adjustment for lost mass, the enrichment and depletion of various elements during weathering can be estimated (Table 4.5-5).

A significant portion of lost mass in Table 4.5-5 is sulfur, which apparently oxidizes and then forms secondary sulfate minerals that are eventually leached away. Many metals typically associated with the sulfur, like iron and zinc, are also removed. Notably, proportionally more zinc than copper is leached. However, a gain, or positive value in the right column of Table 4.5-5, does not necessarily mean no net loss. Based on gold rather than tin as a conservative element, about 40% of initial lead would have been lost.

Boyle (1994) noted that sulfide-rich tailings are often depleted of some metals and primary minerals in the uppermost layers, and thus represent a very young version of massive-sulfide weathering. Similarly, Dumaresq and Michel (1994) examined secondary-mineral crusts forming on top of arsenic-rich tailings during summer months in Ontario, Canada, and found these reflected the supergene alteration reactions of near-surface mineralized rock. Therefore, mass balances (Table 4.5-5) and weathering rates for long-exposed mineralized rock represent analogs for the oxidation and weathering of minesite components in the distant future.

The average rate of weathering and oxidation of massive-sulfide deposits in Canada, Scandinavia, and Russia is approximately 0.01 cm/yr, based on observed depths of oxidation since glaciation exposed the deposits (Boyle, 1994). In contrast, the average rate for high-sulfide tailings is 2 cm/yr, or 200 times greater. This may mean that over several millennia, the rate of oxidation in tailings can decrease by a few orders of magnitude, although differences like grain size make this only a general expectation.

TABLE 4.5-5
Enrichment or Depletion in Oxidized Massive-Sulfide Deposits of the Bathurst Area of Canada
(adapted from Boyle, 1994)

Element (unit of concentration)	Primary Ore	Massive-Sulfide Gossan Zone	% Gain/Loss[1]
S (%)	36.3	0.48	-99
Cd (ppm)	6.9	0.3	-98
Zn (ppm)	3715	245	-96
Cu(ppm)	5620	1000	-90
Fe (%)	33.1	28.2	-50
Al (%)	0.23	0.2	-48
Hg (ppm)	34	36	-38
Ag (ppm)	28.2	39	-18
Sn (ppm)	251	447	0
Bi (ppm)	36	78	+28
Sb (ppm)	380	1000	+55
As (ppm)	3160	9120	+70
Pb (ppm)	1515	6165	+140
Au (ppb)	160	1096	+295

[1] Normalized to Sn and adjusted for loss of mass during weathering; negative value is a loss.

Case Study 4.5-6: Drainage Chemistry from Phosphogypsum Tailings

highlights: mining of phosphate minerals for fertilizer; gypsum-rich tailings; strongly acidic drainage from unneutralized mill effluent

Phosphate mining typically uses open pits to reach phosphate-rich strata for the production of fertilizer. Milling often requires the addition of sulfuric acid to create orthophosphoric acid, leading to “phosphogypsum” tailings. These tailings contain gypsum (or the related dehydrated form of calcium sulfate) and phosphate minerals, and acidic water if not neutralized before discharge. The tailings particles include bladed gypsum crystals, 10-500 µm in length and oriented horizontally, with secondary recrystallization at the tailings’ surface forming a relatively impermeable crust.

The drainage from phosphogypsum tailings impoundments can carry hundreds to thousands of mg SO_4/L and tens to hundreds of mg PO_4/L (Wrench, 1986). In Florida, USA, over a dozen tailings impoundments were studied and their drainages were also found to carry radionuclides and arsenic.

When acidic, the typical pH is 1.2-2.0 (South Africa impoundments, Wrench, 1986) and the drainage from phosphogypsum tailings is progressively neutralized along flowpaths following the sub-region concept defined at the beginning of this section. This results in the precipitation of secondary minerals containing silica, phosphate, and fluoride, which stabilizes aqueous concentrations within definable ranges. However, the secondary phosphate-bearing and fluoride-bearing minerals that precipitate have apparently not been studied in detail.

In addition to the crystalline tailings, phosphate mining of clayey strata produces waste clays discharged from the mill at approximately 3% solids by weight (Bromwell and Carrier, 1983). Florida reportedly generated $36x10^6$ t/yr of phosphate-clay waste around 1983. The area needed to store these low-solids wastes, and the slow rate at which they drain and consolidate, are major problems in remediating phosphate minesites.

4.6 Questions

4-1. A local regulatory limit for copper in minesite drainage is 0.01 mg/L. A kinetic production rate (Rate1, Figure 4.2.2-1) of copper from one minesite's waste rock is 1 mg Cu/kg rock/wk. Below what proportional flow rate (L/wk) will the regulatory limit be exceeded?

4-2. For the Three Stages of Drainage Chemistry, redraw Figure 4.2.2-1 for situations where Rate1 is less than theoretical Rate2, that is, where Rate1 does not lead to secondary-mineral precipitation.

4-3. From Table 4.2.2-1, choose a mineral from each group and locate minesite-specific solubility data for them.

4-4. In Figure 4.2.5-2b, what is the average annual copper concentration at pH 4? What is the maximum annual one-month-duration concentration?

4-5. Based on your answer for Question 3-2 in Chapter 3, an average zinc concentration of 1 mg/L in saturated groundwater (all other flows have zero concentration), and the assumption of simple and complete mixing in the pit, what is the average zinc concentrations when the pit fills to elevations +20, +60, and +100 m?

4-6. Based on your answers for Questions 3-7 and 3-8 in Chapter 3, draw a similar graph showing concentration rather than flow if runoff carries 0.1 mg/L of manganese and subsurface seepage carries 50 mg Mn/L. Assume all runoff and seepage mix completely in ditches to calculate the net concentration.

4-7. Based on concepts in Figure 4.5-1, speculate on what might happen if pH-neutral water began flow into the system at Late Time.

CHAPTER 5
PREDICTION OF DRAINAGE CHEMISTRY

5.1 Overview

One of the best ways to explain the concepts and theory behind drainage chemistry is through the explanation of how it is predicted. In general, prediction inherently supposes that the mechanisms and processes behind drainage chemistry are known and defined — and this leads to the following critical observation about open-environment systems like minesites.

The minesite components (Chapter 2) interact with each other as well as with the open environment around them. This environment includes solid, liquid, and gas phases that can enter and leave a component. As a result, each minesite component, and minesites themselves, are “open systems” in the classic technical sense with no isolating boundaries. Little effort is therefore needed to realize that such open systems cannot be described or predicted in detail unless the entire environment and all its physical, chemical, and biological characteristics are accurately known. Obviously, such intensive assessments and predictions are not possible.

The best-known example of predicting an open-environment system is weather. Daily records and observations of weather conditions have been collected for over a century in many places, some of the world’s fastest and largest computers are dedicated to prediction, and thousands of people are employed in the field. The results of prediction are probabilities of future weather conditions, sometimes with minor probabilities becoming reality.

For drainage chemistry, there are no century-long records of drainage chemistry, no supercomputers dedicated to it, and not many people employed in it. Can we expect to do better than weather prediction? Combined with the observation that weather (climate) is but one variable that can influence drainage chemistry, there is no doubt that drainage prediction and assessment are in their infancy.

With these sobering thoughts and humility in mind, we turn to the techniques developed in the last few decades for predicting drainage chemistry. Later in this chapter, case studies of drainage chemistry will show how these predictive techniques provide some understanding of the mechanisms and processes behind drainage chemistry.

Minesite drainage is sometimes divided into specific classes based on its pH (Table 4.2.3-1). Acidic drainage is often thought to be a major problem for the mining industry. However, as documented in Chapters 4 to 6, other classes sometimes rival or surpass concentrations in acidic drainages. In other words, toxic concentrations of metals at any pH are still toxic. Nevertheless, many of the predictive techniques were originally developed to predict acidic-to-neutral conditions, but are adaptable to the other classes as shown in this chapter.

5.2 Static Tests

Static tests are so named because they are often conducted at one point in time, in contrast to kinetic tests (Sections 5.3 and 5.4) that involve ongoing repetitive analysis. The results of static tests are often used to deduce some future condition of a sample, but the prediction is of course suspect. In fact, only the combined interpretation of static tests, kinetic tests, and drainage chemistry realistically shows how the results of static tests can be extrapolated through time.

5.2.1 Acid-Base Accounting (ABA)

The most popular, most misunderstood, and most abused method for predicting overall drainage chemistry is acid-base accounting (ABA). Developed primarily in the 1960's and 1970's, Sobek et al. (1978) documented an ABA method, also known as EPA 600 ABA (Appendix B). The Sobek ABA now has a track record of usage of a few decades, longer than any other ABA method. Sobek et al. also included procedures for other types of static and kinetic tests, like the Sobek humidity cell (Section 5.3.1 and Appendix C).

Other ABA methods, basically variations on Sobek ABA, have been developed. However, the critical issue is not which method is "best", because no one method is. Instead, the issue is understanding the strengths and weaknesses of an ABA method and interpreting results in light of corresponding kinetic tests and on-site monitoring. Since Sobek ABA has the longest documented existence, well-documented strengths and weaknesses, and a history of comparisons to other tests, it is the obvious choice for ABA. Most of the ABA results discussed in this chapter are derived from the Sobek method.

ABA reflects the awareness that (1) drainage chemistry is a net result of reacting minerals and (2) the minerals which last longest and react fastest will determine long-term and overall chemistry. In reality, the fastest reacting minerals often do not last long and thus affect only short-term chemistry. However, ABA simplifies this complexity to simply predicting the outcome of acidic, near-neutral, or alkaline drainage based primarily on mineral balance.

For example, if the amount of acid-neutralizing minerals exceeds the amount of acid-generating minerals, neutral drainage is predicted indefinitely with no net acidity. Of course, if the acid-neutralizing minerals have slow reaction rates and cannot match the rate of acid generation, then the ABA prediction would be wrong. In this case, acidic drainage would persist until the acid-generating minerals and their secondary minerals are exhausted (First and Second Stages, Figure 4.2.2-1), and then drainage chemistry would approach background values (Third Stage). The lack of reaction rates is one weakness of ABA and highlights the importance of kinetic tests (Sections 5.3 and 5.4) which provide them.

Research on ABA has concentrated on expansions to the basic procedure to estimate better the amounts of reactive minerals, especially since not all minerals may be available and sufficiently reactive. The following subsections explain the basic procedure and various expansions.

5.2.1.1 Paste and Rinse pH

Sobek et al. (1978) provided a procedure to measure the pH of a mixture of distilled water and pulverized sample (Appendix B), known as paste pH. This pH indicates whether the sample was acidic, near-neutral, or alkaline at the time of measurement. If a sample were acidic, for example, then any measured neutralization potential (NP, Section 5.2.1.3) was obviously not reactive.

One criticism of paste pH focusses on the use of pulverized samples. If acid-generating minerals are located preferentially on the outside of particles and creating acidic drainage, crushing could expose internal acid-neutralizing minerals. This could yield an anomalous near-neutral paste pH from rock generating net acidity. To avoid this, an alternative technique not included by Sobek et al. (1978), called rinse pH, simply involves the mixing of distilled water with unpulverized sample (Appendix B). However, the measurements of paste pH far exceed those of rinse pH in reports and publications, and paste pH still reflects aqueous pH while not necessarily matching it (Case Study 5.2.1-1).

If distilled water is used in the measurement of paste or rinse pH, its pH is typically around 5.3. Consequently, any pH measurement less than 5.0 indicates the sample contained net acidity at the time of analysis. Common carbonate minerals can create pH values around 8-10 and thus values above 10.0 are unusually alkaline. Values of paste pH between 5.0 and 10.0 can be considered near neutral at the time of analysis.

5.2.1.2 Sulfur Species and Acid Potentials

ABA identifies the capacity of a sample to generate acidity based on various sulfur analyses. The most common analysis is for total sulfur (Total Sulfur as %S, or %S total) using specialized equipment known as a Leco Furnace, which is relatively simple and automated. The resulting value is converted to a Total Acid Potential by:

$$\text{Total Acid Potential (TAP)} = (\%S\ \text{total}) * 31.25 \qquad (5.2.1\text{-}1)$$

where TAP is provided in any of three equivalent units: kg $CaCO_3$ equivalent/metric tonne (t) of sample, t $CaCO_3$ equivalent/1000 t of sample, or parts per thousand (ppt) $CaCO_3$ equivalent. The second unit of t $CaCO_3$/1000 t is used most often in this book. Other, non-equivalent units include kg H_2SO_4/t (differs by approximately 2%) and %$CaCO_3$ (differs by a factor of 10). TAP is sometimes called Maximum Potential Acidity (MPA).

The conversion factor of 31.25 has a remarkable derivation because of the numerous, restrictive assumptions behind it, which in fact often seem to apply to most minesite components. The "standard" equation for pyrite oxidation on which the factor is based is:

$$FeS_2 + 7/2\, H_2O + 15/4\, O_2 \div Fe(OH)_3 + 2\, SO_4^{2-} + 4\, H^+ \qquad (5.2.1\text{-}2)$$

The assumptions inherent in this equation assume much about mineralogy, reaction pathways, and local environmental conditions at a minesite. They are:

Ø the measured sulfur occurs in the solid phase only as disulfide (S_2^{2-}),
Ù disulfide oxidizes completely to sulfate (SO_4^{2-}),
Ú disulfide originally occurs only as pyrite (FeS_2),
Û oxygen (as O_2) and water are the only oxidants,
Ü iron from pyrite oxidizes to the ferric (Fe^{3+}) state, and
Ý all iron precipitates as $Fe(OH)_3$.

As a result, four parts of acidity (H^+), represented by two parts of $CaCO_3$ equivalent with a molecular weight of 100, are generated by two parts of sulfur with a molecular weight of 32 within FeS_2. This leads to a conversion factor of 2*100/(2*32)=3.125. This is then multiplied by 10 to convert percent (parts per hundred) to parts per thousand, yielding TAP.

Obviously, these assumptions and the resulting Equation 5.2.1-2 are not always appropriate, and thus alternative equations would apply (Morin, 1990a). For example, ferric iron can reportedly oxidize pyrite in the absence of oxygen (Section 5.5). If the ferric iron is originally derived from nearby pyrite, the conversion factor from sulfur to acid potential is 15.63 rather than 31.25. Alternatively, if the ferric iron is derived from nearby ferric-iron minerals, the conversion factor is 125.0.

As another example, the conversion factor to acid potential is 125.0 rather than 31.25 if manganese is the only oxidant and the released iron is not oxidized and precipitated. Also, sulfide minerals other than pyrite (Table 4.2.1-2) are associated with other conversion factors including zero. For example, the oxidation of galena with subsequent precipitation of lead as a hydroxide requires a conversion factor of 31.25 (like Equation 5.2.1-2 but for different assumptions) for acid potential. However, for all conversion factors, frontier-molecular-orbital theory indicates oxidation and acid generation are more complex than suggested by the simple stoichiometry used to calculate the factors (Luther, 1990).

In spite of the foregoing limitations and complications, the conversion factor of Total Sulfur to TAP has been standardized at 31.25 for ABA. Nevertheless, it is clear that there is some uncertainty in the calculated TAP based on this restrictive conversion and thus some uncertainty in predictions. This chapter discusses methods for reducing the uncertainty.

One refinement in acid potential is the use of sulfide instead of total sulfur (Assumption 1 above). Sulfide can be analyzed directly; however, the safest determination of sulfide involves the corresponding measurements of total sulfur, leachable sulfate, and other forms of sulfur that may be relevant like organic sulfur and barite ($BaSO_4$). The appropriate mass-balance equation is:

$$\%S\ \text{total} = (\%S\ \text{sulfide}) + (\%S\ \text{leachable sulfate}) + (\%S\ \text{other}) + (\text{del}\ \%S) \qquad (5.2.1\text{-}3)$$

In this equation, del %S, or)%S, represents any imbalance such as analytical error. If del %S is positive, representing unaccounted for sulfur, it can be added to measured %S sulfide for a safer estimate of acid potential, assuming the sulfide analysis is the source of error. Once the best estimate of sulfide is obtained, a Sulfide Acid Potential is calculated:

Sulfide Acid Potential (SAP) as t $CaCO_3$/1000 t =
(%S sulfide) * 31.25 (5.2.1-4)

Acid Potentials (xAP) are discussed further in Section 5.2.1.4.

In some cases, sulfide is the dominant form of sulfur, and thus SAP and TAP are equivalent (e.g., Figure 5.2.1-1). The advantage to this situation is that analytical efforts and costs are reduced by analyzing for total sulfur only. In other cases, other sulfur species can be significant. A dramatic example is a mine that did not analyze sulfide directly and overestimated it due to underestimates of sulfate values (Case Study 5.2.1-8). All $70x10^6$ t of tailings were originally expected to be net acid generating, and a large dam and impoundment were designed to place them underwater. Upon recalculation of sulfide values, none of the tailings were expected to generate net acidity.

As a preliminary estimate of sulfide reactivity, scatterplots of total sulfur/sulfide against paste pH (Figure 5.2.1-2) may show correlations, suggesting that the greater the amount of sulfide, the greater the amount of oxidation. This can be further assessed, if most sulfate from the oxidation has not been dissolved from samples, by plotting sulfate against total sulfur/sulfide (Figure 5.2.1-3) and against paste pH (Figure 5.2.1-4).

5.2.1.3 Neutralization Potentials

The capacity of rock or tailings to neutralize acidity is commonly called Neutralization Potential (NP). The uncertainty behind accurate determination of Acid Potential seems daunting (Section 5.2.1.2), but is minor in comparison to the uncertainty in NP. The primary cause of this uncertainty lies in the fundamental definition of NP — there is none.

NP has long been defined simply as the result of an analytical procedure, like Sobek (Appendix B). Because there are various versions of the ABA procedure, there can be various NP values for a sample. Some authors have entertained or concerned readers by pointing out that one sample has many NP values (e.g., Case Study 5.2.1-2), sometimes spanning an order of magnitude (Lawrence et al., 1989; Lapakko, 1994a; Calow et al., 1995). In reality, rock and tailings have a certain capacity to neutralize acidity under the site-specific environmental conditions, mineralogy, and rates of mineral reactions. Therefore, there is only one true NP value for a sample, or "effective NP" (also called "empirical NP" by Lapakko, 1994a). The difficulty lies in identifying the effective NP when various methods yield differing values. Which is correct?

To resolve the NP dilemma, there must be a fundamental shift of defining NP from analytical procedures to in-field conditions. A useful definition draws on a previous statement: *the effective Neutralization Potential (ENP) of a sample of rock or tailings is its capacity to neutralize acidity to pH 6.0 or above under the site-specific environmental conditions, mineralogy, grain sizes, and rates of mineral reactions*. A pH of 6.0 is selected because many water-quality guidelines and criteria often list a minimum pH of 6.0 for acceptable quality. With this definition, the issue becomes the delineation of effective NP from a suite of procedures providing various NP values.

As explained in Section 5.2.1, ABA by Sobek et al. (1978) has the longest and widest acceptance for approximately 20 years, and has a history of comparison to other static and kinetic tests. Therefore, the determination of effective NP from Sobek NP is the best approach. As with acid potentials, NP from Sobek and other procedures is traditionally reported in any one of three equivalent units: kg $CaCO_3$ equivalent/metric tonne (t) of sample, t $CaCO_3$ equivalent/1000 t of sample, or parts per thousand (ppt) $CaCO_3$ equivalent. The second unit of t $CaCO_3$/1000 t is used most often in this book. Other, non-equivalent units include kg H_2SO_4/t (differs by approximately 2%) and %$CaCO_3$ (differs by a factor of 10). NP is sometimes called Acid Neutralizing Capacity (ANC).

Unlike several other ABA procedures, the Sobek ABA involves a relatively aggressive method for NP determination. A sample is soaked in excess HCl acid, often around pH 1-2, and then heated to near boiling until all visible reactions cease (Appendix B). Other methods do not include heating, instead use H_2SO_4 acid which can adversely

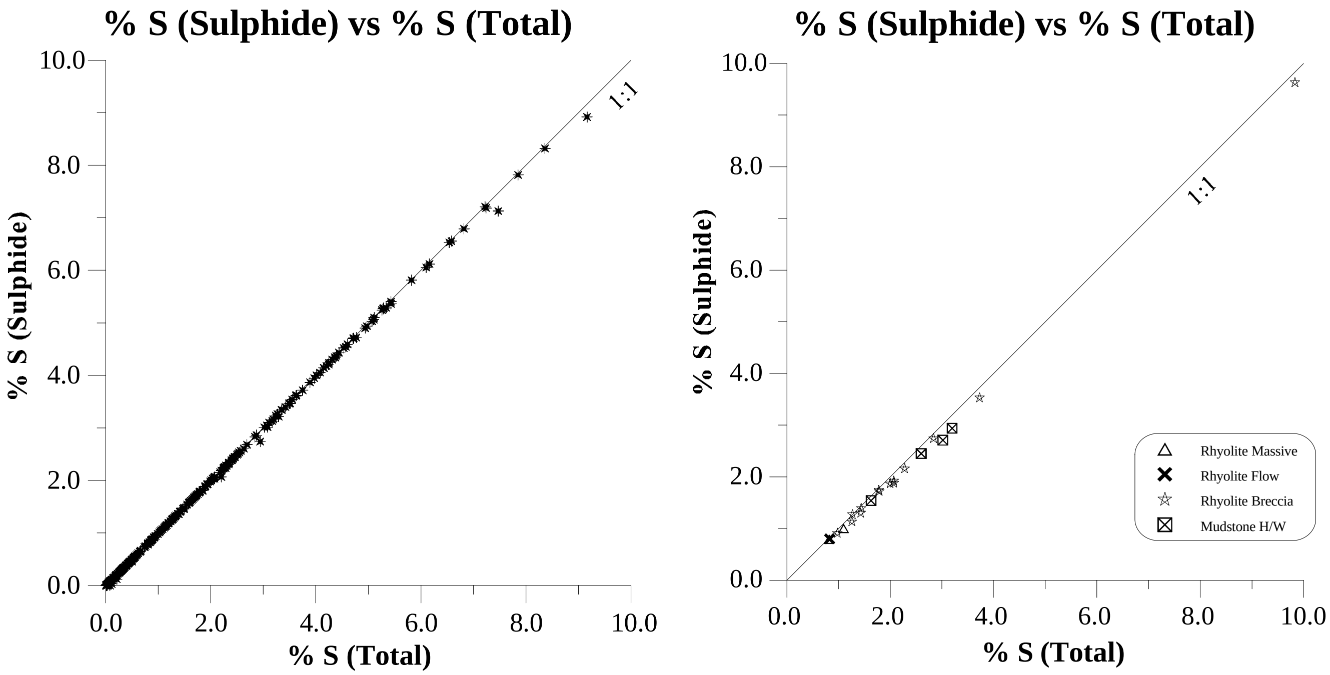

a) total sulfur dominated by sulfide

b) total sulfur dominated by sulfide

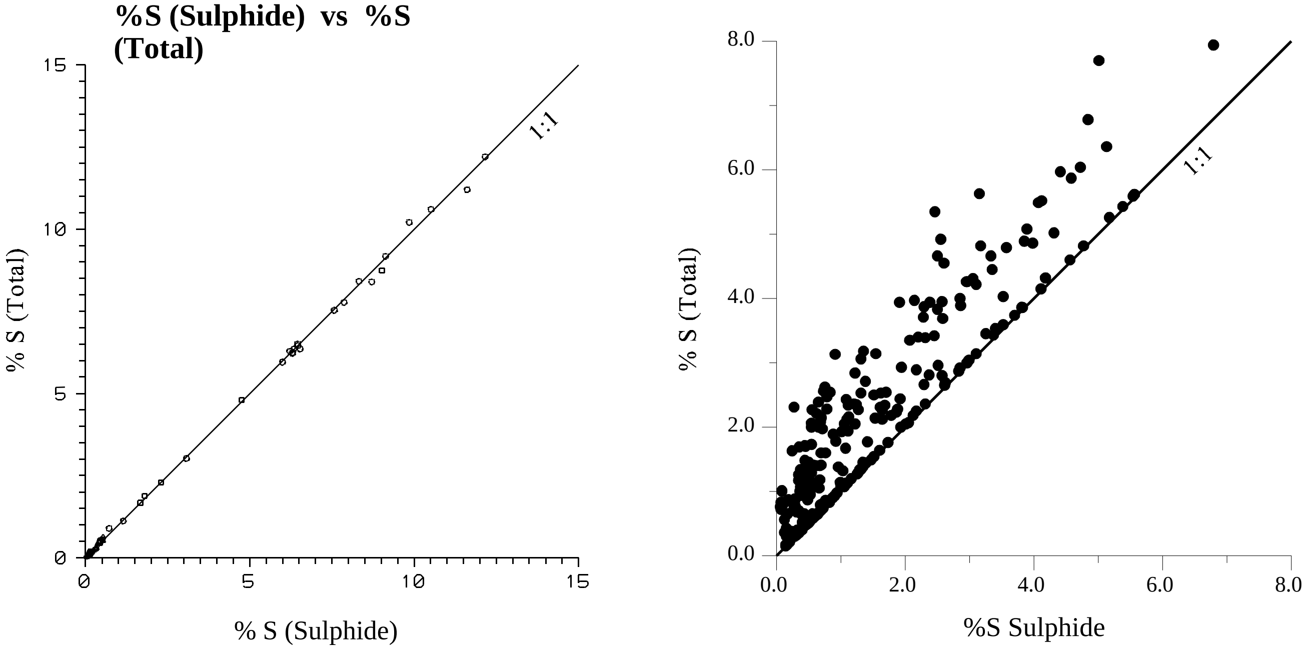

c) total sulfur dominated by sulfide

d) total sulfur dominated by sulfide or sulfate

FIGURE 5.2.1-1. Examples of ABA Total Sulfur vs. Sulfide.

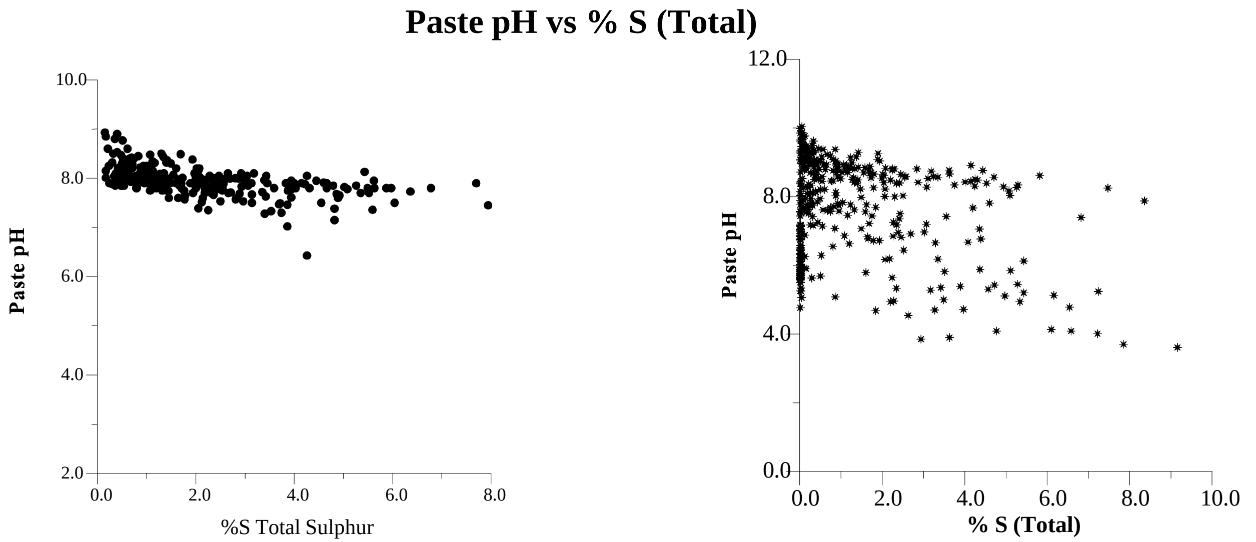

a) early stage of acid generation with available NP and no acidic paste pH

b) net acidity in many samples; no major trend with total sulfur suggesting pH control by NP

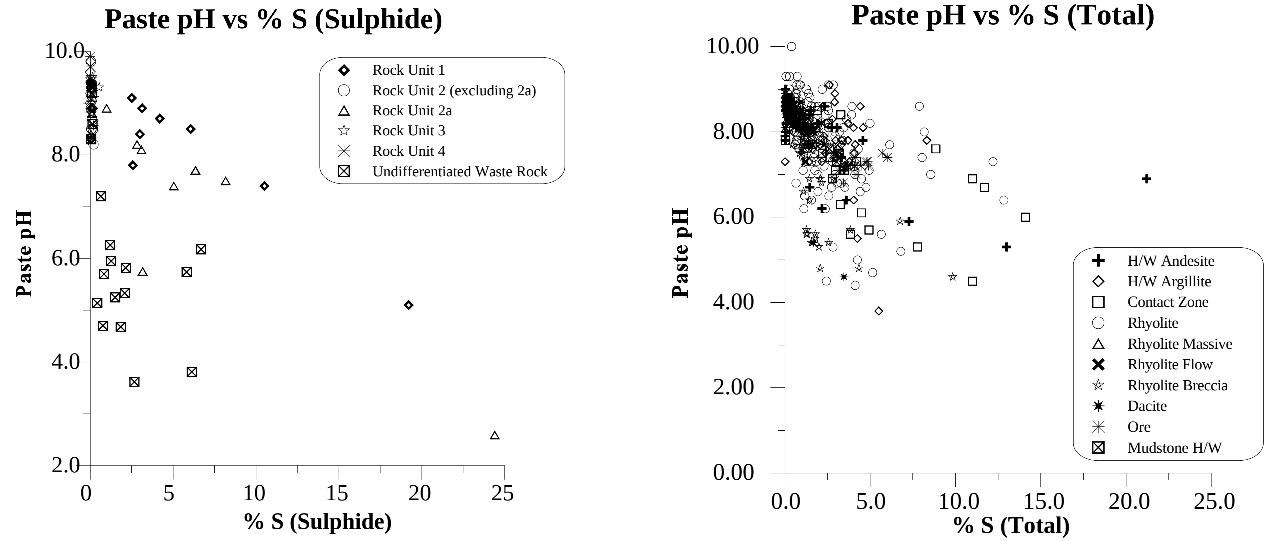

c) net acidity in some rock units; no major trend with sulfide suggesting pH control by NP

d) net acidity in some rock; some trend with total sulphur

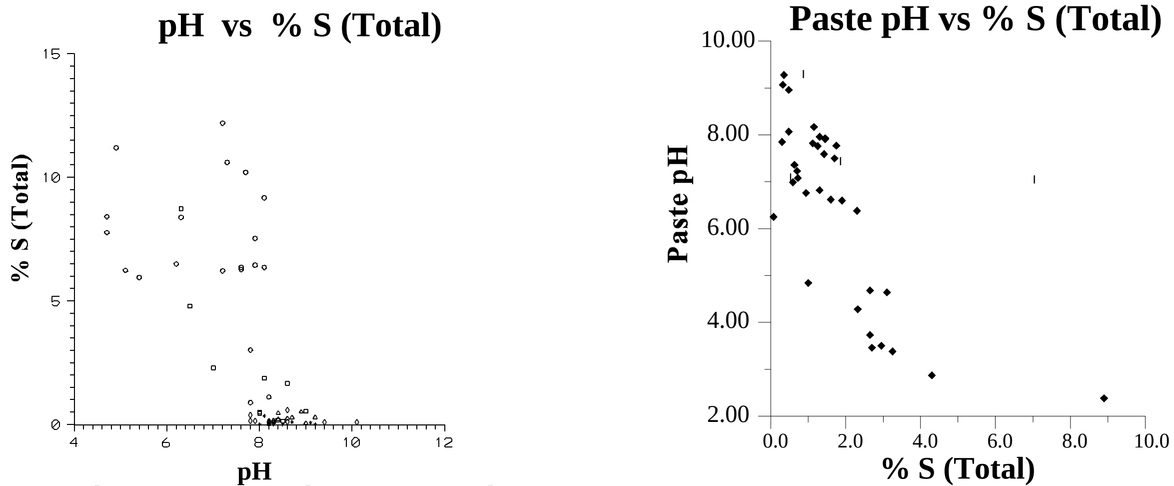

e) net acidity in some samples; minor trend with total sulphur (note pH on x axis)

f) net acidity in some samples; trend of pH with total sulphur

FIGURE 5.2.1-2. Examples of ABA Total Sulfur/Sulfide vs. Paste pH.

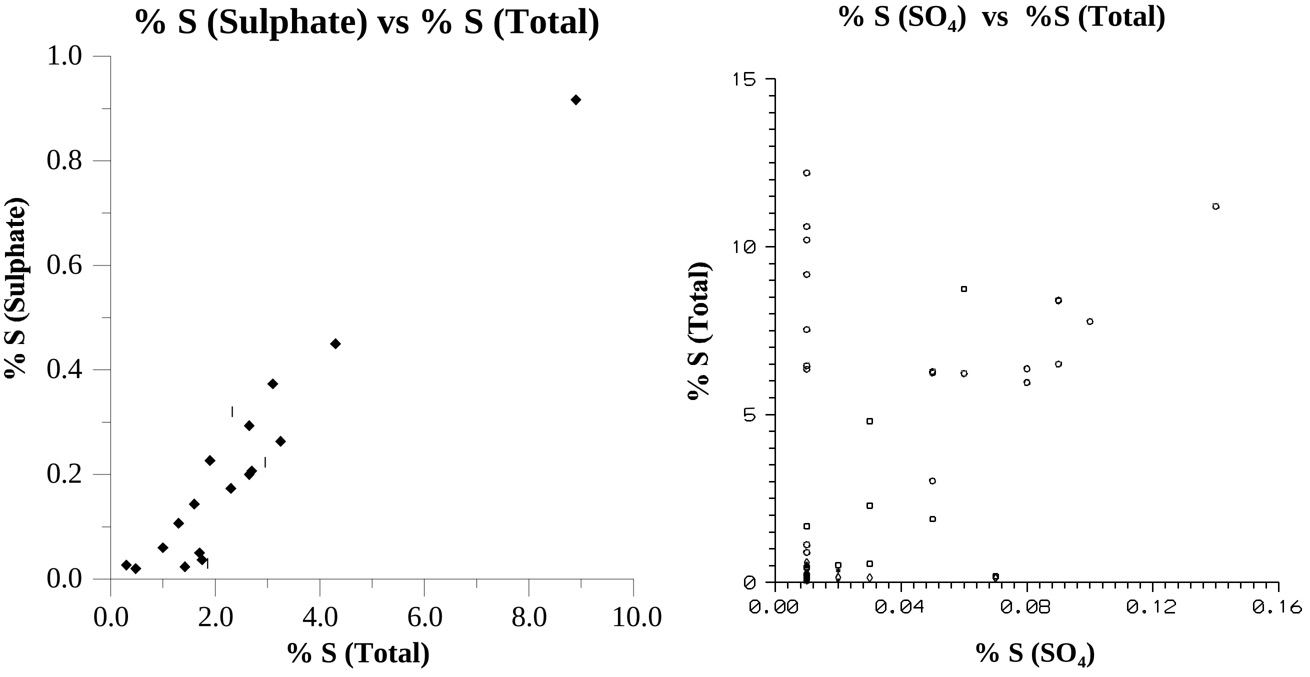

a) correlation suggesting sulfate derived from oxidation of sulfide (total sulfur) by a 1:10 ratio

b) correlation in some samples, others have no detectible sulfate (note sulfate on x axis)

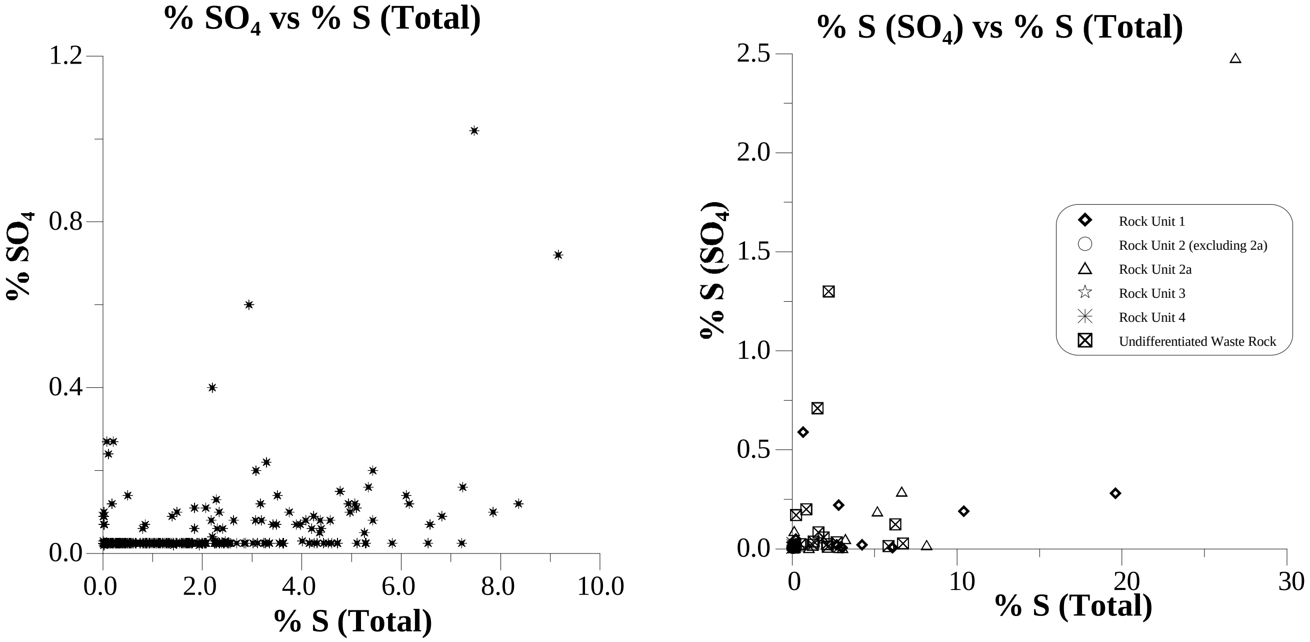

c) no clear correlation with many samples having sulfate less than detection

d) no clear correlation suggesting sulphate not derived from sulphide (total sulphur) oxidation; primary gypsum and other sulphate minerals identified in these samples

FIGURE 5.2.1-3. Examples of ABA Total Sulfur vs. Sulfate.

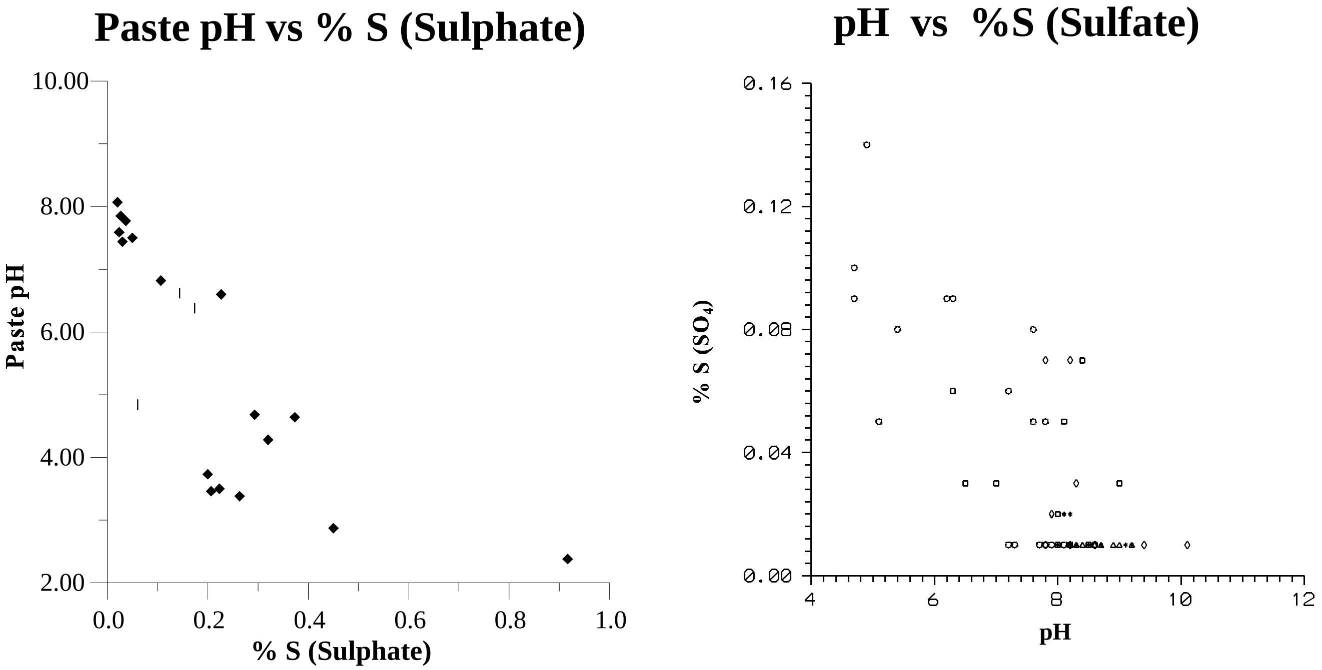

a) correlation suggesting sulfate derived from extent of sulfide oxidation and corresponding acid generation; sulfate retained within samples

b) correlation suggesting sulfate derived from extent of sulfide oxidation and corresponding acid generation; sulfate retained within samples (note paste pH on x axis unlike others)

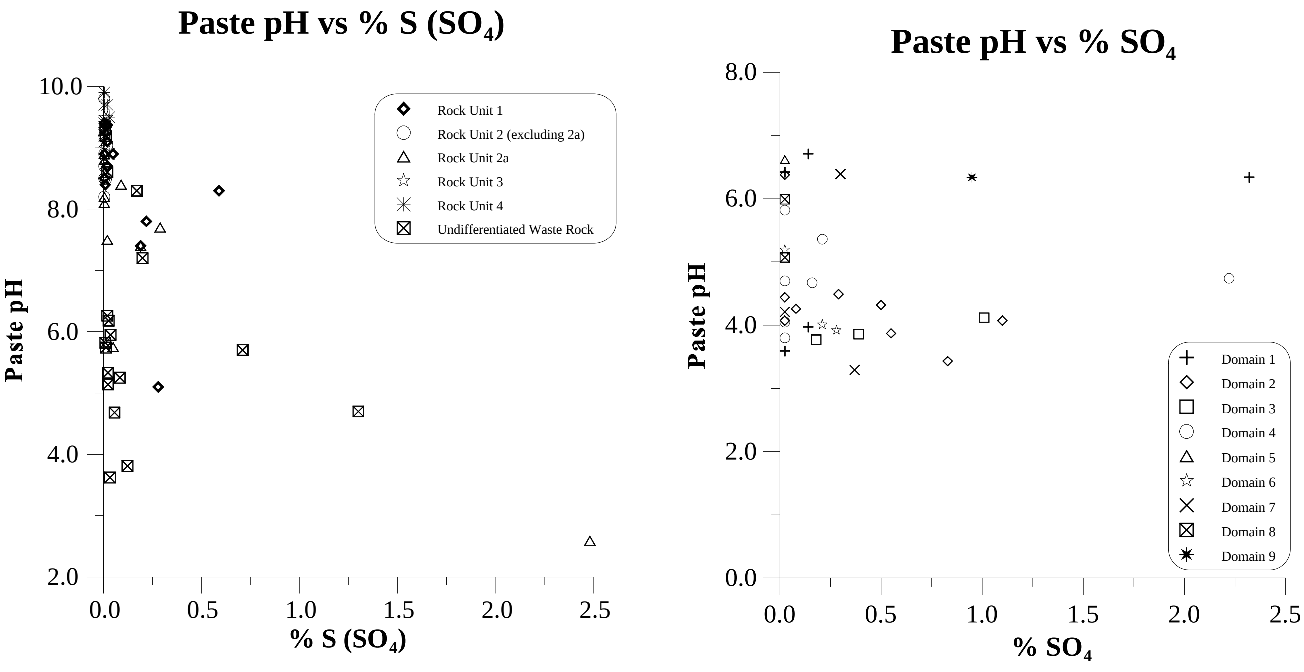

c) general lack of correlation suggesting oxidation-derived sulfate regularly removed from most acidic samples

d) presence of primary (original) sulfate in many sample

FIGURE 5.2.1-4. Examples of ABA Total Sulfur vs. Sulfate.

be affected by the presence of sulfate minerals, or involve an addition of weaker acid around pH 5-6. Consequently, NP from Sobek ABA can be expected to provide reasonable values of ENP where microenvironmental conditions in and around sulfide grains are around pH 1-2, and can overestimate NP when microenvironmental conditions are not as acidic. Other methods may either underestimate or overestimate ENP. For all methods, neutralizing minerals like some aluminosilicates with very slow rates of dissolution will not be detected in NP analyses, and thus ENP could be higher than measured NP (e.g., Case Study 5.3.1-3).

The recommended delineation of effective NP begins with a Sobek NP measurement. The effective NP is then calculated by:

Effective Neutralization Potential (ENP) =
Measured NP -
Unavailable NP(UNP) +
Slow-Reacting NP(SRNP) (5.2.1-5)

Slow-reacting NP (SRNP) is the portion of a sample's NP that does not react during the 24-hour NP analysis, but would react over the residence time of acidic water (if greater than 24 hours) within a minesite component. An interesting modification of NP analyses is extending test times to seven or 30 days, but this is rarely practiced. SRNP is either measured through long-term kinetic tests (Section 5.3) or calculated in a preliminary fashion through mineralogical static tests (Section 5.2.2). Kwong (1993), based on work by Sverdrup (1990), listed a hierarchy of minerals and their generalized relative reaction rates (Table 5.2.1-1), although the rates vary from site to site. In any case, the faster the rate, the greater the amount of that mineral that will appear in an NP analysis.

Morin and Hutt (1994a) provided factors for converting some aluminosilicate minerals to NP CaCO3 equivalent (Table 5.2.1-2). These conversion factors are based on restrictive assumptions like those for acid potentials (Section 5.2.1.2).

Unavailable NP in Equation 5.2.1-5 is best obtained through kinetic tests as is SRNP (Sections 5.3 and 5.4), but an approximate value can sometimes be estimated from ABA data. A scatterplot of NP against paste/rinse pH may show that pH decreases as NP decreases (e.g., Figure 5.2.1-5). The point at which pH approaches or falls below 5.0 corresponds to unavailable NP (see also Section 5.2.1.5). Kinetic tests have shown this estimate is often within 5-10 t $CaCO_3$ equivalent/1000 t of the effective NP, although UNP values up to 60 t/1000 t have been reported. However, rarely has effective NP been used in ABA calculations, interpretations, and predictions in place of measured NP (Section 5.2.1.4).

There is an apparent discrepancy in the preceding approach. The definition of effective NP is based on an aqueous pH of 6.0 and unavailable NP is based on a paste/rinse pH of 5.0. The first reason for this discrepancy is that aqueous pH and paste/rinse pH are not synonymous (Case Study 5.2.1-1). Secondly, aqueous pH is based on water-quality guidelines at pH 6.0, whereas the paste/rinse pH is based on distilled water whose pH as low as 5 would classify it as poor quality under those same guidelines (Section 5.2.1.1). This discrepancy is not a major problem and often does not affect predictions.

The calculation of ENP (to pH 6) from Equation 5.2.1-5 can prove erroneous if (1) the rate of acid generation is relatively high compared to the rate of NP dissolution (Section 5.3) or (2) most of the NP consists of minerals whose equilibrium pH is below 6.0 (Section 4.5). Therefore, an ENP is not a sufficient condition for maintaining near-neutral or alkaline pH. However, minerals like calcium-based carbonate minerals (calcite and dolomite) dissolve relatively rapidly in acid, within a few minutes to hours, and thus can neutralize acidity quickly. In light of this, ABA should be accompanied by mineralogical examinations (Section 5.2.2) and include a determination of Carbonate Neutralization Potential (CaNP).

CaNP can be obtained easily from an analysis of total carbon in some Leco furnaces as sulfur is being analyzed (Section 5.2.1.1). This assumes that all carbon exists as carbonate, which should be confirmed through other static tests (Sections 5.2.2 and 5.2.3).

TABLE 5.2.1-1
Relative Reaction Rates of Minerals Contributing to Acid Neutralization (from Sverdrup, 1990)

Group Name	Typical Minerals	Relative Reactivity
Dissolving	Calcite, aragonite, dolomite, magnesite, brucite	1
Fast Weathering	Anorthite, nepheline, olivine, garnet, jadeite, leucite, spodumene, diopside, wollastonite	0.6
Intermediate Weathering	Epidote, zoisite, enstatite, hypersthene, augite, hedenbergite, hornblende, glaucophane, tremolite, actinolite, anthophyllite, serpentine, chrysotile, talc, chlorite, biotite	0.4
Slow Weathering	Albite, oligoclase, labradorite, vermiculite, montmorillonite, gibbsite, kaolinite	0.02
Very Slow Weathering	K-feldspar, muscovite	0.01
Inert	Quartz, rutile, zircon	0.004

TABLE 5.2.1-2
Factors for Converting Amounts of Selected Aluminosilicate Minerals to NP Values (values corrected from original values in Morin and Hutt, 1994b)

Mineral[1]	Final pH of Neutralization	
	~pH 4[1]	~pH 7[1]
Calcite	1	0.5
Anorthite (Ca feldspar)	1.44	0.72
Albite (Na feldspar)	0.76	0.38
K feldspars (various)	0.72	0.36

[1] Multiply parts-per-thousand of selected minerals by given conversion factor to obtain t $CaCO_3$ equivalent/1000 t; based on restrictive assumptions (see Morin and Hutt, 1994b).

Alternatively, acid can be added to a sample in a sealed chamber and the resulting evolution of carbon dioxide measured through a gas-pressure increase, a gas chromatograph, or gravimetric techniques. CaNP is then calculated through molecular weights:

$$\text{Carbonate Neutralization Potential (CaNP) as t } CaCO_3/1000 \text{ t} = \%C * 83.3 \qquad (5.2.1\text{-}6)$$

or

$$\text{Carbonate Neutralization Potential (CaNP) as t } CaCO_3/1000 \text{ t} = \%CO_2 * 22.7 \qquad (5.2.1\text{-}7)$$

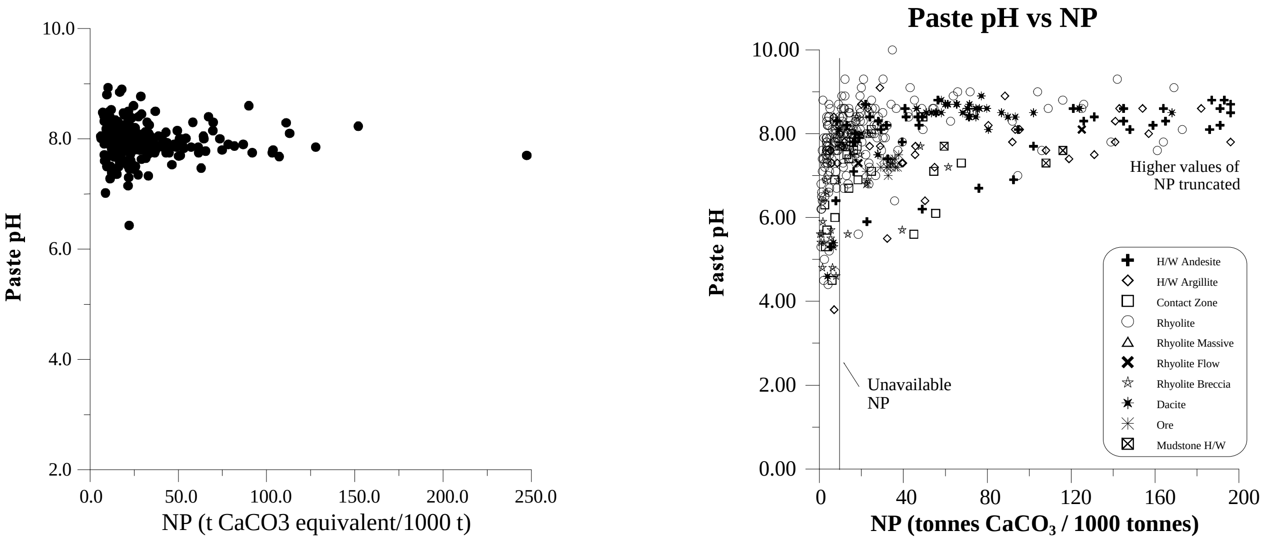

a) early stage of acid generation; no acidic paste pH; preliminary estimate of unavailable NP not possible

b) mature stage of acid generation; unavailable NP ~ 10 t/1000 t

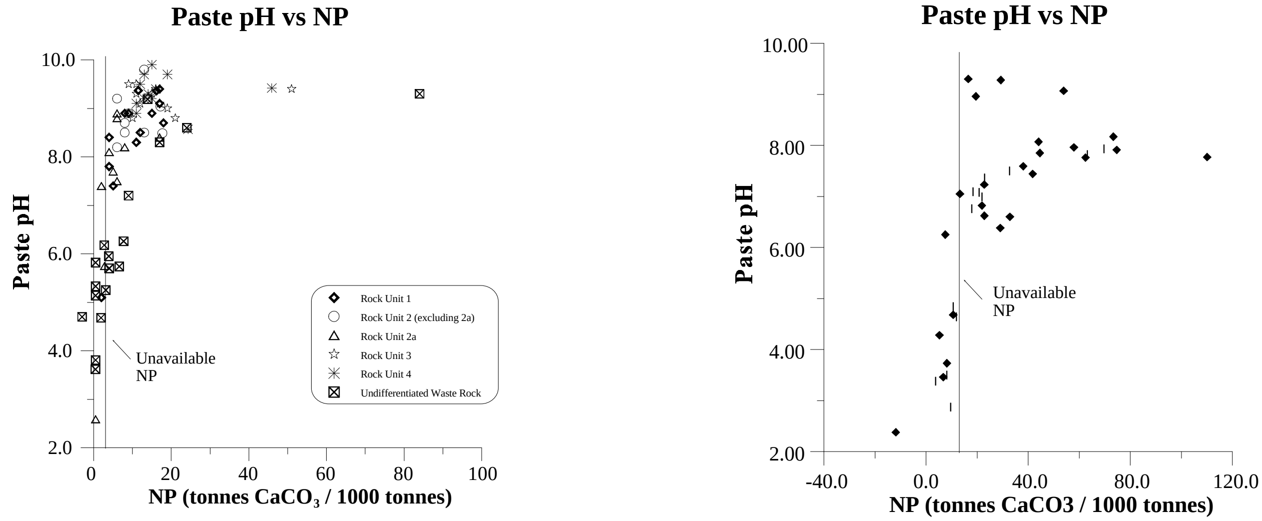

c) mature stage of acid generation; unavailable NP ~ 3 t/1000 t

d) mature stage of acid generation; unavailable NP ~ 15 t/1000 t

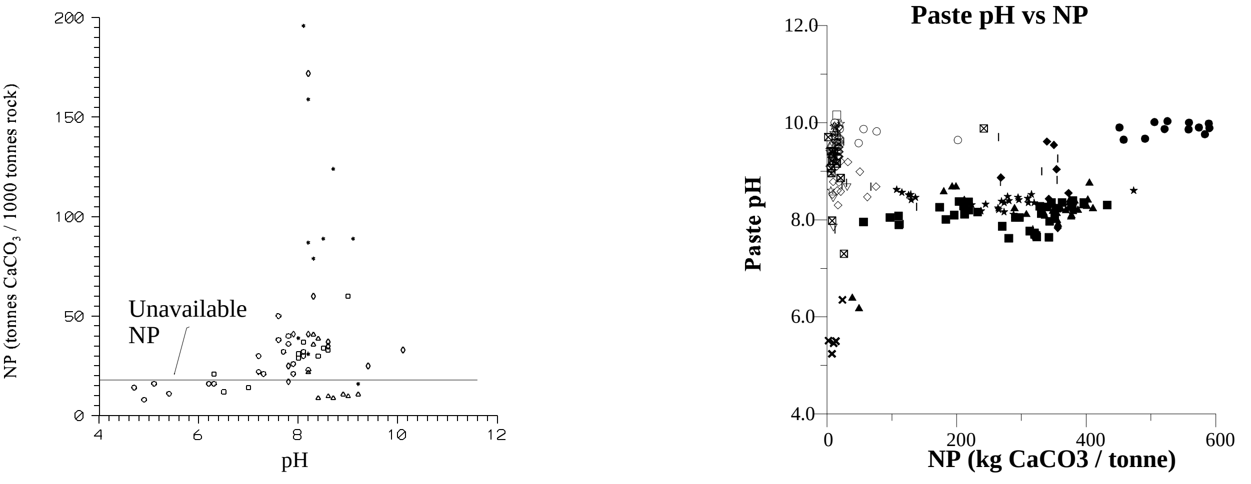

e) mature stage of acid generation (note NP on y axis); unavailable NP ~ 17 t/1000 t

f) very high, non-carbonate NP; one unit capable of alkaline drainage has highest NP and pH values

FIGURE 5.2.1-5. Examples of ABA Neutralization Potential (NP) vs. Paste pH.

The interpretation and use of CaNP for predictions require caution, because not all carbonate minerals are readily reactive. Iron-rich forms like siderite require hundreds of hours to dissolve and may provide little neutralizing capacity (Morin and Cherry, 1986). Consequently, mineralogical examinations are needed (Section 5.2.2) to identify the types of carbonate minerals. Additionally, a scatterplot of CaNP against [bulk] NP can be informative. For example, in Figure 5.2.1-6, (1) a one-to-one correlation indicates most of the NP consists of reactive carbonate minerals, (2) NP much greater than CaNP indicates non-carbonate minerals are major contributors, and (3) CaNP much greater than NP indicates not all carbonate minerals are rapidly reactive or not all carbon is carbonate.

The foregoing discussion has focussed on acidic drainage and neutralization of acidity. The other extreme of alkaline drainage can also be generally assessed with NP analyses. Limestone samples will often generate high NP and CaNP values, typically several hundreds of t $CaCO_3$/1000 t. However, samples with similarly high NP, but negligible CaNP, point to unusual mineralogy (Figure 5.2.1-6f). When these high NP values are accompanied by high paste pH values above 10 (Figure 5.2.1-5f), the potential for long-term alkaline drainage exists and should be resolved with kinetic tests (Section 5.3).

<u>5.2.1.4 Net Potential Ratios and Net Neutralization Potentials</u>

As explained in Sections 5.2.1.2 and 5.2.1.3, sulfur values are converted to various Acid Potentials (xAPs), and various Neutralization Potentials (xNPs) are measured directly or calculated. For ease of comparison, both xAP and xNP are typically reported in equivalent units of kg $CaCO_3$ equivalent/metric tonne (t) of sample, t $CaCO_3$ equivalent/1000 t of sample, or parts per thousand (ppt) $CaCO_3$ equivalent. Other, non-equivalent units include kg H_2SO_4/t (differs by approximately 2%) and %$CaCO_3$ (differs by a factor of 10).

In order to determine the net balance of acid-generating and acid-neutralizing capacities, AP and NP can either be mathematically divided or subtracted. Division yields dimensionless Net Potential Ratios (xNPR):

Total Net Potential Ratio (TNPR) =
NP / TAP (5.2.1-8a)
or

Sulfide Net Potential Ratio (SNPR) =
NP / SAP (5.2.1-8b)

At very high values of xNP or very low values of xAP (sulfur), extreme xNPR values can be obtained (Figure 5.2.1-7).

Subtraction yields various Net Neutralization Potentials (xNNP) in units of t $CaCO_3$/1000 t:

Total Net Neutralization Potential (TNNP) =
NP - TAP (5.2.1-9a)
or

Sulfide Net Neutralization Potential (SNNP) =
NP - SAP (5.2.1-9b)

At relatively high values of xAP (sulfur) or xNP, the xNNP values are dominated by them (Figure 5.2.1-8).

An important note at this point is that xNNP values are not used in all countries. Particularly in Australia, xNNP is replaced by the inverse as Net Acid Producing Potential (NAPP = xAP - NP). For NAPP, a positive value represents the potential for net acid generation.

Carbonate Neutralization Potential (CaNP) or effective NP (ENP, Section 5.1.2.3) can be substituted for measured NP in Equations 5.2.1-8 and -9. However, this is rarely done in the literature, adding to the uncertainty in interpretations and predictions. When CaNP or ENP is used, labels such as Refined NNP (RNNP = CaNP - SAP) or Carbonate NNP (CNNP = CaNP - TAP) should be used (Sections B.6 and B.7).

The interpretation of xNPR and xNNP can be confusing as reported in the literature. In the hopeless drive to use a simple procedure (ABA) for final, conclusive predictions, various types of "universal criteria" have been developed. In their

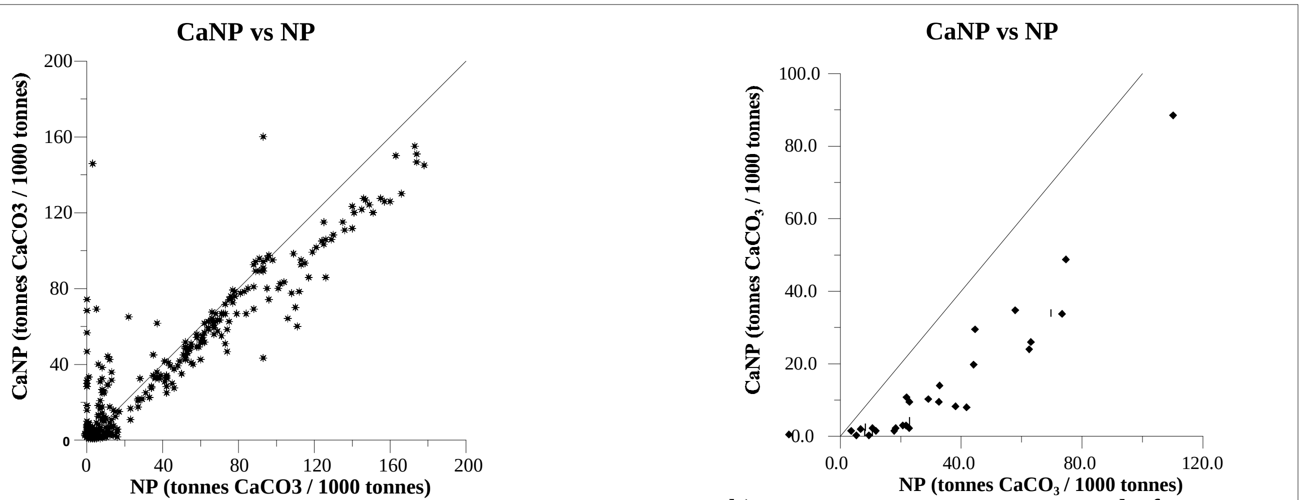

a) a mixture of conditions: 1) NP = CaNP, 2) NP > CaNP at higher NPs,, and 3) CaNP > NP

b) NP > CaNP; NP is comprised of a mixture of carbonate and non-carbonate minerals

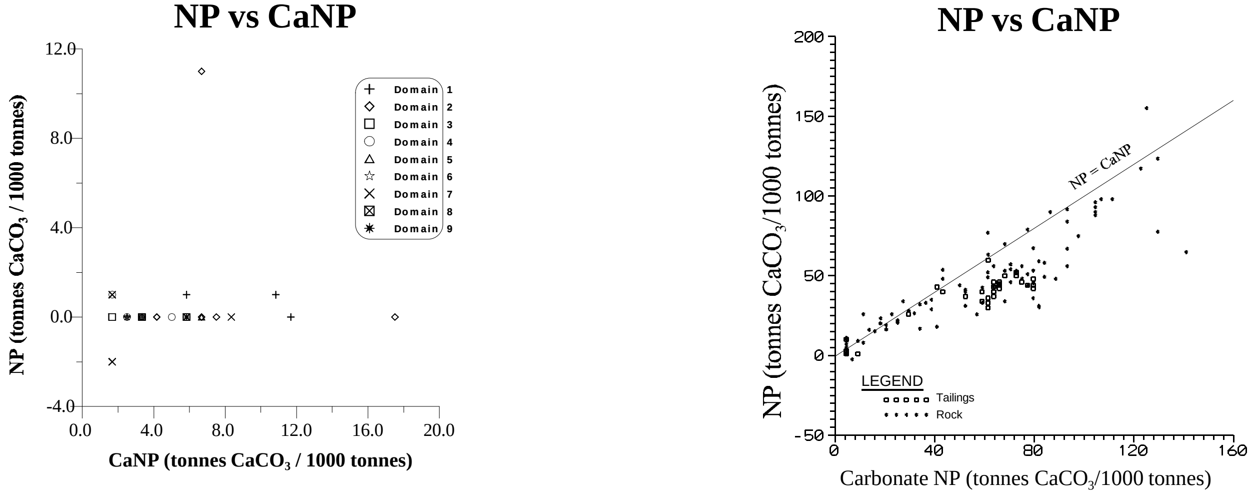

c) CaNP > 0 and NP ~ 0 for many samples (note NP on y axis); virtually none of this CaNP is readily reactive or capable of neutralization in the NP analysis

d) CaNP > NP for many samples (note NP on y axis); a portion of the carbonate minerals do not react quickly or provide neutralization

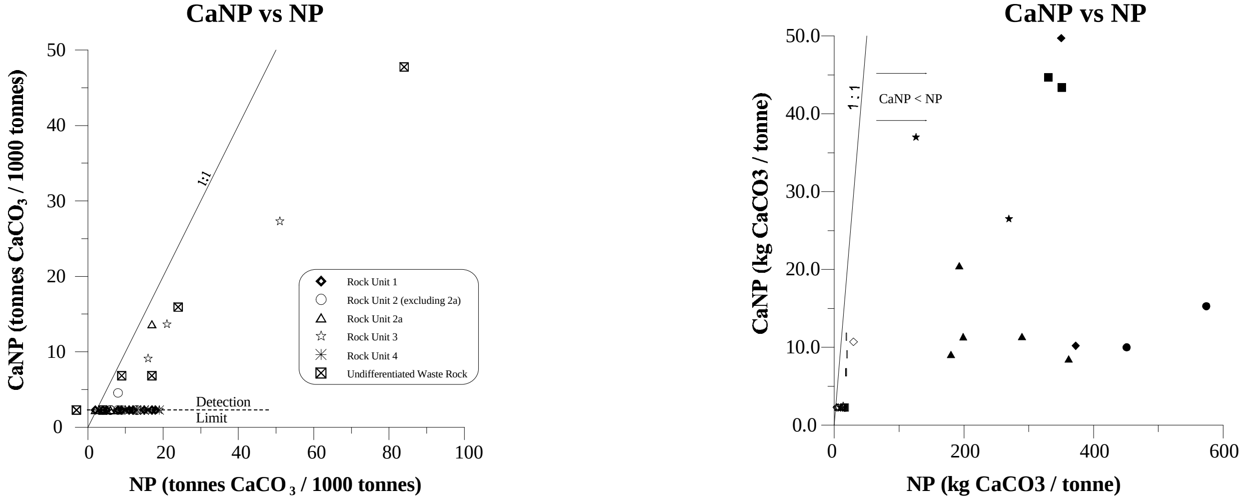

e) CaNP < detection limit for most samples; NP is predominantly non-carbonate minerals

f) CaNP << NP for most samples (note high NP values); warning of alkaline drainage potential

FIGURE 5.2.1-6. Examples of ABA Bulk vs. Carbonate NP (CaNP).

simplest form (Table 5.2.1-3), the criteria state that any sample with an xNPR value less than 1.0, or xNNP value less than 0.0 (zero) t $CaCO_3$/1000 t, has a net deficit of neutralizing capacity. The sample should therefore become acidic when effective NP is depleted.

Conversely, any xNPR value above 1.0, or xNNP value above 0.0 t $CaCO_3$/1000 t, should remain near neutral or alkaline indefinitely. In comparison to one-time paste pH values, this seems reasonable (Figures 5.2.1-9 and 5.1.2-10). However, comparisons to long-term kinetic laboratory and field tests (Sections 5.3 and 5.4) show that rock and tailings with elevated values sometimes become acidic. This led to the creation of a nominal, arbitrary, "uncertain" range of 1.0<xNPR<2.0 and 0.0<xNNP<20.0 t $CaCO_3$/1000 t. In any case, xNPR and xNNP are equivalent, particularly near the critical values (Figure 5.2.1-11).

Not surprisingly, some studies have predicted indefinite near-neutral conditions at xNPR levels of 0.8 (Case Study 5.3.1-3) and acidic drainage for xNPR values up to 4.0. This is the result of site-specific factors and complexities, like unavailable NP and reaction rates (Morin and Hutt, 1994b). Therefore, ABA should only be interpreted in combination with other static and kinetic testwork. This will lead to a particular "critical" or "safe" xNPR or xNNP value for a minesite, or each rock unit or minesite component, that differentiates long-term net-acid-generating from net-acid-neutralizing materials.

For interim or preliminary interpretations, the "universal criteria" with an uncertain range (Table 5.2.1-3) will often suffice, with the recognition that exceptions can and do occur. The International Kinetic Database (Section 5.3.3), which contains more than 400 kinetic tests, shows that the safe xNPR values (based on ENP) are typically within the range of 1.3 and 1.7.

Each minesite often contains more than one rock unit and minesite component, and it is important that the ABA characteristics of each are defined. However, experience for rock units has shown that ABA units can often be defined as containing more than one rock unit, because ranges in ABA values within units are often similar. In fact, in some cases, all rock units can be considered a single ABA unit. One compilation of nearly 6000 analyses of sulfide and total sulfur encompassed several rock units, with

TABLE 5.2.1-3
Universal ABA Criteria for Assessing or Predicting pH Range of Minesite Drainage
(many exceptions are known, so kinetic tests are needed to refine predictions)

Criteria	Prediction/Current Condition
Paste/Rinse pH	
paste/rinse pH < 5.0	currently acidic; future unknown
5.0 # paste/rinse pH # 10.0	currently near-neutral; future unknown
paste/rinse pH > 10.0	currently alkaline; future unknown
xNPR or xNNP	
xNPR < 1.0 or NNP < 0.0 t $CaCO_3$/1000 t	eventually acidic
1.0 # xNPR # 2.0 or 0 # NNP # 20	uncertain future
xNPR > 2.0 or NNP > +20 t $CaCO_3$/1000 t	indefinitely near-neutral or alkaline

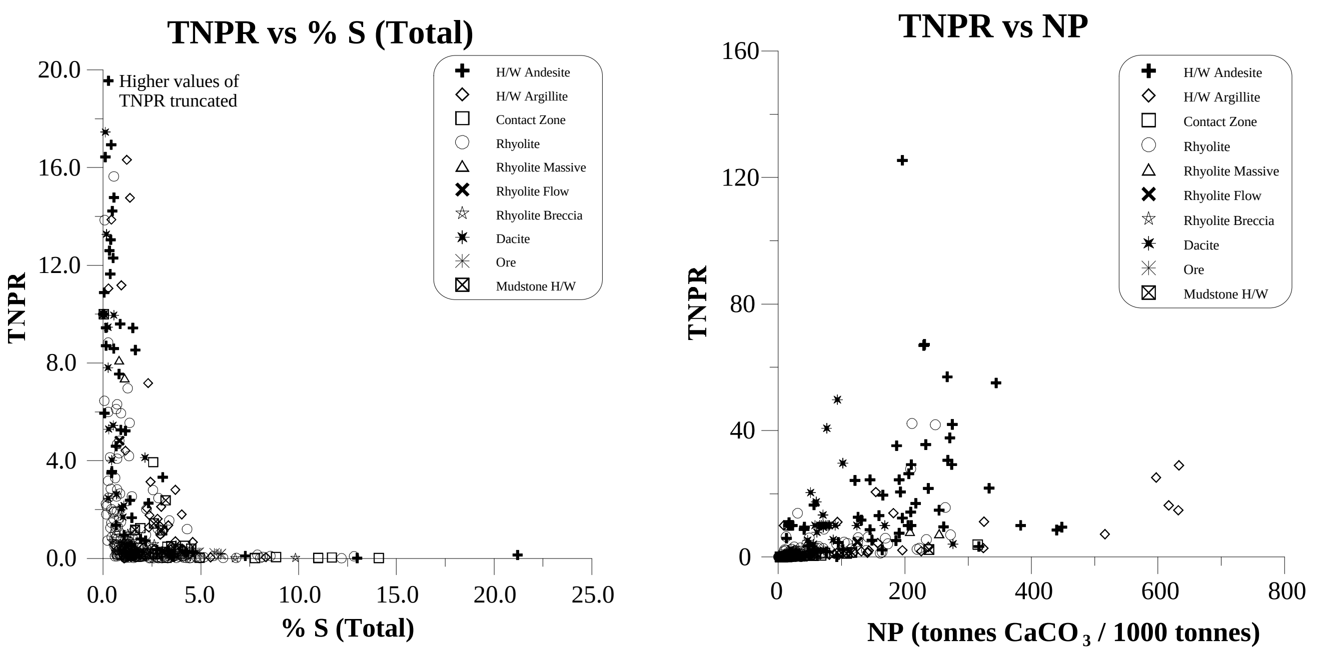

a) relationship of TNPR to total sulfur; all samples with %S>5.0 have TNPR<1.0

b) relationship of TNPR to NP; some samples with high NP have low TNPR

FIGURE 5.2.1-7. Examples of ABA xNPR vs. Total Sulfur and NP.

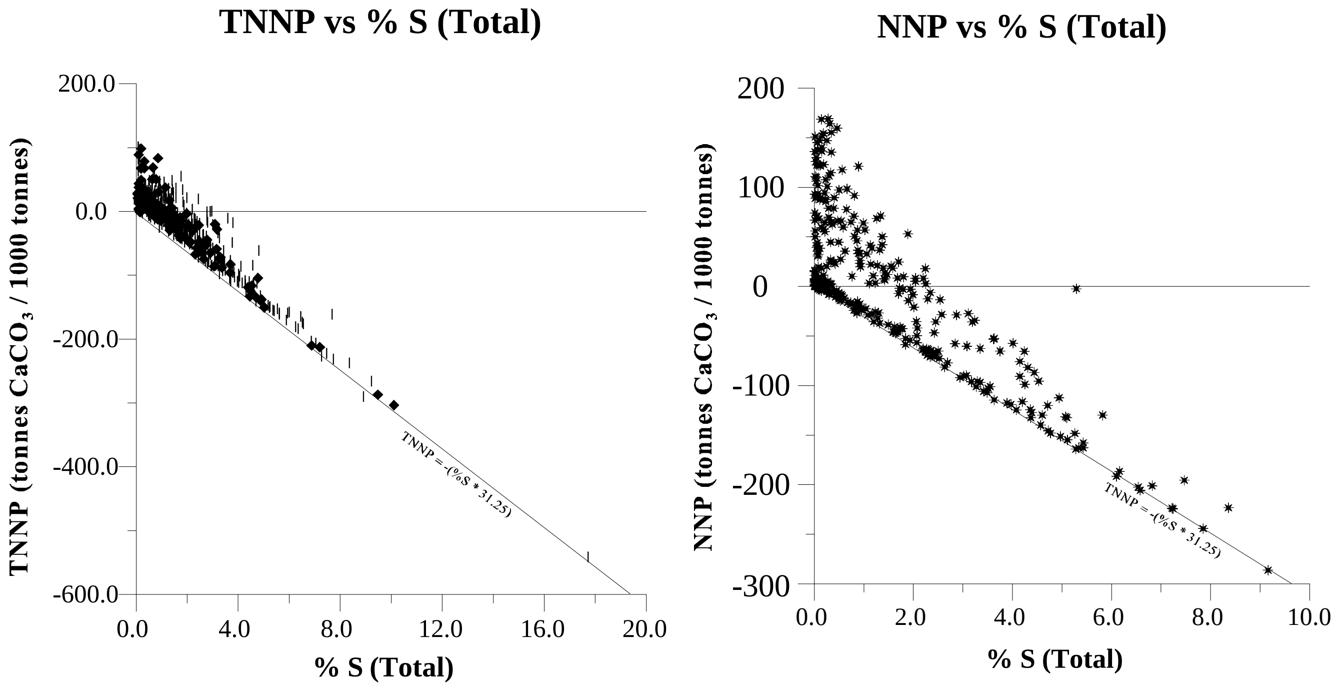

a) for NP~0, TNNP = -[%S total * 31.25] (see line); samples with significant NP above sloping line; samples with negative NP (significant net acidity) below sloping line

b) for NP~0, TNNP = -[%S total * 31.25] (see line); samples with significant NP above sloping line

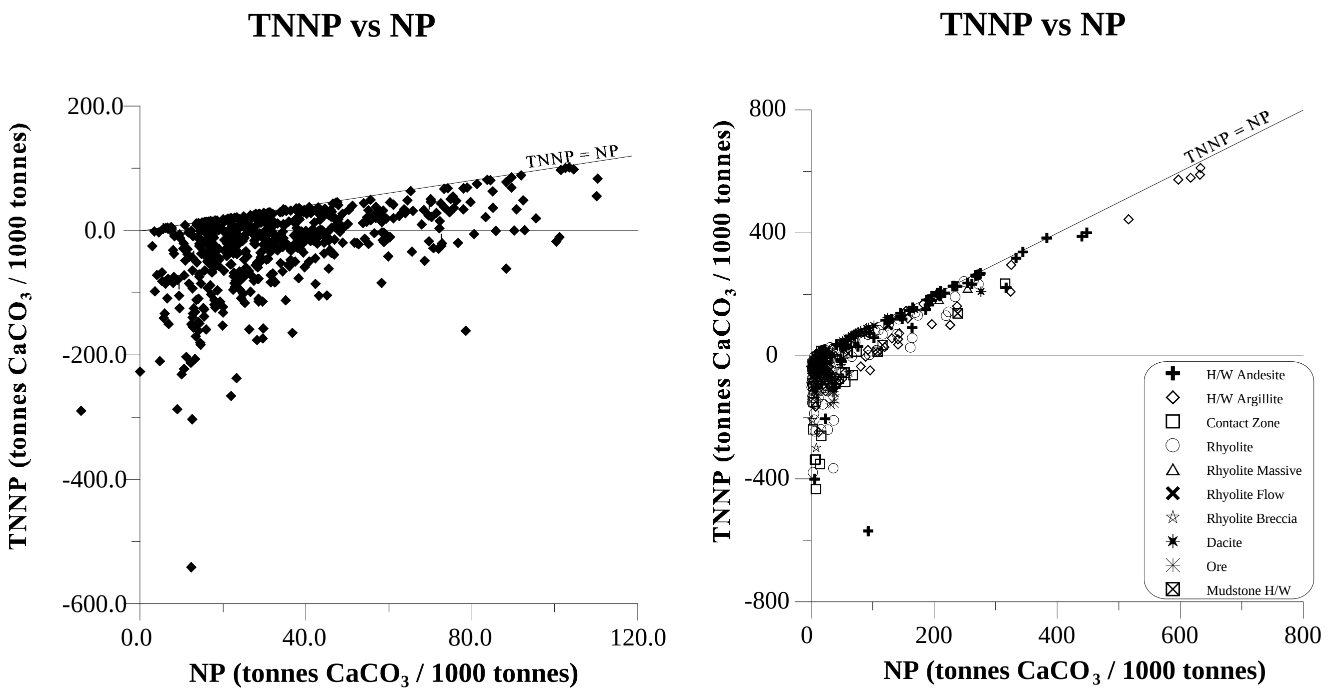

c) for %S~0, TNNP = NP (see line); samples with significant %S below sloping line

d) for %S~0, TNNP = NP (see line); samples with significant %S below sloping line

FIGURE 5.2.1-8. Examples of ABA xNNP vs. NP and Sulfur.

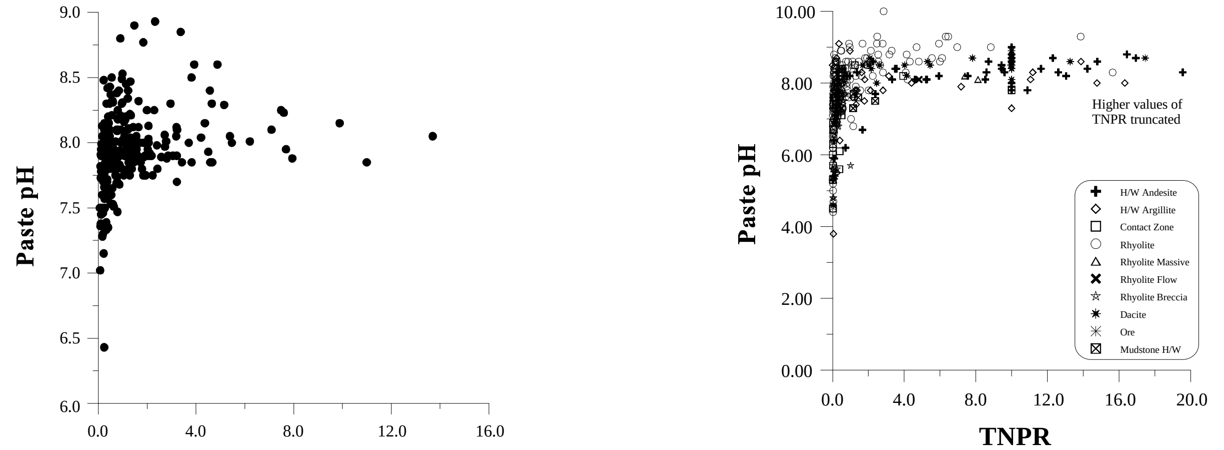

a) early stage of acid generation; no acidic samples

b) onset of net acid generation; only a few samples with TNPR < 1.0 associated with acidic pH

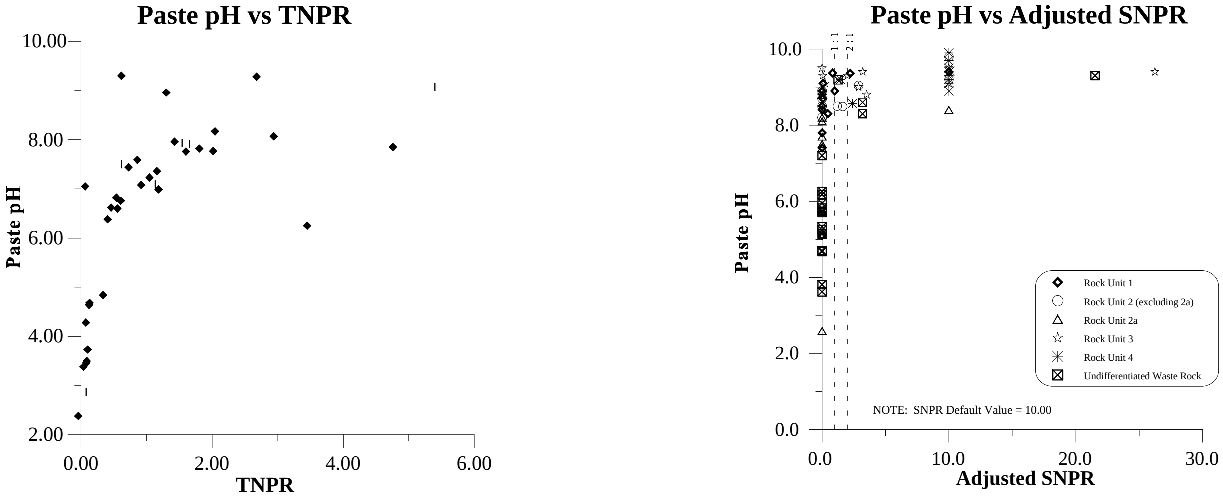

c) all samples with NPR < 0.4 associated with acidic pH except one

d) adjusted SNPR values ~ 0 (unavailable NP subtracted) associated with acidic and neutral/alkaline pH

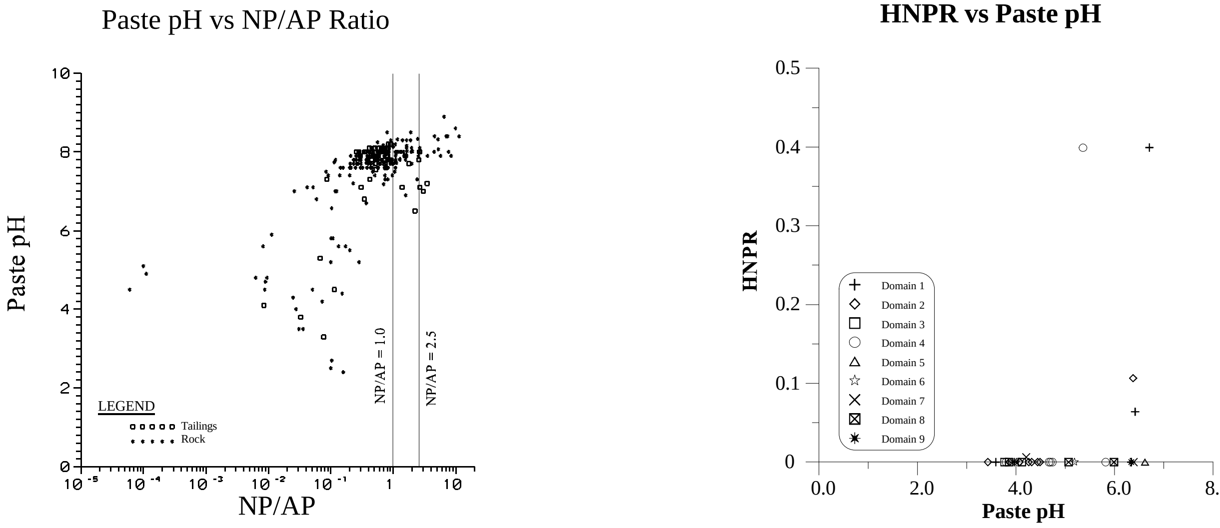

e) only samples with NPR < 0.3 associated with acidic paste pH

f) obvious prognosis for rock at this site (note pH on x axis)

FIGURE 5.2.1-9. Examples of ABA xNPR vs. Paste pH.

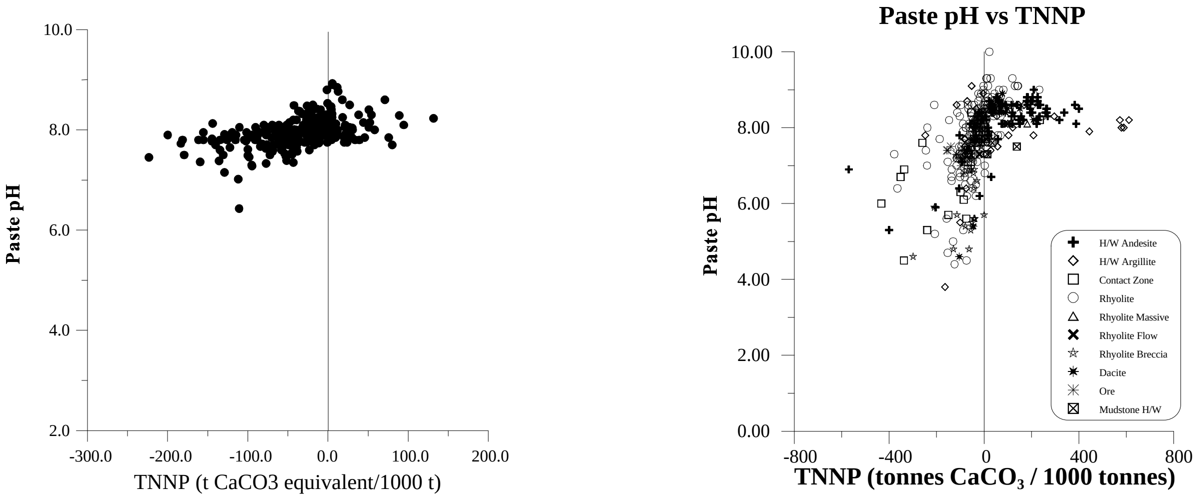

a) early stage of acid generation; no acidic samples

b) some samples with NNP < 0 acidic; some still neutral to alkaline

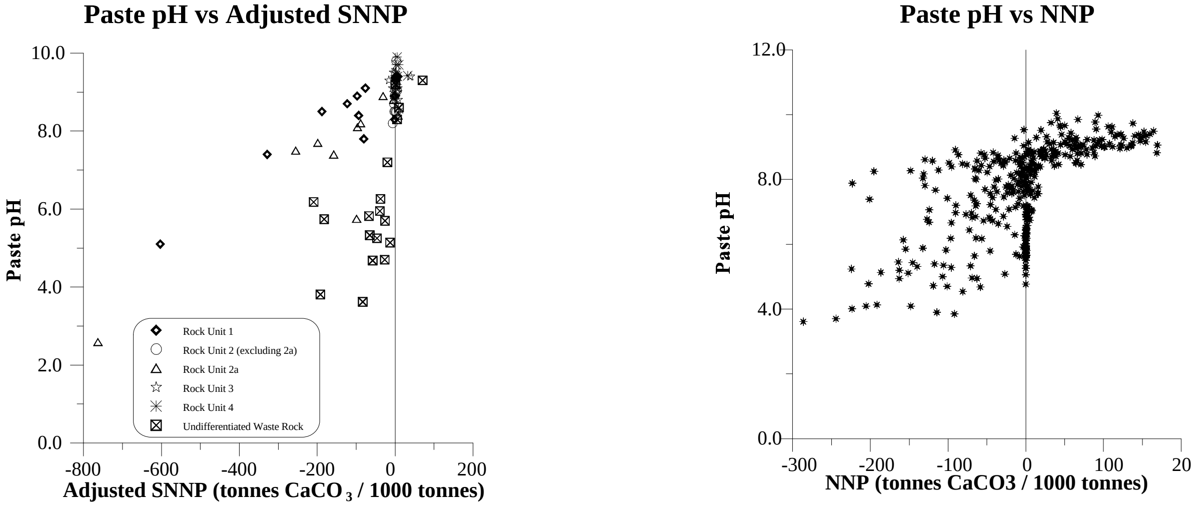

c) some samples with NNP < 0 acidic; some still neutral to alkaline

d) some samples with NNP~0 acidic, reflecting low NP values

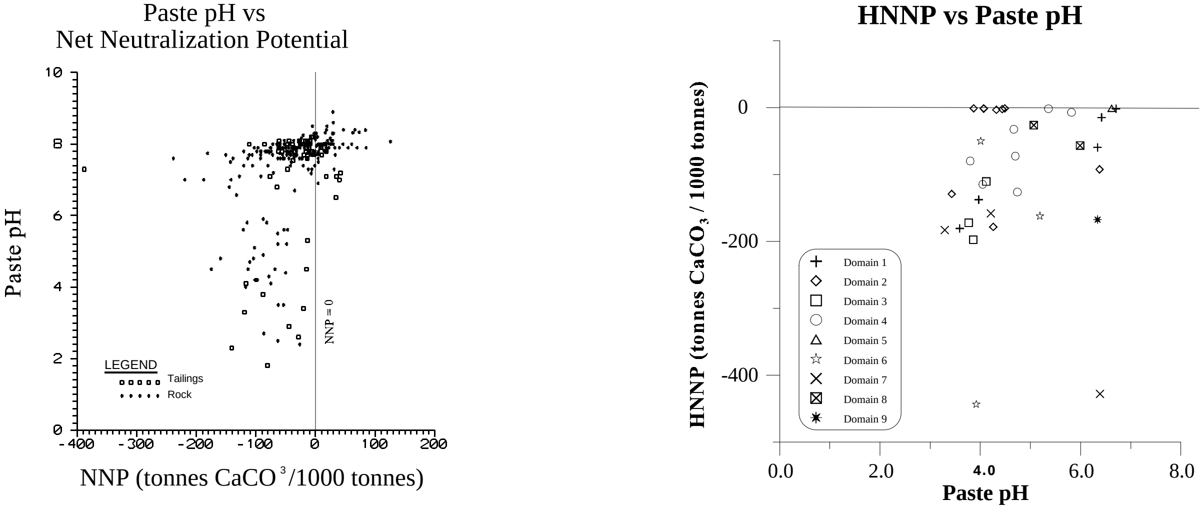

e) some samples with NNP < 0 acidic; some still neutral to alkaline

f) all samples with NNP < 0; some still neutral (note pH on x axis)

FIGURE 5.2.1-10. Examples of ABA xNNP vs. Paste pH.

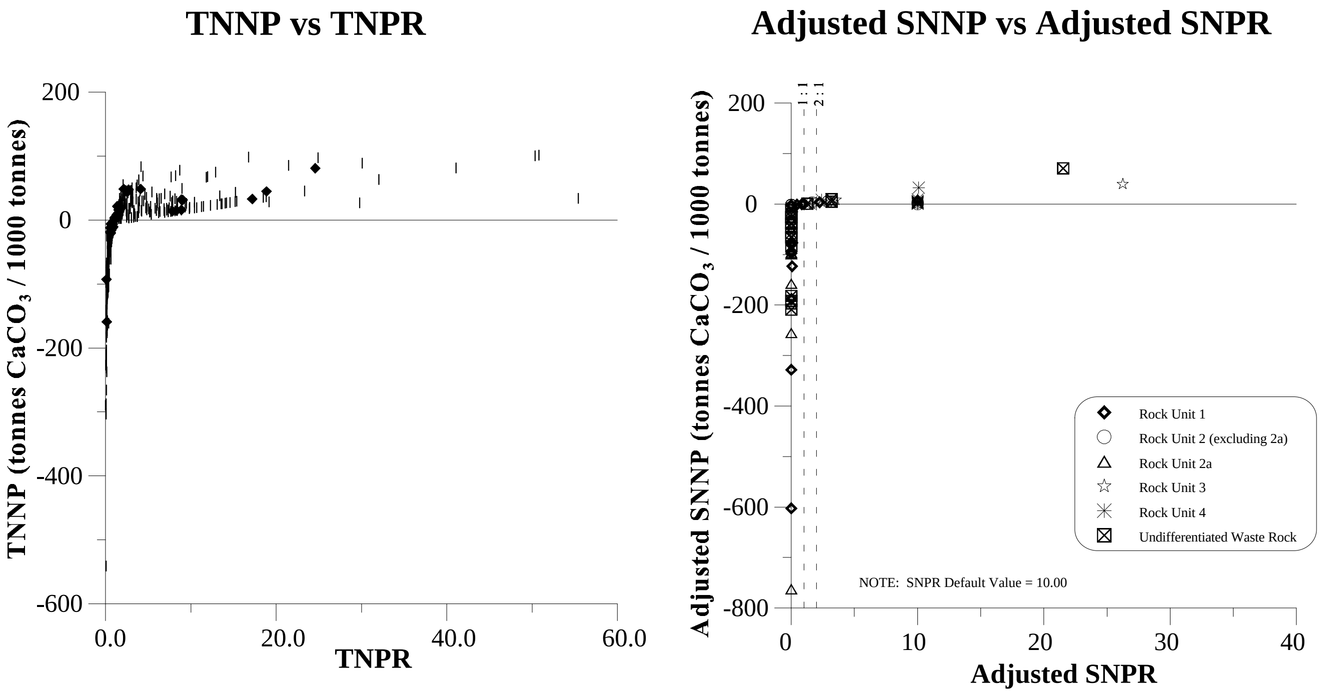

a) relationship of TNNP to TNPR showing TNPR = 1.0 corresponds to TNNP = 0; with some samples with 1.0<TNPR< 2.0 around TNNP=0

b) relationship of adjusted SNNP (unavailable NP subtracted) to adjusted SNPR showing 1.0<SNPR<2.0 equivalent to SNNP~0

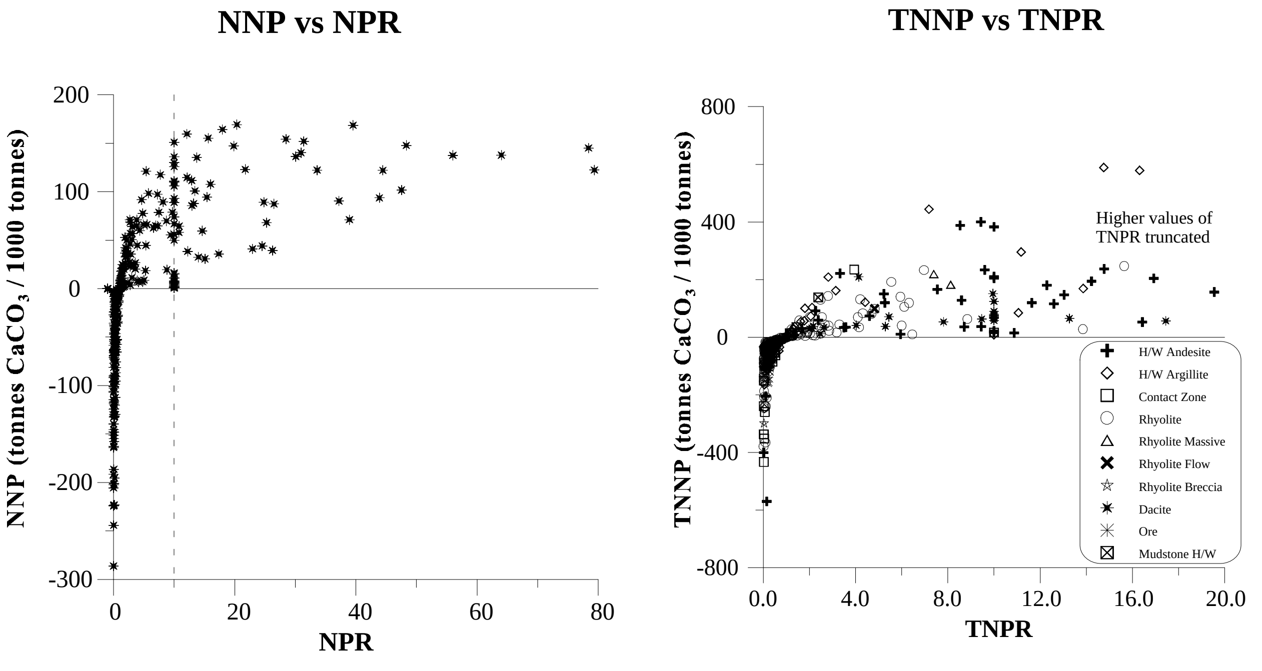

c) relationship of NNP to NPR; samples with %S sulfur < 0.05 assigned default NPR value of 10.0 (see dashed line) showing a range of NP values based on positive NNP values

d) relationship of TNNP to TNPR showing 1.0<TNPR<2.0 corresponds to NNP ~ 0 for all rock units

FIGURE 5.2.1-11. Examples of ABA xNPR vs. xNNP.

varying degrees of silicic, argillic, and sericitic geochemical alteration, and varying degrees of oxidation. The frequency plot showed that total sulfur for the entire minesite, comprised mostly of sulfide, was lognormally distributed. However, the distribution was truncated at high values due to the physical impossibility of having sulfur as sulfide minerals above 30-40%S (Figure 5.2.1-12). Thus all rock at this minesite can be interpreted and predicted as one statistically homogeneous ABA unit.

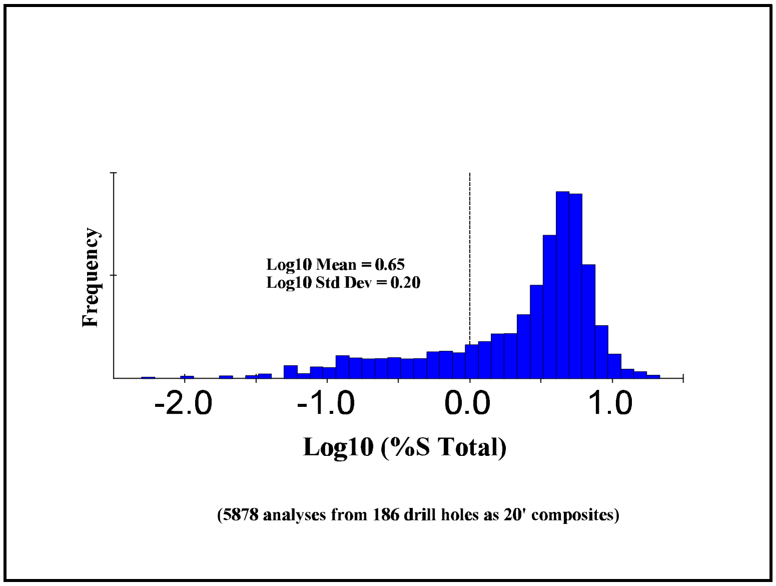

(5878 analyses from 186 drill holes as 20' composites)

FIGURE 5.2.1-12. Lognormal Distribution of Total Sulfur across an Entire Mine.

Mapping of ABA parameters along the lengths of boreholes in rock often reveals irregular distributions with depth and within one stratum (Figures 5.2.1-13a and 13b). This is frequently true of sedimentary, igneous, and metamorphic terrains, and reflects stratification and zonation during sedimentation, diagenesis, emplacement, or alteration.

5.2.1.5 International Static Database

In order to compile and compare ABA data from minesites around the world, the International Static Database (ISD) was recently created (Hutt and Morin, in preparation). The ISD currently contains 20,138 entries from 229 mines. Although the database is currently being evaluated, some initial results are informative. For example, a scatterplot of paste pH against measured NP (Figure 5.2.1-14) shows that unavailable NP (UNP, Section 5.2.1.3) is frequently around 10 t $CaCO_3$ equivalent/1000 t. In other words, oxidized samples with NPs below 10 t/1000 t can be acidic, although there are many exceptions which reflect UNP values close to zero or the lack of oxidation in fresh samples. Additionally, some samples in the ISD show UNP values as high as 60 t/1000 t. This variability highlights the care required in site-specific predictions for a particular minesite.

Case Study 5.2.1-1: Comparison of Paste pH to Groundwater pH in an Acid-Generating Tailings Impoundment

highlights: a vertical profile of paste pH through an acid-generating tailings impoundment; a vertical profile of porewater pH

Davé et al. (1981) conducted a suite of analyses for various solid-phase and aqueous components in the Nordic Main uranium tailings impoundment, Elliot Lake, Canada. This impoundment contains tailings placed between a bedrock valley wall and a coarse-rock dam. The tailings and dam are acid generating due to pyrite (Figures 5.2.1-15 and 5.2.1-16).

Their data allowed a comparison of paste pH, which involves small-scale samples (Section 5.2.1.1), to in-situ aqueous pH which reflects in-field processes over larger volumes. Paste pH (Figure 5.2.1-15) showed that the most acidic zone (pH < 4.0) occurs above the water table, close to the coarse-rock dam, apparently reflecting the ease of oxygen entry through the dam. A small acidic zone (pH < 4.0) also occurred above the relatively impermeable peat layer near the dam.

Below the water table, paste pH was predominantly around 4.5, rising to 6.0 at depth. In comparison, aqueous pH (Figure 5.2.1-16) of groundwater increases from <3.5 to around 7.0 with depth. Consequently, paste pH mimics aqueous pH, but differences of more than one pH unit are common.

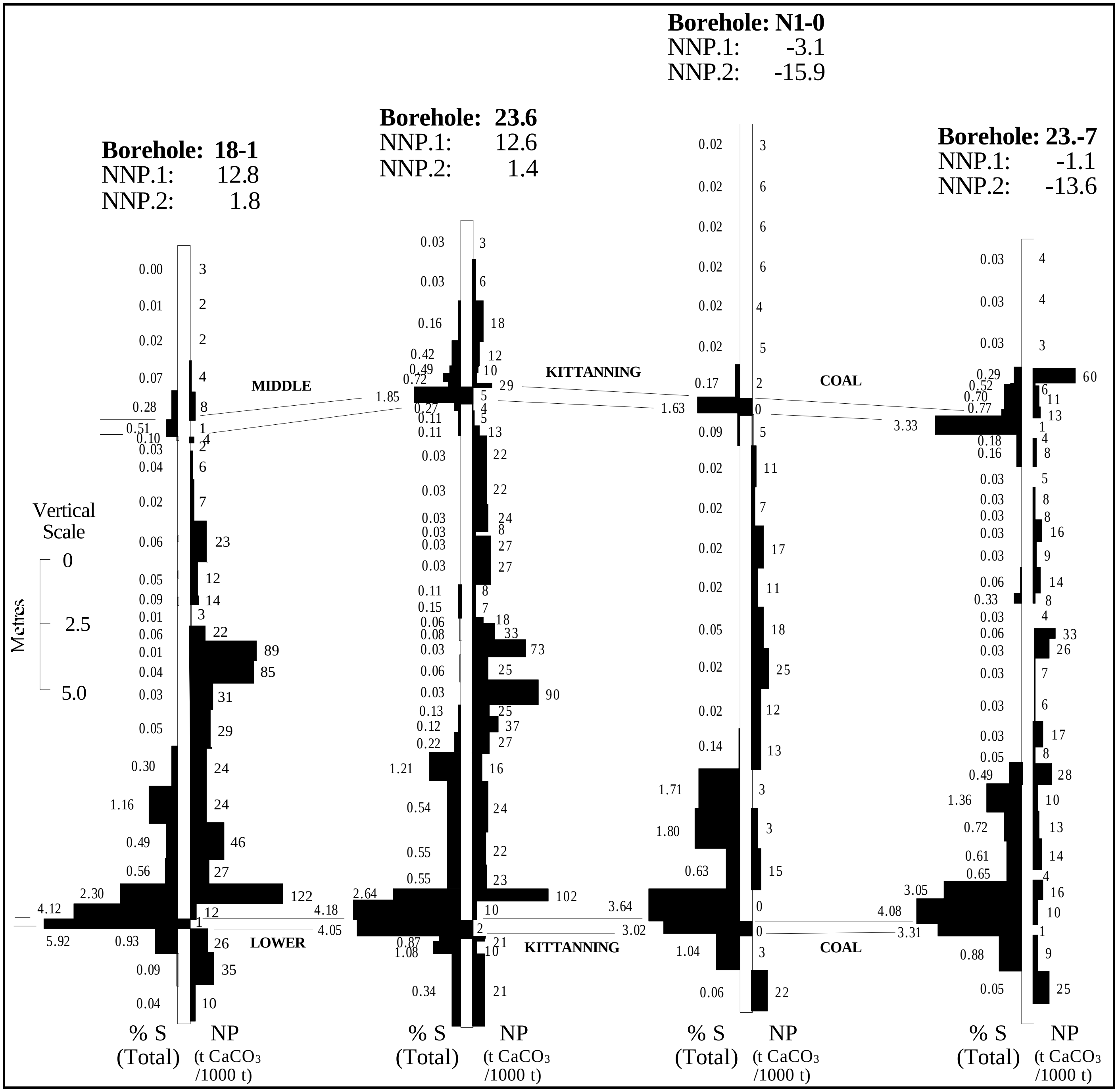

FIGURE 5.2.1-13a. Variability of ABA Parameters Within and Across Strata in a Sedimentary Terrain (adapted from Cravotta et al., 1994).

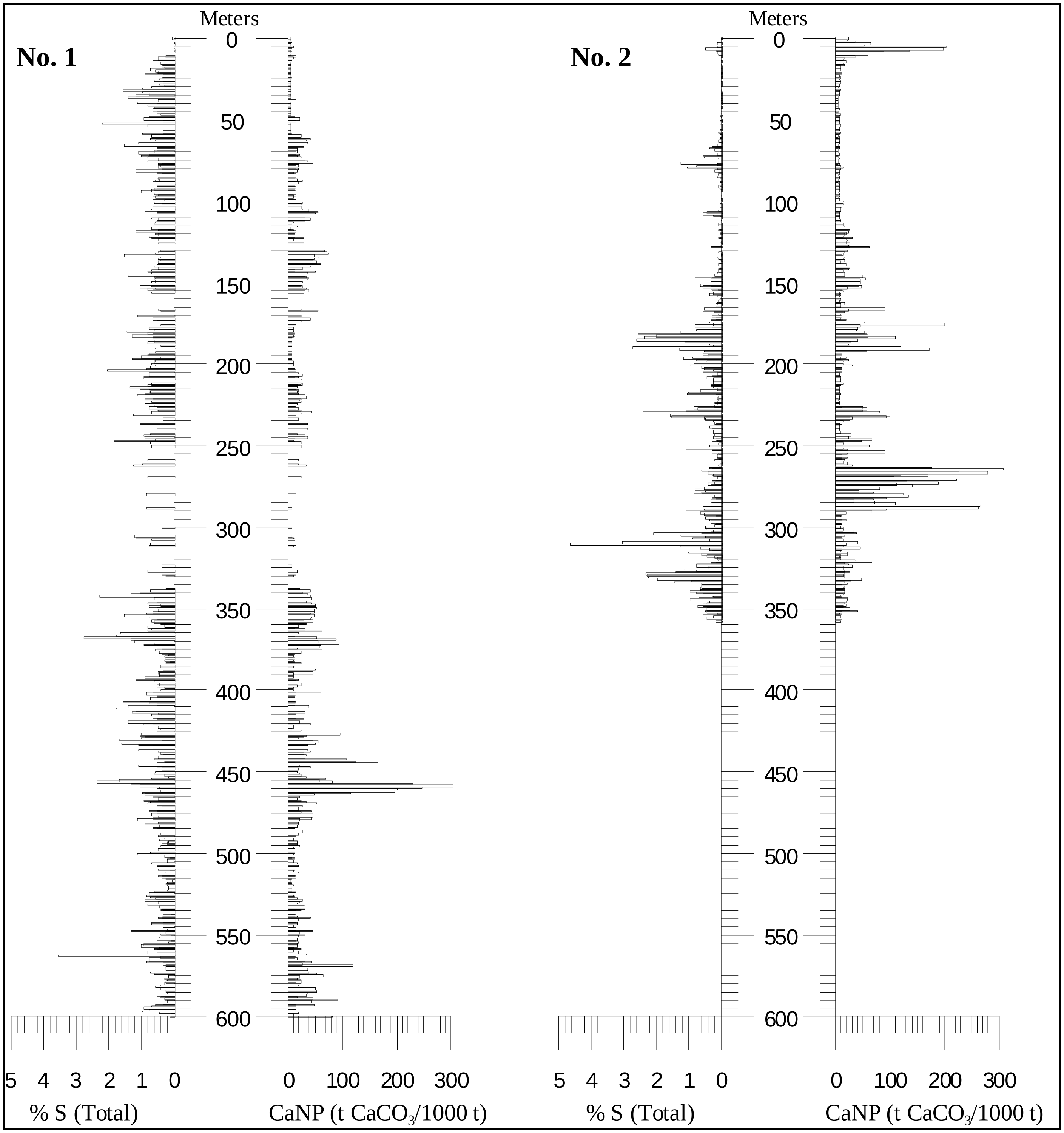

FIGURE 5.2.1-13b. Variability of ABA Parameters Within and Across Strata in a Volcanic Terrain.

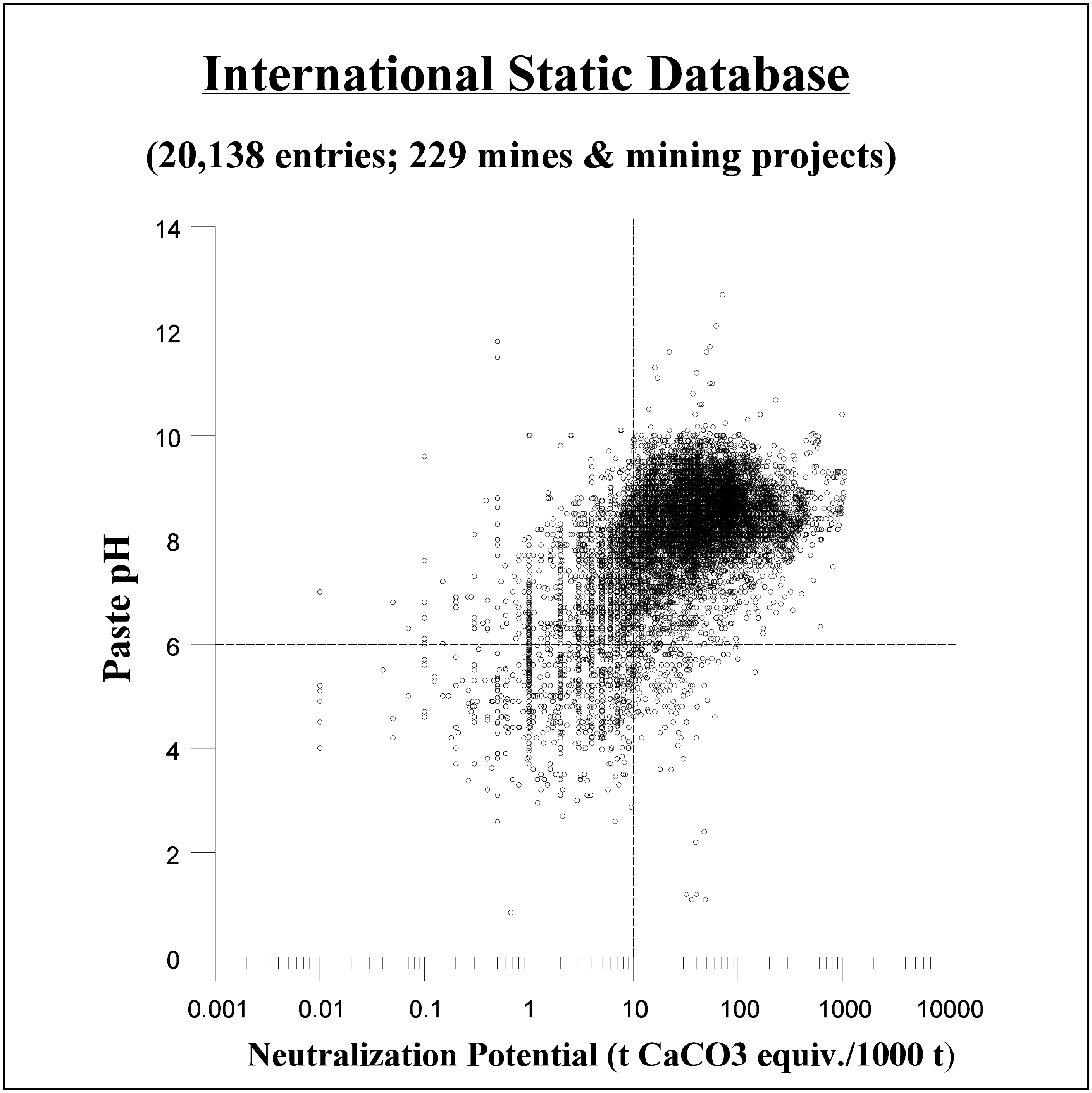

FIGURE 5.2.1-14. Paste pH vs. Neutralization Potential from the International Static Database (adapted from Hutt and Morin, in prep)

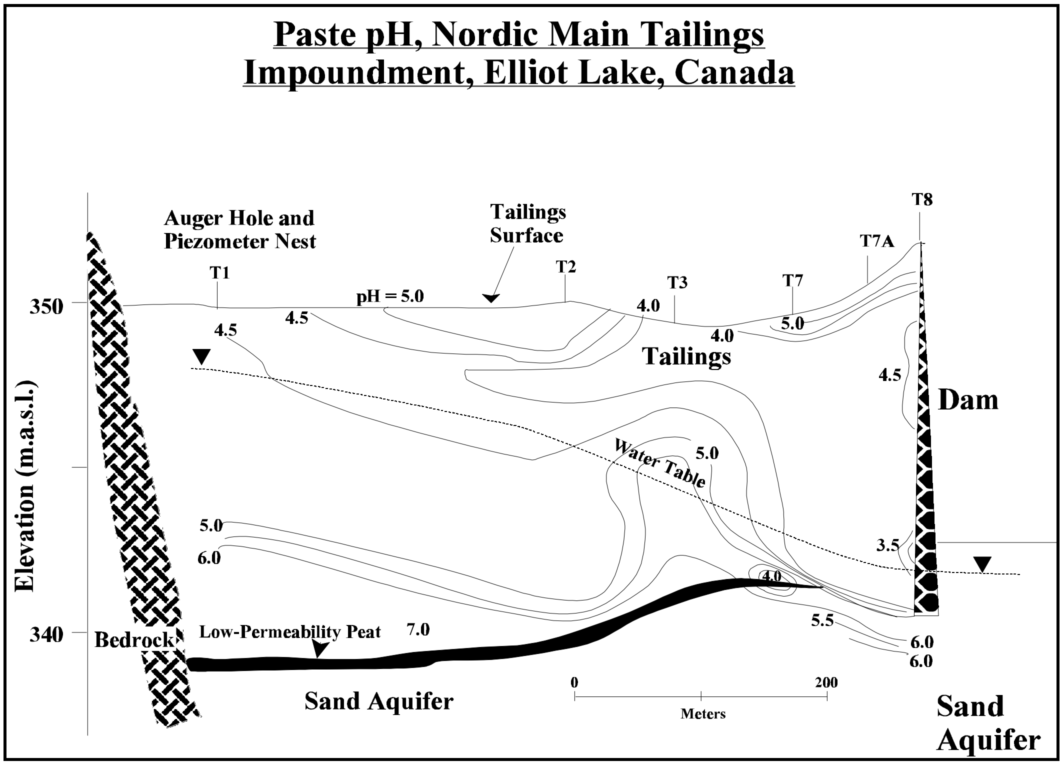

FIGURE 5.2.1-15. Solid-Phase Paste pH in a Cross-section of the Nordic Main Tailings Impoundment (adapted from Davé et al., 1981).

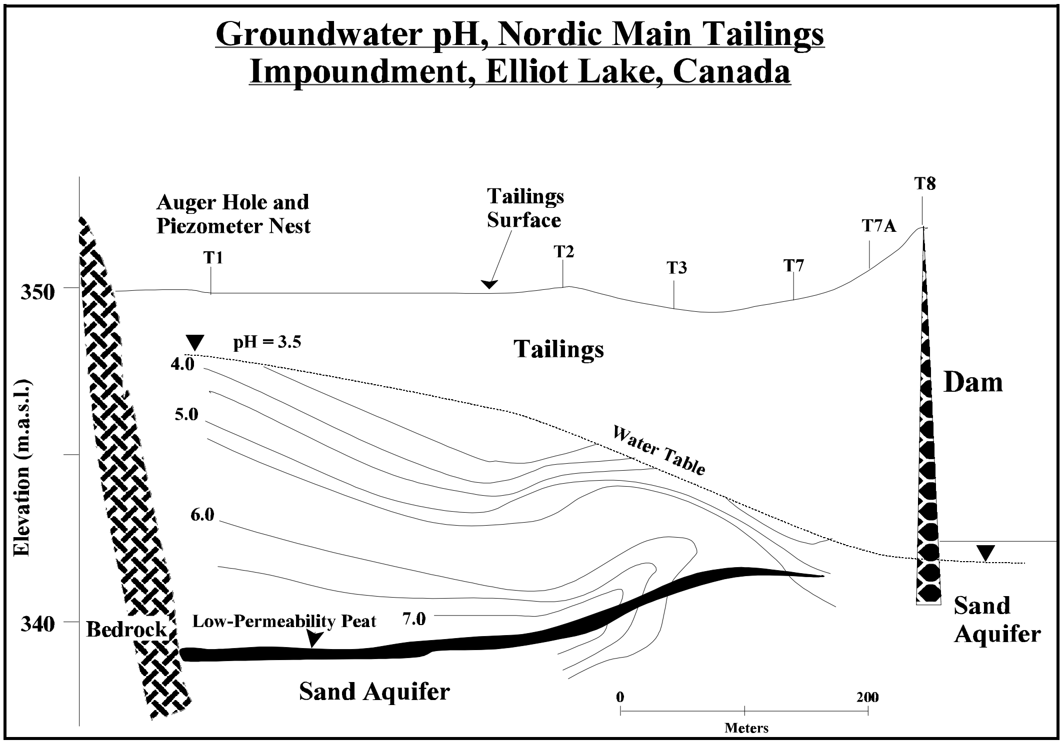

FIGURE 5.2.1-16. Groundwater Aqueous pH in a Cross-section of the Nordic Main Tailings Impoundment (adapted from Davé et al., 1981).

Case Study 5.2.1-2: Study of Various NP Techniques

highlights: various techniques to measure Neutralization Potential; discrepancies among NP techniques; comparison of NP results to mineralogy

Lapakko (1994a) compared results of NP analyses using five different techniques on four waste-rock and six tailings samples (Table 5.2.1-4). Sobek NP is discussed in Section 5.2.1.3 and Appendix B. Modified Sobek NP involved batches of HCl and fresh subsamples until a pH of 1.5-2.0 was maintained for 24 hours at room temperature, rather than at higher temperatures like standard Sobek. Solutions were then titrated with base until pH 8.3 was maintained for 30 seconds. The B.C. Research (BCR) NP involved titration of a pulverized sample with 1.0N H_2SO_4 until pH 3.5 was maintained with less than 0.1 mL added over four hours. The Lapakko Carbonate NP was measured like the BCR NP, except an endpoint pH of 6.0 is used. Mineralogical NP was defined based on the visual content of carbonate minerals:

$$\text{Mineralogical NP} = 10*(\%CaCO_3) + 11.9*(\%MgCO_3) \quad (5.2.1\text{-}10)$$

Also, the Carbonate NP (CaNP) could be calculated from CO_2 analyses in the paper. The latter three methods (Lapakko, Mineralogical, and CaNP) are sensitive primarily to carbonate minerals.

This work by Lapakko (1994a) shows that several analytical values of some type of NP can be made. However, the more important issue is the identification of which NP represents the actual, or effective, NP of each sample (Equation 5.2.1-5). This remains unanswered for these samples.

Nevertheless, some observations on effective NP and for reconciling NP differences can be made from the comparisons. The various NP values were similar for samples RK-1, TL-1, and TL-2. Samples RK-3 and TL-3 contained significant levels of siderite, which was detected by the CO_2 analysis (CaNP) and the BCR method. Sample RK-2 had little carbonate, but the highest amount of feldspar (SRNP, Equation 5.2.1-5) which apparently contributed to the Sobek, Modified Sobek and BCR NPs. Sample TL-5 had higher carbonate-based NP than Sobek-based NP, apparently indicating the carbonate (dolomite and magnesite) was not fully available. Sample TL-6 had the highest amount of carbonate, and yet the Sobek-related NPs are even higher. This suggests that other minerals are contributing to bulk NP, but incomplete mineralogy for this sample prevents confirmation of this.

Case Study 5.2.1-3: Pre-mining Prediction of Acid-Generating Waste Rock and Pit Walls

highlights: pre-mining ABA throughout a proposed open pit; effect of weighting and bench elevation on cumulative ABA characteristics; predictions for waste rock, pit walls, and tailings; comparison of NP to CaNP

In order to predict the drainage chemistry associated with a newly discovered orebody at an existing copper mine in western Canada, Patterson and Ferguson (1994) conducted Sobek acid-base accounting on 151 samples of ore and 244 samples of waste rock from 27 vertical drill holes (Table 5.2.1-5). Each sample represented a 13.7 m composite, based on the proposed bench height in the pit. The ultimate pit was expected to have lateral dimensions of 1000 by 550 by 230 m deep. A total of 109×10^6 t of waste rock and 7.2×10^6 t of overburden would be removed to access 34.7×10^6 t of ore.

ABA showed that no sample of waste rock was yet acidic, but some (almost 40%) were expected to become so based on a TNPR criterion of 1.0 (Table 5.2.1-5). A few samples of ore were acidic at the time of analysis, and many (more than 90%) could become acidic after their effective NP was exhausted.

A correlation of total sulfur with copper levels in waste rock and ore showed that sulfur generally increased with copper. However, sulfur levels spanned more than one order of magnitude at any particular copper level, so sulfur could not be accurately estimated from the less expensive copper analysis.

TABLE 5.2.1-4
Comparison of Five NP Techniques for Acid-Base Accounting
(from Lapakko, 1994a)

Method or Mineral	Sample (RK = rock, TL = tailings)									
	RK-1	RK-2	RK-3	RK-4	TL-1	TL-2	TL-3	TL-4	TL-5	TL-6
NP Data[1]										
Sobek	12	35	15	28	27	18	46	3.8	7.5	99
Modified Sobek pH 1.5	9.6	33	14	28	27	20	61	2.9	3.2	72
BCR pH 3.5	7.7	11	25	33	30	25	82	15	20	58
Lapakko pH 5	4	4	5	29	25	19	34	6	16	57
Lapakko pH 6	3.0	2.8	3.3	28	24	16	30	3.8	15	55
Mineralogical	0	1	5	32	19	16	19	5	12	46
CaNP	2.5	0.7	32	32	20	18	93	5.7	15	46
Mineralogical Data[2]										
%S	0.46	0.64	1.63	2.91	0.96	1.49	2.19	2.30	5.05	5.81
Quartz	24	-	41	34	38	53	42	45	21	12
Feldspar	24	54	29	29	39	30	12	13	52	5
Mica	6	4	12	4	14	10	10	30	10	2
Calcite	-	0.1	0.5	-	1.5	0.7	0.2	0.6	-	4.6
Dolomite	-	-	-	3.0	0.4	0.8	-	-	1.1	-
Ankerite	-	-	-	-	-	-	1.9	-	-	-
Siderite	0.3	-	3.2	-	-	0.2	8.3	-	-	-
Rhodocrosite	-	-	-	-	<.1	-	-	-	-	-
Magnesite	-	-	-	-	-	-	-	-	0.23	-
Chlorite	14	2	2	2	1	-	14	-	-	-
Amphibole	-	4	-	-	-	-	3	-	-	3
Pyroxene	-	18	-	-	-	-	-	-	-	55
Olivine	-	11	-	-	-	-	-	-	-	-
Clay	31	-	8?	21	-	-	-	6?	6?	-

[1] As t CaCO3 equivalent/1000 t; CaNP calculated from CO_2 measurements.

[2] As weight percent.

TABLE 5.2.1-5
ABA Results for the Gibraltar North Project, Canada
(adapted from Patterson and Ferguson, 1994)

Statistic	Paste pH	%S total	NP (t/1000 t)	TNPR
Waste Rock				
Maximum	11.07	6.82	80	170
Mean	9.01	0.66	24	5
Median	9.07	0.31	21	1.8
Minimum	7.45	0.01	3	0.02
Ore				
Maximum	9.31	11.5	62	2.7
Mean	8.03	2.98	17	0.33
Median	8.15	2.47	14	0.18
Minimum	4.98	0.41	3	0.01

A scatterplot of measured NP vs. CaNP showed that nearly all NP consisted of carbonate minerals. In a few samples, CaNP was up to twice the value of NP, indicating up to half the carbonate in those samples was not reactive.

Patterson and Ferguson (1994) noted that the number of samples from each proposed bench was not proportional to the amount of waste rock to be removed. When ABA results were weighted according to the volume of waste rock by bench, the mean sulfur content was 42% less than that of the database. This led to a lower estimate of acid-generating waste rock (28x10^6 t vs. 40x10^6 t). As a result, the authors emphasized the need for careful sample selection. More detailed methods for estimating volumes of net-acid-generating waste are discussed in Case Study 5.2.1-6.

Projecting sulfur values onto proposed pit walls showed that 41% of total exposed wall area would be net acid generating, with most of this rock exposed in the deeper portions of the pit. Because most of the acid-generating walls would be exposed late in the mining operation, contamination of pit water was not expected to be significant. No rates were available to further evaluate this prediction.

Although milling was expected to remove 27% of sulfide from the ore, TNPR values were still sufficiently low that nearly all tailings were net acid generating. As a result, tailings could not be cycloned for use in dam construction or be aerially exposed upon deposition in the tailings impoundment.

Case Study 5.2.1-4: One Weighted ABA Average Per Minesite

highlights: assessments using one weighted ABA value for a minesite; weighted Unavailable Neutralization Potential

Brady et al. (1994) used a novel approach for comparing ABA data to drainage chemistry. They calculated one value of AP, NP, and NNP for each of 38 coal minesites in Pennsylvania, based on weighted averages of all drillholes and ABA data at the sites. The number of drillholes at a site is inversely reflected in the number of hectares represented by one hole (Figure 5.2.1-17). Although possibly misleading on a local scale, these minesite-wide averages were consistent with small-scale observations on unavailable NP (Section 5.2.1.3)

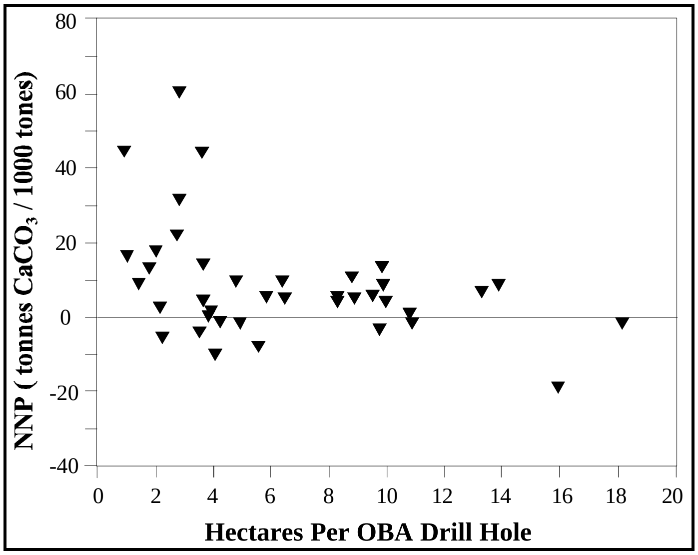

FIGURE 5.2.1-17. Minesite Averages of NNP vs. Hectares Per Hole at Each Minesite (adapted from Brady et al., 1994).

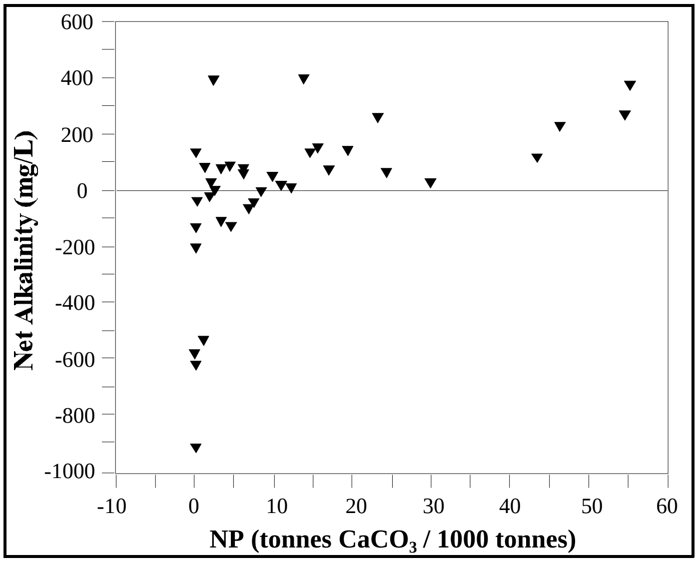

FIGURE 5.2.1-18. Minesite Averages of Net Alkalinity vs. Minesite-Average NP (adapted from Brady et al., 1994).

and an uncertain range for NNP (Section 5.2.1.4). Their plot of NP vs. net alkalinity in drainage (negative net alkalinity is acidic) showed that up to nearly an NP of 10 t/1000 t was unavailable on average (Figure 5.2.1-18). Net alkalinity vs. NNP showed that some NNP values up to +12 t/1000 t could be associated with acidic drainage. This close agreement between unavailable NP and positive NNP suggests that unavailable NP accounts for much of the uncertainty in the near-zero NNP values.

Case Study 5.2.1-5: Net-Acid-Generating Zones in a Type 3 Waste-Rock Pile, and Accumulation of Acidity along Basal Flowpaths

highlights: vertical trends of ABA through a Type 3 waste-rock dump; spatial variation of basal drainage chemistry due to periodic flushing of acidity

Northwest Geochem (1990) reported on a hydrogeologic study at Myra Falls Operations, a polymetallic mine on Vancouver Island, Canada. Based on rock samples collected from 57 drillholes into Waste-Rock Dump #1 (a Type 3 pile; see also Case Study 3.3-2), portions of the dump were classified as (1) mostly neutral with a shallow acidic zone (e.g., Figure 5.2.1-19), (2) mostly neutral with a distinct acidic zone at depth (e.g., Figure 5.2.1-20), or (3) entirely acidic (Table 5.2.1-6). On average, the waste rock was net acid generating based on a negative TNNP value and a TNPR value less than 1.0 (Table 5.2.1-7), although some samples did produce positive values of TNNP.

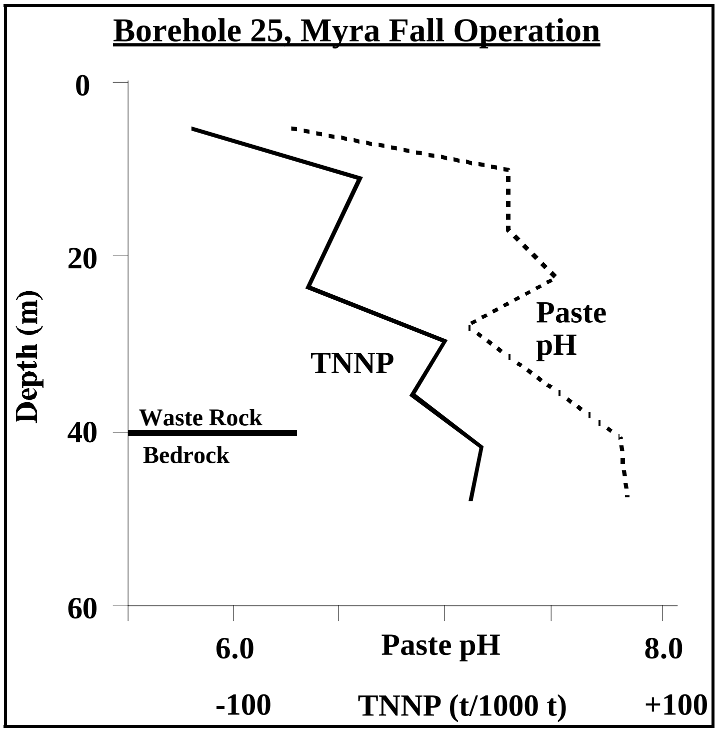

FIGURE 5.2.1-19. ABA Profile along Borehole 25, Myra Falls Operations (adapted from Northwest Geochem, 1990).

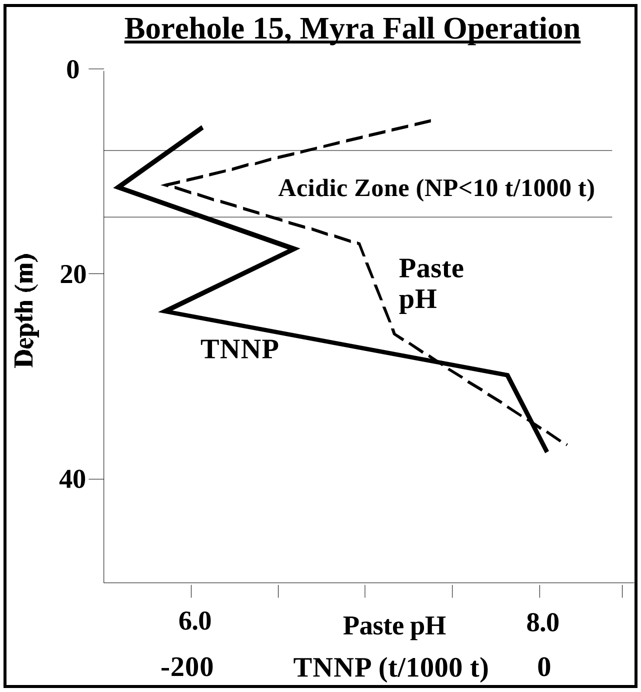

FIGURE 5.2.1-20. ABA Profile along Borehole 15, Myra Falls Operations (adapted from Northwest Geochem, 1990).

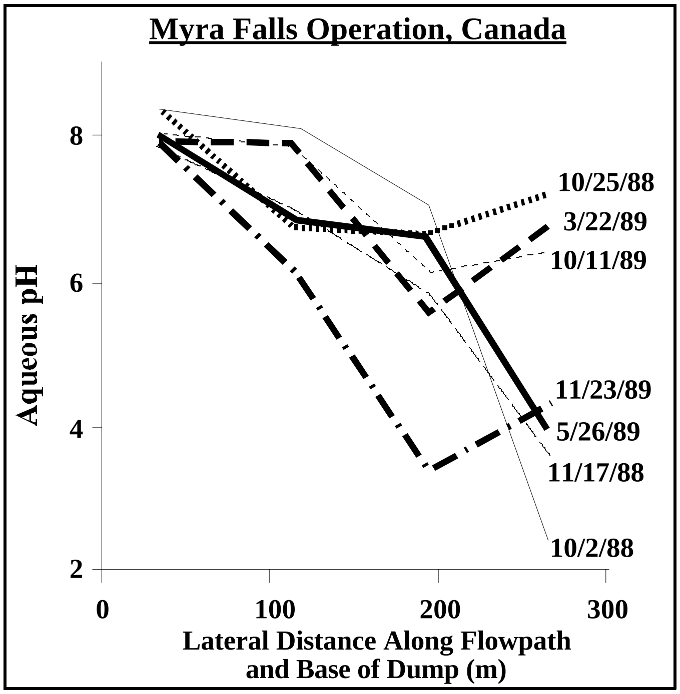

FIGURE 5.2.1-21. Aqueous pH along Basal Flowpath in Dump (adapted from Northwest Geochem, 1990).

Since this is a Type 3 pile (Figure 3.3-3), background groundwater entering the upslope base of the dump had a near-neutral pH. As this water continued to flow downslope along the base, some acidic water was added from the overlying waste rock depending on rainfall levels. This resulted in trends in pH (Figure 5.2.1-21) and aqueous sulfate (not shown) that varied through time along the base.

Compared with laboratory kinetic tests, only 10% of annual acidity was flushed annually from the dump. This corresponds to a retention factor of 90% (Sections 4.2 and 5.2.4).

TABLE 5.2.1-6
Vertical Trends in ABA Parameters in Boreholes, Myra Falls Operations
(from Northwest Geochem, 1990)

Boreholes Showing No Major Trend (Mostly Neutral)
1, 2, 12, 13, 16, 18, 23, 25, 27, 29, 30, 31, 32, 33, 34, 35, 36, 37, 38, 45, 46, 48, 49, 50, 52, 53, 54, 56, 57, 58, 59, 60
Boreholes Showing a Shallow Acidic Zone from the Surface (depth to bottom in m)
3 (14 m), 4 (8 m), 6 (8 m), 9 (8 m), 10 (15 m), 11 (20 m), 19 (14 m), 20 (8 m), 24 (8 m), 26 (8 m), 28 (8 m)
Boreholes Showing Acidic Zones at Depth (top and bottom in m)
5 (9-13 m), 9 (20-26 m), 14 (20-26 m), 15 (8-14 m), 17 (14-26 m), 21 (23-26 m), 22 (9-13 & 27-31 m), 55 (9-20 m)
Boreholes Showing Completely Acidic Profiles
7, 8, 47, 51

TABLE 5.2.1-7
Summary Statistics for Waste-Rock Boreholes at Myra Falls Operations
(from Northwest Geochem, 1990)

Parameter	Minimum	Mean	Maximum
Waste Rock (No. Of Samples = 189)			
Total Acid Potential[1]	0.6	112	438
Neutralization Potential[1]	1.7	24	50
Total Net Neut. Potential[1]	-424	-88	+26
Paste pH	4	7.22	8.16
Natural Organic Material (No. Of Samples = 18)			
Total Acid Potential[1]	0.9	23	176
Neutralization Potential[1]	4	14	29
Total Net Neut. Potential[1]	-159	-9	+25
Paste pH	6.47	7.47	8.13
Bedrock (No. Of Samples = 42)			
Total Acid Potential[1]	0.3	7.3	123
Neutralization Potential[1]	5.1	13	67
Total Net Neut. Potential[1]	-90	+5.6	+67
Paste pH	6.19	7.68	8.45

[1] In units of t $CaCO_3$ equivalent/1000 t.

Case Study 5.2.1-6: Pre-Mining Block Modelling of ABA Data

highlights: "block" models for estimating volumes and locations of ore and waste rock; integration of ABA data into block models; kriging of ABA data; sill and nugget effect for ABA data; timing of rock removal during mining

As part of ore-reserve estimation and mine-plan design, a geologic "block" model is often implemented for a mining project. This type of model divides the ore and associated waste rock into three-dimensional blocks, often several meters on each axis. Geology and chemical assays are then used with geostatistical interpolation to assign to each block a predicted metal level, an ore/waste-rock designation, and a rock unit. In recent years, ABA data have been incorporated into block models to refine the waste rock into net acid generating and net acid neutralizing categories. As a result, for each

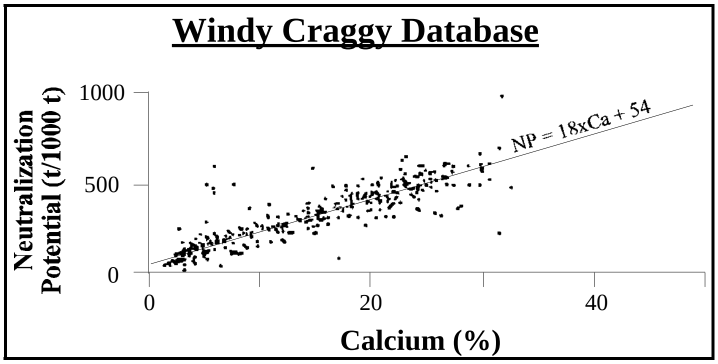

FIGURE 5.2.1-22. Correlation of NP to Calcium in the Windy Craggy Database (adapted from Downing and Giroux, 1993).

category, the total volumes and volumes by depth/spatial location can be delineated, and the scheduling of removal and annual volumes can be adjusted and refined.

Acid Potential (or %S) and NP have to be modelled separately because they are frequently independent variables. After each block has an interpolated AP and NP, the NNP or NPR of the block can be calculated.

Downing and Giroux (1993) described the use of a geologic block model at the Windy Craggy Project in northern British Columbia, Canada. The model contained a total of 100,758 blocks, measuring 20x20x12 m, for estimating levels of copper, cobalt, gold, silver, and zinc. An ABA database of 1247 analyses was considered insufficient to interpolate results to each block properly using geostatistical kriging. Consequently, the more abundant sulfur assays were substituted for %S in ABA and calcium was substituted for NP for samples with Fe < 5% (Figure 5.2.1-22). One weakness in this approach was that the use of Ca overestimated NP and NNP at lower values. As a result, misclassification of some blocks as net acid neutralizing may have occurred in the NNP range of -50 to +50 t/1000 t.

The Windy Craggy block model generated kriging semivariograms (e.g., Davis, 1986; Rautman and Istok, 1996) for calcium in two rock units (Figure 5.2.1-23) and for other parameters (Table 5.2.1-8). In a basic sense, these semivariograms showed that no significant spatial correlation (the "sill") in metal levels beyond lateral distances of 30-180 m, depending on the metal and rock unit. Also, the "nugget effect" indicated that metal levels can change by at least several tens of percent over extremely short distances.

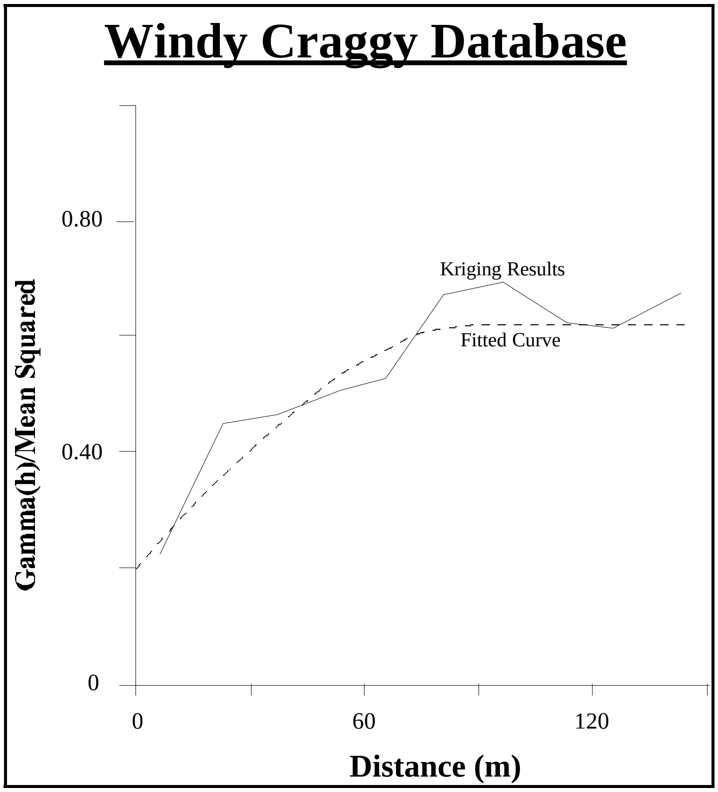

FIGURE 5.2.1-23. Kriging Semivariogram for Argillite at Windy Craggy (adapted from Downing and Giroux, 1993).

The large gold-copper Las Cristinas Project is located in southeastern Venezuela. An expanding ABA database, currently containing more than 2500 ABAs, was integrated into the project's block model with 5x5x10 m blocks (Morin and Hutt, 1995b). Geostatistical kriging was then used to delineate net-acid-generating zones on each pit cross-section and on anticipated final pit walls (Figure 5.2.3-24). This showed that most net-acid-generating rock occurred in discrete intervals, often near mid depth in the pit. As a result, mining could take place for a few years before major management of acid-generating rock was needed.

As with Windy Craggy, kriging variograms for this project showed that neither %S and NP had little correlation over spatial distances greater than 30-150 m depending on the parameter and rock unit (Figure 5.2.3-25). This carries major implications for the amount and degree of ABA sampling to interpolate results properly. Also, the nugget effect for these variograms indicated that NP and %S could vary by at least tens of percent over extremely short distances, in agreement with the Windy Craggy modelling.

TABLE 5.2.1-8
Summary Parameters for Windy Craggy Semivariograms
(adapted from Downing and Giroux, 1993)

Rock Unit	Parameter	Nugget Effect	Sill	Range (m)		
				Maximum Horizontal	Minimum Horizontal	Vertical
Argillite	Cu	1	2	30		
Argillite	Fe	0.05	0.25	120	28	120
Argillite	Ca	0.2	0.62	90		
Volcanics	Cu	0.8	3.6	50		
Volcanics	Fe	0.04	0.31	75	45	150
Volcanics	Ca	0.1	0.5	50		
Gabbro	Cu	0.4	1.05	45		
Gabbro	Fe	0.05	0.2	75		
Gabbro	Ca	0.05	0.5	56		
Stringer	Cu	0.2	1	180	45	100
Stringer	Fe	0.02	0.1	90	38	48
Stringer	Ca	0.15	0.65	45		

Case Study 5.2.1-7: An Inappropriate ABA Analytical Standard

highlights: variability in NP analyses among laboratories; variability due to mineralogy; incorrect use of averaging to obtain a standardized NP value

In order to create an analytical standard for ABA, Leaver and Bowman (1994) obtained 540 kg of non-ore-grade pit-wall rock from the closed Bell Mine in British Columbia, Canada. After careful homogenization, subsamples were sent to various laboratories for ABA analysis.

Total-sulfur analyses showed good clustering (Figure 5.2.1-26), although the range of 0.12%S represented approximately 40% of the mean value of 0.28%S. On the other hand, NP displayed a bimodal distribution (Figure 5.2.1-27), with all values being less than the CaNP value of 65 t $CaCO_3$/1000 t.

Several months earlier, these researchers recognized that some carbonate minerals in this rock occurred as iron-rich ankerite and siderite (Leaver et al., 1994), which can provide little neutralization or neutralization only at a slow rate (Section 5.2.1.3). Consequently, the NP analyses could be expected to deviate among laboratories depending on the fizz rating and strength of acid selected for the NP determination (Appendix B), and this is what occurred.

Furthermore, Morin and Hutt (1993b) conducted a suite of static and kinetic tests on rock at this mine and found that approximately one-third of the carbonate can occur as iron-rich carbonate. As a result, the bimodal distribution may reflect the detection of fast-reacting carbonate around 48 t/1000 t by some laboratories and of fast-reacting and some slow-reacting carbonate up to 62 t/1000 t by others.

Las Cristinas Project

Vertical Section 9400N (looking north)

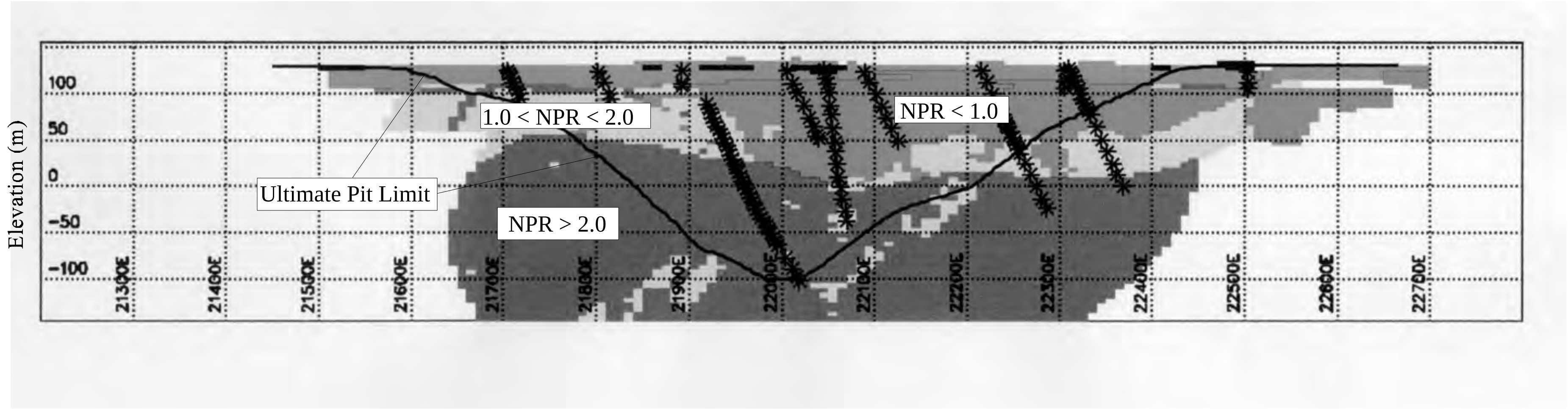

Final East Wall of Pit (looking east)

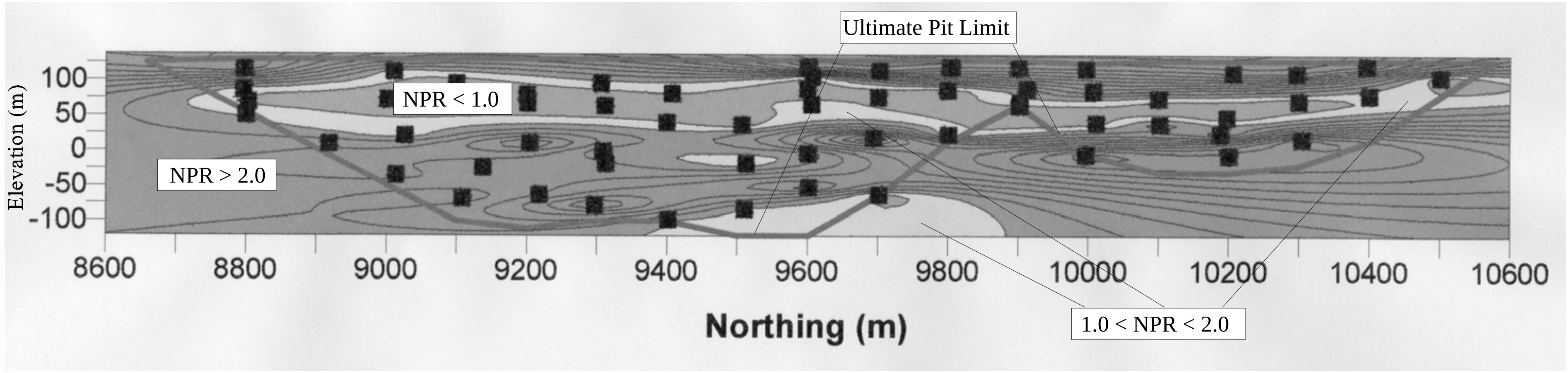

FIGURE 5.2.1-24. Geostatistical Block Modelling of NPR at Las Cristinas (adapted from Morin and Hutt, 1995b).

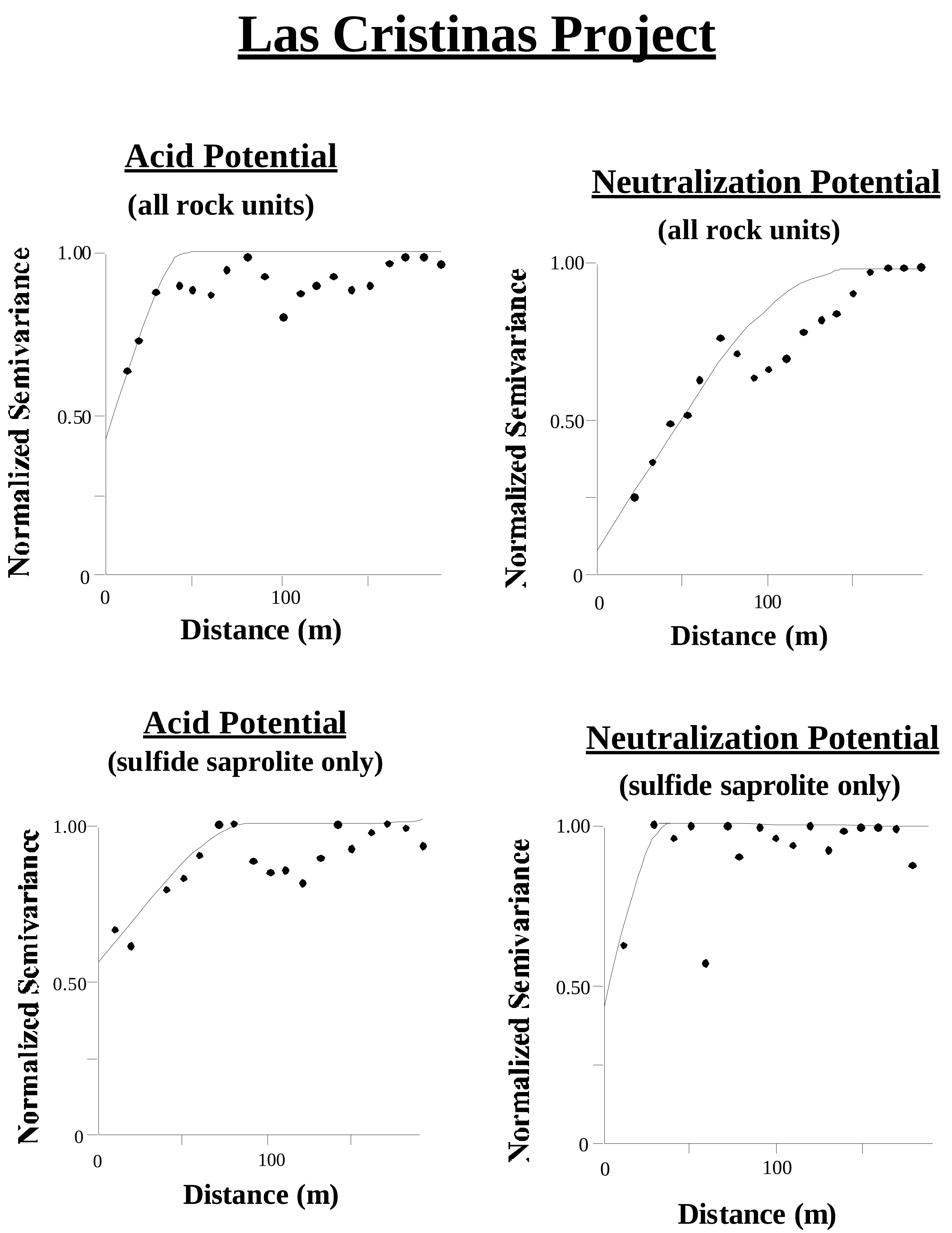

Las Cristinas Project

Acid Potential (all rock units)

Neutralization Potential (all rock units)

Acid Potential (sulfide saprolite only)

Neutralization Potential (sulfide saprolite only)

5.2.1-25. Kriging Variograms for All Rock Units and Sulfide Saprolite Only (adapted from Morin and Hutt, 1995b).

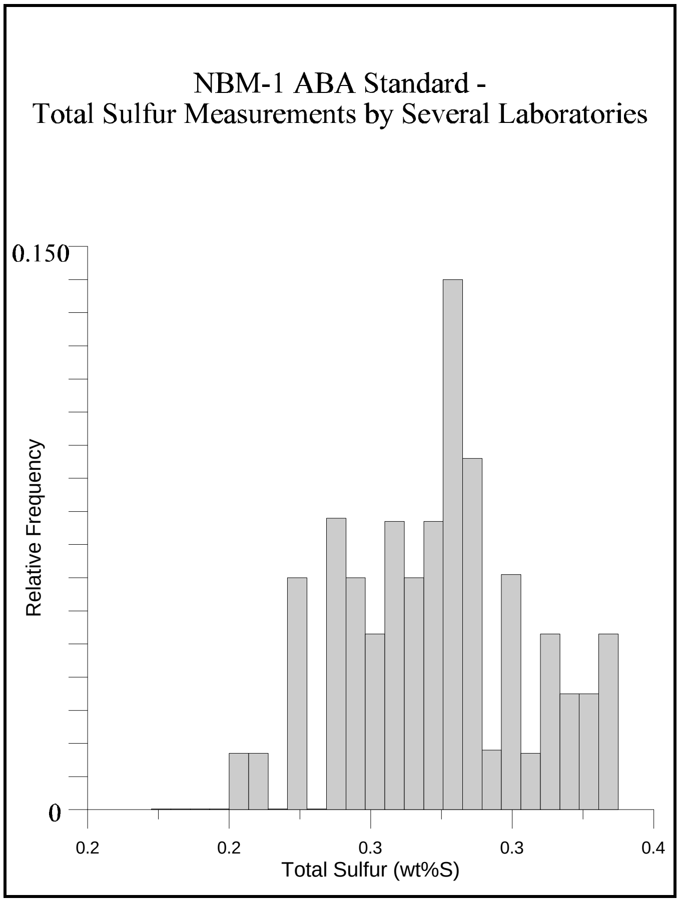

FIGURE 5.2.1-26. Total-Sulfur Analyses for a Standardized ABA Sample by Several Laboratories (adapted from Leaver and Bowman, 1994).

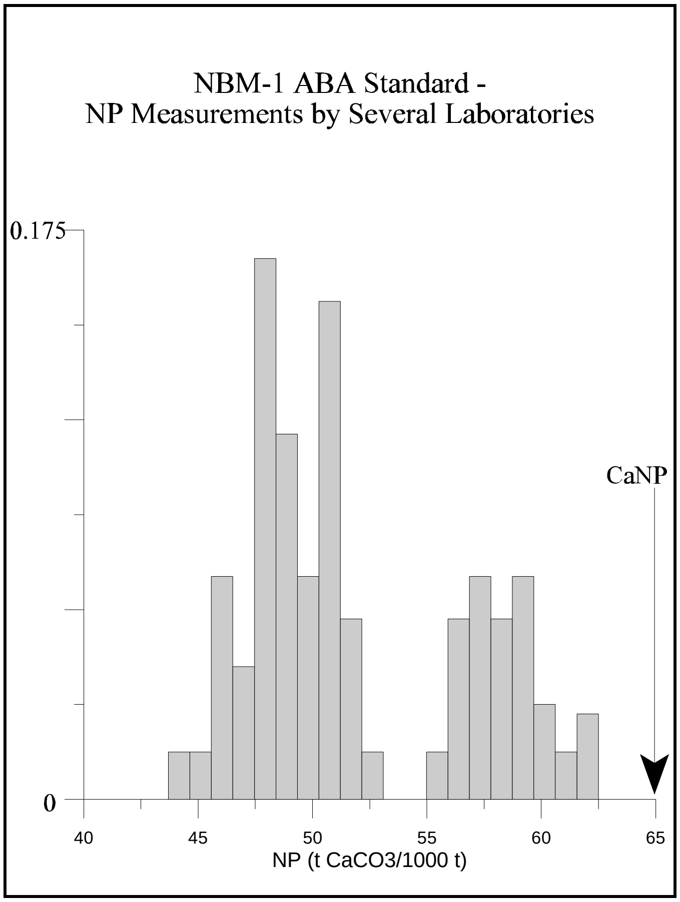

FIGURE 5.2.1-27. NP Analyses for a Standardized ABA Sample by Several Laboratories (adapted from Leaver and Bowman, 1994).

The bimodal distribution implies that an average, standardized value for NP could not be justified for the sample, and Leaver and Bowman (1994) recommended additional work. However, the NBM-1 sample is currently marketed as an ABA standard with an NP value of 52 t/1000 t, which few laboratories actually measured. In other words, laboratories who now measure a standardized NP of 52 t/1000 t for the NBM-1 standard are not performing NP analyses correctly.

While some blame the Sobek technique (Appendix B) for variability in NP results, experienced technicians can generate precise and reproducible NP analyses among laboratories. For example, a set of 34 drillcore samples was submitted to two laboratories with significant experience with the Sobek technique. The results (Figure 5.2.1-28) showed that 50% of the NP analyses agreed within 1 t/1000 t and 97% agreed within 8 t/1000 t.

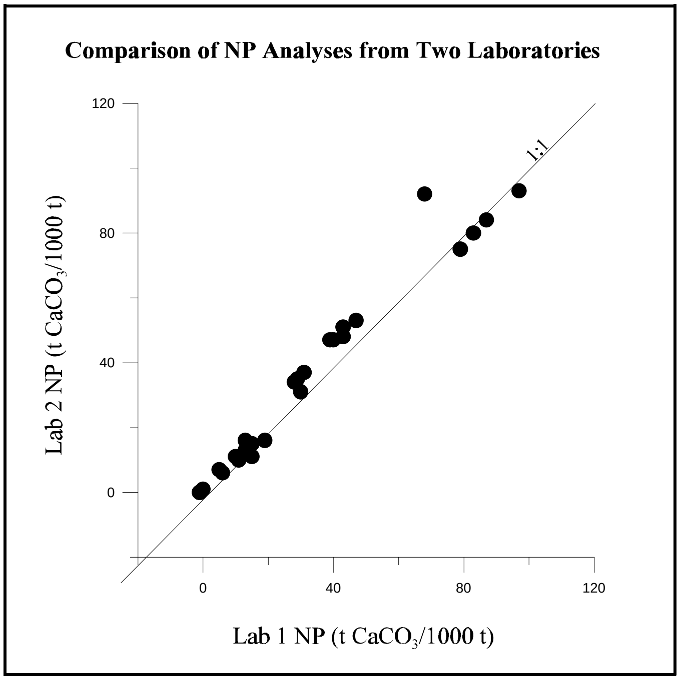

FIGURE 5.2.1-28. Comparison of 34 NP Analyses at Two Laboratories.

Case Study 5.2.1-8: Errors in Predictions Using Static Tests

highlights: errors and uncertainties in drainage-chemistry predictions; regulatory perspective on predictions

Regulatory agencies in British Columbia, Canada, where acidic drainage has been a major concern at several minesites for years, are providing detailed guidelines for the prediction of drainage chemistry (Price et al., 1997). These guidelines are based, in part, on case studies of errors in predictions at British Columbian minesites.

Price et al. (1997) explained that proposed "Minesite A" initially classified all 70×10^6 t of tailings as potentially net acid generating (TNPR < 1.0). Because the tailings contained significant levels of sulfate, SNPR values were calculated, but still showed the tailings would be net acid generating. However, the sulfate levels from the laboratory were as $\%S_{SO4}$, but were incorrectly divided by three in the belief that they were reported as $\%SO_4$. Upon correct calculation of SNPR values at values above 8.0, the tailings were reclassified as net acid neutralizing.

For waste rock at Minesite A, SNPR values were again miscalculated due to the sulfate error and predicted nearly all rock would be net acid generating. Additionally, only average values for each rock unit were used to determine the status of the entire unit. Corrected SNPR values and the use of SNPR ranges revealed that up to 80% of some rock units were actually net acid neutralizing.

Kinetic tests revealed high rates of sulfate production, but this was attributable to the dissolution of the abundant sulfate minerals rather than sulfide oxidation and acid generation. Nevertheless, Minesite A assumed the sulfate did represent significant acid generation, but this was rejected by regulatory agencies.

Detailed engineering designs for Minesite A including a water-retaining dam and submergence of all tailings and waste rock, in public review at the time, were withdrawn. A less expensive flow-through dam using free-draining waste rock was then prepared.

"Minesite B" contains rock with pyrite, chalcopyrite, sphalerite, galena, pyrrhotite, and marcasite (Price et al., 1997). Initial predictions were that waste rock would not generate net acidity because (1) the rock contained little or no sulfides, (2) the climate was subalpine and not conducive to weathering, and (3) the presence of sulfides in outcrops indicated a lack of reactivity. The regulatory agencies countered with (1) sampling revealed sulfide levels between 2 and 20%S and all NPR values less than 0.4, (2) one small area of a waste-rock dump was releasing drainage at pH 3, (3) NP values were 18-40 t $CaCO_3$/1000 t providing the observed lag time to net acidity, and (4) fine particles weathered from outcrops had rinse pHs around 3. Additional testwork is now underway.

"Minesite C" has two of eight waste-rock dumps generating acidic drainage with copper as high as 7 mg/L (Price et al., 1997). ABA results indicated that non-acidic waste rock contains 0.5-4%S, NP of 10-30 t/1000 t providing a lag time to net acidity, and NPR values typically less than 1.0. Short-term column testwork showed that initially acidic samples remained acidic and samples near neutral pH remained neutral. Based on this and generic modelling, the mine concluded that drainage chemistry from the dumps would not become worse. Regulatory agencies remain concerned over the site.

At "Minesite D", tailings were initially predicted to have NPR values above 2.0, but the actual tailings have NPR values less than 1.0. Drainage from the mine area is pH neutral, but carries elevated levels of dissolved zinc requiring treatment. NPR values for the mine walls and waste rock range from 1.0 to 3.0. Regulatory agencies instructed the mine to monitor historic workings in the watershed, which revealed drainages down to pH 2 and zinc as high as 165 mg/L. Additional testwork is underway.

5.2.2 Mineralogy

Because drainage chemistry is created by mineral reactions (Section 4.2), the delineation of the mineralogy within a minesite component or rock unit is critical. Other static tests like acid-base accounting (Section 5.2.1) include assumptions about mineralogy, which affect their predictions of drainage chemistry. For example, the calculation of acid potentials (Section 5.2.1.2) assumes that the reactive sulfide mineral is pyrite, when it could be pyrrhotite or any of the hundreds of other sulfide-bearing minerals. Therefore, optimum predictions require confirmation of mineralogical assumptions.

Mineralogical examinations of samples ideally reveal the types, shapes, sizes, composition, spatial relationships, and abundances of minerals (e.g., Table 5.2.2-1). Accurate estimates of mineral abundances can be assisted by whole-rock and total-metal analyses (Section 5.2.3).

The traditional geological method for determining the mineralogy is through visual, petrographic examination of thin sections, which are thinly shaved, translucent slices of rock mounted on glass slides. This provides the required information on the types, shapes, grain size, and spatial relationships of minerals. However, minerals at levels less than 0.5-1.0% may not be detected. Furthermore, the precise elemental composition of minerals, which can vary significantly from minesite to minesite, cannot usually be determined from thin sections. X-ray diffraction can assist, but still suffers from detection limits around 0.5%.

For better identification of trace minerals and detailed elemental composition, more advanced techniques such as electron microprobes can be employed. However, these techniques focus on individual grains so that larger-scale relationships and overall composition are not readily apparent. Because of the assumptions on mineralogy embedded in many predictive approaches, a combination of techniques may be the best approach for delineating all-important mineralogy.

5.2.3 Total-Metal and Whole-Rock Analysis

This static test of whole-rock/total-metal analysis provides the total amounts of various elements (metals and nonmetals) in a sample, including silica and aluminum. These solid-phase concentrations can then be used to confirm or improve the findings of other static tests (Section 5.2.1 and 5.2.2). For example, if mineralogical examinations (Section 5.2.2) reveal that the only iron-bearing mineral is siderite, a relatively non-neutralizing carbonate mineral (Section 5.2.1.3), then an accurate estimate of its concentration can be obtained from total-metal analysis. In reality, one element rarely occurs entirely in one mineral, which is also one complication in the interpretation of kinetic tests (Section 5.3). In any case, this static test provides information that others cannot, such as the amounts of trace metals like cadmium or mercury. This information is necessary for calculating depletion times for trace metals in kinetic tests (Sections 5.3 and 5.4).

Proper whole-rock/total-metal analyses require near-complete dissolution of a sample in acids or other solvents, followed by elemental analysis. However, incomplete dissolution of a sample can occur, biasing concentrations toward lower values. Some methods such as x-ray fluorescence (XRF) and neutron activation for whole-rock analyses do not require sample dissolution before analysis, and thus avoid the problems with incomplete dissolution.

The basic difference between whole-rock and total-metal analyses is that whole-rock analyses typically have relatively high detection limits (greater than 10-100 ppm) and include a limited number of elements. On the other hand, total-metal analyses detect other, often less abundant elements, often using ICP equipment, but are more prone to incomplete dissolution.

One point of potential confusion in whole-rock analyses is the traditional reporting of concentrations as oxide equivalents like Al_2O_3 and MgO. This does not mean that aluminum and magnesium occur in the sample as these oxide minerals, which can be confirmed with mineralogical examinations (Section 5.2.2). Instead, this is simply an established way of reporting metal contents, and true metal concentrations must be calculated from the oxide equivalents using atomic weights.

TABLE 5.2.2-1
Example of Reactive-Mineral Composition of Tailings

Mineral	Formula	Average Percent
Pyrite	FeS_2	4.5% (2.4%S)
Pyrrhotite	FeS (approximate)	0
Chalcopyrite	$CuFeS_2$	0.3% (0.1%S)
Sphalerite	ZnS	0
Arsenopyrite	FeAsS	0.002%
Gypsum	$CaSO_4 \cdot 2H_2O$	0.085%
Neutralization Potential	$CaCO_3$ equivalent	4.2%
Siderite	$FeCO_3$	2.1%
Iron oxyhydroxides	FeOOH equivalent	0.8%
Phosphate	PO_4	0.15%

5.2.4 Retention of Reaction Products

A comparison of laboratory kinetic tests (Section 5.3) to field tests and monitoring (Sections 5.4 and Chapter 4.2) have shown that more metals and acidity are consistently released for a unit weight and unit time in laboratory tests. This has occasionally been misinterpreted as anomalously accelerated reaction rates in laboratory tests. In reality, laboratory tests typically include relatively large amounts of rinse water whereas field conditions provide relatively little. As a result, an entire minesite component is rarely rinsed completely and thoroughly, providing a lower "reaction" rate based on drainage chemistry (Rate2 vs. Rate1, Figure 4.2.2-1). Additionally, the solubilities of secondary minerals are often exceeded in minesite components, leading to precipitation of those minerals and thus a lower "reaction" rate based on drainage chemistry. Visual evidence of this precipitation, like iron staining with ferric minerals, is common. Therefore, field samples can contain retained reaction products, sometimes at very low concentrations not detectable by mineralogical examinations (Section 5.2.2). Also, these reaction products cannot be distinguished from the primary, or original, metals and nonmetals in whole-rock/total-metal analyses (Section 5.2.3). Therefore, another static test is needed to evaluate retention levels.

In order to determine the amount of retention in a sample, a relatively simple washing or extraction procedure can be employed. The procedure simply uses excess water to ensure most retained products dissolve without solubility limitations, and includes gentle agitation for at least 24 hours to maximize exposure of all grain surfaces to the rinse water. Distilled or acidic water can be used, depending on the data requirements and environmental conditions at the minesite. McGregor et al. (1995) reported that most of the retained heavy metals in a tailings impoundment was in the reducible iron-hydroxide phases and thus acidic water (or iron-reducible solution) would provide a better estimate of total retained heavy metals. The retention tests are concluded with analysis of the water and calculations to obtain original concentration of each element as mg/kg of sample.

A comparison of the retention results to total-metal analyses yields the percentage of the total concentration that is readily soluble and removed upon thorough rinsing. This can be important, for example, where rock or tailings are being relocated and submerged. One study showed that retained copper in net-acid-generating waste rock, approximately 45 years old, ranged from virtually zero to 35% of total copper. Based on reaction rates, this retention corresponded to 0.1 to 48 years of weathering, indicating some waste rock was regularly rinsed by precipitation, whereas other portions were rarely rinsed.

5.2.5 Grain-Size Analysis and Particle-Surface Area

The objective of this static test is to delineate the sizes and amounts of grains or particles in a sample. This information is important for several reasons. First, various size intervals can react at different rates (discussed below). Second, individual grain sizes can be submitted for independent static testing to detect any bias in mineral distribution with size. Third, physical parameters such as hydraulic conductivity and moisture retention are related to grain-size distribution. Fourth, the results can be used to calculate grain/particle surface areas based on geometric shape of the grains.

The surface area can be calculated for a sample under the assumption that the surface area of each particle is proportional to the cubic diameter if a sphere, or width if a cube. This is known as its "geometric surface area". Surface-area-dependent reaction rates from kinetic tests (Section 5.3) can then be calculated if wanted and scaled to other grain sizes, although this is not recommended due to errors in estimates of grain-surface areas.

The use of geometric surface area for surface-area rates is prone to significant errors. Since grains do not necessarily have smooth surfaces and regular shapes, the calculated geometric area may be anomalously low. Other, more direct methods, like BET nitrogen adsorption, which has its own problems, have shown that surface areas can be 100-1000 times higher than the geometric value (White and Peterson, 1990; Case Study 5.2.5-1). However, Nicholson (1994) reported only a factor-of-five discrepancy among geometric and BET areas for quartz and pyrite grains.

The precipitation of secondary minerals onto primary minerals can greatly increase surface area beyond the geometric value. Benjamin and Sletten (1993) reported that, when sand grains with no iron content and a BET surface area of 40 m^2/kg were coated with ferrihydrite, iron content increased to 2.1-3.2 wt-% and BET surface area increased to 2,400-9,100 m^2/kg.

Case Study 5.2.5-1: Grain Size, Surface Area, and Reaction Rates

highlights: uncertainties in measurements of grain-surface area; differences in reaction rates between fresh and weathered feldspar minerals and among grain sizes

Anbeek (1992a, 1992b, 1993) reported that up to three orders of magnitude difference have been noted in reported feldspar reaction rates among freshly crushed and naturally weathered samples. This was attributed, at least in part, to incorrect measurements among surface areas for particles, and reaction sites, pH, P_{CO2}, proportion of mineral surface in contact with solution, organic ligands, other solutes, liquid flux, temperature, and character of mineral surfaces. However, the sources of discrepancy considered most likely by Anbeek were (1) inaccurate surface areas and (2) reactive character of freshly created surfaces. To examine this further, Anbeek conducted surface-area measurements on separated beach sand composed of approximately 50% quartz, 18% albite, 15% microcline, 7% plagioclase ($Ab_{70}An_{30}$), 9% muscovite, and 1% biotite. These mineral percentages were relatively constant with grain size in subsamples ground between 850 and <53 µm in diameter. However, SEM-estimated surface areas increased from 50 to 480 cm^2/g over this range in grain size, whereas BET areas increased from 1730 to 3900 cm^2/g.

Research has shown that some minerals concentrate in the coarser or finer fractions, but intermediate sizes have the highest reaction rate. Anbeek (1992a, 1992b, 1993) examined this trend for crushed vs. naturally weathered feldspar and found that the reaction rate of crushed feldspar decreased toward zero as grain size decreased. The rates of crushed feldspar and naturally weathered feldspar were approximately equal around 50-100 µm. Below this range, naturally weathered feldspar reacted faster, opposite to crushed feldspar. The explanation for this was that natural weathering exposed preferential cleavage planes with a higher density of reaction sites, whereas crushing exposed planes with proportionally less reaction sites per m^2 of surface area. However, ongoing natural weathering leads to the evolution of surfaces that are non-reactive, unless new surfaces are exposed.

A surface roughness factor (8) of mineral grains can be defined as the ratio of the "actual" area to the geometric surface area. These factors can be determined from SEM or BET measurements. Anbeek (1992a, 1992b, and 1993) reported that, for SEM at 10,000x magnification, the 8 factors for fresh and natural feldspar surfaces were 2.1 and 2.8, respectively. For BET, the 8 factors were 4.8 and 34, respectively. These values suggested that natural weathering creates a proportionally larger surface areas than crushing. Also, this complicates laboratory measurements of reaction rates due the existence of fresh and natural surfaces after crushing. Anbeek reported that, upon grinding natural feldspar with 600-850 µm diameter, 10% of total surface was fresh when crushed to 300-425 µm and 85% was fresh when crushed to less than 53 µm.

Possible explanations given for the preceding higher 8 factors from BET vs. SEM were macropores (>50 nm diameter), micropores (<2 nm diameter), and other surface details detected by BET and not apparent to SEM. The relationship between the roughness factor of crushed material greater than 53 µm diameter was: $8 = 0.0477d + 4.8$ ($r^2=0.99$) where d is the average equivalent spherical grain diameter in µm.

Anbeek (1992a, 1992b, 1993) also measured dissolution rates of feldspar at various grain sizes in flow-through cells similar to laboratory kinetic tests (Section 5.3), in order to minimize retention of secondary minerals (Section 5.2.4). At pH 3, the tests generally stabilized within 10-20 weeks. At pH 5, there may have been formation and retention of secondary minerals, especially for aluminum ($Al(OH)_3$ sub-region, Section 4.5). Dissolution rates at pH 3 for crushed samples based on sodium, potassium, and calcium ranged from roughly 5x10^{-17} mol cm^{-2} s^{-1} at a grain diameter of 69 µm to 10-20x10^{-17} mol cm^{-2} s^{-1} at 346 µm. Notably, rates based on silicon were roughly ten times higher. At 612 µm diameter, rates for the freshly crushed material were approximately ten times higher than for naturally weathered material.

5.2.6 NAG Test

Miller et al. (1994 and 1997) and Miller (1996) attempted to identify (1) amounts and balances of reactive sulfur and NP and (2) reaction rates of acid generation and neutralization with one "standalone" test, known as the Net Acid Generation (NAG) Test. This NAG test has also been suggested as a method for determining metal-leaching rates and site-specific criteria of safe xNPR. During the monitored or "kinetic" NAG test, excess hydrogen peroxide and water are added to small amounts of sample, and pH and temperature are monitored for several hours. For the unmonitored or "static" version, pH is simply measured at the end of the test. The hydrogen peroxide vastly accelerates the oxidation of sulfides, sometimes raising water temperatures to near boiling. Additionally, the water and sample are then boiled for approximately two hours, which likely alters sample mineralogy (Section 5.2.2), in order to destroy any remaining hydrogen peroxide before pH and other parameters are measured.

There have been comparisons of NAG results with ABA analyses, but differences and contradictions remain unresolved with the NAG results assumed correct and ABA results assumed incorrect. Comparisons of NAG results with column tests (Miller, 1996; Miller et al., 1997; see also Section 5.3.2), with occasional rinsing and probably some secondary-mineral retention, have shown correlations with lag time to net acidity (Figure 5.2.6-1). However, no other correlations with columns were noted, including NAG temperature which reportedly reflects reaction rates. As a result, the justification that the NAG test provides reasonable estimates of ambient kinetic reaction rates is not presented or obvious.

Because of the vastly accelerated reaction rates and boiling of water and sample for hours, the NAG test likely cannot provide information on ambient rates of metal leaching, acid generation, and acid neutralization. These rates are obtained from true kinetic tests (Section 5.3.1). In fact, data in Miller et al. (1997) show that the NAG test (1) underestimates acid generation in samples with sulfur levels above 3%S, (2) only declares samples with a final NAG pH below 4.0 as "potentially": acid forming, and (3) carries a 5-15% error rate in results. As a result, the NAG test is not acceptable for standalone predictions of drainage chemistry. Additionally, due to the highly accelerated rates of acid generation, NP may not react the same as under ambient conditions and thus predictions of pH and safe xNPR values may not be possible.

In reality, there is no one "standalone" static or kinetic test, like NAG, that can provide valid answers to most predictive questions. The proper and most reliable approach is to use a suite of static and kinetic tests and then to cross-check all results for inconsistencies. Any discrepancies must then be resolved through additional testwork.

The belief that there is one standalone test that can provide most of the required information for prediction is outdated. In fact, problems will arise at minesites that have used the NAG test exclusively. For example, the tolerance for misclassification of net-acid-generating rock during mining, which is then erroneously sent to a net-acid-neutralizing dump, requires detailed knowledge of excess NP in the dump. However, the NAG test does not provide this information. As a result, a net-acid-neutralizing dump may begin releasing acidic drainage.

The primary value of the NAG test is determining the percentage of sulfide that can react under very aggressive oxidizing and boiling conditions. This is in fact the original intent of the hydrogen peroxide method presented by Sobek et al. (1978), which requires the initial removal of NP for proper results. The unoxidized portion of sulfur after this testing can be considered Unavailable Sulfide, similar to the concept of Unavailable NP (Section 5.2.1.3).

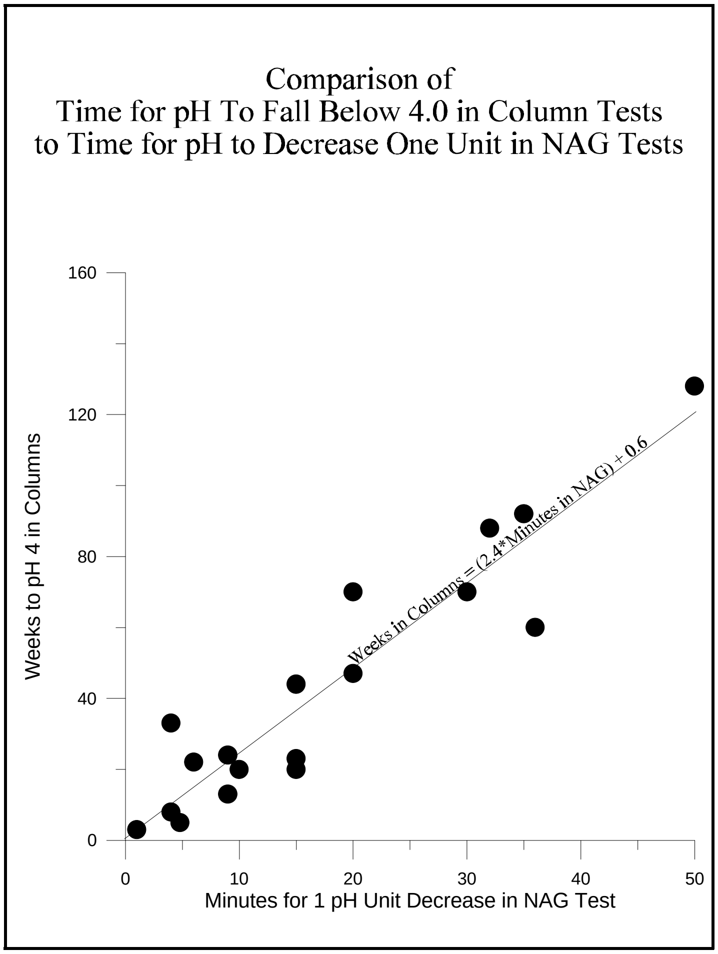

FIGURE 5.2.6-1. Comparison of Times to Acidification in Columns to Times for pH Depression in NAG Tests (adapted from Miller, 1996).

5.3 Laboratory-Based Kinetic Tests

As explained in Section 5.2, static tests characterize tailings and rock at one point in time. Assumptions are then made to extrapolate the one-time results into the future. Among the most important assumptions are that acid-generating and neutralizing minerals are reactive and have equivalent reaction rates. However, studies have shown that this is not necessarily the case.

To obtain reaction rates and depletion times for minerals, kinetic tests are conducted on selected samples, involving repetitive analysis over an extended period. In laboratory kinetic tests, relatively small samples are monitored under controlled conditions, whereas field kinetic tests (Section 5.4) monitor relatively large samples, up to full-scale minesite components, under less controlled conditions. Both types of tests, in addition to static tests, are needed to assess and predict drainage chemistry properly.

5.3.1 Humidity Cells

For approximately 30 years, the laboratory kinetic test of choice is a humidity cell, with more primitive cells used more than 30 years ago. The standardization of the technique and thus the formal creation of humidity cells is attributed to Caruccio (1967) by Sobek et al. (1978). This relatively long existence, with comparisons and calibrations to pre-test static tests and on-site monitoring, lends validity to the use of humidity cells.

The design and operation of a humidity cell are relatively simple, as explained by Sobek et al. (1978), originally involving 200 g of sample spread thinly in the bottom of a well-aerated plastic box and rinsed thoroughly each week. Since then, there have been some refinements, like improved air flow and suspension of samples on perforated plates, but the basic characteristics are the same. Interestingly, there have apparently been extreme variations on the design. In Australia, some humidity cells reportedly involve completely sealed chambers where the consumption of oxygen is monitored. This was never the original intent of humidity cells, but for clarity the traditional humidity cell is referred to here as a Sobek (or EPA 600) humidity cell (Appendix C).

In the United States of America, a standard for humidity cells has been proposed by the Association for Standardized Testing of Materials (ASTM, 1994). However, this procedure (1) does not adhere to the objectives of the Sobek procedure (e.g., water is added as trickle leaching like a column, Section 5.3.2), (2) contains improper instructions (e.g., drying at temperatures above 40°C), and (3) is conceptually flawed (e.g., weekly data are estimated from occasional analyses and then analytical data quality is defined by the interpolated mass balance over the entire testing period). Consequently, this standard is not recommended and cannot draw on the established validity of the Sobek cell.

The primary refinements in cell design and operation in use today from that of Sobek et al. (1978) are:

Ø a larger sample is used (1 kg instead of 200 g),
Ù a larger volume of weekly rinse water is used (500 mL instead of 200 mL),
Ú due to the larger sample which results in a vertical thickness, gentle stirring of fine-grained samples is used to ensure all particle surfaces are exposed to the rinse water, and
Û the sample is suspended on a perforated plate so that air can more easily flow around and through the sample, although this is irrelevant for fine-grained samples remaining near saturation throughout a weekly cycle.

The fundamental purpose of humidity cells is to obtain reaction rates of the primary (or original) minerals in a sample (Rate1, Figure 4.2.2-1). Reaction rates are obtained from the weekly rinses using the formula:

$$\text{Rate (mg/kg/wk)} = \{[\text{Concentration (mg/L)}*\text{Rinse Volume (L)}]/[\text{Sample Wt. (kg)} * \text{Rinsing Interval (wk)}]\} \qquad (5.3.1\text{-}1)$$

Any soluble secondary minerals initially present in a sample are often rinsed away within a few weeks. Thus the early data from a cell represent an alternative to the surface-retention static test (Section 5.2.4) and should not be used for calculations of rates.

There are four major misconceptions about humidity cells in the literature. First, some authors consider the aqueous concentrations in the weekly rinse water as direct predictions of on-site drainage chemistry (Rate2, Figure 4.2.2-1). That is incorrect, because excess rinse water is used to remove thoroughly and to dilute the reaction products so that solubilities of most secondary minerals are not attained. In most minesite components, not all particle surfaces are rinsed regularly and the solubilities of secondary minerals are often attained. Instead, cells provide reaction rates of the primary minerals in the sample, whereas predictions of Rate2 use techniques discussed in Sections 5.4.3 and 4.2).

The second misconception about cells is that some authors believe that reaction rates from cells are accelerated over those in the field. That is often incorrect. For example, field rates in self-heating minesite components can be even higher than those measured at room temperature. The field "rates" that some authors often report are actually chemical loadings (Section 4.2.6) in water draining from the component (e.g., Bennett et al., 1994; Strömberg and Banwart, 1995). Because the loadings are often limited by secondary-mineral precipitation, these loadings (at any temperature) will be less than the rates from cells. In all known cases of comparisons, the field drainage loadings are consistently less than the cell rates, providing a large-scale estimate of reaction-product retention (Section 5.2.4 and 5.3) rather than demonstrating that cell rates are accelerated.

The third major misconception is that cells must be inoculated with *Thiobacillus ferrooxidans* so that bacterially mediated reactions take place. This is unnecessary after several weeks of air flow (Section 4.2.4), because action must be taken only if bacteria are not wanted, as health sciences have shown. If environmental conditions in a cell are appropriate, many species of bacteria will flourish, requiring only an initial acclimatization period of a few weeks (Bhatti et al., 1994). For example, although *T. ferrooxidans* is said to reach optimum activity around 30^{o}C, slow-growing *Thiobacillus* have been reported at the Nanisivik Mine in northern Canada that had apparently acclimatized to cold temperatures. They would generally not reproduce at a warmer temperature of 12^{o}C (Kalin, 1987). In humidity cells where *T. ferrooxidans* has been added, there is either no change in reaction rates, or rates temporarily increase and then return to normal presumably as the in situ population is re-equilibrated (e.g., Figure 4.2.4-1). In any case, some tests for bacteria in cells do not always reveal their presence due to very high detection limits, roughly 10^5 to 10^6 cells a gram. Furthermore, comparisons of sterile and non-sterile oxidation rates for pyrite and pyrrhotite at acidic and neutral pH show that bacterial activity apparently contributed little (Nicholson, 1994; Ziemkiewicz and Lovett, 1994; Van Stempvoort and Krouse, 1994; Kwong et al., 1995). For these reasons, inoculations, explicit examinations, and predictions of bacterial activity are usually unimportant for predicting drainage chemistry.

The fourth misconception is that cells contain relatively fine material (< 6 mm, Appendix C) which may not be representative of some minesite components like coarse-rock dumps. For example, Murray (1977) pointed out that the fines content (< 2 mm) at several precious and base-metal minesites was 0-35% with an average of 15-25%. Based on a simple distribution using two discrete grain sizes (200 and 3.2 mm), a fines content of 10-20% by weight will comprise 87-94% of the reactive particle surface area (Table 5.3.1-1). As a result, the chemical contribution of the coarser particles can often be ignored with little error. Nevertheless, for improved predictive accuracy, kinetic rates (Equation 5.3.1-1) should only be applied to the weight of the finer fraction of a component, which is replenished through time by weathering of the coarser fraction. Walls of pits and underground workings are handled differently (Section 5.4.2).

Examples of results from humidity cells are shown in Figures 5.3.1-1 to 5.3.1-8. The first two figures show temporal trends in sulfate production (representing total acidity generation), acid neutralization (NP consumption), and metal leaching as near-neutral pH remains relatively constant. The next two show trends in cells that turned acidic during the testwork. Figures 5.3.1-5 and -6 show cells that were consistently acidic from the start and Figures 5.3.1-7 and -8 show consistently alkaline cells.

Before a cell is started, the sample should be submitted for static-test analyses (Section 5.2 and Appendix B) for pre-test characterization. As a cell is operated for a few weeks, a trend of decreasing concentrations is sometimes observed as secondary minerals are rinsed out (Figure 5.3.1-1 to 5.3.1-8). Eventually the concentrations reach a general steady state, often requiring 10 to 100 weeks. Meanwhile, short-term peaks in reaction rates may arise, particularly between Weeks 5 and 20, possibly attributable to biological acclimation since physical and chemical conditions are reportedly constant. Also, if pH changes significantly during the test period such as the onset of net acidity, reaction rates may also change sharply and the test should continue until steady state under the new conditions is attained (e.g., Figure 5.3.1-5).

TABLE 5.3.1-1
Effect of Grain Size on Reactive Surface Area
(from Morin and Hutt, 1994a)

Coarse Fraction (200 mm diameter)		Fine Fraction (3.2 mm diameter)		Particle Surface Area	
% Total Weight	Particle Surface Area (m^2)	% Total Weight	Particle Surface Area (m^2)	Total (m^2)	% from Fine Fraction
0	0	100	1040	1040	100
20	3.32	80	832	835	99.6
40	6.64	60	624	631	98.95
60	9.96	40	416	426	97.66
70	11.6	30	312	324	96.42
80	13.3	20	208	221	93.99
90	14.9	10	104	119	87.5
95	15.8	5	52	67.8	76.7
100	16.6	0	0	16.6	0

The point at which a cell reaches steady state and can be terminated is arbitrary. Rarely do the late week-to-week rates remain identical and they can in fact vary by a factor of two or more. Therefore, steady state is arbitrarily defined as the point at which at least the last five weeks fluctuate within a definable and constant range. The average rates over the last five weeks can then be taken as the steady-state values of Rate1 (Figure 4.2.2-1).

The steady-state rates can then be used for predictions of drainage chemistry and depletion times for various acid-generating, acid-neutralizing, alkaline-generating, and metal-leaching minerals (Sections 4.2 and 5.5). Cells can be, and have been, continued for years if wanted to confirm the steady-state rates or to await predicted changes such as the onset of net acidity. Long-term cells show that steady-state rates should persist within a factor of two for at least five years.

Case Study 5.3.1-1: Small-Scale Kinetic Testing highlights: kinetic testing up to 151 weeks; prediction of net acidity based on CaNP consumption; some factors accounting for rate fluctuations through time and among samples

In a laboratory case study of reaction rates and predictive chemistry, Lapakko and Wessels (1995) subjected ten samples of gold-mine tailings to 57-151 weeks of kinetic testing. The ten samples were tested in duplicate, involving the weekly rinsing of 75-g samples with 200 mL of deionized/distilled water. In contrast to Sobek humidity cells (Appendix C), (1) the experimental apparatus resembled a small column, (2) no air was pumped across the samples, (3) water was added slowly to avoid disturbance of the samples, and (4) relative humidity was maintained at an average of 54%. The samples were composed predominantly of quartz and carbonate minerals. Based on acid-base accounting, sulfide, CaNP, and SNPR levels in the ten samples were 0.30-7.87%S, 14-229 ppt $CaCO_3$, and 0.09-24, respectively.

a) waste rock; NP rate about equal to sulfate rate (1:1); rates generally stable to Week 30, then significant increase then decrease; acidic pH predicted after effective NP depleted

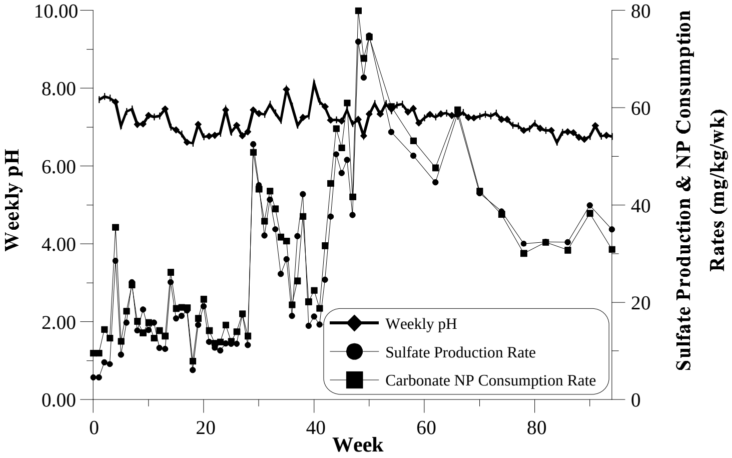

Pre-Test Data:
Paste pH = 8.16 % S (Sulfide) = 1.05 NP (tonnes CaCO3 / 1000 tonnes) = 16

Remaining After Week 94:
% S (Sulfide) = 0.94 NP (tonnes CaCO3 / 1000 tonnes) = 13

b) waste rock; NP rate about 50% higher than sulfate rate over 210 weeks (1.5:1); unlike a) above, rates generally stable after Week 30 with gradual factor-of-two rise and fall around Week 130; abundant sulfide and NP remaining after 210 weeks; acidic pH predicted after effective NP exhausted

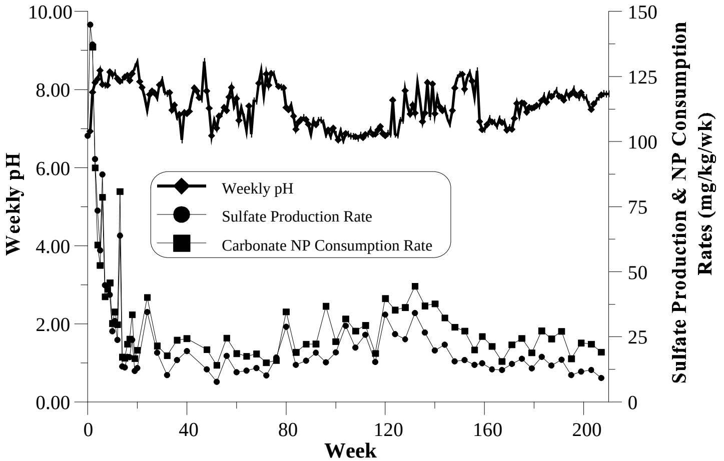

Pre-Test Data:
Paste pH = 8.37 % S (Sulfide) = 4.89 NP (tonnes CaCO3 / 1000 tonnes) = 74

Remaining After Week 210:
% S (Sulfide) = 4.73 NP (tonnes CaCO3 / 1000 tonnes) = 68

c) waste rock; NP rate about 10x higher than sulfate rate after Week 10; rates generally stable after Week 20; no acidic pH because sulfide depleted before NP even at higher NP consumption ratio (10:1)

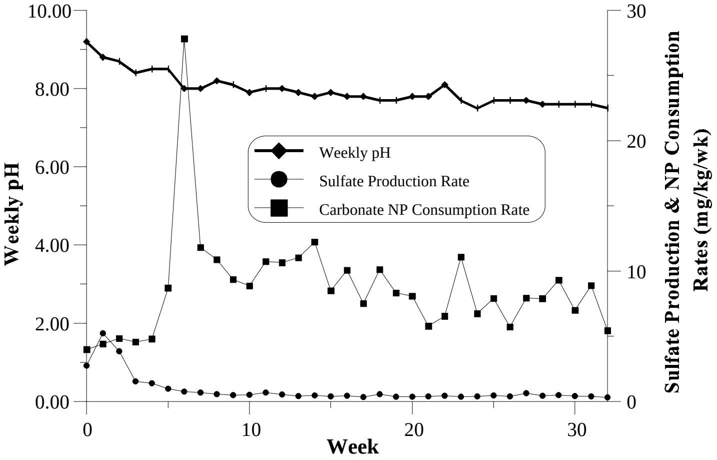

Pre-Test Data:
Paste pH = 9.8 % S (Sulfide) = 0.02 NP (tonnes CaCO3 / 1000 tonnes) = 16

Remaining After Week 32:
% S (Sulfide) = 0.02 NP (tonnes CaCO3 / 1000 tonnes) = 16

FIGURE 5.3.1-1. Examples of Aqueous pH and Rates of Sulfate Production and Acid Neutralization in Humidity Cells Remaining Near Neutral pH.

a) mostly near neutral pH after initial alkaline pH; to Week 35, copper and zinc rates close to detection limit with occasional high peaks; after Week 35, rates variable within defineable ranges

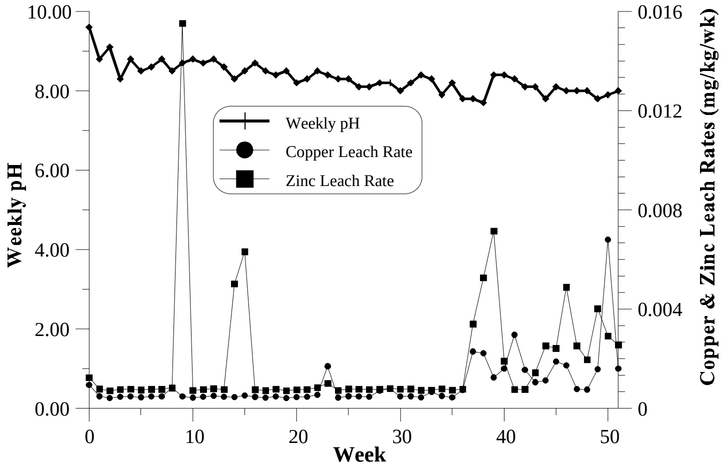

Pre-Test Data:
Paste pH = 9.07 Copper (ppm) = 15 Zinc (ppm) = 52

Remaining After Week 51:
Copper (ppm) = 15 Zinc (ppm) = 52

Post-Test Data:
Paste pH: 8.40 Copper (ppm) = 0.5 Zinc (ppm) = 34

b) consistently near neutral pH; fluctuating copper and zinc rates within defineable ranges throughout test (note log scale for rates)

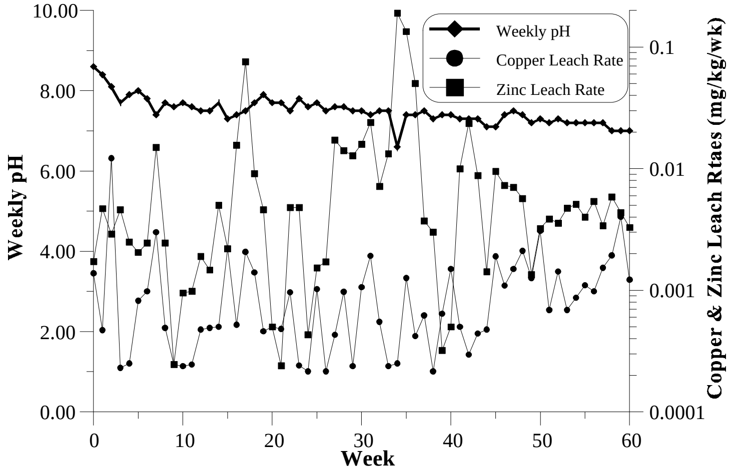

Pre-Test Data:
Paste pH = 9.30 Copper (ppm) = 76 Zinc (ppm) = 86

Remaining After Week 60:
Copper (ppm) = 76 Zinc (ppm) = 85

c) consistently near-neutral pH; fluctuating copper and zinc rates generally within steady ranges throughout test except for peaks in early weeks suggesting rinsing of accumulated secondary minerals

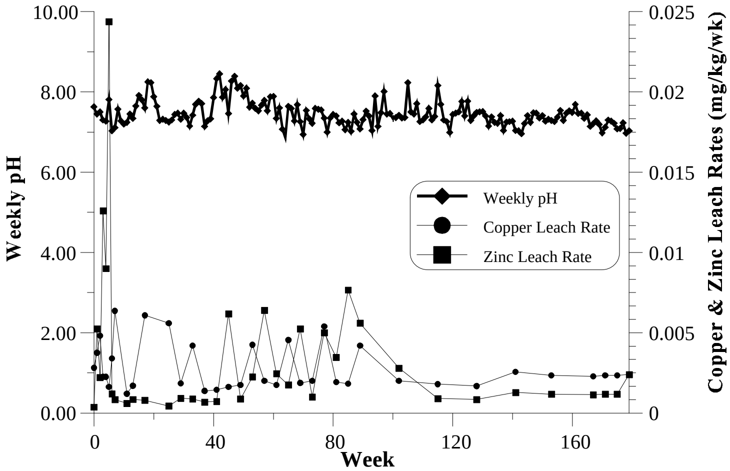

Pre-Test Data:
Paste pH = 7.87 Copper (ppm) = 768 Zinc (ppm) = 159

Remaining After Week 179:
Copper (ppm) = 768 Zinc (ppm) = 159

FIGURE 5.3.1-2. Examples of Leaching Rates of Copper and Zinc in Humidity Cells Remaining Near Neutral pH.

a) waste rock; sulfate and NP rates approximately equal until instability at Weeks 25-35; acidic conditions after Week 24; accelerated sulfate rate below pH 5; NP rate relatively constant around 15-25 mg/kg/wk except during instability; unavailable NP ~ 8 t/1000 t; acceleration factor for sulfate betwen start and end ~ 6x

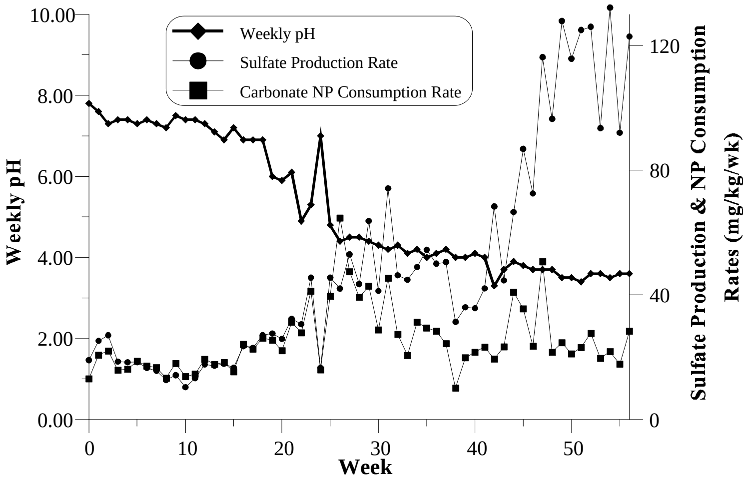

Pre-Test Data:
Paste pH = 8.40 % S (Sulfide) = 0.43 NP (tonnes CaCO3 / 1000 tonnes) = 9

Remaining After Week 56:
% S (Sulfide) = 0.34 NP (tonnes CaCO3 / 1000 tonnes) = 8

b) tailings; pH initially acidic, then near neutral, then acidic around Week 135; sulfate and NP rates erratic, but within defineable ranges; sulfate rate accelerated below pH 5; lateNP rate steady despite onset of acidification; unavailable NP uncertain due to discrepancy between calculated remaining and post-test value, possibly attributable to erroneous pre-test analysis, erroneous weekly analyses, and/or neutralization by non-carbonate minerals; acceleration factor for sulfate betwen start and end ~1.2x

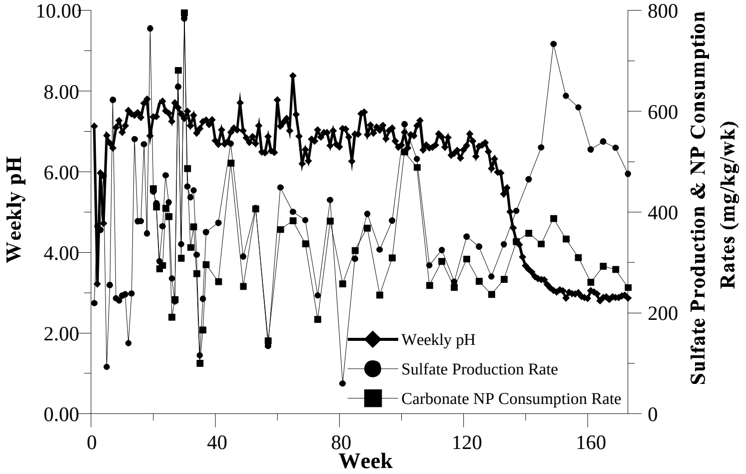

Pre-Test Data:
Paste pH = 6.62 % S (Sulfide) = 12.20 NP (tonnes CaCO3 / 1000 tonnes) = 88
Remaining After Week 173:
% S (Sulfide) = 9.96 NP (tonnes CaCO3 / 1000 tonnes) = 26
Post-Test Data:
% S (Sulfide) = 9.68 NP (Tonnes CaCO3 / 1000 tonnes) = 2

c) granite; %S very low around 0.1; NP rate less than sulfate rate during test; acidic conditions after Week 15-20; accelerated sulfate rate below pH 5; NP rate at lower rate around 10-15 mg/kg/wk after Week 20, suggesting exhaustion of more soluble mineral; unavailable NP ~ 8 t/1000 t; acceleration factor for sulfate betwen start and end ~1.5x

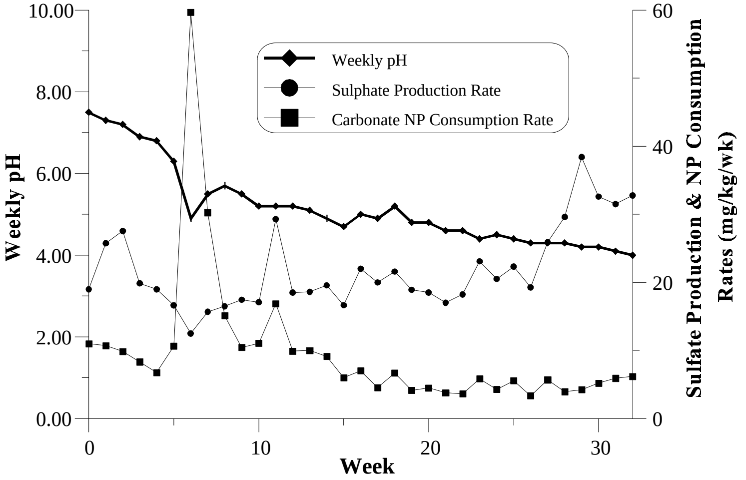

Pre-Test Data:
Paste pH = 9.5 % S (Sulphide) = 0.13 NP (tonnes CaCO3 / 1000 tonnes) = 8

Remaining After Week 32:
% S (Sulphide) = 0.11 NP (tonnes CaCO3 / 1000 tonnes) = 7.7

FIGURE 5.3.1-3. Examples of Aqueous pH and Rates of Sulfate Production and Acid Neutralization in Humidity Cells Becoming Acidic.

a) copper and zinc rates increasing after Week 135 after pH<6; copper and zinc decreasing at end; rates accelerated ~300-1000x between start and end

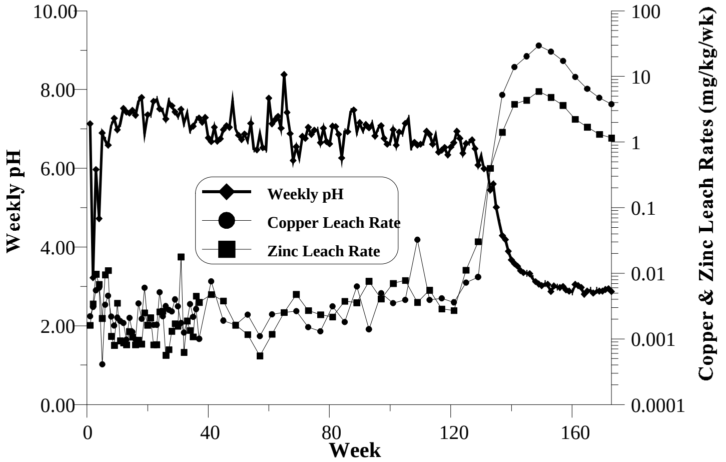

Pre-Test Data:
Paste pH = 6.62 Copper (ppm) = 1282 Zinc (ppm) = 336

Remaining After Week 173:
Copper (ppm) = 746 Zinc (ppm) = 214

Post-Test Data:
Paste pH = 3.03 Copper (ppm) = 700 Zinc (ppm) = 188

b) copper and zinc rates increasing after Week 5 when pH<6; zinc generally stableafter Week 25; copper gradually increasing through test; late-term rates accelerated ~100x over start

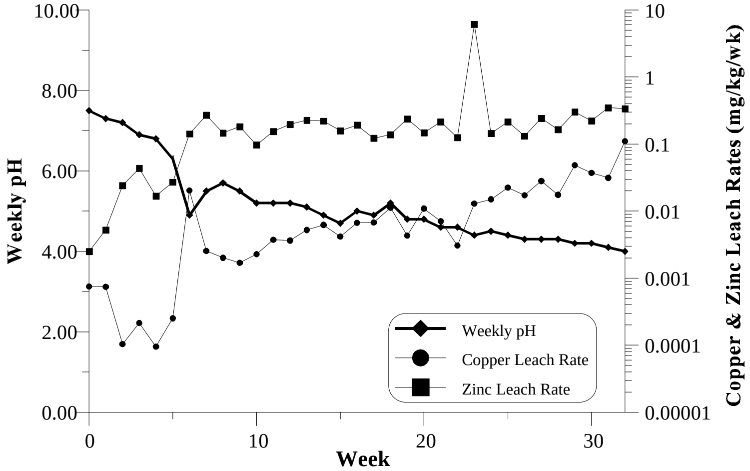

Pre-Test Data:
Paste pH = 9.50 Copper (ppm) = 57 Zinc (ppm) = 96

Remaining After Week 32:
Copper (ppm) = 57 Zinc (ppm) = 85

c) zinc rates increasing after Week 13 when pH<6; zinc generally stable but gradually declining after Week 35; copper rates increasing after Week 25 when pH<5; copper rate stable after Week 50; rates accelerated ~500x between start and end

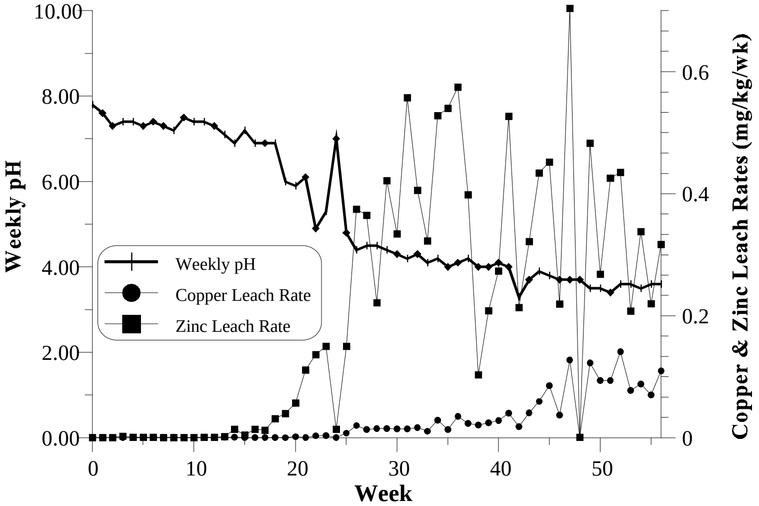

Pre-Test Data:
Paste pH = 8.40 Copper (ppm) = 35 Zinc (ppm) = 90

Remaining After Week 56:
Copper (ppm) = 33 Zinc (ppm) = 78

FIGURE 5.3.1-4. Examples of Leaching Rates of Copper and Zinc in Humidity Cells Becoming Acidic.

a) fine-grained waste rock; NP non-existent from start; NP rate always less than sulfate rate during test, with NP rate falling to 2 mg/kg/wk and sulfate to 30 mg/kg/wk by Week 52 (note log scale for NP and sulfate); pH gradually rises above 3 during test

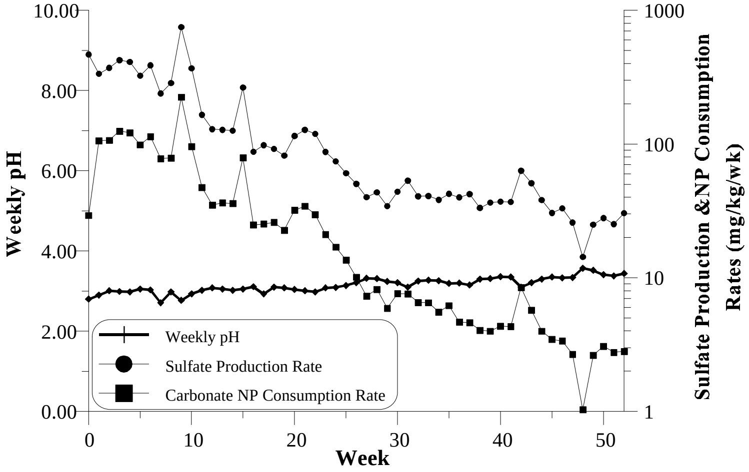

Pre-Test Data:
Paste pH = 3.64 % S (Sulfide) = 1.12 NP (tonnes CaCO3 / 1000 tonnes) = -2

Remaining After Week 52:
% S (Sulfide) = 0.88 NP (tonnes CaCO3 / 1000 tonnes) = 0

b) waste rock; NP non-existent from start; NP rate always less than sulfate rate during test; unlike a) above, sulfate rate increasing and pH decreasing during test; sulfate rate stable around 1000 mg/kg/wk towards end of test

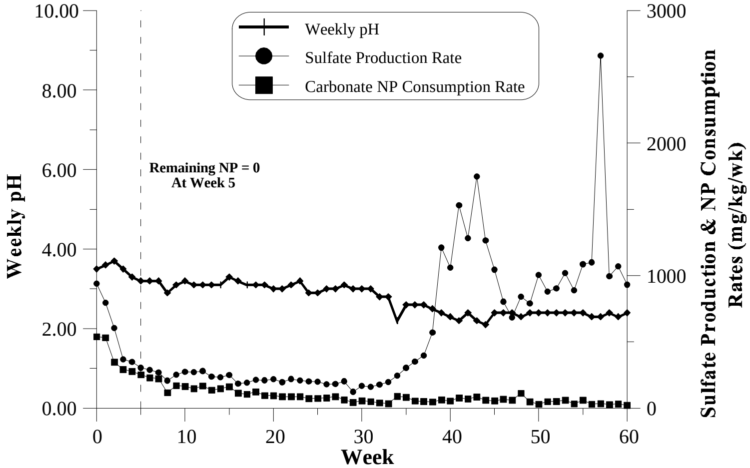

Pre-Test Data:
Paste pH = 5.1 % S (Sulfide) = 19.22 NP (tonnes CaCO3 / 1000 tonnes) = 2

Remaining After Week 60:
% S (Sulfide) = 18.02 NP (tonnes CaCO3 / 1000 tonnes) = 0

c) waste rock; NP non-existent from start; %S very low at 0.08; NP rate always less than sulfate rate during test; sharp decrease in NP and sulfate rates with no effect on pH (note log scale for rates); NP and sulfate rates stabilize quickly around 0.1 and 2 mg/kg/wk, respectively; pH between 4 and 5

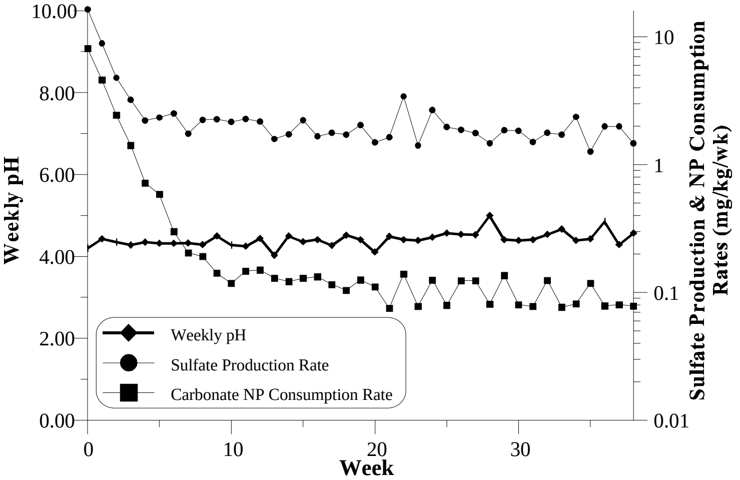

Pre-Test Data:
Paste pH = 5.36 % S (Sulfide) = 0.08 NP (tonnes CaCO3 / 1000 tonnes) = 1
% S (BaSO4) = 0.02

Remaining After Week 38:
% S (Sulfide) = 0.08 NP (tonnes CaCO3 / 1000 tonnes) = 1

FIGURE 5.3.1-5. Examples of Aqueous pH and Rates of Sulfate Production and Acid Neutralization in Humidity Cells Remaining Acidic.

a) consistently acidic; zinc rates often in relatively stable range with gradual decrease through time; copper rates gradually increase through Week 20, then steady

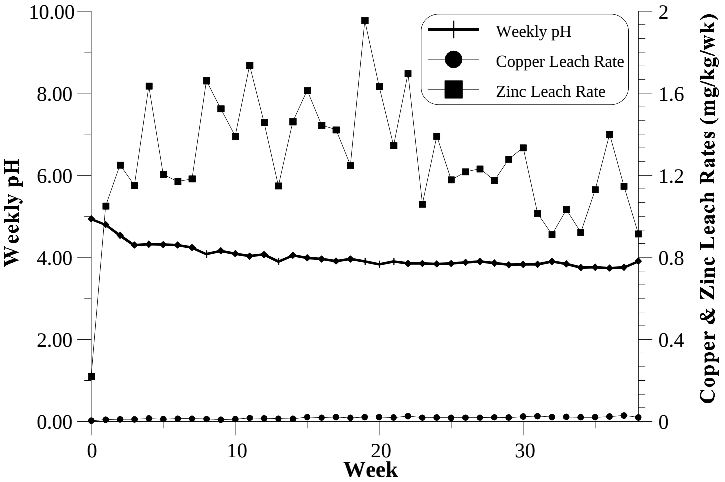

Pre-Test Data:
Paste pH = 6.38 Copper (ppm) = 42 Zinc (ppm) = 187

Remaining After Week 38:
Copper (ppm) = 41 Zinc (ppm) =137

---

b) consistently acidic; falling copper and zinc rates throughout test; zinc often below detection limit beyond Week 20; very low initial zinc at 2 ppm

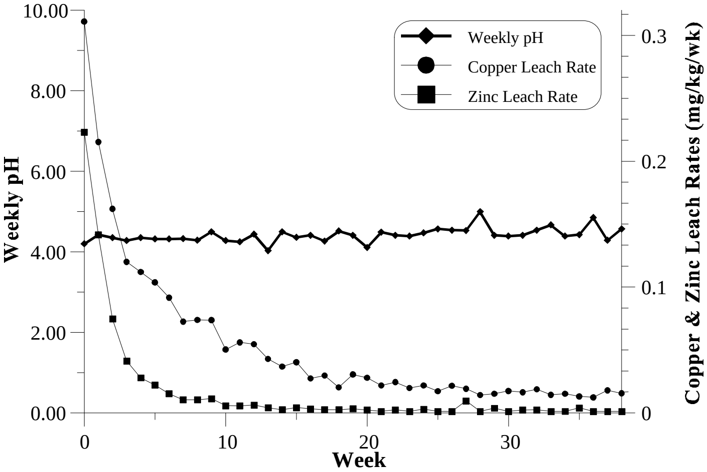

Pre-Test Data:
Paste pH = 5.36 Copper (ppm) = 27 Zinc (ppm) = 2

Remaining After Week 38:
Copper (ppm) = 25 Zinc (ppm) = 1

---

c) consistently acidic; peak copper and zinc rates around Week 40; rates generally steady after Week 50

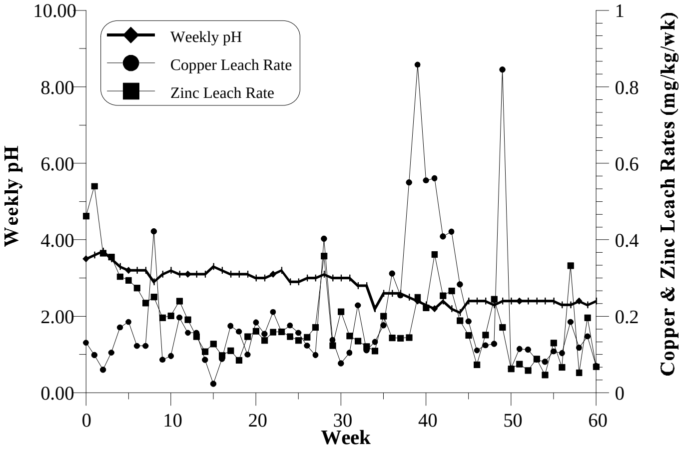

Pre-Test Data:
Paste pH = 5.10 Copper (ppm) = 66 Zinc (ppm) = 62

Remaining After Week 60:
Copper (ppm) = 54 Zinc (ppm) = 51

FIGURE 5.3.1-6. Examples of Leaching of Copper and Zinc in Humidity Cells Remaining Acidic.

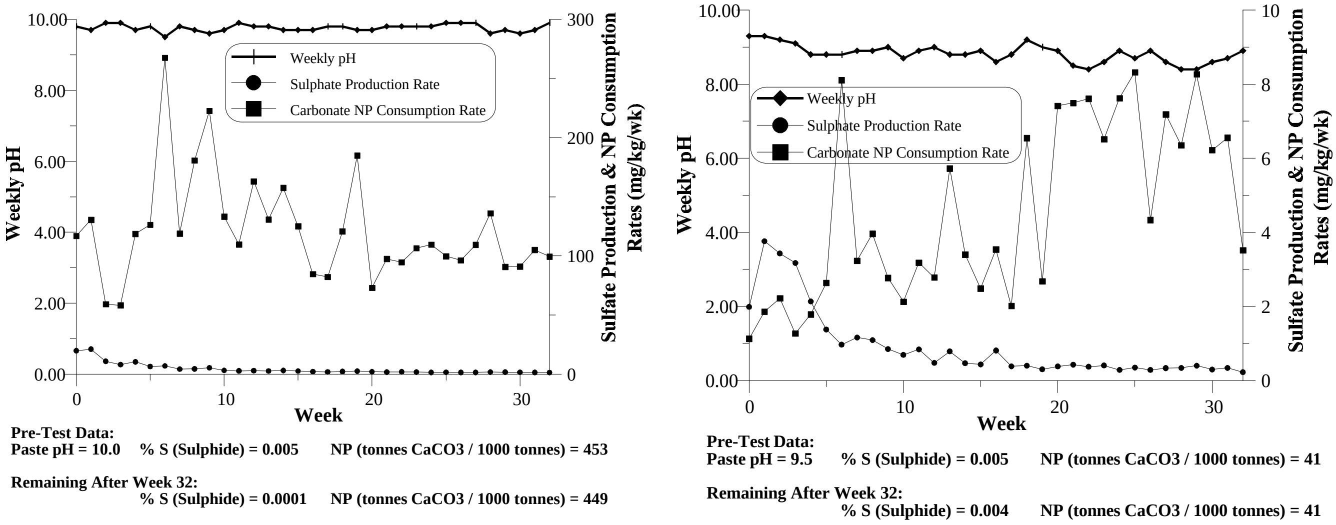

Pre-Test Data:
Paste pH = 10.0 % S (Sulphide) = 0.005 NP (tonnes CaCO3 / 1000 tonnes) = 453

Remaining After Week 32:
% S (Sulphide) = 0.0001 NP (tonnes CaCO3 / 1000 tonnes) = 449

Pre-Test Data:
Paste pH = 9.5 % S (Sulphide) = 0.005 NP (tonnes CaCO3 / 1000 tonnes) = 41

Remaining After Week 32:
% S (Sulphide) = 0.004 NP (tonnes CaCO3 / 1000 tonnes) = 41

a) waste rock; alkaline drainage throughout test; pre-test NP of 453 t/1000 t with negligible sulfide; NP rate about 100x higher than sulfate rate; NP rate stable after Week 20 around 100 mg/kg/wk; prediction of 86 years until NP depletion

b) waste rock; marginal alkaline drainage throughout test; unlike a), pre-test NP of only 41 t/1000 t and NP rate only about 10x higher than sulfate rate; NP rate relatively stable after Week 20 around 6-8 mg/kg/wk; prediction of 130 years until NP depletion

FIGURE 5.3.1-7. Examples of Aqueous pH and Rates of Sulfate Production and Acid Neutralization in Humidity Cells Remaining Alkaline.

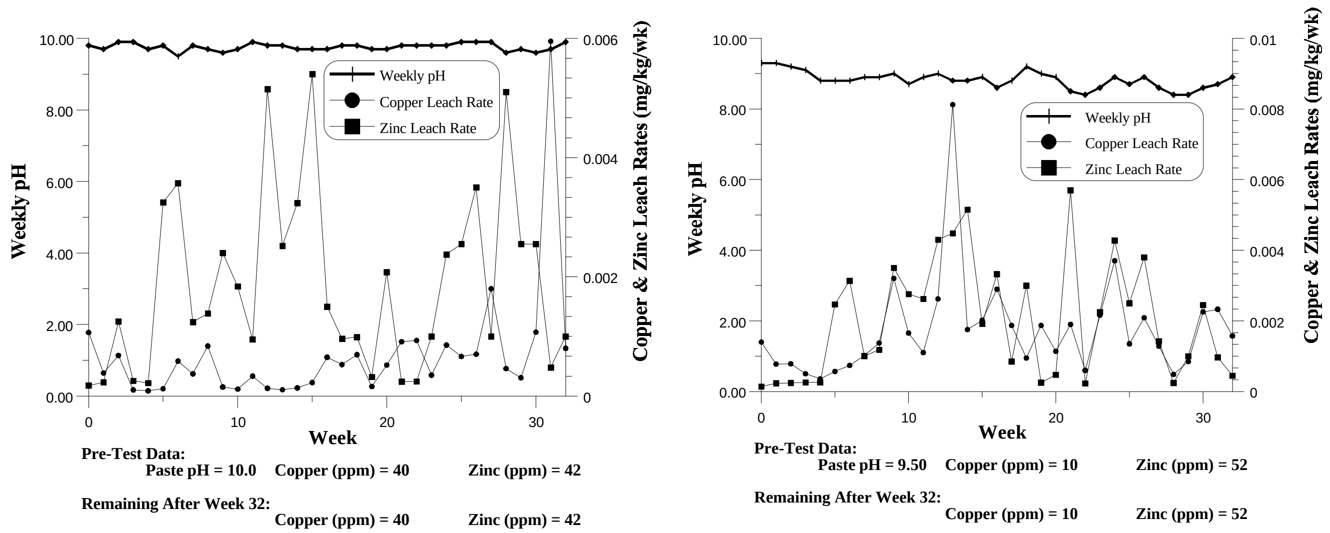

Pre-Test Data:
Paste pH = 10.0 Copper (ppm) = 40 Zinc (ppm) = 42

Remaining After Week 32:
Copper (ppm) = 40 Zinc (ppm) = 42

Pre-Test Data:
Paste pH = 9.50 Copper (ppm) = 10 Zinc (ppm) = 52

Remaining After Week 32:
Copper (ppm) = 10 Zinc (ppm) = 52

a) consistently alkaline; erratic copper and zinc rates with gradual increase through time

b) generally alkaline to near neutral; erratic copper and zinc rates with peak around Week 13 then gradual decline

FIGURE 5.3.1-8. Examples of Leaching of Copper and Zinc in Humidity Cells Remaining Alkaline.

Initially rinsing of soluble primary and accumulated secondary minerals occurred over the first 10-20 weeks, and reaction rates increased in the samples between Weeks 50 and 65, apparently due to elevated humidity levels at that time. Based on extrapolation of rates into the future, several samples were expected to become acidic after several years.

Only one sample became acidic during the testing (Figure 5.3.1-9). The time to net acidity in this sample corresponded to 100% consumption of its CaNP and was predictable, within an error of ten weeks, based on straight-line extrapolation of CaNP consumption from Weeks 20 to 30. The onset of net acidity was preceded by 30 weeks of elevated sulfate concentrations (see also Case Study 4.4-9 and Figure 5.3.1-3), indicating an acceleration in the rate of acid generation.

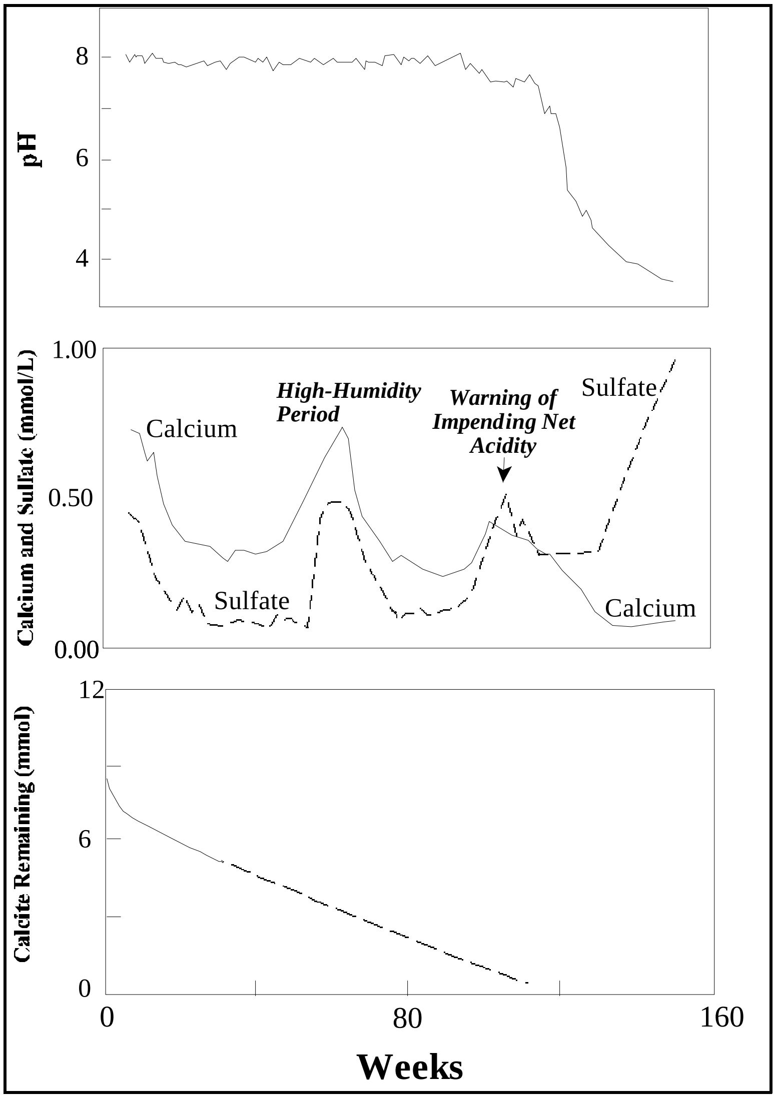

FIGURE 5.3.1-9. Trends in Drainage Chemistry and Remaining Calcite from Small-Scale Kinetic Tests (adapted from Lapakko and Wessels, 1995).

A scatterplot of original sulfide content and the average sulfate production rate over the initial 57 weeks showed a general relationship (Figure 5.3.1-10). The straight-line correlation coefficient indicated 67% of the variation in the rates could be attributed to initial sulfide. However, the increase in rates by a factor of five during high-humidity periods (e.g., Figure 5.3.1-9) showed that the sensitivity to humidity was similar to that of initial sulfide. Furthermore, BET surface areas (Section 5.2.5) of pyrite grains from two samples with similar initial sulfide content were 300 and 1400 m^2/kg. This factor-of-five difference in BET area was consistent with the factor of six difference in their rates. As a result, Lapakko and Wessels (1995) identified three factors that could generate fluctuations of a factor of five or more in weekly reaction rates and among similar samples.

Case Study 5.3.1-2: Effects of Changing Air Flow and Rinse-Water Volume on Humidity Cells

highlights: varying conditions during kinetic testing; difficulty in identifying effects of variable conditions in unstable cells

Pool and Balderrama (1994) attempted to examine the effects of changing air flow and rinse-water volumes on the results of humidity cells while temperature was held constant. Unfortunately, various combinations of these factors were imposed over each cell during the 46-week test, when weekly results can fluctuate even under constant air flow and rinse volume (Case Study 5.3.1-1). Additionally, increased levels of rinse water did not always correspond with higher recovery of rinse water, apparently due to water retention within the samples, and airflow was changed only at Week 8 before the cells had stabilized. In any case, no significant variation with rinse volume was noted outside normal variations in humidity cells.

Case Study 5.3.1-3: Net Acid Generation in Slow Oxidizing, Non-Carbonate Tailings

highlights: static-test characterization of a sulfide-bearing tailings impoundment; discrepancy between static and kinetic tests resolved through mineralogy; safeguard criteria for monitoring of drainage chemistry

A detailed review and geochemical investigation at the closed Boss Mountain molybdenum minesite in British Columbia revealed some geochemical coincidences that would have otherwise resulted in net acid generation within the tailings (Morwijk Enterprises Ltd., 1993). The Boss Mountain deposit was discovered in 1917 and mined from 1965 to 1972 and from 1974 to 1983. For the tailings, visually strong sulfide oxidation and limited static testwork in the early 1980's (TNNP = -13 to -42 t/1000 t) pointed to eventual net acid generation. However, the tailings pond and downstream clarification pond never had a pH below 6.5. Sulfate was frequently below 100 mg/L, that is, below gypsum saturation, so there was little secondary accumulation of sulfate.

Additional, expanded ABAs collected in 1993 yielded an average TNNP value of -19 t/1000 t and an average TNPR value of 0.77. Levels of original sulfate and barite were often detectable, but did not change NNP values significantly. These ABAs also showed that most of the NP consisted of non-carbonate minerals, which was consistent with mineralogy (35% quartz, 50% feldspars, and minor hornblende, biotite, epidote, and sphene).

A composite sample was subjected to humidity-cell testing for 40 weeks. This sample had undetectable CaNP, but a bulk NP of 15 t/1000 t. The late-term, stable rate of sulfide oxidation (36 mg SO_4/kg/wk) was relatively low to moderate compared with other kinetic tests with approximately 1%S (Figure 5.3.3-1a) and the carbonate molar ratio of 1.15 was relatively low (Figure 5.2.2-1b). These results from the cell indicated a calcium-bearing non-carbonate mineral likely accounted for neutralization. Since aluminosilicate minerals do not typically respond to equilibrium conditions (Section 4.2), the ongoing net alkalinity from the tailings was the result of an acid-generation rate that was sufficiently slow to allow full neutralization. A faster acid-generation rate would have likely resulted in net acidity.

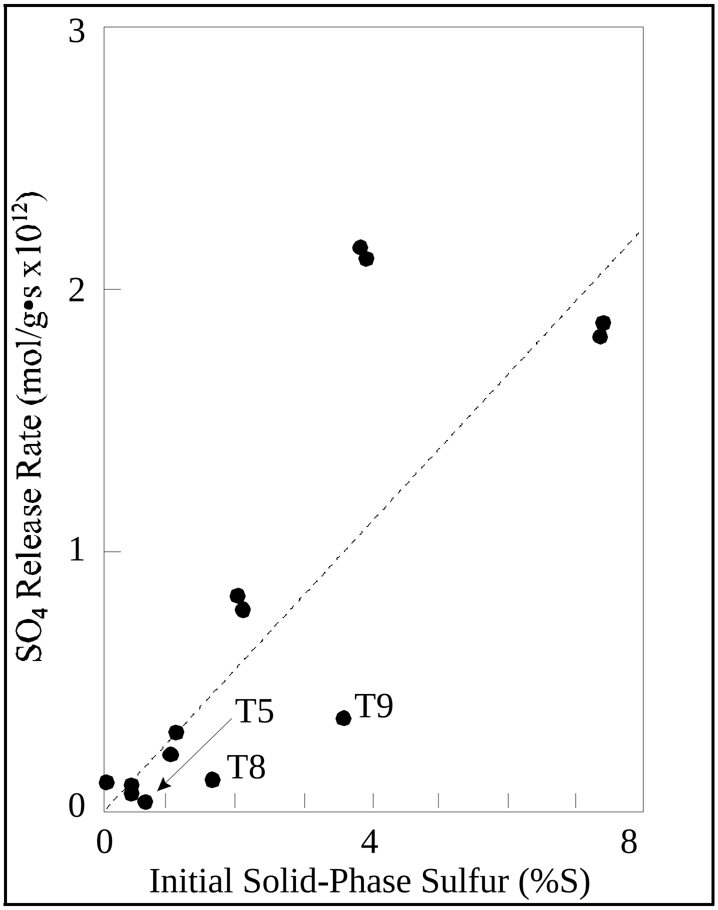

FIGURE 5.3.1-10. Sulfate Release Rate vs. Original Sulfide Content from Small-Scale Kinetic Tests (adapted from Lapakko and Wessels, 1995).

Mathematical conversion of approximately 30% of the calcium-bearing portion of the feldspar to NP yielded highly positive NNP values. The addition of this SRNP (Section 5.2.1.3) to measured NP justified the overall prediction of no net acid generation despite the low NNP values based solely on measured NP. As a safeguard, the tailings drainage is monitored periodically for sulfate which is significantly below gypsum saturation. Sharply increasing sulfate concentrations toward gypsum saturation are often an early warning of impending net acidity (e.g., Case Studies 4.4-9, 5.3.1-1, and 5.3.2-3, and Figure 5.3.1-3).

5.3.2 Columns

An alternative to humidity cells as laboratory kinetic tests are columns, sometimes called "leach columns". These columns are not standardized and reportedly hold samples ranging from 1 kg to more than 20 t.

In addition to the lack of standardization, columns may suffer from other weaknesses that render them inappropriate for predictions of drainage chemistry. Often water is added to columns as "rainfall" or trickling, in an attempt to simulate field conditions. Some column studies even purport to simulate one field year per laboratory week by accelerating all physical, chemical, and biological processes through the simple addition of more water. Also, the rinse concentrations from some columns have been taken directly as predictions of drainage chemistry from full-scale minesite components.

Often, the ratio of solid sample to weekly rinse water is often much higher than humidity cells (Section 5.3.1) so that not all particle surfaces are rinsed and the solubilities of secondary minerals are exceeded. As a result, these columns rarely provide steady-state reaction rates of primary minerals (Rate1, Figure 4.2.2-1), like humidity cells. In fact, Li and St-Arnaud (1997) used columns to examine secondary minerals accumulated on oxidized waste rock.

However, columns may not include reaction-product retention similar to that under field conditions, as provided by field kinetic tests (Section 5.4) and monitoring (Section 4.2), because laboratory conditions may not closely mimic field conditions. Thus they would not provide reliable estimates of Rate2 (Figure 4.2.2-1).

For the preceding reasons, the test conditions under which columns are operated determine the value and approach for interpretation of the resulting data. Despite this complexity, columns are popular for kinetic tests, as demonstrated by the following case studies.

Case Study 5.3.2-1: Five-Year-Duration Column Testing on Acid-Generating Waste Rock

highlights: five-year kinetic column test on 296 kg of acidic rock; ambiguity of test conditions and test results

A five-year column-leaching study was conducted on pyritic waste rock from Woodlawn Mines Pty Ltd in Australia (Jeffery et al., 1988). The PVC column was 300 cm in length with an inside diameter of 30 cm. A basal perforated plate held the sample while allowing water to drain, and a top plate minimized evaporation. The waste rock was primarily gravel sieved through a 25-mm screen and 296 kg was placed into the column, filling 233 cm of its length. The rock had a bulk density of 1.83 g/cm^3 and a porosity of 0.27. Air was periodically pumped through the space between the upper plate and the sample to maintain atmospheric oxygen.

Analysis of various grain-size intervals of the waste rock showed that all intervals were acidic when added to the column (Table 5.3.2-1). Metal contents of all intervals were mostly within 50% of the overall bulk value. Sulfide-bearing minerals were pyrite, chalcopyrite, sphalerite, and galena.

Over a period of 118 days, up to 0.5 L/d of deionized water was added as batches to the top of the column until water began draining through the basal plate. Afterwards, 50 mL/d was added for a total of 125 L over the five years, with 70% recovered through the bottom plate, 20% retained in the column, and 10% lost to evaporation. The rate of water addition was reported as equal to one pore-volume a year and reflected on-site precipitation, but it is unlikely that the water required a year to drain through 233 cm of gravel. It is not stated whether sufficient water was added to rinse thoroughly the grain surfaces like a proper kinetic test, or whether some laboratory-scale retention occurred.

Basal drainage was collected and analyzed weekly. Unfortunately, aqueous concentrations of sulfate were not provided, so that saturation with gypsum cannot be assessed. However, the authors noted that the commonly observed initial flush of soluble ions like sulfate did not occur. This suggests

TABLE 5.3.2-1
Pre-test Analysis of Grain Sizes of Woodlawn Waste Rock
(from Jeffery et al., 1988)

Parameter[1]	Grain Size (mm)				
	<0.2	0.2-0.5	0.5-2.0	2.0-25	Bulk
% of total volume	8.9	7.4	19.4	64.3	100
%S total	1.39	2.57	2.37	2.18	2.18
%S sulfate	0.71	0.66	0.48	0.25	0.37
Paste pH	3.9	5.1	4.3	4.2	4.2
%Fe	5.96	5.63	5.35	4.27	4.73
mg Cd/kg	8.5	9.2	9.6	6.8	7.6
mg Cu/kg	2070	3390	3500	2600	2790
mg Ni/kg	24	22	20	18	19
mg Pb/kg	940	930	990	500	670
mg Zn/kg	2840	3130	3070	2120	2440

[1] All metals are acid soluble, not total, and thus may represent retained metals

that rinse waters remained constantly at saturation with respect to gypsum and thus true oxidation rates cannot be determined.

The formation of secondary minerals, suspected by Jeffery et al. (1988) for copper and lead, is also suggested by elevated average annual concentrations of metals (Table 5.3.2-2, lead was apparently less than detection). However, virtually all cadmium, nickel, and zinc were leached from the column after five years, indicating little retention of those metals.

In the fourth and fifth years, poregas was removed with syringes from septum-covered ports along the column side and was analyzed for oxygen and carbon dioxide. The typical profile showed that oxygen decreased linearly toward <1.0% with depth, whereas carbon dioxide increased (Figure 5.3.2-1). Jeffrey et al. (1988) interpreted the relatively linear oxygen gradient as steady-state evidence that sulfide oxidation was controlled by oxygen diffusion. Sealing the top of the column and measuring oxygen consumption over 48 hours yielded a consumption

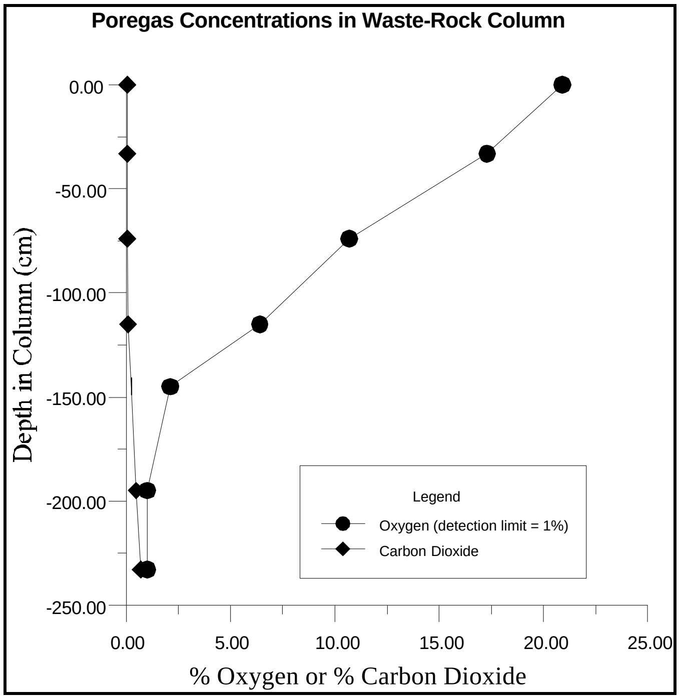

FIGURE 5.3.2-1. Poregas Composition of Woodlawn Waste Rock in Leach Column (from data in Jeffery et al., 1988).

TABLE 5.3.2-2
Metal Concentrations and Release Rates from Woodlawn Waste Rock
(from Jeffery et al., 1988)

Years	Accum Vol (L)	pH	Cd (mg/L)	Cu (mg/L)	Fe (mg/L)	Ni (mg/L)	Zn (mg/L)
0-1	17.343	3.05	88	7550	190	120	22000
1-2	31.982	2.2	91	8300	2590	130	22500
2-3	54.559	2.2	57	5700	4310	120	14000
3-4	71.323	2.27	28	3200	4160	110	6400
4-5	83.052	2.9	18	2500	2150	130	4400
			(mg/kg)	(mg/kg)	(mg/kg)	(mg/kg)	(mg/kg)
0-5	83.052	-	16	1560	786	34	3980

a consumption rate of 4×10^{-10} moles oxygen/($cm^2 \cdot s$). Based on this rate and the oxygen gradient, a diffusion coefficient in the upper 150 cm was calculated at 7.86×10^{-3} cm^2/s. This value was reportedly an order of magnitude less than the coefficient in air due to the low air-filled porosity of less than 0.09.

The trend in carbon dioxide was the inverse of oxygen (Figure 5.3.2-1), but at lower levels, and attributed to neutralization reactions. However, the ongoing lack of carbon dioxide higher in the column suggested consumption, presumably by secondary minerals or microbes.

Case Study 5.3.2-2: Comparison of ABA Data to Kinetic-Test Results

highlights: analysis of 83 rock samples through ABA and three types of kinetic tests; inappropriate TNPR criteria based on incorrect test procedures, durations, and interpretations

Bradham and Caruccio (1995) collected 83 overburden rock samples from coal mines in four eastern states of the USA. The predictions from ABA were compared with effluent chemistry from three types of kinetic tests: humidity cells, leaching columns, and Soxhlet extraction. Disagreements between ABA and kinetic tests were classed as Type I errors, where ABA predicted non-acidic effluent but acidic effluent was obtained, and Type II errors, where acidic conditions were predicted but non-acidic effluent was obtained. The kinetic tests were reportedly operated for a minimum of 12 weeks, whereas diagrams showed that tests were in fact operated for less than 12 weeks.

The major weaknesses in this study are no recognition of lag time in pH changes and of unavailable NP (Section 5.2.1.3). If a sample had a TNPR value less than 1.0 but contained significant NP, then the lag time to acidic conditions could be years. This resulted in Type II errors simply because of the short length of the kinetic tests. On the other hand, low-sulfur, low-NP samples produced high TNPR values, but generated acidic effluent because the minor NP was unavailable, producing Type I errors. Consequently, the errors are not errors in the procedures, but in the simple interpretation of results.

In any case, Bradham and Caruccio (1995) reported a TNPR criterion of 19 was needed to preclude all Type I errors. Of course, this anomalously high criterion resulted in Type II errors for 55 of the 83 samples.

No pH data are given in the text, figures, tables, or appendices. Therefore, the rate of net acidity production from kinetic tests will be used here to identify net acidic samples, although small values of net acidity could still be associated with near-neutral pH. In any case, ABA data compared with significant levels of net acidity production showed that unavailable NP levels were typically less than 20 t $CaCO_3$/1000 t with an extreme value near 40. Bradham and Caruccio in fact reported that an NP greater than 73 was needed to eliminate Type I errors completely.

In the inappropriately short kinetic tests, effects on rinse chemistry were statistically determined for sample temperature, humidity, rinse-water temperature, particle size, and rinsing interval. In general, sample temperature and humidity were found to have little effect on rinse chemistry unless temperatures were above 100°C. Daily production rates only varied within a factor of two when the rinsing interval was varied among 2, 4, and 7 days, although this degree of variation is not unusual in any short-term kinetic test that has not stabilized. The authors concluded that particle size and rinse-water temperature had only minor effects, although the authors discussed statistically significant effects and some differences between cells and columns due to the higher water-to-rock ratio in the cells. There was insufficient data to determine overall solubility effects because, for example, sample weights in the various tests were not given.

Case Study 5.3.2-3: Five-Year Kinetic Studies of Acid-Generating Rock with Added Limestone

highlights: long-term kinetic columns with blended limestone; correlation of column results to pre-test static analyses; accuracy of rate predictions after five years

Norecol, Dames, and Moore (1994) and Day (1994) described a five-year kinetic study involving humidity cells, columns, and 20-t on-site waste-rock piles for the Cinola Gold Project in British Columbia, Canada. The rock units were epithermal, silicified sedimentary rock, hydrothermal breccia, and argillically altered rock. Sulfide content was often around a few percent and predominantly composed of pyrite and less marcasite.

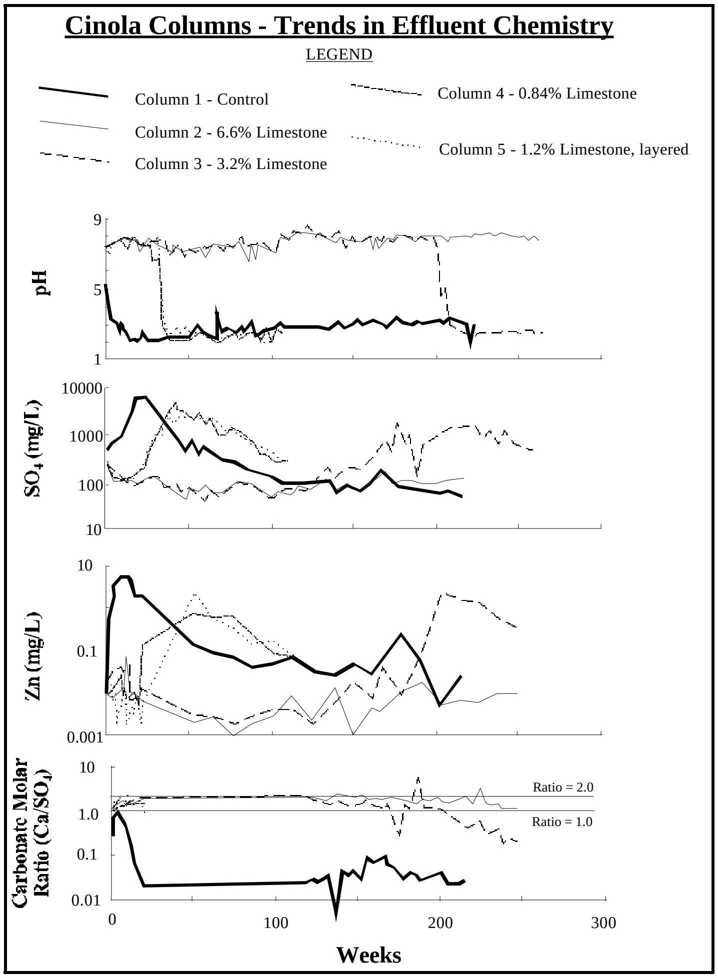

FIGURE 5.3.2-2. Temporal Trends of Effluent Chemistry from Cinola Columns (adapted from Day, 1994).

The Cinola site is located in a cool, wet maritime environment, and has an average annual precipitation of approximately 2 m, with most falling as rain from October to March. Average monthly temperatures are above freezing.

The column tests consisted of 15-cm-diameter columns holding roughly 10-15 kg of sample (Table 5.3.2-3). Water was continuously dripped onto the columns at a rate of 0.4-0.5 mL/min, comparable to 14 m/yr of rainfall for thorough rinsing. The columns were operated for up to 260 weeks (Figure 5.3.2-2). Because weekly carbonate molar ratios indicated NP was consumed at a greater rate than sulfide oxidation (ratios between 1 and 2), none of the columns contained sufficient NP to maintain near-neutral conditions indefinitely.

TABLE 5.3.2-3
Five-Year Column Tests of Limestone Mixed With Net-Acid-Generating Rock[1]
(adapted from Day, 1994)

Column and Description	Sample in Column	%S total	%S sulfide	NP[2]	NNP[2]	NPR	Paste pH
1: no limestone; control	Pre-Test: bulk	2.1	-	8	-58	0.12	6.9
	Post-Test: top	0.53	0.44	-2	-16	0	3.3
	Post-Test: middle	0.55	0.45	-2	-16	0	3.62
2: ~6.6% limestone mixed throughout	Pre-Test: bulk	1.98	-	69	+7	1.12	-
	Post-Test: oxidized	1.12	1.07	3	-30	0.1	5.3
	Post-Test: non-oxidized	1.72	1.71	57	+4	1.07	7.8
3: ~3.2% limestone mixed throughout with 1 cm cap of Column 2 mixture	Pre-Test: bulk	2.05	-	38	-26	0.59	-
	Post-Test: top	0.85	0.8	0	-25	0	4.76
	Post-Test: middle	0.77	0.66	-2	-24	0	4.05
4: ~0.84% limestone mixed throughout with 1 cm cap of Column 2 material	Pre-Test: bulk	2.08	-	16	-49	0.25	-
	Post-Test: bulk	0.65	0.59	-2	-20	0	4.06
5: ~1.2% limestone total as five 1-cm layers of Column 2 material layered with four 10-cm layers of Column 4 material	Pre-Test: bulk	2.08	-	19	-46	0.29	-
	Post-Test: bulk	0.68	0.56	-2	-20	0	4.25

[1] Limestone was ground to less than 0.6 mm diameter with a calculated geometric surface area of 31 m^2/kg; rock was drillcore crushed to less than 3.35 mm with a calculated geometric surface area of 5.4 m^2/kg; columns were 0.15 m in diameter holding sample heights of ~0.5 m holding 10-15 kg of sample.

[2] In units of t $CaCO_3$ equivalent/1000 t; NNP and NPR recalculated here from sulfide where available.

TABLE 5.3.2-4
Results of Mixed Limestone-Rock Columns
(adapted from Day, 1994)

	Column 1: control	Column 2: 6.6% limestone	Column 3: 3.2% limestone	Column 4: 0.84% limestone	Col 5: 1.2% layered limestone
NP (t/1000 t)	8	69	38	16	19
Week when SO_4 began increasing	1	170	100	19	19
Week when pH < 7.0	1	>260	200	31	31
Week to peak SO_4	20	>260	219	40	54
Week to ½ peak SO_4 rate	25	>260	241	58	72
% SO_4 released	62	11	50	61	49

Day (1994) examined relationships among factors like pre-test NP, lag time to acidic conditions (defined as pH < 7.0), and time to peak sulfate production (Table 5.3.2-4 and Figure 5.3.2-3). This showed that the lag time was roughly twice the length of time to the increase in sulfate production, acting as an early warning to net acidity. Based on this, Column 2 with 6.6% limestone would have required at least 340 weeks to become acidic (reportedly 780 weeks based on position of acid front in column and 2600 weeks based on statistical relationships). Day also noted that the time when sulfate production began increasing (TI_{SO4}) was proportional to pre-test NP with a correlation coefficient of 0.991:

$$TI_{SO4} = 2.9NP - 25 \qquad (5.3.2\text{-}1)$$

where TI_{SO4} = the time when sulfate production began increasing in weeks

NP = pre-test NP in t $CaCO_3$/1000 t

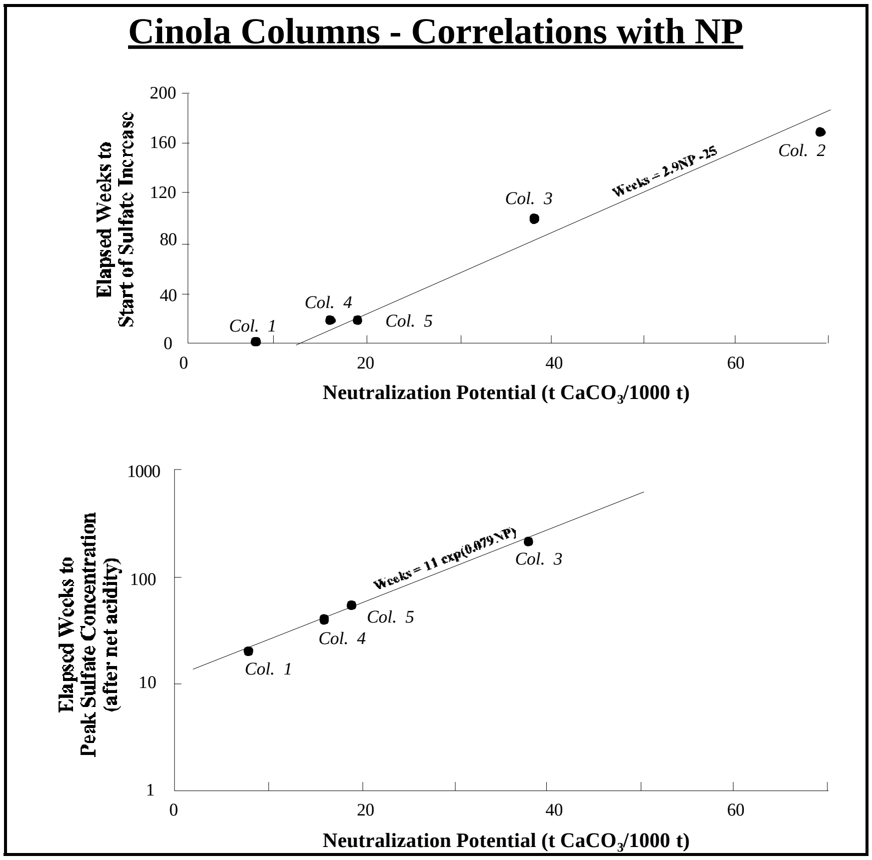

FIGURE 5.3.2-3. Correlations of Geochemical Events with NP from Cinola Columns (adapted from Day, 1994).

Zinc leaching also began increasing at TI_{SO4}, indicating it was driven at least in part by increasing sulfide oxidation, in agreement with the IKD (Section 5.3.3). Copper leaching was not related to TI_{SO4}.

The time to peak sulfate production was also closely related to pre-test NP:

$$TMAX_{SO4} = 11e^{0.079NP} \qquad (5.3.2\text{-}2)$$

where $TMAX_{SO4}$ = the time to peak sulfate production in weeks

NP = pre-test NP in t $CaCO_3$/1000 t

Also, the intensity and sharpness of the sulfate peak decreased with increasing limestone content.

Day (1994) noted that an initial NPR (Section 5.2.1.4) of at least 2.0 would have been required to ensure near-neutral conditions in the columns. This apparently reflected the weekly molar ratios, rather than any unavailable NP. Virtually all limestone was found to be uncoated with secondary-mineral precipitants in near-neutral samples from the columns and almost fully dissolved in acidic samples. Instead, iron from pyrite oxidation remained near the pyrite. No silicate minerals appeared reactive.

Norecol, Dames and Moore (1994) reported similar trends over 140 weeks in original Sobek humidity cells (Appendix C) containing Cinola rock units without added limestone. These were small 200g samples in contrast to the 10-15 kg columns. The initial phase of near-neutral pH and low sulfate production (<20 mg/kg/wk) was followed by peak sulfate production (>1000 mg/kg/wk) below pH 3. This was followed in turn by a decrease in sulfate production by factors of 10-100 as pH rose to 3-4. Pre-test and post-test data were not always consistent with calculated consumption of sulfide and NP, or even with the simple fact there was consumption, due to analytical inaccuracy and subsampling artifacts. Nevertheless, NPR values were generally higher after the tests in samples expected to remain near neutral and lower in those that became acidic.

These pH and sulfate trends were again noted on another scale, 20-30 t waste-rock piles on impermeable liners at the Cinola site (Table 5.3.2-5). Their behavior was less definitive due to climatic effects. However, there seemed to be no major change in pH or sulfate, and this was apparently not the result of secondary-mineral precipitation-dissolution since effluents were undersaturated with respect to gypsum. The leaching of copper and zinc did not show any long-term changes either, but arsenic concentrations falling by 1-3 orders of magnitude toward the end of five years indicated available arsenic was being depleted. This was consistent with the typical less-than-detection values obtained from the start of Pad 1 initially containing five-year-old weathered rock. As with the humidity cells, pre-test and post-test data were not always consistent with calculated consumption of sulfide and NP. Also, post-test mineralogical observations of the rock were not consistent with metal levels obtained with sequential-leach.

Predicted rates of sulfate production for Pad 2 after five years, made in 1988 after less than a year of monitoring, were 33% less than measured (1000 vs. 1500 mg/kg/wk). Also, Pad 2 after five years, which was considered an analog of Pad 1 at its beginning, had a sulfate rate within a factor of two. This indicated that rates could be predicted relatively accurately for at least five years.

Rates from all three scales of testwork at Cinola were similar when expressed as particle-surface rates (mg/m^2/wk) from calculated geometric surface areas. This is in contrast to many other studies and does not reflect the high degree of uncertainty in the calculation (Section 5.2.5).

5.3.3 International Kinetic Database

Ziemkiewicz and Lovett (1994) state that (1) there is little difference in reaction rate among various types of pyrite from sedimentary and hydrothermal sources, (2) particle size affects the rate substantially, (3) pH has little effect on reaction rates, and (4) biotic and abiotic rates are nearly the same. The last two observations are supported by data in this book (e.g., Sections 4.2.4 and 4.2.5). However, the first two observations are not, as shown by the International Kinetic Database (IKD).

TABLE 5.3.2-5
Five-Year On-Site Piles of Net-Acid-Generating Rock
(adapted from Day, 1994)

	Basal Sand[1]	Pad 1	Pad 2	Pad 3	Pad 4
Description	placed on liner	five-year-old weathered Skonun Sediments	fresh Skonun Sediments	argillically altered Skonun Sediments	brecciated Skonun Sediments
Quantity (t)		20	30	30	30
%S total	0.003	1.95	2.96	3.06	1.75
NP (t/1000 t)	3.6	2.2	3.1	-6.4	0.7
TNNP	+3.5	-59	-89	-102	-54
TNPR	38.4	0.04	0.03	0	0.01
Paste pH	7.8	5.3	7.2	3.5	7.1
Geometric Surface Area (m^2/kg)	-	1.81	1.07	2	1.92

[1] Placed on the impermeable liner to channel water into collection buckets.

The IKD is a companion database to the ISD (Section 5.2.1.5) and currently contains the pre-test characterization, overall test results, and late-stage rates from 457 kinetic tests from 63 mines (Morin et al., 1995 c and d; Morin et al., 1996).

Two-dimensional analysis (scatterplots of one parameter against another, e.g., Figure 5.3.3-1) showed that pre-test characteristics like ABA and total metals correlated only weakly with kinetic rates of acid generation/neutralization (Morin et al., 1995c) and metal leaching (Morin et al., 1995d). For example, the inaccuracy (standard deviation) of predicting the rate of sulfide oxidation from initial solid-phase sulfur was a factor of 5.7 and NP below 7-10 t/1000 t was typically unreactive (Figure 5.3.3-1a). This figure also shows that rates can also be qualitatively classified from Very Low to Very High.

The analysis of the IKD was then expanded to three dimensions (scatterplots of one parameter against two others, Morin et al., 1996). This showed, for example, that the relative reactivity of NP decreased with increasing initial sulfur and decreasing initial NP (Figure 5.3.3-2). The leaching rate of copper correlated much better with initial sulfur than initial copper (Figure 5.3.3-3), whereas the zinc rate showed correlations with both initial zinc and initial sulfur (Figure 5.3.3-4).

The ultimate tool for interpreting the IKD and predicting primary-mineral reaction rates would be nonlinear, multidimensional analysis of dozens of factors. However, this may not be possible since potentially relevant factors like sample temperature and infrared flux are rarely measured during kinetic tests.

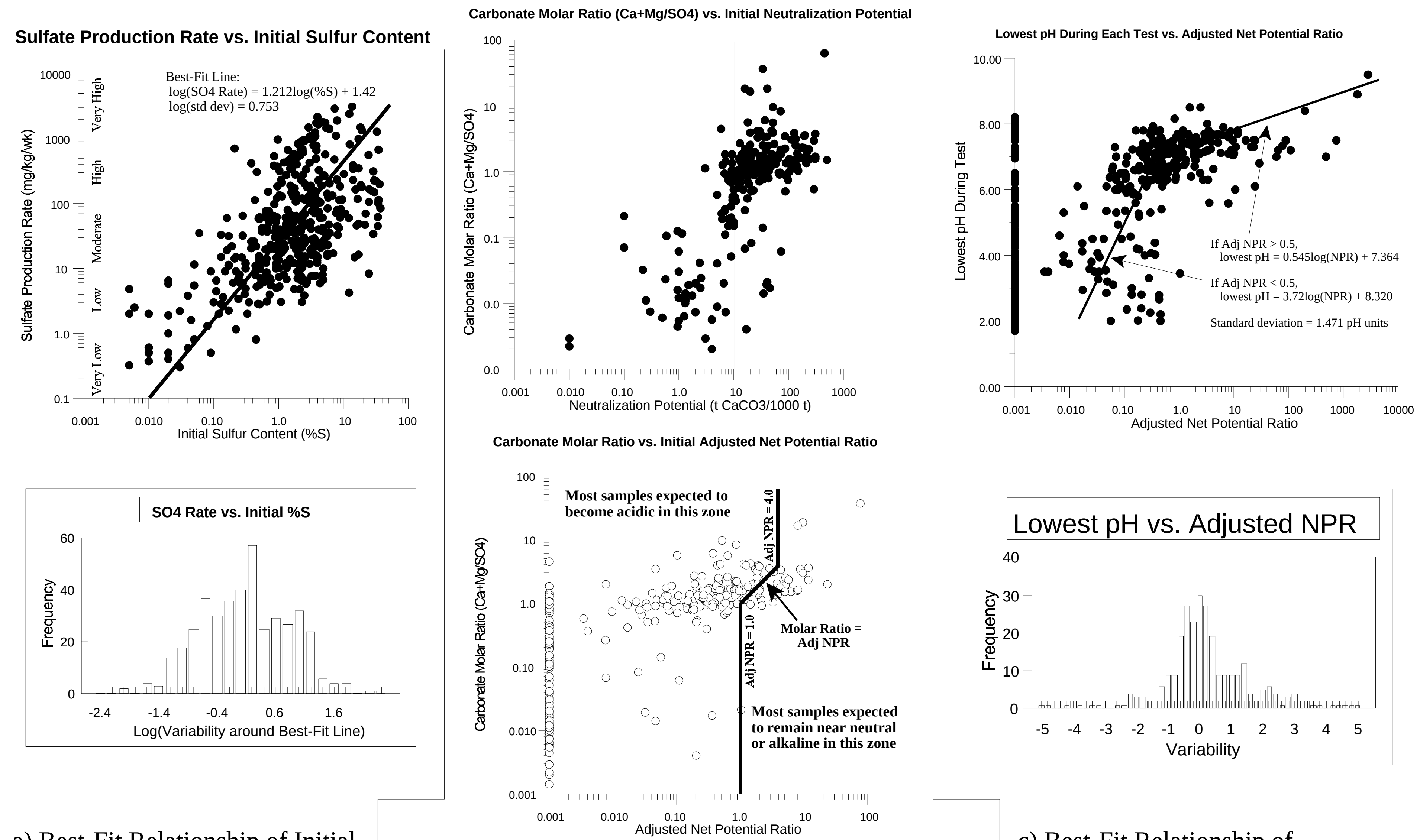

a) Best-Fit Relationship of Initial Sulfur Content to Sulfate Production Rate, and Variability around the Line

b) NP mostly unreactive or unavailable below 7-10 t/1000 t (top), and adjusted NPR (NP decreased by 10 t/1000 t) compared to Carbonate Molar Ratio for identification of samples expected to be acidic at some point

c) Best-Fit Relationship of Adjusted NPR to Lowest pH, and Variability around the Best-Fit Line

FIGURE 5.3.3-1. Examples of Two-Dimensional Plots of IKD Data.

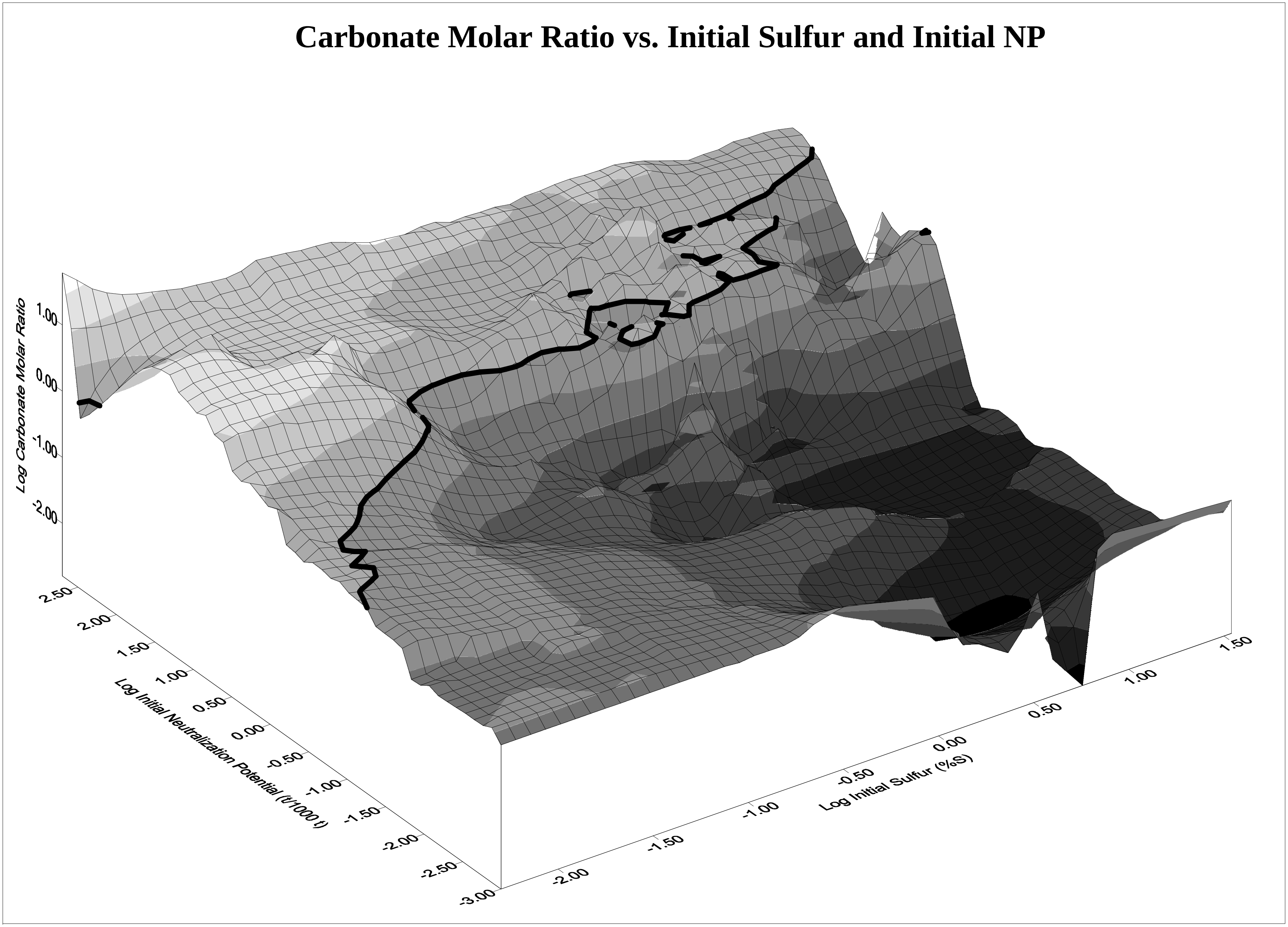

FIGURE 5.3.3-2. Carbonate Molar Ratio vs. Initial Sulfur and Initial NP in the IKD; heavy lines mark a Ratio of 1.0 (adapted from Morin et al., 1996)

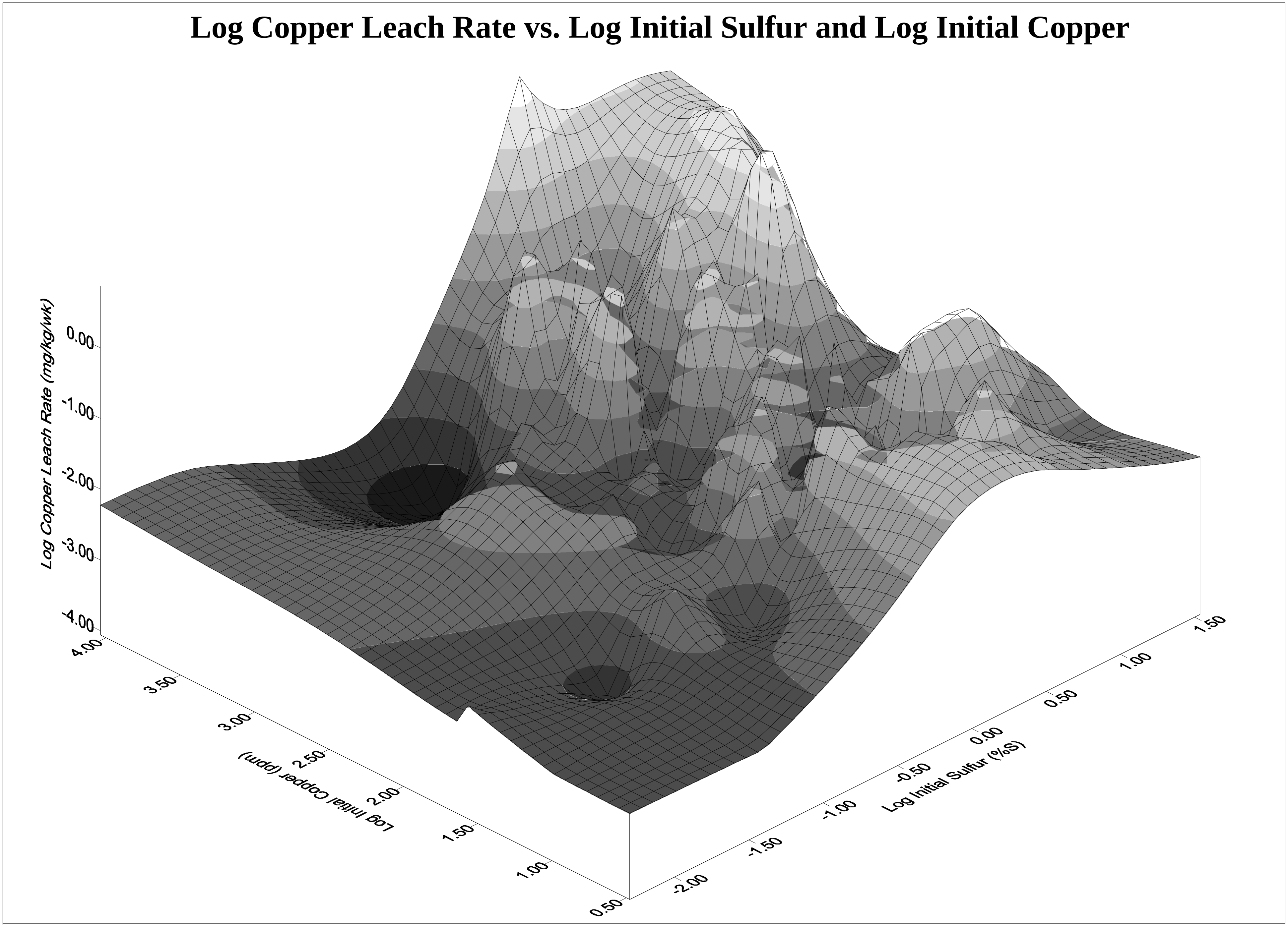

FIGURE 5.3.3-3. Copper Leaching Rates vs. Initial Sulfur and Initial Copper Content in the IKD (adapted from Morin et al., 1996)

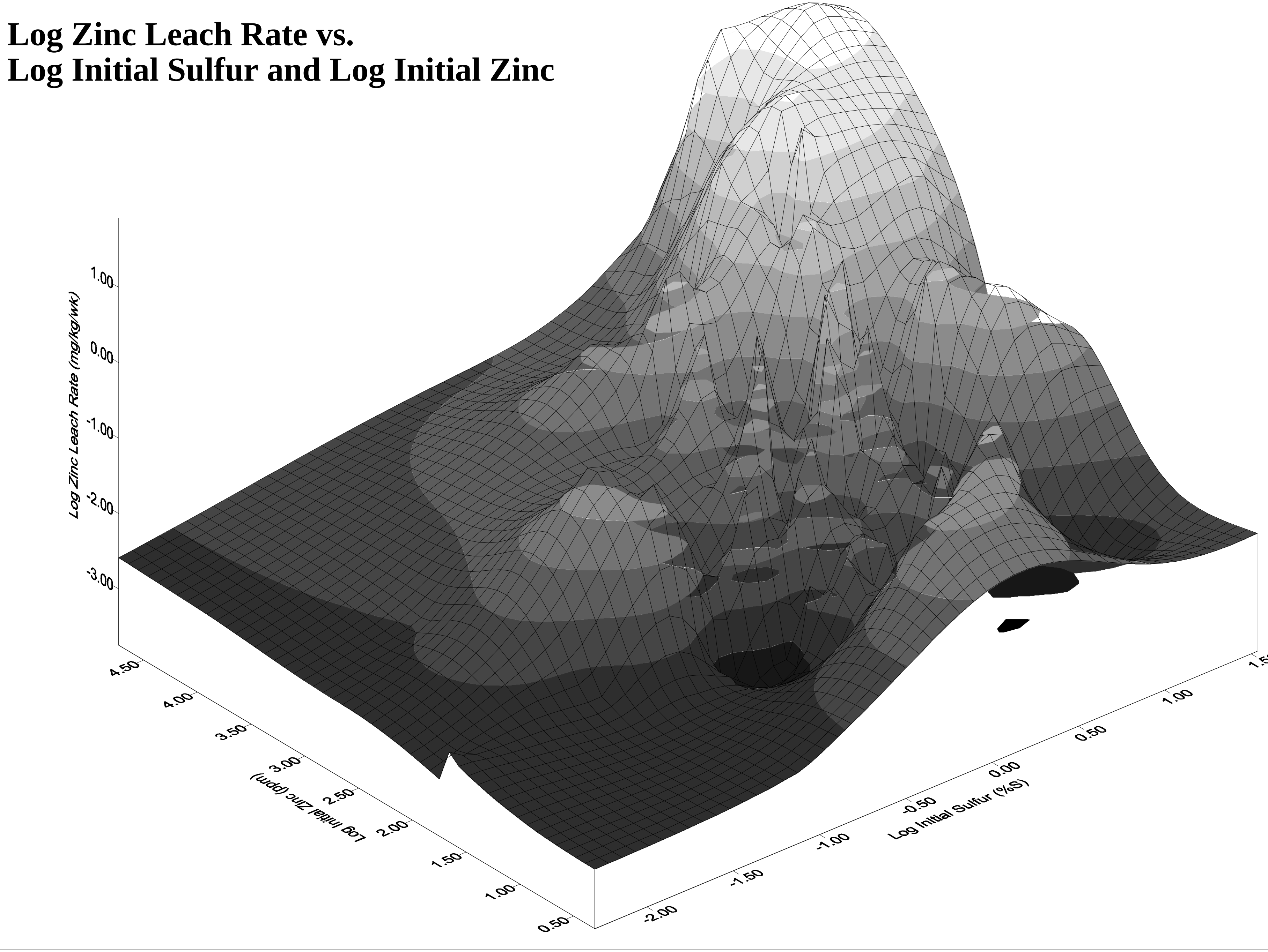

FIGURE 5.3.3-4. Zinc Leaching Rates vs. Initial Sulfur and Initial Zinc Content in the IKD (adapted from Morin et al., 1996)

5.4 Field Kinetic Tests

Unlike laboratory kinetic tests (Section 5.3), field kinetic tests are designed to provide either primary-mineral reaction rates (Rate1, Figure 4.2.2-1) or drainage-chemistry predictions (Rate2) under on-site conditions. The two basic forms of field kinetic tests are large bins that hold rock or tailings (Section 5.4.1) and Minewall Stations that monitor exposed surfaces of rock (Section 5.4.2).

5.4.1 Bins or Cribs

Large-scale bins, cribs, or piles with underdrains can be used to isolate a volume of mined rock or tailings hydraulically so that natural infiltration from precipitation can be collected and analyzed. Due to the relatively large size of sample and the corresponding low flow of water, these tests rarely provide primary-mineral reaction rates (Rate1, Figure 4.2.2-1), but yield field estimates of secondary-mineral controlled Rate2. The following case studies describe the types of field bins and piles and the manner in which the data are interpreted.

Case Study 5.4.1-1: Field Monitoring of Eleven 400-t Waste-Rock Piles

highlights: large-scale field kinetic tests; negligible pH effect of various chemical additions over 11 years; unavailable NP

Donovan and Ziemkiewicz (1994) and Ziemkiewicz and Meek (1994) reported on eleven 400 t waste-rock piles from coal mining constructed in 1982. These piles, containing various amounts of sandstone and shale, were constructed with either (1) no added chemicals in some piles as “controls” for the study, (2) various proportions of neutralizing compounds (limestone, lime, and rock phosphate), or (3) sodium lauryl sulfate to inhibit bacterial activity (Table 5.4.1-1).

The piles were approximately 16 m by 16 m with 2 m height, placed on plastic liners and underdrains to collect the drainage. Rock was sieved to include only the range of 2.5-20 cm, and the lack of fines typically found in waste rock could have distorted the physical and chemical factors that regulate drainage chemistry. The piles with combinations of sandstone/shale and added chemicals either were built in thin layers or blended (Table 5.4.1-1).

The ABA characteristics of each pile were determined from one composite each, consisting of several samples collected during pile construction plus any chemical additions (Donovan and Ziemkiewicz, 1994). As a result, the composite ABA data (Table 5.4.1-1) do not show the lateral and vertical heterogeneity that would affect drainage chemistry. However, Ziemkiewicz and Meek (1994) contradict the composite sampling by saying that ABA was based on one grab sample from each pile, which may not have been representative.

Based on drainage pH less than 5.0 as an indicator of acidic conditions, all control cells except the layered sandstone/shale became acidic in less than a year (Table 5.4.1-1). The piles with lime and the highest limestone addition also became acidic within a year. All other piles remained near neutral pH, although some like Pile #5 displayed trends of decreasing pH. Based on one sample collected 11 years after starting the tests (January 1993), all piles except 4 and 8 were acidic (~pH 5) or close to it, and most sulfate production rates had fallen by an order of magnitude. Notably, Pile 8 with the greatest amount of limestone addition had returned to near-neutral conditions, due to either exhaustion of sulfide or rejuvenation of NP. Peak sulfate rates in the first year indicated that sulfide in Pile 8 would be consumed within 11 years.

According to graphs in Donovan and Ziemkiewicz (1994), molar ratios of (Ca+Mg)/SO_4 were predominantly around 1.0 in early drainage from all piles. The ratios fell below 1.0 when pH turned acidic or toward the end of the one-year monitoring in the near-neutral piles. The cause of the less-than-one ratios with maintenance of near-neutral pH in some piles is not clear, but could be related to neutralization by non-Ca-Mg-carbonate minerals (Section 5.2.1.3).

TABLE 5.4.1-1
Composition of Eleven 400-t Waste-Rock Piles Monitored for One Year (adapted from Donovan and Ziemkiewicz, 1994, and Ziemkiewicz and Meek, 1994)

	Pile #										
	1	2	3	4	5	6	7	8	9	10	11
% sandstone	100	0	57	53	52	0	0	54	59	44	0
% shale	0	100	43	47	48	100	100	46	41	56	100
addition[1]	-	-	-	LS	LS	PH	PH	LS	LI	-	SLS
% added[4]	-	-	-	1.07	0.46	0.31	0.15	1.26	0.15	-	30 lb
mixing	-	-	layer	layer	layer	-	-	layer	layer	blend	-
NP[2,4]	12.3	0.8	1.0	17.2	11.1	0.8	0.8	18.9	8.9	5.8	0.8
%S	0.1	0.31	0.18	0.33	0.64	0.60	0.29	0.25	0.16	0.29	0.41
NPR[4]	3.94	0.08	0.18	1.65	0.56	0.04	0.09	2.38	1.73	0.63	0.06
Lag[3]	200 days	240 days	280 days	>11 yrs	~11 yrs	<11 yrs	~11 yrs	70 days	150 days	<11 yrs	<11 yrs
UNP[2]	12.0	0.3	0.7					18.9	8.6		
Rate[3]	21.0	19.2	14.0	11.1	17.7	17.0	18.3	17.7	16.5	26.5	15.3

[1] LS = crushed limestone; PH = rock phosphate; LI = lime (CaO); SLS = sodium lauryl sulfate.

[2] As t $CaCO^3$ equivalent/1000 t of sample; UNP = unavailable NP (NP remaining after onset of acidic conditions) based on NP consumption from Ca+Mg release.

[3] Lag = approximate lag time to acidic conditions (pH 5); Rate = sulfate production rate in mg SO_4/kg/wk; most sulfate rates less than 1/10 peak rates ten years later; pH of Pile 8 close to 7.0 ten years after onset of acidification suggesting sulfide exhausted or NP rejuvenated; only Piles 4 and 7 had near-neutral pH (> 6) eleven years after start.

[4] There are contradictions between the two references for %added, NP, and NPR (see Table 1 in both references); Donovan and Ziemkiewicz (1994) is used where contradictions exist.

Donovan and Ziemkiewicz (1994) summarized studies of unavailable NP (Section 5.2.1.3), finding that unavailable NPs of less than 10 to greater than 30 t CaCO3 equivalent/1000 t have been reported. Based on graphs in their paper, unavailable NP in the piles was calculated in the range from 0.3 to 19 t CaCO3/1000 t (Table 5.4.1-1). However, there were piles with NP in this range that did not become acidic over the year of monitoring. Therefore, the interpretations of the results and the effect of chemical additions are ambiguous. However, because sulfate rates among the piles were generally consistent (Table 5.4.1-1), there appeared to be little value to the chemical additions.

Case Study 5.4.1-2: Fourteen-Year Monitoring of 1000-t Ore Piles

highlights: long-term field and laboratory kinetic tests; empirical (effective) NP based on kinetic tests

Lapakko (1994b) conducted ongoing field and laboratory kinetic studies of Duluth Complex rock from Minnesota, USA, for nearly 14 years, which is a rare and valuable time frame for such studies. Six piles were constructed in 1977 at the proposed minesite, containing 820 to 1300 t of low-grade copper-nickel ore from underground excavations (Table 5.4.1-2). Pile 4 was dismantled a few years after construction and is thus not reported.

The piles were roughly 4 m high and 15 by 25 m at the base, and the particle size was predominantly sandy gravel. These piles were exposed to natural climatic conditions with (1) an average annual precipitation of 72.1 cm, (2) temperature extremes of -14°C in January to +19.1°C in July with a mean of +3.6°C, and (3) average annual snow coverage for 140 days.

The rock consists of 59% plagioclase (An_{60}), 11% clinopyroxene, 11% olivine, 3.7% orthopyroxene, 3.6% amphibole, and 0.63 to 1.41%S. Analyses of sulfur and metals in various grain sizes from 0.50-2.00 mm to <0.053 mm showed generally increasing concentrations by factors of 2 to 4 with decreasing size over the range.

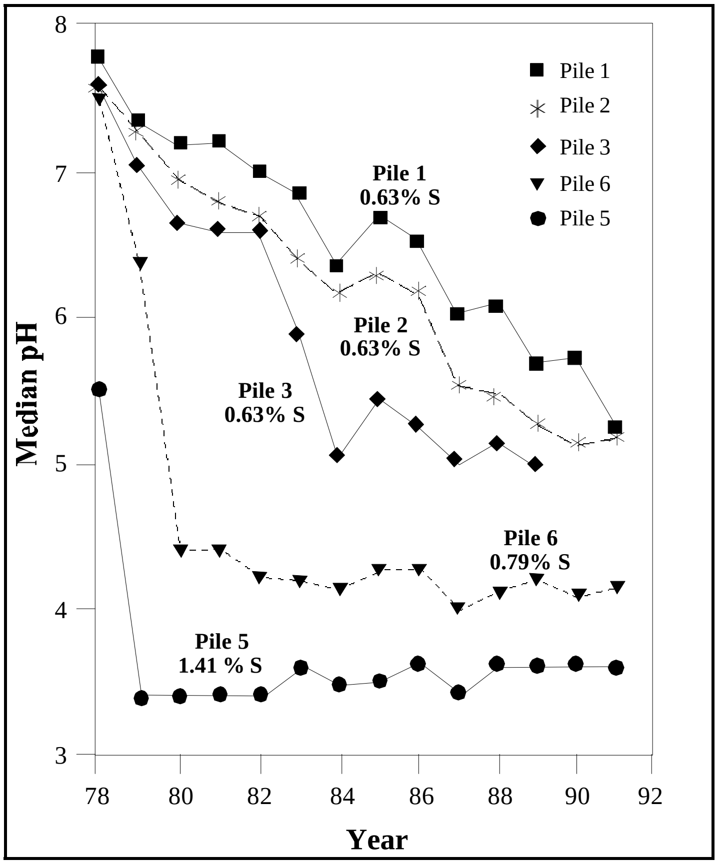

FIGURE 5.4.1-1. Annual Median Drainage pH for In-Field 1000-t Test Piles (adapted from Lapakko, 1994b).

The ore piles typically released drainage between mid March and mid November each year. Annual median pH over these 13 years of drainage showed a general correlation with initial sulfur content (Figure 5.4.1-1). The piles with 0.63%S did not become acidic (pH<5) during the 13 years, although pH was falling toward 5. Sulfate concentrations from most piles were relatively steady, except Pile 5 which had peak levels between 1981 and 1985 that then decreased to those of Pile 6. Also, mean concentrations of calcium and magnesium were relatively constant. It is not clear if aqueous concentrations were regulated by equilibrium or kinetic processes. Lapakko (1994b) noted that release rates from corresponding laboratory tests were qualitatively similar to the field values from the piles. However, the quantitative rates from the piles were typically 10-40% of those from the laboratory, possibly reflecting retention factors in the piles.

TABLE 5.4.1-2
Description of Field Test Piles for Duluth Complex Rock
(adapted from Lapakko, 1994b)

	Pile 1	Pile 2	Pile 3	Pile 5	Pile 6
Completion date	4/20/77	4/20/77	4/20/77	9/10/77	9/30/77
%S	0.63	0.63	0.63	1.41	0.79
%Cu	0.35	0.35	0.35	0.3	0.34
%Ni	0.083	0.083	0.083	0.085	0.084
Weight (t)	1100	1100	830	815	1300
Volume (m^3)	540	530	400	400	630
Lateral area (m^2)	330	450	430	370	390
Cover	none	topsoil	coarse-sand till	sandy till on coarse sand	none
Avg. cover depth (m)	-	0.23	0.34	0.54	-
Vegetation?	no	yes	yes	yes	no

TABLE 5.4.1-3
Values of Effective Neutralization Potential in Duluth Complex Test Piles
(NP as t $CaCO_3$ equivalent/1000 t; adapted from Lapakko, 1994b)

pH Criterion	Pile 1	Pile 2	Pile 3	Pile 5	Pile 6
pH 7	0.346	0.179	0.442	0.044	0.157
pH 6	0.781	0.393	1.254	0.044	0.172
pH 5 [1]	>1.059	>0.642	>1.340	0.096	0.226
pH 4.5	>1.059	>0.642	>1.340	0.13	1.702
pH 4	>1.059	>0.642	>1.340	0.136	>2.074
pH 3.5	>1.059	>0.642	>1.340	>1.889	>2.074

[1] Corresponds to the definition of effective NP in Section 5.2.1.3.

Based on calcium and magnesium concentrations in pile drainage, Lapakko (1994b) defined "empirical neutralization potentials" (ENP) based on the calculated amount of carbonate consumed when aqueous pH fell below various pH levels (Table 5.4.1-3). The ENP for pH 5.0 is synonymous with effective NP as defined in Section 5.2.1.3. Most ENP values for pH 7.0, 6.0, 5.0, 4.5, 4.0, and 3.5 were less than 1 t $CaCO_3$ equivalent/1000 t, which is negligible. Since bulk measured NP was not reported, unavailable NP (measured NP minus effective NP) could not be calculated.

5.4.2 Minewall Stations

The chemistry associated with water in mines is the result of three basic processes:

ì the chemical loading brought into a mine by the various sources of water flowing into it,
í the additional loading provided by the rock exposed on the mine walls and in fractures behind the walls, and
î the geochemical evolution of the water chemistry during its residence in the mine.

An in-field kinetic technique for assessing or predicting the second and third processes is known as Minewall (Morin, 1990b; MEND, 1995; Morin and Hutt, 1995a; Appendix D), based on three decades of studies on the issue (e.g., Morth et al., 1972). During operation of a mine, the basic Minewall mass-balance equation for concentrations in the drained or pumped minewater is relatively simple, using the units of milligram (mg), liters (L), and weeks (wk):

$$\mathrm{Conc}_m = \{[\mathrm{Flow}_1 * \mathrm{Conc}_1] + [\mathrm{Flow}_2 * \mathrm{Conc}_2] + \ldots + \mathrm{MW}_1\} / \{\mathrm{Flow}_1 + \mathrm{Flow}_2 + \ldots\} \qquad (5.4.2\text{-}1)$$

where Conc_m = concentration in pumped/drained minewater (mg/L);
Flow_x = positive (inflow) or negative (outflow) flowrate such as precipitation or groundwater (L/wk);
Conc_x = concentration associated with Flow_x (mg/L); and
MW_1 = loading (mg/wk) from occasional flushing of mine walls (Section 3.2).

A negative value for Conc_m in Equation 5.4.2-1 means there is a net loss of water from the mine.

During mine closure, when active pumping or draining ceases, concentrations in the water filling the mine reflect additional effects like the ongoing accumulation of mine water, additional contributions from chemical retention in the mine walls, and the potential for flow reversals. With units of mg, L, and a time step of one week, the general equation for concentrations in minewater during closure is:

$$\begin{aligned}\mathrm{Conc}_{m,t} = \{&[\mathrm{Conc}_{m,t-1} * \mathrm{Evol}_{m,t-1} * \mathrm{Volume}_{m,t-1}] + \\ &[\mathrm{Flow}_1 * \mathrm{Conc}_1] + [\mathrm{Flow}_2 * \mathrm{Conc}_2] + \ldots + \mathrm{MW}_1 + \mathrm{MW}_2 + \mathrm{MW}_3\} / \mathrm{Volume}_{m,t} \qquad (5.4.2\text{-}2)\end{aligned}$$

and $\mathrm{Volume}_{m,t} = \mathrm{Volume}_{m,t-1} + \mathrm{Flow}_1 + \mathrm{Flow}_2 + \ldots \qquad (5.4.2\text{-}3)$

where $\mathrm{Conc}_{m,t}$ = Closure concentration (mg/L) in ponded minewater at current week, t
$\mathrm{Conc}_{m,t-1}$ = Closure concentration (mg/L) in ponded minewater at previous week, t-1
$\mathrm{Evol}_{m,t-1}$ = factor representing evolution of minewater chemistry between times t-1 and t
$\mathrm{Volume}_{m,t}$ = volume of ponded mine water at current week (L)
$\mathrm{Volume}_{m,t-1}$ = volume of ponded mine water from previous week (L)
MW_1 = loading (mg/wk) from occasional flushing of mine walls (Section 3.2)
MW_2 = loading (mg/wk) from major flushing of recently submerged mine walls (Section 3.2)
MW_3 = loading (mg/wk) from previously submerged mine walls (Section 3.2).

All $Flow_x$ and $Conc_x$ in Equations 5.4.2-1 to 5.4.2-3 must be known to predict minewater chemistry. Most of this required information on flows and concentrations, such as for precipitation and groundwater, can be obtained from routine monitoring of a minesite in any stage of planning, operation, or closure. Also, concentrations in precipitation and evaporation are often negligible and can thus be ignored. As explained below, concentrations in runoff and unsaturated flow can be set to zero and their contributions can be more easily estimated as part of MW_x. The remaining $Conc_x$ for groundwater flow can come from monitor wells at the minesite. Therefore, most of the data requirements for Minewall assessments, except the MW_x factors and $Evol_{m,t-1}$ (Chapter 4), can be relatively easily obtained or estimated. Because operating mines often monitor flow and chemistry ($Conc_m$) in mine drainage/pumpage, Equation 5.4.2-1 can sometimes be solved in reverse to obtain an unknown $Conc_x$ or $Flow_x$.

Again, the primary unknown factors in Equations 5.4.2-1 to 5.4.2-3 are often the MW_x factors, reflecting loadings from the rock surfaces on and behind the mine walls. These loadings are considered "release rates" into the minewater, such as 300 mg Ca/week. These rates are determined by three factors: (1) unit-surface-area production rates, (2) total reactive rock-surface area in a mine, and (3) reaction-product retention and flushing. In other words, for one week of time:

$$\text{Release rate } (MW_x\text{, mg/wk}) = \{[\text{Production rate (mg/m}^2\text{ surface/wk)}*\text{Total rock surface (m}^2)] + [\text{Previously retained products (mg)}]\} * \{\%\text{Flushed from surface}/100\%\} \qquad (5.4.2\text{-}4)$$

There are two basic localities where the geochemical reactions take place: surficial or internal relative to the smallest divisible particle or block at a site. The overall effects of surficial reactions are generally dependent on exposed surface area relative to the water volume. On the other hand, the effects of internal reactions are dependent on exposed surface area, distance to the center of a grain, and the volume of the grain relative to the water volume. Perhaps due to practicality and simplicity, surficial reactions seem to be addressed more often in field-oriented studies (e.g., Morth et al., 1972), while internal reactions appear more often in theory-oriented studies (e.g., Cathles, 1982).

Unit-area production rates can be obtained for Equation 5.4.2-4 from "Minewall Stations" (Appendix D). These stations are relatively simple and inexpensive. Nevertheless, they are effective at allowing reactions to proceed unhindered while preventing removal of reaction products until intended sampling. Examples of unit-area production rates from Minewall Stations are provided in Tables 5.4.2-1 and 5.4.2-2. The currently reported range of pH values measured at stations range from 2.1 to 8.2.

After geochemical reaction rates are obtained for unit surface areas, the next parameter in Equation 5.4.2-4 is the amount of reactive rock surface. This is not synonymous with the observable or exposed surface within a mine. Fractures are invariably present in mine walls, occurring naturally and induced by blasting and excavation (Evans, 1987; Pusch, 1989; Toran and Bradbury, 1988; see also Case Studies 3.2.2-1 and 3.2.2-2). These fractures provide additional reactive surfaces. Morth et al. (1972), for example, found reactive fracture surfaces that extended as far as 15 meters from mine walls. Also, visual observations at a large open-pit mine during a pushback of a pit wall revealed fractures oxidized as far back as 10 meters from the wall (Morin and Hutt, 1995a). Consequently, the fracture surfaces behind the mine walls can provide a much greater reactive surface than that indicated simply by the observable walls.

For example, a pit wall that has (1) spacings for vertical and horizontal fractures of 1 meter and (2) oxidation occurring to 10 meters behind the wall will have 41 m^2 of reactive surface for each m^2 of exposed wall (41:1). The average estimated ratio varied from 27:1 to 161:1 in published Minewall studies. Any waste rock, ore rock, tailings, or backfill placed in the mine can add to this reactive surface area.

TABLE 5.4.2-1
Average Minewall Production Rates (mg/m^2/wk) from an Underground Mine (adapted from Morin and Hutt, 1995a)

Parameter (mg/m^2/wk)	Station 1	Station 2	Station 3	Station 4
pH (pH units)	5	6.39	4.49	5.83
Alkalinity	3.87	52.6	0	199
Acidity	1.62	3.94	27.6	19.6
Sulfate	6.65	6.75	35.3	3.61
Nitrate	0.0321	0.105	0.059	0.0785
Aluminum	0.0937	0.00783	1.96	0.434
Antimony	0.00019	0.00062	0.000217	0.00151
Barium	0.0122	0.0708	0.026	0.0288
Cadmium	0.0054	0.00486	0.0374	0.0288
Calcium	3.55	34.2	9.08	123
Chromium	0.0012	0.00213	0.0026	0.00251
Copper	0.0191	0.0154	1.4	0.462
Iron	0.0212	0.0113	0.0517	0.192
Lead	0.0095	0.00276	0.00816	0.0342
Magnesium	0.242	1.53	0.985	9.91
Manganese	0.0251	1.03	0.138	0.818
Molybdenum	0.00528	0.00021	0.0000204	0.0000174
Nickel	0.003	0.00687	0.00752	0.3
Potassium	0.222	0.228	0.0066	0.355
Selenium	<0.003	<0.0007	0.000479	0.000407
Silver	<6E-06	0.0000355	0.000019	0.000008
Sodium	0.389	0.9	1.02	1.98
Strontium	0.0193	0.178	0.0483	0.11
Zinc	0.0733	0.22	3.19	2.68

TABLE 5.4.2-2
Average Minewall Production Rates ($mg/m^2/wk$) from a Pit
(adapted from Morin and Hutt, 1995a)

Parameter ($mg/m^2/wk$)	Station 1	Station 2	Station 3	Station 4	Station 5	Station 6
pH (units)	7.25	6.95	7.28	6.43	7.2	7
Particulates	878	1060	1250	3930	821	622
Alkalinity	85.5	276	252	21.4	118	62.6
Acidity	2.14	2.47	2.15	8.23	1.36	21.6
Sulfate	181	122	334	2670	200	195
Silicate	<0.3	<1.0	<0.9	<0.6	<0.3	<0.8
Nitrate	0.407	0.00823	1.53	0.36	0.168	0.0807
Aluminum	<0.06	<0.3	<0.2	<0.12	<0.06	<0.16
Cadmium	<0.003	<0.014	<0.008	<0.006	<0.003	<0.008
Calcium	98.1	214	249	69.1	127	40.8
Copper	0.0086	0.0211	0.0244	0.308	0.0423	0.881
Magnesium	17.3	28.7	44.2	525	21	51.5
Manganese	0.0149	0.109	0.0346	2.1	0.0522	0.0384
Molyb.	0.24	<0.04	0.356	0.038	0.00828	<0.025
Potassium	1.97	<3.0	2.31	3.8	1.09	<3
Sodium	1.28	<3.0	2.45	4.18	1.21	<3
Strontium	0.929	0.84	1.46	0.563	1.45	0.344
Zinc	0.0061	0.00829	0.00712	0.0915	0.00219	0.0174

The reaction products on the reactive surfaces are released if water flows over and removes them. Because water flow is often intermittent, this leads to the third and last factor in Equation 5.4.2-4 for estimating M_x (Equations 5.4.2-1 and 5.4.2-2). For open pits, the Minewall technique assumes that certain percentages of the total reactive rock surfaces are flushed (1) regularly by precipitation, condensation, etc., (2) periodically such as during snowmelt or a high-precipitation month, and (3) not at all during operation. Studies to date show that only a few percent of annual reaction products are removed regularly, roughly 10-30% are removed periodically, and 70-90% is retained throughout operation (Morin and Hutt, 1995a). At closure, the latter category can significantly affect water chemistry as the pit-water level rises and flushes reaction products accumulated over the years from flooded surfaces. For walls above the flooded level, the first two categories continue to play an ongoing role in pit-water chemistry for as long as the pit exists.

For underground mines, the removal of reaction products can be viewed differently than open pits according to Morth et al. (1972). According to these researchers, there are three types of reaction-product removal: *diffuse leaching*, *trickle leaching*, and *inundation leaching*. These are the general analogs to the open-pit flushing of rock surfaces regularly, occasionally, and not at all during mine operation. As a result, the open-pit labels are also acceptable for underground mines.

According to Morth et al. (1972), condensation causes a slow, non-point-source leaching of reaction products into minewater (Table 5.4.2-3). However, because there can be other non-point sources of water, *diffuse leaching* is a better label. *Trickle leaching* is a point-source removal of reaction products, such as at a borehole or fracture through which a stream of water flows into the mine. *Inundation leaching* implies full saturation and submergence of some fractures, part of the mine, or even the entire mine. In an underground mine, inundation leaching on a large scale is usually prevented during operation through active water control such as pumping, grouting, and bulkheads (Case Study 3.2.2-6). However, after closure, inundation leaching will often prevail in a pumped Type 1 mine (Figure 2.2-5, Section 3.2.2) when pumping ceases. Such leaching may also occur in a gravity-drained mine if a seal is installed (Case Study 4.3-12) or wall collapse creates a natural plug. The effects of inundation leaching can be significant (e.g., MacGregor, 1966; Wolkersdorfer, 1996).

Once the chemical loadings from the inflows and mine walls have been added to the mine waters, water chemistry may begin to evolve due to various physical, chemical, and biological mechanisms ($Evol_{m,t-1}$ in Equation 5.4.2-2). For example, mineral precipitation/dissolution, controlled by equilibrium or kinetic processes, can change concentrations in ponded water (Section 4.2). Also, redox reactions can change concentrations of some aqueous species through transformation to other ions. Sulfate-reducing bacteria can reduce sulfur from sulfate (SO_4^{2-}) to sulfide (S^{2-}).

In addition to reactions that can affect water chemistry throughout an entire water column, other physical and chemical mechanisms lead to chemical differences along a water column (e.g., Figures 3.2.1-1 to 3.2.1-3, and Case Study 4.3-12). Like lakes, water accumulated in flooded mines can vary physically and chemically in three dimensions. This complexity is often reduced to two dimensions in a vertical plane in which horizontal masses of water are separated by near-horizontal contact zones (Wetzel, 1983). For example, “thermoclines” separate water layers with different temperature and “chemoclines” separate those with different chemistries. Due to seasonal changes in temperature and climate, unstable thermal stratification can arise and lead to some or all of the water layers mixing vertically (“turnover”). At this point, thermoclines and chemoclines essentially disappear (Stevens et al., 1994).

When one or more of the deeper layers do not participate in turnover at any time, the minewater is termed “meromictic”. If fresh metal-laden minewater can be fed to a sulfide-rich monolimnion without destabilizing it, metals may precipitate to low concentrations. The concept of a meromictic pit with sulfate-reducing bacteria (SRB) in the deepest, unmixed monolimnion is a topic of research in some countries. However, establishment of a thriving SRB colony and slow kinetic reactions between metals and sulfide are just two of several problems encountered to date (Case Study 6.1.2-3).

A simple example of a Minewall simulation involved the delineation of rock units, static-test parameters (Table 5.4.2-4), and unit-area production rates from stations. The simulation was calibrated to existing monitoring data from the pit to obtain percentages of surfaces flushed at various intervals. The resulting prediction indicated that, although most of the walls were net acid generating and initial flushing of acidity upon flooding, pH would not be acidic through closure (Figure 5.4.2-1). This was a consequence of inflowing background groundwater (Figures 3.2.1-2 to 3.2.1-4) with sufficient alkalinity to offset the release of retained acidity. This dominance of pit-water pH by inflowing groundwater has been noted at other minesites.

5.4.3 Routine Site Monitoring

Undoubtably the most valuable and representative kinetic test that can be operated at a minesite is the full-scale operation of minesite components. The monitoring of drainage from the components during operation can provide valuable

TABLE 5.4.2-3
Adjusted Rates of Acid Leaching and Flow Dependencies in Underground Mines
(raw data from Morth et al., 1972 normalized to surface area and time)

	McDaniels	---------------- Auger Hole ------------------					Decker #3
		No. 1	No. 3	No. 4	No. 5	No. 6	
Surface area (m^2)	736	574	438	338	94	632	255,000
Trickle leaching, mg acid/m^2/wk	770	630	770	880	1040	2190	-
Inundation,mg acid/m^2/wk	77	710	990	886	550	360	-
Condensation, mg acid/m^2/wk	390	180	31	84	250	190	-
Minimum flows below which:							
- inundation removed no acidity (L/m^2/wk)	10.9	5.3	3.6	6.3	0	4.0	31
- trickle leach removed no acidity (L/m^2/wk)	5.4	3.9	1.8	2.4	0	2.9	3.6
- condensation leaching was determined to be independent of flowrate.							

TABLE 5.4.2-4
Partial Input Data for the Simulation of the Main Zone Pit at Equity Silver Mines
(adapted from Morin, 1990b)

Parameter	Rock Unit #1	Rock Unit #2	Rock Unit #3
Rock Type	Gabbro	Volcanics	Volcanics
NNP from Acid-Base Accounting (t $CaCO_3$/1000 t)	NNP > 0.0	-40 < NNP < 0.0	NNP < -40
Orientation on Pit Wall	Vertical	Vertical	Vertical
Exposed Surface Area (m^2)	315000	234000	214000
Sloping Walls - Percentage of Total Area	35%	35%	35%
Sloping Walls - Angle from Horizontal (degrees)	70	70	70
Exposed Acid-Generating Sulfur (g S/m^2)	48	64	144
Exposed Neutralization Potential (g $CaCO_3$/m^2)	225	100	25
Reactive Surface (m^2) for each m^2 of Pit Wall	21	41	41
Fracture Flushed: - percentage flushed monthly	28%	28%	28%
- percentage flushed once a year	2%	2%	2%
- percentage not flushed during operation	70%	70%	70%

site-specific data for predicting future drainage chemistry.

The techniques to predict future chemistry from routine monitoring data are relatively simple. In fact, they have already been discussed in detail in Section 4.2 and summarized as empirical drainage-chemistry models (e.g., Table 4.2.5-2). In other words, predictions are based on past trends under the assumption that the trends will continue to repeat. Empirical drainage-chemistry models simplify predictions to the estimation of only one or two parameters like pH. Previous subsections (Sections 5.2, 5.3, and 5.4.1) discussed techniques to predict pH, and the following Section 5.5 refines the techniques based on variable exposure to water and air.

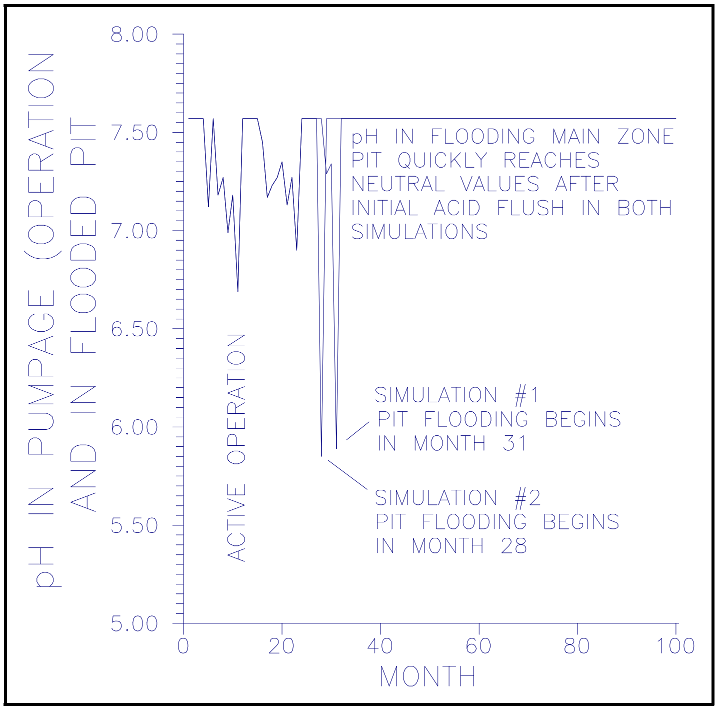

FIGURE 5.4.2-1. Best-Fit Simulation of pH in the Main Zone Pit During Operation and Decommissioning (from Morin, 1990b).

5.5 Adjustments of Static and Kinetic Tests for Full-Scale Minesite Components

The previous sections of Chapter 5 have focussed on various static and kinetic tests to assess or predict mineral balances and reaction rates. For some types of drainage, this information may require adjustment for conditions within each full-scale minesite component. One key adjustment of primary-mineral rates (Rate1, Figure 4.2.2-1) for sulfide-generated acidic drainage (Section 4.2.3) is the availability of oxygen, although residence time of water and partial pressure of carbon dioxide can sometimes also be important. Adjustments for flowrate are not often important for most drainages, except for the basic need for measurable drainage, because concentrations are not often strongly dependent on flowrate (Section 4.2.6). Adjustments for ranges in particle size are only needed where gravel to boulders represent a large proportion of a component (Section 5.3.1 and Table 5.3.1-1).

The weathering and oxidation rates of many primary minerals (Rate1) are often dependent in part on the amount of oxygen in their vicinity. Most kinetic tests allow full exposure to air and oxygen, and thus their reaction rates reflect unlimited oxygen for oxidation and weathering. Predictions from static tests like acid-base accounting (Section 5.2.1.2) are also based on the assumption of unlimited oxygen. Therefore, predictions based on these tests must be adjusted when portions of a minesite component are, or are expected to be, (1) composed of fine-grained particles which limit the transport of air or (2) completely saturated or submerged beneath water.

A major exception to this issue of oxygen availability is minerals from evaporite mining like potash (Case Study 4.2-3). In this case, the simple contact of any waters with the salts for a relatively short period is sufficient to cause dissolution to equilibrium (Rate1=Rate2, Figure 4.2.2-1).

Some caution must be exercised in the following rate adjustments. The adjustments are primarily based on oxygen transport and availability. However, there are other oxidants present in minesite drainage, particularly ferric iron, but published literature is contradictory on whether ferric iron can oxidize minerals in the absence of oxygen (e.g., Morin, 1993). For simplicity, the effects of other oxidants are not considered in the following subsections, but should be included where justified. Also, the following adjustments may be irrelevant in some cases, because dissolution rates of some secondary minerals like calcite and gypsum are generally independent of oxygen availability and respond to equilibrium conditions (Section 4.2).

5.5.1 Portions of Components Exposed to Air and Water

The supply rate of air with gaseous oxygen into a component can be the result of (1) transport, or convection, through minesite components or (2) slow diffusion in the absence of convection. No matter which process controls the transport, there are two basic outcomes, or “scenarios”. With Scenario1, the supply rate of oxygen (RateS) exceeds the consumption rate (RateC), and measurable gaseous oxygen exists continuously near the minerals. For Scenario 2, the consumption rate equals or exceeds the supply rate (RateC $\geq$ RateS), gaseous oxygen is then virtually depleted in the vicinity of the minerals, and primary-mineral rates eventually reflect the supply rate of oxygen (RateC = RateS).

For portions of minesite components that fulfill, or are predicted to fulfill, Scenario 1, no adjustments of kinetic rates from Section 5.3 and 5.4 are necessary for predictions. The predictions from static and kinetic tests are consistent with ample oxygen availability.

For Scenario 2 with RateC $\geq$ RateS and no nearby supply of oxygen (RateS = 0), reaction rates can be set to zero for predictions. This is based on observations that oxidation rates contributing to oxidation decrease sharply or virtually cease below a certain gaseous oxygen level, often reported around 0.1-1.0 %O_2. For example, Myerson (1981) reported 0.3-0.4 mg O_2/L as the limiting level for oxidation by *Thiobacillus ferrooxidans*, and Morin (1993) reported on studies suggesting that zero-order, linear, second-order, and higher relationships of oxidation rate to oxygen level are possible. The assumption of reaction-rate independence above 1% O_2, with no reaction below that level, is generally acceptable for approximate predictions, even when there is some linear dependence. Therefore, the following simplified calculations assume this to be the case.

As explained above, there is some disagreement on the extent that other oxidants, like ferric iron, can oxidize minerals in the absence of oxygen. If this a concern, RateS can be increased by adding the availability of other oxidants to that of oxygen and then the portions of each component falling under Scenario 1 can be reevaluated.

For detailed predictions of Rate1 (Figure 4.2.2-1), the total weight of portions of a component that will have measurable gaseous oxygen nearby is multiplied by rates from humidity cells:

$$\text{Rate1} = \text{OWT} * \text{RHC} \qquad (5.5.1\text{-}1)$$

where Rate1 = total reaction rate of a minesite component in units of mg/wk (see Figure 4.2.2-1)
OWT = total weight of oxidizing material (Scenario 1: RateC < RateS) in the component in units of kg
RHC = humidity-cell rate for acidic or near-neutral conditions in units of mg/kg/wk

As an example, a near-neutral RHC for copper of 25 mg Cu/kg/wk and a OWT of 5,000,000 t from a 30,000,000 t waste-rock dump would provide a Rate1 for the dump of:

$$\begin{aligned} \text{Rate1} &= \\ &= 5{,}000{,}000{,}000 \text{ kg} * (25 \text{ mg Cu/kg/wk}) \\ &= 1.25\text{x}10^{11} \text{ mg Cu/wk} \\ &= 125 \text{ t Cu/wk} \qquad (5.5.1\text{-}2) \end{aligned}$$

A different RHC may apply if the reactive portions became acidic or alkaline and, as a result, Rate1 for the dump would not be constant through the First Stage as suggested by Figure 4.2.2-1.

If desired, Rate1 can be converted to a hypothetical concentration by division with the expected flowrates through the reactive portions, e.g.:

$$\begin{aligned} \text{Rate1}_{\text{conc}} &= \\ &= 1.25\text{x}10^{11} \text{ mg Cu/wk} * 10{,}000{,}000 \text{ L/wk} \\ &= 12{,}500 \text{ mg/L} \qquad (5.5.1\text{-}3) \end{aligned}$$

This concentration of copper is not possible at most minesites, even those with acidic drainage. As a result, one or more secondary copper minerals will precipitate, and the remaining aqueous copper at equilibrium will become Rate2 (Rate2 << Rate1, Figure 4.2.2-1):

$$\text{Rate2} = \text{EQC} * \text{Flow} \qquad (5.5.1\text{-}4)$$

where Rate2 = total release of a component through drainage in units of mg/wk (see Figure 4.2.2-1)
EQC = secondary-mineral equilibrium concentration in mg/L
Flow = total flow through reactive portions of the component in units of L/wk

The amount of retention can then be calculated from:

$$\%\ \text{Retention} = [(\text{Rate1}-\text{Rate2})/\text{Rate1}]*100\% \qquad (5.5.1\text{-}5)$$

For the preceding example, if equilibrium copper were 200 mg/L, then Rate2 would be $2.0\text{x}10^9$ mg Cu/wk (200 mg/L * 10,000,000 L/wk). As a result, the amount retained in the component would be 98.4%, which is typical of higher levels of observed retention (Sections 4.4 and 5.2.4).

Although overlooked above, a critical issue in the prediction of air-exposed portions of minesite components is estimating the portion of a component that will be in contact with oxygen. Anticipated air exposure varies with the type of component (Table 2.1-1) and its physical and chemical composition. Nevertheless, there are a few general expectations (Table 5.5.1-1). For example, in coarse-grained waste rock without covers (Sections 6.2 and 6.3) and in open-pit walls, a reasonable assumption is 100% exposure to air. For underground workings, oxygen availability depends on the layout and ventilation of the workings, so estimates of oxygen availability may be difficult in inactive workings. However, active workings will normally have full oxygen levels for the health of miners.

Internal monitoring of components have shown where portions are poorly aerated (e.g., Case Studies 4.4-2, 4.5-2, and 4.5-4). This typically appears as decreasing oxygen levels with increasing depth or simply as no detectible oxygen. An oxygen gradient with depth is often attributed to diffusion, although slow convection is a possibility that is frequently ignored for unknown reasons. In any case, depths of oxygen diffusion, and thus thicknesses of material in contact with sufficient oxygen for reaction, can be easily estimated with simple equations as illustrated below. More complex models and equations for diffusion are available, but their assumptions, boundary conditions, requirements of infrequently measured input data, and missing processes like barometric pumping do not make their predictions any more reliable.

One difficulty with predicting oxygen diffusion is that there is no agreement in published literature on whether the rate of sulfide oxidation is independent of, linear to, or some power of oxygen level, as discussed above. Again, the following approach is based on oxygen independence with zero rate below some small value like 0.1 or 1.0% O_2.

A column of material in a component, with 1 m^2 lateral area, is conceptually oriented parallel to the path of oxygen diffusion, which is simplified to vertical here (Figure 5.5.1-1). When material has been deposited in the component, diffusion begins to carry oxygen into the upper part of the column (dZ1). This diffusion is regulated by an effective coefficient for oxygen (D) in the material (e.g., Table 5.5.1-2). By definition, the coefficient must lie between the diffusion coefficient of oxygen in air (approximately $1.8\text{x}10^{-5}$ m^2/s) and the diffusion coefficient of oxygen in water (approximately $2.1\text{x}10^{-9}$ m^2/s), with some adjustment for porespace tortuosity, degree of saturation, and other factors. For coarser portions of minesite components that are partially unsaturated, reported values are often in the higher range around 10^{-7} to 10^{-6} m^2/s.

In a simplified adaptation of Fick's First Law of Diffusion (e.g., Freeze and Cherry, 1979):

$$F = D * {}^{dC}/_{dZ1} * TC \qquad (5.5.1\text{-}6)$$

where F = flux of oxygen in units of mol O_2/m^2/wk
D = effective diffusion coefficient of gaseous oxygen within a minesite component in

TABLE 5.5.1-1
General Extent of Air Exposure for Typical Minesite Components

Component	Typical Air Exposure
Open Pits	fully aerated
Underground Workings	fully aerated unless sealed or inactive
Waste-Rock Dumps	fully aerated if coarse; limited oxygen if fine grained
Ore and Low-Grade Ore Stockpiles	fully aerated if coarse; limited oxygen if fine grained
Tailings Impoundments	limited oxygen unless coarse grained
Roads	fully aerated unless sealed
Dams	fully aerated unless fine grained
Disturbed-Rock Foundations for Buildings	fully aerated unless sealed

units of m^2/s (see Table 5.5.1-2)
dC = change in concentration of O_2 from atmospheric to zero in units of mol O_2/m^3 (approximately 8 mol O_2/m^3)
dZ1 = initial depth from the open atmosphere to no oxygen in m (to be calculated)
TC = conversion factor of seconds in one week (604,800 s/wk)

Based on the vertical column of material (Figure 5.5.1-1), the initial total volume of material in this column that would oxidize according to Equation 5.5.1-6 is dZ1 m^3.

The column is assumed to contain sulfide minerals capable of oxidizing in the presence of oxygen. Based on rates from kinetic tests, the consumption of oxygen by a certain weight of material in the column is (Morin and Hutt, 1993b):

$$O2C = RHC * Weight * Conv * Ratio \quad (5.5.1\text{-}7)$$

where O2C = consumption rate of oxygen in units of mol O_2/wk/column; the column has a lateral area of 1 m^2 (Figure 5.5-1)
RHC = humidity-cell rate for applicable pH conditions through time in units of mg SO_4/kg/wk
Weight = weight of material oxidizing at RHC to consume all oxygen in the column in units of kg (to be calculated)
Conv = conversion factor for mg SO_4 to moles S (1/96000)
Ratio = ratio of sulphur in moles to oxygen in moles according to the standard pyrite equation (15/8)

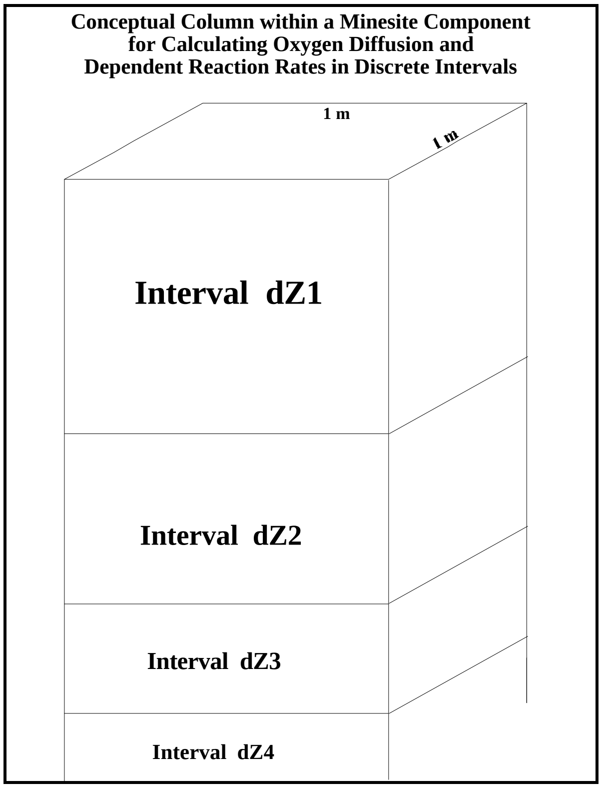

FIGURE 5.5.1-1. Conceptual Column for Calculating Oxygen Diffusion and Depth of Oxidation.

TABLE 5.5.1-2
Examples of Values and Equations for Effective Diffusion Coefficients for Gaseous Oxygen Within Mine-Component Materials

Material	Value (m^2/s) or Equation	Reference
Waste-rock column, Woodlawn Mine, Australia	7.86×10^{-7}	Jeffery et al. (1988)
Waste-rock dump, Woodlawn, Australia	$3.49\text{-}5.07 \times 10^{-6}$	Ritchie (1994)
Waste-rock dump, Aitik Mine, Sweden	$2.25\text{-}6.85 \times 10^{-6}$	Ritchie (1994)
Waste-rock dump, Heath Steele, Canada	$2.65\text{-}3.35 \times 10^{-6}$	Ritchie (1994)
Tailings	$D_{eff} = JD_a^o(1-S)^{"} + JD_w^o/H$ where D_{eff} = effective diffusion coefficient (m^2/s) J and " = fitting parameters from laboratory column data of tailings from an Ontario minesite (J = 0.27 and " = 3.27) D_a^o = coefficient for free diffusion of oxygen in air (1.78×10^{-5} m^2/s) D_w^o = coefficient for diffusion of oxygen in water (2.1×10^{-9} m^2/s) S = dimensionless degree of water saturation (dry = 0.0 to saturated = 1.0) H = modified dimensionless Henry's constant (26.32 at 10°C)	David and Nicholson (1995)
Tailings	$D_{eff} = 3.98 \times 10^{-7}[(G-0.05)/0.95]^{1.7}T^{1.5}$ where D_{eff} = effective diffusion coefficient (m^2/s) G = gas-filled pore space T = temperature (K)	Stuparyk et al. (1995)

When the constants are inserted into Equation 5.5.1-7, the result is:

$$O2C = 1.95 \times 10^{-5} * RHC * Weight \qquad (5.5.1\text{-}8)$$

To estimate the initial depth of oxidation, Weight in Equation 5.5.1-8 is related to dZ1 in Equation 5.5.1-6 through bulk density:

$$Weight = DENS * dZ1 \qquad (5.5.1\text{-}9)$$

where Weight = weight of oxidizing material in kg oxidizing in a column of 1 m^2 lateral area (to be calculated, see Equations 5.5.1-7 and 5.5.1-8)

DENS = bulk density of material in units of kg/m^3

dZ1 = depth from the open atmosphere to no oxygen in m (to be calculated, see Equation 5.5.1-6)

Substituting Equation 5.5.1-9 into 5.5.1-8 and equating F (Equation 5.5.1-6) with O2C (Equation 5.5.1-8) yields:

$$dZ1 = 4.98 \times 10^{5} * [D/(DENS * RHC)]^{0.5} \qquad (5.5.1\text{-}10)$$

As a result, this equation provides a rough estimate of the initial thickness of oxidizing material and is similar to one developed by Gibson et al. (1994) for the same situation in fine-grained waste rock.

This thickness multiplied by the total lateral area of reactive portions provides the total oxidizing volume and weight (= volume * DENS) within a component. In turn, Rate1 and Rate2 can then be determined from the total weight with Equations 5.5.1-1 and 5.5.1-4.

Through time, the uppermost dZ1 is eventually exhausted of oxygen-consuming minerals. As a result, oxygen then moves deeper and initiates oxidation in the next interval (dZ2). To estimate dZ2, Equation 5.5.1-6 must be adjusted to:

$$F = D * {}^{dC}/_{(dZ1+dZ2)} * TC \qquad (5.5.1\text{-}11)$$

Equation 5.5.1-9 must then be adjusted to:

$$Weight = BD * dZ2 \qquad (5.5.1\text{-}12)$$

When these adjusted equations are combined, Equation 5.5.1-10 becomes a quadratic equation:

$$(dZ2)^2 + dZ1dZ2 - 2.48 \times 10^{11} * D/(DENS * RHC) = 0 \qquad (5.5.1\text{-}13)$$

in which only dZ2 is unknown. This equation and, in turn, those for the deeper intervals (dZ3, dZ4, etc.) can be solved as quadratic equations. This typically shows that the thickness of the active interval decreases with depth. Also, the depletion time for sulphide minerals for each interval can also be calculated based on initial sulphide content and the reaction rate (RHC). Gibson et al. (1994) reported less applicable equations for subsequent thicknesses, which for example fail at thicknesses less than 1 m. A plot of time vs. oxidation depth typically shows that the migration rate of the oxidation front (bottom of oxidizing interval) slows with time and eventually becomes negligible.

The thickness of the active dZ interval multiplied by lateral area will provide an estimate of Rate1 (Figure 4.2.2-1) at a particular time, which also decreases as the thickness of the interval decreases with depth. If this Rate1, when divided by flow through the zone, has a concentration less than secondary-mineral solubility, then Rate2 will equal Rate1 and no secondary minerals will form. If Rate1 exceeds Rate2, secondary-mineral retention will occur (Equation 5.5.1-5). For acidic drainage, if the depletion front of NP does not reach the bottom of the component by the time the oxidation-front migration becomes negligible, then acidic drainage from the component is not expected.

5.5.2 Portions of Components Exposed to Water Only

A portion of a minesite component subjected to full porespace saturation or submergence beneath water (e.g., Section 6.3) is exposed to conditions very different from those used or assumed in most static and kinetic testing. As a result, adjustments in the results of standard tests, or the initiation of non-standard tests, are needed. In this section, the adjustments of information from standard tests are addressed.

Initially upon saturation or submergence, a rapid rinsing of retained soluble minerals will occur, causing short-term peaks in concentrations in surface and ground waters. If the component has been exposed to air for some time, the level of retained secondary minerals could be high and thus high concentrations could persist for weeks to years. If the component contains high levels of soluble primary minerals, the elevated concentrations can last for decades to centuries. The static retention test (Section 5.2.4) and early data from kinetic tests (Sections 5.3 and 5.4) can be used to predict the effects of initial rinsing. After the initial peak concentrations have subsided, slower oxidation and/or metal-release rates will prevail and should be predicted separately.

The two basic predictive targets for a submerged component are (1) its porewaters and (2) any surface water lying above it. Laboratory and field studies have shown that overlying water can be affected by transport or diffusion of porewaters upwards if hydraulic gradients are upwards or negligible (Section 6.3), so predictions should focus on porewaters. After that, if porewater movement is upwards through convection or diffusion, then the chemistry of overlying waters can be estimated with information on surface-water residence times and volumes (see also Figure 6-2).

Morin (1993) pointed out that unless the particle size of a component is less than some tailings, approximately 10-50 µm, then dissolved oxygen is supplied primarily by advection of water through, rather than by diffusion into (Section 5.5.1), the component. This is consistent with general knowledge that diffusion is important only where advection is virtually undetectable (e.g., Freeze and Cherry, 1979). Consequently, physical factors like hydraulic conductivity and hydraulic gradients will often determine the extent of long-term oxidation and metal release into a liter of porewater, rather than the diffusion coefficient of oxygen in water (2.1×10^{-9} m^2/s).

Oxygen can dissolve into water to maximum saturation levels of 8 to 12 mg/L (Table 5.5.2-1). The standard equation for pyrite oxidation by oxygen (Equation 4.2.3-1) shows that the maximum amount of sulphate and acidity that would be created by 10 mg/L of dissolved oxygen is 16 mg SO_4/L and 17 mg $CaCO_3$/L, respectively. Therefore, if there is no other oxygen supply to a liter of water and no entrained air bubbles, then acidic conditions cannot develop if alkalinity exceeds the generated acidity of 17 mg $CaCO_3$/L. If ferric iron contributes to sulphide oxidation, then its effect must be included. However, at near-neutral pH levels, the aqueous concentrations of ferric iron are often low and thus minor in importance compared with dissolved oxygen.

In situations where advection of groundwater is virtually zero and diffusion dominates, an approach differing from the preceding simple mass balance is needed. Based on several references, Morin (1993) derived equations for the diffusion of dissolved oxygen into a submerged column of mine materials (Figure 5.5.2-1) and for oxygen concentration at depth.

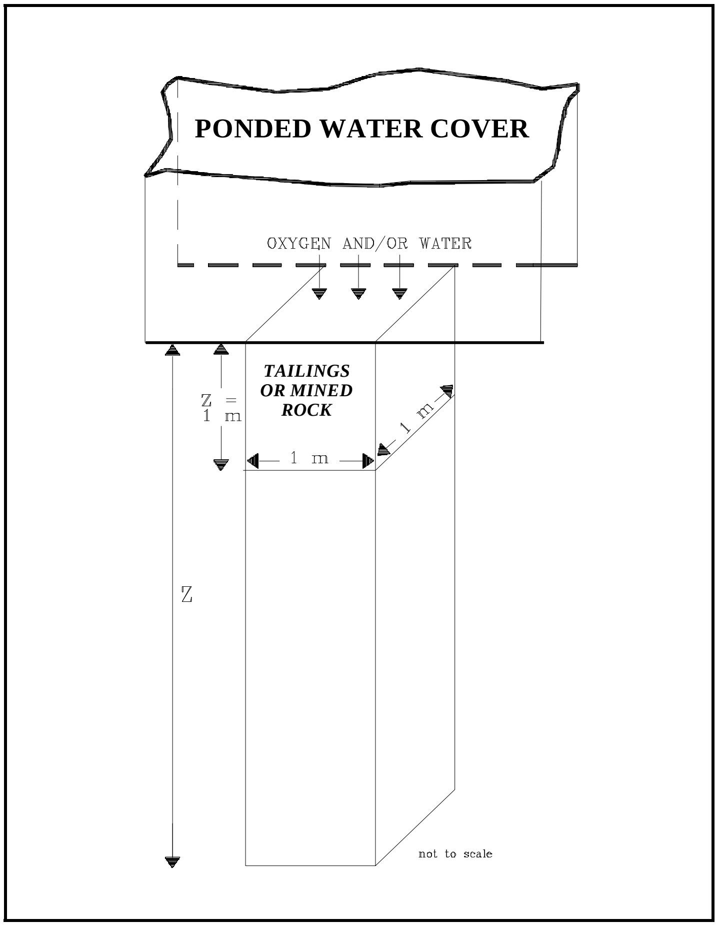

FIGURE 5.5.2-1. Conceptual Submerged Column for Calculating Oxygen Diffusion (adapted from Morin, 1993).

TABLE 5.5.2-1
Saturation Concentrations of Dissolved Oxygen in Water
Based on Temperature and Percentage of Oxygen in the Adjacent Gas Phase[1]
(from Otwinowski, 1994)

T (^{o}C)	Dissolved Oxygen Concentration at Saturation (mg O_2/L)				
	$[O_2]_{gas}$=21%	$[O_2]_{gas}$=15%	$[O_2]_{gas}$=10%	$[O_2]_{gas}$=5%	$[O_2]_{gas}$=1%
5	12.79	9.60	6.02	2.92	0.50
10	11.3	8.03	5.31	2.59	0.41
15	10.11	7.16	4.72	2.27	0.32
20	9.12	6.45	4.23	2.01	0.23
25	8.30	5.86	3.77	1.82	0.14
30	7.60	5.33	3.44	1.56	0.05
35	7.00	4.88	3.12	1.43	0.00
40	6.47	4.47	2.81	1.15	0.00
45	6.00	4.10	2.52	0.94	0.00
50	5.57	3.75	2.25	0.74	0.00
55	5.17	3.55	1.96	0.50	0.00
60	4.89	3.38	1.64	0.25	0.00

[1] calculated by Otwinowski (1994) from various references; water is at atmospheric pressure (1013.25 Pa); best-fit equation is: Diss. O_2 (moles/m^3 water) = $(Y/2.8)^{1.05}(283/T)^{(4.1+9.38/Y)}$, where Y = moles O_2/m^3 air and T in Kelvin.

These equations are:

$$J = 8.2\text{x}10^{-7}\ DO(pond)\ [(n-n^2)\ \text{x}\ \%PYR\ /\ (d\ \text{x}\ T)]^{½} \qquad (5.5.2\text{-}1a)$$

$$DO(z) = DO(pond)\ \exp\{-z\ [0.17\ \text{x}\ \%PYR\ \text{x}\ (1-n)\ \text{x}\ T\ /\ (d\ \text{x}\ n)]^{½}\} \qquad (5.5.2\text{-}1b)$$

where J = flux of dissolved oxygen into a 1 m^2 vertical column of tailings/rock (Figure 5.5.2-1) at the water/material interface (mg O_2 m^{-2} s^{-1})
DO(z) = concentration of dissolved oxygen at depth z below the water/material interface (mg O_2 L^{-1})
z = depth below water/material interface (m)
DO(pond) = concentration of dissolved oxygen in the overlying pond (mg O_2 L^{-1})
n = porosity (dimensionless)
%PYR = percentage of pyrite in material
d = particle diameter (m)
T = tortuosity (dimensionless; assume a value of 3 for rock and 5 for tailings)

Also, rates of pyrite consumption and acid generation can be determined within the 1 m^2 vertical column (Figure 5.5.2-1) for a specific value of J:

$$CP = FACTOR1 \times J \qquad (5.5.2\text{-}2)$$

where CP = rate of pyrite consumption in the 1 m^2 vertical column of tailings/rock ($mgFeS_2\ m^{-2}\ s^{-1}$)
FACTOR1 = factor based in part on ratio of oxygen and pyrite in Equation 4.2.3-1;
=1.00 (corrected from Morin, 1993)

and

$$ACP = FACTOR2 \times J \qquad (5.5.2\text{-}3)$$

where ACP = rate of acidity production in the 1 m^2 vertical column of tailings/rock ($mg\ CaCO_3$ equivalent $m^{-2}\ s^{-1}$)
FACTOR2 = factor based in part on ratio of oxygen and to acidity in Equation 4.2.3-1;
= 1.67 for 2 mol H^+ represented by 1 mole $CaCO_3$;
= 3.33 for 1 mol H^+ represented by 1 mole $CaCO_3$

For types of drainages that are not affected by oxygen availability, residence times of porewaters will be relatively high in submerged materials with a low hydraulic conductivity and thus equilibrium chemistry may be approached or attained. This chemistry can be predicted based on methods discussed in Sections 4.2. On the other hand, if residence times are low due to high hydraulic conductivities or gradients, then kinetic conditions (Table 4.2.1-1) may apply. In this case, chemical reaction rates from submerged samples as well as physical groundwater flowrates will then be required to predict porewater chemistry. In other words, the concentration obtained from diagrams similar to Figure 4.2.1-1 will depend on the site-specific combinations of physical and chemical parameters.

5.6 Questions

5-1. From the ABA Data Table on the next page, calculate TNNP, SNNP, TNPR, and SNPR for the three samples. Are the paste pH values consistent with the predictions from the xNNP and xNPR values? If not, what could account for the discrepancies?

5-2. In the mature-stage diagrams of Figure 5.2.1-5, why are neutral or alkaline values of paste pH sometimes obtained from samples with NP less than the Unavailable NP?

5-3. If no spatial correlation occurs among ABA parameters over distances greater than 50 m (Case Study 5.2.1-6), what is the minimum number of ABA samples needed to carry out kriging and block modelling for a proposed cubic (simplistically shaped like a cube) pit 2 km by 1 km by 300 m deep?

5-4. If the long-term stable rate of sulfide oxidation in a humidity cell is 50 mg SO_4/kg of sample/week, how long can a sample containing pyrite at 1%S continue generating acidity? If this sample also contains 30 ppm selenium leaching steadily at 0.01 mg/kg/wk, when will the selenium be depleted?

5-5. For Hypothetical Mined-Rock Pile “C” (Questions 3-7 and 3-8 in Chapter 3), the copper production rate (Rate1) is 0.17 mg/kg/wk. If only 10% of the rock occurs in a fine grain size typical of a humidity-cell sample and the remaining 90% of coarser material makes little contribution, what is the total production of copper for the entire pile in units of t/yr? If average annual precipitation is 2 m/yr and the average annual copper concentration in drainage (Rate2) is 0.5 mg/L, what is the total release rate of copper in units of t/yr? What is the retention factor of copper in this pile? What processes can account for this retention?

5-6. A stabilized humidity cell produces 50 mg Ca/kg/wk and 40 mg Mg/kg/wk due to dissolution of dolomitic minerals, driven by acid generation at a rate of 100 mg SO_4/kg/wk. What is the carbonate molar ratio for this sample? If

ABA DATA TABLE FOR QUESTION 5-1

Sample ID	Paste pH	Total Sulfur (%S)	Sulfide (%S)	NP (t $CaCO_3$/1000 t)
Sample 1	4.3	1.3	0.5	18
Sample 2	8.1	3.7	3.2	45
Sample 3	10.2	0.3	0.2	300

the sample initially contains an Effective Neutralization Potential of 27 t $CaCO_3$/1000 t, when will the NP be depleted?

5-7. A sample identical to that in Question 5-6, including identical weight, is placed in a laboratory column and receives insufficient rinsing to remove all weekly reaction products. As a result, 86 mg/kg/wk of gypsum ($CaSO_4 \cdot 2H_2O$) precipitates within the column. What would be the apparent carbonate molar ratio and acid-generation rate based on the effluent chemistry? When will the Effective Neutralization Potential be depleted based on the effluent chemistry?

5-8. A humidity cell representative of $1x10^6$ t of fine-grained waste rock yields a stabilized acid-generation rate of 135 mg SO_4/kg/wk. What is the total production of acidity in t/yr? When this rock is submerged, $1x10^8$ L of water in equilibrium with air (21% O_2) at 5°C moves through this rock annually. What is the total production of acidity for the submerged condition in t/yr?

CHAPTER 6
CONTROL OF DRAINAGE CHEMISTRY

This chapter addresses the control of drainage chemistry, that is, the management or adjustment of concentrations carried in waters draining from various minesite components (Table 2.1-1). The most important observation about control of drainage chemistry is that most techniques are relatively simple in concept, but their detailed design, engineering, and implementation can be difficult, expensive, and/or prone to failure, as demonstrated in the following subsections. The practical theory in this chapter focusses on the basic concepts and techniques behind the control of chemistry, rather than detailed design and engineering which is site dependent.

There are two basic types of drainage control: reactive and proactive. Reactive control allows a minesite component to generate its drainage chemistry, the drainage is then collected and treated, and the waste products from treatment like metal precipitants ("sludge") are disposed. Long-term stable disposal of treatment waste is a major problem with reactive control because the treated contaminants are more concentrated.

Proactive control adjusts physical, chemical, and/or biological conditions within a component to create lower concentrations in the drainage as it leaves the component. Any waste products from proactive control are created and retained within the component, which may cause drainage chemistry to evolve differently from standard scenarios (e.g., Figure 4.2.2-1). Because proactive control of most drainages is rarely successful to the degree needed for open discharge to the surrounding environment, some reactive control is frequently included or planned as a contingency. Because of (1) costs for this backup reactive control, (2) the lag time before proactive measures become effective, and (3) the risk of failure of proactive controls (e.g., Case Study 6.2-2), the cost for reactive control alone may be lowest (Geocon, 1995).

On the other hand, two simplified examples illustrate proactive control of drainage and the value in "drainage-chemistry design" of control techniques. In the first example (Figure 6-1), a solid clay cover (Section 6.2) will be placed on a waste-rock dump releasing an aqueous metal. The metal concentrations in seepage and runoff have been characterized using the approaches in Chapters 4 and 5 and are 50 and 0.01 mg/L, respectively. Therefore, to achieve the regulatory release level of 0.5 mg/L without additional reactive control, the clay cover must allow less than 1% of unevaporated rainfall into the dump ($Flow_{runoff}/Flow_{drainage} > 101$). Practical issues like delay of seepage through waste rock (Section 3.3) and degradation of the clay cover through time complicate this scenario.

In the second simplified example (Figure 6-2), tailings under a water cover (Section 6.3) are releasing dissolved metals into the overlying water through diffusion (Sections 5.5.1 and 5.5.2). Because the release rate is partly dependent on the concentration gradient, the thicker the inert cover, the less the release rate, and the less the concentration in the water cover. In this example, a thickness less than 0.2 m would lead to an exceedance of the allowable concentration in the water. Practical issues like porewater advection, cover integrity, and seasonal water-level fluctuations will complicate this scenario.

6.1 Reactive Control of Drainage Chemistry

6.1.1 Active Collection and Treatment

The first step in reactive control is the secure collection of surface and subsurface drainage. Tallin et al. (1990) described methods for collecting contaminant-laden surface and ground waters in and around a component:

Ø Diversion ditching - control of runoff water and surficial seepage;
Ù Basal liners - reduction of seepage into the ground water system, leading to increased flow to surface drainage;

Water Balance:

$$\text{Rain} - \text{Evapotranspiration} = \text{Flow}_{\text{runoff}} + \text{Flow}_{\text{seepage}} = \text{Flow}_{\text{drainage}}$$

Chemical-Loadings Balance:

$$\text{Conc}_{\text{drainage}} = (\text{Conc}_{\text{runoff}}*\text{Flow}_{\text{runoff}} + \text{Conc}_{\text{seepage}}*\text{Flow}_{\text{seepage}})/(\text{Flow}_{\text{runoff}} + \text{Flow}_{\text{seepage}})$$

Example:

Max. $\text{Conc}_{\text{drainage}}$ allowed = 0.5 mg/L
Measured $\text{Conc}_{\text{runoff}}$ = 0.01 mg/L
Measured $\text{Conc}_{\text{seepage}}$ = 50 mg/L
What is the minimum allowable ratio of $\text{Flow}_{\text{runoff}}:\text{Flow}_{\text{seepage}}$ that will not exceed the maximum permissible $\text{Conc}_{\text{drainage}}$?

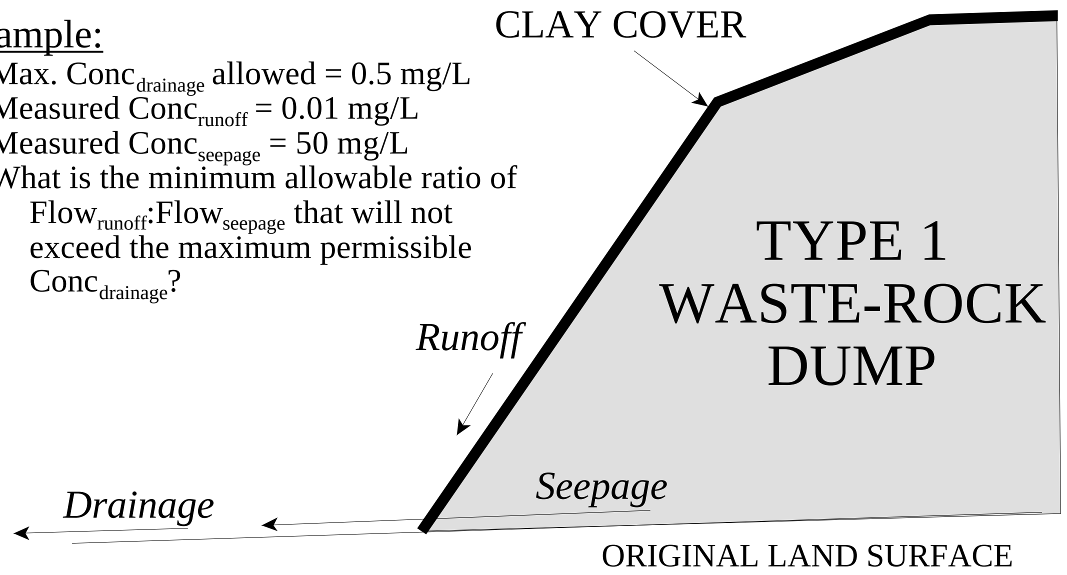

FIGURE 6-1. Example of Designing Drainage-Chemistry Control with a Clay Cover.

Chemical-Loadings Balance (assuming diffusion only):

$$\text{Conc}_{\text{water}} = [\text{Diff. Coeff.}_{\text{inert cover}} * (\text{Conc}_{\text{tailings}} - \text{Conc}_{\text{water}})/\Delta z * \text{Residence Time}_{\text{water}}]*\text{Area}_{\text{tailings}}/\text{Volume}_{\text{water}}$$

Example:

Max. $\text{Conc}_{\text{water}}$ allowed = 0.1 mg/L
Diff. Coeff. $_{\text{inert cover}}$ = 10^{-6} m^2/s
Measured $\text{Conc}_{\text{tailings}}$ = 100 mg/L
Residence Timewater = 10^5 s
$\text{Area}_{\text{tailings}}$ = 10^5 m^2
$\text{Volume}_{\text{water}}$ = $5x10^7$ L
What is the minimum allowable thickness of the inert cover (Δz) that will not exceed the maximum permissible $\text{Conc}_{\text{water}}$?

FIGURE 6-2. Example of Designing Drainage-Chemistry Control with Inert-Soil and Water Covers.

Ú Cutoff walls - “cutoff walls consist of a trench excavated through a permeable strata [sic] and backfilled with a low-permeability material, thus preventing lateral spreading of contaminants through the strata”, which lead to either the need for pumping the trapped groundwater, the redirection of groundwater, or the increase in surface drainage;

Û Interceptor ditches - ditches to divert or collect subsurface seepage through a dike or contamination moving within an aquifer;

Ü Buried drains (subsurface collector drains) - a perforated pipe buried in a trench, surrounded by sand and gravel, which act as a filter between natural soil and the pipe;

Ý Containment wells (“hydrodynamic containment”) - “developing a ground water sink below the disposal site by pumping from one or more wells situated in an aquifer beneath the site”.

The degree of success of each method depends on site-specific conditions. One method, or a combination, can be implemented to reduce the loss of drainage to the surrounding environment. Once the drainage is collected, it is pumped or gravity-drained to a treatment plant.

Murdock et al. (1995) reported that various methods are available for actively treating drainage chemistry at flow rates on the order of 1000 L/min, including carbon adsorption, ion exchange, reverse osmosis, electrodialysis, and ozonation. Where concentrations are controlled by pH (e.g., Figure 4.2.5-1 and 4.2.5-2), pH adjustment toward neutral values results in lower concentrations. For acidic drainage, this involves the addition of lime or limestone. Where concentrations are regulated by equilibrium conditions (Figure 4.2.1-1) but are not significantly affected by pH, the addition of another compound can lower the target element. For example, the dissolution of any calcium compound in gypsum-saturated drainage will cause sulfate concentrations to decrease.

Of the alternatives for acidic drainage, lime/limestone treatment is the most common and preferred method, because it (1) is adaptable to a large range of concentrations, (2) is adaptable to a large range of flow, (3) has moderate capital and operating costs, and (4) is generally considered best practical technology. Gunn (1995) reports that even the simple spreading of lime in catchment basins can be beneficial. Other, passive treatment methods are discussed in Section 6.1.2.

Lime (CaO or $Ca(OH)_2$) treatment depends on the reaction:

aqueous metals + aqueous sulfate + lime 6
metal hydroxides + gypsum (6.1.1-1)

The resulting precipitants are often referred to collectively as “treatment sludge”, and gypsum is desirable in the sludge because it improves chemical stability. Also, the metal hydroxides, like $Fe(OH)_3$, formed during treatment assist in scavenging other metals from the drainage. The primary problem with sludge, however, is that is composed mostly of water, sometimes less than 3% solids, that cannot be disposed of in a compact form. As a result, sludge requires anomalously large storage areas and is difficult to handle.

The chemical composition of sludge from treatment ponds can vary considerably depending on the initial chemical composition of the water, the type of treatment process and the added reagents (Ackman, 1982). Disposal of the sludge can depend mostly on its physical characteristics such as settling behavior and the final volume. Depending on reagents and the process, the sludge may range from “granular dense sludge” to “gelatinous voluminous flocs” (Ackman, 1982). Sludge is often placed in specially designed ponds, in secure landfills, or within tailings impoundments as distinct masses or mixed with tailings where it can affect the physical and chemical characteristics of the tailings. Additionally, if the tailings are generating net acidity, the sludge can redissolve and the treated metals will eventually reappear at the treatment plant.

Murdock et al. (1995) reported on methods for increasing the solids content of sludge, generally known as high-density sludge (HDS), which can reach solids contents of 40-50%. This often requires additional steps in the treatment process and a high ratio of aqueous iron to other metals. Examples of successful HDS treatment plants include (1) 11,500 L/min at pH 4, (2) 22,000 L/min at pH 3.5 with approximately 100 mg/L of aqueous iron and zinc, (3) an unspecified flow rate at pH 6.5 with more than 1 mg/L of copper, nickel, and chromium, and (4) an unspecified flow rate at a pigment plant using acid-chloride digestion (Murdock et al.).

Orava et al. (1995) discussed the capital and operating costs for lime treatment and sludge disposal reflecting options like design of the treatment system, flow rate, concentration of acidity, high-density sludge, and pressure dewatering of sludge. Capital and annual operating costs increased with the complexity of the treatment system and sludge dewatering, but disposal costs for sludge decreased with complexity because of the decreased volume of sludge. Orava et al. estimated the net present value for a century of treatment ranged from $13,550,000 to $32,900,000, and sludge disposal added another $1,060,000 to $11,070,000 to the net present cost. These costs were based on a flow rate of 250 m^3/hr, net acidity of 2,000 mg/L, a treatment period of 100 years, and an interest or discount factor of 3%. Costs are discussed further in Case Study 6.1.1-1.

Case Study 6.1.1-1: Relative Costs of Treatment and Control for Acidic Drainage

highlights: common types of reactive and proactive chemical controls; costs of various controls based on field-scale tests; costs per hectare for tailings and per tonne of waste rock

Meek (1994) compared the economics of proactive prevention techniques to collection and treatment for acidic drainage. The field-scale testing of proactive techniques included (1) selective handling and placement including compaction and soil capping, (2) covering with a PVC liner covered with overburden, (3) various blends and layers of limestone and lime, (4) phosphate addition, and (5) a drainage collection trench filled with limestone and soda ash (see also Sections 6.1.1 and 6.2). The results of these techniques have been monitored since mining from 1979 to 1986 and after reclamation, and detailed records have been kept of costs and reagent consumption.

Meek (1994) presented data and trends for the five techniques and the collect-and-treat site (Table 6.1.1-1). The sources of the temporal curves are not explained in detail, but the curves predict negligible acid generation after approximately 15 years. In any case, the most economical approach on a hectare basis was simply collection and treatment — all proactive techniques were more expensive.

Geocon (1995) also summarized costs for reactive and various proactive control techniques (Table 6.1.1-2), based on a number of assumptions and scenarios. Active collection and treatment were least expensive for waste rock and among the least expensive for tailings. Proactive multilayer covers are discussed in detail in Case Study 6.2-6.

Case Study 6.1.1-2: Loss of Injected Alkaline Process Water at a Solution Mine

highlights: loss of process solution at a solution mine; reactive control of lost solution; cause of solution loss

One of the most serious environmental issues in solution mining (Section 2.2 and Figure 2.2-8) is the loss of injected process water into the surrounding geologic strata before it is captured by retrieval wells or workings. This is a consequence of unacceptable levels of compounds or pH in the process water, like an alkaline-cyanide solution for gold, or in the spent process water, like acidic solutions for copper or oxidizing solutions for uranium (e.g., Bell et al., 1983). Lost process water will be attenuated with distance according to the sub-region concept (Section 4.5), but an ongoing loss will lead to an expanding zone of affected groundwater.

The Moser Mine is a uranium solution mine in southern Texas, USA (Yelderman and Durler, 1983). Economic-grade uranium oxide occurred in sands and silts of a Miocene-Age fluvial deposit known as the Oakville Formation, located 100-200 m beneath the surface. The Oakville Formation consists of interbedded coarse- and fine-grained layers, creating in effect a multiple aquifer-aquitard

TABLE 6.1.1-1
Cost Comparison of Five Proactive Prevention Techniques Against Collection and Treatment for Acidic Drainage
(adapted from Meek, 1994)

Technique	Cost (US$/ha)	Technique	Cost (US$/ha)
Collect and treat	$26,900	Quicklime addition	$56,800
Lime addition	$32,900	Phosphate/apatite addition	$38,500
Clay cover and alkaline trench	$50,200	Controlled layering of acid-generating material	$31,400

TABLE 6.1.1-2
Cost Comparison of Reactive and Proactive Control Techniques for Acidic Drainage from Waste Rock and Tailings
(adapted from Geocon, 1995)

WASTE ROCK		
Control Technique	Initial Capital Cost[1] (1994CDN$/t)	Final Total Cost[1] (1994CDN$/t)
Collect and treat (C&T)	0.03-0.16	0.26-0.64
C&T with simple soil cover	0.16-0.55	0.34-0.85
Multilayer soil cover	0.89-1.12	1.07-1.31
Plastic cover (200-yr lifespan)	1.38	1.59
TAILINGS		
Control Technique	Initial Capital Cost[1] (1994CDN$/ha)	Final Total Cost[1] (1994CDN$/ha)
Collect and treat (C&T)	62,000-97,000	214,000-238,000
C&T with simple soil cover	91,000-182,000	200,000-264,000
C&T with partial water cover	93000	225000
Multilayer soil cover	231,000-307,000	291,000-415,000
Multilayer soil cover with partial water cover	223000	303000
Self-sustained water cover	13,000-254,000	71,000-349,000
Maintained water cover	11000	83000
Plastic cover	257,000-297,000	296,000-404,000

[1] Initial Capital Cost includes implementation costs incurred at the time of minesite closure; Final Total Cost includes Initial Capital Cost plus the Net Present Value of costs incurred after minesite closure, like long-term collection and treatment, inspection and maintenance, and plastic-cover replacement.

system. The hydraulic conductivity of the coarse layers ranges from 0.9 to 4.0 m/day, with an average of 2.4 m/day, yielding average linear groundwater velocities around 3-5 m/yr.

The injected process water was an alkaline oxidizing solution that leaches uranium, molybdenum and other metals. The background water chemistry was predominantly composed of sodium and bicarbonate with a near-neutral pH and total dissolved solids of 600-1200 mg/L. This groundwater was the primary source for drinking water for nearby communities, rural homes, and cattle.

Government operating permits established background concentrations and threshold values that would trigger an unacceptable loss (“excursion”) of process water from the ore zone. For example, an increase of sulfate from 35 to above 235 mg/L, or an increase of ammonia from 0.2 to above 5.2 mg/L, would signal a significant loss requiring control and restoration. Monitor wells in aquifers above the ore zone were monitored semimonthly to delineate any changes to groundwater chemistry. Additionally, groundwater levels were monitored continuously and evaluated daily to detect if the hydraulic gradient in the area turned outward, suggesting an excursion.

In April of 1978, an excursion was identified in a shallow, secondary monitor well that had not been sampled for more than two years. Pumping of the well for several days produced unacceptable water, and thus a significant leak was suspected. The installation of two new wells within 30-45 m of the secondary well also yielded lost process water. A nearby suspected injection well, with cracked well casing, was not the source of the leak after various pressurization tests. On May 16, another injection well was identified as the source and repaired. Nearby monitor wells were then pumped to recover the lost process water. By October, all except one well had returned to background levels. The final well was pumped for another 15 months until its chemistry was at background for five consecutive days. The long restoration time was attributed to retardation of ions in groundwater by clays in the formation.

Investigations into the cause of the leakage found that most active monitor wells were installed in the nearest aquifer above the ore zone, under the assumption that any leakage from injection wells would flow into it first. In fact, the leak occurred into the third aquifer above the ore zone, which was not regularly monitored, due to a bend and crack in the casing against a hard sandstone layer extending partially into the borehole.

Case Study 6.1.1-3: Reactive Control of Potash-Tailings Drainage

highlights: example of drainage chemistry from a potash mine; attempts at initial, proactive control; required efforts for reactive control after failure of proactive controls

As explained in Case Study 4.2-3, drainage from potash tailings carries up to hundreds of thousands of mg/L of chloride, sodium, and potassium. The Rocanville potash minesite in southeastern Saskatchewan, Canada, is built over glacial deposits consisting of interbedded, discontinuous strata of coarse-grained sand and gavel and fine-grained till (Hart, 1985). Groundwater and surface-water drainage migrates 2 km to a nearby river whose water chemistry could be significantly degraded if minesite drainage with 160,000 mg/L Cl reaches it.

Rocanville’s tailings pile is more than 60 m high and covers 55 ha with drainage (brine) ponds around the base covering another 33 ha (Hart, 1985). Water inputs to the impoundment are: 700,000 m^3/yr from the mill, 400,000 m^3/yr from precipitation, and 150,000-250,000 m^3/yr of intercepted contaminated groundwater. Water losses are: 1,000,000 m^3/yr to deep-well injection, 150,000 m^3/yr to evaporation, 100,000 m^3/yr retained in the tailings, and an unknown amount lost to underlying aquifers. Deep-well injection, which can be considered a type of active treatment, at depths of 1100-1380 m reportedly has little local effect on water chemistry, because background water at those depths is also a brine.

To prevent the loss of brine to the shallow aquifers, the six zones within the impoundment were consecutively levelled and smoothed over several years, liners were installed, and 30 cm of soil was placed over the liners. The liners began with low-density polyethylene of 6 mil thickness in Zone 1, increasing to high-density polyethylene of 60 mil thickness in Zone 6. None of the liners were reportedly successful at retaining the brine.

A 10-km system of double ditches was built outside the impoundment dikes to capture any lost brine and to relieve groundwater pressure under the fast-rising tailings pile. The outer ditch was intended to collect uncontaminated groundwater. However, by 1985, both the inner and outer ditches were contaminated with brine. Another, freshwater-diversion ditch around the impoundment was mildly contaminated with brine and was thus used as feed water to the mill.

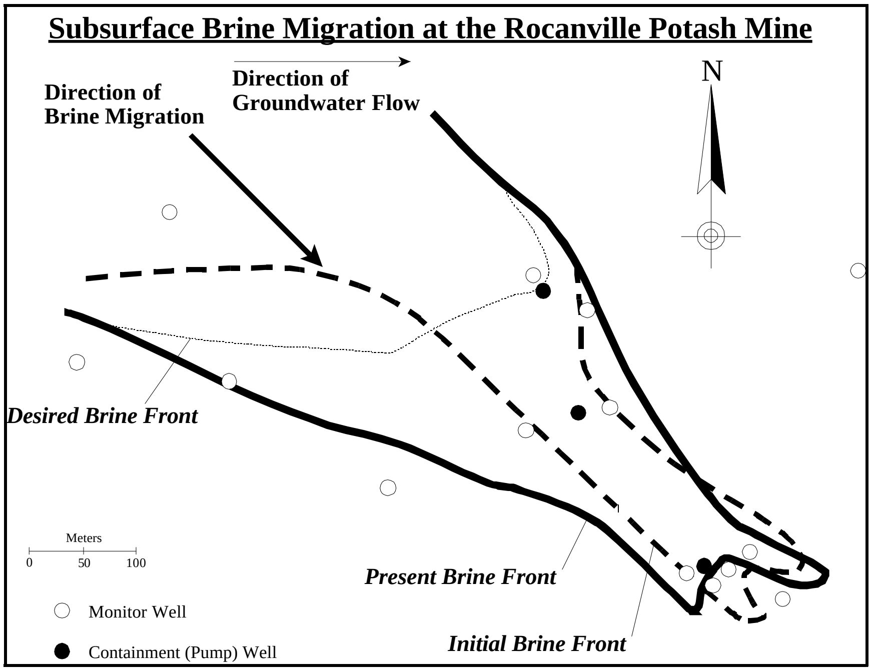

FIGURE 6.1.1-1. Plan View of Subsurface Migration of Potash-Tailings Brine (adapted from Hart, 1985).

A dense brine plume was moving downslope (southeast) at an oblique angle to groundwater flow (east, Figure 6.1.1-1). To control its migration, pump wells were installed and operated at 4 L/s. Although the size of the plume did not change much, the migration of the plume edge slowed from 53 to 3 m/yr. Additional pump wells were anticipated for further control of subsurface brine migration.

One area around a deep injection well was contaminated by brine. This was attributed either to brine spills during construction or leaks from the sumps near the well.

Case Study 6.1.1-4: Remediation Studies at a One-Hundred-Year-Old Minesite

highlights: difficulties in controlling drainage chemistry from a large, old minesite; costs for control defaulting to taxpayers; metal leaching from tailings released into a downstream river

Mount Lyell lies in relatively steep terrain, at approximately 900 m above sea level, near the west coast of Tasmania, Australia. The climate is cool and temperate with 240 days of rainfall a year for an average annual total of 2.5 m. Average annual pan evaporation is estimated at 0.75 m, indicating drainage can be a significant portion of precipitation. Snow and hail can occur in any month.

This copper-silver-gold minesite, covering 13 km^2, has operated almost continuously since 1893 (McQuade et al., 1995; Johnston et al., 1996) and now includes open pits, underground workings, 53x10^6 t of waste-rock dumps, and 100x10^6 t of tailings and smelter slag. The tailings were discharged into the downstream Queen/King River system until 1994 and extend about 20 km into the ocean. A cumulative AUS$4,000,000,000 (1995 dollars) of metals has been mined at Mount Lyell, with costs for control and restoration residing with governments and taxpayers.

Ore units include quartz, sericite, and chlorite with disseminated pyrite and chalcopyrite; massive pyrite and chalcopyrite; native copper in clay; and lenses of pyrite, sphalerite, galena, chalcopyrite, bornite, and chalcocite. Pyrite content exceeds 10% in some waste rock and 6%S in some riverine and deltaic tailings.

Drainage movement through and under the minesite is complex and not well defined, but is predominantly directed into the Queen River. Uncontrolled acidic drainage at pH 2.5-3.5 is currently entering the river, but the riverine tailings reportedly neutralize most of the acidity. Nevertheless, approximately 99% of contaminant loadings (2 t Cu/d) at the ocean are directly attributed to the minesite, whereas the remainder is due to reactions within the riverine and deltaic tailings. Acidic drainage from the waste rock at the minesite is expected to decline gradually, reaching 10% of current levels after 600 years.

Total copper in foreshore ocean waters at Macquarie Harbour are expected to continue decreasing from highs of mg/L because tailings discharge into the river system ceased in 1994 and riverine tailings are stabilizing physically. Nevertheless, deltaic-tailings porewater contains up to 4 mg Cu/L, which represents an ongoing release of copper, particularly if the tailings are disturbed or dredged (Teasdale et al., 1996). Detectable releases are expected for thousands of years (Taylor et al., 1996).

Potential control measures for acidic drainage at Mount Lyell include (1) conventional reactive collection and treatment with lime, (2) an unconventional SX/EW system to recover most of the copper in the drainage (Miedecke and Partners, 1996), or (3) a pipeline for direct discharge of drainage into the ocean (W. Jones, personal communication, 1996). For smaller areas with localized acidic drainage, a series of passive techniques may be used, such as (1) anoxic limestone drains (Case Study 6.1.2-4) discharging into a wetland (Case Study 6.1.2-2), (2) solid covers of waste-rock dumps (Section 6.2), and (3) flooding of underground workings (Case Studies 4.3-12 and 6.4-4).

6.1.2 Passive Collection and Treatment

An important and economic wish for drainage-chemistry control is a passive method requiring no additional expenditures and maintenance after installation. This reason for this wish is clear after reviewing costs in Case Study 6.1.1-1. Several techniques have been touted as "the answer", but research on all techniques to date has revealed significant deficiencies or the need for ongoing maintenance. Such techniques include electrochemical cells in pits, wetlands, and anoxic limestone drains.

Because of the initial deceptive fanfare, some of these methods are now dismissed outright. However, a good understanding of their advantages and limitations allows them to be used properly, at least for partial treatment of drainage chemistry. This is highlighted in the following case studies.

Case Study 6.1.2-1: Passive Treatment of Ponded Acidic and Metal-Laden Drainage with Scrap-Metal Electrodes

highlights: short-term improvement of drainage chemistry using redox changes; exchange of one chemical problem for another; implied need for long-term maintenance

Shelp et al. (1994, 1995, and 1996) described a laboratory-scale test of an electrochemical cell using massive-sulfide rock (45 by 30 by 30 cm) as the cathode and various metals as sacrificial anodes. In approximately 41 L of acidic water, pH was raised from 3.0 to 5.5 and redox potential (Eh) decreased from more than 550 to around 300 mV in about 50 days with a scrap-iron anode. Dissolved oxygen was maintained at 1.0 to 1.2 mg/L while the water was purged with nitrogen to reduce the oxygen levels. This condition reportedly reflected the presence of reduced forms of iron and sulfur. These changes were accompanied by the precipitation of various metals and the formation of a ferric-sulfate mineral.

This increase in pH due to the formation of reduced species, particularly ferrous iron, is simply the reverse of acidification when ferrous-bearing drainage discharges into surface watercourses. As a result, the electrochemical cell will reacidify as reduced species reoxidize unless controlled through careful maintenance of oxygen levels as done in this testwork. Therefore, this method requires long-term maintenance.

In comparison to a neutralized pH of 5.5 after 50 days with an iron anode, an aluminum anode neutralized only to pH 4.4 after six days. For a zinc anode, pH rose above 6.5 after 50 days, and generated a maximum zinc concentration of 70 mg/L at this pH. This zinc concentration is far above most water-quality guidelines and objectives.

Case Study 6.1.2-2: Passive Treatment of Acidic and Metal-Laden Drainage with Wetlands

highlights: comparison of influent and effluent chemistries for six wetlands in a temperate climate; better treatment in warmer climates; one mechanism for metal control in a wetland

Six wetlands constructed in temperate climates with snow cover during winter were monitored for treatment efficiency of acidic drainage over several years (Dietz et al., 1994). Removal levels of metals and acidity often fluctuated through time, did not stabilize, and were not related to season. Examples of flow-weighted averages of influent and effluent (Table 6.1.2-1) showed that the wetlands lowered concentrations, but did not render discharge-quality effluent.

In warm tropical climates, year-round operation of wetlands can provide better treatment efficiency, particularly for near-neutral drainage (Woods and Noller, 1995). However, dry periods can temporarily reduce biological activity and increase aqueous salinity due to evaporation (Tyrrell, 1996). During these periods, diversion of minewater into the wetlands is critical to maintenance (Noller et al., 1994).

Eger et al. (1994) examined the removal processes that operate in wetlands. Although metal levels in the vegetation increased by factors of 3 to 14, the vegetation actually accounted for less than 1% of metal removal. Instead, the peat supporting the vegetation accounted for 99% of metal removal, primarily through organic complexing. If wetlands act simply as sorption media and filters, then they can eventually reach full capacity and cease filtering. This is not the primary concept behind wetland treatment, where continual growth of vegetation would provide an ongoing source of metal removal.

Case Study 6.1.2-3: Passive Treatment of Acidic Drainage by Bacteria

highlights: efforts to passively treat drainage with bacteria; limitations to only low-flow systems in temperate climates

Acidic drainage at an airport was channelled into three clay-lined cells containing straw as the nutrient source for bacteria (Béchard et al., 1995). Over an operational period of 2.4 years, water-quality objectives were met for only 13 weeks, which was not related to colder periods of the year. Fluctuations in flow and drainage chemistry, and maintenance requirements, were considered problems with the wetland system.

Kuyucak and St-Germain (1994) found that, like wetlands, sulfate-reducing bacteria are relatively slow to react at ambient temperatures in many temperate environments. As a result, the bacteria were recommended only for low-flow passive treatment.

Case Study 6.1.2-4: Anoxic Limestone Drains

highlights: effectiveness of 21 anoxic-limestone drains; objectives and weaknesses of anoxic-limestone drains

Hedin and Watzlaf (1994) summarized the treatment success of 21 subsurface anoxic limestone drains (ALD) in the eastern USA. ALDs are used primarily for pre-treatment of drainage to wetlands, since their primary effect is to increase pH and alkalinity (Table 6.1.2-2). The anoxic conditions limit the encapsulation of limestone with iron hydroxides by maintaining iron in the more soluble reduced ferrous state. However, reported equilibrium with calcium-bearing siderite, gypsum, and rhodocrosite suggests that secondary minerals are precipitating and perhaps encapsulating some limestone. Of course, any surface discharge of ALD-treated waters with ferrous iron results in iron oxidation and thus some acidification.

TABLE 6.1.2-1
Examples of Wetland-Treated Drainage in a Temperate Climate (from Dietz et al., 1994)

		Wetland Label					
Parameter[1]		K2	K3	JEEC	CUC1	CUC2	CUC3
Flow		22.7	50.7	129	66.6	7.9	13.6
Lab pH	INFLUENT	4.64	5.20	2.90	2.60	3.27	3.12
	EFFLUENT	4.90	4.41	3.33	2.70	3.51	4.01
Total Iron	INFLUENT	98.3	41.0	22.4	85.6	36.3	10.6
	EFFLUENT	6.7	2.7	14.5	61.9	12.9	5.5
Total Aluminum	INFLUENT	0.80	2.4	18.5	15.0	1.2	4.2
	EFFLUENT	0.42	3.4	14.3	12.0	1.0	3.0
Total Manganese	INFLUENT	12.2	30.7	6.2	3.9	4.2	4.8
	EFFLUENT	8.5	28.0	6.0	4.1	4.8	4.3
Acidity, $CaCO_3$	INFLUENT	126.5	114.3	258.4	392.0	108.3	106.5
	EFFLUENT	6.0	40.6	153.6	272.0	56.2	26.8
SO_4	INFLUENT	594	1388	516	303	718	332
	EFFLUENT	462	1202	519	312	754	313

[1] Flow in L/min; total concentrations in mg/L

TABLE 6.1.2-2
Examples of Twenty-One Anoxic Limestone Drains
(adapted from Hedin and Wetzlaf, 1994)

ALD	Lime-stone (t)	Flow (L/ min)	Limestone/ Flow (t*min/L)	pH		Alkalinity		Fe		Mn	
				In	Out	In	Out	In	Out	In	Out
Rid-2L	114	0.8	143	2.3	6.2	0	469	1416	202	23	11
Ohio	-	-	-	-	6.1	-	400	-	625	-	4250
Hathaway	945	-	-	3.3	6.5	0	385	195	54	44	14
TVA-AROAD	-	265	-	2.8	6.6	0	350	16	38	4	2
Rid-2R	162	0.5	324	3.7	6.3	0	306	217	164	7	7
Rid-1	108	5	24	4.7	6.5	3	290	5	27	23	27
TVA-2	-	-	-	3.5	6.7	0	280	40	24	13	7
Morrison	64	7	9.4	5.3	6.3	23	271	216	151	51	42
Schnepp	132	57	2.3	3.3	6.3	0	191	92	61	28	39
Willi	182	5	36.4	2.7	6.3	0	187	48	<1	45	34
Empire	-	-	-	4	6.2	0	180	37	67	22	29
Jennings	364	92	4	3.3	6.3	0	177	81	62	9	9
Howe-2	132	53	2.5	5.9	6.5	24	174	276	271	39	39
Howe-1	455	92	4.9	5.6	6.2	33	161	279	277	41	40
Maud	-	-	-	-	6.5	-	155	-	<1	-	2
REM-L	125	82	1.5	-	6	-	138	-	184	-	45
Shade	35	15	2.3	3.5	6.6	0	123	3	1	32	36
TVA-4	364	131	2.8	4.9	6.7	-	120	135	<1	24	3
REM-R	124	115	1.1	4.3	5.5	0	69	589	507	136	132
Fawn	-	-	-	3.5	3.7	0	0	417	445	25	29
Ohiopyle	225	218	1	3.3	3.6	0	0	10	3	79	63

6.2 Solid Covers

As explained above, the two basic approaches to drainage-chemistry control are reactive and proactive. Reactive control involves collection and treatment of drainage. Proactive control focusses on reducing concentrations leaving a minesite component. The three types of proactive control are labelled as "solid covers" (this section), "water covers" (Section 6.3), and other techniques (Section 6.4). The concept behind the covers is that the prevention of one or more reactants from entering a component will affect the subsequent concentrations in the drainage.

Solid covers include local soil, clay, till, geomembranes like plastic, cement, wax, desulfurized tailings, and various waste materials like wood bark and paper-waste sludge. The typical purpose of solid covers is to minimize the amount of water entering and draining from a component (Swanson et al., 1995). Also, where oxygen contributes to reaction rates like sulfide oxidation (Section 4.2.3, Equation 4.2.3-1), a solid cover can reduce the entry of air especially when close to saturation.

Although detailed design and engineering are beyond the scope of this book, the selection of the proper cover material and maintenance costs can be seriously affected by slow, long-term mechanisms like freeze-thaw cycling, root penetration, and erosion. For plastic covers, periodic replacement of the covers seems inevitable. Details like this can lead to differences of millions of dollars in the net present value of various covers.

For minesite components that have progressed a few years into the First Stage of Drainage Chemistry (Figure 4.2.2-1), the installation of solid covers will yield little change in drainage concentrations for many years until the retained secondary minerals are removed. In the terminology of Figure 4.2.2-1, a perfect solid cover may cause Rate1 to fall to zero and the Second Stage to begin. However, the Second Stage still generates similar drainage concentrations as the First Stage, probably for 5-50 years for each year in the First Stage. Case Study 6.2-2 illustrates how this Second Stage at one waste-rock dump was expected to be approximately 25 years. The study also discusses how a lack of cover maintenance may cause a dump to re-enter the First Stage.

Case Study 6.2-1: Covers and Other Techniques for Control of Cyanide and Acidic Drainage in a Tropical Climate

highlights: strong attenuation of cyanide in a warm climate; segregation of waste rock by net-acid-generating capacity; problematic manganese release during NP dissolution; implementation, success, and costs of various proactive and reactive controls on drainage chemistry

Kelian Equatorial Mining (KEM) operates Indonesia's largest gold mine in East Kalimantan, Indonesia, on the island of Borneo (van der Linden, 1994a and b; Firth and van der Linden, 1997). Approximately $9x10^6$ t of ore and $21x10^6$ t of waste rock are mined annually from two adjacent pits next to the Kelian River. Ongoing mining of the East Prampus Pit has required the diversion of the Kelian River around the new pit perimeter.

Average annual rainfall at KEM is approximately 4 m, occurring as short-term intense events up to 1.5 cm/hr. Due to the variable rainfall, flow in the Kelian River ranges from 1.9 to 600 m^3/s.

Gold is separated from the ore by conventional cyanide extraction and carbon adsorption (Case Study 4.2-2). Natural degradation is used to control cyanide concentrations entering the Kelian River (van der Linden, 1994a), with concentrations of total cyanide falling from mill discharge levels of 100 ppm CN to 0.02 ppm where drainage enters the river (Figure 6.2-1). More than 99% of degradation occurs in the Namuk Tailings Impoundment where the large surface area, winds, bacteria, and sunlight accelerate the degradation. During times of poor mixing, the tailings pond is stratified with a thermocline, and has total cyanide concentrations at the surface and at depth of 0.1 and 1 ppm, respectively. Concentrations of weak-acid-dissociable cyanide are roughly ½ of total cyanide.

In addition to cyanide, acidic drainage is also a concern at KEM due to reactive sulfide minerals in the ore, waste rock, and tailings at an average of around 2-3%S (van der Linden, 1994b; Firth and van der Linden, 1997). Predicted lag times to significant production of acidity are 32-86 weeks. However, acid generation in the tailings is negligible because they are mostly submerged and will be permanently submerged upon closure. Also, ore is not a concern because it is milled. As a result, control and management strategies focus on waste rock, pit walls, and low-grade ore that might be milled later.

Rock balances indicated that $90x10^6$ t is expected to be net-acid-generating with an average TNNP (Section 5.2.1.4) of -50 t $CaCO_3$/1000 t (van der Linden, 1994b). An additional 40-$45x10^6$ t will be blended to achieve at net-acid-neutralizing TNNP of +30 t $CaCO_3$/1000 t. A final 20-$25x10^6$ t will have high carbonate and low sulfur, providing construction materials for dams. Since the net-acid-generating volume is higher, even simple blending or layering of rock would not be sufficient. The installation of a clay cover on one waste-rock dump, with $8x10^6$ t, followed by revegetation reduced acid drainage by an estimated 80%.

One difficulty in management of drainage chemistry at KEM is the presence of manganese carbonate. In combination with calcite, this manganese carbonate is responsible for natural, desirable in situ neutralization of acidity (Section 5.2.1.3), but as a consequence elevated levels of manganese are released into the drainage. As a result, manganese requires active management and control. To lower manganese to acceptable levels, pH must be raised above 9.0. Current research is focussing on passive-reactive control of manganese by algae and bacteria.

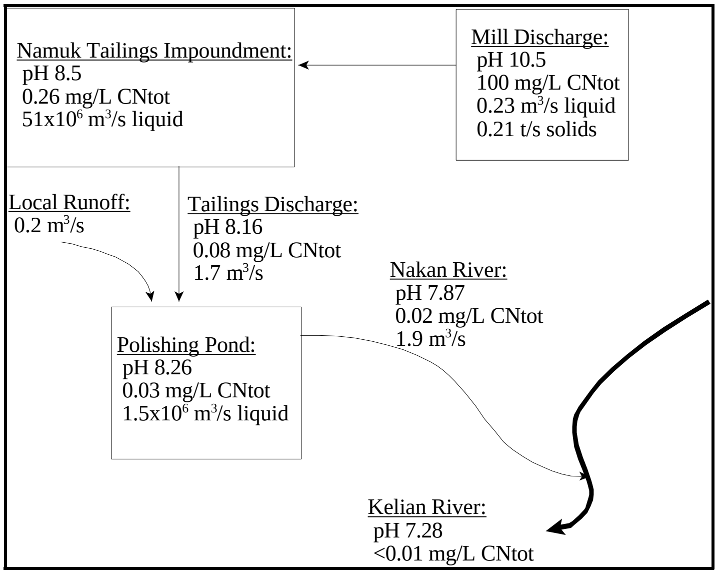

FIGURE 6.2-1. Cyanide Balance from the Mill to the Kelian River at Kelian Equatorial Mining (adapted from van der Linden, 1994a).

To improve drainage-chemistry control, a comprehensive program was initiated involving (van der Linden, 1994b):

❶ addition of lime in drainage pathways,
❷ segregation of acid-generating and non-acid-generating rock,
❸ flooding of acid-generating waste rock behind a large, specially designed dam,
❹ covering of the low-grade stockpile with a high-density polyethylene (HDPE) membrane,
❺ additional clay covers,
❻ wetlands for polishing of water chemistry,
❼ filling the mined out pit with waste rock for eventual submergence, and
❽ maintenance of the water cover over the tailings.

Costs for this comprehensive program were estimated at US$35,000,000 (Firth and van der Linden, 1997).

Lime addition occurs in the upper portion of the minesite drainage system at a rate of 10 t/d, which causes iron to precipitate within downstream waste rock. This addition is usually sufficient to maintain near-neutral pH in the entire drainage system. However, when rainfall exceeds 50 mm/d, additional lime must be added, presumably due to increased flushing of acidity from the minesite components.

Based on pH measurements, the initial onset of acidification at KEM was relatively rapid, which is consistent with the predicted lag times to significant acidity of 32-86 weeks for individual samples. This onset was accompanied by a trend of increasing sulfate concentrations during wet and dry periods. The trend continued until gypsum saturation was apparently reached, indicating that significant precipitation and retention of gypsum was then occurring and obscuring the actual sulfate production in the waste rock.

Due to highly variable precipitation over short periods, high-frequency monitoring was initiated at several locations. In Bayak Stream, pH could vary by two pH units within a 24-hour period accompanied by changes in metal concentrations up to a factor of 10.

Boreholes were drilled into the Low-Grade Stockpile ($10x10^6$ t) which was covered with high-density polyethylene (van der Linden, 1994b). The purpose of the plastic cover was to slow oxidation rates so that less reagents are needed when the low-grade ore is eventually milled. Monitoring at various depths in the boreholes revealed some oxidation was occurring in the stockpile with maximum temperatures around 70°C.

Case Study 6.2-2: Integrated Control of Waste-Rock Drainage and Acidic Pit Water

highlights: implementation of various proactive and reactive controls at a minesite; lag time to drainage-chemistry effects using solid covers; ambiguity in determining effectiveness due to temporal trends and lag times

The Rum Jungle Minesite is located in the Northern Territory of Australia, approximately 150 km south-southwest of Darwin (Ryan and Joyce, 1991; Ritchie, 1994b; Bennett and Lawton, 1995). The climate is tropical and annual rainfall averages 1.5 m with approximately 80% falling between December and March. Monthly mean daily temperature varies from 25°C in July to 30°C in November.

Mining for uranium began at this site in 1954 with White’s orebody, depleted in 1958. This was followed by Dyson’s and Intermediate orebodies, with all mining ceasing in 1965 (Harries and Ritchie, 1982), although Ryan and Joyce (1991) say the site was mined for uranium and copper until 1971. By the time mining ceased, there were three pits and three waste-rock dumps (White’s, Dyson’s, and Intermediate), a copper heap-leach pile, and a tailings impoundment (Figure 6.2-2). Acidic drainage caused by sulfide oxidation and the accompanying metal leaching led to significant releases from these minesite components (Table 6.2-1).

The pits eventually filled with water (Goodman et al., 1981; Northern Territory Department of Mines and Energy, 1986; Water Resources Division, 1986; Henkel and Alcock, 1988). Whites Pit has a lateral area of 10.5 ha, a maximum depth of 50 m, and a volume of 2,700,000 m^3. After 1958, this pit flooded quickly to its equilibrium static level (Figure 3.2.1-4) with the assistance of diverted river water (Figure 3.2.1-3), and at that time had a pH of 4.75 and a sulfate concentration of 180 mg/L. However, unneutralized tailings and treatment raffinate were dumped into the pit through the 1960's so that by 1974 pH had fallen to 2.4 and sulfate increased to 9000 mg/L. The annual flow of water through Whites Pit was estimated at 19,000,000 m^3, but did not include subsurface inflow and outflow.

The East Finniss River which runs through the site (Figure 6.2-2) carried elevated levels of metals even before closure (Table 6.2-2). The river was devoid of biological species up to 8.5 km downstream, with reduced biodiversity over another 15 km (Bennett and Lawton, 1995). In late 1983, a rehabilitation program was started and eventually completed in early 1987 at a cost of AUS$18,600,000. This program was designed to reduce metal levels in the East Finniss River by up to 70%, reduce on-site pollution, and revegetate the minesite. Ryan and Joyce (1991) concluded that the first and primary objective was not accomplished and that diversion of the river may have been a more successful option than all the on-site remediation. On the other hand, Bennett and Lawton (1995) state that metal levels were successfully reduced, but a five-year program is currently underway to delineate carefully the degree of success.

The on-site remediation program included:

Ø reshaping the dumps and placing a three-layer cover with basal clay topped by a moisture-retention layer capped by an erosion-protection layer,

Ù 330,000 m^3 of tailings and soil were retrieved and placed in Dyson’s pit followed by liming and revegetation of the former disposal area,

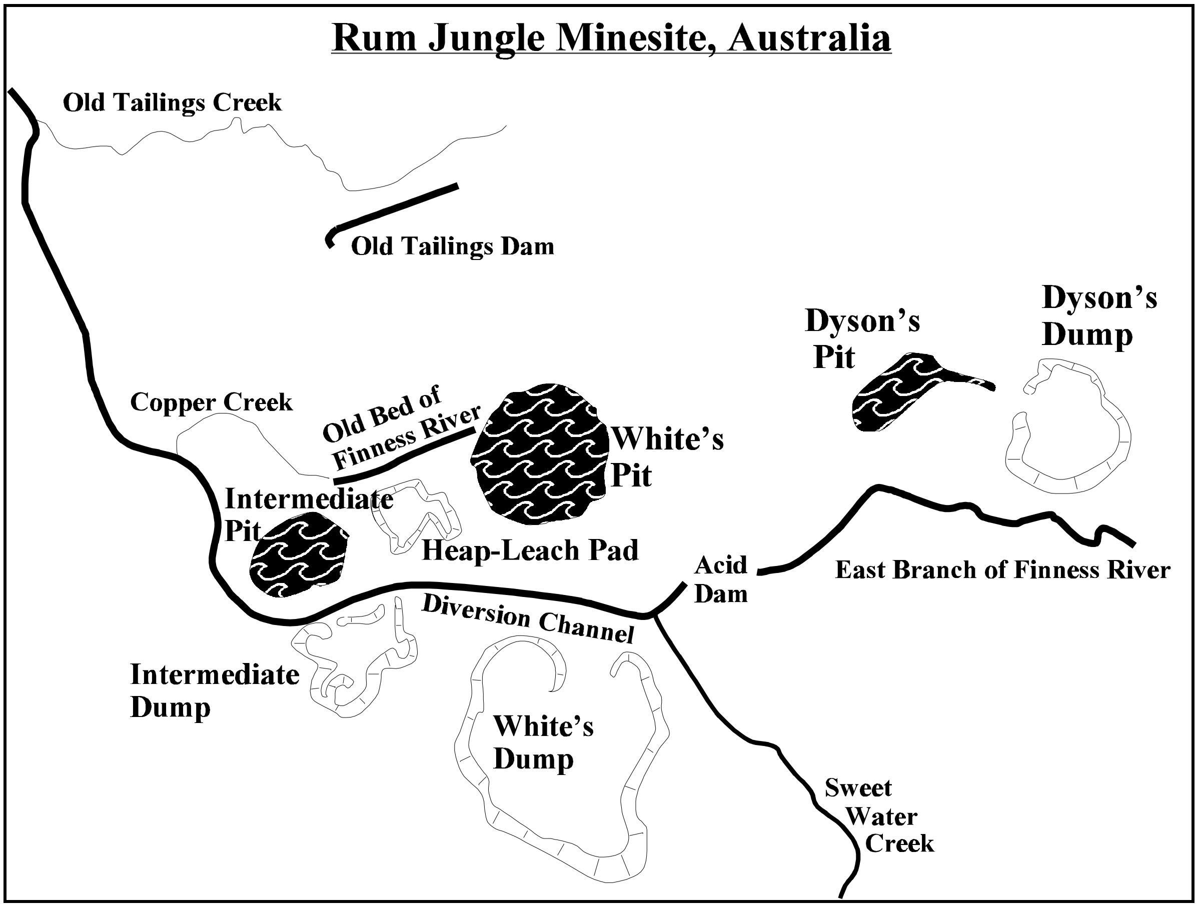

FIGURE 6.2-2. Schematic Map of the Rum Jungle Minesite (adapted from Harries and Ritchie, 1982).

TABLE 6.2-1
Metal-Release Rates from Various Minesite Components during the 1973-1974 Wet Season at the Rum Jungle Minesite
(from Harries and Ritchie, 1982, and Bennett and Lawton, 1995)

Component	Cu (t/yr)	Mn (t/yr)	Zn (t/yr)
White's Pit	8	30	-
White's Waste-Rock Dump	29-53	11-19	17-31
Intermediate Pit	3	3	0.3
Intermediate Waste-Rock Dump	16-30	2.5-4.5	13-25
Dyson's Pit	1	3	-
Dyson's Waste-Rock Dump	0.2	5	-
Copper Heap-leach Pile	32-42	-	-
Tailings Area	5	3.5	-
Old Acid Dam	-	12	-
TOTAL	95-142	70-80	30-56

TABLE 6.2-2
Loadings in the East Finniss River Downstream of the Rum Jungle Minesite
(from Ryan and Joyce, 1991)

	Wet Season						
Parameter	1969-70	70-71	71-72	72-73	73-74	82-83	83-84
Precipitation (mm)	896	1611	1542	1545	2000	1121	1704
Months	Dec-May	Nov-Aug	Nov-Jul	Dec-Jul	Nov-Sep	Dec-Jul	Nov-Jun
Flow (10^6 m^3)	7	33.2	30.9	26	43	9.7	44.8
Cu (t)	44	77	51	45	130	22.7	28
Mn (t)	46	110	64	49	100	6.1	20.8
Zn (t)	-	24	19	16	40	5.2	9.1
SO_4 (t)	3300	12000	6600	5500	13000	1518	3620

Ú treatment of $4x10^6$ m^3 of pit water in a treatment plant and as in situ batch treatment with 82,000 t of treatment sludge placed in a deep clay pit located west of Dyson's pit,
Û transfer of 270,000 m^3 of low-grade ore from the Copper Heap to Dyson's pit followed by covering and revegetation of the former heap area, and
Ü after placement of materials in Dyson's pit apparently to a level above the water table, the pit area was covered with a three-layer cover and revegetated.

The cover systems reportedly reduced infiltration to about 5% of rainfall, cracked during the dry season but resealed during wet periods, and limited oxygen entry to the outer rims of the minesite components. Nevertheless, in 1991, the pits and other components continued to be significant sources of loadings to the river, vegetation on some covers had died raising a concern over capillary rise of metals and acidity, and loadings in the river showed no clear improvement since rehabilitation. Ryan and Joyce (1991) pointed out the difficulty in determining whether rehabilitation efforts at the minesite had failed or whether there was an extended lag time between rehabilitation and improvements in concentrations. As indicated below, the lag time could be 10-20 years, so the success of rehabilitation might not be known until after 2000.

The upper 15 m of White's Pit water was found to have thermoclines and chemoclines (Section 5.4.2). Consequently, treatment of pit water involved pumping of the deeper, denser acidic water and returning the less dense treated water to the top. Although some mixing of the two layers hindered initial treatment efforts, eventually most of the acidic water was treated, pH stabilized at 6.0, and sulfate stabilized at 200 mg/L. Afterwards, water chemistry varied noticeably through the year, improving when the flow of pH-neutral surface water into the pit increased and worsening when evaporation and groundwater inflow (which was found to be acidic) increased. Bennett and Lawton (1995) reported that by 1993 the pit again contained a chemocline with the deeper acidic water carrying 60 mg Cu/L.

The Intermediate Pit has a lateral area of 4 ha, a maximum depth of 78 m, and a volume of 1,100,000 m^3. Like Whites Pit, this pit also flooded to equilibrium level within a year and, in 1974, pH was 3.5 with sulfate at 2000 mg/L. The annual flow of water through the Intermediate Pit was estimated at 18,000,000 m^3, but this did not include subsurface inflow and outflow.

TABLE 6.2-3
Water Balance for Dumps at the Rum Jungle Minesite
(from Daniel, Harries, and Ritchie, 1983; Harries and Ritchie, 1983a and b)

Pathway	White's Dump (% of precipitation)	Intermediate Dump (% of precipitation)
Evaporation	25-35%	25-35%
Runoff over dump	10-22%	10-22%
Toe springs	5%	0%
To underlying groundwater	38-60%	43-65%

Unlike White's Pit, the Intermediate Pit did not contain significant chemoclines and thermoclines, but the reasons for this are not given. Therefore, a different treatment system was designed whereby lime was applied to the top of the pit-water column and the settled sludge removed. As a result, pH increased to 5.9 and sulfate fell to 200 mg/L. Like Whites Pit, pit-water chemistry varies noticeably through the year.

White's Dump has a height of 13-18 m and a lateral area of 26.4 ha, of which 26% is side slope. Total volume was estimated at $4x10^6$ m^3 ($8.0x10^6$ t), comprised predominantly of carbonaceous slates and graphitic schists with 1-3%S as pyrite and 860 mg Cu/kg of rock. Most remedial effort on waste rock was focussed on this dump at a cost of AUS$68,500/ha. Less emphasis was placed on the Intermediate Dump with $1.6x10^6$ t of rock and a 6.9 ha lateral area, of which 30% is side slope, and on Dyson's Dump with $2.3x10^6$ t and a 8.4 ha lateral area.

Water balances for White's and Intermediate Dumps shows that a major portion of the water reported to the underlying groundwater system (Table 6.2-3). The loadings to the underlying groundwater and the nearby river were expected to continue for 10-20 years, apparently reflecting the release of retained reaction products.

Springs at the base of White's Dump had an average pH of 3.6 during the high-flow wet season and 2.8 during the dry season (Harries and Ritchie, 1982). This was accompanied by average concentrations of sulfate, copper, zinc, and manganese at 17,000, 80, 45, and 35 mg/L, respectively. Average concentrations in surficial runoff from the dump were about an order of magnitude less.

Moisture content based on neutron and gamma probes was constant below 2 m depth in White's Dump (Harries and Ritchie, 1983a and b). This suggested that evaporation of water was negligible below 2 m and that water movement was channelized so that it did not affect overall moisture contents. However, flows from springs on the northeast corner continued halfway through the dry season, highlighting the slow migration of water in some areas and suggesting the presence of a perched water table (Figure 3.3-1a). Large cavities and pores noted at the base of the dump apparently did not have a significant effect on drainage, because only 5% of precipitation appeared at the toe (Table 6.2-3).

Oxygen levels in poregas reflected one of three processes in various portions of White's Dump (Harries and Ritchie, 1985 and 1987; see also Case Study 4.4-2 and Figure 4.4-2). A linear decrease in oxygen with depth was attributed to oxygen diffusion into the dump. Thermal convection of air drove oxygen to the base of the dump. Barometric pumping and atmospheric tides caused two maximum and minimum values each day. Emphasis was then placed on limiting oxygen entry into the dump.

After White's Dump was covered as explained above, oxygen levels throughout most of the dump decreased, and remained high (>5% O_2) only within a few meters of the slopes and top surface. Afterwards, these profiles of oxygen, carbon dioxide, and temperature with depth showed minor changes over five years of monitoring. This was taken as evidence that oxygen entry was controlled by diffusion, except for convection in one large area of the dump.

Directions and amounts of oxygen transport in the dump were known to vary significantly over distances of a few meters. However, simplistic simulations with a one-dimensional model, with an assumed heat production of 1.29 J (kg FeS_2)$^{-1}$ ignoring all other exothermic and endothermic reactions, indicated that pyrite oxidation rates varied from 0.3-8.8x10^{-8} kg O_2 (m^3 of dump)$^{-1}$ s^{-1}. This thermal analysis and modelling was later expanded to two dimensions (Bennett et al., 1989; Harries and Ritchie, 1985 and 1987).

The release of sulfate from the dump was reportedly equivalent to the calculated oxidation rate (Harries and Ritchie, 1982). However, additional monitoring appeared to contradict this (Harries and Ritchie, 1983a and b), which is expected from the known retention of reaction products within the dump.

In contrast to debates over the success of remediation at Rum Jungle, the nearby Rum Jungle South Type 1 open-pit uranium mine (Figure 2.2-1) was successfully remediated (Northern Territory Chamber of Mines, 1991; Woods, 1994). Despite some acidic drainage, the pit was flooded and evolved to a slightly alkaline lake. The adjacent waste-rock dump with an average of 0.29%S was recontoured and covered with soil. The minesite is now a pleasant park and swimming area, with only small localized seeps of acidic drainage occasionally seen near the dump.

Case Study 6.2-3: Solid Covers on Waste Rock and Tailings

highlights: increased concentrations after implementation of controls; 70-year lag time to control of oxidation

The closed Bersbo minesite is located 250 km south of Stockholm, Sweden. Underground mining of copper began there around 1760, peaked in 1850-1870, and virtually ceased around 1900 with minor extraction until 1930 (Håkansson et al., 1994). The minesite contains underground workings and shafts, waste rock, and tailings. Rock consists of granite and amphibolite intrusion with hornblende, augite, and calcium-rich feldspar. Sulfide minerals at the site include pyrite, chalcopyrite, sphalerite, and galena. Total mine wastes are estimated at 700,000 m^3.

Waste rock is coarse and well ventilated according to internal oxygen concentrations. During reclamation in 1987-1989, the waste rock was covered. For tailings, approximately 200,000 m^3 was backfilled into shafts (Section 6.4), and the remainder was moved into two piles and covered.

Drainage-chemistry monitoring before and after reclamation activities showed that concentrations of iron and sulfate generally increased after reclamation. This was attributed in part to reduction in infiltration through the covers, resulting in less dilution. However, secondary-mineral equilibrium would eliminate dilution as a factor (Section 4.2), and the values of iron and sulfate reported by Håkansson et al. (1994) could represent equilibrium. However, the lack of pH and other concentrations precludes a better assessment of equilibrium.

In any case, the increased flux of iron from the components was also attributed to chemical reduction of iron through oxidation of sulfide minerals, which also released acidity. Under the assumption that ferric iron is being reduced in the covered components and no oxygen is replenishing the ferric supply, then oxidation of pyrite is expected to cease in 70 years.

Case Study 6.2-4: Cement Covers and Seals

highlights: use of cement-based grout to cap a minesite component; use of cement-based grout to fill porespaces in waste rock

Scheetz et al. (1995) discuss three case studies where cementious (cement-based) grouts have been used to cap or seal coal-minesite components generating acidic drainage. At one site, a pit filled with waste rock was being covered with approximately 400,000 t of grout to reduce infiltration. Bearing strength, chemical stability, and setting time were key requirements for the grout cap at this site. As a result, testing showed that the incorporation of fly and combustion ash from coal improved the stability of the grout and reduced waste management for the ash.

At the second site, strength and setting time were not critical, because the grout was injected into boreholes in the waste where it was expected to flow into and fill adjacent voids. Monitor wells near the injection points showed up to 90% improvement in chemistry, and drainage chemistry at the site boundary was beginning to improve. Rehabilitation of the third site, still in the design phase, will include injection of grout into underground workings

Scheetz et al. (1995) point out that the burning of minerals like sulfates and carbonates at high temperatures will drive off carbon dioxide and sulfur dioxide. This leaves oxides compounds behind, which can generate alkaline drainage (Table 4.2.3-1) if not stabilized.

Jones and Wong (1994) also reported on the use of cementitious mixtures as covers for acid-generating waste rock. Their work focussed on the strength and durability of the mixtures, rather than on the degree of prevention against entry of water and oxygen. Total cost for materials and equipment was placed at CDN\$18.46/m^2 of dump surface.

Case Study 6.2-5: Comparative Testing of Various Solid and Water Covers and Chemical Additions

highlights: small-scale determination of effectiveness of various controls; novel covers using epoxy and wood bark

Payant et al. (1995) reported on small-scale testing of various techniques for reducing acid generation and metal leaching. Laboratory and small-scale field lysimeters examined (Table 6.2-4):

Ø 1 m of water cover (see also Section 6.3),
Ù a triple-layer soil cover with 150 mm of water-saturated clay between two 75-mm sand layers,
Ú addition of limestone at 1% and 3%,
Û addition of phosphate at 1% and 3%, and
Ü a cover of wood bark.

The rock used in all tests contained a sulfide content of 9.7%S, an NP of 17.2 t CaCO$_3$/1000 t, and an SNPR (Section 5.2.1.4) value of 0.06.

Efficiency of the techniques was based on the cumulative amount of acidity drained weekly from the tests, relative to untreated control rock which generated net acidity within six weeks. After three years, the efficiencies showed that the water cover reduced acid generation by 99.7% (Table 6.2-4), whereas wood bark increased the rate presumably due to accelerated bacterial activity. Despite this documented acceleration of acid generation and metal leaching through the addition of bacteria, others still recommend it (e.g., Tremblay, 1994; Stogran and Wiseman, 1995). The triple-layer cover (see also Case Study 6.2-6) was less effective under field conditions, apparently due to freeze-thaw and to entry of oxygen along the sides of the container.

Adams et al. (1994) discussed various sealants for rock surfaces and mine walls as tested in laboratory experiments. An epoxy resin or latex mixed with limestone and applied as a slurry was found best to retard acidic reaction products.

Tremblay (1994) documented a case study of progressive placement of bark on a tailings impoundment since 1984, up to 8 m thick. Fires and contamination of drainage with organic compounds like phenol and tannin were problems. Nevertheless, oxygen concentrations within the bark fell to 1-2% O$_2$ with depth and methane and carbon dioxide increased to nearly 20% CH$_4$. Thus, this type of proactive control may be an exchange of one environmental problem for another.

TABLE 6.2-4
Small-Scale Efficiencies of Techniques for Minimizing Acid Generation
(adapted from Payant et al., 1995)

Technique	Three-Year Cumulative Efficiency(%)[1]
Control	0
1 m water cover - lab	99.7
0.3 m triple-layer clay-sand cover - lab	98.3
0.3 m triple-layer clay-sand cover - field	46.6
1% limestone - lab	82.7
3% limestone - lab	97.7
1% phosphate - lab	9.95
3% phosphate - lab	64
0.15 m uncompacted wood bark - lab	-30 (acceleration of acid generation)
0.15 m uncompacted wood bark - field	-150 (acceleration of acid generation)

[1] Percent reduction in cumulative acidity relative to control.

Case Study 6.2-6: Multilayer Solid Covers

> *highlights: detailed, long-term study of a four-layer cover on 10,000 t of waste rock; increase in concentrations after cover installation*

Bell et al. (1994) presented the results of a large-scale in-field test of a 1.3 m soil cover on a waste-rock pile at the Heath Steele Minesite, New Brunswick, Canada. In 1989, roughly 10,000 t of waste rock was placed onto a level sand layer covering an impermeable membrane, which allowed the collection of drainage. The pile had a lateral surface area of 2100 m^2, an average depth of 2.9 m, and side slopes of 3:1 horizontal to vertical. Overall ABA characteristics (Section 5.2.1) were 7-10% pyrite, or 5-7%S, and a minimal NP of 0.4 t $CaCO_3$/1000 t. With this negligible NP, net acid generation could be expected immediately (Section 5.2.1.3 and 5.3.3).

Intensive monitoring of temperature, oxygen, soil suction, and moisture content was then initiated with depth-specific thermocouples, poregas samplers, and heat-dissipation and electrical-resistance sensors, and time-domain reflectometry. On September 15 of 1991, a four-layer cover was installed, consisting from bottom to top of (1) a 30 cm sand base, (2) 60 cm of compacted glacial till, (3) a 30 cm sand-gravel cover, and (4) a 10 cm erosion-control layer of well-graded gravel. Two large lysimeters were installed just beneath the cover to monitor infiltration through it. The concept behind this and other multilayer covers is that the upper sand-gravel holds periodic precipitation so that the underlying till layer remains moist. At the same time, the deeper sand layer remains drained to residual saturation so that it cannot draw water from the till by capillary action. As a result, the till layer remains near saturation, minimizing the entry of oxygen and infiltration to the underlying waste rock. The selected thicknesses were chosen to maintain saturation of the till for at least 50 days without precipitation.

Oxygen levels ranged from 3.2 to 20.8% before cover installation, falling to 0.2 to 0.7% afterwards at monitoring Station 3 (Figure 6.2-3). Temperature reached a maximum near 50°C at Station 3 in 1989-

1990 and began falling, reaching near-background levels about 1.5 years after cover installation. Monitoring of soil suction and moisture content showed little change from near saturation occurs in the till layer. Lysimeter data over two to three month periods showed that approximately 1-2% of rainfall infiltrates through the cover.

Drainage chemistry from the pile showed an increase in pH after cover installation (Table 6.2-5). However, sulfate and dissolved iron showed general increases by factors of 2 to 4, suggesting the loss of some dilution.

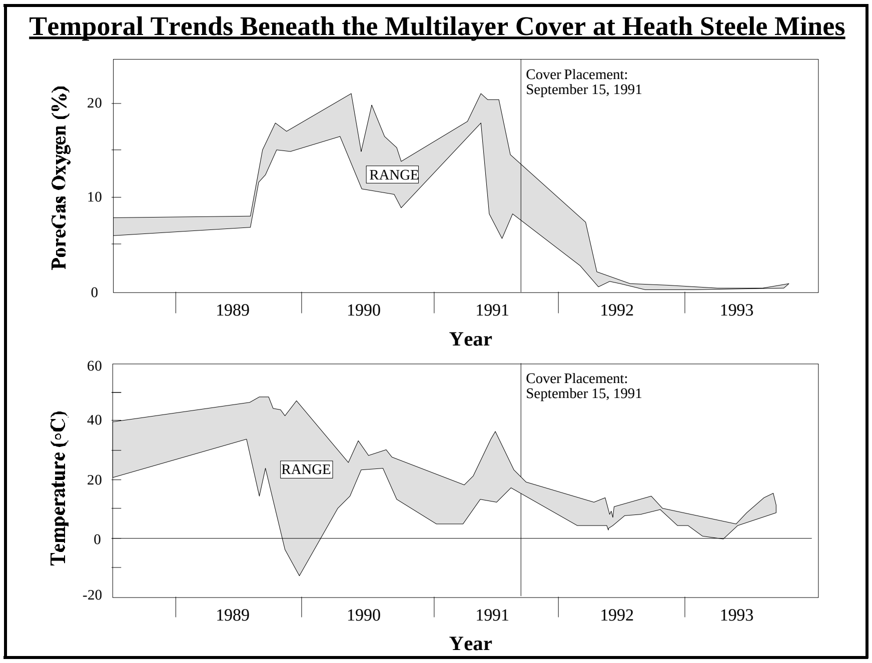

FIGURE 6.2-3. Temporal Trends in Oxygen and Temperature below a Multilayer Cover (adapted from Bell et al., 1994).

TABLE 6.2-5
Trend in Drainage Chemistry from a Waste-Rock Dump with Multilayer Cover (adapted from Bell et al., 1994)

Time	pH	Acidity (mg $CaCO_3$/L)	Sulfate (mg/L)	Diss. Iron (mg/L)
7/89 to 10/90	2.1-2.8	15,800-73,250	12,700-43,440	3,510-13,767
cover placement (9/91)				
1992	2.3-2.9	15,800-54,450	5,140-71,042	15,800-54,000
1993	3.0-3.2	-	9,970-73,854	5,000-30,844

Case Study 6.2-7: Predicted Oxygen Flux through a Non-Reactive Cover

highlights: mathematical delineation of oxygen diffusion through an unreactive solid cover

Aachib et al. (1994) provided equations for the diffusive movement of oxygen and water through non-reactive multilayer covers. Based on adaptations of others' work, the flux of oxygen through a non-reactive layer that is not consuming oxygen is:

$$F(t) = 2C_oG(D/\pi t)^{0.5}\sum_{m=0}^{\infty}\exp[-(2m+1)^2L^2/4Dt] \quad (6.2\text{-}1)$$

where $F(t)$ = flux of oxygen through diffusion at time t as kg/m^2/s
C_o = initial oxygen concentration (atmospheric oxygen) as kg/m^3
G = gas-filled porosity (dimensionless) = $n(1-S)$
where n = porosity (dimensionless)
S = degree of saturation (dimensionless)
D = effective diffusion coefficient for oxygen as m^2/s
t = time in seconds

m = integer incremented from 0 to 4
L = thickness of unreactive layer

Also, the oxygen concentration with depth in the unreactive layer can be calculated from:

$$C(z,t) = C_o \operatorname{erfc}\{z/[2(Dt)^{0.5}]\} \qquad (6.2\text{-}2)$$

where C = oxygen level at depth z and time t in units of kg/m^3
z = depth within unreactive layer in m

The preceding equations were based on the boundary conditions of:

$$C = 0 \text{ for } t=0 \text{ and } z\$0$$
$$C = C_o \text{ for } t\$0 \text{ and } z\#0 \qquad (6.2\text{-}3)$$
$$C = 0 \text{ for } t\$0 \text{ and } z\$L$$

Again, these equations are for a cover that does not consume oxygen, moving only by diffusion. Equations used for oxygen consuming materials are discussed in Section 5.5.1. Convective movement of oxygen, driven by thermal gradients, barometric variations, and winds would lead to greater oxygen fluxes than calculated using the approach in this case study.

Case Study 6.2-8: Thickened Tailings

highlights: lack of acidic-drainage control with thickened tailings

As discussed in Case Study 3.4-1, "thickened" tailings with relatively low moisture content can reduce separation of particle sizes and minerals during deposition. Additionally, by minimizing coarser-grained areas that can drain porewater, an elevated water table can form and reduce the amount of tailings exposed to unsaturated conditions. However, because tailings oxidize downwards from the upper surface, acid generation can continue for a long time before the oxidation front reaches the water table (Section 5.5.1). Consequently, acidic drainage has been reported in thickened-tailings impoundments in Australia (Williams, 1992) and Canada.

Case Study 6.2-9: Reactive Treatment and Subsequent Effect of a Proactive Soil Cover over Acidic Waste Rock

highlights: cost of treating moderate-strength acidic drainage; design, implementation, and costs for a two-layer till cover over waste rock; effects of cover on drainage chemistry

Equity Silver Mine in central British Columbia, Canada, operated from 1980 to 1994 (Aziz and Ferguson, 1997). Approximately $76x10^6$ t of net-acid-generating waste rock was placed in three dumps, with net-acid-neutralizing diverted for use in roads and tailings dams.

Average drainage chemistry from the waste-rock dumps is pH 2.6, acidity of 8,200 mg/L, dissolved iron of 1,300 mg/L, dissolved copper of 120 mg/L, and dissolved zinc of 154 mg/L (Aziz and Ferguson, 1997). This drainage, with an average annual volume of 880,000 m^3, is collected and treated with 5,060 t of lime annually. After treatment, pH is 7.8 and dissolved copper and zinc are 0.01 and 0.04 mg/L, respectively. Annual cost for the treatment is CDN$1,100,000 with lime representing 70% of the cost.

In order to adopt a more proactive approach and to reduce treatment costs, Equity Silver placed fine-grained glacial till over the waste rock beginning in 1990, after long slopes on the dumps were reduced to 20°. The till cover consisted of 0.5 m compacted to 95% of dry proctor overlain by 0.3 m of uncompacted till to protect the lower layer from erosion and to provide soil for vegetation. All this work cost $35,000/ha including revegetation.

Oxygen monitoring within the waste rock shows that levels change with seasons, but there is an overall trend of decreasing oxygen over the last five years. On the other hand, temperatures up to 53°C show no significant changes. Acid loadings from July of one year to June of the next (Figure 6.2-4) show a 25% reduction since 1990/1991, whereas metal loadings have decreased approximately 40%. Lime consumption similarly shows a reduction, and consumption rates now rival those of the mid 1980s (Figure 6.2-5).

The financial security initially placed on this minesite was $32,000,000 plus $5,500,000 for placement of covers and reclamation. However, after a recent review showing lower-than-expected lime consumption and discount rate, the security has been lowered to $21,700,000. Provisions are in place to raise the security should unexpected increases in lime consumption occur.

6.3 Water Covers

As explained in previous sections, the two basic approaches to drainage-chemistry control are reactive and proactive. Reactive control involves collection and treatment of drainage (Section 6.2), whereas proactive control focusses on minimizing concentrations leaving a minesite component. There are three types of proactive control, labelled as "solid covers" (Section 6.2), "water covers" (this section), and other techniques (Section 6.4).

The concept behind covers is that the prevention of one of more reactants from entering a component will affect the subsequent concentrations in the drainage. However, unlike solid covers, water covers obviously do not attempt to reduce water entry. Instead they focus on minimizing air entry and are thus valuable for controlling drainages affected by oxygen like acidic drainage (Section 4.2.3). In contrast, a water cover over potash tailings (Case Studies 4.2-3 and 6.1.1-3), for example, would result in a large, unwanted volume of brine. In moist climates, water covers have become the preferred option around the world (e.g., Case Study 6.2-1).

There are two basic types of water covers: engineered and natural. Engineered water covers are created through construction of water-retaining dams and dikes. Natural water covers consist of lakes, oceans, and other waterbodies that can maintain a constant water column above submerged mined materials. From an engineering perspective, deposition into deep natural waterbodies is preferred because there are less concerns over (1) control of suspended solids, (2) exposure of mined materials during droughts, (3) chemistry of the shallowest water which is in closest contact with the biosphere, and (4) perpetual maintenance of dikes and dams. On the other hand, due to environmental, regulatory, and social concerns, tailings discharged into natural lakes and oceans are being intensively studied and debated. A design manual for proper implementation of water covers is being prepared (Robertson, 1996).

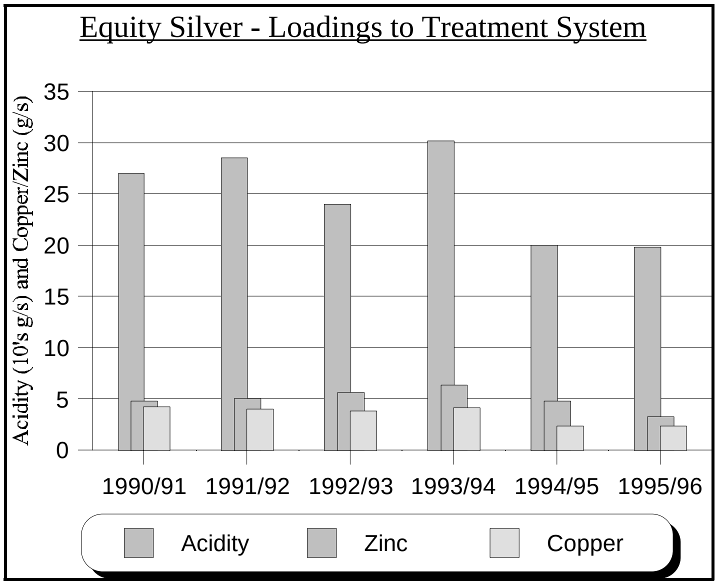

FIGURE 6.2-4. Temporal Trends in Loadings of Acidity, Zinc, and Copper to the Equity Silver Treatment System.

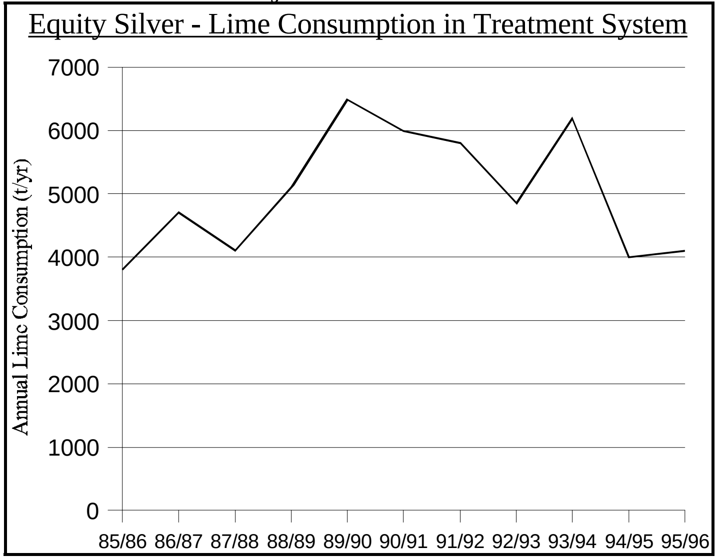

FIGURE 6.2-5. Temporal Trends of Lime Consumption in the Equity Silver Treatment System.

Fraser and Robertson (1994) summarized four detailed field studies of sulfide-bearing tailings discharged into lakes in Canada. The tailings masses ranged from 73,000 t deposited in 1943-1945 to 7,300,000 t discharged in 1979-1995. The studies showed that the reactivity of submerged tailings is decreased below that of aerially exposed tailings. In one case, adjacent mine roads rather than the submerged tailings apparently accounted for a significant portion of detected metals in the lake.

Ellis and Poling (1995) and Ellis (1996a and b) reviewed six cases of submarine (under seawater) tailings deposition, increasingly referred to with the rather unpleasant acronym of STD. The longest case study covered more than 24 years of operation at Island Copper Mine on the west coast of Canada (also discussed in Case Study 4.4-9 and shown on the front cover of this book). Through these years, approximately $300x10^6$ t of tailings were discharged into the adjacent marine fjord (Ellis et al., 1995; Horne, 1996). Ongoing studies show that the tailings-deposition rate in the fjord of 0.01 m/yr had minimal environmental effects and allowed benthic organisms to burrow successfully upwards through the accumulating tailings. The second longest case study from Ellis and Poling, in another fjord, caused environmental problems (see Case Study 6.3-1).

Since 1989, the Misima minesite in Papua New Guinea has discharged tailings from a submerged pipe at 112 m depth (Jones and Ellis, 1995; Mifsud, 1996). The tailings then flow downslope into a deep ocean trench below 900 m depth. Environmental effects are reportedly minimal, although deep-ocean environments are not well understood at this time. All seawater limits specified by Papua New Guinea are met within the 1200 m mixing zone of tailings and seawater.

Case Study 6.3-1: Marine Disposal of Tailings and Waste Rock with Soluble Heavy Metals

> *highlights: placement of weathered tailings and waste rock into a marine fjord; release of tonnes of accumulated metals upon submergence*

The zinc-lead-silver Black Angel Mine on the west coast of Greenland operated from 1973 to 1990, at a rate of approximately 700,000 t/yr of ore. The ore contained an average of 3% lead and 10% zinc, and the mill discharged 600,000 t/yr of tailings at 30 m depth into the adjacent nearby fjord (Asmund, 1992a). A total of $8x10^6$ t of tailings accumulated in a 0.6 km^2 area of the fjord, behind a submerged rock sill at the outlet at a depth of 23 m. The tailings were predominantly composed of calcite, dolomite, and pyrite, with heavy metals occurring in soluble forms.

As tailings were discharged at depth, aqueous metals in the discharge and accumulated soluble minerals (Sections 4.2.5 and 5.2.4) in the tailings were released into the seawater. After the tailings settled, there was an ongoing release of metals (Table 6.3-1). Asmund (1992a) noted that, after 1979, the mining company improved the quality of the discharging tailings, which generally halved the release rates. One year after the mine closed and tailings discharge ceased, metal release rates generally fell by 50-75%. However, there was a larger decrease in lead to the point where the submerged tailings were removing lead from the water (negative rate, Table 6.3-1). The decrease in metal levels in the fjord after closure followed an exponential trend with a half-life of 2.38 years. Consequently, levels were predicted to continue decreasing by a factor of 2 every 2.38 years.

During mining, 320,000 t of waste rock was dumped down a slope extending to the adjacent fjord (Asmund, 1992b). In the fjord, water below the sill depth of 23 m was already "strongly polluted" with zinc, cadmium, and lead from the tailings discussed above. However, the upper 23 m was relatively clean, except the water next to the waste rock. So a decision was made to carry the waste rock out into the fjord and dispose of it with the submerged tailings at 65 m depth. Asmund does not present any pH data, so it is not clear if acidic drainage is involved, but the abundant calcite and dolomite suggest the drainage was near neutral. Additionally, aqueous concentrations in the seepage are not provided, only loadings such as kg/yr.

Leaching tests were conducted on Black Angel waste rock placed in containers below seawater, maintained at 0^oC. After an initial shaking, the containers were not disturbed and upward leaching into the seawater was periodically monitored. As a result of this work, the 320,000 t of waste rock was expected to release 4.7 t of retained soluble zinc immediately (see Section 5.2.4). Afterwards, annual

TABLE 6.3-1
Metal Release Rates from Marine Tailings Disposal, Black Angel Mine, Greenland
(from Asmund, 1992a)

Metal	Metal Release Rate (t/yr)		
	1975-1981	1982-1990	1991[1]
Zn	50	25	6-11
Pb	29	14	-0.3 to 0.2
Cd	0.51	0.25	0.066-0.10

[1] One year after mine closure

leaching of lead from the submerged rock was expected to decrease with the square root of time, from 48 kg/yr to 3.4 kg/yr after 50 years.

The Black Angel waste rock was pushed downslope to the edge of the fjord in June 1990. The dump was partly frozen and required blasting to move it. The rock was loaded on a barge with an 800 t capacity, carried 2 km to the disposal site, and released. Detailed monitoring before, during, and one year after disposal showed good agreement with the preceding predictions. For example, the rapid release of retained metals included approximately 10 t zinc, 57 kg cadmium, and 1 t lead.

Case Study 6.3-2: Reaction Rates of Submerged Rock and Tailings

highlights: laboratory-scale and pilot-scale effectiveness of water covers

Aubé et al. (1995) tested 1 m water covers over 20 kg of initially neutral waste rock with 9.7%S and an NP of 17.2 t $CaCO_3$ equivalent/1000 t. Water flowed from the covers downward through the rock held in the columns and into sample bottles. The columns were subjected to cycles of eight weeks of simulated rain (650 mL/wk) followed by eight weeks of no rain. The tests showed changes in the near-neutral drainage after 2.5 years. These changes included (1) iron release increased by a factor of more than 10, (2) zinc concentrations doubled to more than 5 mg/L, (3) average pH dropped by 1.5 units, and (4) lead became detectable at 1 mg/L (e.g., Figure 6.3-1). Nevertheless, compared with control tests, the overall efficiency of reducing acidity was 99.67%. Based on simplified equations in Morin (1993) and Section 5.5.2 for estimating oxidation rates underwater, the measured rates of sulfate production were about a factor of 100 higher than predicted. This discrepancy may be attributable to initial sulfate in the rock.

St-Arnaud (1994) conducted short-term laboratory tests on submerged tailings. These showed that rates of metal release to overlying water decreased with time and that a sand layer over the tailings limited release, presumably forming an oxidizing or adsorbing bed. In one test of submerging 20-year-old tailings with 33% pyrite and 1.5% sphalerite, zinc concentrations in the overlying water reached 20 mg/L within 152 days. Also, a layer of ferric hydroxide was visibly forming on top of the tailings. This layer could act as a metal adsorber and oxygen barrier as it thickened and compacted, but release of acidity caused by the ferric-iron precipitation could lessen the value of this layer. This points to the need for replenishing overlying water with alkalinity to maintain near-neutral conditions.

Lapakko (1994c) investigated the laboratory oxidation rates of waste rock placed in various submerged environments relative to aerially exposed conditions. The rock was a hornfels containing 32% quartz, 32% opaques (sulfides, oxides, and graphite), 19% clay (kaolinite), 5%

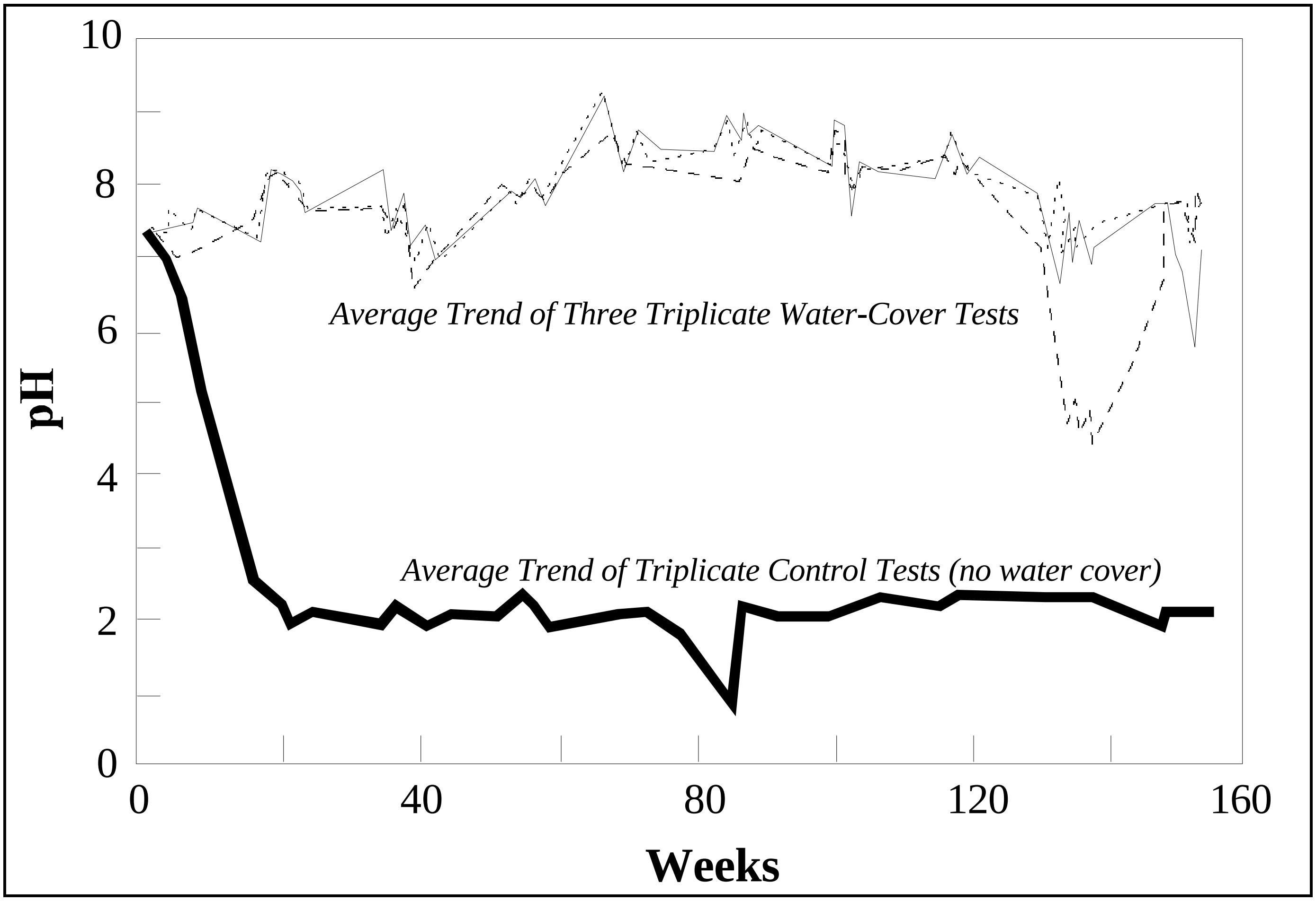

FIGURE 6.3-1. Effluent pH from Waste-Rock Columns with and without Water Covers (adapted from Aubé et al., 1995).

feldspar, 5% chlorite, 4% phlogopite, and 4% muscovite. Opaque minerals included 5-6%S as pyrrhotite.

The scenarios investigated in duplicate for 124 weeks were (1) aerially exposed, (2) submerged, (3) submerged with periodic additions of alkalinity, and (4) initial rinse then periodic additions of alkalinity. The first two scenarios were acidic (pH<5) from the start and the latter two were relatively stable around pH 7. Based on sulfate production, the oxidation rates of pyrrhotite were within 60% in all duplicates of all four scenarios. Late in the testwork, after 90 weeks, pH in the aerially exposed duplicates fell from roughly 3.8 to 3.2. At the same time, the oxidation rates increased by factors of 3-8 over the earlier and submerged rates. This suggested that submerged and aerially exposed rock could have similar oxidation rates. Lapakko (1994c) emphasized the sensitivity of oxidation rates to various physical and chemical hydrogeologic factors.

To compare rates of oxidation and metal leaching under submerged and exposed conditions, one-year-old near-neutral waste rock was excavated from a uranium-mine dump in northen Saskatchewan (Quarshie and Rowson, 1995), then crushed to less than one-inch size in the mine's crushing plant. This rock contained 0.186%S, of which approximately 0.02%S was sulfate, and had an SNPR value of 3.4. The experimental design involved (1) 24.1 t of rock submerged under recirculating lake water, (2) 16.1 t submerged under stagnant lake water, and (3) 42.1 t of free-draining rock exposed to sprayed lake water at 2 L/min for four hours every two days. The first two tests were operated to 42 weeks, whereas the third was operated for 55 weeks.

Based on comparisons of cumulative concentrations at Week 41, the oxidation rate in the exposed waste rock was 5-8 times faster (Quarshie and Rowson, 1995), although the initial sulfate content could have affected the values. Similar factors were also noted for several metals.

Case Study 6.3-3: Flooding of Previously Acidic Tailings

highlights: construction of a full-scale engineered water cover; phased design and implementation using four scales of testwork

Davé and Vivyurka (1994) reported a case study on the design and full-scale implementation of tailings submergence of acid-generating tailings in the Elliot Lake Uranium District of eastern Canada. They noted that the primary benefits of the cover were (1) limitation of oxygen and sulfide oxidation, (2) less surface erosion by wind and water, and (3) formation of chemically reducing conditions for sulfate-reducing and nitrate-reducing bacteria. The studies included laboratory leach columns, in-field studies of partially submerged tailings, a 65 ha "field demonstration" site that was flooded, and full-scale implementation.

The design of the water cover began with 24 laboratory columns of 14.5 cm inside diameter, holding about 14.3 kg each with a vertical tailings height of roughly 45 cm (Table 6.3-2). The submerged Columns 22-24 were rinsed at a relatively high rate to remove retained secondary minerals.

The results of the control columns showed that the whole and coarse tailings became acidic after approximately two and one year, respectively (Table 6.3-2). Exposed coarse tailings (Columns 16 and 17) generated higher levels of sulfate (up to 28,000 mg/L) which decreased to levels of the whole tailings (Columns 1-3) after three years. The corresponding iron concentrations for coarse tailings were equivalent to a cumulative removal of 70-75% of total iron, indicating sulfide oxidation would cease within several years.

Iron removal from the exposed whole tailings was only 0.7% of total iron, probably because pH was not sufficiently acidic to prevent iron-hydroxide precipitation. The lower oxidation rate and higher pH in the whole tailings were attributed to the capillary retention of water which reduced atmospheric oxidation.

The only other columns to become acidic after approximately 4½ years were Columns 18 and 19 with coarse tailings and limestone (Table 6.3-2). This showed that capillary retention of water, fine-grind limestone addition, and submergence were successful options for managing drainage chemistry over the period of several years.

The next step in the study by Davé and Vivyurka (1994) was an investigation of a small wetland basin of 14.5 ha area that contained 236,000 t of tailings covering 12.9 ha in the watershed. Dense wetland vegetation was growing in the basin. Average tailings thickness was 0.92 m, and 88% of the tailings area was submerged under 0.1-0.5 m of water in the west and central portions, and 0.4-1.4 m in the eastern portion. Aerially exposed tailings were located only in the western portion.

Physical and chemical hydrogeology and hydrology were monitored for a year. Surface-water pH was typically between 6 and 8 in the shallow-covered west and central area, with one low pH around 3.8. In the deeper eastern area, surface-water pH was often between 8 and 10. Sulfate concentrations showed the opposite trend, with higher sulfate values (800-1000 mg/L), possibly close to gypsum saturation, in the west and central areas. Groundwater pH at a depth of 1 m below the water interface was between 6-8, with sulfate concentrations around gypsum saturation (800-1600 mg/L) only in the western portion of the basin. Solid-phase paste pH of the tailings ranged from 2.1 to 7.5.

Surface and groundwater data showed that the dense vegetation in the area was not significantly improving chemistry, except for iron precipitation. To the contrary, vegetation was actually related to active oxidation.

The third step in the studies by Davé and Vivyurka (1994) was the 65 ha field demonstration site. This site was confined by internal dikes, and

TABLE 6.3-2
Laboratory Columns for Submergence of Acid-Generating Tailings
(from information in Davé and Vivyurka, 1994)

Column	Contents[1,2]	Results[3]
1-3 (triplicate control)	whole tailings	acidic to pH ~3 after ~ 2 yr
4-6 (triplicate)	whole tailings + 7.5 wt-% limestone < 6.3 mm	always near-neutral pH
7-9 (triplicate)	whole tailings + 7.5 wt-% limestone < 2.4 mm	always near-neutral pH
10-12 (triplicate)	whole tailings + 7.5 wt-% limestone < 0.84 mm	always near-neutral pH
13-15 (triplicate)	whole tailings + 7.5 wt-% wet ground limestone	always near-neutral pH
16-17 (duplicate control)	coarse tailings	acidic to pH 1-2 after~1 yr (1-2 months after change in operation[2])
18-19 (duplicate)	coarse tailings + 7.5 wt-% limestone < 6.3 mm	acidic to pH 2-3 after ~ 2 yr
20-21 (duplicate)	coarse tailings + 7.5 wt-% wet ground limestone	always near-neutral pH
22-24 (triplicate)	coarse tailings	gradually decreasing pH from 8 to 6 after ~4½ yr

[1] whole tailings = fresh and homogenized with 50% less than 74 µm obtained from mill; coarse tailings = fresh and with 94% greater than 74 µm obtained from tailings area.

[2] Operating procedure for all columns except 22-24: aerially exposed; initial inoculation with 100 mL of acidic drainage from underground stope; free drainage of 100 mL of aerated lake water added daily for one year, then 1L of aerated lake water every 2 weeks; operating procedure for 22-24: 40 cm high water cover; initial inoculation with 100 mL of acidic drainage from underground stope; continuous flushing of cover; basal drainage driven by constant-head gradient of 0.9 yielding 1L/day for two years then 1L/wk.

[3] Most drainages were saturated with gypsum, so sulfate was not a reliable indicator of oxidation rate.

flooded by adjacent lake water to a minimum depth of 0.4 m. Before flooding, approximately 50% of the area was levelled and limestone was incorporated into the upper 15 cm of tailings.

Upon initial flooding, pH in the basin was around 3.5, rising to approximately 7 after two months due to lime addition to the incoming lake water. Concurrently, sulfate fell from nearly 400 mg/L to 100 mg/L. Sulfate and pH then remained relatively constant.

The final step in the study was the full-scale implementation of flooding, involving step-wise flooding of segregated cells. Flooding began with the highest cell (Cell 14, Figure 6.3-2), which was in fact the preceding demonstration site. Other cells are now being flooded, although there are no published data for them.

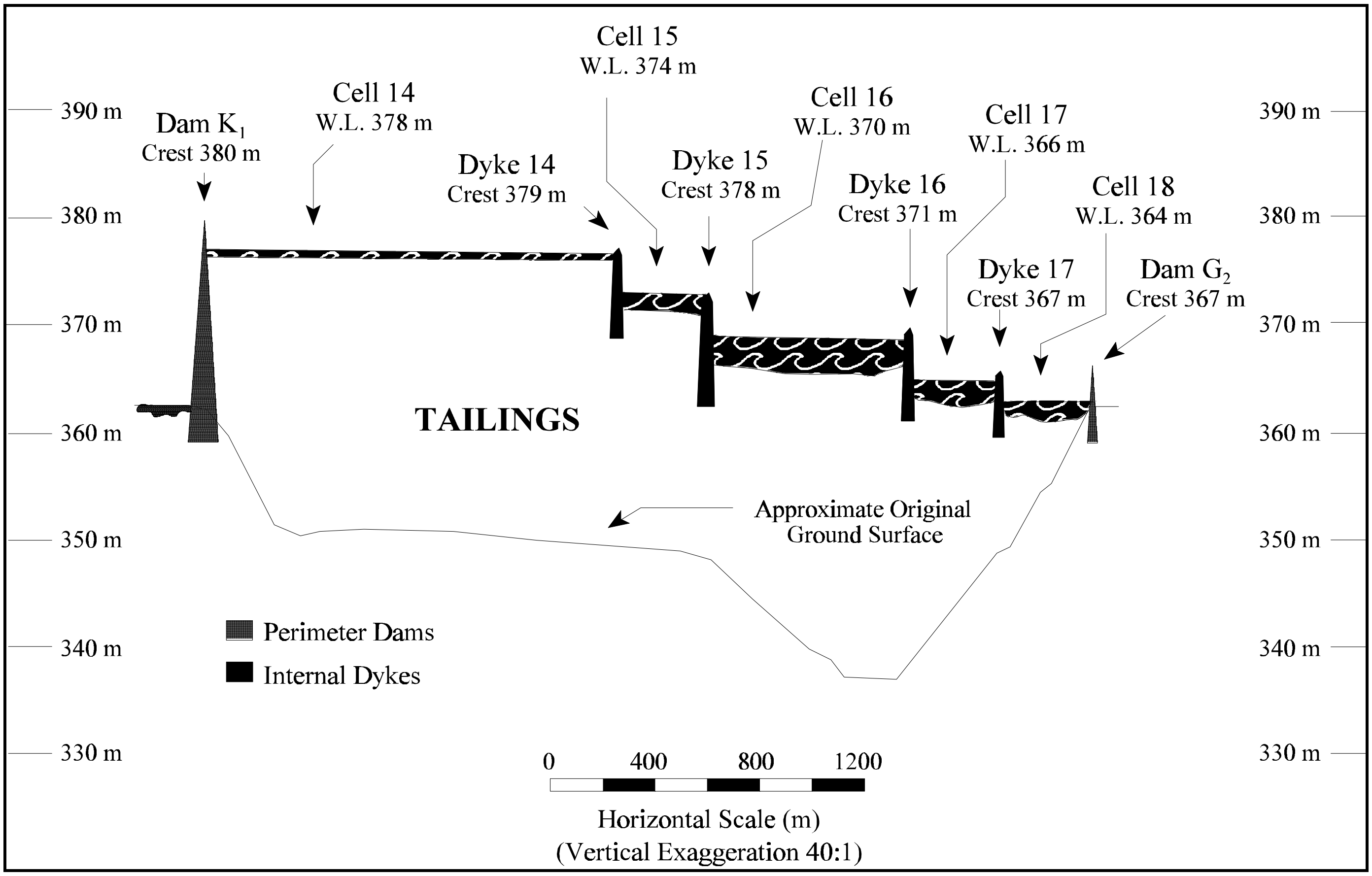

FIGURE 6.3-2. Schematic Flooding of Acid-Generating Quirke Tailings (adapted from Davé and Vivyurka, 1994).

6.4 Other Techniques

As explained in preceding sections of this chapter, there are two basic approaches to drainage-chemistry control: reactive and proactive. Reactive control involves collection and treatment of drainage (Section 6.2), whereas proactive control focusses on minimizing concentrations leaving a minesite component using "solid covers" (Section 6.2), "water covers" (Section 6.3), and other techniques (this section).

As the miscellaneous category, there is a wide variety of other techniques that can control concentrations in drainage from a minesite component, as illustrated in the following case studies. These techniques include moving mine materials elsewhere like underground workings, a pervious "surround" that minimizes water movement through mine materials, layering/blending of mined materials, and sealing of underground workings leading to flooding. The latter technique is also a variant on water covers (Section 6.3).

Other techniques include encapsulation of rock particles or tailings in secondary-mineral coatings consisting of iron or phosphate and bactericides to kill bacteria affecting reaction rates. These coatings and bactericides have not been successful on field scales because they require the physical transport of reactants to virtually all surfaces or all particles. As explained in Chapter 3, water movement in minesite components is not simple and does not lead to the rinsing of most rock surfaces.

Case Study 6.4-1: Backfill of Tailings

highlights: return of mined materials to underground mines ("backfilling"); advantages and disadvantages of backfilling, changing with time

"Backfill" is a term referring to the pumping or hauling of granular material into underground mines to stabilize or seal openings. Coarse-grained materials like sand-sized tailings, typically with a small amount of cement, have been used as backfill in mines for decades. "Paste backfill" refers to mixtures of finer-grained or unsorted tailings and cement pumped into underground mines to seal openings (Brackebusch, 1992). Only relatively small additions of cement (often less than 10%) are needed to stabilize backfill.

While the typical purpose of backfill is to physically stabilize the walls of an opening, backfill has recently gained importance for (1) reducing the surface accumulation of mine wastes (Broicher, 1992) and (2) controlling drainage chemistry from underground mines by isolating workings from air or water (Levens and Boldt, 1992). However, depending on the chemical composition of the backfill, the physical advantages can be offset by the resulting effect on mine water (Hutt and Morin, 1994).

For example, Levens and Boldt (1992) examined the chemistry of drainage waters passing through backfilled zones in two hard-rock polymetallic mines. In one mine, sulfide oxidation and pH neutralization by carbonate and silicate minerals were apparently occurring in water passing through backfill of cemented unsorted tailings. Concentrations of some heavy metals increased in the drainage. In a second mine, backfill consisted of uncemented, sand-sized sorted tailings. Like the first mine, there was evidence of sulfide oxidation and carbonate-mineral dissolution, as well as ferric-iron precipitation where drainage left the backfill. However, unlike the first mine, heavy-metal concentrations were not affected. Levens and Boldt report that backfill is considered "underground injection" in the USA and thus subject to strict regulations regarding water chemistry.

Although geochemical reactivity of tailings is often considered a liability, there are some cases where the benefits reportedly outweigh the liabilities. For example, Patton (1952) reported that sulfide-mineral oxidation enhanced the strength of tailings backfill at Noranda, Quebec, and was thus to be encouraged. This benefit of oxidation was still promoted in the 1980's (Nantel and Lecuyer, 1983), but apparently became a liability by the 1990's. Wheeland and Payant (1991) state,

> "There is currently a legitimate reluctance on the part of mine operators to place reactive material underground due to the uncertainty of the outcome. For example, Brunswick Mining used some high sulphide slimes as uncemented backfill in the upper section of the mine two decades ago, and the resultant 'fire' is still generating sulphur dioxide which is vented via a surface stack, despite herculean efforts to bulkhead the area 'air tight'".

Other types of mining can also use backfill to reduce waste volumes. Potash and salt mines can return soluble tailings and insoluble "slimes" underground (Prugger, 1992; De Souza, 1992; see also Case Study 4.2-3). Lentz (1992) described the excavation of caverns in salt formations using water, with the specific intent of storing sandy waste from oil-sand processing. The brine resulting from cavern excavation can be injected into a deep well for disposal.

Where large-scale backfilling is carried out to control drainage chemistry from tailings, a major issue is the retrieval of tailings from surficial impoundments. However, there are many reported cases of successful tailings retrieval (e.g., Table 6.4-1) using a variety of methods. Costs for retrieval are roughly US$1-5/t (Hutt and Morin, 1994).

Case Study 6.4-2: Pervious Surround

> *highlights: hydraulic isolation of mined materials using a highly permeable envelope; effectiveness dependent on physical and chemical factors that change with time*

St-Arnaud et al. (1994) and Woyshner et al. (1995) reported a case study of a tailings impoundment with natural control of acidic drainage and metal leaching. The Fault Lake tailings impoundment near Sudbury, Canada, contains 6.45×10^6 t of nickel tailings placed in a topographic depression between 1965 and 1978. These tailings cover 22.2 ha of the 55 ha enclosed watershed.

TABLE 6.4-1
Examples of Tailings Retrieval from Surface Impoundments
(adapted from Goode, 1993)

Location	Metal	Rate (tons/month)	Method
Chaffers Plant, Kalgoorlie, Australia	Au	60,000	Monitor with 15% solids feed
Daggafontein, South Africa	Au	1,000,000	Monitors
Eastmaque, Kirkland Lake, Ontario, Canada	Au	58,000	Cutter dredge
ERG, Timmins, Ontario, Canada	Au	1,000,000	Monitors
Freegold Consolidated Mines, South Africa	Au, U, H_2SO_4	1,000,000	Monitors
Giant Yellowknife Mine, Northwest Territories, Canada	Au	250,000	Monitors
Lac Minerals, Kirkland Lake, Ontario, Canada	Au	22,000	Cutter dredge
Mount Morgan, Queensland, Australia	Au	250,000	Bucket wheel dredge
Rand Mines, South Africa	Au, pyrite	370,000	Front-end loaders and monitors
Simmergo, South Africa	Au	174,000	Electric shovel and truck
Anaconda's Darwin Project, California, USA	Ag	120,000	Font-end loader
Santa Julia Plant, Real del Monte y Pachuca, Mexico	Ag	200,000	Monitors
Miami Copper Co., Arizona, USA	Cu	324,000	Monitors
Nchanga, Zambia	Cu	1,500,000	Erosion & monitors
Blyvooruitzicht Gold Mine, South Africa	U, Au	100,000	Bucket wheel
Chemwes, South Africa	U, Au, H_2SO_4	290,000	Monitors & bucket wheel excavator
Eldorado, Port Radium, Northwest Territories, Canada	U	5,000	Suction dredge
ERGO, South Africa	U, Au, H_2SO_4	1,700,000	Monitors

Natural sediments are predominantly fine sand to gravel. In contrast, the fine-grained tailings have a lower hydraulic conductivity by a factor of roughly 100-1000 and thus groundwater flow is preferentially diverted around the tailings mass. Also, most of the tailings are above the water table. As a result, drainage of tailings porewater into the coarser sediments is reduced by capillary tension, which also helps in maintaining saturation except near the tailings surface.

Mineralogy of the tailings is predominantly pyrrhotite (> 30 wt-%) and quartz with minor chlorite and plagioclase in the upper 4 m ("Layer 1"). Pyrrhotite decreased with depth to below detection at 10 m depth ("Layer 2"). This was associated with dominant chlorite and quartz, and minor mica, plagioclase, amphibole, and calcite. Due to typical specific-gravity effects, Layer 1 was laterally limited to the central and northerly portions of the impoundment near the discharge pipes. Acid-base accounting (Section 5.2.1) showed that the upper 2 m of Layer 1 had a paste pH around 3.3, and TNPR and TNNP increased to net-acid-neutralizing levels only at depths greater than 10-14 m. However, the aluminosilicate minerals were considered an additional source of NP not detected by the ABA analyses.

Porewater concentrations of sulfate in the tailings were typically around 1000 mg/L, reflecting gypsum saturation, and concentrations of several other metals were detectible. However, monitor wells in the downgradient natural sediments showed little effect of drainage from the tailings, which was attributed to the contrast in hydraulic conductivity, the relatively high depth to the water table, the limited infiltration into the tailings, and the chemical attenuation of metals. Nevertheless, the primary control was considered the residual NP, because greatly increased porewater concentrations upon exhaustion of NP in the tailings could overwhelm the effect for differing hydraulic conductivities.

Case Study 6.4-3: Placement of Tailings into a Pit

> *highlights: placement of tailings into a mined-out pit; use of a pervious surround to isolate tailings hydraulically; physical, chemical, and geotechnical observations during and after placement*

As a general analog to tailings backfill in underground workings (Case Study 6.4-1), uranium tailings have been placed into the mined-out Rabbit Lake open-pit mine in Saskatchewan since 1984 (Cameco Corporation, 1992; PVS Technologies Ltd., 1994). By the end of 1993, the total weight of tailings placed in the pit was approximately 3,000,000 dry tonnes, filling the lower 60 meters of the pit.

The placement of tailings was conducted after careful design and modelling to create a "pervious surround" (Case Study 6.4-2). This pervious surround, or envelope, of crushed rock was draped upwards onto the pit walls as the pit was filled with tailings. A sand filter was then draped over the crushed rock to prevent tailings from migrating into the rock.

During placement of the tailings, the pervious surround allowed the tailings to drain and consolidate. Drainage flowed downward through the surround to the base of the pit, through a drift, to a raise where the water was then pumped to the surface. This water was then used in the mill, or treated and discharged.

After the Rabbit Lake pit is filled and flooded with a water cover (Section 6.3), the underlying concept of the pervious surround will be to divert regional groundwater flow around the tailings. As a result, no contaminants will be flushed out of the tailings into the surrounding environment. As a result, groundwater is expected to flow only in the crushed rock and sand filter, whereas porewater in the tailings will be stagnant. Nevertheless, molecular diffusion is expected to release a minor amount of contaminants into the pervious surround.

There has been detailed monitoring of the placed tailings shortly after the program was initiated. The results of the monitoring, the success of the program, and the problems encountered during placement provide valuable lessons for similar future efforts.

Tailings were initially transported to the base of the Rabbit Lake Pit by mechanical means, but problems arose with local plugging of the pervious surround and difficulty of moving vehicles over the placed tailings. After regulatory approval in 1990, tailings as approximately 30-40% solids, were placed as a slurry through a moveable pipeline.

The tailings were instrumented with settlement cells, pneumatic piezometers, and thermistors. Several monitoring instruments failed, but sufficient information was obtained to conclude that placement, consolidation, and draining were consistent with expectations.

Rates of settlement in 1992 and 1993 were approximately 0.0009 to 0.0034 m/yr. These rates were in general agreement with modelling predictions.

Piezometric levels in deep piezometers lie tens of meters below the top of the tailings and show no close relationship to the top elevation as tailings were placed over the years. On the other hand, shallow piezometers show piezometric levels near or above the top of the tailings, and these levels increased as tailings were placed. Overall, the hydraulic gradient is downwards.

Partially frozen layers of tailings, formed during winter months and then buried by new tailings, were a concern from the perspective of consolidation. However, thermistors and drilling indicated these layers are slowly thawing.

Particle-size segregation was noted in Rabbit Lake tailings during placement: grain size decreased with increasing distance from the discharge point. However, the segregation apparently did not affect rates of consolidation and draining. The percentage of silt and clay in the tailings (less than 0.044 mm) increased from roughly 30% at the discharge to 100% at a lateral distance of 177 m. The percentage of coarse sand and gravel (greater than 0.55 mm) decreased from approximately 8% at the discharge to 0% at 140 m.

Rabbit Lake Pit can hold approximately 9,000,000 tonnes of tailings. After all tailings have been placed, up to 20 years will be required for dissipation of pore pressures and consolidation based on modelling.

Case Study 6.4-4: Effect of "Wet" Mine Seals on Drainage Chemistry

highlights: effectiveness of flooding underground mines while allowing active water flow; monitoring of 14 sealed mines over 24 years

Case Study 4.3-12 has provided several examples of drainage chemistry from underground mines that were flooded due to solid portal plugs or because of natural flooding (Figures 3.2.2-2 and 3.2.2-3). These examples showed that flooding does not often have significant effects on drainage chemistry, at least for a few decades. This case study focusses on an example of the unexpected effects of natural mine flooding (Hamilton et al., 1994) and on "wet" portal seals which are designed to allow water flow while preventing air entry (Borek et al., 1991). These wet seals minimize one concern over solid portal plugs: the accumulation of pressure and water behind the seal which can lead to catastrophic failure of the seal or surrounding rock. The success of such wet seals at controlling acid generation is based on the assumption that there is no other pathway for oxygen to enter the workings, which is typically incorrect due to fracturing (Case Studies 3.2.2-8 and 4.3-12).

Hamilton et al. (1994) described the closure of an underground tin mine in southwestern England. Closure involved natural flooding and eventual overflow of the workings with the intent of eliminating acidic drainage. Attempts to predict where and when the overflow would occur were not successful due to incomplete mine records and the slow rate of flooding. Also, the rate of overflow was apparently underestimated with overflow rate beginning at 5000 m^3/d, increasing to 40,000 m^3/d, and then averaging 25,000 m^3/d. Drainage chemistry fluctuated through time and with depth, so predictions of chemistry were reportedly "impossible". Pumping and treatment were started to reduce environmental effects of the drainage and, when this was temporarily halted, 50 km^2 of tidal water was polluted. Passive treatment methods

(Section 6.1.2) were being tested.

Borek et al. (1991) examined the effectiveness of wet mine seals at improving acidic drainage chemistry over a period of a few decades in West Virginia, USA. In the late 1960's, 14 wet seals were installed in Type 2 underground coal workings (Figures 2.2-6 and 3.2.2-2) around a 72 km^2 area. Physical inspection of the seals revealed that most were in good condition more than 20 years after installation and therefore any changes in drainage chemistry could be attributed to the seals.

The study area is mountainous and has average temperatures from 0.3°C in January to 21.1°C in July with an annual average of 10.4°C (Borek et al., 1991). Average annual precipitation is 1.16 m with no one quarter consistently producing the greatest amount from year to year. The sulfur level in the local coal was relatively low at 0.6-0.8%S, but non-coal strata could contain up to 10%S.

Monitoring of drainage chemistry through the seals was conducted before sealing in 1968, just after sealing in 1971, in 1980, and again in 1990 (Table 6.4-2). Drainage flows through some seals were generally erratic on a seasonal basis (1980 data), but some showed a decrease by 1990. This apparently indicated flowpaths had changed and water was draining in other directions through time.

Most seals did not create a significant improvement in pH compared to pre-seal values (1966, Table 6.4-1). For acidity, nine of 14 seals showed consistently less acidity after sealing, while three generated more acidity at least at one point after sealing and two had no pre-sealing data. Although Borek et al. (1991) did not explore the drainage chemistry further, the techniques described in Section 4.2.5 indicate that changes in chemistry are related closely to changes in pH (Figure 6.4-1). In other words, the seasonal and longer-term fluctuations in chemistry are primarily the result of pH variation.

Case Study 6.4-5: Layering of Mined Rock to Control Drainage Chemistry

highlights: layering of net-acid-generating and net-acid-neutralizing rock in laboratory columns and a full-scale dump; layer thicknesses from 0.2 m to 6 m; lack of control on reaction rates and drainage chemistry due to physical factors

The Samatosum minesite in southeastern British Columbia, Canada, consists of an open pit, underground workings, a waste-rock dump, and tailings impoundment. Mining began in May 1989 and ended in September 1992 (Denholm and Hallam, 1991; Piteau Associates, 1996).

During the design phase of the mine, static tests (Section 5.2) indicated 5.3x10^6 t (roughly 58%) of the waste rock would be net acid neutralizing and

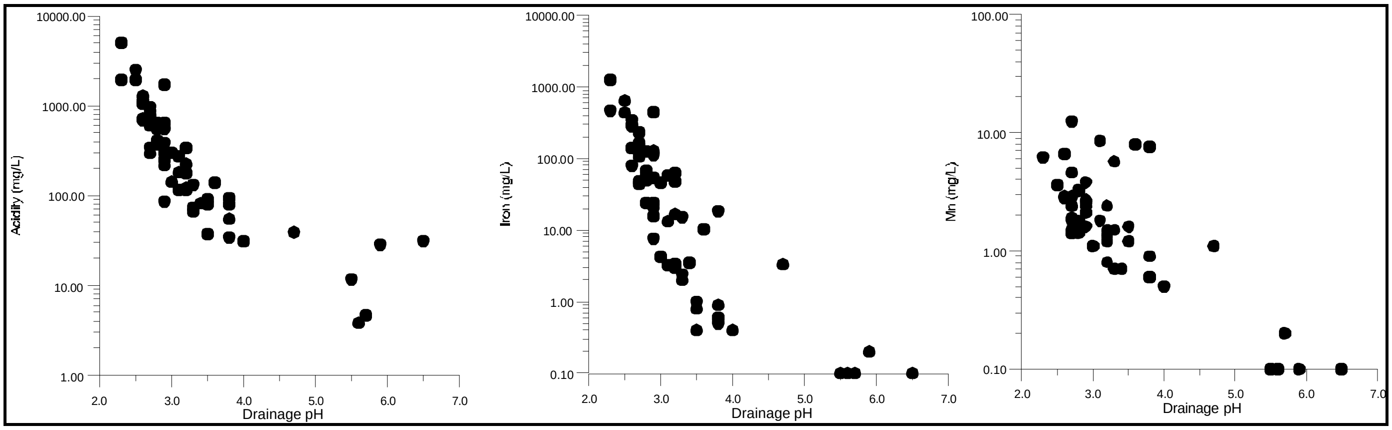

FIGURE 6.4-1. Relationship of Drainage pH to Aqueous Concentrations of Acidity, Iron, and Manganese from Wet Portal Seals (adapted from Borek et al., 1991).

TABLE 6.4-2
Drainage Chemistry Behind Wet Portal Seals in West Virginia, USA
(from Borek et al., 1991)

Year-Month	Flow (L/min)	pH	Acidity (mg/L)	Fe (mg/L)	Mn (mg/L)	Flow (L/min)	pH	Acidity (mg/L)	Fe (mg/L)	Mn (mg/L)
	Seal 1					**Seal 2**				
1966	-	-	-	-	242	NA	3.7	228.1	NA	
1980-3/4	41.6	2.9	86	53	1.6	125	3.2	341	62	1.2
1980-7	30.3	2.8	395	59	1.4	136	3	304	46	1.1
1980-10	30.3	2.7	342	48	1.4	87.1	2.7	297	44	1.4
1990-9	42.3	2.9	644	128	2.1	5.2	2.9	251	23.8	2.7
	Seal 3					**Seal 4**				
1966	183	NA	217	9.4	NA	204.4	2.9	219	7.6	NA
1971	274	NA	164	2.7	NA	-	-	-	-	-
1980-3/4	515	4.7	39	3.3	1.1	519	3.2	116	3.4	1.3
1980-7	174	3.5	80	0.8	1.2	167	3.2	179	3	1.5
1980-10	102	3.5	90	0.4	1.6	37.9	3.1	182	3.2	1.8
1990-9	90.8	3.8	34.3	0.5	0.9	59.6	3.3	133	2.4	1.5
	Seal 5					**Seal 6**				
1966	32.3	2.6	712	80	NA	143.8	3.5	37	1	NA
1971	75.3	NA	388	NA	NA	-	-	-	-	-
1980-3/4	98.4	3.2	225	16.7	2.4	238	5.5	11.7	0.1	0.1
1980-7	56.8	2.9	388	21	2.7	140	5.7	4.6	0.1	0.2
1980-10	8.7	2.8	371	24	3.3	64.3	5.6	3.8	0.1	0.1
1990-9	2.2	2.9	300	15.7	2.5	93.5	6.5	31.2	0.1	0.1
	Seal 7					**Seal 8**				
1966	231	2.5	1942	434.5	NA	-	-	-	-	-
1971	360	2.6	1060	291.3	NA	-	-	-	-	-
1980-3/4	670	2.9	564	112	3.8	189	3.2	341	48	1.4
1980-7	167	2.7	606	120	4.6	28.4	2.8	550	67	1.8
1980-10	159	2.6	692	137	6.6	9.5	2.7	688	105	2.4
1990-9	39	2.7	893	161	12.5	0.8	2.8	409	49	1.7
	Seal 9					**Seal 10**				
1966	1501	NA	307	25.3	NA	53.8	2.3	1958	465	NA
1971	1533	NA	186	10.1	NA	360	2.6	1117	343.7	NA
1980-3/4	2456	3.4	82	3.5	0.7	640	2.8	652	126	3.2
1980-7	1283	3.2	122	3.3	0.8	291	2.7	707	130	2.9
1980-10	515	3	142	4.2	1.1	185	2.6	723	140	2.9
1990-9	673.4	3.3	66.6	2	0.7	72.7	2.7	708	128	2.4
	Seal 11					**Seal 12**				
1966	221	NA	977	117.2	NA	124	NA	264	NA	NA
1971	360	NA	601	NA	NA	53.8	NA	2222	NA	NA
1980-3/4	151	2.9	561	117	1.6	75.7	2.9	1724	439	2.4
1980-7	159	2.7	764	154	1.8	56.8	2.5	2523	639	3.6
1980-10	49.2	2.6	1298	282	2.8	15.1	2.3	5036	1253	6.2
1990-9	26.1	2.7	781	165	1.5	96.9	2.7	973	231	1.9

Year-Month	Flow (L/min)	pH	Acidity (mg/L)	Fe (mg/L)	Mn (mg/L)	Flow (L/min)	pH	Acidity (mg/L)	Fe (mg/L)	Mn (mg/L)
	Seal 13					**Seal 14**				
1966	48.4	2.8	591	NA	NA	98.4	NA	245	22	NA
1971	91.5	3.1	275	58	NA	-	-	-	-	-
1980-3/4	117	3.8	94	18.5	7.6	235	4	31	0.4	0.5
1980-7	64.3	3.6	139	10.2	7.9	117	3.8	55	0.6	0.6
1980-10	34.1	3.1	116	13.2	8.5	45.4	3.8	80	0.9	0.6
1990-9	45.4	3.3	73.3	15.2	5.7	51.6	5.9	28.5	0.2	0.1

the remaining 3.8×10^6 t would be net acid generating. As a result, the mine plan called for the layering of the two types of rock in 6 m layers so that the entire dump would contain sufficient capacity to neutralize all acidity.

To predict the effectiveness of the layering, six kinetic columns (Section 5.3.2), with various layers of the two rock types as thin as 0.2 m, were operated for up to 5.5 years starting in early 1989 (Denholm and Hallam, 1991). Based on the measured alkalinity of column effluents, predictions suggested the columns would never release acidic water. Also, sulfate production rates suggested the layering suppressed rates of oxidation and acid generation.

Within two years of initial dump construction, seepage with pH below 3 was found at one monitoring site, although the columns continued to release near-neutral effluent. Also, drainage at pH 8 was carrying dissolved zinc at levels up to 20 mg/L.

In order to examine the failure of the field-scale layering and the discrepancy with the columns, a detailed review of data and additional analyses were carried out in 1996 (Morin and Hutt, 1997). One problem was that alkalinity in column effluent was equated with dissolution of neutralization potential (NP), whereas alkalinity actually underestimates NP dissolution (Sections 5.2.1.3 and 5.3.1). Although the proper parameters had not been measured in the column effluent, reasonable assumptions based on the International Kinetic Database (Section 5.3.3) indicated all columns would have eventually released acidic effluents. Also, additional analyses showed that the layering as thin as 0.2 m in the columns did not significantly suppress reaction rates. As a result, NP was readily and quickly consumed, which allows the relatively rapid appearance of acidic drainage.

The full-scale dump contained proportionally more NP than the columns, and thus should have remained neutral. However, the unsuppressed reaction rates led to quick generation of acidity and the 6 m layers of relatively net-acid-generating rock preferentially channelled water through and out of these layers. This accounts for the relatively rapid appearance of acidic seepage from the dump. In other words, physical factors like seepage flowpaths led to acidic drainage which was not expected based on chemical factors. In any case, the elevated metal concentrations even at pH 8 highlight the inability of layering in this dump to control drainage chemistry.

6.5 Questions

6-1. The selection of the optimum reactive or proactive control of drainage chemistry at a minesite is based on many site-specific factors, including technical, engineering, economic, and political issues. List some factors that would lead to reactive collection and treatment for centuries as the optimum control.

6-2. Based on Figure 6-1, what maximum proportion of unevaporated rainfall could be allowed through the cover if the allowable regulatory concentration in the drainage were (a) 5 mg/L and (b) 0.05 mg/L?

6-3. Based on Figure 6-2, what is the minimum thickness of the inert cover if the allowable regulatory concentration in the overlying water were (a) 1 mg/L and (b) 0.01 mg/L?

6-4. Based on Table 6.1.1-2, costs for reactive collection and treatment from tailings impoundments are within the cost range for proactive self-sustaining water covers. Under which conditions would this water cover be less expensive than collection and treatment? Give a numerical example.

6-5. At a minesite, the acidic drainage has pH 2.5 and 30,000 mg/L of acidity. Would you expect passive treatment of this drainage by wetlands or anoxic limestone drains (ALD) to be successful? Why? Would a series of passive controls, like an ALD followed by wetland treatment, have a higher chance of success?

6-6. Case Study 6.2-2 is one of the most detailed published studies of integrated drainage controls for several minesite components. Although the detailed assessment of overall successes and failures is not yet completed, what successes and failures do you perceive or expect? Would you do anything differently?

6-7. What are some technical and political issues surrounding the underwater placement of tailings and waste rock in lakes, rivers, and oceans?

6-8. How might adverse environmental effects be caused by the retrieval of tailings from a surface impoundment?

6-9. Is the sealing or flooding of underground workings generally successful in controlling acidic drainage and metal leaching?

REFERENCES

Aachib, M., M. Aubertin, and R.P. Chapuis. 1994. Column tests investigation of milling wastes properties used to build cover systems. IN: International Land Reclamation and Mine Drainage Conference and Third International Conference on the Abatement of Acidic Drainage, Pittsburgh, PA, USA, April 24-29, Volume 2, p. 128-137. U.S. Bureau of Mines Special Publication SP 06A-94.

Ackman, T.E. 1982. Sludge Disposal from Acid Mine Drainage Treatment. U.S. Bureau of Mines, Report of Investigations 8672, 25 p.

Adams, R.L., J.J. Ninesteel, and H.W. Rauch. 1994. Laboratory testing of coatings for prevention of acid drainage in underground coal mines. IN: International Land Reclamation and Mine Drainage Conference and Third International Conference on the Abatement of Acidic Drainage, Pittsburgh, PA, USA, April 24-29, Volume 2, p. 218-225. U.S. Bureau of Mines Special Publication SP 06A-94.

Agricola, G. 1556. De Re Metallica. Translated from the first Latin edition of 1556 by H.C. Hoover and L.H. Hoover. Dover Publications Inc, New York, 1950.

Aitchison, J., and J.A.C. Brown. 1976. The Lognormal Distribution. University of Cambridge, Department of Applied Economics Monograph 5. Cambridge University Press. 176 p.

Al, T.A., and D.W. Blowes. 1995. Storm-water hydrograph separation of run off from the Kidd Creek Mine-Tailings Impoundment, Timmins, Ontario. 1995. IN: T.P. Hynes and M.C. Blanchette, eds., Proceedings of Sudbury ‘95, Mining and the Environment, Sudbury, Canada, May 28-June 1, Volume 2, p.693-701.

Al, T.A., D.W. Blowes, and J.L. Jambor. 1994. A geochemical study of the Main Tailings Impoundment at the Falconbridge Limited, Kidd Creek Division Metallurgical Site, Timmins, Ontario. IN: J.L. Jambor and D.W. Blowes, eds, The Environmental Geochemistry of Sulfide Mine-Wastes, Mineralogical Association of Canada Short Course Handbook Volume 22, p.333-379.

Aljoe, W.W. 1994. Hydrologic and water quality characteristics of a partially-flooded, abandoned underground coal mine. IN: International Land Reclamation and Mine Drainage Conference and Third International Conference on the Abatement of Acidic Drainage, Pittsburgh, PA, USA, April 24-29, Volume 2, p. 178-187. U.S. Bureau of Mines Special Publication SP 06A-94.

Aljoe, W.W., and J.W. Hawkins. 1993. Neutralization of Acidic Discharges from Abandoned Underground Coal Mines by Alkaline Injection. U.S. Bureau of Mines Report of Investigation 9468. 37 p.

Aljoe, W.W., and J.W. Hawkins. 1991a. Investigation and characterization of groundwater flow systems in abandoned underground coal mines. IN: Proceedings of the 1991 National Meeting of the American Society for Surface Mining and Reclamation, Durango, Colorado, USA, May 14-17,. P.241-259.

Aljoe, W.W., and J.W. Hawkins. 1991b. Hydrologic characterization and in-situ neutralization of acidic mine pools in abandoned underground coal mines. IN: Proceedings of the Second International Conference on the Abatement of Acidic Drainage, Montreal, Quebec, September 16-18, Tome 1, p. 69-89.

Allen, D.F. 1983. Quarry site rehabilitation and after use. IN: Surface Mining and Quarrying, the Second International Surface Mining and Quarrying Symposium, Institution of Mining and Metallurgy, Great Britain, October 4-6, p.89-97.

Alpers, C.N., D.K. Nordstrom, and J.M. Thompson. 1994. Seasonal variations of Zn/Cu ratios in acid mine water from Iron Mountain, California. IN: C.N Alpers and D.W. Blowes, eds., Environmental Geochemistry of Sulfide Oxidation, American Chemical Society Symposium Series 550, p.324-344.

Anbeek, C. 1993. The effect of natural weathering on dissolution rates. Geochemica et Cosmochimica Acta, 57, p.4963-4975.

Anbeek, C. 1992a. Surface roughness of minerals and implications for dissolution studies. Geochimica et Cosmochimica Acta, 56, p.1461-1469.

Anbeek, C. 1992b. The dependence of dissolution rates on grain size for some fresh and weathered feldspars. Geochimica et Cosmochimica Acta, 56, p.3957-3970.

Armstrong, D. 1982. Problems associated with the rapid dewatering of a multilayered aquifer and mining of a trial coal pit at Bowmans, South Australia. IN: Proceedings of the First International Mine Water Congress of the International Mine Water Association, April 19-24, Budapest, Hungary, Section B, p. 354-372.

Asmund, G. 1992a. Pollution from the marine tailings disposal at the lead-zinc mine at Maarmorilik, West Greenland. IN: R.K. Singhal, A.K. Mehotra, K. Fytas, and J-L. Collins, eds., Environmental Issues and Management of Waste in Energy and Mineral Production, Volume 1, p. 587-594. A.A. Balkema Publishers, Brookfield, Vermont, USA.

Asmund, G. 1992b. Lead and zinc pollution for marine dumping of waste rock from lead/zinc mining. IN: S. Bandopadhyay and F.J. Skudrzyk, eds., Proceedings of the 1st International Symposium on Mining in the Arctic, July 17-19, Fairbanks, Alaska, p.105-112.

Association for the Standardized Testing of Materials. 1994. Draft Method: Standard Test Method for Accelerated Weathering of Solid Waste Using a “Modified” Humidity Cell. Draft dated November 30, 1994.

Aubé, B.C., L.C. St-Arnaud, S. Payant, and E.K. Yanful. 1995. Laboratory evaluation of the effectiveness of water covers for preventing acid generation from pyritic rock. IN: T.P. Hynes and M.C. Blanchette, eds., Proceedings of Sudbury ‘95, Mining and the Environment, Sudbury, Canada, May 28-June 1, Volume 2, p.495-504.

Aziz, M.A., and K.D. Ferguson. 1997. Equity Silver Mine - integrated case study. IN: Proceedings of the Fourth International Conference on Acid Rock Drainage, Vancouver, Canada, May 31 - June 6.

Bain, J.G., D.W. Blowes, and W.D Robertson. 1995. The hydrogeochemistry of a sand aquifer affected by discharge from the Nickel Rim Tailings, Sudbury, Ontario. IN: T.P. Hynes and M.C. Blanchette, eds., Proceedings of Sudbury ‘95, Mining and the Environment, Sudbury, Canada, May 28-June 1, Volume 2, p.715-723.

Banks, D., P.L. Younger, and S. Dumpleton. 1996. The historial use of mine-drainage and pyrite-oxidation waters in central and eastern England, United Kingdom. Hydrogeology Journal, 4, p.55-68.

Bean, J.J. 1972. Tailing as an ore body. IN: C.L. Alpin and G.O. Argall, Jr., eds., Tailings Disposal Today, Proceedings of the First International Tailing Symposium, Tucson, USA, October 31 to November 3, p.606-614.

Béchard, G., R.G.L. McCready, D.W. Koren, and S. Rajan. 1995. Microbial treatment of acid mine drainage at Halifax International Airport. IN: T.P. Hynes and M.C. Blanchette, eds., Proceedings of Sudbury ‘95, Mining and the Environment, Sudbury, Canada, May 28-June 1, Volume 2, p.545-554.

Bell, A.V., M.D. Riley, and E.K. Yanful. 1994. Evaluation of a composite soil cover to control acid waste rock pile drainage. IN: International Land Reclamation and Mine Drainage Conference and Third International Conference on the Abatement of Acidic Drainage, Pittsburgh, PA, USA, April 24-29, Volume 2, p. 113-121. U.S. Bureau of Mines Special Publication SP 06A-94.

Bell, A.V., F.E. Baechler, and R. Parker. 1992. Management of coal wastes: a state-of-the-art review. IN: R.K. Singhal, A.K. Mehotra, K. Fytas, and J-L. Collins, eds., Environmental Issues and Management of Waste in Energy and Mineral Production, Volume 1, p. 367-378. A.A. Balkema Publishers, Brookfield, Vermont, USA.

Bell, N.E., W.J. Deutsch, and R.J. Serne. 1983. Laboratory studies on natural restoration of ground water after in situ leach uranium mining. IN: D.M. Nielsen, ed., Proceedings of the Third National Symposium on Aquifer Restoration and Ground-Water Monitoring, May 25-27, The Fawcett Center, Columbus, Ohio, USA, p.162-168.

Benjamin, M., and R. Sletten. 1993. Metals treatment at Superfund sites by adsorptive filtration. U.S. Environmental Protection Agency Emerging Technology Summary EPA/540/SR-93/515.

Bennett, J.W., and M.D. Lawton. 1995. Assessment of the Rum Jungle Strategy for acid mine drainage control. IN: N.J. Grundon and L.C. Bell, eds., Proceedings of the Second Australian Acid Mine Drainage Workshop, Charters Towers, Queensland, Australia, March 28-31.

Bennett, J.W., D.K. Gibson, A.I.M. Ritchie, Y Tan, P.G. Broman, and H. Jönsson. 1994. Oxidation rates and pollution loads in drainage: correlation of measurements in a pyritic waste rock dump. IN: International Land Reclamation and Mine Drainage Conference and Third International Conference on the Abatement of Acidic Drainage, Pittsburgh, PA, USA, April 24-29, Volume 1, p. 400-409. U.S. Bureau of Mines Special Publication SP 06A-94.

Bennett, J.W., J.R. Harries, G. Pantelis, and A.I.M. Ritchie. 1989. Limiations on pyrite oxidation rates in dumps set by air transport mechanisms. IN: International Symposium on Biohydrometallurgy, Jackson Hole, Wyoming, August 13-18.

Bhatti, T.M., J.M. Bigham, A. Vuorinen, and O.H. Tuovinen. 1994. Alteration of mica and feldspar associated with the microbiological oxidation of pyrrhotite and pyrite. IN: C.N Alpers and D.W. Blowes, eds., Environmental Geochemistry of Sulfide Oxidation, American Chemical Society Symposium Series 550, p.90-105.

Blight, G.E. 1979. The Disposal of Mining and Industrial Waste - Viewpoint. Die Sivielle Ingenieur in Suid-Afrika, June, 1979, p. 133.

Blowes, D.W. 1990. The Geochemistry, Hydrogeology, and Mineralogy of Decommissioned Sulfide Tailings: A Comparative Study. Ph.D. Thesis, Department of Earth Sciences, University of Waterloo, Ontario, Canada.

Blowes, D.W., and C.J. Ptacek. 1994. Acid-neutralization mechanisms in inactive mine tailings. IN: J.L. Jambor and D.W. Blowes, eds, The Environmental Geochemistry of Sulfide Mine-Wastes, Mineralogical

Association of Canada Short Course Handbook Volume 22, p.271-292.

Blowes, D.W., C.J. Ptacek, E.O. Frind, R.H. Johnson, W.D. Robertson, and J.W. Molson. 1994. Acid-neutralization reactions in inactive mine tailings impoundments and their effect on the transport of dissolved metals. IN: International Land Reclamation and Mine Drainage Conference and Third International Conference on the Abatement of Acidic Drainage, Pittsburgh, PA, USA, April 24-29, Volume 1, p. 429-437. U.S. Bureau of Mines Special Publication SP 06A-94.

Bochenska, T., P. Limisiewicz, and L. Poprawski. 1995. Long-term changes in the shallow water table in a mining area: The Lubin-Glogow copper region, southwestern Poland. Hydrogeology Journal, 3, p.41-52.

Bocker, T., and B. Vizy. 1982. Protection against underground waters of bauxite mining at Nyirad, Hungary, and its impact on the environment. IN: Proceedings of the First International Mine Water Congress of the International Mine Water Association, April 19-24, Budapest, Hungary, Section C, p. 5-26.

Booth, C.J. 1986. Strata-movement concepts and the hydrogeological impact of underground coal mining. Ground Water, 24, p.507-515.

Boreck, D.L., and J.M. Goris. 1992. Reduction of surface mineral waste through underground in situ leaching of fragmented ore and fill material. IN: R.K. Singhal, A.K. Mehotra, K. Fytas, and J-L. Collins, eds., Environmental Issues and Management of Waste in Energy and Mineral Production, Volume 2, p. 951-959. A.A. Balkema Publishers, Brookfield, Vermont, USA.

Boreck, D.L., W.W. Lutzens, and R.A. Speirer. 1990. Ore leaching in underground stopes. Mineral Resource Engineering, 3, p.31-46.

Borek, S.L., T.E. Ackman, G.R. Wetzlaf, R.W. Hammack, and J.R. Lipscomb. 1991. The long-term evaluation of mine seals constructed in Randolph County, WV [USA] in 1967. IN: Proceedings of the Twelfth Annual West Virginia Surface Mine Drainage Task Force Symposium, Morgantown, West Virginia, April 3-4.

Boyle, D.R. 1994. Oxidation of massive sulfide deposits in the Bathurst Mining Camp, New Brunswick. IN: C.N Alpers and D.W. Blowes, eds., Environmental Geochemistry of Sulfide Oxidation, American Chemical Society Symposium Series 550, p.535-550.

Brackebusch, F.W. 1992. Basics of paste backfill systems. IN: R.K. Singhal, A.K. Mehotra, K. Fytas, and J-L. Collins, eds., Environmental Issues and Management of Waste in Energy and Mineral Production, Volume 2, p. 879-883. A.A. Balkema Publishers, Brookfield, Vermont, USA.

Bradham, W.S., and F.T. Caruccio. 1995. Sensitivity Analysis of Laboratory Based Mine Overburden Analytical Techniques for the Prediction of Acidic Mine Drainage. U.S. Department of Interior, Office of Surface Mining, Cooperative Agreement #GR 196451 [USC# 13040-F-151], 267 p.

Brady, K.B.C., E.F. Perry, R.L. Beam, D.C. Bisko, M.D. Gardner, and J.M. Tarantino. 1994. Evaluation of acid-base accounting to predict the quality of drainage at surface coal mines in Pennsylvania, U.S.A. IN: International Land Reclamation and Mine Drainage Conference and Third International Conference on the Abatement of Acidic Drainage, Pittsburgh, PA, USA, April 24-29, Volume 1, p. 138-147. U.S. Bureau of Mines Special Publication SP 06A-94.

Braney, M.C., A. Haworth, N.L. Jeffries, and A.C. Smith. 1993. A study of the effects of an alkaline plume from a cementitious repository on geological materials. Journal of Contaminant Hydrology, 13, p.379-402.

Brawner, C.O. 1979. General report on mine drainage. IN: Mine Drainage, Proceedings of the First International Mine Drainage Symposium, edited by G.O. Argall, Jr., and C.O. Brawner, Denver, Colorado, May. Published by Miller Freeman Publications, Inc., San Francisco, CA, 848 p.

Brealey, S.C. 1965. Groundwater control in opencast mining. IN: Opencast Mining, Quarrying, and Alluvial Mining, p.309-415. The Institution of Mining and Metallurgy, London.

Broicher, H.F. 1992. High-density pumped fill, the perfect solution for disposal of waste from energy and mineral production. IN: R.K. Singhal, A.K. Mehotra, K. Fytas, and J-L. Collins, eds., Environmental Issues and Management of Waste in Energy and Mineral Production, Volume 2, p. 945-950. A.A. Balkema Publishers, Brookfield, Vermont, USA.

Bromwell, L.G., and W.D. Carrier III. 1983. Reclamation alternatives for phosphatic clay disposal areas. IN: D.H. Graves and R.W. De Vore, eds., Proceedings of the 1983 Symposium on Surface Mining, Hydrology, Sedimentology, and Reclamation, November 28-December 2, University of Kentucky, p.371-376.

Bunge, A.L., and C.J. Radke. 1982. Migration of alkaline pulses in reservoir sands. Society of Petroleum Engineers Journal, December, p.998-1012.

Calow, R.W., D. Hevenor, and D. Masson-Stogran. 1995. Comparison of the B.C. Research and EPA acid mine drainage predictive static tests. IN: T.P. Hynes and M.C. Blanchette, eds., Proceedings of Sudbury '95, Mining and the Environment, Sudbury, Canada, May 28-June 1, Volume 2, p.605-612.

Cameco Corporation. 1992. Environmental Impact Statement: Collins Bay A-Zone D-Zone and Eagle Point Development (Revised - 1992). Prepared for the Federal Environmental Assessment Review Panel.

Cameron, E.M. 1979. Effect of graphite on the enhancement of surficial geochemical anomalies originating from the oxidation of sulphides. Journal of Geochemical Exploration, 12, p.35-43.

Cameron, E.M. 1977. Geochemical dispersion in mineralized soils of a permafrost environment. Journal of Geochemical Exploration, 7, p.301-326.

Carlsson, H. 1981. The Stripa Project: An International Project in Radioactive Waste Management. Underground Space, Vol. 6, July/August 1981, pp. 43-45. Pergamon Press.

Caruccio, F.T. 1967. An Evaluation of Factors Influencing Acid Mine Drainage Production from Various Strata of the Allegheny Group and the Groundwater Interactions in Selected Areas of Western Pennsylvania. Ph.D. Thesis, The Pennsylvania State University, State College, Pennsylvania, USA.

Castelo Branco, M.A., M.E. Balsa, M.R. Gusmao, J.M. Vieira e Silva, M.L. Fernandes, and E.M. Sequeira. 1996. Use of pyrite in the reclamation of degraded calcareous soils. Applied Geochemistry, 11, p.347-349.

Cathles, L.M. 1994. Attempts to model the industrial-scale leaching of copper-bearing mine waste. IN: C.N Alpers and D.W. Blowes, eds., Environmental Geochemistry of Sulfide Oxidation, American Chemical Society Symposium Series 550, p.123-131.

Cathles, L.M. 1982. Acid Mine Drainage. Earth and Mineral Sciences, 51, p.37-41.

Cavers, D.S. 1987. Rock engineering for surface gold mines. IN: Gold Mining 87, First International Conference on Gold Mining, edited by C.O. Brawner, Society of Mining Engineers, Vancouver, B.C., November 23-25, 1987, pp.

Chen, L., and Xianjin Huang. 1995. Environmental problems and their treatments in Chinese coal mines. IN: T.P. Hynes and M.C. Blanchette, eds., Proceedings of Sudbury ‘95, Mining and the Environment, Sudbury, Canada, May 28-June 1, Volume I, p.109-115.

Cherry, J.A., T.A. Shepherd, and K.A. Morin. 1982. Chemical composition and geochemical behavior of contaminant groundwater at uranium tailings impoundments. SME-AIME Annual Meeting, Dallas, Texas, February, 1982. Preprint 82-114.

Cherry, J.A., R.J. Blackport, N.M. Dubrovsky, R.W. Gillham, T.P. Lim, D. Murray, E.J. Reardon, D.J.A. Smyth. 1980. Subsurface hydrology and geochemical evolution of inactive pyritic tailings in the Elliot Lkae uranium district, Canada. IN: Proceedings of the Third Symposium on Uranium Mill Tailings Management, Colorado State University, Fort Collins, Colorado, USA, p.353-385.

Cliffe, K.A., D. Gilling, N.L. Jeffries, and T.R. Lineham. 1993. An experimental study of flow and transport in fractured slate. Journal of Contaminant Hydrology, v. 13, p.73-90.

Comba, P.G., R.B. Dix, and S.L. McGill. 1992. A field study to assess natural degradation of cyanide species in an incative leached ore heap. IN: R.K. Singhal, A.K. Mehotra, K. Fytas, and J-L. Collins, eds., Environmental Issues and Management of Waste in Energy and Mineral Production, Volume 1, p. 535-543. A.A. Balkema Publishers, Brookfield, Vermont, USA.

Craft,J.L., and T.M. Crandall. 1988. Mine configuration and its relationship to surface subsidence. IN: Mine Drainage and Surface Mine Reclamation, Volume II: Mine Reclamation, Abandoned Mine Lands, and Policy Issues, U.S. Bureau of Mines Circular 9184, p.373-382.

Cravotta, C.A., III. 1994. Secondary iron-sulfate minerals as soruces of sulfate and acidity. IN: C.N Alpers and D.W. Blowes, eds., Environmental Geochemistry of Sulfide Oxidation, American Chemical Society Symposium Series 550, p.345-364.

Cravotta, C.A., III, K.B.C. Brady, L.C. Gustafson-Minnich, and M.R. DiMatteo. 1994. Geochemical and geohydrological characteristics of bedrock and spoil from two methods of mining at a reclaimed surface coal mine, Clarion County, PA, USA. IN: International Land Reclamation and Mine Drainage Conference and Third International Conference on the Abatement of Acidic Drainage, Pittsburgh, PA, USA, April 24-29, Volume 2, p. 242-249. U.S. Bureau of Mines Special Publication SP 06A-94

Cruickshank, M.J. 1965. Mining offshore alluvials. IN: Opencast Mining, Quarrying and Alluvial Mining, The Institution of Mining and Metallurgy, London, p. 125-155.

Daniel, J.A., J.R. Harries, and A.I.M. Ritchie. 1983. The quality and quantity of runoff and groundwater in two overburden dumps undergoing pyritic oxidation. AWWA ‘83, p.24-1 to 24-8.

Davé, N.K., and A.J. Vivyurka. 1994. Water cover on acid-generating uranium tailings - laboratory and field studies. IN: International Land Reclamation and Mine Drainage Conference and Third International Conference on the Abatement of Acidic Drainage, Pittsburgh, PA, USA, April 24-29, Volume 1, p. 297-306. U.S. Bureau of Mines Special Publication SP 06A-94.

Davé, N.K., T.P. Lim, and A.J. Vivyurka. 1981. Chemical and radioisotopic distribution profiles in an abandoned uranium tailings pile. IN: Proceedings of the 4th Symposium on Uranium Mill Tailings

Management, Fort Collins, Colorado, October.

David, D.J., and R.V. Nicholson. 1995. Field measurements for determining rates of sulphide oxidation. IN: T.P. Hynes and M.C. Blanchette, eds., Proceedings of Sudbury '95, Mining and the Environment, Sudbury, Canada, May 28-June 1, Volume I, p.201-210.

Davis, A., and D. Ashenberg. 1989. The aqueous geochemistry of the Berkeley Pit, Montana. Applied Geochemistry, 4, p.23-36.

Davis, J.C. 1986. Statistics and Data Analysis in Geology, Second Edition.. John Wiley & Sons, New York. 646 p.

Dawson, R.F., and K.A. Morin. 1996. Acid Mine Drainage in Permafrost Regions: Issues, Control Strategies and Research Requirements. Canadian Mine Environment Neutral Drainage (MEND) Report 1.61.2.

Day, S.J. 1994. Evaluation of acid generating rock and acid consuming rock mixing to prevent acid rock drainage. IN: International Land Reclamation and Mine Drainage Conference and Third International Conference on the Abatement of Acidic Drainage, Pittsburgh, PA, USA, April 24-29, Volume 2, p. 77-86. U.S. Bureau of Mines Special Publication SP 06B-94.

De Souza, E. 1992. Geotechnical and environmental benefits of salt tailings disposal underground. IN: R.K. Singhal, A.K. Mehotra, K. Fytas, and J-L. Collins, eds., Environmental Issues and Management of Waste in Energy and Mineral Production, Volume 1, p. 617-626. A.A. Balkema Publishers, Brookfield, Vermont, USA.

De Vos, K.J., D.W. Blowes, W.D Robertson, and J.P Greenhouse. 1995. Deineation and evaluation of a plume of tailings derived water, Copper Cliff, Ontario. IN: IN: T.P. Hynes and M.C. Blanchette, eds., Proceedings of Sudbury '95, Mining and the Environment, Sudbury, Canada, May 28-June 1, Volume 2, p.673-682.

Denholm, E., and R. Hallam. 1991. A review of acid generation research at the Samatosum Mine. IN: Proceedings of the Second International Conference on the Abatement of Acidic Drainage, Montreal, Quebec, September 16-18, Tome 2, p. 561-578.

Dietz, J.M., R.G. Watts, and D.M. Stidinger. 1994. Evaluation of acidic mine drainage treatment in constructed wetland systems. IN: International Land Recalamation and Mine Drainage Conference and Third International Conference on the Abatement of Acidic Drainage, Pittsburgh, PA, USA, April 24-29, Volume 1, p. 70-79. U.S. Bureau of Mines Special Publication SP 06A-94.

Donovan, J.J., and P.F. Ziemkiewicz. 1994. Early weathering behavior of pyritic coal spoil piles interstratified with chemical amendments. IN: International Land Recalamation and Mine Drainage Conference and Third International Conference on the Abatement of Acidic Drainage, Pittsburgh, PA, USA, April 24-29, Volume 1, p. 119-128. U.S. Bureau of Mines Special Publication SP 06A-94.

Down, C.G., and J. Stocks. 1976. The Environmental Problem of Tailings Disposal at Metal Mines. Department of the Environment, United Kingdom, 1976, 33 p.

Downing, B.W., and G.H. Giroux. 1993. Estimation of a waste rock ARD block model for the Windy Craggy massive sulfide deposit, northwestern British Columbia. Exploration and Mining Geology, 2, p.203-215.

Dria, M.A., S.L. Bryant, R.S. Schecter, and L.W. Lake. 1987. Interacting precipitation/dissolution waves: the movement of inorganic contaminants in groundwater. Water Resources Research, 23, p.2076-2090.

Dubrovsky, N.M. 1986. Geochemical Evolution of Inactive Pyritic Tailings in the Elliot Lake Uranium District. Ph.D. Thesis, Department of Earth Sciences, University of Waterloo, Ontario, Canada.

Dudgeon, C.R. 1987. A study of the effects of mining on a groundwater flow regime. IN: Proceedings of the International Conference on Groundwater Systems under Stress, May 11-16, Brisbane, Australia, p.419-429.

Dumaresq, C.G., and F.A. Michel. 1994. The alteration of arsenic-bearing tailings, and the release of contaminants to surface waters in Cobalt, Ontario. IN: International Land Reclamation and Mine Drainage Conference and Third International Conference on the Abatement of Acidic Drainage, Pittsburgh, PA, USA, April 24-29, Volume 2, p. 410. U.S. Bureau of Mines Special Publication SP 06A-94.

Eger, P., J.R. Wagner, Z. Kessa, and G.D. Melchert. 1994. Metal removal in wetland treatment systems. IN: International Land Recalamation and Mine Drainage Conference and Third International Conference on the Abatement of Acidic Drainage, Pittsburgh, PA, USA, April 24-29, Volume 1, p. 80-88. U.S. Bureau of Mines Special Publication SP 06A-94.

ElBoushi, I.M. 1975. Amount of water needed to initiate flow in rubbly rock particles. Journal of Hydrology, 27, pp.275-284.

Ellis, D.V. 1996a. A review of environmental issues associated with different tailings disposal practices. IN: Proceedings of the 3rd International and 21st Annual Minerals Council of Australia Environmental Workshop, Newcastle, New South Wales, Australia, October 14-18, Volume 1, p. 253-263.

Ellis, D.V. 1996b. Regulations controlling submarine tailings disposal in the USA and Canada. IN: Proceedings of the 3rd International and 21st Annual Minerals Council of Australia Environmental Workshop, Newcastle, New South Wales, Australia, October 14-18, Volume 2, p. 197.

Ellis, D.V., and G.W. Poling. 1995. Marine Georesources and Geotechnology, 13, no. 1-2, 233 p.

Ellis, D.V., T.F. Pedersen, G.W. Poling, C. Pelletier, and I. Horne. 1995. Review of 23 years of STD: Island Copper Mine, Canada. Marine Georesources and Geotechnology, 13, p.59-99.

Emrich, G.H., and G.L. Merritt. 1969. Effects of mine drainage on ground water. Ground Water, 7, p.27-32.

Erickson, P.M., R.L.P. Kleinmann, E.T. Posluszny, and P.J. Leonard-Mayer. 1982. Hydrogeochemistry of a large mine pool. IN: Proceedings of the First International Mine Water Congress of the International Mine Water Association, Budapest, Hungary, April 19-24, Section A, p.27-42.

Evans, R.S. 1987. A regional groundwater model for open cut coal winning in the Latrobe Valley, Victoria. IN: Proceedings of the International Conference on Groundwater Systems under Stress, May 11-16, Brisbane, Australia, p.555-564.

Everitt, R.A., P. Chernis, D. Good, and A. Grogan. 1989. Mapping of the excavation damage zone around the circular access shaft at Atomic Energy of Canada Limited's Underground Research Laboratory. IN: Proceedings of an NEA Workshop on Excavation Response in Geological Repositories for Radioactive Waste, Winnipeg, April 26-28, p.271-282. Atomic Energy of Canada Limited.

Ficklin, W.H., K.S. Smith, and G.S. Plumlee. 1994. Geological and geochemical controls on the composition of waters draining from diverse mineral deposits. IN: International Land Reclamation and Mine Drainage Conference and Third International Conference on the Abatement of Acidic Drainage, Pittsburgh, PA, USA, April 24-29, Volume 2, p. 412. U.S. Bureau of Mines Special Publication SP 06A-94.

Firth, I.C., and J. van der Linden. 1997. ARD control at P.T Kelian Equatorial Mining. IN: Proceedings of the Fourth International Conference on Acid Rock Drainage, Vancouver, Canada, May 31 - June 6.

Forsyth, B., A. Cameron, and S. Miller. 1995. Explosives and water quality. IN: T.P. Hynes and M.C. Blanchette, eds., Proceedings of Sudbury ‘95, Mining and the Environment, Sudbury, Canada, May 28-June 1, Volume 2, p.795-803.

Fraser, W.W., and J.D. Robertson. 1994. Subaqueous disposal of reactive mine waste: an overview and update of case studies - MEND/Canada. IN: International Land Reclamation and Mine Drainage Conference and Third International Conference on the Abatement of Acidic Drainage, Pittsburgh, PA, USA, April 24-29, Volume 1, p. 250-259. U.S. Bureau of Mines Special Publication SP 06A-94.

Fredrickson, P. 1996. Mining and water quality with a freshwater aquifer at Tea Gardens, NSW. IN: Proceedings of the 3rd International and 21st Annual Minerals Council of Australia Environmental Workshop, Newcastle, New South Wales, Australia, October 14-18, Volume 2, p. 101-115.

Freeze, R.A., and J.A. Cherry. 1979. Groundwater. Prentice-Hall Canada.

Frost, B.D. 1983. Restoration to agriculture of sand and gravel workings - a practical approach. IN: Surface Mining and Quarrying, the Second International Surface Mining and Quarrying Symposium, Institution of Mining and Metallurgy, Great Britain, October 4-6, p.75-87.

Fuge, R., M. Billet, and O. Selinus, eds. 1996. Selected Papers from the 3rd International Symposium on Environmental Geochemistry, Kraków, Poland, 12-16 September 1994. Applied Geochemistry, 11, 1&2.

Galbraith, D.M. 1990. Mt. Washington Mine Reclamation Project, Brief Status Report (March 19). British Columbia Ministry of Energy, Mines and Petroleum Resources.

Gascoyne, M., S. Stroes-Gascoyne, and F.P. Sargent. 1995. Geochemical influences on the design, construction and operation of a nuclear waste vault. Applied Geochemistry, 10, p.657-671.

Gélinas, P., R. Lefebvre, M. Choquette, D. Isabel, J. Locat, and R. Guay. 1994. Monitoring and Modelling of Acid Mine Drainage from Waste Rocks [sic] Dumps: La Mine Doyon Case Study. Canadian Mine Environment Neutral Drainage (MEND) Report.

Geocon. 1995. Economic Evaluation of Acid Mine Drainage Technologies. Canadian Mine Environment Neutral Drainage (MEND) Report 5.8.1.

Germain, M.D., N. Tassé, and M. Bergeron. 1994. Limit to self-neutralization in acid mine tailings. IN: C.N Alpers and D.W. Blowes, eds., Environmental Geochemistry of Sulfide Oxidation, American Chemical Society Symposium Series 550, p.365-392.

Gibson, D.K., G. Pantelis, and A.I.M. Ritchie. 1994. The relevance of the intrinsic oxidation rate to the evolution of polluted drainage from a pyritic waste rock dump. IN: International Land Reclamation and Mine Drainage Conference and Third International Conference on the Abatement of Acidic Drainage, Pittsburgh, PA, USA, April 24-29, Volume 2, p. 258-264. U.S. Bureau of Mines Special Publication SP

06A-94.

Golder Associates Ltd. 1989. Report to Environment Canada on the Drilling Program at the Mt. Washington Mine Site, British Columbia. Report 882-1441.

Goode, J.R. 1993. The relocation of tailings. IN: CIM Metsoc Meeting Symposium, Advances in Environmental Protection for Metallurgical Industries, Quebec City, August 30 - September 1.

Goodman, A.E., A.M. Khalid, and B.J. Ralph. 1981. Microbial Ecology of Rum Jungle. II: Environmental Study of Two Flooded Opencuts and Smaller Associated Water Bodies. Australian Atomic Energy Commission Establishment, Report AAEC/E-527.

Gunn, J.M. 1995. International experience with catchment liming for the improvement of water quality. IN: T.P. Hynes and M.C. Blanchette, eds., Proceedings of Sudbury ‘95, Mining and the Environment, Sudbury, Canada, May 28-June 1, Volume 2, p.659-665.

Haji-Djafari, S., P.E. Antommaria, and H.L. Crouse. 1979. Attenuation of radionuclides and toxic elements by in situ soils at a uranium tailings pond in central Wyoming. IN: T.F. Zummer and C.O. Riggs, eds., Permeability and Groundwater Contaminant Transport, ASTM Symposium, Philadelphia, p.221-242.

Håkansson, K., S. Karlsson, and B. Allard. 1994. Effects of increased iron concentration on the mobility of cadmium, copper and zinc in leachates after remedial actions at an old sulphidic mine waste site. IN: International Land Reclamation and Mine Drainage Conference and Third International Conference on the Abatement of Acidic Drainage, Pittsburgh, PA, USA, April 24-29, Volume 1, p. 337-345. U.S. Bureau of Mines Special Publication SP 06A-94.

Hall, G.E.M., G.F. Bonham-Carter, A.J. Horowitz, K. Lum, C. Lemieux, B. Quemerais, and J.R. Garbarino. 1996. The effect of using different 0.45 µm filter membranes on ‘dissolved’ element concentrations in natural waters. Applied Geochemistry, 11, p.243-249.

Hamilton, R.M., R.R.J. Waite, N.A. Postlethwaite, and M. Cambridge. 1994. Wheal Jane, its abandonment and treatment of the resultant discharge. IN: International Land Reclamation and Mine Drainage Conference and Third International Conference on the Abatement of Acidic Drainage, Pittsburgh, PA, USA, April 24-29, Volume 2, p. 414. U.S. Bureau of Mines Special Publication SP 06A-94.

Harries, J.R., and A.I.M. Ritchie. 1987. The effect of rehabilitation on the rate of oxidation of pyrite in a mine waste rock dump. Environmental Geochemistry and Health, 17, p.27-36.

Harries, J.R., and A.I.M. Ritchie. 1985. Pore gas composition in waste rock dumps undergoing pyritic oxidation. Soil Science, 140, p.143-152.

Harries, J.R., and A.I.M. Ritchie. 1983a. Runoff fraction and pollution levels in runoff from a waste rock dump undergoing pyritic oxidation. Water, Air, and Soil Pollution, 19, p.155-170.

Harries, J.R., and A.I.M. Ritchie. 1983b. The microenvironment within waste rock dumps undergoing pyritic oxidation. IN: Proceedings of an International Symposium on Biohydrometallurgy, Calgary, Alberta, May 1-4.

Harries, J.R., and A.I.M. Ritchie. 1982. Pyrite oxidation in mine wastes: its incidence, its impact on water quality and its control. IN: E.M. O’Loughlin and P. Cullen, eds., Prediction in Water Quality: Proceedings of a Symposium on the Prediction in Water Quality, Australian Academy of Science and the Institute of Engineers, Canberra, November 30-December 2, p.347-377.

Hart, R.T. 1985. Waste Management in the Saskatchewan Potash Industry: Two Case Histories. Report by PCS Mining to CANMET, Project Number 350204, 26SQ.23440-3-9177. 92 p.

Hawkins, J.W., and W.W. Aljoe. 1991. Hydrologic characteristics of a surface mine spoil aquifer. IN: Proceedings of the Second International Conference on the Abatement of Acidic Drainage, Montreal, Quebec, September 16-18, Tome 1, p.47-68.

Hawkins, J.W., and W.W. Aljoe. 1990. Hydrologic characterization and modeling of a heterogeneous acid-producing surface coal mine spoil, Upshur County, WV. IN: Proceedings of the 1990 National Symposium on Mining, May 14-18, Knoxville, Tennessee, USA.

Hearn, R.L., and R. Hoye. 1988. Copper Dump Leaching and Management Practices That Minimize the Potential for Environmental Releases. U.S. Environmental Protection Agency Report EPA/600/S2-88/005.

Hedin, R.S., and G.R. Watzlaf. 1994. The effects of anoxic limestone drains on mine water chemistry. IN: International Land Reclamation and Mine Drainage Conference and Third International Conference on the Abatement of Acidic Drainage, Pittsburgh, PA, USA, April 24-29, Volume 1, p. 185-194. U.S. Bureau of Mines Special Publication SP 06A-94.

Henkel, C.H.R.F., and J.F. Alcock. 1988. Rum Jungle Mine Rehabilitation Project: Whites Open Cut and Intermediate Open Cut Water Quality, 1986-1987. Power and Water Authority Report 97/1988, Northern Territory, Australia.

Hofedank, R.H. 1979. Computation of and experience on lignite opencast mine drainage. IN: G.O. Argall, Jr., and C.O. Brawner, eds., Mine Drainage: Proceedings of the First International Mine Drainage Symposium, Denver, May, p.383-408. Miller Freeman Publications Inc., San Francisco.

Horne, I.A. 1996. Submarine tailings disposal at Island Copper Mine. IN: Proceedings of the 3rd International and 21st Annual Minerals Council of Australia Environmental Workshop, Newcastle, New South Wales, Australia, October 14-18, Volume 2, p. 318-350.

Howe, D.J. 1997. The Physical and Chemical Characteristics of Kimberlite Fines. M.A.Sc. Thesis, Department of Mining and Mineral Process Engineering, University of British Columbia. 217 p.

Hu, Z. 1995. Coal waste disposal and management in Chinese Shuoli Mine. IN: T.P. Hynes and M.C. Blanchette, eds., Proceedings of Sudbury ‘95, Mining and the Environment, Sudbury, Canada, May 28-June 1, Volume 3, p.1183-1188.

Hutt, N.M., and K.A. Morin. In preparation. The International Static Database: initial results of the compilation.

Hutt, N.M., and K.A. Morin. 1994. Assessment of the Underground Disposal of Tailings. Atomic Energy Control Board of Canada Report 5.147.1.

Jakubick, A.T., R. Klein, M.N. Gray, L.D. Keil. 1989. Characteristics of the excavation response zone as applied to shaft sealing. IN: Proceedings of an NEA Workshop on Excavation Response in Geological Repositories for Radioactive Waste, Winnipeg, April 26-28, p.157-174. Atomic Energy of Canada Limited.

Jambor, J.L., and D.W. Blowes, eds. 1994. The Environmental Geochemistry of Sulfide Mine-Wastes. Mineralogical Association of Canada Short Course Handbook Volume 22. 438 p.

James, P., and N.Thorpe. 1994. Ancient Inventions. Random House of Canada Limited, Toronto. 672 p.

Jardine, K., L. Smith, and T. Clemo. 1996. Monitoring networks in fractured rocks: a decision analysis approach. Ground Water, 34, p.504-518.

Jeffery, J.J., R.T. Lowson, J.V. Sarbutt, and R.J. Bowdler. 1988. Sulphide oxidation in pyritic overburden: a controlled leach column study. IN: The Third International Mine Water Congress, Melbourne, Australia, Australia Institute of Mining and Metallurgy, p.157-164.

Johnson, A.N., and D.M. Cregger. 1986. Groundwater contamination problems in the Iron River Mining District of Michigan. IN: H-Y. Fang, ed., International Symposium on Environmental Geotechnology, Volume 1, p.185-196. Envo Publishing Company, Inc.

Johnson, R.F. 1984. Investigation of the Physical and Chemical Characteristics of Potash Tailings in Saskatchewan. Report from the Potash Corporation of Saskatchewan Mining Limited for the Canada Center for Mineral and Energy Technology, 26SQ.23440-3-9177.

Johnston, J., P. McBride, and J. Miedecke. 1996. Assessing the acid mine drainage problem from historical operations at Mount Lyell, Western Tasmania: a case study from the wet temperate zone. IN: Proceedings of the 3rd International and 21st Annual Minerals Council of Australia Environmental Workshop, Newcastle, New South Wales, Australia, October 14-18, Volume 2, p. 380-391.

Jones, C.E., and J.Y. Wong. 1994. Shotcrete as a cementitious cover for acid generating waste rock piles. IN: International Land Reclamation and Mine Drainage Conference and Third International Conference on the Abatement of Acidic Drainage, Pittsburgh, PA, USA, April 24-29, Volume 2, p. 104-112. U.S. Bureau of Mines Special Publication SP 06A-94.

Jones, S.G., and D.V. Ellis. 1995. Deep water STD at the Misima Gold and Silver Mine, Papua New Guinea. Marine Georesources and Geotechnology, 13, p.183-200.

Jurjovec, J., D.W. Blowes, and C.J. Ptacek. 1995. Acid neutralization in mill tailings and the effect of natrojarosite addition. IN: T.P. Hynes and M.C. Blanchette, eds., Proceedings of Sudbury ‘95, Mining and the Environment, Sudbury, Canada, May 28-June 1, Volume I, p.29-38.

Kalin, M. 1987. Ecological Engineering for Gold and Base Metal Mining Operations in the Northwest Territories. Northern Affairs Program, Ministry of Indian Affairs and Northern Development, Environmental Studies No. 59. p. 64.

Kipp, J.A., F.W. Lawrence, and J.S. Dinger. 1983. A conceptual model of ground-water flow in the eastern Kentucky coal field. IN: D.H. Graves and R.W. DeVore, eds., Proceedings of the 1983 Symposium on Surface Mining, Hydrology, Sedimentology, and Reclamation, University of Kentucky, November 27-December 2, p.543-548.

Kiusalaas, J., and E.K. Albert. 1984. SPASID: A computer program for subsidence prediction. IN: A.B. Szwilski and C.O. Brawner (eds.), Proceedings of the Second International Conference on Stability in Underground Mining, August 6-8, Lexington, Kentucky, SME-AIME, p. 524-540.

Koyanagi, V.M., and A. Panteleyev. 1992. Natural acid drainage in the Mount McIntosh/Pemberton Hills Area, northern Vancouver Island (92L/12). British Columbia Geological Survey Branch, Geological Fieldwork 1992, paper 1993-1, p.445-450.

Kuyucak, N., and P. St-Germain. 1994. In situ treatment of acid mine drainage by sulphate reducing bacteria in open pits: scale-up experiences. IN: International Land Reclamation and Mine Drainage Conference and Third International Conference on the Abatement of Acidic Drainage, Pittsburgh, PA, USA, April 24-29, Volume 2, p. 303-310. U.S. Bureau of Mines Special Publication SP 06A-94.

Kwong, Y.T.J. 1993. Prediction and Prevention of Acid Rock Drainage from a Geological and Mineralogical Perspective. Canadian Mine Environment Neutral Drainage (MEND) Report 1.32.1.

Kwong, E.C.M., J.M. Scharer, J.J. Byerley, and R.V. Nicholson. 1995. Prediction and control of bacterial activity in acid mine drainage. IN: T.P. Hynes and M.C. Blanchette, eds., Proceedings of Sudbury ‘95, Mining and the Environment, Sudbury, Canada, May 28-June 1, Volume I, p.211-216.

Lang, P.A. 1989. Room 209 excavation response test in the underground research laboratory. IN: Proceedings of an NEA Workshop on Excavation Response in Geological Repositories for Radioactive Waste, Winnipeg, April 26-28, p.295-329. Atomic Energy of Canada Limited.

Lapakko, K.A. 1994a. Evaluation of neutralization potential determinations for metal mine waste and a proposed alternative. IN: International Land Reclamation and Mine Drainage Conference and Third International Conference on the Abatement of Acidic Drainage, Pittsburgh, PA, USA, April 24-29, Volume 1, p. 129-137. U.S. Bureau of Mines Special Publication SP 06A-94.

Lapakko, K.A. 1994b. Comparison of Duluth Complex rock dissolution in the laboratory and field. IN: International Land Reclamation and Mine Drainage Conference and Third International Conference on the Abatement of Acidic Drainage, Pittsburgh, PA, USA, April 24-29, Volume 1, p. 419-428. U.S. Bureau of Mines Special Publication SP 06A-94.

Lapakko, K. 1994c. Subaqueous disposal of mine waste: laboratory investigation. IN: International Land Reclamation and Mine Drainage Conference and Third International Conference on the Abatement of Acidic Drainage, Pittsburgh, PA, USA, April 24-29, Volume 1, p. 270-278.. U.S. Bureau of Mines Special Publication SP 06A-94.

Lapakko, K.A., and J.N. Wessels. 1995. Release of acid from hydrothermal quartz-carbonate hosted gold-mine tailings. IN: T.P. Hynes and M.C. Blanchette, eds., Proceedings of Sudbury ‘95, Mining and the Environment, Sudbury, Canada, May 28-June 1, Volume 1, p.139-148.

Larson, W.C. 1980. Uranium in situ leach mining - environmental controls. IN: C.O. Brawner, ed., First International Conference on Uranium Mine Waste Disposal, Vancouver, Canada, Society of Mining Engineers of AIME, p.175-192.

Lawrence, R.W., G.M. Ritcey, G.W. Poling, and P.B. Marchant. 1989. Strategies for the prediction of acid mine drainage. IN: Proceedings of the Thirteenth Annual British Columbia Mine Reclamation Symposium, Vernon, British Columbia, Canada, June 7-9, p.52-67.

Leatherwood, J., and L. Kunzler. 1989. Coal refuse weathering under cold desert conditions. IN: G.E. Cordy, ed., Geology and Hydrology of Hazardous-Waste, Waste-Water, and Repository Sites in Utah, Utah Geological Association Publication 17, p.159-164.

Leaver, M.E., and W.S. Bowman. 1994. Interlaboratory Measurement Program for the Standard ARD Material NBM-1. Mineral Sciences Laboratories Division Report MSL 94-28(CR), CANMET, Canadian Department of Natural Resources, for the Canadian Mine Environment Neutral Drainage (MEND) Program 1.16.2a.

Leaver, M.E., W.S. Bowman, R.P. Beaudoin, and R.H. McCorkill. 1994. ARD Standard Rock. Mineral Sciences Laboratories Division Report MSL 94-12(CR), CANMET, Canadian Department of Natural Resources, for Environment Canada.

Lentz, R.W. 1992. The disposal of sand produced with heavy oil into a salt cavern. IN: R.K. Singhal, A.K. Mehotra, K. Fytas, and J-L. Collins, eds., Environmental Issues and Management of Waste in Energy and Mineral Production, Volume 1, p. 677-684. A.A. Balkema Publishers, Brookfield, Vermont, USA.

Levens, R.L., and C.K.M. Boldt. 1992. Hydrochemical impacts of mine waste backfill in underground sulfide mines. IN: R.K. Singhal, A.K. Mehotra, K. Fytas, and J-L. Collins, eds., Environmental Issues and Management of Waste in Energy and Mineral Production, Volume 2, p. 891-902. A.A. Balkema Publishers, Brookfield, Vermont, USA.

Li, M., and L. St-Arnaud. 1997. Hydrogeochemistry of secondary mineral dissolution: column leaching experiment using oxidized waste rock. IN: Proceedings of the Fourth International Conference on Acid Rock Drainage, Vancouver, Canada, May 31 - June 6.

Lin, Z., and U. Qvarfort. 1996. A study of the Lilla Bredsjön tailings impoundment in mid-Sweden — a comparison of observations with RATAP model simulations. Applied Geochemistry, 11, p.293-298.

Loofbourow, R.L. 1979. Controlling mine water. IN: Mine Drainage, Proceedings of the First International Mine Drainage Symposium, edited by G.O. Argall, Jr., and C.O. Brawner, Denver, Colorado, May. Published by Miller Freeman Publications, Inc., San Francisco, CA, 848 p.

Lopaschuk, R.S. 1979. Drainage control and mine dewatering at Faro open pit mine. IN: G.O. Argall, Jr., and C.O. Brawner, eds., Mine Drainage: Proceedings of the First International Mine Drainage Symposium, Denver, May, p.233-257. Miller Freeman Publications Inc., San Francisco.

Lowson, R.T. 1982. Aqueous oxidation of pyrite by molecular oxygen. Chemical Reviews, 82, p.461-497.

Luther, G.W, III. 1990. The frontier-molecular-orbital theory approach in geochemical processes. IN: W. Stumm, ed., Aquatic Chemical Kinetics: Reaction Rates of Processes in Natural Waters, John Wiley & Sons, Inc., Toronto. 545 p.

MacGregor, R.A. 1966. Recovery of U_3O_8 by underground leaching. Canadian Mining and Metallurgical Bulletin for May, p. 583-587.

Maki, T.D., and J.B. Taylor. 1987. Precious metal slag treatment using an electrostatic separator. IN: T.M. Li and T.M. Plouf, eds., Small Mines Development in Precious Metals, Society of Mining Engineers of AIME, p.245-252.

Martin, R., and A. Thomas. 1974. An example of the use of bacteriophage as a groundwater tracer. Journal of Hydrology, 23, p. 73-78.

Martin, R.R., J. Li, and J.A. MacPhee. 1993. Colorimetric studies of the reduction of Fe^{3+} by coal. Canadian Journal of Chemistry, 71, p. 1970-1973.

McCurry, G.N., and H.W. Rauch. 1986. Characterization of ground water contamination associated with coal mines in West Virginia. IN: Proceedings of the Sixth National Symposium and Exposition on Aquifer Restoration and Ground Water Monitoring, National Water Well Association, May 19-22, The Ohio State University, p.669-685.

McFarland, W.H.S. 1965. Operations of the Yukon Consolidated Gold Corporation, Canada. IN: Opencast Mining, Quarrying and Alluvial Mining, The Institution of Mining and Metallurgy, London, p. 180-195.

McGregor, R.G., D.W. Blowes, and W.D. Robertson. 1995. The application of chemical extractions to sulphide tailings at the Copper Cliff Tailings Area, Sudbury, Ontario. IN: T.P. Hynes and M.C. Blanchette, eds., Proceedings of Sudbury '95, Mining and the Environment, Sudbury, Canada, May 28-June 1, Volume 3, p.1133-1142.

McQuade, C.V., J.F. Johnston, and S.M. Innes. 1995. Review of Historical Literature and Data on the Sources and Quality of Effluent from the Mount Lyell Lease Site. Mount Lyell Remediation Research and Demonstration Program, Commonwealth of Australia, Report 104. 78 p.

Meek, F.A., Jr. 1994. Evaluation of acid prevention techniques used in surface mining. IN: International Land Reclamation and Mine Drainage Conference and Third International Conference on the Abatement of Acidic Drainage, Pittsburgh, PA, USA, April 24-29, Volume 2, p. 41-48. U.S. Bureau of Mines Special Publication SP 06A-94.

MEND (Mine Environment Neutral Drainage Program). 1995. MINEWALL 2.0. Series of four reports (Literature Review, User's Guide, Application of MINEWALL to Three Minesites, and Programmer's Notes and Source Code) plus one diskette. Canadian Mine Environment Neutral Drainage (MEND) Reports 1.15.2.

Merrington, G., and B.J. Alloway. 1994. The transfer and fate of Cd, Cu, Pb and Zn from two historic metalliferrous mine sites in the U.K. Applied Geochemistry, 9, p.677-687.

Miedecke, J., and Partners Pty. Ltd. 1996. Remediation Options to Reduce Acid Drainage from Historical Mining Operations at Mount Lyell, Western Tasmania. Mount Lyell Remediation Research and Demonstration Program, Commonwealth of Australia, Report 108. 90 p.

Mifsud, J. 1996. Deep sub-marine tailings disposal at the Misima Gold Mine in Papua New Guinea. IN: Proceedings of the 3rd International and 21st Annual Minerals Council of Australia Environmental Workshop, Newcastle, New South Wales, Australia, October 14-18, Volume 2, p. 305-317.

Millenacker, D.J. 1992. Developing an in situ mining method for copper oxide minerals. IN: R.K. Singhal, A.K. Mehotra, K. Fytas, and J-L. Collins, eds., Environmental Issues and Management of Waste in Energy and Mineral Production, Volume 2, p. 903-910. A.A. Balkema Publishers, Brookfield, Vermont, USA.

Miller, S.D. 1996. Advances in acid drainage: prediction and implications for risk management. IN: Proceedings of the 3rd International and 21st Annual Minerals Council of Australia Environmental Workshop, Newcastle, New South Wales, Australia, October 14-18, Volume 1, p. 149-157.

Miller, S.D., A. Robertson, and T.A. Donohue. 1997. Advances in acid drainage prediction using the Net Acid Generation (NAG) test. IN: Proceedings of the Fourth International Conference on Acid Rock Drainage, Vancouver, Canada, May 31 - June 6.

Miller, S.D., J.J. Jeffrey, and T.A. Donohue. 1994. Developments in predicting and management of acid forming mine wastes in Australia and Southeast Asia. IN: International Land Reclamation and Mine Drainage Conference and Third International Conference on the Abatement of Acidic Drainage, Pittsburgh, PA, USA, April 24-29, Volume 1, p. 177-184. U.S. Bureau of Mines Special Publication SP 06A-94.

Mitchell, A., and W.O. Mackasey. 1995. The identification, location, and assessment of abandoned mine hazards - the first step toward rehabilitation. IN: T.P. Hynes and M.C. Blanchette, eds., Proceedings of Sudbury ‘95, Mining and the Environment, Sudbury, Canada, May 28-June 1, Volume I, p.289-298.

Morgan, M.G., and M. Henrion. 1990. Uncertainty — A Guide to Dealing with Uncertainty in Quantitative Risk and Policy Analysis. Cambridge University Press. 332 p.

Morin, K.A. 1993. Rates of sulfide oxidation in submerged environments: Implications for subaqueous disposal. Proceedings of the 17th Annual Mine Reclamation Symposium, Port Hardy, British Columbia, May 4-7, p.235-247. Mining Association of British Columbia.

Morin, K.A. 1990a. Problems and proposed solutions in predicting acid drainage with acid-base accounting. Acid Mine Drainage - Designing for Closure, Geological Association of Canada/Mineralogical Association of Canada Conference, Vancouver, British Columbia, May 16-18, p.93-107, p.93-107.

Morin, K.A. 1990b. Acid Drainage from Mine Walls: The Main Zone Pit at Equity Silver Mines. Report for the British Columbia Acid Mine Drainage Task Force and the federal Mine Environment Neutral Drainage Program.

Morin, K.A. 1988a. Groundwater contamination from precious-metal, base metal, uranium, and potash mining operations. Proceedings of the International Groundwater Symposium of the International Association of Hydrogeologists, Halifax, Nova Scotia, May 1-4, 1988, p.165-174.

Morin, K.A. 1988b. Physical and chemical hydrogeology of uranium tailings in Canada and the United States of America. Proceedings of the International Groundwater Symposium of the International Association of Hydrogeologists, Halifax, Nova Scotia, May 1-4, 1988, p.175-187.

Morin, K.A. 1983. Prediction Of Subsurface Contaminant Transport In Acidic Seepage From Uranium Tailings Impoundments. Ph.D. Thesis, Department of Earth Sciences, University of Waterloo, Ontario, Canada.

Morin, K.A., and N.M. Hutt. 1997. Control of Acidic Drainage in Layered Waste Rock at the Samatosum Minesite: Laboratory Studies and Field Monitoring. Canadian Mine Environment Neutral Drainage (MEND) Report 2.37.3.

Morin, K.A., and N.M. Hutt. 1995a. MINEWALL 2.0: A technique for predicting water chemistry in open-pit and underground mines. Proceedings of the Conference on Mining and the Environment, Sudbury, Ontario, May 28 - June 1, Volume 3, p.1007-1016

Morin, K.A., and N.M. Hutt. 1995b. Assessment of the Potential for Acidic Drainage at the Las Cristinas Project, Venezuela: Phase 2. Report to Placer Dome Inc.; geostatistical modelling by Placer Dome staff (C. Keech).

Morin, K.A., and N.M. Hutt. 1994a. An empirical technique for predicting the chemistry of water seeping from mine-rock piles. IN: Proceedings of the Third International Conference on the Abatement of Acidic

Drainage, Pittsburgh, Pennsylvania, USA, April 24-29, Volume 1, p.12-19.

Morin, K.A., and N.M. Hutt. 1994b. Observed preferential depletion of neutralization potential over sulfide minerals in kinetic tests: Site-specific criteria for safe NP/AP ratios. IN: Proceedings of the Third International Conference on the Abatement of Acidic Drainage, Pittsburgh, Pennsylvania, USA, April 24-29, Volume 1, p.148-156.

Morin, K.A., and N.M. Hutt. 1993a. The use of routine monitoring data for assessment and prediction of water chemistry. Proceedings of the 17th Annual Mine Reclamation Symposium, Port Hardy, British Columbia, May 4-7, p.191-201. Mining Association of British Columbia.

Morin, K.A., and N.M. Hutt. 1993b. Mine-Rock and Tailings Geochemistry, and Prediction of Water Chemistry. Support Document E, Bell Mine Closure Plan, Noranda Mining and Exploration. 400 p.

Morin, K.A., and J.A. Cherry. 1988. Migration of acidic groundwater seepage from uranium-tailings impoundments, 3. Simulation of the conceptual model with application to Seepage Area A. Journal of Contaminant Hydrology, 2, p.323-342.

Morin, K.A., and J.A. Cherry. 1986. Trace amounts of siderite near a uranium-tailings impoundment, Elliot Lake, Ontario, and its implication in controlling contaminant migration in a sand aquifer. Chemical Geology, 56, p.117-134.

Morin, K.A., N.M. Hutt, and K.D. Ferguson. 1996. The International Kinetic Database: Rates of acid generation, neutralization, and metal leaching from mines around the world. IN: Proceedings of the 3rd International and 21st Annual Minerals Council of Australia Environmental Workshop, Newcastle, New South Wales, Australia, October 14-18, Volume 1, p. 132-148.

Morin, K.A., N.M. Hutt, and I.A. Horne. 1995a. Prediction of future water chemistry from Island Copper Mine's On-Land Dumps. 19th Annual British Columbia Mine Reclamation Symposium, Dawson Creek, B.C., June 19-23, p. 224-233.

Morin, K.A., N.M. Hutt, and R. McArthur. 1995b. Statistical assessment of past water chemistry to predict future chemistry at Noranda Minerals' Bell Mine. Proceedings of the Conference on Mining and the Environment, Sudbury, Ontario, May 28 - June 1, Volume 3, p.925-934

Morin, K.A., N.M. Hutt, and K.D. Ferguson. 1995c. Measured rates of sulfide oxidation and acid neutralization in humidity cells: Statistical lessons from the database. Proceedings of the Conference on Mining and the Environment, Sudbury, Ontario, May 28 - June 1, Volume 2, p.525-536

Morin, K.A., N.M. Hutt, and K.D. Ferguson. 1995d. Measured rates of copper and zinc leaching in the International Kinetic Database. 19th Annual British Columbia Mine Reclamation Symposium, Dawson Creek, B.C., June 19-23, p.255-263.

Morin, K.A., I.A. Horne, and D. Riehm. 1994a. High-frequency geochemical monitoring of toe seepage from mine-rock dumps, BHP Minerals' Island Copper Mine, British Columbia. IN: Proceedings of the Third International Conference on the Abatement of Acidic Drainage, Pittsburgh, Pennsylvania, USA, April 24-29, Volume 1, p.346-354.

Morin, K.A., N.M. Hutt, and R. McArthur. 1994b. Prediction of minewater chemistry from available monitoring data, Noranda Minerals' Bell Mine, British Columbia. IN: Proceedings of the Third International

Conference on the Abatement of Acidic Drainage, Pittsburgh, Pennsylvania, USA, April 24-29, Volume 2, p.422.

Morin, K.A., C.E. Jones, and R.P. van Dyk. 1994c. Internal hydrogeologic monitoring of an acidic waste-rock dump at Westmin Resources' Myra Falls Operations, British Columbia. IN: Proceedings of the Third International Conference on the Abatement of Acidic Drainage, Pittsburgh, Pennsylvania, USA, April 24-29, Volume 1, p.355-364.

Morin, K.A., I.A. Horne, and D. Flather. 1993. The appropriate geochemical monitoring of toe seepage from a mine-rock dump. Proceedings of the 17th Annual Mine Reclamation Symposium, Port Hardy, British Columbia, May 4-7, p.119-129. Mining Association of British Columbia.

Morin, K.A., E. Gerencher, C.E. Jones, and D.E. Konasewich. 1991. Critical Literature Review of Acid Drainage from Waste Rock. Canadian Mine Environment Neutral Drainage (MEND) Report 1.11.1.

Morin, K.A., J.A. Cherry, N.K. Dave, T.P. Lim, and A.J. Vivyurka. 1988a. Migration of acidic groundwater seepage from uranium-tailings impoundments, 1. Field study and conceptual hydrogeochemical model. Journal of Contaminant Hydrology, 2, p.271-303.

Morin, K.A., J.A. Cherry, N.K. Dave, T.P. Lim, and A.J. Vivyurka. 1988b. Migration of acidic groundwater seepage from uranium-tailings impoundments, 2. Geochemical behavior of radionuclides in groundwater. Journal of Contaminant Hydrology, 2, p.305-322.

Morin, K.A., J.A. Cherry, T.P. Lim, and A.J. Vivyurka. 1982. Contaminant migration in a sand aquifer near an inactive tailings impoundment, Elliot Lake, Ontario. Canadian Geotechnical Journal, 19, p.49-62.

Morth, A.H., E.E. Smith, and K.S. Shumate. 1972. Pyrite Systems: A Mathematical Model. Contract Report for the U.S. Environmental Protection Agency, EPA-R2-72-002.

Morwijk Enterprises Ltd. 1993. Potential for Acidic Drainage from Tailings, Boss Mountain Minesite, Hendrix Lake, British Columbia. Report for Noranda Minerals submitted to the British Columbia government. 95 p.

Murdock, D.J., J.R.W. Fox, and J.G. Bensley. 1995. Treatment of acid mine drainage by the high density sludge process. IN: T.P. Hynes and M.C. Blanchette, eds., Proceedings of Sudbury ‘95, Mining and the Environment, Sudbury, Canada, May 28-June 1, Volume 2, p.431-439.

Murray, D.R. 1977. Pit Slope Manual 10-1: Reclamation by Vegetation, Volume 1, Mine Waste Description and Case Histories. Canadian CANMET Report, Ottawa, Canada.

Myerson, A.S. 1981. Oxygen Mass Transfer Requirements during the Growth of *Thiobacillus ferroxidans* on iron pyrite. Biotechnology and Bioengineering, Vol. XXIII, p. 1413-1416.

Nantel, J., and N. Lecuyer. 1983. Assessment of slag backfill properties for the Noranda Chadbourne Project. CIM Bulletin, 76, No. 849, p. 57-60.

Neller, R.R., J.D. Sandy, and V.H.R Oliver. 1973. How Mufulira Has Been Rehabilitated. World Mining, United States Edition, September, 1973, pp. 30-37.

Nichols, R.S. 1986. Rock segregation in waste dumps. IN: Proceedings of the International Symposium on

Flow-Through Rock Drains, Cranbrook, British Columbia, Canada, p.105-120.

Nicholson, R.V. 1994. Iron-sulfide oxidation mechanisms: laboratory studies. IN: J.L. Jambor and D.W. Blowes, eds, The Environmental Geochemistry of Sulfide Mine-Wastes, Mineralogical Association of Canada Short Course Handbook Volume 22, p.163-182.

Noller, B.N., P.H. Woods, and B.J. Ross. 1994. Case studies of wetland filtration of mine waste water in constructed and naturally occurring systems in northern Australia. Water Science Technology, 29., p.257-264.

Nordstrom, D.K., and C.N. Alpers. 1995. Remedial investigations, decisions, and geochemical consequences at Iron Mountain, California. IN: T.P. Hynes and M.C. Blanchette, eds., Proceedings of Sudbury '95, Mining and the Environment, Sudbury, Canada, May 28-June 1, Volume 2, p.633-642.

Nordstrom, D.K., T. Olsson, L. Carlsson, and P. Fritz. 1989. Introduction to the hydrogeochemical investigations within the international Stripa Project. Geochimica et Cosmochimica Acta, 53, pp.1717-1726.

Norecol, Dames, and Moore. 1996. Guide for Predicting Water Chemistry. Canadian Mine Environment Neutral Drainage (MEND) Report 1.27.1a.

Norecol, Dames, and Moore. 1994. Long Term Acid Generation Studies Cinola Project, Queen Charlotte Islands British Columbia. Canadian Mine Environment Neutral Drainage (MEND) Report 1.19.1.

Northern Territory Chamber of Mines. 1991. The Rum Jungle Creek South Rehabilitation Project. Down to Earth, November, p.10-11.

Northern Territory Department of Mines and Energy. 1986. The Rum Jungle Rehabilitation Project: Final Project Report.

Northwest Geochem. 1992. Physical and Chemical Hydrogeology of the Lynx Area of the Westmin Myra Falls Operations [Westmin Resources Limited]. Mine Report submitted to the British Columbia Ministry of Energy, Mines, and Petroleum Resources.

Northwest Geochem. 1990. Hydrogeological Assessment and Development of AMD Control Technology for Myra Falls Waste Rock. Report for Westmin Mines Ltd.

Norton, G.A., R.G. Richardson, and R. Markuszewski. 1991. Precipitation of jarosite compounds as a method for removing impurities from acidic wastes from chemical coal cleaning. Environmental Science and Technology, 25, p.449-455.

Norton, P.J. 1982. Advance dewatering and control of groundwater in surface coal mining. IN: Proceedings of the First International Mine Water Congress of the International Mine Water Association, April 19-24, Budapest, Hungary, Section B, p. 517-530.

Oertel, A.O., and W.C. Hood. 1983. Changes in ground water quality associated with cast overburden in southwest Perry County, Illinois. IN: D.H. Graves and R.W. DeVore, eds., Proceedings of the 1983 Symposium on Surface Mining, Hydrology, Sedimentology, and Reclamation, University of Kentucky, November 27 - December 2, p.73-79.

Orava, D., C.E. Hallam, and R. Swider. 1995. Evaluating alterantive long-term treatment strategies for treatment of acid mine drainage (AMD). IN: T.P. Hynes and M.C. Blanchette, eds., Proceedings of Sudbury '95, Mining and the Environment, Sudbury, Canada, May 28-June 1, Volume 2, p.505-514.

O'Steen, W.N., and H.W. Rauch. 1983. Effects of coal mining on ground-water quality in West Virginia. IN: D.H. Graves and R.W. DeVore, eds., Proceedings of the 1983 Symposium on Surface Mining, Hydrology, Sedimentology, and Reclamation, University of Kentucky, November 27-December 2, p.355-363.

Otwinowski, M. 1994. Quantitative analysis of chemical and biological kinetics for the acid mine drainage problem. Canadian Mine Environment Neutral Drainage (MEND) Program Report 1.51.1.

Pakianathan, S., and P. Simpson. 1965. General practices on large-scale hydraulic mines in Malaysia. IN: Opencast Mining, Quarrying and Alluvial Mining, The Institution of Mining and Metallurgy, London, p. 180-195.

Parker, G.K., B.N. Noller, and P.H. Woods. 1996. Water quality and its origin in some mined-out open pits of the monsoonal zone of the Northern Territory, Australia. IN: Proceedings of the 3rd International and 21st Annual Minerals Council of Australia Environmental Workshop, Newcastle, New South Wales, Australia, October 14-18, Volume 1, p. 50-63.

Patterson, R.L., and K.D. Ferguson. 1994. The Gibraltar North Project assessing acid rock drainage. IN: International Land Reclamation and Mine Drainage Conference and Third International Conference on the Abatement of Acidic Drainage, Pittsburgh, PA, USA, April 24-29, Volume 2, p. 12-21. U.S. Bureau of Mines Special Publication SP 06A-94.

Payant, S., L.C. St-Arnaud, and E.K. Yanful. 1995. Evaluation of techniques for preventing acidic rock drainage. IN: T.P. Hynes and M.C. Blanchette, eds., Proceedings of Sudbury '95, Mining and the Environment, Sudbury, Canada, May 28-June 1, Volume 2, p.485-494.

Patton, F.E. 1952. Backfilling at Noranda. Canadian Mining and Metallurgical Bulletin, April, p. 191-197.

Peng, S.S., and D.Y. Geng. 1984. Surface subsidence, overburden behavior, and structural damages due to longwall mining - two case studies. IN: A.B. Szwilski and C.O. Brawner (eds.), Proceedings of the Second International Conference on Stability in Underground Mining, August 6-8, Lexington, Kentucky, SME-AIME, p. 497-523

Pentz, D.L. 1979. Case examples of open pit drainage. IN: G.O. Argall, Jr., and C.O. Brawner, eds., Mine Drainage: Proceedings of the First International Mine Drainage Symposium, Denver, Colorado, May, p.324-341. Miller Freeman Publications Inc., San Francisco.

Piteau Associates. 1996. Assessment of ARD Mitigation Measures for the Open Pit and Waste Rock Dump, Volumes 1 and 2. Report for Inmet Mining, Project 1464, April 1996.

Pollard, J.H. 1977. A Handbook of Numerical and Statistical Techniques. Cambridge University Press. 349 p.

Pool, D.L., and R.M. Balderrama. 1994. Evaluation of humidity cell parameters their effect on precision and repeatability. IN: International Land Reclamation and Mine Drainage Conference and Third International Conference on the Abatement of Acidic Drainage, Pittsburgh, PA, USA, April 24-29, Volume 2, p. 326-333. U.S. Bureau of Mines Special Publication SP 06A-94.

Popovich, J.M., and R.F.J. Adam. 1985. Hydraulic transportation of coal mine refuse. IN: Proceedings from the Tenth International Conference on Slurry Technology, March 26-28, Lake Tahoe, Nevada, pp.327-332. Slurry Technology Association, Washington, DC.

Price, W.A., J. Errington, and V. Koyanagi. 1997. Guidelines for the prediction of acid rock drainage and metal leaching for mines in British Columbia: Part I. Policies and principles, case studies and general procedures and information requirements. IN: Proceedings of the Fourth International Conference on Acid Rock Drainage, Vancouver, Canada, May 31 - June 6.

Prugger, F.F. 1992. Tailings disposal in potah mines. IN: R.K. Singhal, A.K. Mehotra, K. Fytas, and J-L. Collins, eds., Environmental Issues and Management of Waste in Energy and Mineral Production, Volume 1, p. 545-554. A.A. Balkema Publishers, Brookfield, Vermont, USA.

Ptacek, C.J., and D.W. Blowes. 1994. Influence of siderite on the pore-water chemistry of inactive mine-tailings impoundments. IN: C.N Alpers and D.W. Blowes, eds., Environmental Geochemistry of Sulfide Oxidation, American Chemical Society Symposium Series 550, p.172-189.

Pufahl, D.E., and R.F. Johnson. 1987. The engineering properties of slimes and their application to the design and operation of waste management systems of potash mines in Saskatchewan. IN: Geotechnique in Resource Development, 40th Canadian Geotechnical Conference, Preprint Volume, October 19-21, Regina, Saskatchewan, Canada, p.285-290.

Pusch, R. 1989. Alteration of the hydraulic conductivity of rock by tunnel excavation. International Journal of Rock Mechanics and Mining Sciences & Geomechanical Abstracts, 26, p. 79-83.

PVS Technologies Ltd. 1994. Tailings Disposal in Rabbit Lake Pit: 1993 Annual Report. Prepared for Cameco Corporation. Report No. 94-01, dated 15 February 1994.

Quarshie, L., and J. Rowson. 1995. Waste rock leach tests at the Cluff Mining Operation in northern Saskatchewan. IN: T.P. Hynes and M.C. Blanchette, eds., Proceedings of Sudbury '95, Mining and the Environment, Sudbury, Canada, May 28-June 1, Volume I, p.217-226.

Ralston, D.R., and A.G. Morilla. 1974. Ground-water movement through an abandoned tailings pile. IN: Water Resources Problems Related to Mining, Proceedings No. 18, American Water Resources Association, June, p.174-183.

Rautman, C.A., and J.D. Istok. 1996. Probabilistic assessment of ground-water contamination: 1. geostatistical framework. Ground Water, 34, p.899-909.

Raven, K.G. 1986. Hydraulic Characterization of a Small Ground-water Flow System in Fractured Monzonitic Gneiss. Canadian National Hydrology Research Institute Paper No. 30. 133 p.

Reardon, E.J., and P.M. Moddle. 1985. Gas diffusion coefficient measurements on uranium mill tailings: implications to cover layer design. Uranium, 2, p.111-131.

Ritchie, A.I.M. 1994a. The waste-rock environment. IN: J.L. Jambor and D.W. Blowes, eds, The Environmental Geochemistry of Sulfide Mine-Wastes, Mineralogical Association of Canada Short Course Handbook Volume 22, p.133-161.

Ritchie, A.I.M. 1994b. Sulfide oxidation mechanisms: controls and rates of oxygen transport. IN: J.L. Jambor and D.W. Blowes, eds, The Environmental Geochemistry of Sulfide Mine-Wastes, Mineralogical Association of Canada Short Course Handbook Volume 22, p.201-245.

Roberts, A. 1981. Applied Geotechnology. Pergamon Press, New York.

Robertson, J.D. 1996. Subaqueous tailings disposal - the best option available. IN: Proceedings of the 3rd International and 21st Annual Minerals Council of Australia Environmental Workshop, Newcastle, New South Wales, Australia, October 14-18, Volume 2, p. 428-440.

Robertson, J.D. 1994a. The prediction and assessment of acid rock drainage potential: a summary of Placer Dome's Corporate Program. IN: Proceedings of the Mining Environmental Management Conference, Reno, Nevada, USA, October 16-19.

Robertson, W.D. 1994b. The physical hydrogeology of mill-tailings impoundments. IN: J.L. Jambor and D.W. Blowes, eds, The Environmental Geochemistry of Sulfide Mine-Wastes, Mineralogical Association of Canada Short Course Handbook Volume 22, p.1-17.

Ross, A., S. Matte, and F. Belle-Isle. 1994. Monitoring the Solbec Pit: first year observations. Preprint for the Third International Conference on the Abatement of Acidic Drainage, Pittsburgh, Pennsylvania, USA, April 24-29.

Ryan, P., and C. Joyce. 1991. Prevention and remediation of acid drainage from mine waste rock in Australia. IN: Proceedings of the Randol Gold Forum, Cairns ‘91, Cairns, Australia, April 16-19, p. 87-99.

Saskatchewan Environment and Resource Management. 1993. Environmental Monitoring of the Flooded D-Pit at Cluff Lake, Saskatchewan. Government report.

Saskatchewan Environment and Public Safety. 1990. Environmental Monitoring of the Flooded "D" Pit at Cluff Lake, Saskatchewan. Government report.

Schafer, W.A., S. Smith, C. Luckay, and T. Smith. 1994. Monitoring gaseous and liquid flux in sulfide waste rock. IN: Proceedings of the Third International Conference on the Abatement of Acidic Drainage, Pittsburgh, Pennsylvania, USA, April 24-29, Volume 1, p.410-418.

Scheetz, B.E., M.R. Silsbee, and J. Schuek. 1995. Field applications of cementitious grouts to address the formation of acid mine drainage. IN: T.P. Hynes and M.C. Blanchette, eds., Proceedings of Sudbury ‘95, Mining and the Environment, Sudbury, Canada, May 28-June 1, Volume 3, p.935-944.

Seweryn, L. 1982. Large open-pit drainage system and its effect on environment. IN: Proceedings of the First International Mine Water Congress of the International Mine Water Association, April 19-24, Budapest, Hungary, Section C, p. 115-128.

Shastkewich, U. 1966. Permafrost and ground temperature of the Alpine part of Udokan ridge. Zabaikalskij North’s Geocryology, Moscow, Nauka, 1960, p. 53-54.

Shelp, G., W. Chesworth, and G. Spiers. 1996. The amelioration of acid mine drainage by an *in situ* electrochemical method; part 2: employing aluminum and zinc sacrificial anodes. Applied Geochemistry, 11, p.425-432.

Shelp, G., W. Chesworth, and G. Spiers. 1995. The amelioration of acid mine drainage by an *in situ* electrochemical method - I. Employing scrap iron as the sacrificial anode. Applied Geochemistry, 10, p.705-713.

Shelp, G., W. Chesworth, G. Spiers, and L. Liu. 1994. A demonstration of the feasibility of treating acid mine drainage by an in situ electrochemical method. IN: International Land Reclamation and Mine Drainage Conference and Third International Conference on the Abatement of Acidic Drainage, Pittsburgh, PA, USA, April 24-29, Volume 2, p. 348-355. U.S. Bureau of Mines Special Publication SP 06A-94.

Sims, W.N. 1972. Remining of Tailings by Hydraulicking and Other Methods. IN: Tailings Disposal Today, Proceedings of the First International Tailing Symposium, Tuscon, Arizona, October 31 - November 3, 1972, pp. 615-633.

Singer, P.C., and W. Stumm. 1970. Acidic mine drainage: the rate determining step. Science, 167, p.1121-1123.

Singh, R.N., and S.M. Reed. 1988. Mathematical modelling for estimation of minewater inflow to a surface mining operation. International Journal of Mine Water, v. 7, no. 3, September, p.1-34.

Smith, A. 1994. The geochemistry of cyanide in mill tailings. IN: J.L. Jambor and D.W. Blowes, eds, The Environmental Geochemistry of Sulfide Mine-Wastes, Mineralogical Association of Canada Short Course Handbook Volume 22, p.293-332.

Smith, L., D.L. López, R. Beckie, K.A. Morin, R. Dawson, and W.Price. 1995. Hydrogeology of Waste Rock Dumps. Report for Natural Resources Canada, Contract No. 23440-4-1317/01-SQ. 130 p.

Sobek, A.A., W.A. Schuller, J.R. Freeman, and R.M. Smith. 1978. Field and Laboratory Methods Applicable to Overburdens and Minesoils. Report EPA-600/2-78-054, U.S. National Technical Information Report PB-280 495. 403 p.

St-Arnaud, L. 1994. Water covers for the decommissioning of sulfidic mine tailings impoundments. IN: International Land Reclamation and Mine Drainage Conference and Third International Conference on the Abatement of Acidic Drainage, Pittsburgh, PA, USA, April 24-29, Volume 1, p. 279-287. U.S. Bureau of Mines Special Publication SP 06A-94.

St-Arnaud, L.C., and S.R. Aiken. 1991. Hydrogeology and geochemistry of the Brunswick Mining No. 6 Open Pit Mine Site. IN: Proceedings of the Second International Conference on the Abatement of Acidic Drainage, Montreal, Quebec, September 16-18, Tome 1, p.400-420.

St-Arnaud, L.C., B.C. Aubé, M.E. Wiseman, and S.R. Aiken. 1994. Mitigation of acid mine drainage by the porous envelope effect. IN: International Land Reclamation and Mine Drainage Conference and Third International Conference on the Abatement of Acidic Drainage, Pittsburgh, PA, USA, April 24-29, Volume 2, p. 87-95. U.S. Bureau of Mines Special Publication SP 06A-94.

Stevens, C., G. Lawrence, C. Rogers, and P. Hamblin. 1994. Modeling the thermal stratification of water filled mine pits. IN: Proceedings of the Eighteenth Annual British Columbia Mine Reclamation Symposium, Vernon, British Columbia, April 11-14, p. 109-117.

Stogran, S.W., and M.E. Wiseman. 1995. A comparison of organic and inorganic covers for long term prevention or amelioration of acid mine drainage. IN: T.P. Hynes and M.C. Blanchette, eds., Proceedings of Sudbury ‘95, Mining and the Environment, Sudbury, Canada, May 28-June 1, Volume 2, p.555-563.

Straskraba, V., and L.E. Kissinger. 1982. Dewatering of the Jenkins open pit uranium mine. IN: Proceedings of the First International Mine Water Congress of the International Mine Water Association, April 19-24, Budapest, Hungary, Section B, p. 559-577.

Strömberg, B., and S. Banwart. 1995. Laboratory investigation of alkalinity producing reactions in sulphide containing waste rock. IN: T.P. Hynes and M.C. Blanchette, eds., Proceedings of Sudbury ‘95, Mining and the Environment, Sudbury, Canada, May 28-June 1, Volume I, p.39-48.

Strömberg, B., and S. Banwart. 1994. Kinetic modelling of geochemical processes at the Aitik mining waste rock site in northern Sweden. Applied Geochemistry, 9, p.583-595.

Stuart, W.T., and T.A. Simpson. 1961. Variations of pH with depth in anthracite mine-water pools in Pennsylvania. U.S. Geological Survey Professional Paper 424-B, p. B-82 to B-84.

Stucki, J.W., G.W. Bailey, and H. Gan. 1993. Oxidation-reduction mechanisms in iron-bearing phyllosilicates. U.S. Environmental Protection Agency Emerging Technology Summary EPA/600/S-93/002.

Stuparyk, R.A., W.B. Kipkie, A.N. Kerr, and D.W. Blowes. 1995. Production and evaluation of low sulphur tailings at INCO’s Clarabelle Mill. IN: T.P. Hynes and M.C. Blanchette, eds., Proceedings of Sudbury ‘95, Mining and the Environment, Sudbury, Canada, May 28-June 1, Volume I, p.159-169.

Sumer, S.M., J.J. Elton, and J.A. Tapics. 1987. Dewatering optimization using a groundwater flow model at the Whitewood open-pit coal mine, Alberta. IN: Geotechnique in Resource Development, Preprint Volume, 40th Canadian Geotechnical Conference, October 19-21, Regina, p.79-87.

Sumioka, S.S. 1991. Quality of Water in an Inactive Uranium Mine and Its Effects on the Quality of Water in Blue Creek, Stevens County, Washington, 1984-1985. U.S. Geological Survey Water-Resources Investigations Report 89-4110. 62 p.

Sverdrup, H.U. 1990. The Kinetics of Base Cation Release Due to Chemical Weathering. Lund University Press, Lund. 246 p

Swanson, D.A., S.L. Barbour, G.W. Wilson, and M. O’Kane. 1995. Modelling the performance of engineered soil covers for acid generating mine waste. IN: T.P. Hynes and M.C. Blanchette, eds., Proceedings of Sudbury ‘95, Mining and the Environment, Sudbury, Canada, May 28-June 1, Volume 3, p.861-868.

Tallin, J.E., D.E. Pufahl, and S.L. Barbour. 1990. Waste management schemes of potash mines in Saskatchewan. Canadian Journal of Civil Engineering, 17, pp 528-542.

Taylor, D.A.R. 1995. The North American Bats and Mines Project: a cooperative approach for integrating wildlife, ecosystem management, and mine land reclamation. IN: T.P. Hynes and M.C. Blanchette, eds., Proceedings of Sudbury ‘95, Mining and the Environment, Sudbury, Canada, May 28-June 1, Volume I, p.319-327.

Taylor, J.R., T.R Weaver, D.C. McPhail, and N.C. Murphy. 1996. Characterisation and Impact Assessment of Mine Tailings in the King River System and Delta, Western Tasmania. Mount Lyell Remediation Research and Demonstration Program, Commonwealth of Australia, Report 105. 122 p.

Taylor, M.J. 1980. Radionuclide movement in seepage and its control. IN: Proceedings of the First International Conference on Uranium Mine Waste Disposal, May 19-21, Vancouver, Canada, Society of

Mining Engineers of AIME, Chapter 17.

Taylor, M.J., and P.E. Antommaria. 1978. Immobilization of radionuclides at uranium tailings disposal sites. IN: Symposium on Uranium Mill Tailings Management, Fort Collins, Colorado, USA, November 20-21, Colorado State University.

Teasdale, P., S. Apte, G. Batley, and P. Ford. 1996. The Behaviour of Copper in Sediments and Waters of Macquarie Harbour, Western Tasmania. Mount Lyell Remediation Research and Demonstration Program, Commonwealth of Australia, Report 111. 118 p.

Thornton, I. 1996. Impacts of mining on the environment; some local, regional and global issues. Applied Geochemistry, 11, p.355-361.

Toran, L., and K.R. Bradbury. 1988. Ground-water flow model of drawdown and recovery near an underground mine. Ground Water, 26, p.724-733.

Tremblay, R.L. 1994. Controlling acid mine drainage using an organic cover: the case of the East Sullivan Mine, Abitibi, Québec. IN: International Land Reclamation and Mine Drainage Conference and Third International Conference on the Abatement of Acidic Drainage, Pittsburgh, PA, USA, April 24-29, Volume 2, p. 122-127. U.S. Bureau of Mines Special Publication SP 06A-94.

Trexler, B.D., Jr. 1979. Hydrogeology of a lead-zinc mine. IN: G.O. Argall, Jr., and C.O. Brawner, eds., Mine Drainage: Proceedings of the First International Mine Drainage Symposium, Denver, Colorado, USA, May 1979, p.552-570.

Trexler, B.D., Jr., D.R. Ralston, W. Renison, and R.E. Williams. 1974. The hydrology of an acid mine problem. IN: Water Resources Related to Mining, Proceedings No. 18, American Water Resources Association, June 1974, p.32-40.

Trudell, M.R., and S.R. Moran. 1982. Spoil hydrology and hydrochemistry at the Battle River Site in the Plains of Alberta. IN: D.H. Graves and R.W. DeVore, eds., 1982 Symposium on Surface Mining Hydrology, Sedimentology, and Reclamation, University of Kentucky, USA.

Tyrrell, W.R. 1996. Potential for wetlands to treat coal mine wastewaters, particularly in low rainfall environments in Australia. IN: Proceedings of the 3rd International and 21st Annual Minerals Council of Australia Environmental Workshop, Newcastle, New South Wales, Australia, October 14-18, Volume 1, p. 237-252.

van der Linden, J. 1994a. Environmental monitoring at Kelian Equatorial Mining. IN: M. Simatupang and B.N. Whaju, eds., Environmental Aspects of Mining in Indonesia, Seminar of the IMA AusIMM Two-Day Seminar on Environment, Jakarta, November 9-10, 1993, Indonesian Mining Association, p. 106-115.

van der Linden, J. 1994b. Acid mine drainage from mining in a tropic environment: monitoring, prediction and prevention, the Kelian Experience. IN: Workshop on Sound Environmental Management for Mining in Indonesia, Bandung, Indonesia, August 29-31.

Van Stempvoort, D.R., and H.R. Krouse. 1994. Controls of *^{18}O in sulfate. IN: C.N Alpers and D.W. Blowes, eds., Environmental Geochemistry of Sulfide Oxidation, American Chemical Society Symposium Series 550, p.446-480.

Vance, J.B., J.R. Walmsley, and M.C. Bétournay. 1995. Inactive mines database. IN: T.P. Hynes and M.C. Blanchette, eds., Proceedings of Sudbury '95, Mining and the Environment, Sudbury, Canada, May 28-June 1, Volume 3, p.969-978.

Veska, E. 1983. PhD Thesis, Department of Chemistry, University of Waterloo.

Vonhof, J.A. 1983. Hydrogeological and Hydrochemical Investigation of the Waste Disposal Basin at I.M.C.C. K2 Potash Plant, Esterhazy, Saskatchewan. National Hydrology Research Institute (NHRI) Paper No. 13, Inland Water Directorate (IWD) Scientific Series No. 116. 203 p. plus maps.

Vranesh, G. 1979. Mine drainage: the common enemy. IN: G.O. Argall, Jr., and C.O. Brawner, eds., Proceedings of the First International Mine Drainage Symposium, Denver, Colorado. Miller Freeman Publications, Inc., San Francisco, 848 p.

Water Resources Division. 1986. Rum Jungle Mine Rehabilitation: The Treatment of Whites and the Intermediate Open Cut Waters. Water Resources Division Report No. 7/1986, Department of Mines and Energy, Northern Territory, Australia.

Wei, L., and J.A. Hudson. 1990. Permeability Variation Around Underground Openings in Jointed Rock Masses: A Numerical Study. IN: Proceedings of the International Symposium on Rock Joints, Leon, Norway, June 4-6, 1990, pp.565-569. A.A. Balkema, Rotterdam, ISBN 90 6191 1095.

Weimer, W.C., R.R. Kinnison, and J.H. Reeves. 1981. Survey of Radionuclide Distributions Resulting from the Church Rock, New Mexico, Uranium Mill Tailings Pond Dam Failure. Pacific Northwest Laboratory for the U.S. Nuclear Regulatory Commission, December 1981, NUREG/CR-2449 PNL-4122, Washington, D.C.

Weingart, R.L. 1982. Reclamation - evolution of a hard rock miner's perspective. IN: 1982 Symposium on Surface Mining Hydrology, Sedimentology, and Reclamation, University of Kentucky, Lexington, December 5-10, p.187-192.

Wetzel, R.G. 1983. Limnology. Saunders. 743 p.

Wheeland, K., and S. Payant. 1991. Criteria for Underground Disposal of AMD-Generating Materials. IN: Proceedings of the Second International Conference on the Abatement of Acidic Drainage, September 16-18, Montreal, Quebec, Volume 1, p. 577-579.

Whittaker, B.N., and D.J. Reddish. 1984. Mining subsidence in longwall mining with special reference to the prediction of surface strains. IN: A.B. Szwilski and C.O. Brawner (eds.), Proceedings of the Second International Conference on Stability in Underground Mining, August 6-8, Lexington, Kentucky, SME-AIME, p. 576-588.

Whittaker, B.N., D.J. Reddish, and X.L. Yao. 1992. Environmental issues arising from subsidence occurrence at underground operational and abandoned mine sites. IN: R.K. Singhal, A.K. Mehotra, K. Fytas, and J-L. Collins, eds., Environmental Issues and Management of Waste in Energy and Mineral Production, Volume 1, p. 641-649. A.A. Balkema Publishers, Brookfield, Vermont, USA.

White, A.F., and M.L. Peterson. 1990. Role of Reactive-Surface-Area Characterization in Geochemical Kinetic Models. IN: D.C. Melchoir and R.L. Bassett, eds., Chemical Modeling of Aqueous Systems II, Chapter 35, p.461-475. American Chemical Society ACS Symposium Series 416.

Williams, D.J. 1996. Broadening the options - innovative tailings disposal concepts and practices. IN: Proceedings of the 3rd International and 21st Annual Minerals Council of Australia Environmental Workshop, Newcastle, New South Wales, Australia, October 14-18, Volume 1, p. 264-278.

Williams, M.P.A. 1992. Australian experince with the central thickened discharge method for tailings disposal. IN: R.K. Singhal, A.K. Mehotra, K. Fytas, and J-L. Collins, eds., Environmental Issues and Management of Waste in Energy and Mineral Production, Volume 1, p. 567-577. A.A. Balkema Publishers, Brookfield, Vermont, USA.

Williams, R.E. 1979. Waste Production and Disposal in Mining, Milling, and Metallurgical Industries. Miller Freeman Publications, Inc.

Williams, R.E., G.V. Winter, G.L. Bloomsburg, and D.R. Ralston. 1986. Mine Hydrology. Society of Mining Engineers of AIME, Littleton, Colorado, USA.

Williams, R.E., J. Baldwin, and D.R. Ralston. 1979. Coping with mine drainage regulations. IN: G.O. Argall, Jr., and C.O. Brawner, eds., Mine Drainage: Proceedings of the First International Mine Drainage Symposium, Denver, Colorado, May, p.185-218. Miller Freeman Publications Inc., San Francisco.

Witherspoon, P.A., N.G. Cook, and J.E. Gale. 1981. Geologic storage of radioactive waste: Field studies in Sweden. Science, 211, February 27 1981, pp. 894-900.

Wolkersdorfer, C. 1996. Hydrogeochemical investigations of an abandoned uranium mine in the Erzgebirge/Germany. Appiled Geochemistry, 11, p.237-241.

Wong, D.K.H., and S.L. Barbour. 1987. Studies of the infiltration and migration of brine in potash tailings. Canadian Journal of Civil Engineering, 14, p.638-648.

Wood, P.A. 1983. Underground Stowing of Mine Waste. IEA Coal Research, Report No. ICTIS/TR23, London, England, April 1983, 67 p.

Woods, P.H. 1994. Uranium and radium-226 in runoff from the rehabilitated Rum Jungle Creek South Uranium Mine, Northern Territory: interim results and health implications. Radiation Protection in Australia, 12, p.18-21.

Woods, P.H., and B.N. Noller. 1995. Medium-term performance of wetlands improving water quality of near-neutral mine drainage in the Northern Territory. IN: Proceedings of the National Conference on Wetlands for Water Quality Control, Townsville, Australia, September 25-29, p.29-39.

Woyshner, M.R., and L. St-Arnaud. 1994. Hydrogeological evaluation and water balance of a thickened tailings deposit near Timmins, ON, Canada. IN: International Land Reclamation and Mine Drainage Conference and Third International Conference on the Abatement of Acidic Drainage, Pittsburgh, PA, USA, April 24-29, Volume 2, p. 198-207. U.S. Bureau of Mines Special Publication SP 06A-94.

Woyshner, M.R., L. St-Arnaud, and M.E. Wiseman. 1995. Neutralization potential and the porous envelope effect: two favourable conditions for decommissioning of the Fault Lake Tailings Site, Falconbridge, Ontario. IN: T.P. Hynes and M.C. Blanchette, eds., Proceedings of Sudbury '95, Mining and the Environment, Sudbury, Canada, May 28-June 1, Volume 2, p.785-793.

Wrench, B.P. 1986. Surface water management and vegetation at a phosphogypsum tailings impoundment.

IN: Geotechnical and Geohydrological Aspects of Waste Management, Proceedings of the 8th Annual Symposium on Geotechnical and Geohydrological Aspects of Waste Management, Fort Collins, Colorado, February 5-7, p.173-182. A.A. Balkema.

Yelderman, J.C., Jr., and D.L. Durler. 1983. Detection, correction and restoration of mining in a confined aquifer at an in situ uranium mine. IN: D.M. Nielsen, ed., Proceedings of the Third National Symposium on Aquifer Restoration and Ground-Water Monitoring, May 25-27, The Fawcett Center, Columbus, Ohio, USA, p.151-161.

Ziemkiewicz, P.F., and R.J. Lovett. 1994. The rate of pyrite dissolution: comparison of field and laboratory studies. IN: International Land Reclamation and Mine Drainage Conference and Third International Conference on the Abatement of Acidic Drainage, Pittsburgh, PA, USA, April 24-29, Volume 2, p. 430. U.S. Bureau of Mines Special Publication SP 06A-94.

Ziemkiewicz, P.F., and F.A. Meek, Jr. 1994. Long term behavior of acid forming rock: results of 11-year field studies. IN: International Land Reclamation and Mine Drainage Conference and Third International Conference on the Abatement of Acidic Drainage, Pittsburgh, PA, USA, April 24-29, Volume 2, p. 49-56. U.S. Bureau of Mines Special Publication SP 06A-94.

SUBJECT INDEX

MINESITE/MINING PROJECT/MINING AREA INDEX

CASE STUDY INDEX

AUTHOR INDEX

APPENDIX
A. GLOSSARY

(note: words in *italics* are defined separately in this glossary)

Acid Base Accounting (ABA) - a *static test* that defines the amounts, and relative balance, of potentially acid-generating and acid-neutralizing minerals in a sample; the most common static test for prediction of *acid mine drainage*.

Acid-Leachable Sulfate Sulfur - a part of *acid-base accounting* that provides the acid-leachable sulfate content of a sample, expressed as %S; typically represents gypsum content; see also *total sulfate sulfur*.

Acid Mine Drainage (AMD) - *minesite drainage* with an acidic pH; an acidic pH is often defined through government regulations as a value less than 6.0 or 6.5; technically, an acidic pH from the perspective of impacts can be any value less than 5.0 since dilute, unimpacted water can have a natural pH of approximately 5.3.

Acid Potentials (xAP) - part of *acid base accounting* yielding the potential capacity for acid generation based on sulfur analyses; see *Total Acid Potential* and *Sulfide Acid Potential*.

Acid Rock Drainage (ARD) - a variation on *acid mine drainage* that includes natural *acidic drainage* from rock not related to mining activity.

Acidic Drainage (AD) - a general term applied to any drainage with a acidic pH; see *acid mine drainage* for discussion of acidic pH.

Adit - horizontal or near-horizontal *underground working*; see also *drift* and *crosscut* and *level*.

Alkaline Mine Drainage (LMD) - *minesite drainage* with an alkaline pH; an alkaline pH is often defined through government regulations as a value greater than 9.0 or 8.5.

Barium Sulfate Sulfur - a part of *acid-base accounting* that yields the (unleachable) barium-bound sulfate content of a sample assuming all barium occurs as barite, expressed as %S; calculated from barium content obtained by *total-metal* or *whole-rock* analyses.

Bench - a relatively flat, lateral surface within an *open pit*, often identified by elevation or depth.

Carbonate Net Neutralization Potential (CNNP) - as part of *acid-base accounting*, *Carbonate Neutralization Potential* minus *Total Acid Potential*, in units of kilogram of $CaCO_3$ equivalent per metric tonne of sample (kg $CaCO_3$/t), t $CaCO_3$ equivalent/1000 t of sample, or parts per thousand (ppt) $CaCO_3$ equivalent [all are equal].

Carbonate Net Potential Ratio (CNPR) - as part of *acid-base accounting*, *Carbonate Neutralization Potential* divided by *Total Acid Potential* (dimensionless).

Carbonate Neutralization Potential (CaNP) - as part of *acid-base accounting*, the amount of inorganic carbon converted to $CaCO_3$ equivalent, in units of kilogram of $CaCO_3$ equivalent per metric tonne of sample (kg $CaCO_3$/t), t $CaCO_3$ equivalent/1000 t of sample, or parts per thousand (ppt) $CaCO_3$ equivalent [all are equal]; assumed to represent neutralizing capacity attributable only to carbonate minerals.

Classes of Drainage Chemistry - primarily based on pH: Acidic, Near Neutral, Alkaline, and Other (pH generally irrelevant); see *acid mine drainage*, *neutral mine drainage*, and *alkaline mine drainage*.

Concentrator - see *mill*.

Consumption Rate - see *production rate*.

Crosscut - horizontal or near-horizontal *underground working* or *adit* excavated at an angle to a *drift* to access *ore* or another *drift*.

Cutoff Grade - a general term for differentiating *ore* from *waste rock*.

Decline - a sloping *underground working* used for a roadway for transportation of workers and/or *ore* and *waste rock* from a *portal*; see also *incline*.

del %S - as part of *acid-base accounting*, *total sulphur* minus all other measured sulfur species such as *sulfide sulfur*, *total sulfate sulfur*, and *organic sulfur*, in units of %S; represents error in measurements of sulfur species and assumed to be acid-generating *sulfide sulfur*.

Drainage - see *minesite drainage*.

Drainage Chemistry - concentrations of elements and other aqueous parameters in *minesite drainage* from minesite components through surface or subsurface pathways.

Drift - horizontal or near-horizontal *underground working* or *adit* parallel to, but not excavated in, *ore*; see also *crosscut*.

Effective Neutralization Potential (ENP) - the capacity of mined materials to neutralize acidity to pH 6.0 or above under the site-specific in-field (1) environmental conditions, (2) mineralogy, (3)grain sizes, and (4) rates of mineral reactions; see also *Neutralization Potential*.

Equilibrium - chemical equilibrium is one of two theoretical processes for assessing or predicting drainage, described through equilibrium concentrations that do not change through time; see also *kinetics*.

Evapotranspiration - precipitation returning to the atmosphere as water vapor due to evaporation by thermal processes and transpiration by biological processes.

Fracture - a general term used in this book indicating a physical discontinuity in a rock mass, including small “cracks” to large-scale faults that are open to water and air or are sealed with fault gouge or secondary-mineral precipitants.

Gob - see *waste rock*.

Heap Leaching - a type of mill processing in which stockpiled ore is subjected to a leaching solution that removes the target metals, leaving a waste-rock dump after leaching ceases.

Humidity Cell - a type of *kinetic test* in which a small sample (about 1 kg) is placed in an enclosed chamber in a laboratory, moist and/or dry air is constantly pumped through the chamber, and once a week the sample is rinsed with water; chemical analysis of rinse water yields calculated bulk reaction *rates*; beware of highly variable procedures internationally.

Incline - a primary sloping *underground working* for hoist-based transportation of workers and/or *ore* and *waste rock*; see also *shaft*.

Infiltration - precipitation penetrating the surface of a minesite component and migrating through it, eventually appearing as *minesite drainage*.

Kinetics - one of two theoretical processes assessing or predicting *drainage chemistry*, described through reaction *rates* that imply concentrations continue to increase or decrease indefinitely through time; see also *equilibrium*.

Kinetic Test - a procedure for characterizing the physical, chemical, or biological status of a sample through time during continued exposure to a known set of environmental conditions, such as a *humidity cell*; see also *static test*.

Level - a primary *adit* at an identified elevation or depth.

Loading - concentration multiplied by flow, providing a mass per unit time flowing through or from a *minesite component*.

Low-Grade-Ore Stockpile - a *mined-rock pile* containing low-grade *ore* that may someday be sent to a *mill*; see also *ore stockpile*.

Metal Leaching - the removal of a metal from its solid-phase mineral into *minesite drainage*; described by bulk leach *rates* obtained from *kinetic tests*.

Mill - a facility for milling *ore* in order to remove and concentrate economic metals or minerals; may be called a "cleaner" for coal milling.

Mine - a *minesite component* from which *ore* and *waste rock* are extracted; see also *open pit* and *underground workings*.

Minesite Component - a physically distinct portion of a *minesite* such as a *tailings* impoundment, *waste-rock* dump, *ore* stockpile, *open pit*, *underground workings*, a building foundation, or a road.

Mined-rock Piles - a general term referring to any accumulation of rock at a mine, including *waste-rock* dumps, *ore* and low-grade-ore stockpiles, roads, *heap-leach* piles, and building foundations.

Minesite - location of one or more *minesite components*.

Minesite Drainage - water that runs off or flows through a *minesite component*, including surface and subsurface (groundwater) flow; see also *acid mine drainage*, *neutral mine drainage*, *alkaline mine drainage*, and *drainage chemistry*.

Net Neutralization Potential (xNNP) - see *Total Net Neutralization Potential, Sulfide Net Neutralization Potential, Refined Net Neutralization Potential, Carbonate Net Neutralization Potential*.

Net Potential Ratio (xNPR) - see *Total Net Potential Ratio, Sulfide Net Potential Ratio, Refined Net Potential Ratio, Carbonate Net Potential Ratio*.

Neutral Mine Drainage (NMD) - *minesite drainage* with a near-neutral pH; a near-neutral pH is generally defined as a value between 6.0-6.5 and 8.5-9.0; see also *acid mine drainage* and *alkaline mine drainage*.

Neutralization - the raising of acidic pH or the lowering of alkaline pH to near-neutral values; see also *neutral mine drainage*.

Neutralization Potential (NP) - as part of *acid-base accounting*, the analytical bulk capacity of a sample for neutralizing acidity, in units of kilogram of $CaCO_3$ equivalent per metric tonne of sample (kg $CaCO_3$/t), t $CaCO_3$ equivalent/1000 t of sample, or parts per thousand (ppt) $CaCO_3$ equivalent [all are equal]; see also *Effective Neutralization Potential, Unavailable Neutralization Potential, Carbonate Neutralization Potential, Slow Reacting Neutralization Potential* (collectively labelled xNP).

Open Pit - any open area created by human excavation; also referred to as open cast mine in some countries or as a quarry; alternative to *underground workings*; also known as open cut or mine void in some countries.

Ore - rock, sediments, or soil that contains economically recoverable levels of metals or minerals, often stockpiled near a *mill* until processed; accompanying rock with uneconomic levels of target metals or minerals is typically called *waste rock*; rock close to the *cutoff grade* of waste and ore is typically called low-grade ore, which may be milled at a later time; after milling, the uneconomic waste material is typically called *tailings*.

Ore Stockpile - a *mined-rock pile* containing *ore* destined for a *mill*; see also *low-grade-ore stockpile*.

Organic Sulfur - the portion of *total sulfur* bound to organic compounds, which can be significant in some materials like coal and soil samples.

Overburden - a general term referring to soil and broken rock, lying above *ore* and *waste rock*, that can usually be removed without blasting; at mines in soft sedimentary rock like coal, overburden can be synonymous with waste rock.

Paste pH - a part of *acid-base accounting* that yields the pH of a mixture of distilled water and pulverized sample; see also *rinse pH*.

Pit - see *open pit*.

Placer Mining - a type of mining in which unconsolidated ore and waste can be removed without blasting by shovel, dredging, water jetting, etc.

Portal - surface entrance into an *adit*, *level*, or *decline*.

Primary Minerals - minerals that existed in rock prior to disturbance by human activity, often occurring as (but not limited to) sulfide, aluminosilicate, and oxide minerals; see also *secondary minerals*.

Production Rate - a chemical reaction rate, obtained from a *kinetic test*, expressed in units of mg of parameter/kg of sample/week (mg kg^{-1} wk^{-1}).

Raise - vertical or inclined *underground working* excavated upwards to another *level*; see also *adit*.

Rate - a geochemical reaction rate of *sulfide oxidation*, *neutralization*, or *metal leaching*; based on the amount of element produced (e.g., 10 mg) over a period of time (e.g., 1 week) from a known amount of material (e.g., 1 kg); see also *kinetics* and *equilibrium*.

Refined Net Neutralization Potential (RNNP) - as part of *acid-base accounting*, *Carbonate Neutralization Potential* minus *Sulfide Acid Potential*, in units of kilogram of $CaCO_3$ equivalent per metric tonne of sample (kg $CaCO_3$/t), t $CaCO_3$ equivalent/1000 t of sample, or parts per thousand (ppt) $CaCO_3$ equivalent [all are equal].

Refined Net Potential Ratio (RNPR) - as part of *acid-base accounting*, *Carbonate Neutralization Potential* divided by *Sulfide Acid Potential* (dimensionless).

Retention - amount of reacted *primary minerals* not released to drainage, but held within rock and *tailings*; reflects physical processes such as lack of rinsing water and geochemical processes such as *secondary minerals*.

Rinse pH - a variation on *paste pH* in which the sample is not pulverized, but simply mixed with distilled water to obtain the diluted pH of grain-surface moisture.

Runoff - precipitation falling onto a minesite component and running over its surface; see also *minesite drainage*, *evapotranspiration*, and *infiltration*.

Secondary Minerals - minerals that formed in or on a *minesite component* after disturbance by human activity, often occurring as (but not limited to) sulfate, carbonate, and hydroxide minerals; see also *kinetic test*, *primary minerals*, and *retention*.

Shaft - a primary vertical *underground working* for hoist-based transportation of workers and/or *ore* and *waste rock*; see also *incline*.

Slow Reacting Neutralization Potential (SRNP) - the neutralizing capacity of mined materials under on-site field conditions which is not detected and included in the analytical *Neutralization Potential*; in units of kilogram of $CaCO_3$ equivalent per metric tonne of sample (kg $CaCO_3$/t), t $CaCO_3$ equivalent/1000 t of sample, or parts per thousand (ppt) $CaCO_3$ equivalent [all are equal]; see also *Unavailable Neutralization Potential*.

Solution Mining - a type of mining through which ore is dissolved and pumped to a processing plant, leaving solution cavities.

Spoils - see *waste rock*.

Stages of Drainage Chemistry - First Stage: dissolution of primary minerals, often accompanied by precipitation of secondary minerals; Second Stage: dissolution of any accumulated secondary minerals; Third Stage: return to background concentrations.

Static Test - a procedure for characterizing the physical, chemical, or biological status of a sample at one point in time, such as *acid-base accounting*.

Subsurface Flow - a type of *minesite drainage*.

Sulfide Acid Potential (SAP) - as part of *acid-base accounting*, [*sulfide sulfur* as %S plus *del %S*] multiplied by 31.25, in units of kilogram of $CaCO_3$ equivalent per metric tonne of sample (kg $CaCO_3$/t), t $CaCO_3$ equivalent/1000 t of sample, or parts per thousand (ppt) $CaCO_3$ equivalent [all are equal].

Sulfide Net Neutralization Potential (SNNP) - as part of *acid-base accounting*, *Neutralization Potential* minus *Sulfide Acid Potential*, in units of kilogram of $CaCO_3$ equivalent per metric tonne of sample (kg $CaCO_3$/t), t $CaCO_3$ equivalent/1000 t of sample, or parts per thousand (ppt) $CaCO_3$ equivalent [all are equal].

Sulfide Net Potential Ratio (SNPR) - as part of *acid-base accounting*, *Neutralization Potential* divided by *Sulfide Acid Potential* (dimensionless).

Sulfide Oxidation - oxidation of chemically reduced sulfur, such as sulfide (S_2^{2-}) and elemental sulfur to a partially or fully oxidized form, such sulfate (SO_4^{2-}).

Sulfide Sulfur - a part of *acid-base accounting* that provides the sulfide content of a sample, expressed as %S.

Surface Flow- a type of *minesite drainage*.

Tailings - the waste material from a mill or concentrator that removed the economic metals, minerals, or coal from the *ore*; derived from the use of "heads" as the ore material fed to a *mill*, "concentrate" as the economically valuable and recoverable portion of the heads, and "tails" as the remaining waste portion of the heads; often stored in a surface impoundment with or without confining dams, but also placed elsewhere such as in *underground workings* and non-impounded river valleys.

Tailings Impoundment - a waste-disposal area for *tailings*, often surrounded by one or more confining dams.

Total Acid Potential (TAP) - as part of *acid-base accounting*, total sulfur as %S multiplied by 31.25, in units of kilogram of $CaCO_3$ equivalent per metric tonne of sample (kg $CaCO_3$/t), t $CaCO_3$ equivalent/1000 t of sample, or parts per thousand (ppt) $CaCO_3$ equivalent [all are equal].

Total Net Neutralization Potential (TNNP) - as part of *acid-base accounting*, *Neutralization Potential* minus *Total Acid Potential*, in units of kilogram of $CaCO_3$ equivalent per metric tonne of sample (kg $CaCO_3$/t), t $CaCO_3$ equivalent/1000 t of sample, or parts per thousand (ppt) $CaCO_3$ equivalent [all are equal].

Total Net Potential Ratio (TNPR) - as part of *acid-base accounting*, *Neutralization Potential* divided by *Total Acid Potential* (dimensionless).

Total Sulfate Sulfur - a procedure that provides the total sulfate content of a sample, expressed as %S; see also *acid-leachable sulfate sulfur*.

Total Sulfur - a part of *acid-base accounting* that provides the total sulfur content of a sample, expressed as %S; see also *sulfide sulfur*, *acid-leachable sulfate sulfur*, *total sulfate sulfur*, *organic sulfur, del %S.*

Unavailable Neutralization Potential (UNP) - the portion of the analytical *Neutralization Potential* that is not reactive or available under on-site field conditions; in units of kilogram of $CaCO_3$ equivalent per metric tonne of sample (kg $CaCO_3$/t), t $CaCO_3$ equivalent/1000 t of sample, or parts per thousand (ppt) $CaCO_3$ equivalent [all are equal]; see also *Slow Reacting Neutralization Potential*.

Underground Workings - any open area underground created by human excavation, including *adits*, *crosscuts*, *declines*, *drifts*, *inclines*, *levels*, *portals*, *raises*, and *shafts*; also referred to as galleries in some countries and in some types of mining; alternative to *open pit* mines.

Waste Rock - rock that contains less-than-economic levels of metals, minerals, or coal as opposed to *ore*; often placed in dumps on the land surface or occasionally returned to *open pits* or *underground workings*; in coal mining, may be referred to as “spoils”, “gob”, or “rejects”, but these terms sometimes imply some milling; see also *mined-rock piles*.

Waste-Rock Dump - a *mined-rock pile* containing *waste rock*.

APPENDIX
B. METHODS FOR STATIC TESTS

B.1 Sulfur Species

The recommended procedures for determining sulphur species follow the basic procedures of Sobek et al. (1978), also known as EPA-600 acid-base accounting (ABA). Recommended expansion and minor modifications of the EPA-600 method are provided in *italics* (see also Section 5.2.1.2)

Chemicals (from Sobek et al., 1978)

1. Hydrochloric acid (HC1), 2 parts acid to 3 parts water: mix 400 mL of concentrated HCl with 600 mL of distilled water.
2. Nitric acid (HNO_3), 1 part acid to 7 parts water: Mix 125 mL of concentrated HNO_3 with 875 mL of distilled water.
3. Silver Nitrate ($AgNO_3$), 10%: Dissolve 10.0 g of $AgNO_3$ in 90 mL of distilled water. Store in amber bottle away from light.
4. Nesslar's Solution (Fisher Scientific Co. No. So-N-24 or equivalent).

Materials (from Sobek et al., 1978)

1. Leco Induction Furnace and Automatic Sulfur Titrator, *prepared and operated according to the Operator's Manual and internal laboratory QA/QC and operating procedures.*
2. Funnels, 28" I.D. polyethylene.
3. Filter paper, 5.5" glass fiber.
4. Flasks, Erlenmeyer, 250 mL.
5. Beakers, 100 mL.
6. Syringe.
7. Balance, can be read to 0.001 g.

Procedure (from Sobek et al., 1978)

1. Take three 0.500 g subsamples of less than 60 mesh material.
2. Take one subsample and analyze for total sulfur.
3. Taking care not to sharply crease the glass fibers, fold filter paper to fit a polyethylene funnel.
4. Place second subsample in filter. NOTE: Make sure all material is placed in the filter.
5. Place subsample and filter onto funnel holder in sink or other suitable pan which can receive outflow from funnel.
6. Using a syringe, pipette, or other graduated dispenser, add 2:3 HCl to almost the top of the filter paper. Caution: During this step and all other leaching steps, be careful not to lose any sample by runover, splashing, or breaking through the filter paper.
7. Repeat step 6 until a total of 50 mL of acid has been added.
8. Place funnel holder, containing funnel and subsample, over a 100 mL beaker.
9. Leach subsample with 50 mL of distilled and deionized water. Discard leachate. NOTE: Stop here if procedure cannot be completed in one day. CAUTION: Samples must be kept moist.
10. Leach subsample with another 50 mL of distilled and deionized water.
11. Test leachate for chlorides by adding 3 drops of 10% AgNO3 with a dropper. NOTE: The presence of

chlorides wil1 be detected by a white precipitate.

12. Discard leachate and repeat steps 10 and 11 until no precipitate forms.
13. Discard leachate.
14. Air dry subsample and filter ovemight.
15. Carefully fold glass fiber filter around the sample and transfer to ceramic crucible for [residual] total sulfur analysis.
16. Place third subsample in a 250 mL Erlenmeyer flask. NOTE: Make sure all of the subsample is placed in the flask.
17. Add 50 mL of HNO_3 (1:7).
18. Let stand overnight at room temperature.
19. Taking care not to sharply crease the glass fibers, fold a filter to fit a polyethylene funnel.
20. Place a funnel holder over a sink or other suitable pan which can receive outflow from funnel.
21. Carefully pour subsample and acid from the Erlenmeyer flask into the funnel. NOTE: Do not get material above top of filter paper.
22. Repeat step 21 using distilled and deionized water to wash all materials remaining in the Erlenmeyer flask into the funnel.
23. Place funnel holder containing funnel and subsample over a 100 mL beaker. NOTE: Stop here if procedure cannot be completed in one day. CAUTION: Sample must be kept moist.
24. Leach subsample with 50 mL of distilled and deionized water. Discard leachate.
25. Leach subsample with another 50 mL of distilled and deionized water.
26. Test leachate for presence of nitrates by adding 3 drops of Nessler's Solution with a dropper. NOTE: If nitrates are present, the leachate will turn yellow within 30 seconds as seen against a white background.
27. Discard leachate and repeat steps 25 and 26 until no nitrates are detected.
28. Discard leachate.
29. Air dry subsample and filter overnight.
30. Carefully fold glass fiber filter around the sample and transfer to a ceramic crucible for [residual] total sulfur analysis.

Comment: It is necessary to remove chlorides and nitrates by water leachings after the hydrochloric and nitric acid (respectively) extractions before running total sulphur.

Calculations (adapted from Sobek et al., 1978)

1. Total sulphur (%S_{total})= total sulphur of untreated sample.

2. Acid-leachable sulphate (%$S\text{-}SO4_{leachable}$) = (%S_{total}) - (Total sulfur after HCl treatment).

3. Sulphide (%$S_{sulphide}$) = (Total sulfur after HCl treatment) - (Total sulfur after HNO_3 treatment).

*4. Insoluble sulphate (%$S\text{-}SO4_{insoluble}$)= (Barium as %Ba from total-metal analyses) * (32.06/137.34); assumes all insoluble sulphate occurs as barite and all barium occurs as barite.*

5. Sulphur discrepancy (%S_{del}) = (%S_{total}) - (%$S\text{-}SO4_{leachable}$ + %$S\text{-}SO4_{insoluble}$ + %$S_{sulphide}$); if positive in value, assumed to be acid-generating sulphide unless demonstrated otherwise.

B.2 Bulk Neutralization Potential

This procedure is from Sobek et al. (1978), also known as the EPA-600 method. It involves soaking a sample in excess acid, heating the mixture to ensure good dissolution, and then determining the remaining, un-neutralized acidity. The NP is then reported in any of three equal units: tonnes (t) of $CaCO_3$ equivalent/1000 t of sample, or kg of $CaCO_3$ equivalent/t of sample, or parts per thousand (ppt) $CaCO_3$ equivalent (see also Section 5.2.1.3). This procedure includes an initial determination of the rate of NP dissolution ("fizz rating" of carbonate dissolution) to ensure sufficient acid is added to dissolve all readily reactive NP.

Method (from Sobek et al., 1978)

During digestion, do not boil samples. If boiling occurs, discard sample and rerun. Before titrating with acid, fill buret with acid and drain completely. Before titrating with base, fill buret with base and drain completely to assure that free titrant is being added to the sample.

Chemicals

1. Carbon dioxide-free water: Heat distilled water just to boiling in the beaker. Allow to cool slightly and pour into a container equipped with ascarite tube. Cool to room temperature before using.
2. Hydrochloric acid (HCl) solution, 0.1 N, certified grade.
3. Sodium hydroxide (NaOH), approximately 0.5 N: Dissolve 20.0 g of NaOH pellets in carbon dioxide-free water and dilute to 1 liter. Protect from CO_2 in the air with ascarite tube. Standardize solution by placing 50 mL of certified 0.1 N HCl in a beaker and titrating with the prepared 0.5 N NaOH until a pH of 7.00 is obtained. Calculate the normality of the NaOH using the following equation:

   N2 = (NlV1)/V2, where:
   V1= Volume of HCl used.
   N1= Normality of HCl used.
   V2 = Volume of NaOH used.
   N2 = Calculated normality of NaOH.

   Note: Other methods of standardizing prepared NaOH solutions, such as the use of triplicate accurately weighed samples of potassium acid phthalate, can be employed and should be consistent with a laboratories QA/QC procedures.

4. Sodium hydroxide (NaOH) approximately 0.1 N: Dilute 200 mL of 0.5 N NaOH with carbon dioxide-free water to a volume of 1 liter. Protect from CO_2 in air with ascarite tube. Standardize solution by placing 20 mL of certified 0.1 N HCl in a beaker and titrating with the prepared 0.1 N NaOH until a pH of 7.00 is obtained. Calculate the normality of the NaOH using the equation in No. 3 above.

   Note: Other methods of standardizing prepared NaOH solutions, such as the use of triplicate accurately weighed samples of potassium acid phthalate, can be employed and should be consistent with a laboratories QA/QC procedures.

5. Hydrochloric acid (HCl), approximately 0.5 N: Dilute 42 mL of concentrated HCl to a volume of 1 liter with distilled water. Standardize solution by placing 20 mL of the known normality NaOH prepared in No. 3 above in a beaker and titrating with the prepared HCl until a pH Of 7.00 is obtained.

   Calculate the normality of the HCl using the following equation:

   N1 = (N2V2)/V1, where:

V2 = Volume of NaOH used.
N2 = Normality of NaOH used.
V1 = Volume of HCl used.
N1 = Calculated Normality of HC1.

6. Hydrochloric acid (HC1), approximately 0.1 N: Dilute 200 mL of 0.5 N HCl to a volume of 1 liter with distilled water. Standardize solution as in step 5 above, but use 20 mL of the known normality NaOH prepared in No. 4 above.
7. Hydrochloric acid (HC1), 1 part acid to 3 parts water: Dilute 250 mL of concentrated HCl with 750 mL of distilled water.

Materials

1. Flasks, Erlenmeyer, 250 mL.
2. Buret, 100 mL (one required for each acid and one for each base).
3. Hotplate, steam bath can be substituted.
4. pH meter equipped with combination electrode.
5. Balance, can be read to 0.01 g.

Procedure

1. Place approximately 0.5 g of sample (less than 60 mesh) on a piece of aluminum foil.
2. Add one or two drops of 1:3 HCl to the sample. The presence of $CaCO_3$ is indicated by a bubbling or audible "fizz."
3. Rate the bubbling or "fizz" in step 2 as indicated in Table B-1.

TABLE B-1
Volumes and Normalities of Acid Addition for NP Determination Based on Fizz Rating (from Sobek et al., 1978)

Fizz Rating	Add mL of HCL	Normality of Added HCl
None	20	0.1
Slight	40	0.1
Moderate	40	0.5
Strong	80	0.5

4. Weigh 2.00 g of sample (less than 60 mesh) into a 250 mL Erlenmeyer flask.
5. Carefully add HCl indicated by Table B-1 into the flask containing sample.
6. Heat nearly to boiling, swirling flask every 5 minutes, until reaction is complete. NOTE: Reaction is complete when no gas evolution is visible and particles settle evenly over the bottom of the flask.
7. Add distilled water to make a total volume of 125 mL.
8. Boil contents of flask for one minute and cool to slightly above room temperature. Cover tightly and cool to room temperature. CAUTION: Do not place rubber stopper in hot flask as it may implode upon cooling.
9. Titrate using 0.1 N NaOH or 0.5 N NaOH (concentration exactly known), to pH 7.0 using a pH meter and

buret. The concentration of NaOH used in the titration should correspond to the concentration of the HCl used in No. 5 above. NOTE: Titrate with NaOH until a constant reading of pH 7.0 remains for at least 30 seconds.

10. If less than 3 mL of the NaOH is required to obtain a pH of 7.0, it is likely that the HCl added was not sufficient to neutralize all of the base present in the 2.00 g sample. A duplicate sample should be run using the next higher volume or concentration of acid as indicated in Table B-1.
11. Run a blank for each volume or normality of acid using steps 5, 7, 8, and 9 above.

Calculations

1. Constant (C) = (mL acid in blank)/(mL base in blank).

2. mL acid consumed = (mL acid added) - (mL base added multiplied by C).

3. Neutralization Potential (as t $CaCO_3$ equivalent/1000 t material) = (mL of acid consumed) * (25.0) * (N of acid).

B.3 Carbonate Neutralization Potential

Leco equipment for analysis of sulfur also includes the option for total carbon analysis. If static tests indicate inorganic carbon is the only significant form of carbon in a sample, the value of Leco total carbon can be used to calculate the Carbonate Neutralization Potential (CaNP; see also Section 5.2.1.3). If organic carbon is present, it must be determined separately as explained below and subtracted from the Leco total-carbon value.

Method

1) Obtain total carbon value from Leco equipment.
2a) If Leco total carbon is reported as %C:
    CaNP (as t $CaCO_3$ equivalent/1000 t sample) = (Leco %C) * (100.09/12.01) * (10).
2b) If Leco total carbon is reported as %CO_2:
    CaNP (as t $CaCO_3$ equivalent/1000 t sample) = (Leco %C) * (100.09/44.01) * (10).
3) If there are other significant sources of non-carbonate carbon, an independent determination of inorganic carbonate is required. This determination can be made in one of several ways:
    (1) measurement of Leco total carbon before and after the bulk NP analysis (Section B.3); the subtraction of the two values provides the amount of carbon dissolved by acid and assumed to be inorganic carbonate (should be confirmed by mineralogical examinations - Section 5.2.2);
    (2) dissolution of carbonate in acid within a sealed chamber, followed by analysis of the evolved gas by Gas Chromatograph to determine the original, solid-phase carbonate content; or,
    (3) dissolution of carbonate in acid within a sealed chamber; the measurement of gas-pressure increase will indicate the carbonate content after calibration of the chamber with known carbonate standards.

B.4 Paste pH

In addition to sulphur species and neutralization potential, the measurement of sample pH is a fundamental part of acid-base accounting (ABA). Because samples are usually not saturated, sufficient water must be added to create a “paste”. A combination pH electrode is then inserted into the paste and the pH value recorded. The primary difference between crushed pH and rinse pH is the use of only fine material in crushed pH, which is obtained either by pulverizing a sample. Simple sorting of grains without crushing would be classified as rinse pH.

Like all static tests, crushed pH characterizes a sample at one point in time, but does not indicate how sample pH will change in the future. Kinetic tests are required for these predictions. Furthermore, crushed pH is subject to many interferences and inaccuracies including prior wetting and drying of samples, final ratio of water to sample, amount of sample handling and preparation, and geochemical effects of particle surfaces and aqueous diffusion rates on the combination pH electrode. Therefore, crushed pH should not be considered any more accurate and representative than ½ to one pH units, and is not directly comparable to an aqueous pH.

The basic procedure for crushed pH is taken from Sobek et al. (1978), also known as the EPA-600 paste pH. Modifications to the original procedure are in *italics*.

Method (from Sobek et al., 1978)

Care must be taken to insure electrode life and accurate pH measurements: (1) Electrode should not remain in the sample longer than necessary for a reading, especially if more alkaline than pH 9.0 *or more acidic than pH 2.0*. (2) Electrode should be washed with a jet of distilled water from a wash bottle after every measurement (sample or buffer solution). (3) Electrode should be dipped in dilute (*0.1 N*) hydrochloric acid for a few seconds and washed with distilled water to remove any calcium carbonate film which may form, especially from alkaline samples. (4) Drying out of the electrode should be avoided. Electrode is cleaned and suspended in distilled water (which is protected from evaporation) for storage. (5) Place pH meter in standby position when electrode is not in a solution.

The pH meter and electrode should be standardized with buffers differing by 3 or 4 pH units, such as 4.0 and 7.0, before beginning a series of measurements. After every tenth measurement, recheck the standardization with both buffers. Care should be taken not to contaminate one buffer with the other buffer or with the test solution. Never return used standard buffers to their stock bottles. The procedure describes the technique for measuring pH with a glass electrode and meter. If pH is taken in the field using color paper strips or indicator solutions, modification will have to be made by qualified personnel to the procedure.

Chemicals

1. Standard buffer solutions, pH 4.00 and pH 7.00.
2. Distilled water (H_2O).

Materials

1. pH meter equipped with combination electrode.
2. Paper cups, 30 mL capacity.
3. Plastic cups.
4. Stirring rod.
5. Wash bottle containing distilled water.
6. Balance, can be read to 0.1 g.

Procedure

1. Turn on pH meter, adjust temperature setting, and "zero" pH meter per instruction manual.
2. Place pH 4.0 and pH 7.0 standard buffers in two plastic cups (one buffer in each cup). NOTE: NEVER return used buffers to stock bottles.
3. Place electrode in the pH 7.0 buffer.
4. Adjust pH meter to read 7.0.
5. Remove electrode from buffer solution and wash with a jet of distilled water from a wash bottle.
6. Place electrode in the pH 4.0 buffer and check the pH reading. NOTE: If pH meter varies more than ±0.1 pH units from 4.0, something is wrong with the pH meter, electrode, or buffers.
7. Weigh 10 g of less than 60 mesh material (*obtained by pulverizing and/or sorting the sample*) into a paper *or plastic* cup. *Record whether the sample has been pulverized or sorted.*
8. Add 5 mL of distilled water to sample. NOTE: Do not stir. Allow water to wet sample by capillary action without stirring. With soft overburden and minesoils materials, the 2:1 (soil:water) ratio provides a satisfactory paste for pH measurements; however, for the very coarse textured and the very fine textured material, more material or water can be added to bring the soil near saturation. At near saturation conditions, water should not be puddled nor dry soil appear at the surface. *If additional water or sample is required, record each of the amounts and report the ratio of sample:water along with the rinse pH.*
9. Stir sample with a spatula until a thin paste is formed adding more water or soil as required to keep soil at saturation point. NOTE: At saturation, the soil paste glistens as it reflects light and the mixture slides off the spatula easily. Wash the spatula with a jet of distilled water before stirring another sample.
10. Place electrode in paste and move carefully about to insure removal of water film around the electrode. CAUTION: Do not trap particles between electrode and inside surface of the sample container. Electrodes are easily scratched. Contact between paste and electrode should be gentle to avoid both impact and scratching damage, especially in sandy samples.
11. When reading remains constant, record pH and remove electrode from paste. Carefully wash electrode with distilled water to insure removal of the paste. If all pH measurements are completed, the electrode should be stored in a beaker of distilled water. NOTE: After every 10 samples, check meter calibration with standard buffers.

B.5 Rinse pH

Like crushed pH, rinse pH characterizes a sample at one point in time. However, whereas crushed pH involves pulverizing, rinse pH uses a sample as received with the <2 mm fraction used and the coarser grains discarded. Because samples are usually not saturated, sufficient water must be added to allow the pH electrode to work properly.

The basic procedure for rinse pH is adapted from the procedure for paste pH in Sobek et al. (1978), also known as the EPA-600 method. Modifications to the original procedure are in *italics*. The primary modification is the use of a weight ratio of 1:1 sample:water, rather than 2:1 used for crushed pH.

Method (from Sobek et al., 1978)

Care must be taken to insure electrode life and accurate pH measurements: (1) Electrode should not remain in the sample longer than necessary for a reading, especially if more alkaline than pH 9.0 *or more acidic than pH 2.0*. (2) Electrode should be washed with a jet of distilled water from a wash bottle after every measurement (sample or buffer solution). (3) Electrode should be dipped in dilute (*0.1 N*) hydrochloric acid for a few seconds and washed with distilled water to remove any calcium carbonate film which may form, especially from alkaline samples. (4) Drying out of the electrode should be avoided. Electrode is cleaned and suspended in distilled water (which is protected from evaporation) for storage. (6) Place pH meter in standby position when electrode is not in a solution.

The pH meter and electrode should be standardized with buffers differing by 3 or 4 pH units, such as 4.0 and 7.0, before beginning a series of measurements. After every tenth measurement, recheck the standardization with both buffers. Care should be taken not to contaminate one buffer with the other buffer or with the test solution. Never return used standard buffers to their stock bottles. The procedure describes the technique for measuring pH with a glass electrode and meter. If pH is taken in the field using color paper strips or indicator solutions, modification will have to be made by qualified personnel to the procedure.

Chemicals

1. Standard buffer solutions, pH 4.00 and pH 7.00.
2. Distilled water (H_2O).

Materials

1. pH meter equipped with combination electrode.
2. Paper cups, 30 mL capacity.
3. Plastic cups.
4. Stirring rod.
5. Wash bottle containing distilled water.
6. Balance, can be read to 0.1 g.

Procedure

1. Turn on pH meter, adjust temperature setting, and "zero" pH meter per instruction manual.
2. Place pH 4.0 and pH 7.0 standard buffers in two plastic cups (one buffer in each cup). NOTE: return used buffers to stock bottles.
3. Place electrode in the pH 7.0 buffer.
4. Adjust pH meter to read 7.0.
5. Remove electrode from buffer solution and wash with a jet of distilled water from a wash bottle.
6. Place electrode in the pH 4.0 buffer and check the pH reading. NOTE: If pH meter varies more than ±0.1 pH units from 4.0, something is wrong with the pH meter, electrode, or buffers.
7. Weigh 10 g of *sample as received, preferably using the <2 mm fraction,* into a paper *or plastic* cup. *If the sample is coarse grained, additional weight can be used to obtain a more representative sample. In this case, the amount of water (next step) must also be increased. Record the grain size of the sample.*
8. Add *at least 10* mL of distilled water to sample. NOTE: Do not stir. Allow water to wet sample by capillary action without stirring. With soft overburden and minesoils materials, the *1*:1 (soil:water) *weight* ratio provides a satisfactory paste for pH measurements; however, for the very coarse textured and the very fine textured material, more material or water can be added to bring the soil near saturation. At near saturation conditions, water should not be puddled nor dry soil appear at the surface. *If additional water or sample is required, record each of the amounts and report the ratio of sample:water along with the rinse pH.*
9. Stir sample with a spatula until *well mixed,* adding more water or soil as required to keep soil at saturation

point. NOTE: At saturation, *water should just cover the entire sample*. Wash the spatula with a jet of distilled water before stirring another sample.

10. Place electrode in *sample* and move carefully about to insure removal of water film around the electrode. CAUTION: Do not trap particles between electrode and inside surface of the sample container. Electrodes are easily scratched. Contact between paste and electrode should be gentle to avoid both impact and scratching damage, especially in sandy samples.
11. When reading remains constant, record pH and remove electrode from paste. Carefully wash electrode with distilled water to insure removal of the paste. If all pH measurements are completed, the electrode should be stored in a beaker of distilled water. NOTE: After every 10 samples, check meter calibration with standard buffers.

B.6 Net Neutralization Potentials

Net Neutralization Potential (NNP) is a part of acid-base accounting, like sulphur species, neutralization potential, and paste/rinse pH. However, NNP does not involve chemical analysis, but is simply a calculated parameter (see also Section 5.2.1.4).

1. Obtain $\%S_{total}$, $\%S_{sulphide}$, and $\%S_{del}$ from Section B.1.
2. Calculate: Total Acid Potential (TAP, as t $CaCO_3$/1000 t) = $\%S_{total} * 31.25$
   Sulphide Acid Potential (SAP, as t $CaCO_3$/1000 t) = $(\%S_{sulphide} + \%S_{del}) * 31.25$
3. Obtain bulk NP and CaNP from Sections B.2 and B.3.
4. Calculate: Total NNP (TNNP, as t $CaCO_3$/1000 t) = NP-TAP
   Sulphide NNP (SNNP as t $CaCO_3$/1000 t) = NP-SAP
   Carbonate NNP (CNNP, as t $CaCO_3$/1000 t) = CaNP-TAP
   Refined NNP (RNNP, as t $CaCO_3$/1000 t) = CaNP-SAP
5. Interpretation of NNPs is discussed in Chapter 5.

NOTE: Other calculations are possible and in use in some countries. In Australia, Net Acid Producing Potential (NAPP) is calculated from xAP-NP.

B.7 Net Potential Ratios

Net Potential Ratio (NPR) is a part of acid-base accounting, like sulphur species, neutralization potential, paste/rinse pH, and net neutralization potentials. Like NNP, NPR does not involve chemical analysis, but is simply a calculated parameter (see also Section 5.2.1.4).

1. Obtain $\%S_{total}$, $\%S_{sulphide}$, and $\%S_{del}$ from Section B.1
2. Calculate: Total Acid Potential (TAP, as t $CaCO_3$/1000 t) = $\%S_{total} * 31.25$
   Sulphide Acid Potential (SAP, as t $CaCO_3$/1000 t) = $(\%S_{sulphide} + \%S_{del}) * 31.25$
3. Obtain bulk NP and CaNP from Sections B.2 and B.3.
4. Calculate: Total NPR (TNPR, dimensionless) = NP/TAP
   Sulphide NPR (SNPR, dimensionless) = NP/SAP
   Carbonate NPR (CNPR, dimensionless) = CaNP/TAP
   Refined NPR (RNPR, dimensionless) = CaNP/SAP
5. Interpretation of NPRs is discussed in Chapter 5.

APPENDIX
C. METHODS FOR KINETIC TESTS

This chapter describes the recommended technique for laboratory and field-based kinetic tests. The recommended laboratory test is a humidity cell, and the given procedure should be followed unless a deviation is justified. The recommended field-based test is an on-site leach pad and/or site monitoring. Kinetic tests are not optional, but are critical in predicting drainage chemistry even in the absence of acid generation.

C.1 Initial Comments

Humidity cell testing is one form of kinetic test. This testing provides data on the rates of metal leaching, acid generation, and acid neutralization for a selected sample. In turn, these rates provide important information needed to predict drainage chemistry. Kinetic tests differs from static tests such as acid-base accounting (ABA), in that the static tests only provide data on the composition of the sample, such as the amount of sulphur and the sample neutralization potential. A large suite of static and kinetic tests are needed to predict or assess drainage chemistry.

C.2 Laboratory-Based Tests

The recommended laboratory kinetic test is a humidity cell (Figure C-1 and C-2). Humidity cells have been in use for almost 30 years.

A humidity cell is typically a plexiglass cylinder fitted with a base plate equipped with a drain hole and tubing nipple. Approximately 1 inch from the bottom of the base plate is a removable perforated plate or screen which supports the sample. In some cases materials such as landscape fabric may be used to prevent particularly fine samples from passing through the perforated plate.

The size and shape of the humidity cell will vary whether the sample is waste rock or tailings. A waste-rock humidity cell is usually tall and slender, ~8 inches high and 4 inches wide (Figure C-1), whereas a cell for tailings samples tends to be shorter and wider than the waste-rock cell (Figure C-2).

Approximately 1 kg (dry weight) of sample is placed in a humidity cell, forming a relatively flat surface. Then air is continuously pumped into and through the cell. However, the pattern of air flow differs between the tailings and waste-rock cells. This difference reflects in part the deposition pattern and water-retention characteristics in the field. Tailings are typically fine materials with a high moisture content and are usually placed as a slurry into an impoundment. Usually the only air in constant contact with the tailings is that which passes over the top of the tailings mass. Subsequent air diffusion into the tailings is a slow process (Section 5.5.1) and limits the movement of oxygen down through the tailings. Waste rock, on the other hand, is usually coarser than tailings, and is placed in piles or dumps. The larger particle size allows for better drainage, more contact between the waste rock and air, and greater air circulation. As a result, air is

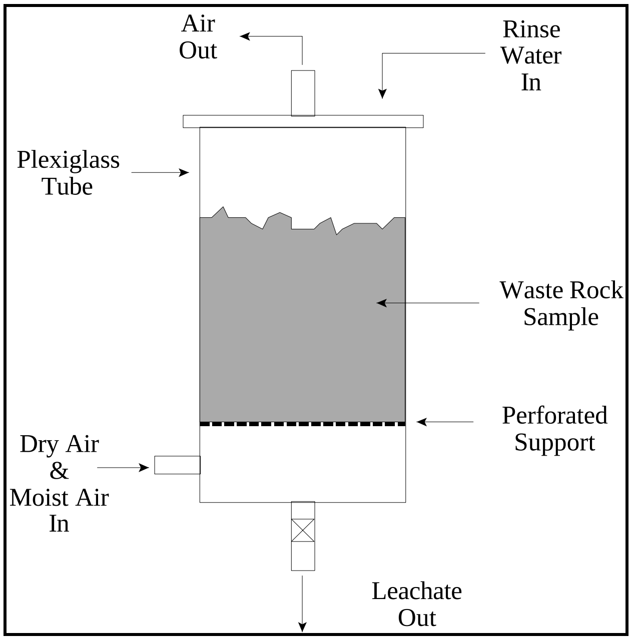

FIGURE C-1. Humidity Cell for Rock

introduced below the sample in a waste rock cell so that it can more freely circulate through it.

One testing "cycle" takes place over seven days. The first three days of the cycle is the "dry" portion of the cycle during which background laboratory air is passed over a tailings sample and through a waste-rock sample. The next three-day period is the "wet" portion of the testing cycle, when laboratory air is first pumped through a humidifier unit and then into a cell.

On the final day of the testing cycle a sample "rinse/leach" is done. A known amount of distilled/deionized water is added to the top of the cell, allowed to soak the sample for a specified period, and then drained for analysis. The purpose of the weekly rinse/leaching is to wash out any weathering reaction products that have accumulated in the cell during the wet and dry segments of the cycle. After the sample rinse/leach, another cycle is initiated with the introduction of dry air. A detailed description of the startup, operating, and closedown procedures are presented below.

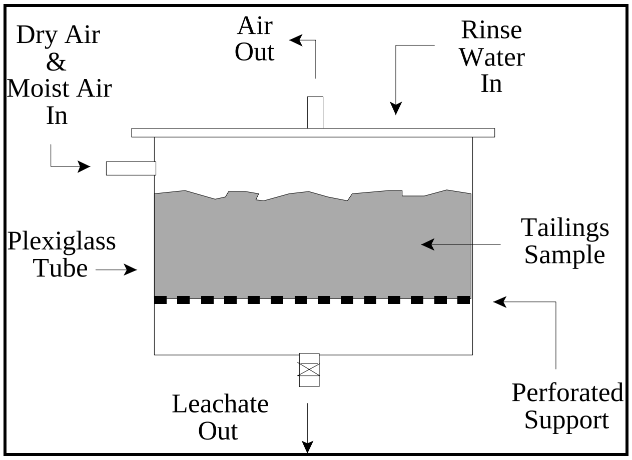

FIGURE C-2. Humidity Cell for Tailings

The weekly "leachate" or rinse water is usually analysed for pH, sulphate, conductivity, acidity, alkalinity, and ICP metals. Metal samples should be filtered to provide dissolved concentrations. From the analyses, leaching rates can be calculated, typically in units of mg of parameter/kg of sample/week (Table C-1 and Section C.2.4). Also, along with pre-test static tests such as ABA and ICP metals analysis, depletion times can be calculated.

The duration of humidity cell test is usually at least 40 weeks, or until the rates of sulphate generation and metal leaching have stabilized at relatively constant rates for at least five weeks. Experience has shown that stabilization can take over 60 weeks, and significant changes may take place even after several years. Therefore, the criteria on which to close down a cell depend on the site-specific objectives and uncertainty of predictions. Particularly because of uncertainty and associated risks, some mines have continued kinetic tests for up to five years (and some are still continuing).

C.2.1 Humidity Cell Startup Procedure

1. Collect a minimum of 2 kg of sample for humidity cell testing. Record sample information on a humidity cell pre-test sample information sheet (Figure C-3).
2. The beginning of the humidity cell test program will be Week 0. Humidity cells are operated on a weekly cycle.
3. If the sample is rock (ie. waste rock, ore, etc.), crush the sample to 80% minus ¼ inch. If the sample is tailings, crushing is not required and is normally tested as received.
4. Split out sufficient representative portions of the sample and send for all static tests discussed in Chapter 5. Record information on pre-test sample information sheet. Label these results “pre-test data”.
5. Accurately weigh 1000 g of the sample and carefully place in the appropriate humidity cell, either for waste rock or tailings (Figures C-1 and C-2). If the sample is moist, determine water content so a dry weight can be calculated. Ensure the sample has a relatively level surface in the cell.

[Procedures For Week 0:]

6. Clamp the drain hose at the bottom of the cell. Carefully add a known volume of demineralized water, approximately 750 mL, to the top of the humidity cell. Enough demineralized water should be added to the sample to thoroughly moisten the sample and allow for collection of at least 300-500 mL of leachate. Record the amount of water added on a weekly data sheet (Figure C-4). Put a collection flask under the cell with the hose draining into it. All samples must have good contact with the water, therefore gently agitate fine, semi-permeable samples for about one minute.

7. Allow rock samples to soak for ~2 hour and tailings samples to soak for ~4 hours allowing any suspended particles to settle. Disconnect the hose clamp and drain off the leachate into the collection flask. If the cell will not drain in a reasonable time (ie. about an hour) check to see if the drainage hose is blocked. If the leachate still will not drain carefully decant the leachate off the top of the sample. Record the volume of leachate collected (Figure C-4).

   NOTE: if excess solids flow from the humidity cell with the leachate it may be necessary to filter the leachate through coarse filter paper into a clean weighed filter flask. Transfer as much of the solids as possible from the collection flask to the filter apparatus by swirling before transferring. Weigh the filtrate plus the filter flask; record the weight. Record the volume of the filtrate. Keep a record of all weights and calculations.

8. Immediately filter the leachate through a 0.45-micrometer filter into a 500 mL polyethylene bottle ("raw") and a 100 mL polyethylene bottle acidified with HNO_3 to a pH < 1.5. Label the bottles with the project name, sample id., cycle number, and date. Record all data for this initial rinse as Week or Cycle 0.

HUMIDITY CELL TESTING PROGRAM
PRE-TEST SAMPLE INFORMATION SHEET

Company: ____________________

Project: ____________________

Sample Id.: ____________________

Sample Type (waste rock, tailings, etc.): ____________________

Sample Submission Date: ____________________

Submitted To: ____________________

Submitted By: ____________________

Sample Description (colour, smell, textured, size distribution, moisture content, etc.): ____

____

____

FIGURE C-3. Pre-Test Sample-Description Form for Kinetic-Test Samples

KINETIC TEST - WEEKLY DATA SHEET

PROJECT: Mine A
CELL NO.: A-4
SAMPLE ID./DESCRIPTION: Sample 45964 (Dump #6 - Waste Rock)

Week/Cycle	Date	Water Volume Added (mL)	Leachate Volume Recovered (mL)	pH	Conductivity (µS/cm)	Humidifier Water Temp. (°C)	Comments /Analyst
0	35106	750	430	6.68	425	30.5	Filtered solids returned to cell. Water drained well. NH
1	35113	500	427	6.96	505	30.5	Filtered solids returned to cell. Water drained well. KM
2	35120	500	471	7.21	311	30.5	Filtered solids returned to cell. NH
3	35127	500	453	7.01	353	30.5	Filtered solids returned to cell. NH

FIGURE C-4. Weekly Report Form for Kinetic Testing

9. Place ~25 mL of the "raw" leachate in a 30 mL beaker and perform pH and conductivity measurements on the sample using calibrated instruments, record all results. Keep a record of the instruments used, all QA/QC procedures, and any data resulting from calibration.
10. Submit the remaining "raw" leachate immediately for acidity, alkalinity, and sulphate analysis. Submit the acidified sample for ICP metals. This suite of analyses is a standard request, but may vary somewhat according to the sample and the type of information needed (i.e. some samples may require low level arsenic and/or mercury analyses, etc.).
11. Carefully scrap any residue in the filter apparatus back into the humidity cell. Place the filter paper on top of the humidity cell to dry ensuring it will not be disturbed. When the filter paper and residue have dried return any solids back to the humidity cell.

[QA/QC Procedures for Week 0:]

12. Take a sample of the demineralized water used as humidity cell rinse water, and process through a blank cell, handle, and filter the sample as was done with the humidity cell leachate. Measure pH and conductivity in the sample. Label the sample "Method Blank” and submit it for analysis.
13. Take a sample of demineralized water used for leaching the cells (do not process in any way). Label it “DDI H_20" and submit it for analysis.

C.2.2 Humidity Cell Weekly Operating Procedure

1. For the first three days after the weekly rinse, dry air is passed over and through the sample within the humidity cell. Connect the humidity cell to a dry air source, use a gentle flow rate to move the air past

the sample. If more than one humidity cell is running, splits can be taken from a main air line leading to each humidity cell. Use hose clamps to ensure that each cell receives roughly the same air flow rate.

2) On the morning of the fourth day, a three day wet air cycle begins. Switch the air supply from a dry source to a humid one. Disconnect each humidity cell from the main dry air supply line. Connect each cell to a nipple on the humidifier. The humidifier should be roughly half full of water, and contain an immersion heater which is set to 30°C. The air from the main dry air supply is switched to pass through the humidifier unit. This air passes through the humidifier and exits from an aquarium-type diffuser. The air pressure is adjusted to provide an adequate air flow without causing rolling waves in the humidifier. Again, if more than one humidity cell is running, use hose clamps associated with each humidity cell to ensure that each cell receives roughly the same air flow rate.

3) On the seventh day, sampling procedures begin. Shut off the main air supply. Disconnect the air supply hose from each of the waste rock humidity cells and clamp shut. Note: the waste rock cells have the air inlet at the bottom and will allow leach water to drain back into the humidifier if not clamped. Disconnect the immersion heater and record the water temperature and pH of each humidifier.

4) Ensure that the drain hose at the bottom of the cell is clamped. Place a clean 500 mL beaker under each cell with the hose draining into it. Carefully add 500 mL of water, taken from the demineralized water reservoir, to the top of each humidity cell. Record the amount of water added. All samples must have good contact with the water, therefore gently agitate fine, semi-permeable samples for about one minute before and/or after the addition of water. Note how each cell is treated in the weekly records (Figure C-4).

5) Allow rock samples to soak for ~2 hour and tailings samples to soak for ~4 hours allowing any suspended particles to settle. Disconnect the hose clamp and drain off the leachate into the collection flask. If the cell will not drain in a reasonable time (i.e. about an hour) check to see if the drainage hose is blocked. If the leachate still will not drain carefully decant the leachate off the top of the sample. Record the volume of leachate collected.

NOTE: if excess solids flow from the humidity cell with the leachate it may be necessary to filter the leachate through coarse filter paper into a clean weighed filter flask. Transfer as much of the solids as possible from the collection flask to the filter apparatus by swirling before transferring. Weigh the filtrate plus the filter flask record the weight. Record the volume of the filtrate. Keep a record of all weights and calculations.

6) Immediately filter the leachate through a 45 micrometer filter into a 500 mL polyethylene bottle ("raw") and a 100 mL polyethylene bottle acidified with HNO_3 to a pH < 1.5. Label the bottles with the project name, sample id., cycle number, and date.

7) Place ~25 mL of the "raw" leachate in a 30 mL beaker and perform pH and conductivity measurements on the sample using calibrated instruments, record all results. Keep a record of the instruments used, all QA/QC procedures, and any data resulting from calibration.

8) Submit the remaining "raw" leachate immediately for acidity, alkalinity, and sulphate analysis. Also, send the acidified sample for ICP metals, and arsenic and mercury analysis. This suite of analyses is a standard request, but may vary somewhat according to the sample and the type of information needed (i.e., some samples may not require arsenic analysis, etc.).

9) Carefully scrap any residue in the filter apparatus back into the humidity cell. Place the filter paper on top of

the humidity cell to dry, ensuring it will not be disturbed. When the filter paper and residue have dried, return any solids back to the humidity cell.

[QA/QC Procedures for Weekly Operation:]

10) Take a sample of the demineralized water used as humidity cell rinse water, and process through the blank cell, handle, and filter the sample as was done with the humidity cell leachate. Measure pH and conductivity in the sample. Label the sample "Method Blank” and send it for analysis.

11) Take a sample of the demineralized water used for leaching the cells (do not process in any way). Label it “DDI H_20" and submit it for analysis.

12) Humidifier maintenance: Humidifiers should be cleaned out every three months or if water appears turbid. Also replace tubing whenever necessary.

13) Calculations are discussed in Section C.2.4.

C.2.3 Humidity Cell Closedown Procedure

1) When the cell has stabilized geochemically (Section 5.3.1), it can be terminated if desired. To properly interpret cell results from the beginning of the test, specific closedown procedures must be carried out and included in data interpretation.

2) Collect leachate after the last cycle rinse as per the humidity cell operational procedures (Section C.2.2). Note: the rinse from the last cycle must be submitted for the full suite of analysis.

3) Remove the sample from the test cell and place it into a clean 4 L polyethylene rotary jar. To ensure that the test cell has been thoroughly cleaned, and all of the sample and its precipitates have been transferred to the rotary jar, use a known amount of demineralized water of known composition to wash the cell. Add enough demineralized water to the rotary jar so that a total of 3 L of demineralized water has been added.

4) Gently agitate the sample on a rotary extractor for a period of 24 hours. On completion of the 24 hour agitation, let the sample stand for a minimum of three hours allowing suspended materials to settle.

5) Collect the supernatant, recording its volume. Handle and prepare the sample the same as was done during normal humidity cell operation. Label the sample "Final Leach" and submit it for leachate analysis.

6) Transfer the wet solid from the rotary jar to a pre-weighed drying tray, ensuring all the sample has been moved. Record the weight of the wet sample.

7) Air dry the wet sample for 24 hours, or dry in an oven on low heat (<40°C) if necessary. Record the final weight of the dry sample. If sample was dried in an oven, cool in a desiccator prior to weighing.

8) Take a representative split from the sample and label it "Final Residue". Submit the split for all static tests defined in Chapter 5. These analyses will be known as "post-test data”.

9) Package the remaining sample, label it "Final Residue". Place it in cold storage for later examination.

10) Calculations are discussed in Section C.2.4.

C.2.4 Humidity Cell Calculations

The key objectives of laboratory kinetic tests are (a) long-term stable reaction rates under kinetic conditions and (b) depletion times for acid-generating, acid-neutralizing, and metal-leaching minerals. Therefore, interpretations of the tests focus on calculating these values. Recommended equations are listed in Table C-1. Examples of humidity-cell results are shown in Figures 5.3.1-1 to 5.3.1-8.

After a kinetic test is terminated, the closedown procedure (Section C.2.3) includes a final rinse to determine the amount of accumulated reaction products. These retained products should be redistributed evenly over all weeks of the test, based on the assumption that the weekly amount of retained product was constant. As a result, all calculated weekly rates will increase somewhat after the termination of the test. If the weekly increase is significant, the sample was not properly rinsed during the test (Section C.2.2).

TABLE C-1
Recommended Equations for Interpreting Laboratory Kinetic Tests

Acid Generation

Acidity Production Rate (mg $CaCO_3$/kg/wk) = Acidity (mg $CaCO_3$/L) * Volume Leachate Collected (L) / Sample Weight (kg)

Sulphate Production Rate (mg/kg/wk) = Sulphate (mg/L) * Volume Leachate Collected (L) / Sample Weight (kg)

Remaining S_{total} (% of original) = {[Initial %S_{total} - ((Cumulative Sulphate Production Rate (mg/kg) * 32.06 / 96.06) / 10000))] / Initial S_{total} as %S} * 100%

Remaining $S_{sulphide}$ (% of original) = {[Initial %$S_{sulphide}$ - ((Cumulative Sulphate Production Rate (mg/kg) * 32.06 / 96.06) / 10000))] / Initial $S_{sulphide}$ as %S} * 100%

Sulphate Production Rate By Surface Area (mg/m^2/wk) = Sulphate Production Rate (mg/kg/wk) / Surface Area (m^2/kg)

Molar Ratios

Carbonate Molar Ratio = [(Ca (mg/L)/40.08) + (Mg (mg/L)/24.31) + (Sr (mg/L)/ 87.62)] / (SO_4 (mg/L)/96.06)

Feldspar Molar Ratio = [(Ca (mg/L)/40.08) + (K (mg/L)/(2*39.1) + (Na (mg/L)/(2* 22.99)] / (SO_4 (mg/L)/96.06)

TABLE C-1
Recommended Equations for Interpreting Laboratory Kinetic Tests

Acid Neutralization and NP Consumption

Alkalinity Production Rate (mg $CaCO_3$/kg/wk) = Alkalinity (mg $CaCO_3$/L) * Volume Leachate Collected (L) / Sample Weight (kg)

Carbonate Ratio NP Consumption (mg $CaCO_3$/kg/wk) = Carbonate Molar Ratio * Theoretical NP Consumption (mg/kg/wk);

based on: $2H^+ + SO_4^{2-} + (Ca_xMg_{1-x})CO_{3(s)} \rightarrow xCa^{2+} + (1-x)Mg^{2+} + SO_4^{2-} + H_2CO_3^0$

or $2H^+ + SO_4^{2-} + 2(Ca_xMg_{1-x})CO_{3(s)} \rightarrow 2xCa^{2+} + (2-2x)Mg^{2+} + SO_4^{2-} + 2HCO_3^-$

Feldspar Molar Ratio Total NP Consumption (mg $CaCO_3$ equivalent/kg/wk) = Feldspar Molar Ratio * Theoretical NP Consumption (mg/kg/wk);

based on:

$2H^+ + SO_4^{2-} + 6H_2O + CaAl_2Si_2O_8 \rightarrow Ca^{2+} + SO_4^{2-} + 2Al(OH)_3 + 2H_4SiO_4^0$

$2H^+ + SO_4^{2-} + 6H_2O + 2KAlSi_3O_8 \rightarrow 2K^+ + SO_4^{2-} + 2Al(OH)_3 + 4H_4SiO_4^0$

$2H^+ + SO_4^{2-} + 6H_2O + 2NaAlSi_3O_8 \rightarrow 2Na^+ + SO_4^{2-} + 2Al(OH)_3 + 4H_4SiO_4^0$

Theoretical NP Consumption at pH 6 (mg $CaCO_3$/kg/wk) = Sulphate Production Rate (mg SO_4/kg/wk) * 100.09 / 96.06;

based on: $2H^+ + SO_4^{2-} + CaCO_{3(s)} \rightarrow Ca^{2+} + SO_4^{2-} + H_2CO_3^0$

Empirical Open-System NP Consumption around neutral pH (mg $CaCO_3$/kg/wk) = Theoretical NP Consumption (mg/kg/wk) + Alkalinity Production Rate (mg/kg/wk) - Acidity Production Rate (mg/kg/wk);

based on: $2H^+ + SO_4^{2-} + CaCO_{3(s)} \rightarrow Ca^{2+} + SO_4^{2-} + H_2CO_3^0$

plus $H_2CO_3^0 + CaCO_{3(s)} \rightarrow Ca^{2+} + 2HCO_3^-$

minus un-neutralized acidity

Theoretical Closed-System NP Consumption above pH 6.5 (mg $CaCO_3$/kg/wk) = [Theoretical NP Consumption (mg/kg/wk) * 2] - Acidity Production Rate (mg/kg/wk);

based on: $2H^+ + 2CaCO_{3(s)} \rightarrow 2Ca^{2+} + 2HCO_3^-$

minus un-neutralized acidity

Remaining NP (% of original) = {[Initial NP (t $CaCO_3$/1000 t) - (Cumulative NP Depletion Rate (mg/kg) / 1000)] / Initial NP (tonnes $CaCO_3$/1000 tonnes)} * 100%

TABLE C-1
Recommended Equations for Interpreting Laboratory Kinetic Tests

Metal Leaching

Metal Leach Rates (mg/kg/wk) = Metal Concentration (mg/L) * Volume of Leachate Collected (L) / Sample Weight (kg)

Remaining Metal (%of original) = {[Initial Metal Content (mg/kg) - Cumulative Metal Leach Rate (mg/kg)] / Initial Metal Content (mg/kg)} * 100%

NOTES: At later stages of some humidity cell testing programs, analyses for sulphate, alkalinity, and metals are not necessarily done on a weekly basis but may be decreased to monthly. In this circumstance, weekly values for rates can be calculated through interpolation of the preceding and subsequent measured values.

C.3 Field-Based Tests

Because humidity cells are carefully operated under controlled conditions (Section C.2), they are not subjected to annual patterns and unusual climatic events that can occur at a minesite. For this reason, in-field kinetic tests should be used to verify that humidity cells are providing reasonable information applicable to field conditions.

C.3.1 On-Site Kinetic Tests

Field kinetic tests show that they behave like either humidity cells (Section C.2), providing Rate1 (Figure 4.2.2-1), or full-scale minesite components (Section C.3.2) providing Rate2 (Figure 4.2.2-1), depending on the volume of rock and the amount of precipitation. Higher volumes of rock or proportionally less precipitation lead to significant geochemical retention (Section 5.2.4) typical of full-scale behavior. Lower volumes or proportionally more precipitation provide more complete rinsing of reaction products typical of humidity cells.

Method

1) Obtain or build a large container, open on top and with a basal drain hole. Some designs that have been used include (1) portable drilling mud tanks that hold about 2 t, (2) V-shaped trenches lined with geotextile holding 20 t, and (3) above-ground cribs holding over 100 t. The important criteria are (a) the volume of rock is known, (b) this volume is isolated from runoff and only exposed to precipitation, and (c) all water passing through the rock is collected at one point.

2) Daily measurements of temperature ranges and precipitation are required from a nearby location.

3) Whenever a significant rainfall event occurs, a clean bucket should be placed at the collection point to collect all water. After flow from the container ceases, retrieve the bucket, determine water volume, and process the water for chemical analysis (filter, preserve, etc.).

4) Interpretation of the results is discussed in Chapter 5.

C.3.2 On-Site Monitoring of Minesite Components

Although not often recognized as a kinetic test, on-site monitoring in and around minesite components is an excellent type of kinetic test, because it shows the in-field full-scale behaviour of a component. However, due to complexities such as geochemical retention (Section 5.2.4), these full-scale kinetic tests must be interpreted with caution (Section 4.2) and in conjunction with humidity cells (Section 5.3). The comparison of field monitoring and humidity cells has shown reasonable and compatible results when retention is taken into account.

The interpretation of on-site monitoring requires that any and all drainage-chemistry data for a minesite be regularly compiled into spreadsheets and occasionally re-examined for trends. The techniques of Section 4.2 and 5.5 should then be used to complete interpretations and predictions.

APPENDIX
D. METHODS FOR MINEWALL STATIONS

Installation and Operation of Monitoring Stations for Minewall Investigations

K. Morin, Version 1/96

Equipment (for each station):

Ø 3 m of 90°-bent, flexible plastic bathtub edging
Ù 2 tubes of pure silicon bathroom sealant (must be pure silicon)
Ú 1 sheet of clear plastic 1 m by 1 m
Û 8 black metal clasps often used for holding unbound reports
Ü 1 L of distilled water in a squeeze bottle which allows the direction and pressure of water to be controlled

Installation Procedure (see Figure D-1):

Ø Select a relatively flat surface of rock, preferably with no surface fractures, measuring no more than 1 m by 1 m.
Ù Mark the intended perimeter of the station on the surface with a pencil, with three, four, or five limbs of plastic edging.
Ú The lowest, or bottom, limb must slope downwards from horizontal so that all water caught on it will drain in one direction for collection and later analysis.
Û Cut the plastic edging to the length required for each limb.
Ü Install each limb by using pure silicon sealant as glue.
Ý Ensure silicon sealant fills all open spaces between the edging and the rock surface so that no water can pass underneath.
Þ Ensure each limb overlaps so that no large gaps exist at any junction; seal any smaller gaps with silicon.
ß Ensure the upper limb(s) will divert wall runoff around the sides of the station so that the water will not flow over the isolated area.
à With 1 L of distilled water, wash the entire isolated surface within the edging, rinsing out any loose rock/dust and ensuring all water is caught by the edging and directed to the bottom limb where the water can then be caught in a bottle.
á Cut the clear plastic sheet to extend 2 cm over each limb, then loosely attach the plastic sheet with the metal clasps, ensuring the plastic sheet does not touch the rock surface but prevents all precipitation or runoff from reaching the isolated rock surface.

Regular Sampling:

Ø Carefully remove the plastic sheet and place it somewhere clean and dry.
Ù Inspect the station for loose edging and broken seals against the rock; repair any problems AFTER sampling (below), but avoid losing rinse water through any broken seals.
Ú Record a note if there is any condensation and if any water may have condensed and trickled out of the station between sampling events.
Û Place a calibrated collection bottle at the downstream (outflow) end of the lower limb (trough) to catch all subsequent rinse water.
Ü With a calibrated squeeze bottle, spray at least 200 mL onto the isolated rock surface to rinse the entire area thoroughly; use as little water as possible; it is important to catch all rinse water in the collection bottle; record the volume of water sprayed on the rock.
Ý Record the amount of water recovered in the collection bottle.
Þ Analyze the water in the collection bottle like any other water sample, including pH, acidity, alkalinity,

sulfate, dissolved metals, and total metals as desired.

❽ As a quality-assurance procedure for one round of sampling, also filter a similar volume of the distilled water through a 0.45 µm filter, then analyze like all other water samples

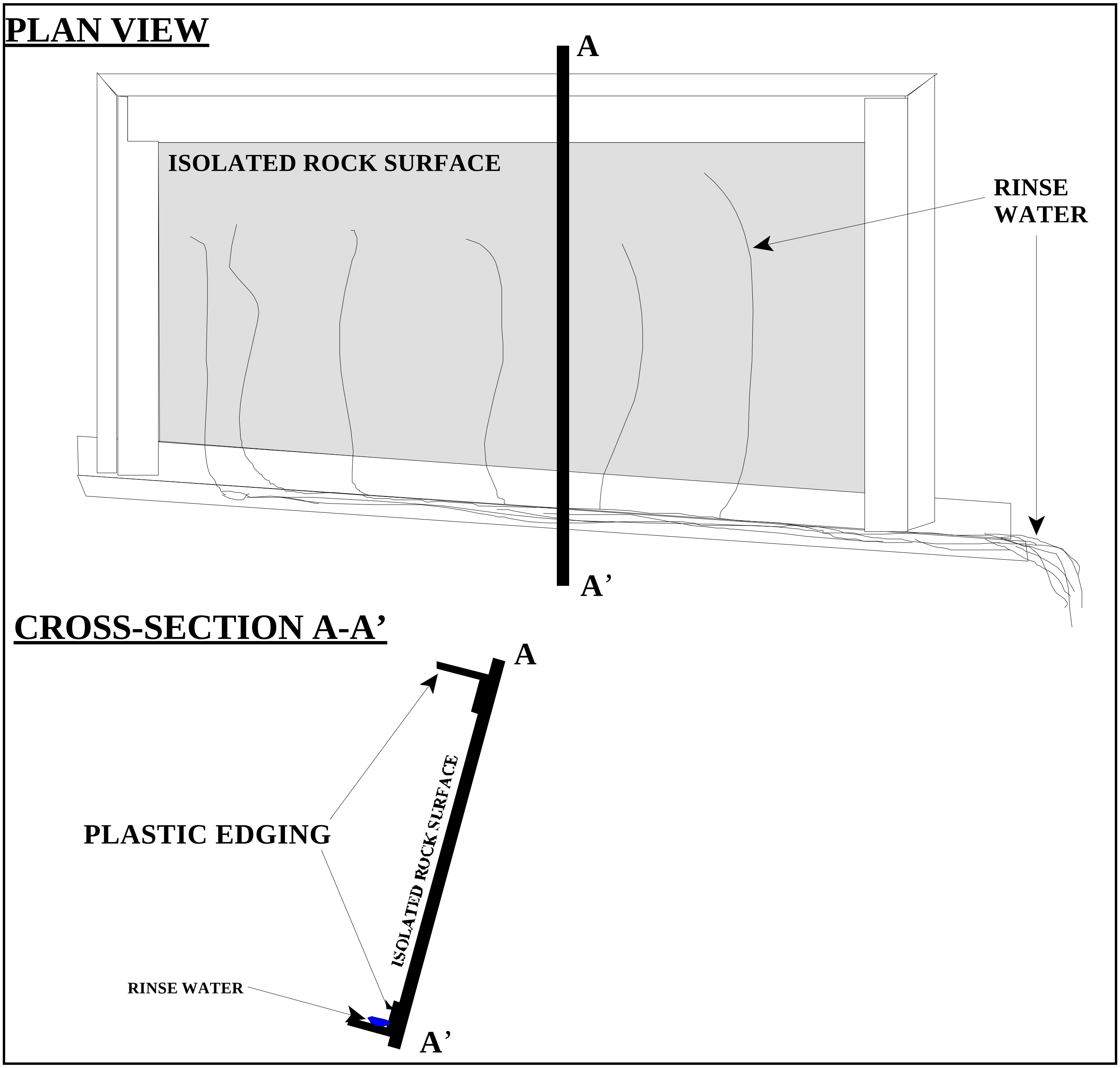

FIGURE D-1. Example of a MINEWALL Station (Plan View and Cross-Section).